


5th Edition

# Handbook of ICP-QQQ Applications using the Agilent 8800 and 8900

Primer



Agilent ICP-QQQ

**10**   
Years  
of enabling  
industry advances

## Foreword

Agilent Technologies launched its 8800 Triple Quadrupole ICP-MS (ICP-QQQ) at the 2012 Winter Conference on Plasma Spectrochemistry in Tucson, Arizona, USA.

By the time the first ICP-QQQ was launched, ICP-MS had already been around for almost three decades and was widely praised for its low limits of detection. In fact, it was considered as the technique-par-excellence for multi-element (ultra-)trace analysis in a wide variety of fields. However, spectral interferences were still causing concern in some applications. Significant progress had been made in providing ICP-MS users with adequate tools to cope with spectral overlaps compared to the early commercial instruments introduced in 1983. By using a double-focusing sector-field mass spectrometer instead of a quadrupole filter for mass analysis, many spectral interferences can be resolved, but this approach requires expensive instrumentation. Quadrupole-based instruments could be equipped with a multipole-based collision/reaction cell (CRC), which alleviated spectral interferences to a significant extent, for instance, by using a non-reactive collision gas such as helium to slow down polyatomic interfering ions to a larger extent than the atomic analyte ions, such that the former could be selectively discriminated against on the basis of their lower kinetic energy. The analytical community first saw Agilent's 8800 ICP-QQQ instrumentation as an improved version of a quadrupole-based ICP-MS equipped with a CRC. But the unique applications being performed using Agilent ICP-QQQ instruments installed in hundreds of laboratories across industry, research and academia clearly demonstrates that it is much more than that.

In Agilent's ICP-QQQ, an octopole CRC is preceded by an additional quadrupole, enabling double mass selection, i.e. before the ions enter the CRC and afterwards. When the first quadrupole is used as an ion guide only, the ICP-QQQ system can be used as a "traditional" quadrupole-based ICP-MS instrument. This mode could be useful for carrying out routine analysis not significantly challenged by spectral interferences. When operated in tandem or MS/MS mode, however, the double mass selection only allows the analyte ion and the interfering ion(s) with the same mass-to-charge ratio to enter the CRC; all ions with a different mass-to-charge ratio are removed at this stage. Consequently, the control over the processes in the cell is greatly improved as the reaction of other (e.g. matrix) ions with the cell gas no longer hinders the desired reaction process. In case of a mass-shift reaction—i.e. chemical conversion of the analyte ion into a reaction product ion that can be measured interference-free at another mass-to-charge ratio—the absence of other ions at the new "location" of the product ion in the mass spectrum is guaranteed. As a result, interesting but challenging elements, such as S and P in biochemical applications, As and Se in environmental and food applications, or Si in nanoparticle applications can be easily assayed, interference-free.

Profiting from the analytical advantages offered by MS/MS functionality, some ICP-QQQ users have demonstrated a larger degree of creativity by using very reactive gases such as  $\text{NH}_3$  or  $\text{CH}_3\text{F}$  in the CRC and monitoring reaction product ions at much higher mass-to-charge ratios than could be adequately exploited previously. Although this might initially sound complicated, the ICP-QQQ's software offers tools like product ion scanning, precursor ion scanning and differential mass scanning that provide the user with a clear insight into the reactions proceeding in the cell and allow the product ion that will provide the best, often unprecedented limits of detection to be easily identified. This level of freedom and ease of use leads to a situation in which every type of spectral overlap – whether caused by a polyatomic ion, doubly charged ion or isobaric nuclide – can be successfully overcome. Moreover, ICP-QQQ users have also been charmed by the additional advantages provided by this type of instrumentation, such as the unparalleled abundance sensitivity, which is an added benefit of double mass selection.

In 2016, the 8800 ICP-QQQ was replaced by the Agilent 8900 ICP-QQQ series. While maintaining the performance to resolve spectral interferences, this second generation ICP-QQQ instrument provides enhanced sensitivity and a faster detector system with a 100  $\mu\text{s}$  minimum dwell time. The latter feature is of specific importance in single-nanoparticle analysis, a rapidly emerging type of application, and in handling fast transient signals, such as those generated via laser ablation systems equipped with ultra-fast ablation cells.

In my opinion, ICP-QQQ has not only fulfilled its initial promises, but has greatly surpassed the anticipations of the diverse community of ICP-MS users.

**Frank Vanhaecke**

Department of Analytical Chemistry  
Ghent University, Belgium  
[www.analchem.ugent.be/A&MS](http://www.analchem.ugent.be/A&MS)

# Table of contents

Title	Elements	Page
Introduction to Agilent Triple Quadrupole ICP-MS		8
<b>Semiconductor</b>		12
<b>Process chemicals</b>		
Ultrapure process chemicals analysis by ICP-QQQ with hot plasma conditions	Multiple	13
Determination of ultratrace elements in SEMI Grade 5 high purity hydrogen peroxide	Multiple	19
Automated analysis of semiconductor grade hydrogen peroxide and DI water using ICP-QQQ	Multiple	22
Ultratrace measurement of calcium in ultrapure water	Ca	31
Ultratrace measurement of potassium and other elements in UPW using ICP-QQQ in cool plasma/reaction mode	Multiple	34
Ultralow level determination of phosphorus, sulfur, silicon, and chlorine using the Agilent 8900 ICP-QQQ	P, S, Si, Cl	37
Direct analysis of trace metal impurities in high purity nitric acid using ICP-QQQ	Multiple	42
Direct determination of V, Cr, Ge, and As in high-purity 20% hydrochloric acid	Multiple	49
Analysis of trace metal impurities in high purity hydrochloric acid using ICP-QQQ	Multiple	52
Determination of Ti, V, and Cr in 9.8% sulfuric acid	Ti, V, Cr	62
Determination of trace elements in ultrapure semiconductor grade sulfuric acid using the Agilent 8900 ICP-QQQ in MS/MS mode	Multiple	64
Multielement nanoparticle analysis of semiconductor process chemicals using spICP-QQQ	Multiple	70
<b>Silicon wafers</b>		
Silicon wafer analysis: Determination of phosphorus and titanium in a high silicon matrix	P, Ti	77
Analysis of ultratrace impurities in high silicon matrix samples by ICP-QQQ	Multiple	80
<b>Organic chemicals</b>		
Analysis of sulfur, phosphorus, silicon, and chlorine in N-methyl-2-pyrrolidone	S, P, Si, Cl	86
Analysis of silicon, phosphorus, and sulfur in 20% methanol	Si, P, S	90
Automated ultratrace element analysis of isopropyl alcohol with the Agilent 8900 ICP-QQQ	Multiple	93
Analysis of nanoparticles in organic reagents by Agilent 8900 ICP-QQQ in spICP-MS mode	Fe	104
Analysis of 15 nm iron nanoparticles in organic solvents by spICP-MS	Fe	109
<b>Semiconductor gases</b>		
GC-ICP-QQQ achieves sub-ppb detection limits for hydride gas contaminants	P, Ge, As, S	112
Determination of trace impurities in electronic grade arsine by GC-ICP-QQQ	Si, P, Ge, S	116

Title	Elements	Page
<b>Materials</b>		122
<b>Rare earth oxides</b>		
Direct measurement of trace rare earth elements in high purity REE oxides	REEs	123
Removal of MH <sup>+</sup> interferences in refined REE material analysis	REEs	126
Direct analysis of trace REEs in high purity Nd <sub>2</sub> O <sub>3</sub>	REEs	129
Direct determination of challenging trace rare earth elements in high purity lanthanide REE oxides	REEs	132
<b>Metals</b>		
Arsenic measurement in cobalt matrix using MS/MS mode with oxygen mass-shift	As	135
Analysis of ultratrace impurities in high purity copper using the Agilent 8900 ICP-QQQ	Multiple	138
Determination of sulfur, phosphorus, and manganese in high purity iron	S, P, Mn	145
The benefits of improved abundance sensitivity with MS/MS for trace elemental analysis of high purity metals	Multiple	148
Ultratrace copper analysis in a semiconductor grade organometallic titanium complex	Cu	152
<b>Nanomaterials</b>		
Analysis of 10 nm gold nanoparticles using the high sensitivity of the Agilent 8900 ICP-QQQ	Au	155
High sensitivity analysis of SiO <sub>2</sub> nanoparticles using the Agilent 8900 ICP-QQQ	Si	158
Accurate determination of TiO <sub>2</sub> nanoparticles in complex matrices using the Agilent 8900 ICP-QQQ	Ti	161
<b>Environmental</b>		168
Routine soil analysis using the Agilent 8800 ICP-QQQ	Multiple	169
The accurate measurement of selenium in reference materials using online isotope dilution	Se	172
ICP-QQQ with oxygen reaction mode for accurate trace-level arsenic analysis in complex samples	As	176
Avoidance of spectral overlaps on reaction product ions with O <sub>2</sub> cell gas: comparison of quadrupole ICP-MS and ICP-QQQ	Ti	181
Removal of complex spectral interferences on noble metal isotopes	Ru, Rh, Pd, Ag, Os, Ir, Pt, Au	184
Analysis of platinum group elements (PGEs), silver, and gold in roadside dust using triple quadrupole ICP-MS	Ru, Rh, Pd, Ag, Os, Ir, Pt, Au	190
Direct analysis of ultratrace rare earth elements in environmental waters by ICP-QQQ	REE	199
Solving doubly charged ion interferences using an Agilent 8900 ICP-QQQ	Ca, Sc, Zn, As, Se	205
Removal of REE <sup>++</sup> interference on arsenic and selenium	As, Se	211
Removal of molybdenum oxide interference on cadmium	Cd	215
Rapid analysis of radium-226 in water samples by ICP-QQQ	Ra	218
Feasibility study of fluorine detection by ICP-QQQ	F	222
HPLC-ICP-MS/MS: fluorine speciation analysis	F	225

Title	Elements	Page
<b>Foods and consumer products</b>		228
<b>Elemental analysis</b>		
Benefits of the Agilent 8900 ICP-QQQ with MS/MS operation for routine food analysis	Multiple	229
Routine elemental analysis of dietary supplements using an Agilent 8900 ICP-QQQ	Multiple	241
Accurate and sensitive analysis of arsenic and selenium in foods using ICP-QQQ to remove doubly-charged REE interferences	As, Se	250
Analysis of TiO <sub>2</sub> nanoparticles in foods and personal care products by single particle ICP-QQQ	Ti	254
Accurate analysis of trace mercury in cosmetics using the Agilent 8900 ICP-QQQ	Hg	263
Sulfur isotope fractionation analysis in mineral waters using an Agilent 8900 ICP-QQQ	S	269
<b>Speciation</b>		
Fast analysis of arsenic species in infant rice cereals using LC-ICP-QQQ	As	275
High throughput determination of inorganic arsenic in rice using hydride generation-ICP-QQQ	As	282
Fast determination of inorganic arsenic (iAs) in food and animal feed by HPLC-ICP-MS	As	286
Multielement analysis and selenium speciation in cattle and fish feed using LC-ICP-QQQ	Multiple	295
Arsenic speciation analysis in apple juice using HPLC-ICP-MS with the Agilent 8800 ICP-QQQ	As	304
Speciated arsenic analysis in wine using HPLC-ICP-QQQ	As	312
Fast analysis of arsenic species in wines using LC-ICP-QQQ	As	319
Simultaneous iodine and bromine speciation analysis of infant formula by HPLC-ICP-MS	I, Br	326
Determination of pesticides using phosphorus and sulfur detection by GC-ICP-QQQ	P, S	333
<b>Petrochemicals</b>		336
Determination of P, Si and S in acid digested lubricating oil using the Agilent 8800 triple quadrupole ICP-MS	P, Si, S	337
Accurate sulfur quantification in organic solvents using isotope dilution mass spectrometry	S	342
Determination of chloride in crude oils using an Agilent 8900 ICP-QQQ	Cl	346
Single nanoparticle analysis of asphaltene solutions using ICP-QQQ	Fe, Mo	351
Gas chromatographic separation of metal carbonyls in carbon monoxide with detection using the Agilent 8800 ICP-QQQ	Ni, Fe	358
<b>Geology and geochemistry</b>		363
Lead isotope analysis: removal of <sup>204</sup> Hg isobaric interference on <sup>204</sup> Pb using ICP-QQQ MS/MS reaction cell	Pb	364
Fractionation of sulfur isotope ratio analysis in environmental waters	S	368
Measurement of <sup>87</sup> Sr/ <sup>86</sup> Sr isotope ratios in rocks by ICP-QQQ in mass-shift mode	Sr	372
Direct strontium isotopic analysis of solid samples by LA-ICP-MS/MS	Sr	378
Resolution of <sup>176</sup> Yb and <sup>176</sup> Lu interferences on <sup>176</sup> Hf to enable accurate <sup>176</sup> Hf/ <sup>177</sup> Hf isotope ratio analysis using an Agilent 8800 ICP-QQQ with MS/MS	Hf	382

Title	Elements	Page
<b>Nuclear</b>		390
Analysis of radioactive iodine-129 using MS/MS with O <sub>2</sub> reaction mode	I	391
Feasibility study on the analysis of radioisotopes: Sr-90 and Cs-137	Sr, Cs	395
Determination of trace <sup>236</sup> U as UOO <sup>+</sup> using ICP-QQQ O <sub>2</sub> mass-shift method	U	398
Measurement of neptunium in the presence of uranium: benefits of low abundance sensitivity and oxygen reaction mode	Np, U	401
Direct analysis of zirconium-93 in nuclear site decommissioning samples by ICP-QQQ	Zr	404
<b>Clinical research</b>		410
Manganese analysis in whole blood: expanding the analytical capabilities of ICP-MS	Mn	411
Measurement of titanium to assess joint replacements	Ti	415
Measurement of selenium in the presence of Gd-based MRI contrasting agents	Se	418
Evaluation of the elemental content of a single cell using fast time-resolved analysis (TRA) ICP-MS	Mg, P, Fe, Zn	421
<b>Life science</b>		428
Simultaneous quantitation of peptides and phosphopeptides by capLC-ICP-QQQ	P, S	429
Analysis of selenoproteins in rat serum using HPLC-ICP-QQQ	Se	432
Absolute quantification of intact proteins in snake venom by capLC-ICP-QQQ	S	435
<b>Pharmaceutical</b>		441
Quantitative analysis of active pharmaceutical ingredients using heteroatoms as elemental labels	S, P, Cl	442
Fast and accurate absolute-quantification of proteins and antibodies using ID-ICP-QQQ	S	446
Determination of diclofenac and its related compounds using RP-HPLC-ICP-QQQ	Cl	449
Characterization of rare earth elements used for radiolabeling applications by ICP-QQQ	REE	456
<b>Glossary</b>		464

# Introduction to Agilent Triple Quadrupole ICP-MS

Agilent introduced the world's first triple quadrupole ICP-MS (ICP-QQQ) in 2012.

The Agilent 8800 ICP-QQQ signaled a major advance in ICP-MS technology and redefined performance for trace element analysis. Compared to existing quadrupole ICP-MS instruments, the 8800 ICP-QQQ offered significant analytical benefits across many applications in both industry and academic research laboratories. Building on this success, the Agilent 8900 ICP-QQQ was launched four years later, in 2016.

## Configuration of Agilent's ICP-QQQ instrumentation

According to IUPAC (term 538 from the 2013 Recommendations), a triple quadrupole mass spectrometer is a *"Tandem mass spectrometer comprising two transmission quadrupole mass spectrometers in series, with a (non-selecting) RF-only quadrupole (or other multipole) between them to act as a collision cell."*

The cell containing the ion guide—the Octopole Reaction System (ORS) in the case of Agilent ICP-QQQ—can be pressurized with a collision or reaction gas to allow the selective attenuation of potential interfering ions.

In MS/MS operation, where both quadrupoles are operated as unit mass filters, ions at the target analyte mass are selected by the first quadrupole (Q1) and passed to the ORS cell, where the analyte ions are separated from overlapping interfering ions. The resulting product ions that emerge from the cell are then filtered by the second quadrupole (Q2) before being passed to the detector. This configuration releases the full potential of reaction cell gas methods to resolve spectroscopic interferences including isobaric and doubly-charged interferences, as well as polyatomic ion overlaps.

As a result, ICP-QQQ can determine a wider range of analytes at much lower concentrations with greater reliability and higher confidence.

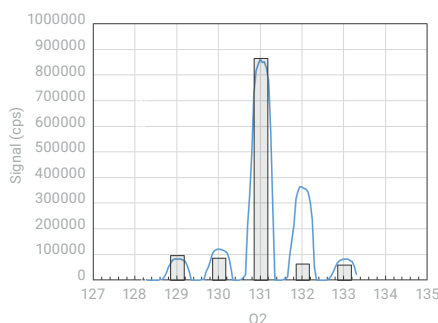




Figure 1. Cutaway diagram of the Agilent 8900 ICP-MS.

## ICP-MS/MS technology

Ti<sup>+</sup>(NH)(NH<sub>3</sub>)<sub>4</sub> spectrum; Δm = 2.1 u of Q1



Ti<sup>+</sup>(NH)(NH<sub>3</sub>)<sub>4</sub> spectrum; Δm = 0.7 u of Q1

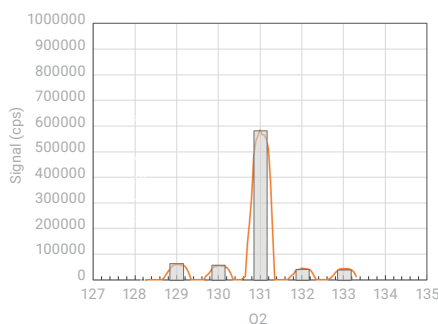


**Figure 2.** Ti + (NH)(NH<sub>3</sub>)<sub>4</sub> product ion spectrum of five Ti isotopes obtained with NH<sub>3</sub> cell gas mode: <sup>46</sup>Ti (8.25%), <sup>47</sup>Ti (7.44%), <sup>48</sup>Ti (73.72), <sup>49</sup>Ti (5.41%), and <sup>50</sup>Ti (4.29%). A Ti standard solution was analyzed using ICP-QQQ with NH<sub>3</sub> cell gas. Top: Q1 was set at Δm = 2.1 u. Bottom: spectrum was acquired with Q1 set at Δm = 0.7 u.

The tandem MS configuration of Agilent ICP-QQQ instruments – with two fully functioning mass filters, one either side of the ORS cell – allows unprecedented control over the ions that enter the collision/reaction cell (CRC). Q1 rejects all non-target masses/elements, ensuring more consistent reaction processes in the CRC, even when the sample composition varies. Precise mass selection by the first quadrupole, Q1, is crucial to the accurate analytical performance in MS/MS mode. For reliable, consistent control of reaction processes, Q1 must allow only ions at the target mass-to-charge ratio ( $m/z$ ) to pass into the cell. Inefficient mass filtering would cause results to be compromised by interferences arising from non-target ions entering the cell. To ensure the most effective mass filtering and the best quality data, Agilent ICP-QQQ instruments use the same hyperbolic quadrupole mass spectrometer for Q1 and Q2. Both quadrupoles are placed in the high vacuum region to ensure optimum mass filtering. This arrangement allows both quadrupoles to operate at unit mass resolution and low abundance sensitivity while maintaining high transmission and sensitivity.

The impact of varying Q1 mass filter performance is illustrated in the comparison of product ion spectra for Ti–NH<sub>3</sub> cluster ions shown in Figure 2. The product ion spectrum (top) was obtained using Q1 settings that provide compromised mass resolution, with Q1 passing all masses in a 2.1 u window. This wider Q1 mass window allowed non-target ions to enter the cell, so the reaction processes and product ions formed were not under control. In this case, the overlapping ions were derived from different NH<sub>3</sub> clusters formed from the other Ti isotopes. For example, when <sup>49</sup>Ti is the target analyte but Q1 fails to exclude <sup>48</sup>Ti from the cell, <sup>48</sup>Ti(NH<sub>2</sub>)(NH<sub>3</sub>)<sub>4</sub><sup>+</sup> forms in the cell and overlaps <sup>49</sup>Ti(NH)(NH<sub>3</sub>)<sub>4</sub><sup>+</sup> at  $m/z$  132. In contrast, the Ti isotopic pattern (bottom) was obtained with Q1 set to operate with mass resolution of 0.7 u; i.e. as a true mass filter providing genuine MS/MS operation. The Ti–NH<sub>3</sub> product ions fit the expected Ti isotopic pattern perfectly, confirming that each Ti isotope entered the cell in isolation to react with the NH<sub>3</sub> cell gas, i.e. <sup>48</sup>Ti<sup>+</sup> + NH<sub>3</sub> → <sup>48</sup>Ti(NH)(NH<sub>3</sub>)<sub>4</sub><sup>+</sup>. The results show that if the mass resolution of Q1 is greater than 0.7 u, precise analysis of the specific target analyte ion/isotope is impossible. Without true MS/MS operation (both quadrupoles operating with unit mass resolution), analytical results acquired for any analyte could be compromised because unexpected reaction product ions can be formed and cause overlap on the target product ion.

## Second-generation triple quadrupole ICP-MS: the Agilent 8900 ICP-QQQ

Building on the success of the 8800, the 8900 ICP-QQQ provides performance and productivity improvements to address a wider range of applications:

- Double the sensitivity of the 8800: users of the 8900 can achieve lower detection limits or improve matrix robustness by diluting samples, without degrading detection capability. Note that the sensitivity of the Agilent 8900 Semiconductor configuration ICP-QQQ now exceeds 1Gcps/ppm (1,000,000,000 counts per second per ppm).
- Axial Acceleration on the 8900 Advanced Applications and Semiconductor configurations controls the energy of ions in the cell. This increases the sensitivity in reaction cell mode and reduces potential product ion overlaps due to slow moving ions.
- Lower contribution from instrumental background: the 8900 ICP-QQQ is designed and manufactured to control background signals arising from the instrument itself. This attention to detail allows users to achieve even lower BECs than the 8800. The DL specification of the 8900 Advanced Applications and Semiconductor configurations for sulfur and silicon is < 50 ppt.
- 0.1 ms dwell time: the 8900 ICP-QQQ uses a new fast detector with fast time resolved analysis (TRA) capability suitable for the accurate analysis of single nanoparticles (sNPs). High speed is combined with effective interference removal and specialized software to process the signals and reveal the particle size and size distribution.

With true triple quadrupole performance, the advanced features and the robustness of the 8900 ICP-QQQ make it a supremely powerful and flexible multi-element analyzer. Agilent's Triple Quadrupole ICP-MS instruments will continue to open up new possibilities for analysts, especially for the most challenging applications.

# Semiconductor

<b>Title</b>	<b>Page</b>
<b>Process chemicals</b>	
Ultrapure process chemicals analysis by ICP-QQQ with hot plasma conditions	13
Determination of ultratrace elements in SEMI Grade 5 high purity hydrogen peroxide	18
Automated analysis of semiconductor grade hydrogen peroxide and DI water using ICP-QQQ	22
Ultratrace measurement of calcium in ultrapure water	31
Ultratrace measurement of potassium and other elements in UPW using ICP-QQQ in cool plasma/reaction mode	34
Ultralow level determination of phosphorus, sulfur, silicon, and chlorine using the Agilent 8900 ICP-QQQ	37
Direct analysis of trace metal impurities in high purity nitric acid using ICP-QQQ	42
Direct determination of V, Cr, Ge, and As in high-purity 20% hydrochloric acid	49
Analysis of trace metal impurities in high purity hydrochloric acid using ICP-QQQ	52
Determination of Ti, V, and Cr in 9.8% sulfuric acid	62
Determination of trace elements in ultrapure semiconductor grade sulfuric acid using the Agilent 8900 ICP-QQQ in MS/MS mode	64
Multielement nanoparticle analysis of semiconductor process chemicals using spICP-QQQ	70
<b>Silicon wafers</b>	
Silicon wafer analysis: Determination of phosphorus and titanium in a high silicon matrix	77
Analysis of ultratrace impurities in high silicon matrix samples by ICP-QQQ	80
<b>Organic chemicals</b>	
Analysis of sulfur, phosphorus, silicon, and chlorine in N-methyl-2-pyrrolidone	86
Analysis of silicon, phosphorus, and sulfur in 20% methanol	90
Automated ultratrace element analysis of isopropyl alcohol with the Agilent 8900 ICP-QQQ	93
Analysis of nanoparticles in organic reagents by Agilent 8900 ICP-QQQ in spICP-MS mode	104
Analysis of 15 nm iron nanoparticles in organic solvents by spICP-MS	109
<b>Semiconductor gases</b>	
GC-ICP-QQQ achieves sub-ppb detection limits for hydride gas contaminants	112
Determination of trace impurities in electronic grade arsine by GC-ICP-QQQ	116

# Ultrapure Process Chemicals Analysis by ICP-QQQ with Hot Plasma Conditions

## Authors

Kazuhiro Sakai and  
Yoshinori Shimamura  
Agilent Technologies, Inc.

Meeting single- and sub-ppt guideline levels for ASTM/SEMI elements in ultrapure water using an Agilent 8900 ICP-QQQ

## Introduction

Contamination control is critical in semiconductor device fabrication (FAB) facilities (1). Contaminants may be introduced via the wafer substrate, or the chemicals and reagents used during the manufacturing process. Impurities—particularly metal ions and particles—adversely affect device performance and production yield, so FABs use the highest purity reagents and follow strict protocols to control contaminants during the manufacturing process. Ultrapure water (UPW) is used throughout the wafer fabrication process including in the RCA standard cleaning (SC-1/SC-2) procedure to remove chemical contaminants and particulate impurities from the wafer surface. UPW is one of the most critical process chemicals for contamination-control as the water is in direct contact with the wafer surface at many stages of manufacturing. Any impurities present in the UPW could directly affect the electrical properties of the finished device, for example, by reducing dielectric breakdown voltage.

ASTM International and Semiconductor Equipment and Materials International (SEMI) publish standards regarding the specifications for semiconductor process chemicals and reagents, including UPW. ASTM D5127-13, 2018 and SEMI F63-0521, 2021 provide guidance for the quality of UPW needed to produce devices with linewidths < 0.045 microns (2, 3). Both standards require detection limits (DLs) of less than 0.5 ppt (boron has a higher limit of 15 ppt) and background equivalent concentrations (BECs) less than 1 ppt (50 ppt for B). The semiconductor industry standard method for monitoring trace element contaminants is ICP-MS, with laboratories increasingly switching to triple quadrupole ICP-MS (ICP-QQQ or ICP-MS/MS) for its superior detection limits. The Agilent 8900 ICP-QQQ is a tandem MS instrument, which uses MS/MS operation to further improve the performance of the technique compared to single quadrupole ICP-MS instruments.

The 8900 ICP-QQQ meets the electronic and semiconductor industry's need for trace and ultratrace element analysis due to its high sensitivity, low background, and interference removal capabilities. The 8900 has the flexibility to operate in several modes to give optimum performance across different applications. For example, semiconductor labs often use cool plasma conditions to achieve the lowest BECs and DLs for interfered elements and easily ionized elements (EIEs). Cool plasma reduces EIE backgrounds and suppresses the formation of intense argon-based interferences such as  $\text{Ar}^+$ ,  $\text{ArH}^+$ , and  $\text{ArO}^+$ , allowing low-level analysis of  $^{40}\text{Ca}$ ,  $^{39}\text{K}$ , and  $^{56}\text{Fe}$ , respectively.

Cool plasma gives excellent results in low matrix samples, such as UPW, H<sub>2</sub>O<sub>2</sub>, HNO<sub>3</sub>, and HCl (4). However, high matrix samples, such as silicon and metal digests, are difficult to run using cool plasma due to the higher level of matrix suppression. More robust, hot plasma (low CeO/Ce ratio) conditions are preferred for such sample types. For labs wishing to use only hot plasma, the 8900 ICP-QQQ can be fitted with an optional skimmer cone and m-lens that provide optimum performance in hot plasma conditions. In a recent study, an 8900 fitted with the optional m-lens was used to determine 38 elements in two digested silicon samples prepared at 10 and 100 ppm Si (5). The m-lens and the skimmer cone that it is paired with have an optimized geometry that minimizes EIE backgrounds when using normal, hot plasma conditions. Using m-lens, the 8900 was able to measure all required elements at ppt levels in the Si matrix without using cool plasma.

The 8900 with m-lens can also be used to analyze ultratrace elements in low matrix semiconductor samples – such as UPW – using only normal, hot plasma conditions. In this study, hot plasma was combined with no gas mode and two cell gas modes to resolve spectral interferences, achieving single- or sub-ppt BECs and DLs for all analytes.

## Experimental

### Reagents and sample preparation

UPW (Organo Corp, Tokyo, Japan) was acidified to 0.1% with high purity 68% HNO<sub>3</sub> (TAMAPURE AA-100, Japan). Acidification ensures that elements are retained as soluble ions in solution, although adding acid can potentially contribute to the level of contamination.

### Calibration standards

The 8900 ICP-QQQ was calibrated using the method of standard addition (MSA), as is typical for the analysis of high-purity semiconductor samples. A mixed multi-element standard (SPEX CertiPrep, NJ, US) was prepared and spiked into the UPW to give standard additions at 5, 10, 20, and 40 ppt.

### Instrumentation

The 8900 Semiconductor Configuration ICP-QQQ was fitted with standard components including a PFA-100 MicroFlow nebulizer, quartz spray chamber, quartz torch with 2.5 mm injector, and Pt sampling cone. The standard s-lens was replaced with an optional m-lens (part number G3666- 67500) and optional Pt-tipped, Ni-based skimmer cone for m-lens (part number G3666-67501). The 8900 includes the ORS<sup>4</sup> collision/reaction cell (CRC) and two quadrupoles (Q1 and Q2), one either side of the CRC, enabling double mass selection (MS/MS). Q1 rejects all nontarget ions before they enter the cell, allowing only analyte ions and on-mass interference ions to pass to the cell. The analyte and interfering ions can then be separated using predictable, consistent, and reproducible reaction chemistry (6, 7). Q2 then ensures that only the analyte ions (on-mass mode) or analyte-product ions (mass-shift mode) pass to the detector, free of interferences.

Agilent ICP-MS MassHunter instrument control software for the 8900 provides simple method setup to measure analytes in different cell gas modes using a single multitune acquisition. In this analysis no gas mode, ammonia reaction mode (using a mixture of ammonia and hydrogen cell gases), and oxygen reaction mode were used to remove interferences using a combination of on-mass and mass-shift measurement. During data acquisition, the cell gases and measurement modes were switched automatically, giving a fast and automated analysis using the best mode for each analyte. Instrument acquisition and operating parameters are given in Table 1.

**Table 1.** Agilent 8900 ICP-QQQ operating conditions.

	No Gas	NH <sub>3</sub> +H <sub>2</sub>	O <sub>2</sub>
<b>Acquisition Parameters</b>			
Scan Mode	MS/MS		
Replicates (standards)	3		
Replicates (blank)	10		
Integration Time per Mass (s)	1.0		
<b>Plasma</b>			
RF Power (W)	1600		
Sampling Depth (mm)	8.0		
Nebulizer Gas (L/min)	0.70		
CeO <sup>+</sup> /Ce <sup>+</sup> (%)	2		
<b>Cell</b>			
He Flow Rate (mL/min)	-	1	-
H <sub>2</sub> Flow Rate (mL/min)	-	2	-
*NH <sub>3</sub> Flow Rate (mL/min)	-	2.0 (20%)	-
O <sub>2</sub> Flow Rate	-	-	0.45 (30%)
KED (V)	3	-10	-7

\*Mix of 10% NH<sub>3</sub> in 90% He

## Results and discussion

### Calibration curves

Four representative MSA calibration curves for K, Ca, Fe, and Ni in UPW are shown in Figure 1. No background subtraction or blank correction was performed. The four analytes are representative of the EIEs (K), elements with severe background interferences (Ca), elements of particular importance for the semiconductor industry (Fe), and elements that could indicate contamination from the ICP-MS interface (Ni). All the SEMI element calibrations showed excellent linearity ( $r > 0.999$ ) and low BECs. This performance confirms the high sensitivity of the 8900 and the effectiveness of the reaction cell method with m-lens to control elemental backgrounds and resolve interferences.

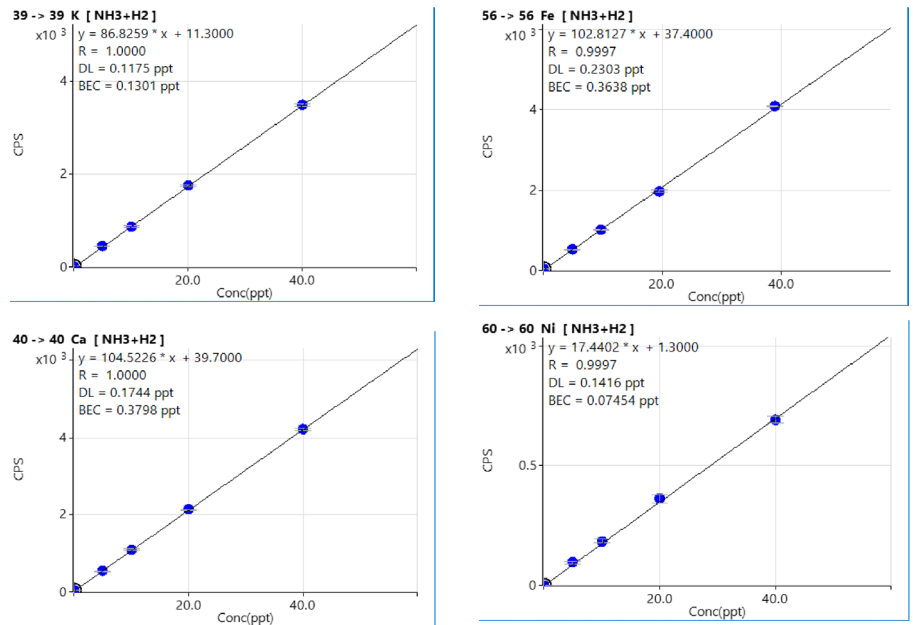


Figure 1. Representative MSA calibration plots for K, Ca, Fe, and Ni in UPW.

### BECs and DLs

BECs and DLs for 26 elements were calculated automatically by the ICP-MS MassHunter software (Table 2). BECs below 0.5 ppt and DLs below 0.3 ppt were obtained for 25 SEMI elements, easily meeting the limits for UPW specified by ASTM and SEMI. The higher specified limits for boron (50 ppt BEC and DL of 15 ppt) were also easily achieved (measured BEC of 1.11 ppt and DL of 1.18 ppt). Backgrounds are highly dependent on water quality, but the BEC achieved in this work was a factor of 50 lower than the SEMI guideline, easily meeting current industry requirements. Critical metallic (conductive) contaminants such as Al, Cr, Fe, Co, Ni, Cu, Zn, and Mo were measured with BECs and DLs substantially below 0.5 ppt, again easily meeting industry requirements.

The results, which are also shown in Figure 2, demonstrate the suitability of the 8900 ICP-QQQ using hot plasma for the analysis of ultratrace contaminants in high purity semiconductor process chemicals.

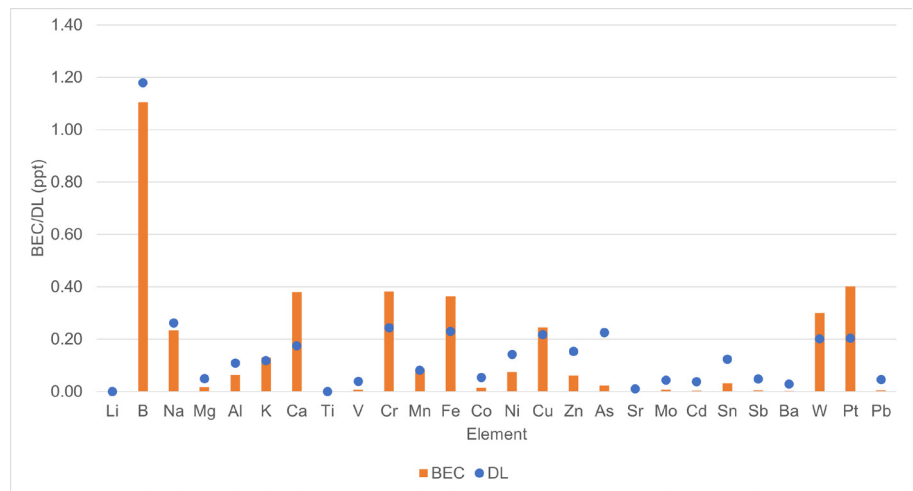


Figure 2. BECs and DLs for SEMI specified elements in UPW measured using the 8900 ICP-QQQ with hot plasma conditions.



## Conclusion

The study has demonstrated the suitability of the Agilent 8900 ICP-QQQ with optional m-lens for the measurement of ultratrace-level contaminants in low-matrix semiconductor reagents such as UPW. The m-lens ensured that background signals for the EIEs – K, Na, Ba, and Li – were minimized, allowing all 26 SEMI-critical elements to be measured at ppt levels using hot plasma conditions (CeO/Ce ratio < 2%). All potential spectral interferences were resolved by operating the 8900 in MS/MS mode using a single multitune method with no gas and two reaction gas modes.

Standard addition calibration curves from 0 ppt to 40 ppt concentration range showed excellent linearity and sensitivity for all elements. The low BECs showed that the method successfully removed all spectral interferences, including argon-based interferences that typically form under hot plasma conditions. The 8900 method resolved the intense interferences such as Ar<sup>+</sup>, ArH<sup>+</sup>, and ArO<sup>+</sup>, allowing sub-ppt analysis of <sup>40</sup>Ca, <sup>39</sup>K, and <sup>56</sup>Fe, respectively.

The BECs and DLs for all elements were well below the recommendations set by ASTM and SEMI for the quality of UPW related to semiconductor-industry manufacturing at < 0.045 m linewidths.

**Table 2.** Agilent 8900 ICP-QQQ DLs and BECs and ASTM/SEMI requirements for 26 elements in UPW.

Analyte	Tune Mode	Measured in UPW by 8900		ASTM D5127-13 (2018) Requirements	SEMI F63-0521 (2021) Requirements			
		Q1	Q2	DL (ppt)	BEC (ppt)	BEC (ppt)	BEC (ppt)	MDL (ppt)
Li	No gas	7		0	0	<1	<1	0.5
B	No gas	11		1.18	1.11	<50	<50	15
Na	No gas	23		0.26	0.23	<1	<1	0.5
Mg	NH <sub>3</sub> +H <sub>2</sub>	24		0.05	0.02	<1	<1	0.5
Al	NH <sub>3</sub> +H <sub>2</sub>	27		0.11	0.06	<1	<1	0.5
K	NH <sub>3</sub> +H <sub>2</sub>	39		0.12	0.13	<1	<1	0.5
Ca	NH <sub>3</sub> +H <sub>2</sub>	40		0.17	0.38	<1	<1	0.5
Ti	O <sub>2</sub>	48	64	0	0	<10	<1	0.5
V	NH <sub>3</sub> +H <sub>2</sub>	51		0.04	0.01	<10	<1	0.5
Cr	NH <sub>3</sub> +H <sub>2</sub>	52		0.24	0.38	<1	<1	0.5
Mn	NH <sub>3</sub> +H <sub>2</sub>	55		0.08	0.09	<10	<1	0.5
Fe	NH <sub>3</sub> +H <sub>2</sub>	56		0.23	0.36	<1	<1	0.5
Co	NH <sub>3</sub> +H <sub>2</sub>	59		0.05	0.01	<1	<1	0.5
Ni	NH <sub>3</sub> +H <sub>2</sub>	60		0.14	0.07	<1	<3	1.6
Cu	NH <sub>3</sub> +H <sub>2</sub>	63		0.22	0.24	<1	<1	0.5
Zn	NH <sub>3</sub> +H <sub>2</sub>	64		0.15	0.06	<1	<1	0.5
As	O <sub>2</sub>	75	91	0.23	0.02	<1	<1	0.5
Sr	NH <sub>3</sub> +H <sub>2</sub>	88		0.01	0.002	<1	<1	0.5
Mo	NH <sub>3</sub> +H <sub>2</sub>	98		0.04	0.01	<1	<1	0.5
Cd	NH <sub>3</sub> +H <sub>2</sub>	114		0.04	0.004	<10	<1	0.5
Sn	NH <sub>3</sub> +H <sub>2</sub>	118		0.12	0.03	<10	<1	0.5
Sb	NH <sub>3</sub> +H <sub>2</sub>	121		0.05	0.01	<1	<1	0.5
Ba	NH <sub>3</sub> +H <sub>2</sub>	138		0.03	0.003	<1	<1	0.5
W	O <sub>2</sub>	184	216	0.20	0.30	<1	<1	0.5
Pt	O <sub>2</sub>	195		0.20	0.40	<1	<1	0.5
Pb	NH <sub>3</sub> +H <sub>2</sub>	208		0.05	0.005	<1	<1	0.5

BEC and DL values of “0” are reported for Li and Ti because zero counts per second were measured for these elements in all 10 replicates of the blank UPW.

## References

1. Applications of ICP-MS: Measuring Inorganic Impurities in Semiconductor Manufacturing, Agilent publication [5991-9495EN](#)
2. ASTM D5127-13, Standard Guide for Ultra-Pure Water Used in the Electronics and Semiconductor Industries, <https://www.astm.org/Standards/D5127.htm>
3. SEMI F63 - Guide for Ultrapure Water Used in Semiconductor Processing, <https://store-us.semi.org/products/f06300-semi-f63-guide-for-ultrapure-water-used-in-semiconductor-processing>
4. Kazuo Yamanaka, Determination of Ultratrace Elements in High Purity Hydrogen Peroxide with Agilent 8900 ICP-QQQ, Agilent publication [5991-7701EN](#)
5. Yu Ying, Analysis of Ultratrace Impurities in High Silicon Matrix Samples by ICP-QQQ, Agilent publication [5994-2890EN](#)
6. Technical Overview of Agilent 8900 Triple Quadrupole ICP-MS, Agilent publication [5991-6942EN](#)
7. Naoki Sugiyama and Kazumi Nakano, Reaction data for 70 elements using O<sub>2</sub>, NH<sub>3</sub> and H<sub>2</sub> with the Agilent 8800 Triple Quadrupole ICP-MS, Agilent publication [5991-4585EN](#)

# Determination of Ultratrace Elements in SEMI Grade 5 High Purity Hydrogen Peroxide

## Author

Kazuo Yamanaka  
Agilent Technologies, Japan

## Keywords

SEMI, H<sub>2</sub>O<sub>2</sub>, hydrogen peroxide, semiconductor, high purity chemicals

## Introduction

Hydrogen peroxide (H<sub>2</sub>O<sub>2</sub>) is one of the most important process chemicals used in semiconductor device manufacturing. As a strong oxidizer, it is used for cleaning silicon wafers, removing photoresists, and etching metallic copper on printed circuit boards.

Semiconductor Equipment and Materials International (SEMI) publishes standards regarding the specifications for semiconductor process chemicals including H<sub>2</sub>O<sub>2</sub> (SEMI C30-1110). SEMI Grade 5 is the highest purity level, with maximum contamination levels of 10 ppt for most trace elements. The industry therefore requires analytical methods capable of measuring the trace elements at single- or sub-ppt level background equivalent concentrations (BECs). SEMI C30-1110 also includes specifications for the maximum concentrations of sulfate and phosphate allowed in high purity H<sub>2</sub>O<sub>2</sub>, with a limit of 30 ppb. This limit equates to elemental concentrations of sulfur and phosphorus of 10 ppb. These two contaminants are not currently measured by ICP-QMS. However, the recent development of triple quadrupole ICP-MS (ICP-QQQ) permits much lower limits of detection for S and P. It is now possible to monitor all SEMI elements using a single technique.

## Experimental

**Instrumentation:** Agilent 8900 Semiconductor configuration ICP-QQQ.

**Tuning:** To achieve the lowest DLs, a multi-tune method was used. The tuning parameters are summarized in Table 1. For data acquisition, a 2 s integration time was used for all isotopes with three replicates (10 replicates for the blank to calculate the DLs).

**Table 1.** ICP-QQQ tuning conditions.

	Cool	Cool-NH <sub>3</sub> (1)	Cool-NH <sub>3</sub> (2)	No gas	H <sub>2</sub>	He	O <sub>2</sub> (1)	O <sub>2</sub> (2)
Scan mode	Single Q			MS/MS				
RF power (W)	600			1500				
Nebulizer gas flow (L/min)				0.70				
Make-up gas flow (L/min.)	0.90			0.48				
Sampling depth (mm)	18.0			8.0				
Ex1 (V)	-150.0	-100.0	4.2	4.7	4.2	4.5	3.5	
Ex2 (V)	-18.0	-17.0	-12.0	-250.0		-120.0		
Omega (V)	-70.0			-140.0				
Omega Bias (V)	2.0			10.0	8.0	-10.0	10.5	4.0
Q1 Entrance (V)	-15.0			-50.0				
Cell gas	-	NH <sub>3</sub>		-	H <sub>2</sub>	He	O <sub>2</sub>	
Cell gas flow (ml/min)	2.0		2.0	7.0		5.0	0.3	0.3
Axial Acceleration (V)	0.0	1.5		0.0		1.0		
KED (V)	15.0	-5.0		5.0	0.0	3.0	-7.0	

## Sample Preparation

TAMAPURE-AA-10 hydrogen peroxide (35%, Tama Chemicals, Japan) was used as the sample matrix. To stabilize the spiked elements, ultrapure nitric acid (TAMAPURE-AA-10) was added to the H<sub>2</sub>O<sub>2</sub> samples at one part of 70% HNO<sub>3</sub> to 1000.

## Results and discussion

Table 2 shows quantitative results and detection limits for the SEMI specification elements in high purity 35% H<sub>2</sub>O<sub>2</sub>. Comparative quantitative results and DLs are also shown for the same elements in ultrapure water. Long-term stability was evaluated by measuring a H<sub>2</sub>O<sub>2</sub> sample spiked at 10 ppt for most elements and 100 ppt for sulfur. Calibration curves were generated at the beginning of the sequence. The spiked samples were then run as unknown samples for a total analysis period of 3 h 40 min. The RSDs of the 13 results are shown in Table 2 (Stability RSD %).

**Table 2.** ICP-QQQ tuning conditions.

Element	Q1	Q2	Scan mode	Tune	Hydrogen peroxide			Ultrapure water	
					Conc. (ppt)	DL (ppt)	Stability RSD (%)	Conc. (ppt)	DL (ppt)
Li		7	single quad	Cool	< DL	0.003	4.7	< DL	0.004
B	11	11	MS/MS	No gas	7.7	0.69	8.1	4.6	0.57
Na		23	single quad	Cool	0.39	0.031	3.3	0.5	0.069
Mg		24	single quad	Cool	0.017	0.017	4.1	< DL	0.012
Al		27	single quad	Cool	0.39	0.071	2.9	0.11	0.11
P	31	47	MS/MS	O <sub>2</sub> (1)	4.2	0.89	3.3	3.4	0.91
S	32	48	MS/MS	O <sub>2</sub> (1)	190	5.1	7.8	41	3.8
K	39	39	MS/MS	cool+NH <sub>3</sub> (2)	0.21	0.11	2.2	0.2	0.088
Ca	40	40	MS/MS	cool+NH <sub>3</sub> (2)	< DL	0.23	1.9	< DL	0.10
Ti	48	64	MS/MS	O <sub>2</sub> (2)	0.097	0.045	2.6	< DL	0.028
V	51	67	MS/MS	O <sub>2</sub> (2)	0.067	0.027	2.6	< DL	0.023
Cr	52	52	MS/MS	cool+NH <sub>3</sub> (1)	0.13	0.075	3.5	< DL	0.031
Mn	55	55	MS/MS	cool+NH <sub>3</sub> (1)	< DL	0.012	2.7	< DL	0.004
Fe	56	56	MS/MS	cool+NH <sub>3</sub> (1)	0.13	0.074	3.3	< DL	0.027
Ni	60	60	MS/MS	cool+NH <sub>3</sub> (1)	0.16	0.14	3.7	< DL	0.030
Cu	63	63	MS/MS	cool+NH <sub>3</sub> (1)	< DL	0.048	5.0	0.19	0.18
Zn	64	64	MS/MS	He	0.22	0.14	4.5	0.35	0.17
As	75	91	MS/MS	O <sub>2</sub> (2)	< DL	0.087	3.5	< DL	0.081
Cd	114	114	MS/MS	No gas	< DL	0.02	2.3	< DL	0.017
Sn	118	118	MS/MS	No gas	0.088	0.063	2.0	< DL	0.037
Sb	121	121	MS/MS	H <sub>2</sub>	< DL	0.015	1.6	< DL	0.022
Ba	138	138	MS/MS	H <sub>2</sub>	0.061	0.033	1.2	< DL	0.004
Pb	208	208	MS/MS	No gas	0.081	0.053	1.0	0.056	0.035

## Conclusion

All the elements specified in SEMI C30-1110 were measured at sub-ppt to ppt levels in high purity 35% hydrogen peroxide using the Agilent 8900 ICP-QQQ. For almost all elements, sub ppt quantitative results were obtained, with the remaining elements having single-ppt detection limits (except Si, 25 ppt). Reproducibility between 1.0 – 8.1 % RSD was obtained at the 10 ppt level (100 ppt for S) for the spiked analytes in a high purity 35% hydrogen peroxide sample analysis sequence that lasted 3 hours 40 minutes. This performance demonstrates the suitability of the Agilent 8900 Semiconductor configuration ICP-QQQ instrument for the routine analysis of the highest-purity semiconductor reagents and process chemicals.

## More information

Determination of ultratrace elements in high purity hydrogen peroxide with Agilent 8900 ICP-QQQ, Agilent publication, [5991-7701EN](#)

# Automated analysis of semiconductor grade hydrogen peroxide and DI water using ICP-QQQ

## Authors

Kazuhiro Sakai  
Agilent Technologies, Japan  
Austin Schultz  
Elemental Scientific, USA

Online MSA calibration using prepFAST S automated sample introduction and Agilent 8900 ICP-QQQ

## Introduction

Maximizing product yield and performance of semiconductor devices requires manufacturers to address the potential for contamination at every stage of the production process. Contamination from particles, metals, and organic residues can affect the electrical properties of the semiconductor, reducing the quality and reliability of the final product. For example, following each photolithography step during wafer processing, the organic photoresist mask must be completely removed from the silicon wafer surface. A mixture of sulfuric acid ( $H_2SO_4$ ) and hydrogen peroxide ( $H_2O_2$ ) known as a sulfuric/peroxide mix (SPM) is used for this cleaning procedure. SPM is also used for degreasing the wafer surface.  $H_2O_2$  is also used in the RCA Standard Clean steps (SC-1 and SC-2) used to clean silicon wafers, and for etching metallic copper on printed circuit boards.

Ultrapure water (UPW) is used throughout the wafer fabrication process. As well as working as a rinse solution between processing steps, UPW is also the diluent for many process chemistries such as SC-1 and SC-2 solutions. As these chemicals are in frequent and prolonged contact with the wafer surface, minimizing metal impurities is essential to prevent wafer surface contamination.

Semiconductor Equipment and Materials International (SEMI) publishes standards for semiconductor process chemicals. The standard for  $H_2O_2$  is SEMI C30-1110 – Specifications for Hydrogen Peroxide (1). SEMI Grade 5 is the highest purity level, with maximum contamination levels of 10 ppt for most trace elements.

Quadrupole ICP-MS (ICP-QMS) is the standard technique used to monitor trace element contaminants in the semiconductor industry. However, the drive for ever smaller device architectures and higher yields requires an increasing number of contaminant elements to be monitored at lower concentrations.

In addition to trace elements, SEMI Standard C30-1110 specifies the maximum concentration of sulfate and phosphate allowed in high purity  $H_2O_2$ , with a limit of 30,000 ppt. This limit equates to an elemental concentration of sulfur (S) and phosphorus (P) of 10,000 ppt. Due to the relatively high detection limits achievable with conventional single quadrupole ICP-MS, these two elements are not currently measured using ICP-MS.

Triple quadrupole ICP-MS (ICP-QQQ) provides much lower limits of detection for S and P (among many other elements). Uniquely, the technique offers the potential for the sulfate and phosphate analysis to be combined with the other trace metals. The adoption of ICP-QQQ therefore enables all SEMI specified elements to be monitored using a single technique (2, 3).

## Contamination control

Ultratrace analysis at the pg/g (ppt) or fg/g (ppq) level is susceptible to contamination from the lab environment, reagents, or errors arising from manual tasks, such as pipetting. To deliver consistently accurate results at these ultratrace concentrations, a skilled and experienced analyst is typically required.

One approach to simplifying the analysis for less expert analysts is to use an automated sample introduction system. These systems automate typical sample handling steps such as dilution, acidification, and spiking. They can also automatically generate a calibration curve using either external standards or Method of Standard Additions (MSA).

In this study, an automated procedure was developed to quantify ultratrace elemental impurities in de-ionized (DI) water and H<sub>2</sub>O<sub>2</sub> using an Agilent 8900 ICP-QQQ fitted with an ESI prepFAST S automated sample introduction system. The prepFAST S automates sample preparation and calibration, saving time and minimizing the risk of sample-contamination from manual sample handling operations.

## Experimental

### Reagents and samples

TAMAPURE-AA-10 hydrogen peroxide (35%, Tama Chemicals, Japan) and ultrapure DI water (Milli-Q water, Molsheim, France) were used as the samples.

Standard stock solution for MSA: a 1000 ppt mixed multi-element standard solution was prepared by diluting a 10 ppm mixed multi-element standard solution (SPEX CertiPrep, NJ, US) with 1% HNO<sub>3</sub>.

Nitric acid for sample acidification: a 10% nitric acid solution was prepared by diluting 68% ultrapure HNO<sub>3</sub> (TAMAPURE-AA-10) with DI water. HNO<sub>3</sub> was automatically added to the H<sub>2</sub>O<sub>2</sub> samples, giving a final concentration of 0.5% HNO<sub>3</sub> to stabilize the spiked elements. UPW samples are often also acidified to ensure trace element stability (see reference 2). However, in this work, the DI water was analyzed unacidified, without the addition of a HNO<sub>3</sub> spike, providing results that can be compared with the earlier work.

The standard stock and HNO<sub>3</sub> spike solutions were loaded on the prepFAST S. All solutions run in the analysis were automatically prepared from these stock solutions by the prepFAST S system. The prepFAST S method used DI (Milli-Q) water as the carrier solution, at a flow rate of 100 µL/min.

All preparation and analysis steps were performed in a Class 10,000 clean room.

### Instrumentation

A standard Agilent 8900 semiconductor configuration ICP-QQQ instrument was equipped with a PFA concentric nebulizer that is included with the prepFAST S automated sample introduction system. The semiconductor configuration ICP-QQQ is fitted with a Peltier cooled quartz spray chamber, quartz torch (2.5 mm id), platinum-tipped sampling and skimmer cones, and s-lens.

The 8900 ICP-QQQ was connected to the ESI prepFAST S automated sample introduction system. The prepFAST S is a specialized, semiconductor version of the standard ESI prepFAST. The S version has a high purity, low-contamination, inert sample path and features an automated MSA spike addition mode. ICP-QQQ

instrument operating conditions are given in Table 1. Tuning: To achieve the lowest DLs, a multi-tune method was used. The tuning parameters are summarized in Table 1. For data acquisition, a 2 s integration time was used for all isotopes with three replicates (10 replicates for the blank to calculate the DLs).

**Table 1.** ICP-QQQ operating conditions.

	Cool-no gas	Cool-NH <sub>3</sub> (1)	Cool-NH <sub>3</sub> (2)	No gas	H <sub>2</sub>	He	O <sub>2</sub> (1)	O <sub>2</sub> (2)	
Acquisition mode	Single Q	MS/MS							
RF power (W)	600			1500					
Carrier gas (L/min)	0.70								
Make-up gas (L/min.)	0.90			0.48					
Sampling depth (mm)	18.0			8.0					
Ex1 (V)	-150.0		-100.0	4.2	4.7	4.2	4.5	3.5	
Ex2 (V)	-18.0	-17.0	-12.0	-250.0			-120.0		
Omega bias (V)	-70.0			-140.0			-70.0		
Omega lens (V)	2.0			10.0	8.0	10.0	10.5	4.0	
Q1 entrance (V)	-15.0		-50.0						
NH <sub>3</sub> flow (mL/min)*	-	3.0 (30%)**		-	-	-	-	-	
He flow (mL/min)	-	1.0		-	-	5.0	-	-	
H <sub>2</sub> flow (mL/min)	-	-	-	-	7.0	-	-	-	
O <sub>2</sub> flow (mL/min)	-	-	-	-	-	-	4.5 (45%)**		
Axial acceleration (V)	0.0	1.5		0.0			1.0		
Energy discrimination (V)	15.0	-5.0		5.0	0.0	3.0	-7.0		

\*10% NH<sub>3</sub> balanced with 90% He

\* Values in parentheses are % of the maximum flow of the gas controller, as displayed in the tuning pane of ICP-MS MassHunter software

The most advanced semiconductor manufacturing facilities require the lowest possible levels of contamination, so they require analytical techniques that can deliver the lowest possible detection limits (DLs). This requirement is critical in the analysis of trace contaminants in process chemicals such as UPW and H<sub>2</sub>O<sub>2</sub>, which are used at multiple stages of the wafer fabrication process. UPW and H<sub>2</sub>O<sub>2</sub> also come into direct contact with the wafer surface.

The 8900 ICP-QQQ satisfies this requirement by offering the flexibility to optimize the measurement parameters (plasma conditions, quadrupole scan mode, cell gas type, and flow rate) to give the highest sensitivity and lowest background for each analyte.

In this work, several reaction cell gases (He, H<sub>2</sub>, O<sub>2</sub>, and NH<sub>3</sub>) were used in the collision/reaction cell (CRC) of the 8900, as appropriate for the large number of analytes being measured. Since DI water and H<sub>2</sub>O<sub>2</sub> are low-matrix samples, cool plasma conditions were also applied for the elements where this mode provides the lowest background equivalent concentrations (BECs).

The tuning steps were applied sequentially during the measurement of each solution. This approach allows the tuning conditions to be optimized for the removal of different types of interferences, while maintaining maximum sensitivity for the analytes. Q1 and Q2 settings are shown in Table 2 along with DLs, BECs, and quantification results.

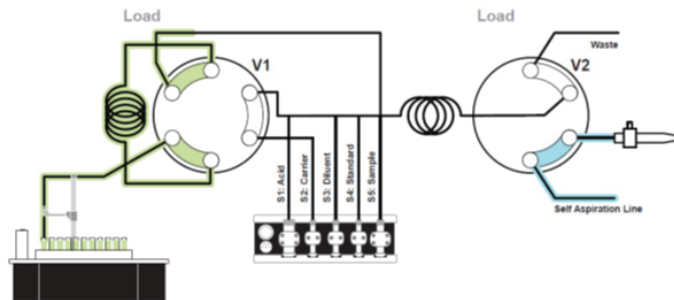


## ESI prepFAST S operation

The prepFAST S automated sample introduction system combines an autosampler with a system of ultrapure valves (S1 -5), and a set of high precision syringe pumps. Undiluted chemicals can be placed on the autosampler and the system will perform the actions—such as dilution, acidification, and spiking—required to prepare the sample for introduction to the ICP-MS or ICP-QQQ. The operation of the prepFAST S is outlined in the four schematics shown in Figure 1.

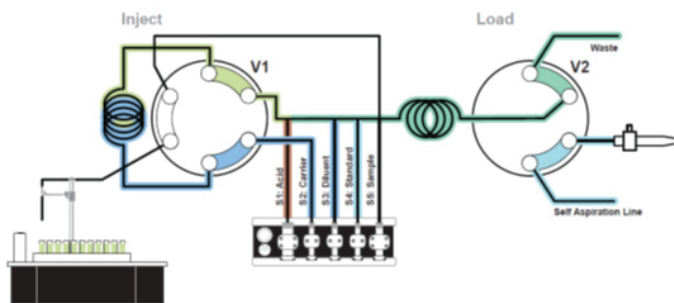
**1. Loading of sample:** Syringe S5 loads a precise amount of sample to the loop of valve 1 (V1).

### Step 1: Fill Loop



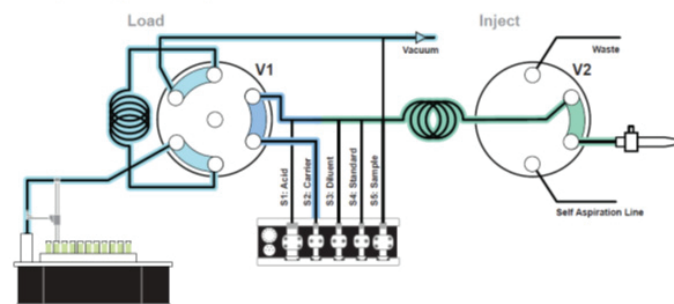
**2. Sample dilution and sample spiking:** Syringes S1, S2, S3, and S4 mix the acid, sample, diluent, and spike solution into a loop connecting V1 and V2.

### Step 2: Dilute Sample



**3. Sample injection:** The prepared sample is introduced into the ICP-QQQ via the carrier solution pumped by S2. S2 provides a precise flow rate regardless of sample type. The V1 loop is washed simultaneously.

### Step 3: Inject Sample



**4. Valve wash:** UPW or acidified UPW is used to clean the lines between V1 and V2.

**Step 4: Clean Valves**

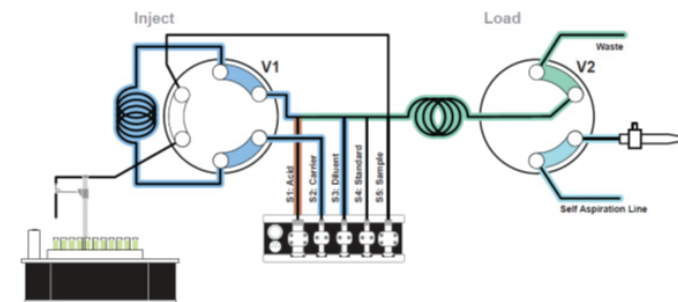


**Figure 1.** ESI prepFAST S system schematic, illustrating four distinct steps: sample loading during spray chamber rinse, sample preparation, injection, and cleaning.

The prepFAST S removes the need for analyst intervention in the analysis of semiconductor grade chemicals, reducing the risk of sample contamination. The integrated system offers the following advantages for the ultratrace elemental analysis of semiconductor samples:

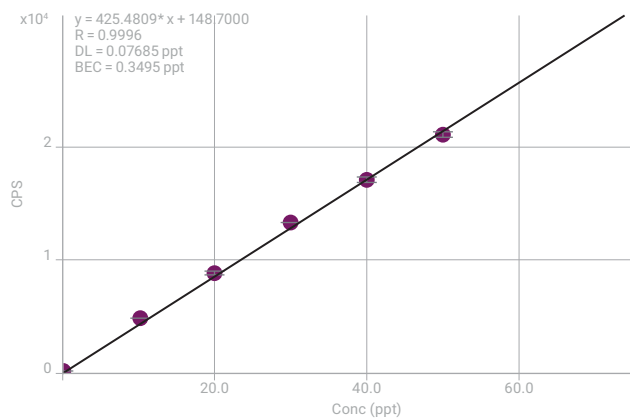
1. Automated dilution of samples
2. Automated creation of external or MSA calibrations
3. Automated acidification of samples
4. Injection of samples at a precise flow rate
5. High speed rinsing of the ICP-MS sample introduction system

## Results and discussion

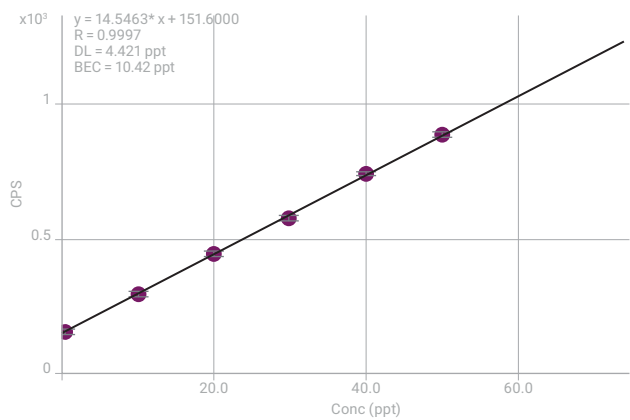
Figures 2 and 3 show calibration curves for Na, K, Si, P, and S in DI water and Ca, Zn, and As in  $H_2O_2$ , respectively. All elements were measured using the MSA calibration prepared automatically using the prepFAST S. These elements are difficult to analyze at low levels due to raised backgrounds. The analytes Si, P, and S are not commonly measured with conventional single quadrupole ICP-MS, due to the presence of intense polyatomic interferences. However, the controlled reaction chemistry of the 8900 ICP-QQQ operating in MS/MS mode gives far superior control of background interferences. MS/MS mode allows these elements to be calibrated and quantified at ppt concentrations.

Good linearity at the ppt level was observed for all elements measured in both sample matrices, although Si, P, and S had relatively high BECs of 85, 10, and 118 ppt, respectively. These elements are typically present at higher levels than the trace metals, as they are more difficult to control in the lab environment and in reagents. They are also less critical contaminants, as reflected in the higher levels for P and S (of 30 ppb for phosphate and sulfate) permitted in high purity  $H_2O_2$ . However, despite the higher BECs, the calibration curves for Si, P, and S were still linear over the calibration range from 10 to 50 ppt. The same calibration levels were used for all analytes, as the mixed stock standard contained all elements at the same concentration.

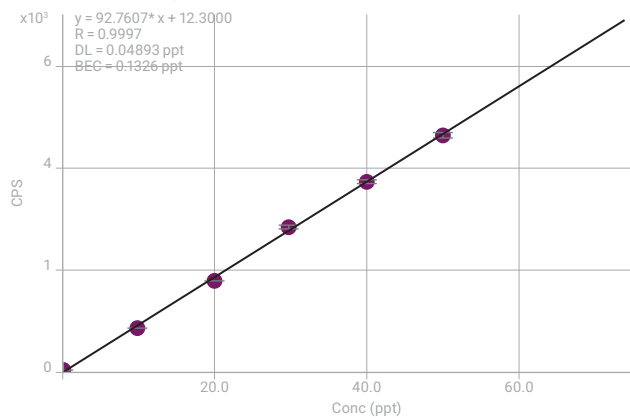
23 Na [No gas]



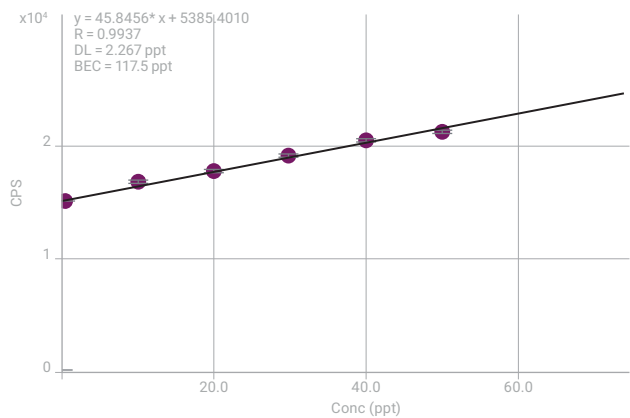
31 → 47 P [Ox]



39 → 39 K [Cool NH<sub>3</sub><sup>-2</sup>]



32 → 48 S [Ox]



28 → 28 Si [H<sub>2</sub>]

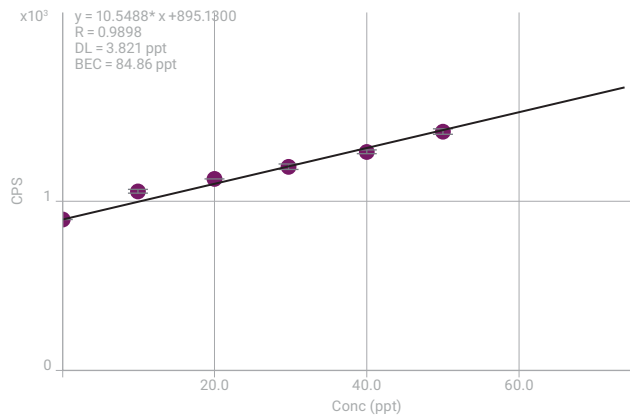


Figure 2. Calibration plots for Na, K, Si, P, and S in DI water. All values in ng/L (ppt).

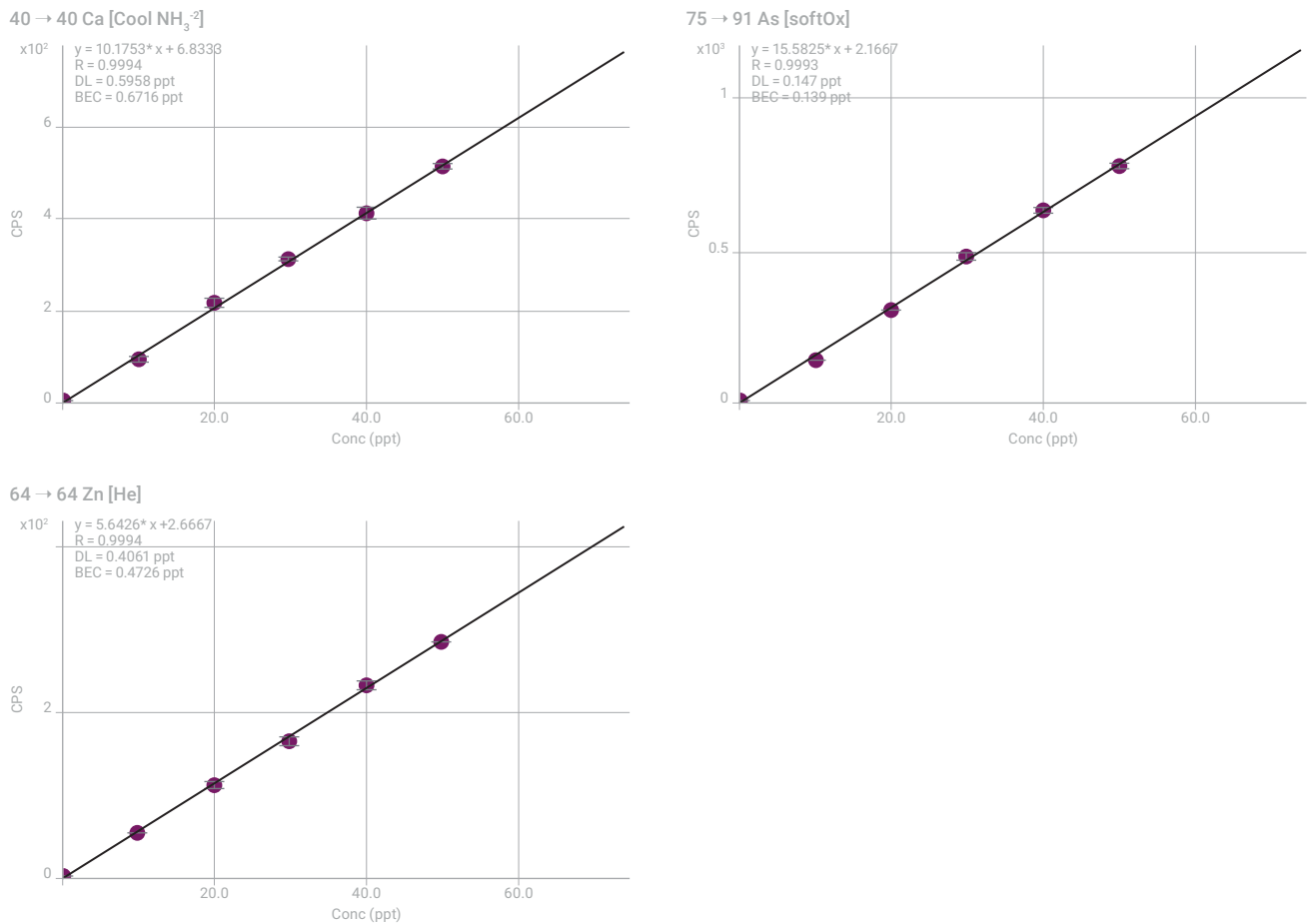


Figure 3. Calibration plots for Ca, Zn, and As in H<sub>2</sub>O<sub>2</sub>. All values in ng/L (ppt).

### DLs and quantitative results

Forty-nine elements in total, including all the elements listed in SEMI C30-1110, were measured by MSA in DI water and H<sub>2</sub>O<sub>2</sub>, using the 8900 multi-tune mode method. Data was acquired in an automated sequence of cool plasma, no gas, and gas modes, during a single visit to the sample vial. Data for each of the modes was combined automatically into a single report for each sample.

Quantitative results, DLs, and BECs for all analytes—including all the SEMI specified elements—are shown in Table 2. Detection limits were calculated as 3-sigma of 10 replicate measurements of the blank DI water or H<sub>2</sub>O<sub>2</sub> sample.

DLs <1 ng/L (ppt) were obtained for 46 elements in DI water. The DLs for the remaining 3 elements, Si, P, and S, were at the single-ppt level. Measured concentrations of all elements apart from B, Si, P, and S were <1 ng/L or <DL, confirming the purity of the sample. This analytical performance easily meets the requirements for monitoring UPW in semiconductor manufacturing.

In H<sub>2</sub>O<sub>2</sub>, DLs <1 ng/L were obtained for 45 elements. The DLs for B, P, and S, were at the single-ppt level, while the DL for Si was 26 ppt. All elements were measured at <1 ng/L or <DL apart from B (22 ppt), Na (1.1 ppt), Si (500 ppt), P (9.4 ppt), and S (220 ppt) in 35% H<sub>2</sub>O<sub>2</sub>. Only B and Si exceed the 10 ppt maximum limit in the SEMI specifications, and of these, only B is a SEMI specified element. P and S were quantified well below the 10,000 ppt SEMI specified limit in H<sub>2</sub>O<sub>2</sub>.

**Table 2.** Quantification of trace elements in DI water and 35% H<sub>2</sub>O<sub>2</sub>. SEMI specification elements are in bold.

	Q1	Q2	Scan type	Tune mode	DI Water			H <sub>2</sub> O <sub>2</sub>		
					DL (ng/L)	BEC (ng/L)	Conc (ng/L)	DL (ng/L)	BEC (ng/L)	Conc (ng/L)
Li		7	SQ	Cool no gas	0.003	0.001	<DL	0.025	0.022	<DL
Be	9	9	MS/MS	No gas	0.096	0.040	<DL	0.089	0.017	<DL
B	11	11	MS/MS	No gas	0.52	1.7	1.7	1.9	22	22
Na		23	SQ	Cool no gas	0.077	0.35	0.35	0.11	1.1	1.1
Mg		24	SQ	Cool no gas	0.015	0.009	<DL	0.040	0.053	0.053
Al		27	SQ	Cool no gas	0.040	0.028	<DL	0.22	0.63	0.63
Si	28	28	MS/MS	H <sub>2</sub>	3.8	85	85	26	500	500
P	31	47	MS/MS	O <sub>2</sub>	4.4	10	10	2.6	9.4	9.4
S	32	48	MS/MS	O <sub>2</sub>	2.3	120	120	7.5	220	220
K	39	39	MS/MS	Cool NH <sub>3</sub> (2)	0.049	0.13	0.13	0.19	0.45	0.45
Ca	40	40	MS/MS	Cool NH <sub>3</sub> (2)	0.082	0.044	<DL	0.60	0.67	0.67
Ti	48	64	MS/MS	O <sub>2</sub> (2)	0.042	0.021	<DL	0.24	0.21	<DL
V	51	67	MS/MS	O <sub>2</sub> (2)	0.021	0.026	0.026	0.058	0.068	0.068
Cr	52	52	MS/MS	Cool NH <sub>3</sub> (1)	0.085	0.047	<DL	0.24	0.69	0.69
Mn	55	55	MS/MS	Cool NH <sub>3</sub> (1)	0.010	0.010	0.010	0.039	0.020	<DL
Fe	56	56	MS/MS	Cool NH <sub>3</sub> (1)	0.070	0.076	0.076	0.29	0.17	<DL
Co	59	59	MS/MS	Cool NH <sub>3</sub> (1)	0.017	0.002	<DL	0.025	0.005	<DL
Ni	60	60	MS/MS	Cool NH <sub>3</sub> (1)	0.080	0.016	<DL	0.24	0.18	<DL
Cu	63	63	MS/MS	Cool NH <sub>3</sub> (1)	0.12	0.11	<DL	0.17	0.12	<DL
Zn	64	64	MS/MS	He	0.063	0.28	0.28	0.41	0.47	0.47
Ga		71	SQ	Cool no gas	0.011	0.001	<DL	0.032	0.031	<DL
Ge	74	74	MS/MS	He	0.36	0.32	<DL	0.27	0.20	<DL
As	75	91	MS/MS	O <sub>2</sub> (2)	0.072	0.035	<DL	0.15	0.14	<DL
Se	78	78	MS/MS	H <sub>2</sub>	0.20	0.14	<DL	0.40	0.13	<DL
Rb		85	SQ	Cool no gas	0.031	0.015	<DL	0.052	0.035	<DL
Sr	88	88	MS/MS	He	0.024	0.002	<DL	0.000*	0.000*	0.000*
Nb	93	93	MS/MS	He	0.018	0.010	<DL	0.030	0.029	<DL
Mo	98	98	MS/MS	He	0.093	0.045	<DL	0.065	0.063	<DL
Ru	101	101	MS/MS	He	0.077	0.058	<DL	0.075	0.014	<DL
Rh	103	103	MS/MS	O <sub>2</sub> (2)	0.057	0.10	0.10	0.018	0.097	0.097
Pd	105	105	MS/MS	No gas	0.078	0.12	0.12	0.055	0.090	0.090
Ag	107	107	MS/MS	No gas	0.099	0.14	0.14	0.031	0.016	<DL
Cd	114	114	MS/MS	No gas	0.045	0.021	<DL	0.047	0.009	<DL
In	115	115	MS/MS	No gas	0.009	0.003	<DL	0.022	0.019	<DL
Sn	118	118	MS/MS	No gas	0.038	0.059	0.059	0.20	0.17	<DL
Sb	121	121	MS/MS	H <sub>2</sub>	0.029	0.032	0.032	0.028	0.005	<DL
Te	125	125	MS/MS	No gas	0.18	0.043	<DL	0.000*	0.000*	0.000*
Cs		133	MS/MS	Cool no gas	0.074	0.020	<DL	0.088	0.059	<DL
Ba	138	138	MS/MS	H <sub>2</sub>	0.023	0.014	<DL	0.039	0.018	<DL
Ta	181	181	MS/MS	No gas	0.024	0.041	0.041	0.12	0.28	0.28
W	182	182	MS/MS	No gas	0.037	0.009	<DL	0.044	0.044	0.044
Re	185	185	MS/MS	No gas	0.040	0.037	<DL	0.062	0.056	<DL
Ir	193	193	MS/MS	H <sub>2</sub>	0.023	0.016	<DL	0.040	0.027	<DL
Pt	195	195	MS/MS	No gas	0.28	0.33	0.33	0.088	0.39	0.39
Au	197	197	MS/MS	No gas	0.051	0.048	<DL	0.22	0.15	<DL
Tl	205	205	MS/MS	No gas	0.036	0.082	0.082	0.015	0.010	<DL
Pb	208	208	SQ	No gas	0.042	0.066	0.066	0.056	0.035	<DL
Bi	209	209	MS/MS	No gas	0.034	0.048	0.048	0.027	0.054	0.054
U	238	238	MS/MS	No gas	0.004	0.001	<DL	0.012	0.008	<DL

SQ: single quadrupole. \*Measured value was zero counts in all replicates.

## Conclusion

By combining ultra low detection limits with a high degree of automation, the Agilent 8900 ICP-QQQ fitted with ESI's prepFAST S automated sample introduction system provides performance ideally suited to the high demands of the semiconductor industry. The method also simplifies the elemental analysis of semiconductor process chemicals.

User handling of the samples is limited to loading the multielement stock standards, acid used for spiking, and samples into the prepFAST S automated sample introduction system. All subsequent steps, including introduction of the sample to the ICP-QQQ, are performed automatically by the prepFAST S. Benefits of the method include:

- Autodilution of samples
- Auto-acidification of samples
- Auto-creation of MSA calibrations
- Injection of samples at a precise flow rate
- High-speed rinsing of the ICP-MS sample introduction system.

A complete analysis of the two samples, measured using separate, automated MSA calibrations, was achieved in less than 30 minutes.

Automating the sample handling steps speeds up the analytical procedure, while also making the overall analysis easier for the analyst to perform.

Eliminating manual tasks such as sample dilution and spiking lowers the risk of contamination during ultratrace analysis. Limiting the handling of reagents and samples also reduces the likelihood of errors arising during the experimental procedure, leading to an increased confidence in the data quality.

All the elements specified in SEMI C30-1110, including P and S, were measured at sub-ppt to ppt levels in DI water and high purity 35% H<sub>2</sub>O<sub>2</sub>. The results easily meet the current SEMI Grade 5 specifications for H<sub>2</sub>O<sub>2</sub>.

## References

1. SEMI C30-1110, Specifications for hydrogen peroxide, 2010.
2. Kazuo Yamanaka, Determination of ultratrace elements in high purity hydrogen peroxide with Agilent 8900 ICP-QQQ, Agilent publication, 2016, [5991-7701EN](#)
3. Kazumi Nakano, Ultra-low level determination of phosphorus, sulfur, silicon, and chlorine using the Agilent 8900 ICP-QQQ, Agilent publication, 2016, [5991-6852EN](#)

# Ultratrace Measurement of Calcium in Ultrapure Water

## Authors

Albert Lee, Vincent Yang, Jones Hsu, Eva Wu and Ronan Shin, BASF Taiwan Ltd., Taipei, Taiwan

Katsuo Mizobuchi, Agilent Technologies, Japan

## Keywords

semiconductor, process chemicals, ultra pure water, UPW, calcium, method of standard additions, hydrogen on-mass

## Introduction

In the semiconductor industry, the control of metal impurities in the process chemicals used in the manufacture of semiconductor devices is critical to achieve the required product performance and yield. As device performance is continually increasing, the required impurity control becomes ever more stringent. For example, metal content of the ultra-pure water (UPW) used in the manufacturing process must be at the sub-ppt level. ICP-MS is the standard technique used for the trace metals analysis of semiconductor chemicals and devices. The most common instrument and measurement technique used in the semiconductor industry is single quadrupole ICP-MS (ICP-QMS) with cool plasma. The cool plasma technique [1], developed in the mid 1990s, enables the quantification of key contaminant elements at the single ppt level. Collision and reaction cell ICP-QMS, developed from 2000 onwards, enabled the direct analysis of more complex semiconductor matrices, but did not improve on the DLs or BECs of cool plasma for low-matrix samples. To achieve measurement at the sub-ppt level, reduction of the BEC is required. As outlined in this paper, the Agilent 8800 ICP-QQQ provides new reaction cell technology that enables a significant reduction in the BEC that can be achieved for Ca, to 100 ppq.

**Table 1.** Cool plasma operating conditions.

Parameter	Unit	Tuning value
RF	W	600
Sampling depth	mm	18
Carrier gas flow	L/min	0.7
Make-up gas flow	L/min	1.0
Spray chamber temp.	°C	2

## Experimental

**Instrumentation:** Agilent 8800 #200.

**Plasma conditions:** For the ultratrace measurement of Ca, cool plasma operating conditions were used (Table 1). The sample was self-aspirated at a carrier gas flow rate of 0.7 L/min.

**Reagents and sample preparation:** A Ca standard was prepared in UPW acidified with 0.1% high purity HNO<sub>3</sub>. This was used to make 50 ppt and 100 ppt additions to a UPW blank acidified with 0.1% high purity HNO<sub>3</sub>.

## Results and discussion

### Ultra-low BEC for Ca using MS/MS mode

Figure 1 shows the BECs obtained for Ca, measured at its major isotope of  $^{40}\text{Ca}$ , using the method of standard additions (MSA) under three different operating conditions on the 8800 ICP-QQQ: Single Quad mode with no cell gas, MS/MS mode with no cell gas, and finally MS/MS mode with a  $\text{H}_2$  cell gas flow of 1 mL/min. The Single Quad mode uses operating conditions with Q1 acting as an ion guide, to emulate the Agilent 7700 ICP-QMS. The obtained BEC of 6.8 ppt is similar to that routinely achieved with the Agilent 7700 operated in cool plasma mode.

Using MS/MS mode (without cell gas) improved the Ca BEC to 1.4 ppt. MS/MS mode with  $\text{H}_2$  at 1 mL/min in the cell further improved the BEC down to 0.041 ppt (41 ppq). The obtained MSA plot is shown in Figure 2. The Agilent 8800 ICP-QQQ in MS/MS mode with  $\text{H}_2$  cell gas achieved a BEC for Ca in UPW two orders of magnitude lower than the BEC obtained using conventional ICP-QMS.

Figure 3 shows the spectrum obtained for UPW using cool plasma conditions in Single Quad mode with no cell gas. As can be seen,  $\text{Ar}^+$  ( $m/z$  40) is suppressed under the lower temperature plasma conditions, but two intense background peaks are observed at  $m/z = 19$  and 30. These are  $(\text{H}_2\text{O})\text{H}^+$  and  $\text{NO}^+$  respectively. In Single Quad mode, all ions formed in the plasma, including these two intense ions, pass through to the cell. Even with no gas added to the cell, a reaction occurs in the cell which causes a new interfering ion at  $m/z = 40$ . The likely reaction occurring in the cell is:  $\text{NO}^+ + \text{Ar} \rightarrow \text{Ar}^+ + \text{NO}$  (charge transfer reaction), which increases the BEC for Ca by several ppt. Although the ionization potential (IP) of NO (IP = 9.26 eV) is lower than that of Ar (IP = 15.7 eV), a metastable ion,  $\text{NO}^+$ , exists close to the ionization potential of Ar [2]. So it is reasonable to assume that the charge transfer reaction shown occurs in the cell.

With MS/MS mode on the 8800 ICP-QQQ, Q1 rejects all non-target ions such as  $\text{NO}^+$  and  $(\text{H}_2\text{O})\text{H}^+$ , preventing unwanted reactions from occurring in the cell, which lowers the Ca BEC. The addition of  $\text{H}_2$  in the cell also removes any residual  $^{40}\text{Ar}^+$  that is formed even under cool plasma conditions.



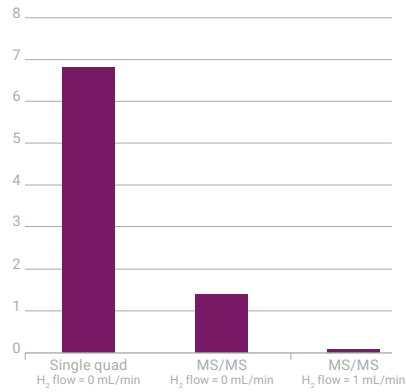


**Figure 1.** BECs for Ca obtained using Single Quad mode with no cell gas [6.8 ppt], MS/MS mode with no cell gas [1.4 ppt], and MS/MS mode with an H<sub>2</sub> cell gas flow of 1 mL/min [0.041 ppt].

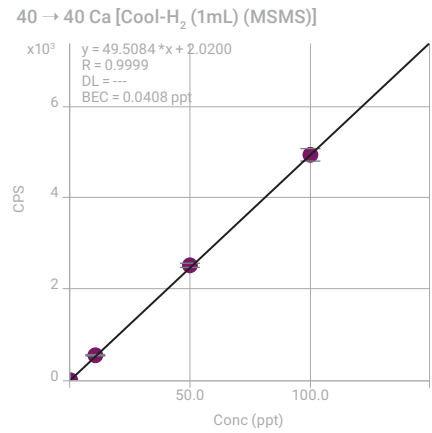


**Figure 2.** MSA calibration plot for Ca using MS/MS mode with H<sub>2</sub> flow of 1 mL/min.

[1] Spectrum No. 1 [187.530 sec]DIW\_COOL.D/Tune#1[CPS][Log]

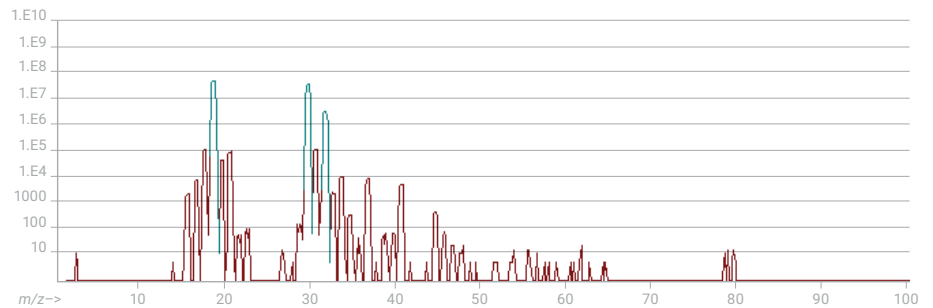


**Figure 3.** Spectrum of UPW acquired using cool plasma conditions in Single Quad mode with no gas mode.

## References

1. K. Sakata and K. Kawabata, Reduction of fundamental polyatomic ions in inductively coupled plasma mass spectrometry, *Spectrochimica Acta, Part B*, **1994**, 49, 1027.
2. R. Marx, Y.M. Yang, G. Mauclaire, M. Heninger, and S. Fenistein, Radioactive lifetimes and reactivity of metastable NO<sup>+</sup>(a<sup>3</sup>Σ<sup>+</sup>,v) and O<sub>2</sub><sup>+</sup>(α<sup>4</sup>Π<sub>u</sub>,v) , *J.Chem. Phys.*, Vol. 95, No. 4, 2259-2264, **1991**.

# Ultratrace Measurement of Potassium and Other Elements in UPW Using ICP-QQQ in Cool Plasma/Reaction Mode

## Authors

Katsuo Mizobuchi and  
Masakazu Yukinari  
Agilent Technologies, Tokyo, Japan

## Keywords

semiconductor, process chemicals,  
ultra pure water, UPW, potassium, cool  
plasma, ammonia on-mass

## Introduction

The level of metal contaminants is strictly controlled in semicon device manufacturing processes, but the elements K, Ca and Fe are difficult to determine by ICP-MS due to argide interferences e.g. ArH<sup>+</sup> on <sup>39</sup>K<sup>+</sup>, Ar<sup>+</sup> on <sup>40</sup>Ca<sup>+</sup> and ArO<sup>+</sup> on <sup>56</sup>Fe<sup>+</sup>. Cool plasma employs a relatively low temperature plasma to remove the argide interferences allowing the analyst to measure these elements at trace levels. The low temperature plasma also reduces the background signal from any Easily Ionized Elements (EIEs) such as Li and Na that may deposit of on the interface of the ICP-MS. Even after the introduction of high concentration of EIEs, cool plasma ensures a low background level of these elements is maintained.

The Agilent 8800 ICP-QQQ provides improved cool plasma performance in combination with reaction cell technology, to enable a BEC of 30 ppq for K to be achieved in ultrapure water (UPW), and BECs at the ppq level for all the other elements studied: Li, Na, Mg, Al, Ca, Cr, Mn, Fe, Ni and Cu.

**Table 1.** Cool plasma operating conditions.

Parameter	Unit	Tuning value
RF	W	600
Carrier gas	L/min	0.7
Make-up gas	L/min	0.8
Sampling depth	(mm)	18
NH <sub>3</sub> (10% in He) cell gas flow rate	mL/min	1

## Experimental

**Instrumentation:** Agilent 8800 #200 (semiconductor configuration).

**Plasma conditions:** Cool plasma operating conditions (Table 1).

**Reagents and sample preparation:** The blanks and samples were acidified using high purity HNO<sub>3</sub> (TAMAPURE-AA-10, TAMA Chemicals Co. Ltd. Kanagawa, Japan). Standard solutions were prepared by serial dilution from a SPEX 331 mixed standard (SPEX CertiPrep, NJ, USA).

### Cool plasma/NH<sub>3</sub> reaction cell mode

Investigation of the signal at *m/z* 39 under cool plasma conditions indicated the presence of <sup>38</sup>ArH<sup>+</sup> which decreases with lowering plasma temperature, indicating a reduction in the ionization of the polyatomic ion. However, there was also a contribution from a water cluster ion, (H<sub>3</sub>O<sup>+</sup>)(H<sub>2</sub>O), which is likely to form under low temperature plasma conditions. The combination of these two interferences means that there is no plasma temperature at which both interferences can be minimized (Figure 1). As the water cluster ion is known to react with deuterated ammonia (ND<sub>3</sub>) via a fast proton transfer reaction [1], it was assumed that reaction with NH<sub>3</sub> would proceed at a similar rate, so this cell gas mode was investigated in order to remove the water cluster ion in cool plasma conditions.

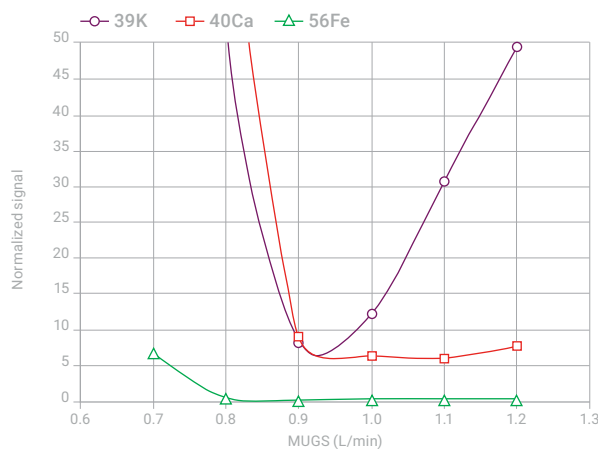


**Figure 1.** Investigation of the background signal under cool plasma conditions. BEC of K, Ca and Fe as a function of make-up gas (MUGS) flow rate.

## Results and discussion

### Ultra-low BEC for K using MS/MS mode

Ammonia reaction gas mode under cool plasma conditions was used to determine K in UPW. The BEC of K was measured at 30 ppq. A comparative study carried out using a 7500cs quadrupole ICP-MS in cool plasma/ $\text{NH}_3$  reaction mode achieved a BEC of 500 ppt for K [2]. It would be reasonable to attribute the improvement of BEC achieved with the 8800 to the MS/MS reaction capability of the ICP-QQQ. In conventional quadrupole ICP-MS, ions formed under cool plasma conditions enter the reaction cell and react with  $\text{NH}_3$  or with impurity residues present in the cell to form product ions at  $m/z$  39. MS/MS prevents any unwanted precursor ions from entering the cell, thus minimizing the production of undesired product ions.

### Multielement analysis

The cool plasma/ $\text{NH}_3$  reaction mode method was applied to the multielement analysis of UPW. As can be seen from the results in Table 2, a BEC < 150 ppq was achieved for all elements, including K, Ca and Fe.

**Table 2.** DL and BEC of elements in UPW.

Mass/Element	Sensitivity, cps/ppt	DL, ppt	BEC, ppt
7 Li	6.2	0.000	0.000
23 Na	94.0	0.014	0.035
24 Mg	44.0	0.010	0.005
27 Al	42.7	0.010	0.002
39 K	96.8	0.000	0.030
40 Ca	42.5	0.035	0.091
52 Cr	36.5	0.029	0.037
55 Mn	64.5	0.020	0.011
56 Fe	42.2	0.488	0.134
60 Ni	13.4	0.270	0.101
65 Cu	15.5	0.014	0.029

## Conclusion

The Agilent 8800 ICP-QQQ was used to show the background signal at  $m/z$  39 under cool plasma conditions was due to a water cluster ion,  $H_3O(H_2O)^+$ , which was removed using  $NH_3$  cell gas. The ICP-QQQ BEC for  $^{39}K$  was more than a factor of 10 lower than that achieved using a conventional quadrupole ICP-MS. This demonstrates the benefit of MS/MS mode for reaction gas methods: MS/MS mode prevents all non-target ions from entering the cell, and thereby eliminates the possibility of unwanted reactions from occurring.

## References

1. V. G. Anicich (2003.11), An Index of the Literature for Bimolecular Gas Phase Cation-Molecule Reaction Kinetics (p369), NASA
2. Junichi Takahashi et al., Use of collision reaction cell under cool plasma condition in ICP-MS, Asia Pacific Winter Plasma Conference 2008 (O-10)

## More information

Ultratrace measurement of potassium and other elements in ultrapure water using the Agilent 8800 ICP-QQQ in cool plasma reaction cell mode, Agilent publication [5991-5372EN](#)

# Ultralow level determination of phosphorus, sulfur, silicon, and chlorine using the Agilent 8900 ICP-QQQ

## Author

Kazumi Nakano,  
Agilent Technologies, Japan

## Introduction

Quadrupole ICP-MS (ICP-QMS) is one of the most sensitive and versatile analytical tools used in inorganic analysis. With sensitivity approaching 1,000 million counts per second/part per million (1 G cps/ppm) and background signals typically less than 1 cps, the latest instrumentation achieves detection limits (DL) in the ppq (pg/L) range for most of the elements in the periodic table. Detection limits tend to be lowest for elements at masses higher than 80 u, while some lower mass elements are more difficult to measure at trace levels due to the presence of spectral overlaps from polyatomic interferences. ICP-QMS can utilize cool plasma and/or collision/reaction cell methods to address the problem of background interferences, with successful results in many applications.

More recently, the introduction of triple quadrupole ICP-MS (ICP-QQQ) has dramatically improved the reliability and performance of reaction cell methods by allowing a double mass filter (MS/MS) to be applied to control reaction chemistry in the cell. This now allows analysts to resolve interferences on a wide range of elements in a controlled and effective manner.

With the introduction of Agilent's second generation ICP-QQQ instrument, the Agilent 8900 Triple Quadrupole ICP-MS, reaction cell operation with MS/MS mode has been further refined. This note describes the performance of the 8900 ICP-QQQ for the analysis of some of the most challenging elements for ICP-MS: phosphorus (P), sulfur (S), silicon (Si), and chlorine (Cl). The first ionization potentials of these elements are relatively high, which reduces the degree of ionization and therefore the analyte signal. Furthermore, the background signals are elevated due to plasma-, solvent- and matrix-based polyatomic ions, making low-level analysis even more difficult. As ICP-MS technology has developed, there has been a growing demand and expectation to measure these difficult elements together with more conventional elements in high purity chemicals and materials. Details of the methods used to control the interferences on the four elements are presented, together with background equivalent concentrations (BECs) and detection limits (DLs) for P, S, Si and Cl in ultra-pure water (UPW), and P, S and Si in the highest grade hydrogen peroxide (H<sub>2</sub>O<sub>2</sub>).

## Experimental

### Instrumentation

An Agilent 8900 ICP-QQQ (#200, Semiconductor Configuration) was used for all measurements. The sample introduction system comprised a PFA concentric nebulizer, a quartz spray chamber and torch, and platinum interface cones. The 8900 #200 ICP-QQQ is fitted with a new argon gas flow control system specially designed to minimize sulfur/silicon contamination from the gas line components.

Normal, hot plasma conditions were used throughout. Extraction lens voltages were optimized for maximum sensitivity using an Agilent 1 ppb tuning solution containing Li, Y, Ce and Tl. Operating and tuning parameters are summarized in Table 1.

**Table 1.** Agilent 8900 ICP-QQQ operating parameters.

Parameter	Unit	Value
RF power	W	1500
Sampling depth	mm	8.0
Carrier gas flow rate	L/min	0.70
Make-up gas flow rate	L/min	0.52
Extraction lens 1	V	4.0
Extraction lens 2	V	-210
Omega lens bias	V	-80
Omega lens	V	8.0

### Method and cell tuning

Based on previous studies, oxygen (O<sub>2</sub>) mass-shift mode was used for the analysis of P and S, hydrogen (H<sub>2</sub>) on-mass mode was used for Si, and Cl was determined using H<sub>2</sub> mass-shift mode [1]. The reaction processes used for removal of the primary interference on each analyte were as follows:

#### *Sulfur by oxygen mass-shift mode*

The intense polyatomic interference from <sup>16</sup>O<sub>2</sub><sup>+</sup> on the primary isotope of S, <sup>32</sup>S<sup>+</sup> at *m/z* 32, is avoided by shifting S<sup>+</sup> away from the interfering O<sub>2</sub><sup>+</sup> ion, using an O-atom addition reaction. S<sup>+</sup> reacts readily with O<sub>2</sub> cell gas to form the product ion SO<sup>+</sup>, which can be measured free of interference at *M* + 16 u (*m/z* 48 for the primary <sup>32</sup>S<sup>16</sup>O<sup>+</sup> isotope product ion), as shown in the following equations:



#### *Phosphorus by oxygen mass-shift mode*

A similar mass-shift approach is used for the measurement of P as PO<sup>+</sup>. The native mass of P (*m/z* 31) suffers an intense background interference from <sup>14</sup>N<sup>16</sup>O<sup>1</sup>H<sup>+</sup>, <sup>15</sup>N<sup>16</sup>O<sup>+</sup>, and <sup>14</sup>N<sup>17</sup>O<sup>+</sup>. These background polyatomic ions are avoided by reacting P<sup>+</sup> with O<sub>2</sub> cell gas, shifting the P<sup>+</sup> away from the interfering ions, and measuring it as the PO<sup>+</sup> product ion at *m/z* 47:



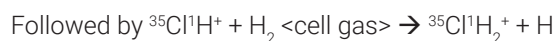
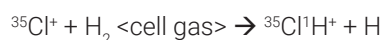
#### *Silicon by hydrogen on-mass mode*

The analysis of Si uses on-mass measurement with H<sub>2</sub> cell gas, as the primary interferences on the major Si isotope at *m/z* 28, <sup>14</sup>N<sub>2</sub><sup>+</sup> and <sup>12</sup>C<sup>16</sup>O<sup>+</sup>, react readily with H<sub>2</sub>, while Si<sup>+</sup> does not react. Thus, the N<sub>2</sub><sup>+</sup> and CO<sup>+</sup> interferences can be removed, and <sup>28</sup>Si<sup>+</sup> can be measured free from the interferences at its original mass:



### Chlorine by hydrogen mass-shift mode

Cl is a difficult element to analyze at low concentrations using ICP-MS, because it is a common contaminant and is often present in reagents used in the laboratory environment. In addition, its first ionization potential of 12.967 eV is higher than that of any other commonly measured element, meaning that Cl is very poorly ionized, so the sensitivity for Cl<sup>+</sup> is extremely low. A further issue for low-level Cl analysis is the presence of a polyatomic interference from <sup>16</sup>O<sup>18</sup>O<sup>1</sup>H<sup>+</sup> on the primary Cl isotope at *m/z* 35. The O<sub>2</sub>H<sup>+</sup> overlap can be avoided by measuring Cl as a ClH<sub>2</sub><sup>+</sup> product ion, produced from sequential reaction with H<sub>2</sub> reaction gas:



In all of these methods, the Agilent 8900 ICP-QQQ was operated in MS/MS mode (where both Q1 and Q2 function as mass filters) ensuring that only the target ion or product ion was measured. MS/MS means that potentially overlapping ions are excluded from the collision/reaction cell, so the reaction chemistry is controlled and consistent, even if other matrix elements or analytes are present in the sample. For example, in the case of <sup>32</sup>S<sup>16</sup>O<sup>+</sup> product ion measured at *m/z* 48, the product ion mass could be overlapped by other ions, such as <sup>48</sup>Ca<sup>+</sup>, <sup>48</sup>Ti<sup>+</sup>, and <sup>36</sup>Ar<sup>12</sup>C<sup>+</sup>, if these ions were not rejected by Q1. This is the main reason for the improved reaction mode performance of ICP-QQQ compared to ICP-QMS, as ICP-QMS has no mass filter step before the collision/reaction cell.

The ORS<sup>4</sup> collision/reaction cell of the 8900 #200 instrument has the facility to utilize an axial acceleration voltage, which was found to be effective to increase sensitivity in the O<sub>2</sub> mass-shift method used for the determination of P and S. Cell parameters were optimized separately for each mode while aspirating a 1 ppb standard solution of each of the elements. Cell tuning parameters are summarized in Table 2.

**Table 2.** Cell mode related tuning parameters.

Parameter	Unit	O <sub>2</sub> mass-shift	H <sub>2</sub> on-mass	H <sub>2</sub> mass-shift
Element		<sup>31</sup> P, <sup>32</sup> S	<sup>28</sup> Si	<sup>35</sup> Cl
Mass pair	(Q1 → Q2)	(31 → 47), (32 → 48)	(28 → 28)	(35 → 37)
Cell gas		O <sub>2</sub>		H <sub>2</sub>
Flow rate	mL/min	0.41		5.0
OctpBias	V	-3		-18
KED	V	-8		0
Axial acceleration	V	1		0
Cell exit	V	-90		-70
Deflect	V	8		-6
Plate bias	V		-60	

## Reagents

Standard solutions for P, S and Si were prepared from single element standards purchased from SPEX CertiPrep (NJ, USA), by serial dilution with UPW. The UPW was supplied from ORGANO Corp (Tokyo, Japan). The Cl standard was prepared from high purity HCl purchased from Wako Pure Chemicals Industries Ltd (Osaka, Japan). The highest purity grade H<sub>2</sub>O<sub>2</sub>, TAMAPURE-AA-10, was purchased from TAMA Chemicals Co Ltd (Kanagawa, Japan). The calibration standard addition spikes were added directly to the undiluted H<sub>2</sub>O<sub>2</sub>. A 1% TMAH alkaline rinse was used during the analysis of Cl to maximize the effectiveness of the washout between samples and prevent any carryover. All pipette tips, vials and bottles were thoroughly cleaned using diluted high purity acids and rinsed in UPW prior to use.

## Results and discussion

To prepare the ICP-QQQ for the analysis, a 1% HNO<sub>3</sub> solution was aspirated overnight to thoroughly clean the sample introduction system. Running the plasma for several hours would also help to remove any contaminants in the Ar gas flow line. P, S and Si were measured together, and Cl was analyzed in a separate batch since it benefited from an alkaline rinse between solutions. Figures 1 and 2 show the calibration curves of the four elements in UPW and P, S and Si in H<sub>2</sub>O<sub>2</sub>, respectively, measured using the method of standard addition (MSA). The background level of Cl present in the H<sub>2</sub>O<sub>2</sub> sample was too high to permit accurate analysis at the spike levels used.

Good linearity at low and sub-ppb levels was observed for all elements measured in both of the sample matrices. The DL for each element was calculated as 3 times the standard deviation of 10 replicates of the blank using an integration time of 1 sec for each element. The results are summarized in Table 3.

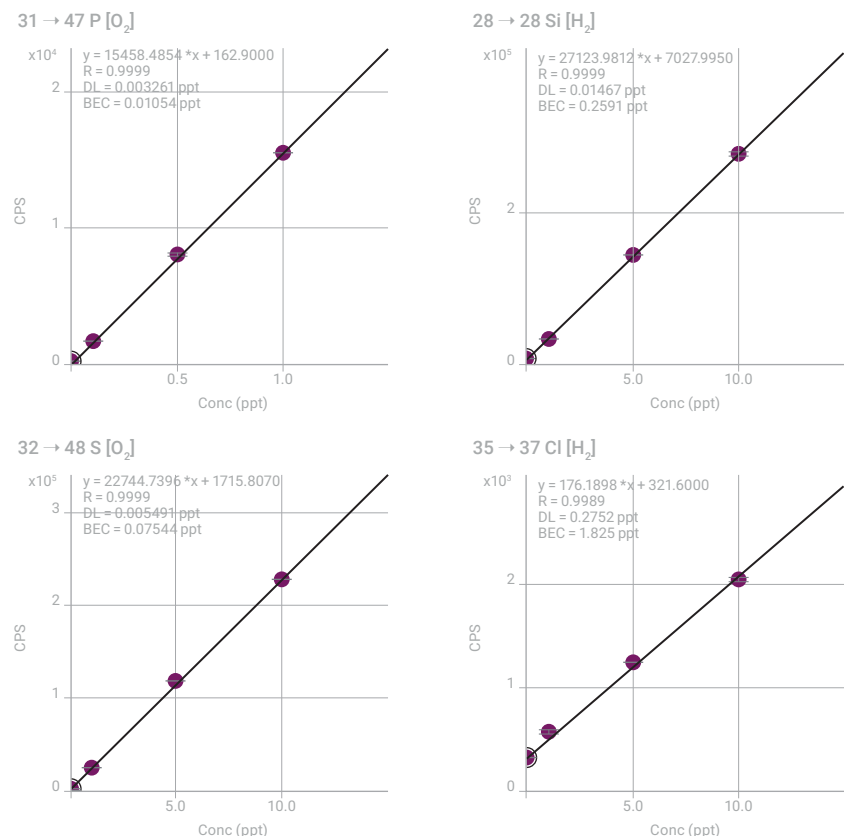


Figure 1. Calibration plots of P, S, Si and Cl in UPW. All values in ug/L (ppb).



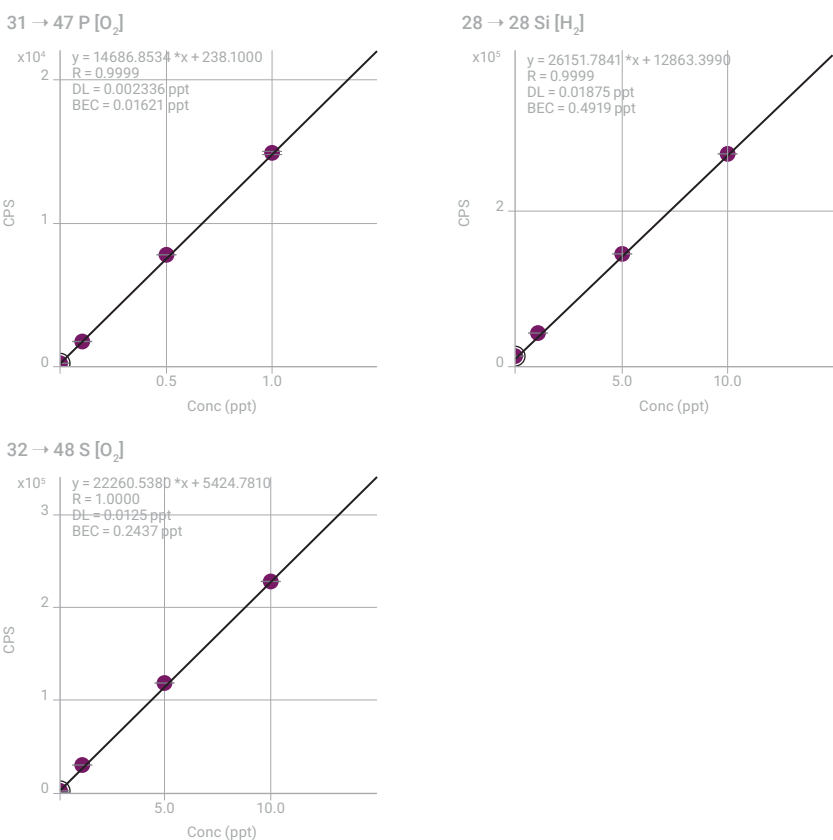


Figure 2. Calibration plots of P, S and Si in H<sub>2</sub>O<sub>2</sub>.

Table 3. BEC and DL of P, S, Si and Cl in UPW and P, S and Si in the highest grade H<sub>2</sub>O<sub>2</sub>.

Element	P (ppt)		S (ppt)		Si (ppt)		Cl (ppt)	
	BEC	DL	BEC	DL	BEC	DL	BEC	DL
UPW	10.5	3.3	75.4	5.5	259	14.7	1.83	0.28
H <sub>2</sub> O <sub>2</sub>	16.2	2.3	244	12.5	492	18.8		

## Conclusion

The Agilent 8900 ICP-QQQ operating in MS/MS mode with O<sub>2</sub> and H<sub>2</sub> cell gases successfully eliminated problematic spectral interferences on non-metallic impurities P, S, Si and Cl in UPW and P, S and Si in H<sub>2</sub>O<sub>2</sub>. The results highlight the advanced performance of the second generation ICP-QQQ for the analysis of challenging elements, by achieving the lowest ever reported BECs for the four elements in UPW.

## References

1. N. Sugiyama, Trace level analysis of sulfur, phosphorus, silicon and chlorine in NMP using the Agilent 8800 Triple Quadrupole ICP-MS, Agilent application note, 2013, [5991-2303EN](#)

# Direct analysis of trace metal impurities in high purity nitric acid using ICP-QQQ

## Authors

Kazuo Yamanaka and Kazuhiro Sakai  
Agilent Technologies, Tokyo, Japan

## Introduction

The manufacturing yield of semiconductor devices has always been susceptible to contamination from trace metals. As the industry continues to progress towards devices with smaller features and a higher density of integration, susceptibility to contamination in microfabrication processing presents an increasing challenge. Controlling contamination at these small scales requires ever-higher purity of process chemicals and manufacturing conditions.

The semiconductor device fabrication industry uses well-established cleaning procedures to remove organic and metallic residues and impurities from the surface of silicon wafers. The purity of reagents used during manufacturing processes and the air quality in the fabrication plant are important considerations.

Nitric acid ( $\text{HNO}_3$ ) plays an important role in the fabrication of semiconductor devices so needs to be of ultrahigh purity. A mix of nitric and hydrofluoric acid is used to etch single crystal silicon and polycrystalline silicon.  $\text{HNO}_3$  is also combined with phosphoric acid and acetic acid for wet etching of aluminum. As a reagent,  $\text{HNO}_3$  is used in the preparation of other semiconductor materials.

SEMI standard C35-0708 Tier-B protocol for  $\text{HNO}_3$  (69.0–70.0%) specifies contaminant levels of  $<1 \mu\text{g/L}$  (ppb) for several elements [1]. The concentration of industrial grade  $\text{HNO}_3$  is usually 60–68%, depending on the method of production.

In this study, undiluted  $\text{HNO}_3$  was analyzed directly by triple quadrupole ICP-MS (ICP-QQQ). This approach simplified sample preparation and avoided the potential introduction of contaminants during dilution.

## Experimental

### Samples and standards

Two samples of  $\text{HNO}_3$  were used in this study:

- Sample 1: 68 %  $\text{HNO}_3$  (high purity-grade)
- Sample 2: 61 %  $\text{HNO}_3$  (electronic-grade - lower purity)

No further sample preparation was necessary as all samples were introduced directly into the ICP-QQQ.

Calibration and quantification were done using the method of standard additions (MSA). Standard solutions were prepared by spiking a multi-element standard solution (SPEX CertiPrep, NJ, US) into each  $\text{HNO}_3$  sample to give spike levels of 5, 10, 20, 30 and 40 ppt. The density of the nitric acid solution varies with the concentration of the acid, which affects the sample transport, nebulization and droplet evaporation processes in the ICP-MS sample introduction. Therefore, for the most accurate analysis, the acid grade (concentration) used for the spiked MSA calibration solutions should be approximately matched to the acid concentration of the samples. ICP-MS MassHunter allows an MSA calibration to be converted to an external calibration to determine contaminant levels in other nitric acid samples with similar acid concentration. The solutions were prepared just before analysis. All preparation and analyses were performed in a Class 10,000 clean room.

## Instrumentation

An Agilent 8900 Semiconductor configuration ICP-QQQ instrument was used in this study. The instrument is fitted as standard with a PFA-100 nebulizer, Peltier-cooled quartz spray chamber, quartz torch, platinum-tipped sampling and skimmer cones, and s-lens. The nebulizer was operated in self-aspiration mode to minimize the potential for sample contamination from contact with the peristaltic pump tubing. If large numbers of undiluted HNO<sub>3</sub> samples are run routinely, it is recommended that the large (18 mm) insert Pt cone is fitted. Long-term corrosion of internal ICP-MS components can be minimized by fitting the dry pump option and ball-type interface valve kit.

In advanced semiconductor applications, the key requirement is to deliver the absolute lowest possible detection limits (DLs) for each analyte. To achieve this goal, laboratories measuring ultratrace levels of contaminants can use a multitune method, where several tuning steps are applied sequentially during the measurement of each solution. This approach allows the tuning conditions to be optimized for the removal of different types of interferences, while maintaining sensitivity for each analyte. In this work, several reaction cell gases (He, H<sub>2</sub>, O<sub>2</sub>, and NH<sub>3</sub>) and both hot and cool plasma conditions were used as appropriate for the large number of analytes being measured. Tuning conditions are shown in Table 1 and other acquisition parameters are shown in Table 2.

**Table 1.** ICP-QQQ operating conditions.

	Cool-NH <sub>3</sub>	No gas	H <sub>2</sub>	He	O <sub>2</sub>	O <sub>2</sub> -soft
Acquisition mode	MS/MS					
RF power (W)	600	1500				
Sampling depth (mm)	18.0	8.0				
Nebulizer gas (L/min)	0.70					
Make-up gas (L/min)	0.78	0.36				
Ex1 (V)	-150	4.2	4.7	4.2	4.5	3.5
Ex2 (V)	-17.0	-250.0				-120.0
Omega bias (V)	-70.0	-140.0				-70.0
Omega lens (V)	2.0	10.0	8.0	10.0	10.5	4.0
Q1 entrance (V)	-15.0	-50.0				
He flow (mL/min)	1.0	-	-	5.0	-	-
H <sub>2</sub> flow (mL/min)	-	-	7.0	-	-	-
*NH <sub>3</sub> flow (mL/min)	2.0 (20%)**	-	-	-	-	-
O <sub>2</sub> flow (mL/min)	-	-	-	-	4.5 (30%)**	
Axial acceleration (V)	1.5	0.0				1.0
Energy discrimination (V)	-5.0	5.0	0.0	3.0	-7.0	

\*10% NH<sub>3</sub> balanced with 90% He

\*\* Values in parentheses are % of the maximum flow of the gas controller, as displayed in the tuning pane of ICP-MS MassHunter

**Table 2.** Acquisition parameters.

Parameter	Setting
Q2 peak pattern	1 point
Replicates	3 (spiked samples) 10 (unspiked solution for DL measurement)
Sweeps/replicate	10
Integration time	2 s for all isotopes

## Results and discussion

### DLs and BECs

In total, 49 elements were measured using the 8900 ICP-QQQ operating in multiple tune modes, switched automatically during a single visit to each sample vial. Data for each of the modes was combined automatically into a single report for each sample. DLs and Background Equivalent Concentrations (BECs) in undiluted 68% HNO<sub>3</sub> (Sample 1) are given in Table 3. The stability test results are discussed in the “long-term stability” section of the report.

**Table 3.** DLs and BECs in high purity 68% HNO<sub>3</sub>.

Element	Tune	Q1	Q2	DL (ng/L)	BEC (ng/L)	30 ppt Recovery %	Stability test RSD %
Be	No gas	9	9	0.12	0.071	92	3.5
B	No gas	11	11	0.43	3.5	94	6.3
Na	Cool-NH <sub>3</sub>	23	23	0.53	2.3	93	3.1
Mg	Cool-NH <sub>3</sub>	24	24	0.085	0.049	93	2.0
Al	Cool-NH <sub>3</sub>	27	27	0.10	0.16	93	3.6
P	O <sub>2</sub>	31	47	8.1	83	95	—**
S	O <sub>2</sub>	32	48	2.6	65	93	—**
K	Cool-NH <sub>3</sub>	39	39	0.38	0.73	93	2.9
Ca	Cool-NH <sub>3</sub>	40	40	0.54	0.38	93	1.2
Sc	O <sub>2</sub>	45	61	0.007	0.013	93	0.5
Ti	O <sub>2</sub> -soft	48	64	0.039	0.081	93	3.3
V	O <sub>2</sub> -soft	51	67	0.041	0.17	93	1.5
Cr	Cool-NH <sub>3</sub>	52	52	0.42	0.25	93	3.0
Mn	Cool-NH <sub>3</sub>	55	55	0.084	0.014	93	2.5
Fe	Cool-NH <sub>3</sub>	56	56	0.75	1.1	92	4.7
Co	Cool-NH <sub>3</sub>	59	59	0.21	0.075	93	4.3
Ni	O <sub>2</sub> -soft	60	60	0.067	0.38	93	2.0
Cu	Cool-NH <sub>3</sub>	63	63	0.12	0.50	94	3.8
Zn	He	64	64	0.52	0.46	93	2.9
Ga	Cool-NH <sub>3</sub>	71	71	0 cps	0 cps	92	2.5
Ge	H <sub>2</sub>	74	74	0.060	0.10	93	1.4
As	O <sub>2</sub> -soft	75	91	0.082	0.081	93	1.8
Se	H <sub>2</sub>	78	78	0.78	0.41	93	5.5
Rb	Cool-NH <sub>3</sub>	85	85	0.089	0.030	93	3.0
Sr	He	88	88	0.014	0.012	93	0.8

Element	Tune	Q1	Q2	DL (ng/L)	BEC (ng/L)	30 ppt Recovery %	Stability test RSD %
Zr	O <sub>2</sub>	90	106	0.22	1.0	93	0.4
Nb	He	93	93	0.012	0.014	93	0.8
Mo	He	98	98	0.088	0.10	93	1.0
Ru	He	101	101	0.032	0.034	93	1.2
Pd	No gas	105	105	0.066	0.14	92	1.0
Ag	No gas	107	107	0.029	0.025	93	0.9
Cd	No gas	114	114	0.058	0.046	92	1.4
In	No gas	115	115	0.004	0.004	93	0.6
Sn	No gas	118	118	0.099	0.35	93	0.9
Sb	H <sub>2</sub>	121	121	0.056	0.028	93	1.6
Te	H <sub>2</sub>	125	125	0.57	0.45	93	5.2
Cs	Cool-NH <sub>3</sub>	133	133	0 cps	0 cps	93	2.4
Ba	H <sub>2</sub>	138	138	0.014	0.010	93	0.4
Hf	No gas	178	178	0.014	0.005	93	0.9
Ta	He	181	181	0.052	0.065	93	0.5
W	No gas	182	182	0.030	0.022	93	0.7
Ir	No gas	193	193	0.016	0.011	93	0.9
Au	No gas	197	197	0.049	0.068	93	1.7
Tl	No gas	205	205	0.090	0.46*	93	0.6
Pb	No gas	208	208	0.060	0.21	93	0.7
Bi	No gas	209	209	0.018	0.025	93	0.4
Th	No gas	232	232	0.004	0.003	93	0.8
U	No gas	238	238	0.025	0.013	93	0.6

DLs were calculated as 3-sigma of 10 replicate measurements of a blank HNO<sub>3</sub> sample (cps refers counts per second).

\*The BEC of Tl was higher than expected, most likely due to residual signal from the ICP-MS tuning solution.

\*\*P and S concentration in the mixed spike (30 ppt) was too low for reliable quantification above the blank (83 ppt and 65 ppt, respectively).

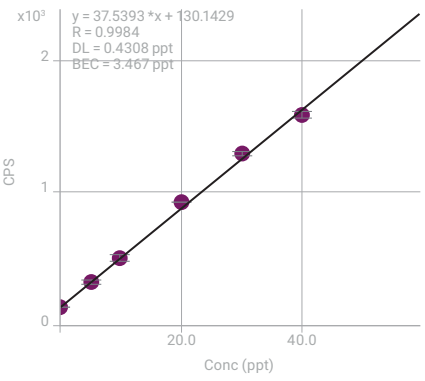
Table 4 shows quantitative data for all SEMI specification elements [1] in high purity 68% HNO<sub>3</sub> and electronic-grade 61% HNO<sub>3</sub> determined by MSA. For the greatest accuracy, the two different concentration grades of nitric acid measured in this study were calibrated using separate MSA calibrations. However, if additional samples of similar grade (acid concentration) are measured, the MSA calibration can be easily and automatically converted to an external calibration plot. External calibration allows subsequent samples to be measured without requiring MSA spike additions into each additional sample. Good linearity was obtained for all SEMI target elements, as shown in the representative calibration curves for B, Na, Al, K, Ca, As, and Pb (Figure 1). Normally, the concentration in each sample is obtained by multiplying the quantitative value by the dilution factor (usually about 10 times for nitric acid). However, in this study, the quantitative value equals the sample concentration in the original sample, as the acids were measured undiluted. The results given in Table 4 show that all 49 elements studied can be analyzed at significantly lower levels than the <1 ppb maximum limit specified for HNO<sub>3</sub> in SEMI standard C35-0708 Tier-B [1].

**Table 3.** Quantitative results for SEMI specification elements [1] in high purity 68% HNO<sub>3</sub> and electronic-grade 61% HNO<sub>3</sub>.

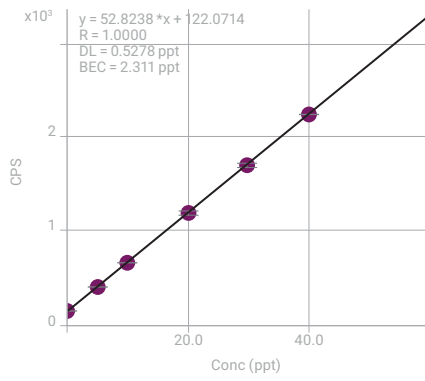
Element	High-purity grade 68% HNO <sub>3</sub> , ng/L	Electronic grade 61% HNO <sub>3</sub> , ng /L	SEMI C35-0708 Tier-B max limit, ng/L
Li	<0.061	0.19	<1000
B	3.5	270	<1000
Na	2.3	130	<1000
Mg	<0.085	11	<1000
Al	0.16	93	<1000
K	0.73	6.5	<1000
Ca	<0.54	50	<1000
Ti	0.081	1.1	<1000
V	0.17	0.24	<1000
Cr	<0.42	70	<1000
Mn	<0.084	3.4	<1000
Fe	1.1	270	<1000
Ni	0.38	28	<1000
Cu	0.50	0.99	<1000
Zn	<0.52	3.8	<1000
As	<0.082	0.25	<1000
Cd	<0.058	0.80	<1000
Sn	0.35	13	<1000
Sb	<0.056	0.11	<1000
Ba	<0.014	0.43	<1000
Pb	0.21	0.31	<1000

Measured values shown as "<" indicate that the measured concentration was below the detection limit.

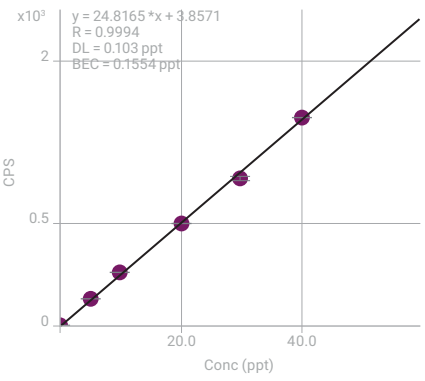
11 → 11 B



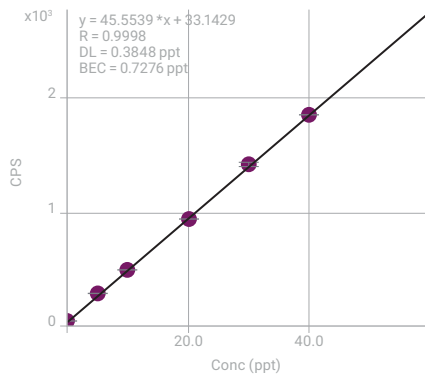
23 → 23 Na



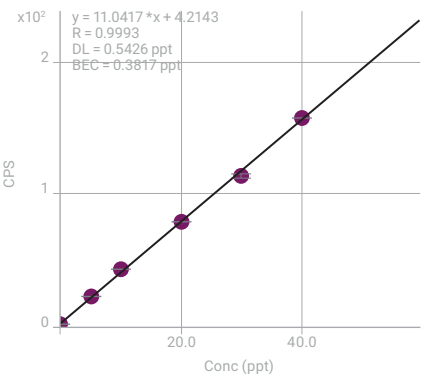
27 → 27 Al



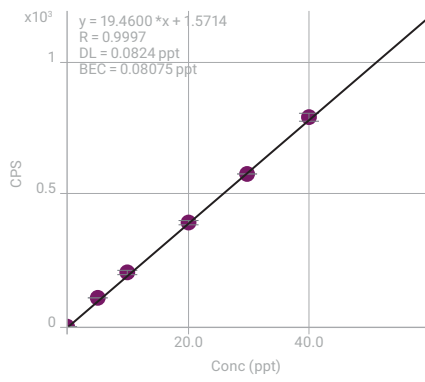
39 → 39 K



40 → 40 Ca



75 → 91 As



208 → 208 Pb

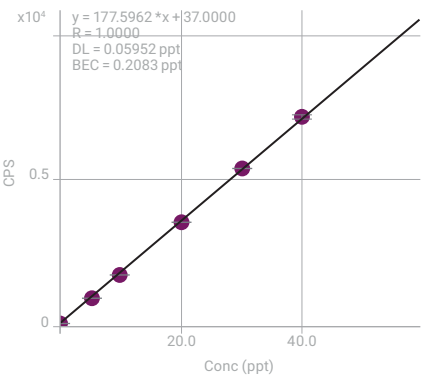


Figure 1. Calibration curves for several SEMI specification elements in high purity 68% HNO<sub>3</sub>.

### Long-term stability

Long-term stability was evaluated by measuring a 68% HNO<sub>3</sub> sample spiked at 30 ppt for all elements. Calibration curves were generated at the beginning of the sequence. The spiked samples were then run as unknown samples for a total analysis period of 6.5 hours. The RSDs of the 21 analysis results are shown in Table 3 (stability test RSD (%)). Good stability was maintained throughout the run, with RSDs between 0.4 and 5.5 %. S and P gave less reliable long-term results due to the low concentration of the spike (30 ppt) measured above the relatively high concentration (83 ppt for P; 65 ppt for S) in the unspiked sample.

### Conclusion

The Agilent 8900 ICP-QQQ operating in MS/MS mode provides the sensitivity, low backgrounds, and effective control of interferences required for the analysis of ultratrace elements in high purity nitric acid.

Forty-nine elements were measured at sub-ppt to ppt levels in undiluted high purity 68% HNO<sub>3</sub>. Calibrations were linear for all elements between 0–40 ppt. SEMI-specified elements were quantified at the single-figure ppt or sub-ppt level in high purity 68% HNO<sub>3</sub>. The reproducibility results for 30 ppt spikes in high purity undiluted 68% HNO<sub>3</sub> were between 0.4–5.5 % RSD for all elements except P and S, in a sequence lasting 6.5 hours.

The results demonstrate the suitability of the Agilent 8900 Semiconductor configuration ICP-QQQ for the routine analysis of the highest-purity semiconductor-grade reagents and process chemicals.

### References

1. SEMI C35-0708, Specifications and guidelines for nitric acid (2008).

### More information

For more information on Agilent ICP-MS products and services, visit our website at [www.agilent.com/chem/icpms](http://www.agilent.com/chem/icpms)

When analyzing 61–68 % HNO<sub>3</sub> on a routine basis, it is recommended to use the following options:

- G3280-67056 Pt sampling cone (18 mm insert)
- G4915A Upgrade to dry pump
- G3666-67030 Interface valve kit – ball type valve



# Direct Determination of V, Cr, Ge, and As in High-Purity 20% Hydrochloric Acid

## Author

Junichi Takahashi  
Agilent Technologies, Japan

## Keywords

semiconductor, RCA Standard Clean, silicon wafer, hydrochloric acid, vanadium, chromium, germanium, arsenic, ammonia on-mass, ammonia mass-shift, oxygen mass-shift

## Introduction

Since the 1970s, the RCA Standard Clean (SC) method has been used extensively in many countries for cleaning silicon wafer surfaces. SC-2 refers to a mixture of HCl and H<sub>2</sub>O<sub>2</sub> that is used to remove ionic and metallic contaminants from the surface of silicon wafers. Because cleaning solutions are in direct contact with semiconductor devices, ultra high purity is required for these solutions. The SEMI standard Tier-D protocol for HCl defines the contaminant level to be <10 ppt for each element. Some elements have been very difficult to determine at ppt level by quadrupole ICP-MS (ICP-QMS) due to significant spectral interferences arising from the Cl matrix, even when analyzed by ICP-MS equipped with a collision/reaction cell (CRC). Consequently, some methods for the analysis of high purity HCl by ICP-MS have recommended sample pre-treatment steps to remove the chloride matrix, which can lead to analyte loss and sample contamination. In this study, ICP-QQQ was used to analyze undiluted HCl directly. Using MS/MS mode with mass-shift to remove polyatomic ions, the most problematic elements, such as V, Cr, Ge and As could be determined in HCl at single-figure ppt detection limits.

## Experimental

**Instrumentation:** Agilent 8800 #200. Operating parameters are given in Table 1.

**Reagents:** 20% TAMAPURE-AA-100 HCl (metallic impurities are guaranteed to be below 100 ppt) was purchased from Tama Chemicals Co., Ltd. (Kanagawa, Japan). The undiluted HCl was introduced directly into the ICP-QQQ.

**Table 1.** ICP-QQQ operating conditions.

		O <sub>2</sub> MS/MS <sup>1)</sup>	NH <sub>3</sub> MS/MS <sup>2)</sup>
RF power	W	1600	
Sampling depth	mm	8	
Carrier gas flow rate	L/min	0.8	
Make-up gas flow rate	L/min	0.41	
Octopole bias V	V	-20	
KED	V	-20	
He	mL/min	3	1
O <sub>2</sub>	mL/min	0.4	0
NH <sub>3</sub>	mL/min	0	3

1) 100% O<sub>2</sub> (purity 99.995%)

2) 10% NH<sub>3</sub> balanced with 90% He (purity 99.995%)

## Results and discussion

### Determination of BECs of V, Cr, Ge, and As in high purity HCl

ICP-QMS with a CRC using He collision mode can successfully eliminate some polyatomic ions such as ArCl [1], and the use of NH<sub>3</sub> as a reaction gas also works to remove the ClO<sup>+</sup> ion for the determination of V. However, ICP-QMS has some serious limitations when highly reactive cell gases (such as NH<sub>3</sub>) are used in the CRC. Principal among these limitations is the fact that all ions enter the CRC, so predicted reaction pathways can be disrupted and new reaction product ion overlaps can be formed if the analyte levels in the sample change. ICP-QQQ with MS/MS removes this limitation, as the first quadrupole mass filter (Q1) allows precise selection of the ions that are allowed to enter the cell. This ensures that reaction processes and product ions are strictly controlled, dramatically improving detectability of the analyte ions shown in Table 2.

**Table 2.** Spectral interferences arising from the Cl matrix on some key elements.

Polyatomic interference	<i>m/z</i>	Analyte ion
ClO <sup>+</sup>	51, 53	<sup>51</sup> V <sup>+</sup>
ClOH <sup>+</sup>	52, 54	<sup>52</sup> Cr <sup>+</sup> , ( <sup>54</sup> Fe <sup>+</sup> )*
ClCl <sup>+</sup>	70, 72, 74	<sup>70</sup> Ge <sup>+</sup> , <sup>72</sup> Ge <sup>+</sup> , <sup>74</sup> Ge <sup>+</sup>
ArCl <sup>+</sup>	75, 77	<sup>75</sup> As <sup>+</sup> , ( <sup>77</sup> Se <sup>+</sup> )*

\*Alternative isotopes can be chosen to avoid spectral interferences on Fe and Se.

The MS/MS acquisition mode using O<sub>2</sub> or NH<sub>3</sub> as the reaction gas enables the determination of trace <sup>51</sup>V (measured directly as V<sup>+</sup> using NH<sub>3</sub> cell gas), Cr as <sup>52</sup>Cr<sup>16</sup>O<sup>+</sup> (using O<sub>2</sub>), Ge as <sup>74</sup>Ge<sup>14</sup>NH<sub>2</sub><sup>+</sup> (using NH<sub>3</sub>) and As as <sup>75</sup>As<sup>16</sup>O<sup>+</sup> (using O<sub>2</sub>). In the case of As, the <sup>91</sup>Zr<sup>+</sup> ion is removed by Q1 (which is set to the As<sup>+</sup> precursor ion mass of *m/z* 75), so the potential overlap from Zr on the AsO<sup>+</sup> product ion at *m/z* 91 is also removed. The complete cut-off of cluster ions by Q1 also eliminates the possibility that <sup>14</sup>NH<sub>2</sub><sup>35</sup>Cl is created in the cell, so the potential new product ion interference on <sup>51</sup>V is avoided. Representative calibration curves for V and Ge are shown in Figure 1. BECs and DLs determined by the ICP-QQQ for V, Cr, Ge, and As are given in Table 3.

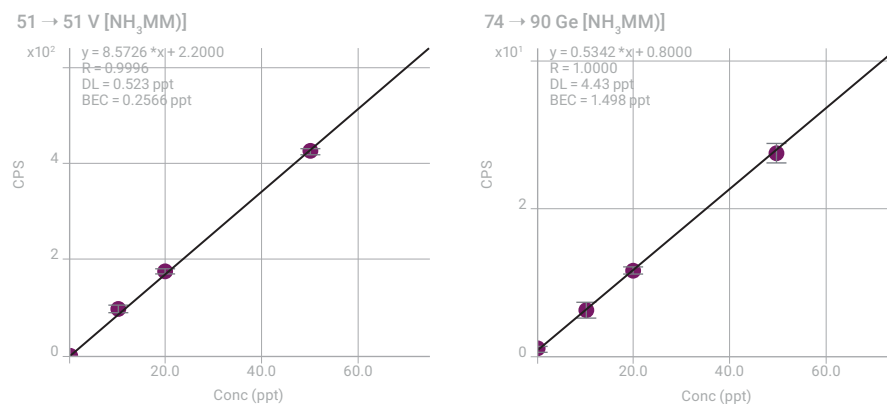


**Figure 1.** Calibration curves of V (NH<sub>3</sub> on-mass mode) and Ge (NH<sub>3</sub> mass-shift mode) in 20% HCl.

**Table 3.** BECs and DLs for V, Cr, Ge and As in 20% HCl.

Element	Ti	Cr	Ge	As
Mode (cell gas)	MS/MS (NH <sub>3</sub> )	MS/MS (O <sub>2</sub> )	MS/MS (NH <sub>3</sub> )	MS/MS (O <sub>2</sub> )
Measured ion	<sup>51</sup> V <sup>+</sup>	<sup>52</sup> Cr <sup>16</sup> O <sup>+</sup>	<sup>74</sup> Ge <sup>14</sup> NH <sub>2</sub> <sup>+</sup>	<sup>52</sup> Cr <sup>16</sup> O <sup>+</sup>
Mass pair	Q1 = Q2 = 51	Q1 = 52, Q2 = 68	Q1 = 74, Q2 = 90	Q1 = 75, Q2 = 91
BEC - ppt	0.3	8.0	1.5	19.7
DL - ppt	0.5	1.1	4.4	3.4

### Investigation of arsenic contamination

As the BEC for arsenic in high purity HCl was relatively high (Table 3), the signal count at *m/z* 91 was investigated further. The signals of the mass-pairs 75/75, 77/77, 75/91 and 77/91 were measured by ICP-QQQ with MS/MS, the mass pair number represents the set mass of Q1 followed by the set mass of Q2, so an MS/MS mode acquisition of mass pair 75/91 represents a mass-shift mode with Q1 = 75 and Q2 = 91, for example. The four mass pairs were measured in HCl blanks from three different lots, and the results are shown in Table 4. The following observations were made:

1. The ratio of the signal of 75/75 to 77/77 is around four, which is close to the ratio of the abundance of <sup>35</sup>Cl to <sup>37</sup>Cl, i.e. 3.13.
2. The ratio of the signal of 75/91 to 77/93 is 200–1000, which is far in excess of the ratio of <sup>35</sup>Cl to <sup>37</sup>Cl.
3. While the signals of 75/75 and 77/77 are similar for the three HCl blanks, those of 75/91 and 77/93 vary.

**Table 4.** Comparison of background counts (cps) in 3 different lots of 20% HCl\*.

Mass pair	75->75	77->77	75->91	77->93
Sample A	509.3	133.5	584.4	2.5
Sample B	508.4	126.0	1172.6	1.9
Sample C	612.7	130.0	3175.6	2.6

\*All the samples were obtained from the new bottles of high purity HCl.

Finding #1 suggests that the remaining signal on 75/75 and 77/77 was mostly from ArCl<sup>+</sup>. This is a reasonable assumption since ArCl<sup>+</sup> doesn't react with O<sub>2</sub> very efficiently so most ArCl<sup>+</sup> remains at the original masses of 75 and 77. Finding #2 suggests that the signal of 75/91 is not due to ArCl<sup>+</sup>. Assuming that all counts of 77/93 arise from <sup>40</sup>Ar<sup>37</sup>Cl, the contribution of <sup>40</sup>Ar<sup>35</sup>Cl to the signal of 75/91 in the HCl blank is estimated to be just 7-8 cps, which is two orders of magnitude lower than the signal that is actually observed. Observation #3, together with #1 and #2, suggests the high count obtained for 75/91 in HCl is due to As impurity in the acid.

### Reference

1. Direct analysis of trace metallic impurities in high purity hydrochloric acid by Agilent 7700s ICP-MS, Agilent application note, [5990-7354EN](#).

# Analysis of trace metal impurities in high purity hydrochloric acid using ICP-QQQ

## Authors

Kazuo Yamanaka and Kazuhiro Sakai  
Agilent Technologies, Japan

## Introduction

Hydrochloric acid (HCl) is a component of the standard RCA cleaning process used to remove organic and metallic residues and impurities from the surface of silicon wafers used in semiconductor manufacturing. The cleaning steps are performed before high temperature processing steps such as oxidation and chemical vapor deposition (CVD). RCA Standard Clean 2 (SC-2) removes ionic contaminants from the wafer surface. SC-2 follows SC-1, which removes organic residues and particles. SC-2 consists of HCl combined with hydrogen peroxide ( $H_2O_2$ ) and de-ionized water (DIW). Since the cleaning solutions are in direct contact with the silicon wafer surface, ultrahigh purity reagents are required for these solutions.

SEMI standard C27-0708 Tier-C protocol for HCl specifies a maximum contaminant level of 100 ppt for each element (HCl 37.0 - 38.0 %) [1]. The concentration of industrial grade HCl is usually 20 or 35%, depending on the method of production. The Cl matrix leads to the formation of several polyatomic ions, which cause significant spectral interferences on some key elements. For example,  $H_2^{37}Cl^+$  on  $^{39}K^+$ ,  $^{35}Cl^{16}O^+$  on  $^{51}V^+$ ,  $^{35}Cl^{16}OH^+$  on  $^{52}Cr^+$ ,  $^{37}Cl^{16}O^+$  on  $^{53}Cr^+$ ,  $^{35}Cl^{37}Cl^+$  on  $^{72}Ge^+$ ,  $^{37}Cl_2^+$  on  $^{74}Ge^+$ , and  $^{40}Ar^{35}Cl^+$  on  $^{75}As^+$ . As a result of these polyatomic interferences, it has been difficult to determine these elements at the required levels using conventional single quadrupole ICP-MS (ICP-QMS). Even ICP-QMS instruments fitted with a collision/reaction cell (CRC) or bandpass filter can only offer limited reduction of the spectral interferences arising from the Cl matrix. Consequently, some methods for the analysis of high purity HCl by ICP-QMS have recommended sample pretreatment steps to remove the chloride matrix, which can lead to analyte loss and/or sample contamination.

In this study, triple quadrupole ICP-MS (ICP-QQQ) was used to analyze 50 elements in HCl, using MS/MS mode to resolve the polyatomic interferences. All analytes, including the most problematic elements such as K, V, Cr, Ge, and As, could be determined directly in the undiluted HCl with single digit ppt detection limits.

## Experimental

### Instrumentation

An Agilent 8900 Semiconductor configuration ICP-QQQ was used in this study. The instrument was fitted with a PFA-100 nebulizer, Peltier-cooled quartz spray chamber, quartz torch, platinum-tipped sampling and skimmer cones and s-lens.

The nebulizer was operated in self-aspiration mode to minimize the potential for sample contamination from the peristaltic pump tubing. In advanced semiconductor applications, the key requirement is to deliver the absolute lowest possible detection limits (DLs) for each analyte. To achieve this goal, laboratories measuring ultratrace levels of contaminants can use a multi-tune method, where several tuning steps are applied sequentially during the measurement of each solution. This approach allows the tuning conditions to be optimized for the removal of different types of interferences, while maintaining maximum sensitivity for each analyte. In this work, several reaction cell gases ( $H_2$ ,  $O_2$ , and  $NH_3$ ) were

used as appropriate for the large number of analytes being measured. He was used as a buffer gas in the NH<sub>3</sub> reaction gas modes. Tuning conditions are shown in Table 1 and other acquisition parameters are shown in Table 2.

**Table 1.** ICP-QQQ operating conditions.

	Cool	Cool-NH <sub>3</sub>	No gas	H <sub>2</sub>	O <sub>2</sub>	NH <sub>3</sub>	O <sub>2</sub> -soft
Acquisition mode	MS/MS						
RF power (W)	600	1500					
Sampling depth (mm)	18.0	18.0 8.0					
Nebulizer gas (L/min)	0.70						
Make-up gas (L/min)	0.90	0.48					
Extract 1 (V)	-150	4.2	4.7	4.5	3.5		
Extract 2 (V)	-18.0	-17.0	-250.0				-120.0
Omega bias (V)	-70.0	-140.0					-70.0
Omega lens (V)	2.0	10.0	8.0	10.5		4.0	
Q1 entrance (V)	-15.0	-50.0					
He flow (mL/min)	-	1.0	-	-	-	1.0	-
H <sub>2</sub> flow (mL/min)	-	-	-	7.0	-	-	-
NH <sub>3</sub> flow (mL/min)		2.0 (20%)	-	-	-	2.0 (20%)	-
O <sub>2</sub> flow (mL/min)	-	-	-	-	0.45 (30%)		0.45 (30%)
Axial acceleration (V)	0.0	1.5	0.0		1.0	0.2	1.0
Energy discrimination (V)	15.0	-5.0	5.0	0.0	-7.0		

**Table 2.** Acquisition parameters.

Parameter	Setting
Q2 peak pattern	1 point
Replicates	3 (spiked samples) 10 (unspiked solution)
Sweeps/replicate	10
Integration time	2 s for all isotopes

### Samples and standards

The samples of HCl used in this study included:

- Sample 1: 20% HCl (high purity grade).
- Sample 2: 36% HCl (non-high purity grade).
- Sample 3: 20% HCl (34% high purity grade diluted to 20% with DIW).

No further sample preparation was necessary as all samples were introduced directly into the ICP-QQQ. To run undiluted HCl routinely, it is recommended that the large (18 mm) insert Pt cone is fitted. Long-term corrosion of internal ICP-MS components can be minimized by fitting the dry pump option.

Calibration and quantification were done using the method of standard additions (MSA). Standard solutions were prepared by spiking a multi-element standard solution (SPEX CertiPrep, NJ, US) into each HCl sample type to give spike levels of 10, 20, 30, and 40 ppt. The MSA calibrations were then automatically converted to external calibrations in the ICP-MS MassHunter data analysis table. This conversion allows other samples of the same type (HCl concentration) to be quantified without requiring separate MSA spike additions into each sample. All solutions were prepared just before analysis.

All preparation and analysis was performed in a Class 10,000 clean room.

## Results and discussion

### DLs and BECs

In total, 50 elements including all SEMI specification analytes were measured using the 8900 ICP-QQQ operating in multiple tune modes. Data for each mode was combined automatically into a single report for each sample. Detection limits (DLs) and background equivalent concentrations (BECs) in 20% HCl are given in Table 3.

**Table 3.** DLs and BECs in high purity 20% HCl\*.

Element	Cell gas mode	Q1 mass	Q2 mass	DL ng/L	BEC ng/L
Li	Cool-NH <sub>3</sub>	7	7	0.032	0.016
Be	No gas	9	9	0.022	0.021
B	No gas	11	11	0.55	4.1
Na	Cool-NH <sub>3</sub>	23	23	0.064	0.15
Mg	Cool-NH <sub>3</sub>	24	24	0.077	0.056
Al	Cool-NH <sub>3</sub>	27	27	0.20	0.19
P	O <sub>2</sub> -soft	31	47	1.1	2.6
K	Cool-NH <sub>3</sub>	39	39	0.087	0.17
Ca	Cool-NH <sub>3</sub>	40	40	0.44	0.68
Sc	O <sub>2</sub> -soft	45	61	0.014	0.012
Ti	O <sub>2</sub> -soft	48	64	0.051	0.074
V	NH <sub>3</sub>	51	51	0.11	0.19
Cr	Cool-NH <sub>3</sub>	52	52	0.18	0.12
Mn	Cool-NH <sub>3</sub>	55	55	0.016	0.006
Fe	Cool-NH <sub>3</sub>	56	56	0.24	0.27
Co	Cool-NH <sub>3</sub>	59	59	0.10	0.038
Ni	Cool-NH <sub>3</sub>	60	60	0.66	0.26
Cu	Cool-NH <sub>3</sub>	63	63	0.10	0.12
Zn	NH <sub>3</sub>	66	66	0.14	0.097
Ga	NH <sub>3</sub>	71	71	0.015	0.026
Ge	NH <sub>3</sub>	74	107	0.90	3.0
Ge	NH <sub>3</sub>	74	107	0.32	0.77
As	O <sub>2</sub>	75	91	1.4	48
As	O <sub>2</sub>	75	91	0.73	6.2
Se	H <sub>2</sub>	78	78	0.44	0.52

\* Shaded rows for Ge and As indicate results measured in Sample 3, due to suspected contamination for these elements in Sample 1.

Element	Cell gas mode	Q1 mass	Q2 mass	DL ng/L	BEC ng/L
Rb	Cool-NH <sub>3</sub>	85	85	0.041	0.013
Sr	NH <sub>3</sub>	88	88	0.003	0.001
Y	O <sub>2</sub> -soft	90	106	0.010	0.006
Zr	O <sub>2</sub> -soft	93	125	0.012	0.004
Nb	O <sub>2</sub>	93	125	0.004	0.005
Mo	He	98	98	0.13	0.57
Ru	He	101	101	0.016	0.003
Pd	He	105	105	0.010	0.001
Ag	He	107	107	0.032	0.014
Cd	He	114	114	0.090	0.10
In	He	115	115	0.035	0.021
Sn	He	118	118	0.57	3.3
Sb	He	121	121	0.66	1.5
Te	H <sub>2</sub>	125	125	0.37	0.31
Cs	NH <sub>3</sub>	133	133	0.008	0.019
Ba	NH <sub>3</sub>	138	138	0.005	0.005
Hf	No gas	178	178	0.005	0.004
Ta	He	181	181	0.013	0.010
W	No gas	182	182	0.039	0.062
Re	No gas	185	185	0.12	0.50
Ir	No gas	193	193	0.017	0.012
Au	He	197	197	0.027	0.022
Tl	No gas	205	205	0.007	0.004
Pb	H <sub>2</sub>	208	208	0.028	0.023
Bi	No gas	209	209	0.024	0.030
Th	No gas	232	232	0.017	0.021
U	No gas	238	238	0.009	0.005

### Quantitative results

Table 4 shows quantitative data for all SEMI specification elements in high purity 20% HCl and non-high purity 36% HCl determined by MSA. The results show that the 8900 ICP-QQQ can measure contaminants in HCl at a much lower level than the 100 ppt maximum limit specified in the SEMI specifications. It is important to note that the concentration specified by SEMI is for 37–38% HCl while the data presented here is for 20 and 36% HCl. Even taking this difference into account, the 8900 ICP-QQQ is clearly able to measure contaminants at levels far lower than current industry requirements for high-purity HCl.

**Table 4.** Quantitative results for SEMI specification elements in high purity 20% HCl (Sample 1) and non-high purity 36% HCl (Sample 2).

Element	Cell gas mode	Q1	Q2	Sample 1 20% HCl, ng/L	Sample 2 36% HCl, ng/L	DL, ng/L
Li	Cool-NH <sub>3</sub>	7	7	<DL	<DL	0.032
B	No gas	11	11	4.1	15	0.55
Na	Cool-NH <sub>3</sub>	23	23	0.15	6.4	0.064
Mg	Cool-NH <sub>3</sub>	24	24	<DL	6.5	0.077
Al	Cool-NH <sub>3</sub>	27	27	<DL	23	0.20
K	Cool-NH <sub>3</sub>	39	39	0.17	1.5	0.087
Ca	Cool-NH <sub>3</sub>	40	40	0.68	13	0.44
Ti	O <sub>2</sub> -soft	48	64	0.074	1.4	0.051
V	NH <sub>3</sub>	51	51	0.19	4.6	0.11
Cr	Cool-NH <sub>3</sub>	52	52	<DL	0.55	0.18
Mn	Cool-NH <sub>3</sub>	55	55	<DL	0.071	0.016
Fe	Cool-NH <sub>3</sub>	56	56	0.27	7.6	0.24
Ni	Cool-NH <sub>3</sub>	60	60	<DL	<DL	0.66
Cu	Cool-NH <sub>3</sub>	63	63	0.12	0.57	0.10
Zn	NH <sub>3</sub>	66	66	<DL	1.1	0.14
As	O <sub>2</sub>	75	91	48	39	0.73*
Cd	He	114	114	0.10	0.34	0.090
Sn	He	118	118	3.3	2.3	0.57
Sb	He	121	121	1.5	0.95	0.66
Ba	NH <sub>3</sub>	138	138	0.005	<DL	0.005
Pb	H <sub>2</sub>	208	208	0.023	0.13	0.028

\*DL for As measured in Sample 3, due to suspected contamination for this element in Sample 1.

### Cr and K determination

Cool plasma is a proven technique used to remove plasma-based interferences. Although it has been largely superseded by CRC methodology, cool plasma remains the most effective analytical mode for some elements in certain matrices. Combining cool plasma with CRC technology has been shown to be a powerful mode for interference removal [2]. Because the major isotope of chromium ( $^{52}\text{Cr}^+$ ) suffers an interference from  $^{35}\text{Cl}^{16}\text{OH}^+$  in high purity HCl, Cr was determined using cool plasma with ammonia cell gas. The calibration curve for  $^{52}\text{Cr}$  shows that  $^{35}\text{Cl}^{16}\text{OH}^+$  interference was removed successfully, allowing a BEC of 0.12 ng/L (ppt) to be achieved, with a detection limit of 0.18 ppt (Figure 1). The DL and BEC displayed in the ICP-MS MassHunter calibration plots are based on the 10 replicates of the unspiked high-purity 20% HCl sample.



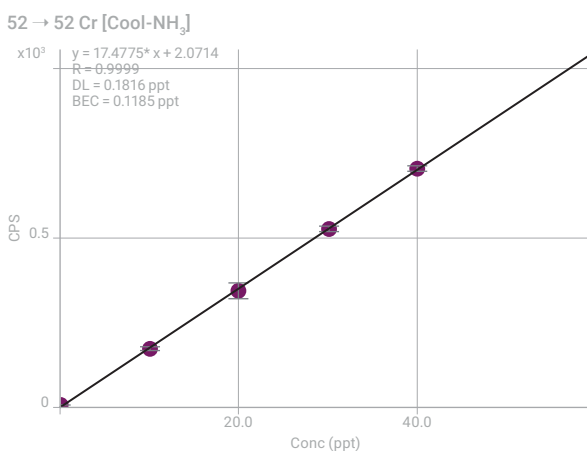


**Figure 1.** <sup>52</sup>Cr calibration curve obtained using cool plasma and NH<sub>3</sub> cell gas, showing low BEC and good linearity.

The same approach is effective for the determination of other interfered elements such as K. Figure 2 shows that the interference from H<sup>237</sup>Cl<sup>+</sup> on <sup>39</sup>K<sup>+</sup> was suppressed using cool plasma and NH<sub>3</sub> cell gas, giving a BEC and DL for K of 0.17 ppt and 0.09 ppt, respectively.

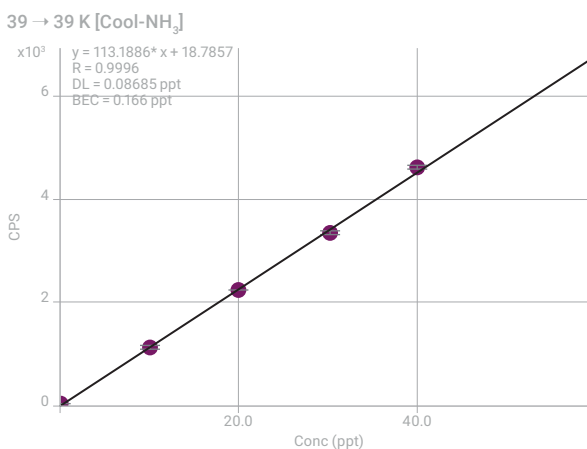


**Figure 2.** <sup>39</sup>K calibration curve obtained using cool plasma and NH<sub>3</sub> cell gas.

### V and Ge determination

ICP-QMS fitted with a CRC operating in helium collision mode can successfully eliminate many polyatomic ions using He collision cell gas and kinetic energy discrimination (KED) [3]. However, ICP-QMS has some serious limitations when highly reactive cell gases, such as NH<sub>3</sub>, are used in the CRC.

ICP-QMS has no mass selection step before the cell, so all ions enter the CRC. It is likely, therefore, that new reaction product ions will form in the CRC that may overlap the target analyte mass of interest. Bandpass ICP-QMS instruments, where all ions within a certain mass range (usually about 10 u) of the target analyte can enter the cell and react, have similar limitations to traditional ICP-QMS in terms of controlling reaction chemistry with highly reactive cell gases.

ICP-QQQ with MS/MS removes this limitation, as the first quadrupole mass filter (Q1), which is located before the CRC, allows precise selection of the specific mass of ions that are allowed to enter the cell. This extra mass selection step ensures that reaction processes in the cell are controlled, which removes the

potential for non-target product ion overlaps and dramatically improves the detectability of the analyte ions.

MS/MS acquisition mode using  $\text{NH}_3$  as the reaction cell gas was used for the trace determination of V and Ge. The  $\text{ClO}^+$  interference on  $^{51}\text{V}$  was removed using  $\text{NH}_3$  on-mass mode. Potentially,  $^{14}\text{NH}_2^{35}\text{Cl}^+$  could form in the cell and interfere with V at  $m/z$  51. However, the unit mass resolution of Q1 on the 8900 ICP-QQQ ensures that only ions at  $m/z$  51 can enter the cell. All other matrix and analyte ions, e.g.  $^{35}\text{Cl}^+$ , are prevented from entering the cell and cannot, therefore, contribute to the signal at the analyte mass. This simple approach avoids the formation of any new product ion interferences on  $^{51}\text{V}$ .

The  $\text{ClCl}^+$  interference on  $^{74}\text{Ge}$  was avoided by measuring a Ge-ammonia cluster ion,  $^{74}\text{Ge}[^{14}\text{NH}_2(^{14}\text{NH}_3)]^+$ , in mass-shift mode at mass 107. Q1 (set to  $m/z$  74 to allow the  $^{74}\text{Ge}^+$  precursor ions to enter the cell) rejects all non-target masses, including  $^{107}\text{Ag}^+$ , which would otherwise overlap the Ge- $\text{NH}_3$  product ion mass. Q1 (in contrast to a bandpass filter) also rejects all other nearby analyte ions,  $^{70}\text{Zn}^+$ ,  $^{71}\text{Ga}^+$ ,  $^{73}\text{Ga}^+$ ,  $^{75}\text{As}^+$ ,  $^{78}\text{Se}^+$ , etc., preventing them from forming potentially overlapping ammonia clusters at the target product ion mass.

Representative calibration curves for V and Ge are shown in Figure 3, again illustrating the low BEC (0.19 ppt for V and 0.77 ppt for Ge) and DL (0.11 ppt for V and 0.32 ppt for Ge) achieved with the 8900 with  $\text{NH}_3$  cell gas in MS/MS mode.

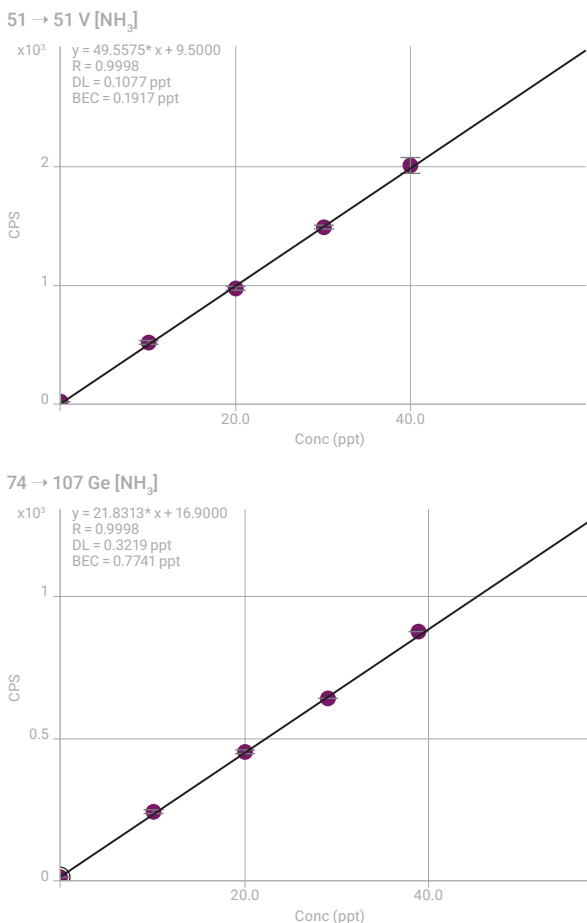


Figure 3.  $^{51}\text{V}$  and  $^{74}\text{Ge}$  calibration curve obtained using  $\text{NH}_3$  cell gas.

## Determination of As

Arsenic has a single isotope at  $m/z$  75 that suffers an interference from the polyatomic ion  $^{40}\text{Ar}^{35}\text{Cl}^+$ . Since  $\text{ArCl}^+$  readily forms in a chloride matrix, the polyatomic interference compromises the determination of As at ultratrace levels in concentrated HCl using ICP-QMS. Oxygen can be used as the cell gas to avoid this overlap, with As being measured as the  $\text{AsO}^+$  product ion at  $m/z$  91. However, with ICP-QMS, the  $\text{AsO}^+$  product ion at mass 91 suffers an interference from  $^{91}\text{Zr}^+$ . Helium collision mode in the Agilent ORS cell can reduce  $\text{ArCl}^+$  effectively, allowing a BEC of less than 20 ppt to be achieved by ICP-QMS [3]. But, as semiconductor industry demands become more stringent, this sensitivity may not be sufficient for the lowest level of ultratrace analysis.

Using the 8900 ICP-QQQ with MS/MS, the  $^{91}\text{Zr}^+$  ion is removed by Q1, which is set to the  $\text{As}^+$  precursor ion mass of 75. MS/MS mode allows  $\text{O}_2$  cell gas to be used successfully, with As being measured as the  $\text{AsO}^+$  product ion at  $m/z$  91 without overlap from  $^{91}\text{Zr}^+$ . A further benefit of  $\text{O}_2$  cell gas is that measuring  $\text{AsO}^+$  provides more sensitivity than direct measurement of  $\text{As}^+$  in He mode.

A calibration curve for As in 20% HCl (Sample 3) is shown in Figure 4, demonstrating a BEC of 6.17 ppt and a DL of 0.73 ppt. While lower than the industry requirements for high-purity HCl, this BEC doesn't represent the best performance that can be achieved with the 8900 ICP-QQQ, so further investigation was done to identify the cause of the relatively high background.

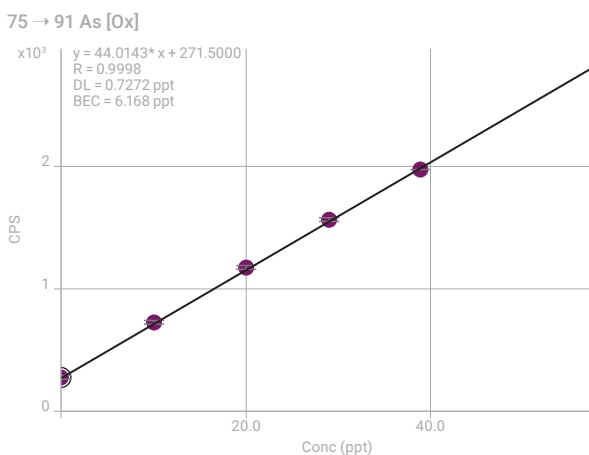
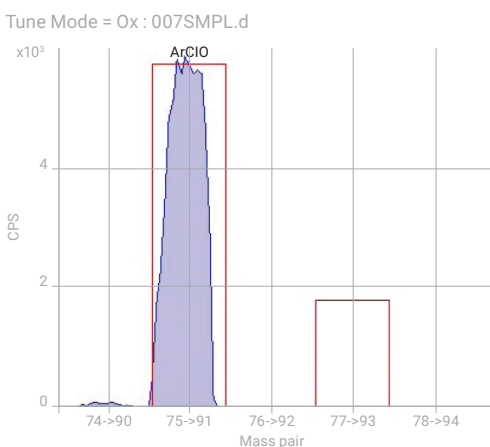


Figure 4.  $^{75}\text{As}$  MSA calibration curve obtained in Sample 1 using  $\text{O}_2$  cell gas.

## Investigation of arsenic contamination

As the measured result for As was relatively high in high purity HCl Sample 1 (Table 4), the signal count at  $m/z$  91 (mass of the product ion  $\text{AsO}^+$ ) was investigated further. In a high Cl matrix, the polyatomic ion  $^{40}\text{Ar}^{35}\text{Cl}^+$  forms in the plasma and during ion extraction. This polyatomic ion has the same nominal mass as the target  $^{75}\text{As}^+$  precursor ion, so it passes through Q1 and enters the cell. While not thermodynamically favored, the  $\text{ArCl}^+$  might react with the  $\text{O}_2$  cell gas to form  $\text{ArClO}^+$ , which would therefore remain as an interference on  $\text{AsO}^+$  at  $m/z$  91. This possibility can be checked by comparing the isotopic signature of the Cl-based product ions observed in the mass spectrum. Since chlorine has two isotopes, 35 and 37, the ratio of the natural abundances of these isotopes (75.78%: 24.22%) can be used to confirm whether a product ion is Cl-based.

The signals of the mass-pairs 75/91 and 77/93, representing the potential Cl interferences  $^{40}\text{Ar}^{35}\text{Cl}^{16}\text{O}^+$  and  $^{40}\text{Ar}^{37}\text{Cl}^{16}\text{O}^+$  respectively, were measured by ICP-QQQ with MS/MS. A neutral gain scan spectrum (where Q1 and Q2 are scanned synchronously, with a fixed mass difference between them) was measured and the scan is presented in Figure 5. For this neutral gain scan, Q1 was scanned across the mass range from 74 to 78 u to pass any precursor ions to the CRC, and Q2 was scanned synchronously at Q1 + 16, monitoring any product ions formed by O-atom addition. The peak at mass-pair  $m/z$  75/91 that caused the relatively high BEC for As in Sample 1 is clearly visible. However, if the signal at 75/91 was due to interference from  $^{40}\text{Ar}^{35}\text{Cl}^{16}\text{O}^+$ , there would also be a corresponding signal from  $^{40}\text{Ar}^{37}\text{Cl}^{16}\text{O}^+$  at mass-pair 77/93. Since there was no signal observed at 77/93, we can conclude that the signal at  $m/z$  75/91 is not due to any contribution from  $\text{ArClO}^+$ , and the high reported concentration of As in Sample 1 is due to contamination.



**Figure 5.** Neutral gain scan spectrum for 20% high purity HCl showing the theoretical isotope template for  $^{40}\text{Ar}^{35}\text{Cl}^{16}\text{O}^+$  and  $^{40}\text{Ar}^{37}\text{Cl}^{16}\text{O}^+$ . Q1 was scanned from  $m/z$  74 to 78, while Q2 was set to Q1 + 16.

## Conclusion

The high performance of Agilent ICP-QQQ systems for the analysis of trace metallic impurities in concentrated HCl has been described previously [4]. Now, the Agilent 8900 Semiconductor configuration ICP-QQQ with flexible cell gas support, powerful MS/MS capability, and proven cool plasma performance, further improves the detection limits for the analysis of a wide range of trace metal contaminants in high purity acids. The advanced reaction cell methodology supported by the 8900 ICP-QQQ allows the SEMI elements, including those elements with potential matrix-based interferences such as K, V, Cr, Ge, and As, to be determined at lower concentrations in a chloride matrix than was previously possible.

## References

1. SEMI C27-0708, Specifications and guidelines for hydrochloric acid (2008)
2. Junichi Takahashi and Katsuo Mizobuchi, Use of Collision Reaction Cell under Cool Plasma Conditions in ICP-MS, 2008 Asia Pacific Winter Conference on Plasma Spectroscopy
3. Junichi Takahashi, Direct analysis of trace metallic impurities in high purity hydrochloric acid by Agilent 7700s/7900 ICP-MS, Agilent publication, 2017, [5990-7354EN](#)

## More information

When analyzing 20–36% HCl on a routine basis, it is recommended to use the following options:

- G3280-67056 Pt sampling cone (18 mm insert)
- G4915A Upgrade to dry pump
- G3666-67030 Interface valve kit – ball type valve

Since hydrochloric acid is corrosive, avoid placing open sample bottles near the instrument.

# Determination of Ti, V, and Cr in 9.8% Sulfuric Acid

## Author

Junichi Takahashi  
Agilent Technologies, Japan

## Keywords

semiconductor, process chemicals, ultra pure water, UPW, calcium, method of standard additions, hydrogen on-mass

## Introduction

High purity  $H_2SO_4$  is frequently used in the manufacturing of semiconductor devices, in processes such as the removal of organic substances from the surface of silicon wafers. The required metallic impurity level is lower than 100 ppt in the concentrated (usually 98%) acid. ICP-MS is the technique of choice for the measurement of trace metal impurities in semiconductor process chemicals. There are, however, some limitations for the measurement of elements such as Ti, V and Cr in  $H_2SO_4$ . Because of its high viscosity of 27 cP, it is not possible to introduce  $H_2SO_4$  directly into the ICP without dilution. A 10 times dilution in UPW is normally applied, thus the BEC of the calibration curve must be lower than 10 ppt in the 9.8%  $H_2SO_4$  solution measured. In addition, spectral interferences from  $SO^+$ ,  $S_2^+$  and  $ArS^+$  originating from  $H_2SO_4$  make it difficult to determine elements such as Ti and Cr at low concentration even by quadrupole ICP-MS (ICP-QMS) equipped with collision/reaction cell (CRC). As outlined in this report, the Agilent 8800 ICP-QQQ with MS/MS mode allows the successful determination of the most problematic elements including Ti, V and Cr in  $H_2SO_4$ .

## Experimental

**Instrumentation:** Agilent 8800 #200. Operating parameters are given in Table 1.

**Reagents and sample preparation:** Highly purified  $H_2SO_4$ , TAMAPURE-AA-100 (98%  $H_2SO_4$ ) was purchased from Tama Chemicals Co., Ltd. (Kanagawa, Japan). 5 g of  $H_2SO_4$  was diluted by a factor of 10 in a chilled PFA bottle.

Table 1. ICP-QQQ operating conditions.

		O <sub>2</sub> MS/MS <sup>1)</sup>	NH <sub>3</sub> MS/MS <sup>2)</sup>
RF power	W	1600	
Sampling depth	mm	8	
Carrier gas flow rate	L/min	0.8	
Make-up gas flow rate	L/min	0.41	
Octopole bias V	V	-20	
KED	V	-20	
He	mL/min	3	1
O <sub>2</sub>	mL/min	0.4	0
NH <sub>3</sub>	mL/min	0	3

1) 100% O<sub>2</sub> (purity 99.995%)

2) 10% NH<sub>3</sub> balanced with 90% He (purity 99.995%)

## Results and discussion

Of the potential polyatomic interferences formed from the  $H_2SO_4$  matrix, the  $SO^+$  ion is very stable and difficult to eliminate because its dissociation energy is as high as 5.44 eV. In addition, its ionization potential is 10.3 eV, which is almost the same as that of S, 10.36 eV. The spectral interferences caused by  $SO^+$  and  $SOH^+$  overlap with  $^{48}Ti$  ( $^{32}S^{16}O$ ),  $^{51}V$  ( $^{33}S^{18}O$ ,  $^{34}S^{16}OH$  and  $^{32}S^{18}OH$ ) and  $^{52}Cr$  ( $^{34}S^{18}O$ ). Quadrupole ICP-MS operating in He

collision mode provides BECs of 60 ppt for  $^{47}\text{Ti}$  (the BEC for the preferred isotope  $^{48}\text{Ti}$  is much higher), 3 ppt for V and 8 ppt for Cr in 9.8%  $\text{H}_2\text{SO}_4$ . The BEC of Ti, in particular, is not acceptable for producers and users of semiconductor grade  $\text{H}_2\text{SO}_4$ .

Appropriate reaction gases to remove  $\text{SO}^+$  successfully in ICP-QMS are difficult to find.  $\text{NH}_3$  can reduce  $\text{SO}^+$  by two orders of magnitude but the background signal remains too high for this application. Additionally, cluster ions of  $\text{NH}_3$  such as  $\text{N}_m\text{H}_n$  produced by the reaction between  $\text{Ar}^+$  and the  $\text{NH}_3$  cell gas lead to new reaction product ion interferences that increase the background at  $m/z$  51, for example.

The 8800 ICP-QQQ operating in MS/MS mass-shift mode with  $\text{NH}_3$  or  $\text{O}_2$  reaction gas provides reliable and consistent measurement of Ti as  $^{48}\text{Ti}^{14}\text{NH}(^{14}\text{NH}_3)_3$  (Figure 1) and Cr as  $^{52}\text{Cr}^{16}\text{O}$  in  $\text{H}_2\text{SO}_4$ . Furthermore, in MS/MS mode, the  $\text{Ar}^+$  ion is removed by Q1, preventing it from reacting with  $\text{NH}_3$  to form new product ion interferences in the cell. This reduces the background at  $m/z$  51 improving the BEC for V, as shown in Figure 2. The final BECs obtained by ICP-QQQ in 9.8% high purity  $\text{H}_2\text{SO}_4$  are summarized in Table 2.

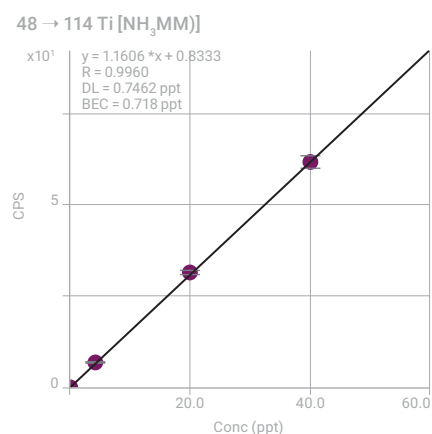


Figure 1. Calibration curve of Ti in 9.8%  $\text{H}_2\text{SO}_4$ .

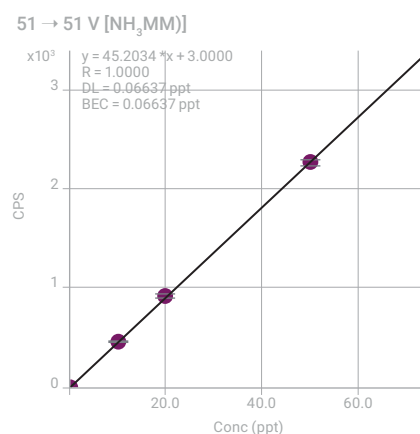


Figure 2. Calibration curve of V in 9.8%  $\text{H}_2\text{SO}_4$ .

Table 2. BECs of Ti, V and Cr in 10x diluted 98%  $\text{H}_2\text{SO}_4$ , measured by ICP-QQQ.

Element	Ti	V	Cr
Mode (cell gas)	MS/MS ( $\text{NH}_3$ )	MS/MS ( $\text{NH}_3$ )	MS/MS ( $\text{O}_2$ )
Measured ion	$^{48}\text{Ti}^{14}\text{NH}(^{14}\text{NH}_3)_3^+$	$^{51}\text{V}^+$	$^{52}\text{Cr}^{16}\text{O}^+$
Mass pair	Q1 = 48, Q2 = 114	Q1 = Q2 = 51	Q1 = 52, Q2 = 68
BEC - ppt	0.72	0.07	3.70

## Conclusion

ICP-QQQ operating in MS/MS mode provides a reliable means for manufacturers of high purity  $\text{H}_2\text{SO}_4$  to guarantee all metallic impurity concentrations at less than 100 ppt in the concentrated acid.

## More information

Determination of challenging elements in ultrapure semiconductor grade sulfuric acid by Triple Quadrupole ICP-MS, Agilent publication, [5991-2819EN](#)

# Determination of trace elements in ultrapure semiconductor grade sulfuric acid using the Agilent 8900 ICP-QQQ in MS/MS mode

## Authors

Michiko Yamanaka, Kazuo Yamanaka  
and Naoki Sugiyama,

Agilent Technologies, Japan

## Introduction

In the semiconductor industry, it is extremely important to reduce contamination within the manufacturing process, as particle-, metallic-, or organic-based contaminants degrade the quality and reliability of the final device. Organic materials, such as photoresist polymer patterns, must be thoroughly removed from the surface of the silicon wafer following ion implantation; this cleaning step is performed using a piranha solution; a mixture of sulfuric acid ( $\text{H}_2\text{SO}_4$ ) and hydrogen peroxide ( $\text{H}_2\text{O}_2$ ). Ensuring a low level of metal impurities in these chemicals is vital to ensure that contamination of the wafer surface is avoided at this stage in the manufacturing process.

Since its inception, ICP-MS has been widely utilized for the analysis of elemental impurities in chemicals and materials used by semiconductor-related industries. More recently, collision/reaction cell (CRC) technology, which was first developed for quadrupole ICP-MS (ICP-QMS), has been implemented to remove polyatomic ions that cause problematic spectral interferences on many analytes. In certain sample matrices, however, not all polyatomic species can be completely removed using CRC-ICP-QMS, hindering accurate measurement of a few important elements at low-levels. For example, high concentration sulfur matrices generate polyatomic ions with a low ionization potential, such as  $\text{SO}^+$ , which interferes with Ti. Since  $\text{SO}^+$  has a high dissociation energy of 5.4 eV, it is not easily dissociated using a CRC operating in collision mode with an inert cell gas.

The Agilent 8900 Triple Quadrupole ICP-MS (ICP-QQQ) has a unique tandem MS configuration, comprising two quadrupole mass filters (Q1 and Q2), separated by an octopole reaction system (ORS<sup>4</sup>) cell. The MS/MS configuration allows reaction chemistry to be applied to the most complex and challenging interference problems that hinder ICP-QMS. As more reactive gases (e.g.  $\text{NH}_3$  or  $\text{O}_2$ ) can be used in ICP-QQQ in a controlled way, the reaction pathways and product ions formed in the cell are not affected by changes in the sample matrix or by other co-existing analyte ions. Using MS/MS, Ti can be analyzed in a sulfur matrix, using  $\text{NH}_3$  reaction gas mode, by measuring a suitable ammonia cluster product ion that is free from polyatomic ion interference. In addition, the new axial acceleration technology of the 8900 ICP-QQQ, which accelerates product ions generated in the ORS<sup>4</sup> cell, leads to an increase in sensitivity of product ions, including  $\text{Ti}/\text{NH}_3$  cluster ions.

In this study, the Agilent 8900 ICP-QQQ was used for the analysis of 42 analytes in sulfuric acid, including Ti and other elements which are difficult to determine at trace levels in a high sulfur matrix.



## Experimental

### Sample preparation

All sulfuric acid samples were prepared using pre-cleaned PFA containers. High purity 98%  $\text{H}_2\text{SO}_4$  (TAMA Chemicals Co. Ltd. Japan) was diluted ten-fold with ultrapure water (UPW). All calibration and quantification was done using the method of standard additions (MSA). Standard solutions were prepared from a mixture of XSTC-331, XSTC-7, XSTC-8 (SPEX CertiPrep, USA) and a Si single element standard (Kanto Chemical Co., Inc., Japan).

### Instrumentation

An Agilent 8900 ICP-QQQ (#200, Semiconductor configuration) was used throughout. The sample introduction system comprised a quartz torch with a 2.5 mm i.d. injector, quartz spray chamber, a PFA concentric nebulizer and platinum-tipped interface cones. The sample was self-aspirated using an Agilent I-AS autosampler. MS/MS mode, in which Q1 and Q2 both act as unit mass filters, was used for all measurements. To run ten-fold diluted sulfuric acid routinely, it is recommended that the large (18 mm) insert Pt cone is fitted. Long-term corrosion of internal ICP-MS components can be minimized by fitting the dry pump option and ball-type interface valve kit.

### Evaluation of different reaction gases

For multi-element trace analysis,  $\text{O}_2$ ,  $\text{NH}_3$ ,  $\text{H}_2$  and He were evaluated as cell gases.  $\text{O}_2$  is often used in mass-shift methods to move the target analyte from its elemental ion mass to its oxide product ion mass ( $\text{MO}^+$ ) by setting Q2 to 16 amu higher than Q1 [1].  $\text{NH}_3$  is highly reactive and used as a cell gas in both on-mass mode and mass-shift mode depending on the interference to be removed.  $\text{H}_2$  and He were used with  $\text{O}_2$  or  $\text{NH}_3$ , to assist the cell gas reaction process. He cell gas was used in collision mode to eliminate many common background polyatomic interferences.

### Results and discussion

As is typical with analyses at the ultra-trace level, the optimum plasma mode (normal or cool plasma) and cell gas type was selected for each element. Most higher-mass analytes are free from significant interference in high-purity reagents, but element-specific optimization is particularly important for the ultra-trace analysis of Ti, V, Cr, Zn, Ge and As, which suffer from S-based polyatomic interferences in a sulfur-matrix. Instrument operating parameters used are shown in Table 1.

Oxygen mass-shift mode detects analyte ions ( $\text{M}^+$ ) as reaction product ions at the oxide ion mass ( $\text{MO}^+$ ). For example,  $^{75}\text{As}^+$  is detected as  $\text{AsO}^+$  at  $m/z$  91. This method is used when the analyte ion reacts efficiently with  $\text{O}_2$  gas to form an oxide ion, while the interfering ion reacts slowly or not at all with the  $\text{O}_2$  gas, so does not contribute significantly to the signal at the new mass of the analyte product ion. The lowest detection limits (DLs) and background equivalent concentrations (BECs) for Si, As and Se were obtained with a relatively high  $\text{O}_2$  cell gas flow rate (0.7 mL/min), which encourages the formation of O-atom addition product ions for these analytes, especially Se.

**Table 1.** ICP-QQQ operating parameters.

	Cool-NH <sub>3</sub>	NH <sub>3</sub> -1 (for Ti and V)	NH <sub>3</sub> -2 (for Zn)	O <sub>2</sub>	O <sub>2</sub> + H <sub>2</sub> (for P)	He mode <sup>1</sup>
RF power, W	600	1600				
Sampling depth, mm	18.0	8.0				
Carrier gas, L/min	0.7					
Makeup gas, L/min	0.75	0.49				
Extraction lens 1, V	-150	5.3	5.1	5.0		4.5
Extraction lens 2, V	-15	-200		-250	-190	-155
Octopole bias, V	-10.0	-17.0	-13.5	-11.0	-4.0	-100.0
Axial acceleration, V	1.0		0.2	1.0		0.0
Energy discrimination, V	-5.0	-18.2	-20.0	-13.0	-8.0	5.0
NH <sub>3</sub> flow <sup>1</sup> , mL/min	2	1	4.5	-	-	-
O <sub>2</sub> flow, mL/min	-	-	-	0.7	0.2	-
He flow, mL/min	1	9	1	-	-	9
H <sub>2</sub> flow, mL/min	-	-	-	-	1	-

<sup>1</sup> High energy He mode conditions<sup>2</sup> 10% NH<sub>3</sub> balanced with 90% He

### O<sub>2</sub> + H<sub>2</sub> mass-shift mode for P

In a sulfur matrix, on-mass measurement of <sup>31</sup>P is affected by the peak tail of the large adjacent <sup>32</sup>S peak. This can be addressed using ICP-QQQ, which benefits from the high abundance sensitivity (AS) of MS/MS mode. The AS in MS/MS mode is the product of the AS of the two quadrupoles, so Q1 AS x Q2 AS. On the Agilent 8900, each of the two quadrupoles has an AS specification of 10<sup>-7</sup>, so the overall AS is theoretically 10<sup>-14</sup>, meaning that peak tailing, even from very intense background peaks, is practically eliminated. However, on-mass measurement (e.g. using He mode) does not give sufficiently low backgrounds for the measurement of P at ultra-trace levels. As an alternative, O<sub>2</sub> mass-shift mode can be used to effectively eliminate the NO<sup>+</sup> or NOH<sup>+</sup> interference on P<sup>+</sup>, since the oxidation of P<sup>+</sup> is exothermic, while the oxidation of NO<sup>+</sup> or NOH<sup>+</sup> is endothermic. Hence, these background polyatomic ions are avoided by shifting the P<sup>+</sup> away from the interfering ions, and measuring it as the PO<sup>+</sup> product ion at m/z 47. Interestingly, P sensitivity was improved 1.5 times by adding H<sub>2</sub> gas to the cell together with O<sub>2</sub>. In this study, O<sub>2</sub> + H<sub>2</sub> mass-shift mode was used for P analysis to obtain maximum sensitivity. However, O<sub>2</sub> alone would deliver sufficient performance for the analysis of semiconductor grade H<sub>2</sub>SO<sub>4</sub>. Optimum gas conditions were 0.2 mL/min of O<sub>2</sub> and 1 mL/min of H<sub>2</sub>.

### NH<sub>3</sub> mass-shift mode for Ti

The two most abundant isotopes of titanium, <sup>48</sup>Ti and <sup>46</sup>Ti, suffer interferences from <sup>32</sup>S<sup>16</sup>O and <sup>32</sup>S<sup>14</sup>N respectively, so the minor isotope, <sup>47</sup>Ti, is usually selected for analysis using ICP-QMS. However, MS/MS mode with ICP-QQQ allows control of the complex reaction chemistry that occurs with ammonia cell gas, allowing the major Ti isotopes to be measured as a suitable Ti-NH<sub>3</sub> cluster ion and thereby avoiding the S-based interferences. Single ng/L level BECs can be achieved using this approach [2]. <sup>48</sup>Ti could also potentially suffer an isobaric overlap from the minor <sup>48</sup>Ca isotope (0.187% abundance), but this is not a problem in semiconductor reagents as the concentration of Ca is low.

When a heavy cell gas such as O<sub>2</sub> or NH<sub>3</sub> is used at a high flow rate, analyte ions entering the cell significantly slow down due to suffering multiple collisions with the cell gas molecules, resulting in an increased transit time through the cell.

Some ions may even lose so much energy that their progress through the cell stops, which causes a loss of sensitivity. Furthermore, product ions formed in the cell are generally very slow as a result of the reaction with cell gas molecules. If the transmission of these product ions through the cell reduces, so does the sensitivity. The ORS<sup>4</sup> CRC of the 8900 Semiconductor configuration ICP-QQQ benefits from axial acceleration; an electrical field is established by a potential gradient in the axial direction of the cell so that positively charged analyte ions are accelerated towards the cell exit. Axial acceleration can improve the transmission of slow-moving product ions, and thus increase the sensitivity for certain analytes. In practice, changing the axial acceleration voltage from 0 V to +1 V resulted in a 5-fold increase in the sensitivity of the ammonium cluster ion selected for titanium analysis, <sup>48</sup>TiNH(NH<sub>3</sub>)<sub>3</sub><sup>+</sup> (*m/z* = 114). An axial acceleration voltage of 1 V was used for Ti analysis using MS/MS mass-shift mode with NH<sub>3</sub> cell gas.

### Multi-element analysis

Representative calibration curves obtained using MSA are shown in Figure 1. Good linearity was observed for all analytes (*R* > 0.9995), and sub-ppt detection limits were achieved for all elements apart from Si (44 ppt), P (3 ppt), and Zn (1.5 ppt). The quantitative results of the analysis of 9.8% H<sub>2</sub>SO<sub>4</sub> are shown in Table 2. The DLs were determined from 10 x replicate measurements of the blank 9.8% H<sub>2</sub>SO<sub>4</sub> solution. Recoveries and RSDs were determined from 10 replicate measurements of a 20 ng/L spiked solution of 9.8 % H<sub>2</sub>SO<sub>4</sub>. Excellent performance was achieved for all elements, including Ti, V and Zn, indicating the effective suppression of S-based matrix interferences.

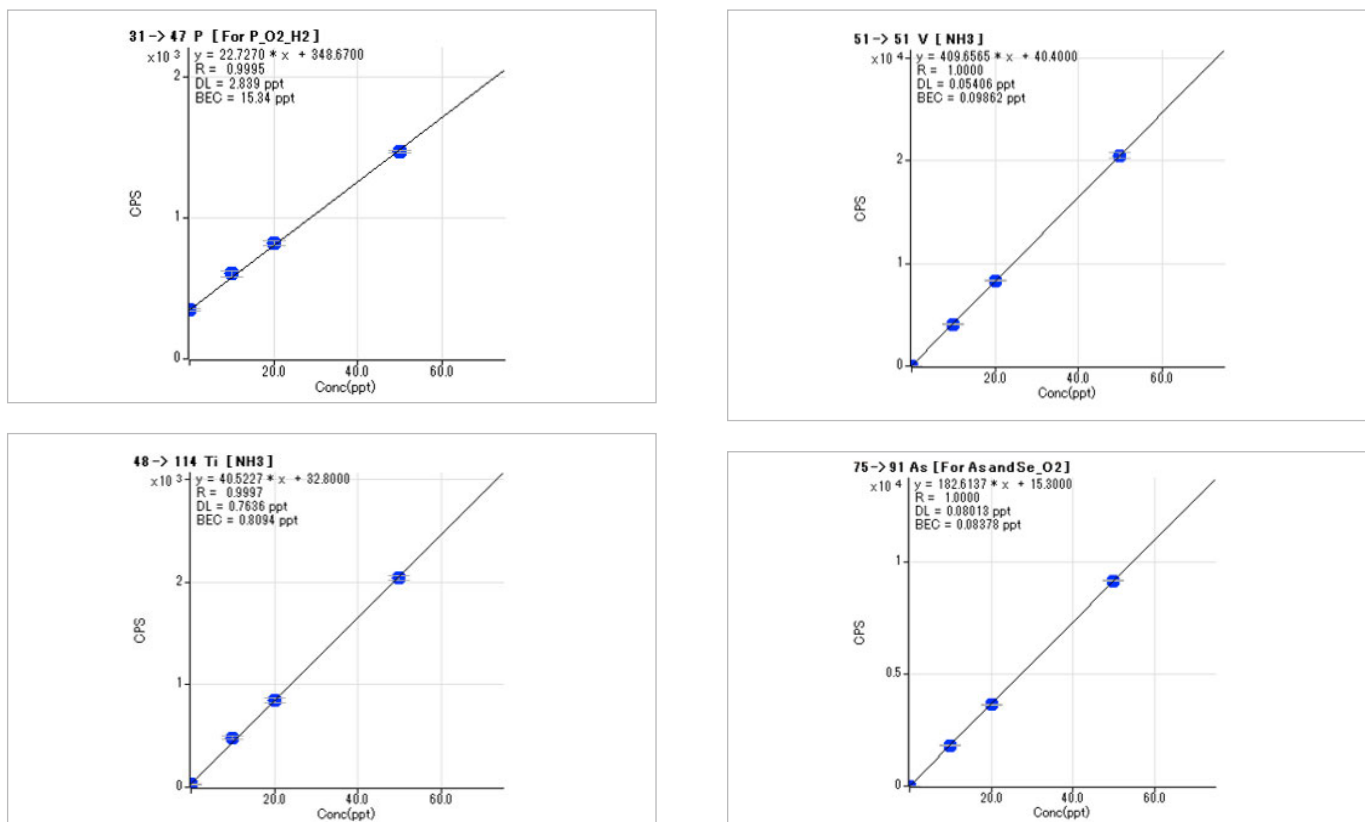


Figure 1. Calibration curves of P, Ti, V and As in 9.8% H<sub>2</sub>SO<sub>4</sub>

**Table 2.** Quantitative results for 42 elements in 9.8% H2SO4.

Analyte	Mode	Q1 Mass	Q2 Mass	DL (ng/L)	BEC (ng/L)	20 ng/L Spike Recovery (%)	20 ng/L RSD (%)
Li	Cool-NH <sub>3</sub>	7	7	0.13	0.13	104	2.1
Na	Cool-NH <sub>3</sub>	23	23	0.37	0.73	102	1.8
Mg	Cool-NH <sub>3</sub>	24	24	0.15	0.05	106	2.4
Al	Cool-NH <sub>3</sub>	27	27	0.18	0.09	107	1.8
Si	O <sub>2</sub>	28	44	44	480	*98	*1.7
P	O <sub>2</sub> + H <sub>2</sub>	31	47	2.8	15	96	3.5
K	Cool-NH <sub>3</sub>	39	39	0.36	0.66	104	2.1
Ca	Cool-NH <sub>3</sub>	40	40	0.57	0.18	106	1.8
Ti	NH <sub>3</sub> -1	48	114	0.76	0.81	99	2.9
V	NH <sub>3</sub> -1	51	51	0.05	0.10	101	0.5
Cr	Cool-NH <sub>3</sub>	52	52	0.51	0.37	106	2.8
Mn	Cool-NH <sub>3</sub>	55	55	0.16	0.11	103	3.0
Fe	Cool-NH <sub>3</sub>	56	56	0.40	0.28	101	2.7
Ni	Cool-NH <sub>3</sub>	58	58	0.12	0.02	100	3.6
Co	Cool-NH <sub>3</sub>	59	59	0.23	0.03	102	2.3
Cu	Cool-NH <sub>3</sub>	63	63	0.57	0.58	101	2.8
Zn	NH <sub>3</sub> -2	68	85	1.5	1.8	99	4.1
Ga	Cool-NH <sub>3</sub>	69	69	0.08	0.01	102	2.0
Ge	He	74	74	0.40	0.24	101	3.3
As	O <sub>2</sub>	75	91	0.08	0.08	101	1.1
Se	O <sub>2</sub>	78	94	0.14	0.22	103	2.0
Rb	Cool-NH <sub>3</sub>	85	85	0.12	0.03	102	2.6
Sr	He	88	88	0.02	0.004	100	1.9
Zr	He	90	90	0.03	0.005	101	1.1
Nb	He	93	93	0.03	0.05	100	1.3
Mo	He	98	98	0.19	0.12	104	1.9
Ru	He	101	101	0.19	0.10	101	3.6
Pd	He	105	105	0.04	0.004	102	3.1
Ag	He	107	107	0.16	0.15	99	1.2
Cd	He	114	114	0.16	0.04	102	3.5
In	He	115	115	0.02	0.008	101	1.1
Sn	He	118	118	0.35	0.33	102	2.3
Sb	He	121	121	0.09	0.03	101	3.1
Cs	He	133	133	0.10	0.17	103	1.7
Ba	He	138	138	0.03	0.007	102	1.3
Ta	He	181	181	0.26	0.42	100	1.6
W	He	182	182	0.28	0.07	99	4.4
Au	He	197	197	0.41	0.30	99	3.3
Tl	He	205	205	0.09	0.07	100	2.6
Pb	He	208	208	0.56	0.93	95	4.1
Bi	He	209	209	0.03	0.004	100	2.2
U	He	238	238	0.02	0.003	101	2.7

\*2 µg/L spike

## Conclusions

Forty-two elements were determined successfully at ultra-trace levels in semiconductor grade  $H_2SO_4$  using the Agilent 8900 Semiconductor configuration ICP-QQQ. Excellent spike recoveries for all elements were achieved at the 20 ppt level (2 ppb for Si) in the 1/10 diluted  $H_2SO_4$ , demonstrating the suitability of the 8900 ICP-QQQ method for the routine analysis of high purity process chemicals.

Problematic spectral interferences that hinder the measurement of some key elements by ICP-QMS were eliminated using ICP-QQQ in MS/MS mode with suitable reaction cell gas conditions. The axial acceleration function of the 8900 ICP-QQQ provided significant improvements in the product ion sensitivity used for the determination of Ti, Zn and P etc. Sub-ppt level DLs and BECs were obtained for almost all analytes in 9.8 %  $H_2SO_4$ .

## References

1. 'Agilent 8800 Triple Quadrupole ICP-MS: Understanding oxygen reaction mode in ICP-MS/MS', Agilent publication, 2012, 5991-1708EN.
2. J. Takahashi, 'Determination of challenging elements in ultrapure semiconductor grade sulfuric acid by Triple Quadrupole ICP-MS', Agilent publication, 2015, 5991-2819EN

## More information

When analyzing 9.8% sulfuric acid on a routine basis, it is recommended to use the following options:

- G3280-67056 Pt sampling cone (18 mm insert)
- G4915A Upgrade to dry pump
- G3666-67030 Interface valve kit - ball type valve

# Multielement Nanoparticle Analysis of Semiconductor Process Chemicals Using spICP-QQQ

## Authors

Yoshinori Shimamura, Donna Hsu,  
and Michiko Yamanaka  
Agilent Technologies, Inc.

Characterization of Ag, Fe<sub>3</sub>O<sub>4</sub>, Al<sub>2</sub>O<sub>3</sub>, Au, and SiO<sub>2</sub> NPs  
in TMAH in a single analytical run

## Introduction

Technologies such as smartphones, cloud computing, the Internet of Things (IoT), and development of autonomous vehicles continue to drive demand for semiconductor products. To meet the requirements for higher integrated circuit (IC) performance and improved device yield, contamination must be controlled in the wafer substrate and on the surface of the device during fabrication. Given the nanometer scale of device features, there is a critical need to monitor metallic nanoparticles (NPs), as well as dissolved metals. Analysis of NPs present in bulk chemicals, silicon wafers, and cleaning bath solutions is important. If a particle is present between two metal lines, it may cause electrical shorting to occur, and surface defects can affect the growth of new layers on the silicon wafer. To fully investigate the cause/source of any particle contamination, multi-element analysis of NPs is necessary. ICP-MS is used increasingly to measure nanoparticles directly in sample solutions, using single particle inductively coupled plasma mass spectrometry (spICP-MS). With growing interest in characterizing NPs in various semiconductor samples, the technique is currently being evaluated within the industry.

The Single Nanoparticle Analysis software module available for ICP-MS MassHunter provides the method setup, analysis, and data interpretation tools for single particle ICP-MS analysis. spICP-MS has been used for a range of studies, from the analysis of gold NPs in simple matrices to TiO<sub>2</sub> NPs in complex samples (1–4). To facilitate multiple element NP analysis, Agilent has developed Rapid Multi-Element Nanoparticle Analysis software. The software can collect data sequentially for up to 16 elements in a single sample analysis, using optimum conditions for the measurement of each individual element (6). This function saves time and reduces the risk of sample contamination compared to conventional spICP-MS analysis, as data for multiple elements can be obtained with only one visit to the sample vial.

In this study, multiple element NPs including Ag, Fe<sub>3</sub>O<sub>4</sub>, Al<sub>2</sub>O<sub>3</sub>, Au, and SiO<sub>2</sub> were measured in semiconductor grade tetra methyl ammonium hydroxide (TMAH). TMAH is widely used as a basic solvent in the development of photoresist in the photolithography processing of ICs. Since TMAH comes into direct contact with the wafer surface, avoiding contamination of the chemical is critical. The Agilent 8900 Triple Quadrupole ICP-MS (ICP-QQQ) was used for the analysis because of its high sensitivity, low background, and effective interference removal capability.

## Experimental

### Sample reagents and NP standards

A 60 nm silver NP (Sigma Aldrich, P/N 730815) reference material (RM) was used to measure the nebulization efficiency, which is required for the calculation of particle size and particle concentration. The value was calculated using RM size and the sensitivity of an ionic Ag solution (Kanto Chemical, Japan).

Solutions containing 30 nm iron oxide ( $\text{Fe}_3\text{O}_4$ ) NPs (Sigma Aldrich, P/N 747408), 30~60 nm aluminum oxide ( $\text{Al}_2\text{O}_3$ ) NPs (Sigma Aldrich, P/N 642991), 200 nm silica ( $\text{SiO}_2$ ) NPs (nanoComposix, P/N SISI200), and 60 nm gold NPs (NIST 8013) were used as NP standards. The sample comprised 25 wt% TMAH diluted to 1 wt% (25 times dilution) with de-ionized water (Organo, Japan).

### Sample preparation

To verify the method for the measurement of multiple element NPs, the Ag RM and four NP standards were dispersed in 1 wt% TMAH using the preparation procedure shown in Figure 1. To prepare the intermediate solutions, 1% TMAH was used as the diluent for  $\text{Al}_2\text{O}_3$  NPs, while DIW was used for the other NPs. Better dispersion was obtained for  $\text{Al}_2\text{O}_3$  NPs using TMAH as the diluent.

### Instrumentation

An Agilent 8900 ICP-QQQ (Semiconductor configuration) was used for all measurements. The sample introduction system comprised a quartz torch with a 1.5 mm i.d. injector, quartz spray chamber, a PFA concentric nebulizer, and platinum-tipped interface cones. The samples were self-aspirated using an Agilent I-AS integrated autosampler.

The 8900 ICP-QQQ was operated in MS/MS mode for all measurements, with Q1 and Q2 acting as unit mass filters. Q1 selects which elements enter the ORS<sup>4</sup> collision/reaction cell (CRC), allowing controlled reaction chemistry to take place in the cell when a reactive cell gas such as hydrogen ( $\text{H}_2$ ) or ammonia ( $\text{NH}_3$ ) is used. The 8900 can also operate in helium (He) collision mode, which is effective for the elimination of many common polyatomic ions using kinetic energy discrimination (KED).

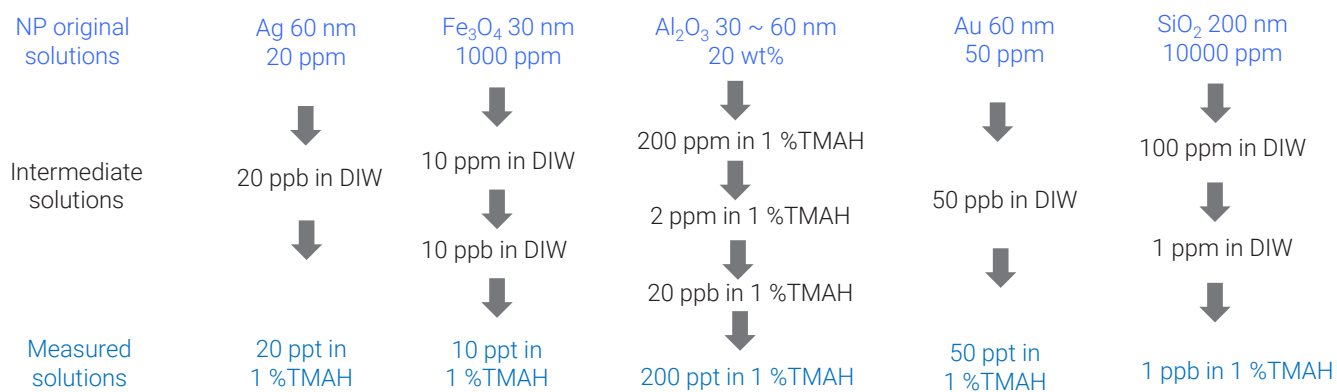


Figure 1. Sample preparation procedure.

NPs containing  $^{28}\text{Si}$ ,  $^{197}\text{Au}$ ,  $^{27}\text{Al}$ ,  $^{56}\text{Fe}$ , or  $^{107}\text{Ag}$  were measured in fast Time Resolved Analysis (fast TRA) mode. Fast TRA allows single element acquisition at a sampling rate of 100  $\mu\text{s}$  (10,000 measurements per second) with no settling time between measurements (7). All elements were measured on-mass in MS/MS mode, with Q1 and Q2 set to the same mass.  $\text{H}_2$  cell gas was used to eliminate any on-mass polyatomic interferences on  $^{28}\text{Si}$ , such as  $^{12}\text{C}^{16}\text{O}$  and  $^{14}\text{N}_2$ .  $\text{NH}_3$  mode was used to control the  $\text{ArO}$  and  $\text{C}_2\text{O}_2$  interference on Fe at  $m/z$  56 and the  $\text{C}_2\text{H}_3$  and  $\text{CNH}$  interferences on Al at  $m/z$  27.  $\text{NH}_3$  was also used to eliminate any of potential interferences from the carbon matrix on Ag at  $m/z$  107. Au is less susceptible to polyatomic interference so can be measured using He or no gas mode. During the analysis, ICP-MS MassHunter changes between each tune step sequentially, ensuring that optimum conditions are used for the measurement of each element.

Multiple element NP data acquisition and analysis were performed using the Rapid Multi-Element Nanoparticle Analysis mode of the Single Nanoparticle Application Module of ICP-MS MassHunter. In Rapid Multi-Element Nanoparticle Analysis mode, multi-element data is collected sequentially from a single sample acquisition, with the multi-element data being combined into a single data file. This approach saves time, as only one sample uptake and rinse time is required for all analytes. Data quality is likely to be improved, as the risk of sample contamination using a single analysis-approach is significantly reduced compared to performing multiple, separate analyses.

The operating conditions of the Agilent 8900 ICP-QQQ are detailed in Table 1.

**Table 1.** ICP-MS operating conditions.

Parameter	Value		
	$\text{H}_2$ mode	He mode	$\text{NH}_3$ mode
RF power (W)	1200		
Sampling depth (mm)	12		
Nebulizer gas (L/min)	0.70		
Makeup gas (L/min)	0.20		
Sample uptake rate (mL/min)	0.216 (self aspiration)		
Spray chamber temp. ( $^{\circ}\text{C}$ )	2		
Extraction lens 1 (V)	-100		
Extraction lens 2 (V)	-10		
Octopole bias (V)	-18	-8	-8
Axial acceleration (V)	1	1	1.5
Energy discrimination (V)	3	3	-10
$\text{H}_2$ cell gas flow rate (mL/min)	6	0	0
He cell gas flow rate (mL/min)	0	2	1
$\text{NH}_3$ cell gas flow rate (mL/min)	0	0	3.0 (30 % of full scale)
Dwell time ( $\mu\text{s}$ )	100		
Masses monitored ( $m/z$ )	Si (Q1:28, Q2:28)	Au (Q1:197, Q2:197)	Al (Q1:27, Q2:27) Fe (Q1:56, Q2:56) Ag (Q1:107, Q2:107)
Data acquisition time (s/element)	30		



## Results and discussion

### Nebulization efficiency measurement

To convert the signals measured using spICP-MS to the particle content of the original sample, it is necessary to calculate the nebulization efficiency. The nebulization efficiency is the ratio of the amount of analyte entering the plasma to the amount of analyte delivered to the nebulizer. Here, the nebulization efficiency was calculated by measuring a reference material (Ag NP) of known particle size. A 60 nm Ag NP RM dispersed in 1% TMAH and an ionic Ag solution (in 1% TMAH base) were measured. The Single Nanoparticle software automatically calculated the nebulization efficiency as 0.081 (8.1%). The signal distribution and the size distribution graphs of Ag NPs in 1% TMAH are shown in Figure 2.

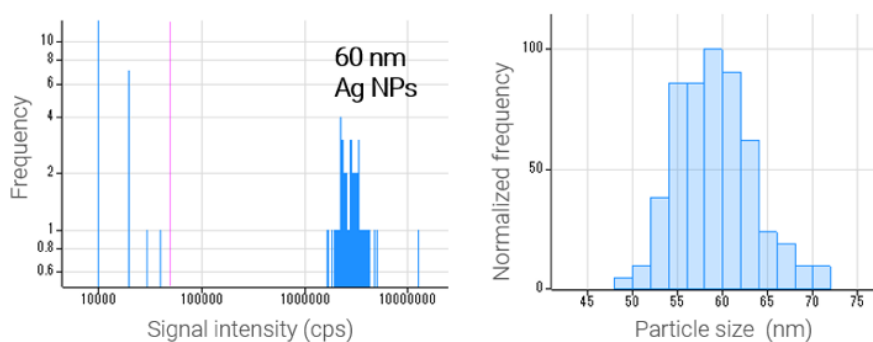


Figure 2. Signal distribution (left) and size distribution (right) of Ag NPs in 1% TMAH solution.

### Analysis of various kinds of NPs in TMAH

Blank TMAH and TMAH solution spiked with  $\text{Fe}_3\text{O}_4$ ,  $\text{Al}_2\text{O}_3$ , Au, or  $\text{SiO}_2$  NPs were measured using the multi-element spICP-MS method. The time resolved signal, signal distribution, and size distribution for  $\text{Fe}_3\text{O}_4$ ,  $\text{Al}_2\text{O}_3$ , Au, and  $\text{SiO}_2$  NPs are shown in Figure 3.

The Rapid Multi-Element Nanoparticle Analysis software enabled multiple element NP data to be quickly collected. Less than six minutes were required for the measurement of all elements, which equates to a saving of 7 minutes compared to separate, single sample analyses. The time-saving per sample can be calculated using the following equation, which means that more time can be saved if more elements are measured.

$$\text{Time saving per sample} = (\text{number of measured elements} - 1) \times (\text{sample uptake time} + \text{rinse time})$$

The improved Single Nanoparticle Application Module software automatically sets the signal baseline in the TRA data, which is shown in light blue in the time charts in Figure 3. The improved software also sets the particle threshold, which separates particle-generated signals from the background or ionic signals. The particle threshold is shown by the vertical red/pink line in the signal distribution graphs in Figure 3.

The measured size and size distribution data for all four spiked NP samples agreed with the expected results (Figure 3). The results for  $\text{Fe}_3\text{O}_4$  and  $\text{SiO}_2$  NPs show that both NPs were present in the blank TMAH solution analyzed in this study, although not all TMAH solutions are likely to contain NPs.

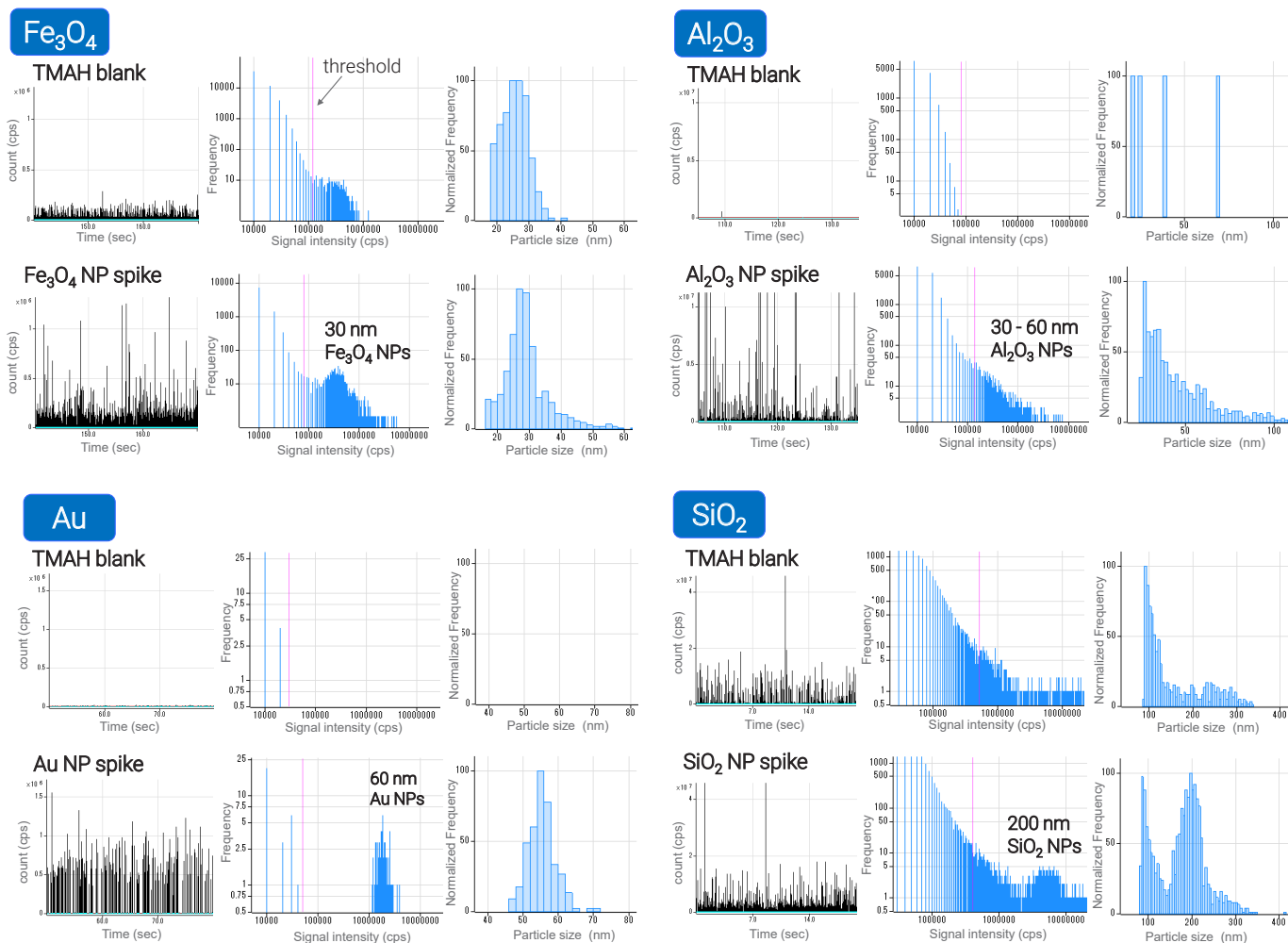


**Figure 3.** Time resolved signal, signal distribution, and size distribution graphs for  $\text{Fe}_3\text{O}_4$ ,  $\text{Al}_2\text{O}_3$ , Au, and  $\text{SiO}_2$  NPs. The upper graphs for each NP show the results from 1% TMAH without NP spike; the lower graphs show the results with NP spike.

Figure 4 summarizes the size data for multiple element NPs in 1% TMAH. The blue histograms show NPs present in the unspiked (original) TMAH solution. The green histograms show NPs present in the spiked TMAH solution. The results show that all five NPs were detected separately, even in the mixed NP TMAH solution. Using the multiple element spICP-MS method, small particles (e.g. 30 nm  $\text{Fe}_3\text{O}_4$ ) can be clearly measured with good accuracy even in the presence of larger particles (e.g. 200 nm  $\text{SiO}_2$ ).

#### Long-term stability test

Figure 5 shows the stability of particle concentration and particle size for five NPs in 1% TMAH over 10 hours. For Ag NPs, both the particle concentration and the size decreased over time, suggesting that Ag NPs are easily dissolved in 1% TMAH solution. For  $\text{Fe}_3\text{O}_4$  NPs, the size was constant, but the particle concentration decreased over time. Rather than being dissolved in TMAH,  $\text{Fe}_3\text{O}_4$  NPs are likely to settle or be adsorbed onto the surface of the sample container.  $\text{Al}_2\text{O}_3$  and  $\text{SiO}_2$  NPs were stable in terms of particle concentration and size over 10 hours. The size profile of the Au NPs remained constant over 10 hours, while the particle concentration remained broadly stable over 10 hours after a slight change during the first three hours.

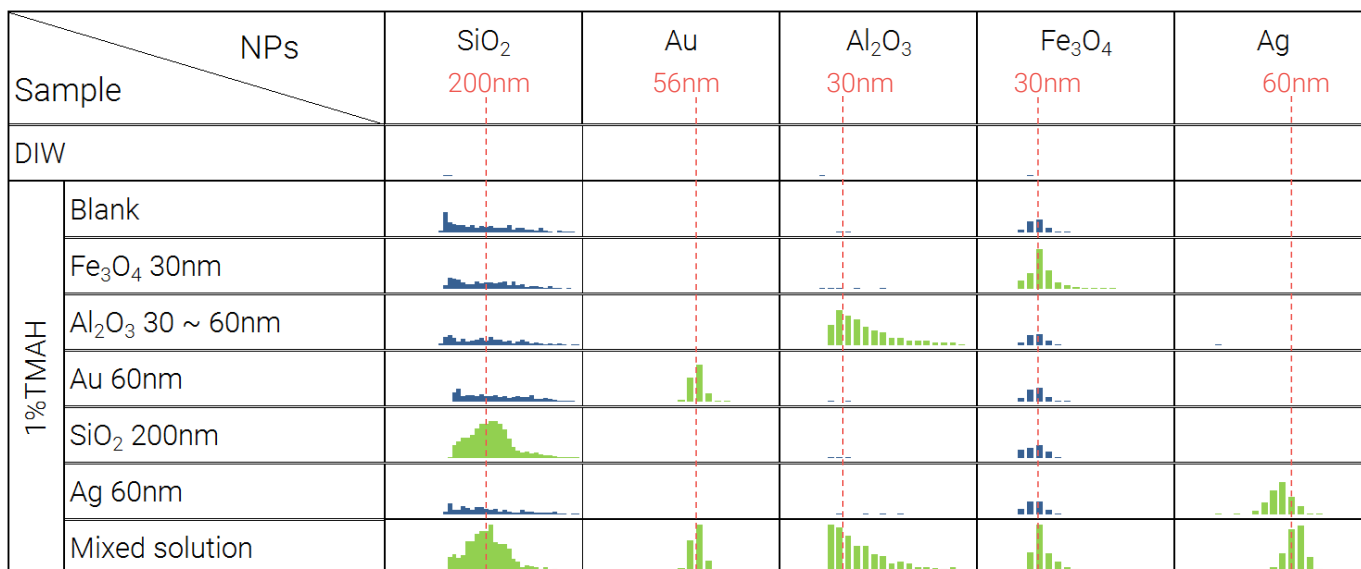


**Figure 4.** Size distribution overview for multiple element NPs in 1% TMAH. The results for the unspiked TMAH solution are shown in blue and the spiked TMAH solution results are shown in green.

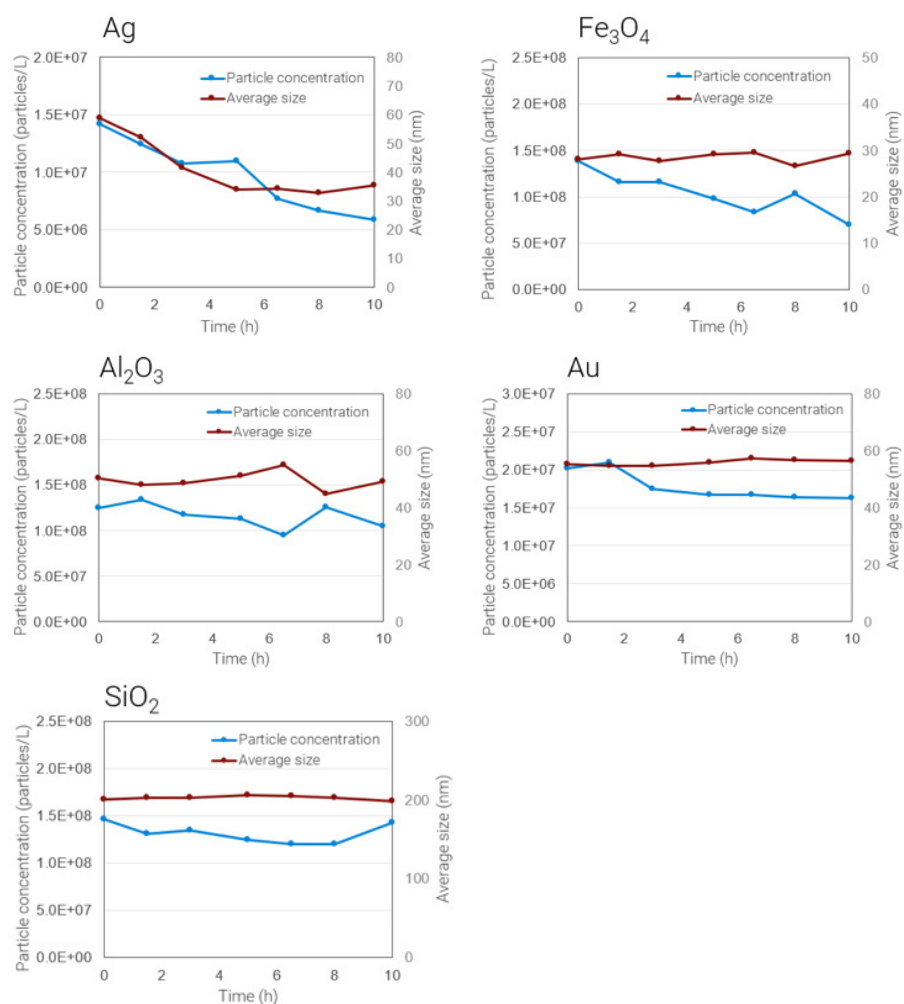


**Figure 5.** Long-term stability of NP solutions of Ag, Fe<sub>3</sub>O<sub>4</sub>, Al<sub>2</sub>O<sub>3</sub>, Au, and SiO<sub>2</sub>. The blue line shows the particle concentration and the red line shows the average particle size.

## Conclusion

Multiple element nanoparticles were determined and characterized in 1% TMAH using the Agilent 8900 ICP-QQQ operating in multi-element spICP-MS mode. The MS/MS method delivered the low background, high sensitivity, and interference control necessary for the analysis of multiple element NPs in semiconductor grade chemicals.

Using specially developed Rapid Multi-Element Nanoparticle Analysis software, multi-element data for Ag, Al<sub>2</sub>O<sub>3</sub>, Fe<sub>3</sub>O<sub>4</sub>, Au, and SiO<sub>2</sub> NPs were collected from a single sample acquisition and combined into a single table of results. The table provides comprehensive information about the nanoparticles containing each of the measured elements. The results showed that small particles such as 30 nm Fe<sub>3</sub>O<sub>4</sub> NPs could be measured in solutions containing larger particles, such as 200 nm SiO<sub>2</sub> NPs. The particle size and particle concentration of Al<sub>2</sub>O<sub>3</sub> and SiO<sub>2</sub> NPs were stable in 1% TMAH solution over 10 hours, while the particle concentration of Fe<sub>3</sub>O<sub>4</sub> and Ag NPs decreased over time. The results suggest that Fe<sub>3</sub>O<sub>4</sub> and Ag NPs in TMAH solutions should be measured as soon as they are prepared. While the particle size of Fe<sub>3</sub>O<sub>4</sub> NPs remained stable in 1% TMAH, the variation in the concentration of NPs over time requires further investigation.

The study showed that samples containing nanoparticles composed of different and/or multiple elements can be determined quickly and accurately using spICP-MS. Compared to acquiring data separately for each NP, the Rapid Multi-Element Nanoparticle Analysis software simplifies the analytical method and shortens the sample run times by seven minutes. If more elements are measured, more time can be saved.

## References

1. Susana Nunez, Heidi Goenaga Infante, Michiko Yamanaka, Takayuki Itagaki, Steve Wilbur, Analysis of 10 nm gold nanoparticles using the high sensitivity of the Agilent 8900 ICP-QQQ, [Agilent publication, 5991-6944EN](#)
2. Jenny Nelson, Michiko Yamanaka, Francisco Lopez-Linares, Laura Poirier, Estrella Roge, Single Nanoparticle Analysis of Asphaltene Solutions using the Agilent 8900 ICP-QQQ: ICP-MS MassHunter software module simplifies spICP-MS analysis, [Agilent publication, 5991-9498EN](#)
3. Michiko Yamanaka, Steve Wilbur, Accurate Determination of TiO<sub>2</sub> Nanoparticles in Complex Matrices using the Agilent 8900 ICP-QQQ, [Agilent publication, 5991-8358EN](#)
4. Michiko Yamanaka, Takayuki Itagaki, Steve Wilbur, High sensitivity analysis of SiO<sub>2</sub> nanoparticles using the Agilent 8900 ICP-QQQ in MS/MS mode, [Agilent publication, 5991-6596EN](#)
5. Michiko Yamanaka and Steve Wilbur, Measuring Multiple Elements in Nanoparticle using spICP-MS: Acquire NP data for up to 16 elements in Rapid Multi-Element Nanoparticle Analysis Mode, [Agilent publication, 5994-0310EN](#)
6. Craig Jones, Emmett Soffey, Mark Kelinske, Rapid Multielement Nanoparticle Analysis Using Single-Particle ICP-MS/MS, *Spectroscopy*, **2019**, 34, 5, 10–20. [Link](#).
7. Steve Wilbur, Michiko Yamanaka, and Sebastien Sannac, Characterization of nanoparticles in aqueous samples by ICP-MS, [Agilent publication, 5991-5516EN](#)

# Silicon Wafer Analysis by ICP-QQQ: Determination of Phosphorus and Titanium in a High Silicon Matrix

## Author

Junichi Takahashi  
Agilent Technologies, Japan

## Keywords

semiconductor, silicon wafer, phosphorus, titanium, Vapor Phase Decomposition, VPD, oxygen mass-shift

## Introduction

The semiconductor industry first used ICP-MS for trace element analysis in the early 1980s. Nowadays the technique is widely used for control of trace impurities in materials and chemicals, particularly by silicon device manufacturers. The major challenge for quadrupole ICP-MS (ICP-QMS) is the presence of spectroscopic interferences on key contaminant elements, although performance has been gradually improved through developments such as cool plasma and collision/reaction cells (CRC), and improved performance has also been provided by high resolution ICP-MS. Consequently, metallic impurity control of silicon wafers can be successfully monitored by ICP-MS in the case of low silicon samples such as Vapor Phase Decomposition (VPD) of native silicon wafers. However, difficulties of Si-based spectral interferences, particularly on P and Ti, still affect the analysis of samples that contain high concentrations of Si, such as VPD samples of thermally oxidized wafers and samples relating to bulk silicon wafers. These interferences cannot be reduced adequately by ICP-QMS and have required HR-ICP-MS. In this paper, we evaluate triple quadrupole ICP-MS with MS/MS technology for the determination of ultratrace P and Ti in a high Si matrix.

## Experimental

**Instrumentation:** Agilent 8800 #200 with an inert sample introduction kit including a low flow nebulizer (PFA-20) and a Pt/Ni skimmer cone. The actual sample uptake rate was 36  $\mu\text{L}/\text{min}$ . The sample was self-aspirated from an Agilent I-AS autosampler.

**Plasma conditions:** Robust tuning conditions were applied as summarized in Table 1.

**Ion lens tune:** Extract 1 = 0 V was used and other lens voltages were optimized using Auto tune.

**Sample preparation:** Silicon wafer samples were dissolved in TAMAPURE HF/HNO<sub>3</sub> and the final Si concentration was adjusted to 2000 ppm.

**Table 1.** Robust tuning conditions.

		O <sub>2</sub> MS/MS	H <sub>2</sub> MS/MS
RF power	W	1600	
Sampling depth	mm	8	
Carrier gas flow rate	L/min	0.6	
Make-up gas flow rate	L/min	0.6	
He	mL/min	3	0
O <sub>2</sub>	mL/min	0.4	0
H <sub>2</sub>	mL/min	0	10

## Results and discussion

Phosphorus is monoisotopic at  $m/z$  31, and suffers an interference from  $^{30}\text{SiH}$ . While  $\text{P}^+$  can be detected as  $\text{PO}^+$  under cool plasma conditions, it is difficult to maintain cool plasma when the matrix concentration is high. Si sample solutions always contain HF, so Si will form SiF (IP: 7.54 eV) that also interferes with Ti. Table 2 shows the Si-based spectral interferences on P and Ti. Using the 8800 ICP-QQQ operating in MS/MS mode with  $\text{O}_2$  mass-shift, P and Ti can be determined as their oxide ions, avoiding the Si-based interferences.

**Table 2.** Spectral interferences of Si on P and Ti.

Polyatomic interference	$m/z$	Analyte ion
$^{30}\text{SiH}^+$	31	$^{31}\text{P}^+$
$^{30}\text{Si}^{16}\text{O}^+$	46	$^{46}\text{Ti}^+$
$^{28}\text{Si}^{19}\text{F}^+$ , $^{30}\text{Si}^{16}\text{OH}^+$	47	$^{47}\text{Ti}^+$ , $^{31}\text{P}^{16}\text{O}^+$
$^{29}\text{Si}^{19}\text{F}^+$ , $^{30}\text{Si}^{18}\text{O}^+$	48	$^{48}\text{Ti}^+$
$^{30}\text{Si}^{19}\text{F}^+$	49	$^{49}\text{Ti}^+$

For Ti analysis, Q1 is set to  $m/z$  48, and so will transmit  $^{48}\text{Ti}^+$  and any other interfering ions at mass 48, such as  $^{29}\text{Si}^{19}\text{F}^+$  and  $^{30}\text{Si}^{18}\text{O}^+$ . But only  $^{48}\text{Ti}$  reacts with oxygen in the CRC, producing the product ion  $^{48}\text{Ti}^{16}\text{O}^+$ , which is transmitted by setting Q2 to  $m/z$  64.  $\text{NH}_3$  can be used as an alternative reaction gas, as it produces  $^{48}\text{Ti}^{14}\text{NH}^+$  that can be detected at  $m/z$  63.

$^{31}\text{P}^+$  reacts readily with  $\text{O}_2$  to form  $^{31}\text{P}^{16}\text{O}^+$ . The selection of ions at  $m/z$  31 by Q1 eliminates the spectral interference of  $^{28}\text{Si}^{19}\text{F}$ . However,  $^{30}\text{SiH}$  passes through Q1 and reacts with  $\text{O}_2$  to create  $^{30}\text{Si}^{16}\text{OH}$ . In order to determine P in a high Si matrix,  $\text{H}_2$  mass-shift is a preferred option, despite the relatively low efficiency of production of  $\text{PH}_3^+$  or  $\text{PH}_4^+$  ions. The MSA calibration curves for P and Ti in a matrix of 2000 ppm Si are shown in Figure 1. The calculated BECs are summarized in Table 3. A long term stability test was carried out by analyzing a spiked sample repeatedly over five hours (Figure 2).

**Table 3.** BECs of P and Ti in 2000 ppm Si.

Element	P	Ti
Mode (cell gas)	MS/MS ( $\text{H}_2$ )	MS/MS ( $\text{O}_2$ )
Measured ion	$^{31}\text{PH}_4^+$	$^{48}\text{Ti}^{16}\text{O}^+$
Mass pair	Q1 = 31, Q2 = 35	Q1 = 48, Q2 = 64
BEC - ppt	227	13

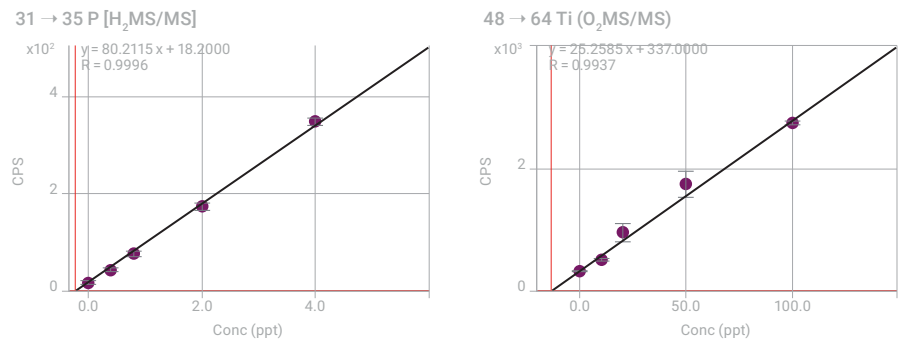


Figure 1. MSA curves of P and Ti in 2000 ppm Si.

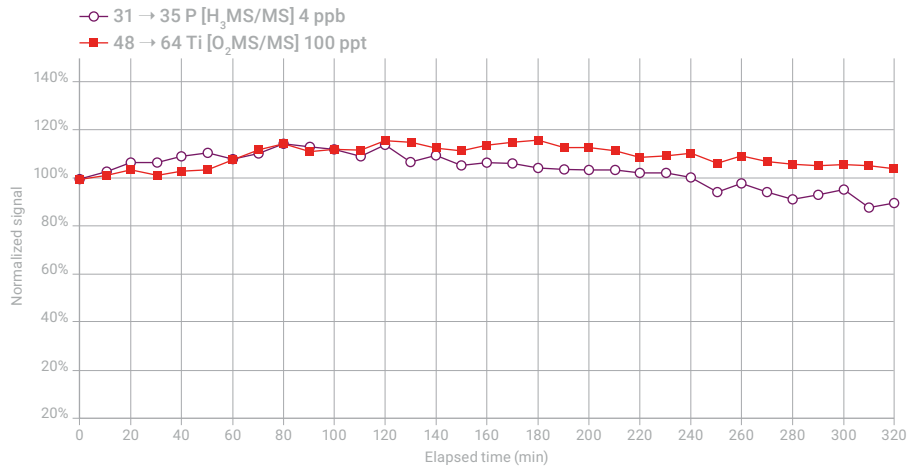


Figure 2. Five-hours test of P and Ti spiked in 2000 ppm Si.

## Conclusion

The MS/MS mass-shift mode of the ICP-QQQ is effective for the determination of P, Ti and other trace elements in high purity silicon matrices, providing effective removal of the potential Si-based polyatomic interferences.

## More information

Improvement of ICP-MS detectability of phosphorus and titanium in high purity silicon samples using the Agilent 8800 Triple Quadrupole ICP-MS, Agilent publication [5991-2466EN](#)

# Analysis of Ultratrace Impurities in High Silicon Matrix Samples by ICP-QQQ

## Authors

Yu Ying  
Agilent Technologies (China) Co., Ltd.

Determination of 38 elements in high matrix samples using an Agilent 8900 ICP-QQQ with optional m-lens

## Introduction

Rapid developments in the emerging fields of artificial intelligence (AI) and the Internet of Things (IoT) are driving innovation in the integrated circuit (IC) sector of the semiconductor industry. IC fabrication plants (known as FABs or IC foundries) are increasing production of ICs to meet the requirements of this expanding market, as well as serving ongoing demand from other high-tech industries. Silicon (Si) is essential to the IC industry, as most modern electronics are based on Si semiconductors. These devices are made from millions of individual transistors (or switches) packed onto a Si wafer chip. Smaller transistors give higher core density, faster processing speed, lower power consumption, and less heat generation, critical factors for mobile devices. Currently, FABs are producing chips with transistor "gates" 10, 7, or even 5 nanometers (nm) long, with ongoing research projects to reduce the gate length even further. Manufacturing ICs at this small scale and high density requires excellent control of the quality of the Si substrate and process chemicals. It is important that the performance of the analytical instruments used to detect metallic impurities in raw materials evolves to meet the needs of the semiconductor industry.

Single quadrupole ICP-MS is the most widely used atomic spectrometry technique for the measurement of trace elements in many semiconductor applications due to its sensitivity and multi-element capability (1). However, more advanced semiconductor processes require elemental impurities on the Si wafer to be less than  $1.0 \times 10^7$  atom/cm<sup>2</sup> level. While it is difficult to meet these specifications using single quadrupole ICP-MS, triple quadrupole ICP-MS (ICP-QQQ) with MS/MS operation has further improved the sensitivity, background, and interference removal capabilities of the technique. With detection limits (DLs) for many elements at the sub-ppt level, ICP-QQQ is increasingly used in the semiconductor industry for the accurate analysis of the highest purity semiconductor materials (1).

Another challenge of measuring trace metal impurities in a high Si matrix by ICP-MS relate to physical effects arising from the matrix. The high levels of Si in the sample can lead to deposition of Si on the sampling cone and suppression of analytes, leading to instability and signal drift. Operating single quadrupole ICP-MS with a "cool" or reduced-energy plasma has been widely used in the semiconductor industry for many years for the analysis of high-purity chemicals and materials. Cool plasma suppresses the formation of intense argon-based interferences such as Ar<sup>+</sup> and ArO<sup>+</sup>, allowing low-level analysis of <sup>40</sup>Ca and <sup>56</sup>Fe, respectively. A lower-temperature plasma also causes less re-ionization of traces of easily ionized elements (EIEs) from the cones and ion lens, giving lower



background signals for these elements than normal plasma conditions. However, the lower power used with cool plasma conditions provides insufficient energy to decompose some sample matrices, including high Si matrix samples.

The Agilent 8900 ICP-QQQ fitted with an optional “m-lens” ion lens uses normal plasma conditions to analyze silicon-rich samples. The m-lens has an optimized geometry that minimizes background signals from EIEs deposited on the ICP-MS interface components. The 8900 with m-lens provides ppt-level background equivalent concentrations (BECs) for the elements of interest in the semiconductor industry, including the easily-ionized alkaline elements. The low BECs enable the monitoring of ultra-trace ppt-level impurities in high Si matrices using high-power, robust, matrix tolerant plasma conditions.

In this study, the 8900 ICP-QQQ was used to analyze two Si samples prepared at matrix levels that are typically analyzed in the semiconductor industry. Excellent precision was achieved for the measurement of 50 ppt spikes in the Si matrix samples over a 1 hour analytical run, demonstrating the effectiveness, robustness, and sensitivity of the method.

## Experimental

### Reagents

All samples and standards were prepared in semiconductor grade TAMAPURE AA-100 nitric acid (HNO<sub>3</sub>) and hydrofluoric acid (HF) bought from Tama Chemicals Co. Ltd, Kanagawa, Japan. The ultrapure water (UPW) was supplied from Organo Corp (Tokyo, Japan).

### Sample preparation

Pieces of electronic grade (9N purity) poly-silicon were weighed to the nearest 0.05 g and the sample surfaces were cleaned with HNO<sub>3</sub> and rinsed with UPW. To prepare a 1000 ppm Si matrix solution, the Si pieces were digested in a 1:1 (w/w) acid mix of 38% HF and 55% HNO<sub>3</sub>. The Si matrix solution was then diluted to provide two typical Si matrix samples. A 10 ppm Si solution was used to represent the Si matrix level in a sample prepared by scanning the wafer using a vapor phase decomposition (VPD) device. A 100 ppm Si matrix solution was used to represent the matrix level that would be present in a digested poly-silicon sample.

### Calibration standards

Simple, aqueous (no Si matrix) calibration standards were prepared in the same acid concentration as the 10 and 100 ppm Si samples using Agilent stock solutions. Multi-element calibration standards included “2A” (p/n 8500-6940) and “4” (p/n 8500-6942). Single element standards at 1000 µg/mL were used for antimony (p/n 5190-8562) and tin (p/n 5190-8583).

A multi-element spike solution containing all elements was also prepared from the stock solutions. The spike solution was added to the 10 and 100 ppm Si matrix samples at 50 ng/L (ppt).

## Instrumentation

An Agilent 8900 ICP-QQQ was used for the analysis. The 8900 was fitted with an inert (HF-resistant) sample introduction system comprising a 200  $\mu\text{L}/\text{min}$  MicroFlow PFA nebulizer, a PFA spray chamber, endcap, and connector tube, and a demountable torch with a 2.5 mm internal diameter (i.d.) sapphire injector. A Pt-tipped sampling cone was used, together with the optional m-lens (G3666-67500), and Pt-tipped, Ni-based skimmer cone for m-lens (G3666-67501). The PFA nebulizer and Pt tipped sampling cone are standard on the 8900 #200 (Semiconductor Applications model). The other sample introduction parts (PFA spray chamber, endcap, connecting tube, and demountable torch) are included in the Inert Kit (G4912A #001). The sample introduction and interface parts listed are also compatible with the 8900 #100 (Advanced Applications model).

A high Si matrix leads to the formation of several polyatomic ions, which cause significant spectral interferences on some important elements such as Ti, Fe, Ni, Cu, and Ge (Table 1). To achieve the lowest BEC for each analyte in the silicon-rich samples, optimized ICP-QQQ acquisition conditions were used for different elements. Using ICP-MS MassHunter instrument control software, it is simple to measure different analytes in different cell gas modes using a single multitune method. During data acquisition, the ORS<sup>4</sup> cell gases and measurement modes are switched automatically, giving a fast and automated analysis using the best mode for each analyte.

In this study, several reaction cell gases ( $\text{He}$ ,  $\text{H}_2$ ,  $\text{O}_2$ , and  $\text{NH}_3$ ) were used as appropriate for the large number of analytes being measured. Details of the configuration and principles of ICP-QQQ and MS/MS are explained elsewhere (2, 3). The operating parameters of the 8900 ICP-QQQ are given in Table 2.

## Results and discussion

### Background equivalent concentrations

The blank, 10 ppm, and 100 ppm Si samples were measured by external calibration method and the BECs of each sample were calculated using ICP-MS MassHunter. The BECs of all 38 analytes were lower than 50 ng/L in both the 10 and 100 ppm Si matrix blank samples, with most below 5 ng/L (Table 3). The low BECs show the effectiveness of the ICP-QQQ method at removing interferences on all analytes, including Si-based interferences on Ti, Fe, Ni, Cu, and Ge (Table 1). The relatively high BECs for some analytes may be due to the contamination during sample preparation.

### Spike-recovery and stability test

The stability, robustness, and matrix tolerance of the instrument and method were tested over an hour of continual measurements. The unspiked (blank) Si samples were measured three times and each spiked sample was measured 11 times over the 60 minute run. The average recoveries of the 50 ng/L spikes ranged from 90 to 110% for all elements apart from Fe at 112% in the 10 ppm Si sample (Table 3). The slightly higher recovery of Fe was likely due to sample contamination from the laboratory environment. The 8900 ICP-QQQ also provided excellent sensitivity and accuracy for all elements, including EIEs, as shown by the spike recoveries in both Si matrices.

The relative standard deviation (RSD) of the measurements (n=11) was <6% for all 38 elements in both Si matrices, indicating minimal signal drift during the run using the 8900 with m-lens. Figure 1 shows the stability test results of some typical elements of importance to IC foundries such as Fe in the 100 ppm Si matrix sample.

**Table 1.** Potential spectral interferences in a Si matrix digest with HF.

Analyte Ion	Interference	Analyte Ion	Interference
$^{46}\text{Ti}^+$	$^{30}\text{Si}^{16}\text{O}^+$	$^{56}\text{Fe}^+$	$^{28}\text{Si}^{28}\text{Si}^+$
$^{47}\text{Ti}^+$	$^{28}\text{Si}^{19}\text{F}^+$ $^{30}\text{Si}^{16}\text{OH}^+$	$^{63}\text{Cu}^+$	$^{28}\text{Si}^{16}\text{O}^{19}\text{F}^+$
$^{48}\text{Ti}^+$	$^{29}\text{Si}^{19}\text{F}^+$ $^{30}\text{Si}^{18}\text{O}^+$	$^{65}\text{Cu}^+$	$^{30}\text{Si}^{16}\text{O}^{19}\text{F}^+$ $^{28}\text{Si}^{18}\text{O}^{19}\text{F}^+$
$^{49}\text{Ti}^+$	$^{30}\text{Si}^{19}\text{F}^+$	$^{72}\text{Ge}^+$	$^{28}\text{Si}^{28}\text{Si}^{16}\text{O}$
$^{58}\text{Ni}^+$	$^{28}\text{Si}^{30}\text{Si}^+$ $^{29}\text{Si}^{29}\text{Si}^+$	$^{74}\text{Ge}^+$	$^{28}\text{Si}^{28}\text{Si}^{18}\text{O}$ $^{30}\text{Si}^{28}\text{Si}^{16}\text{O}$
$^{60}\text{Ni}^+$	$^{28}\text{Si}^{16}\text{O}_2^+$ $^{30}\text{Si}^{30}\text{Si}^+$		

**Table 2.** ICP-QQQ operating conditions.

	No Gas	H <sub>2</sub>	NH <sub>3</sub>	He
<b>Acquisition Parameters</b>				
Scan Mode	MS/MS			
Stabilization Time (s)	15	25	25	20
Replicates	3			
Sweeps/Replicate	100			
Integration Time (s)	0.6			
<b>Plasma</b>				
RF Power (W)	1550			
Sampling Depth (mm)	8.0			
Carrier Gas (L/min)	0.8			
Makeup Gas (L/min)	0.4			
<b>Lenses</b>				
Extract 1 (V)	1.5			
Extract 2 (V)	-70			
Omega Bias	-20			
Omega Lens	6			
<b>Cell</b>				
He Flow Rate (mL/min)				4.0
H <sub>2</sub> Flow Rate (mL/min)		10.0		
*NH <sub>3</sub> Flow Rate (mL/min)			2.0	
Octopole Bias (V)	-8	-18	-6	-20
Axial Acceleration (V)	0	1	1.5	0
KED (V)	3	-8	-10	5

**Table 3.** Analysis results of 10 and 100 ppm Si matrix samples and matrix-spiked samples, n = 11.

Element	Q1/Q2	Cell Gas	10 ppm Si Matrix Sample			100 ppm Si Matrix Sample		
			BEC (ng/L)	%RSD of 50 ppt-Spiked Samples	50 ppt Spike Recovery Average (%)	BEC (ng/L)	%RSD of 50 ppt-Spiked Samples	50 ppt Spike Recovery Average (%)
Li	7/7	No gas	0.38	3.7	101.4	0.60	3.4	107.3
Be	9/9	No gas	0.00	3.6	99.4	0.87	4.7	105.7
B	11/11	No gas	16.1	4.0	105.9	30.2	3.2	109.7
Na	23/23	H <sub>2</sub>	5.13	5.6	101.8	13.3	2.9	96.7
Mg	24/24	H <sub>2</sub>	1.45	3.0	93.9	5.82	4.4	108.2
Al	27/27	H <sub>2</sub>	8.52	3.8	103.1	46.6	2.6	97.7
K	39/39	H <sub>2</sub>	10.8	2.3	93.6	10.3	2.6	105.1
Ca	40/40	H <sub>2</sub>	7.99	2.1	95.8	7.79	3.3	108.9
Ti	48/114	NH <sub>3</sub>	5.35	5.4	101.3	4.55	5.4	101.7
V	51/67	NH <sub>3</sub>	0.00	2.5	90.8	0.30	4.6	102.3
Cr	52/52	NH <sub>3</sub>	4.30	2.5	95.9	9.71	2.8	101.4
Mn	55/55	NH <sub>3</sub>	35.7	3.8	103.8	43.3	1.5	96.2
Fe	56/56	H <sub>2</sub>	21.6	6.0	112.0	23.6	3.9	106.9
Ni	58/58	NH <sub>3</sub>	6.75	2.4	90.0	4.69	3.2	99.1
Co	59/59	NH <sub>3</sub>	2.37	4.0	92.2	5.56	2.3	96.7
Zn	64/64	NH <sub>3</sub>	1.92	5.6	99.4	34.8	5.9	94.5
Cu	65/65	NH <sub>3</sub>	4.19	5.1	101.1	33.6	5.7	95.7
Ga	69/69	H <sub>2</sub>	0.34	2.4	94.8	6.13	2.8	109.8
Ge	74/74	H <sub>2</sub>	4.26	2.0	90.7	4.30	1.7	98.1
As	75/75	H <sub>2</sub>	0.86	4.7	90.3	0.29	5.9	100.4
Se	78/78	H <sub>2</sub>	1.24	5.0	90.4	1.60	4.5	97.2
Rb	85/85	H <sub>2</sub>	0.62	2.0	96.5	18.4	4.5	100.6
Sr	88/88	H <sub>2</sub>	0.02	2.0	95.3	0.03	2.5	101.2
Zr	90/90	H <sub>2</sub>	0.08	1.9	94.9	0.03	2.3	102.2
Nb	93/93	He	0.43	2.6	91.5	0.12	2.7	98.2
Mo	95/95	He	0.12	2.9	93.8	0.53	4.3	98.0
Ag	107/107	No gas	0.12	1.9	98.2	0.18	1.6	100.8
Cd	114/114	NH <sub>3</sub>	0.02	1.7	95.9	0.00	2.5	98.1
Sn	118/118	NH <sub>3</sub>	0.51	2.5	96.7	1.12	2.1	97.6
Sb	121/121	NH <sub>3</sub>	0.14	2.3	93.9	0.24	2.6	95.3
Cs	133/133	He	0.03	2.7	94.6	0.03	1.8	97.0
Ba	138/138	H <sub>2</sub>	0.42	2.3	97.6	0.43	1.9	98.4
Ta	181/181	He	0.17	2.2	98.8	0.09	1.6	96.4
W	182/182	He	3.48	4.2	99.2	0.12	2.2	96.1
Re	185/185	He	0.00	2.9	95.8	0.01	1.9	95.9
Tl	205/205	No gas	0.15	3.0	104.2	0.12	1.3	103.2
Pb	208/208	NH <sub>3</sub>	0.31	2.2	98.0	0.19	1.9	96.1
U	238/238	No gas	0.00	3.3	103.2	0.00	1.0	101.2

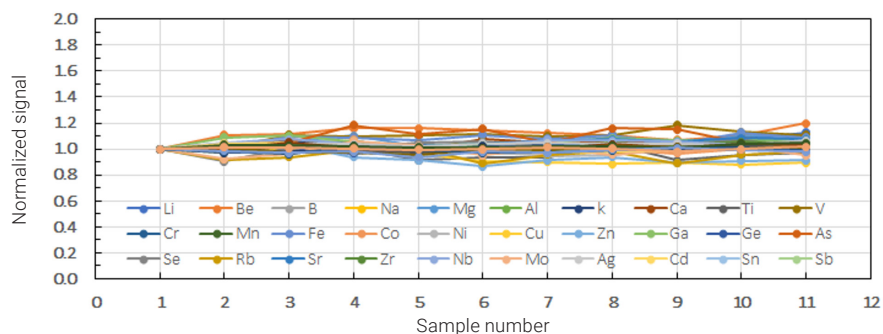


**Figure 1.** Stability results for multiple elements spiked at 50 ppt in a 100 ppm Si matrix sample.

## Conclusion

The robustness of the Agilent 8900 ICP-QQQ with m-lens was demonstrated for the determination of 38 elements in two digested silicon samples containing 10 and 100 ppm Si. The optional m-lens ensured that the background signals for the EIEs were minimized, allowing all elements to be measured at ppt levels using matrix tolerant, high-power plasma conditions.

The best BECs for all elements were achieved by operating the 8900 ICP-QQQ in MS/MS mode using a single multitune method with different cell gases. The low BECs showed that the method successfully removed all spectral interferences, including Si-based interferences on Ti, Fe, Ni, Cu, and Ge.

The reproducibility (stability) results for the 50 ppt spikes in the two high silicon samples were between 1 and 6% RSD for all elements in a sequence lasting 1 hour. These results showed that there was minimal signal suppression or drift caused by Si deposition on the interface under the robust plasma conditions.

The study demonstrates the suitability of the 8900 ICP-QQQ for the characterization of trace metals in silicon-matrix samples. The method has the potential to meet the evolving needs and future specifications of the most advanced manufacturing processes that are required to meet the demand for higher IC performance.

## References

1. Applications of ICP-MS: Measuring Inorganic Impurities in Semiconductor Manufacturing, Agilent publication, [5991-9495EN](#)
2. Eduardo Bolea-Fernandez, Lieve Balcaen, Martin Resano, Frank Vanhaecke. Overcoming spectral overlap via inductively coupled plasma-tandem mass spectrometry (ICP-MS/MS). A tutorial review, *J. Anal. At. Spectrom.*, **2017**, 32, 1660–1679
3. Ed McCurdy, Glenn Woods, Naoki Sugiyama. Method Development with ICP-MS/MS: Tools and Techniques to Ensure Accurate Results in Reaction Mode, *Spectroscopy*, **2019** (9):20–27, <http://www.spectroscopyonline.com/method-development-icp-msms-tools-and-techniques-ensure-accurate-results-reaction-mode>

# Analysis of Sulfur, Phosphorus, Silicon, and Chlorine in N-methyl-2-pyrrolidone

## Author

Naoki Sugiyama  
Agilent Technologies, Japan

## Keywords

N-methyl-2-pyrrolidone, NMP, semiconductor, process chemicals, sulfur, phosphorus, silicon, chlorine, method of standard additions, oxygen mass-shift

## Introduction

N-Methyl-2-Pyrrolidone (NMP), chemical formula:  $C_5H_9NO$ , is a stable, water-soluble organic solvent that is widely used in the pharmaceutical, petrochemical, polymer science and especially semiconductor industries. Electronic grade NMP is used by semiconductor manufacturers as a wafer cleaner and photo resist stripper and as such the solvent comes into direct contact with wafer surfaces. This requires NMP with the lowest possible trace metal (and non-metal) contaminant levels. ICP-MS is the technique of choice for the measurement of trace metal impurities in semiconductor process chemicals. It is a challenge, however for ICP-MS to measure non-metallic impurities such as sulfur, phosphorus, silicon, and chlorine in NMP. The low ionization efficiency of these elements greatly reduces analyte signal, while the elevated background signal (measured as background equivalent concentration, BEC) due to N-, O-, and C-based polyatomic ions formed from the NMP matrix makes low-level analysis even more difficult (Table 1).

**Table 1.** ICP-QMS BECs obtained in no gas mode for selected analytes in NMP.

Element	<i>m/z</i>	Ionization potential (eV)	Ionization ratio (%)	BEC without cell (ppm)	Interference
Si	28	8.152	87.9	>100	$^{14}N_2^+$ , $^{12}C^{16}O^+$
P	31	10.487	28.8	0.39	$^{14}N^{16}OH^+$ , $COH_3^+$
S	32	10.360	11.5	9.5	$^{16}O_2^+$ , $NOH_2^+$
Cl	35	12.967	0.46	0.26	$^{16}O^{18}OH^+$

## Experimental

**Instrumentation:** Agilent 8800 #200 with narrow injector (id =1.5 mm) torch (G3280-80080) typically used for the analysis of organic solvents. A C-flow 200 PFA nebulizer (G3285-80000) was used in self-aspiration mode. An option gas flow of 20%  $O_2$  in Ar was added to the carrier gas to prevent carbon build up on the interface cones.

**Plasma conditions:** NMP analysis requires hotter plasma conditions than normal. This was achieved by reducing Make-up Gas (MUGS) by 0.2 L/min. Plasma tuning conditions are summarized in Table 2.

**Table 2.** Plasma conditions for NMP analysis.

Parameter	Unit	Tuning value
RF	W	1550
Sampling depth	mm	8.0
Carrier gas flow	L/min	0.50
Make-up gas flow	L/min	0.10
Option gas flow	L/min	0.12 (12% of full scale)
Spray chamber temperature	°C	0

**CRC conditions:** Table 3 summarizes the cell tuning parameters (gas flow rate and voltages) used.

**Table 3.** CRC operating conditions.

Parameter	Unit	O <sub>2</sub> reaction cell		H <sub>2</sub> reaction cell	
		On-mass	Mass-shift	On-mass	Mass-shift
Cell gas	-	O <sub>2</sub>		H <sub>2</sub>	
Gas flow rate	mL/min	0.30		4.0	
Octopole bias	V	-14		-10	
KED	V	-5	-5	0	-5

**Reagents and sample preparation:** Electronic industry grade NMP was distilled at 120 °C and acidified by adding high purity HNO<sub>3</sub> to a concentration of 1% w/w.

## Results and discussion

NMP was analyzed directly using the method of standard additions (MSA). Three replicate measurements (ten replicates for the blank) were acquired for S, P, Si and Cl using an integration time of 1 s per isotope.

### P and S measurement in NMP

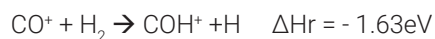
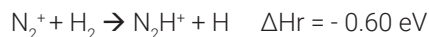
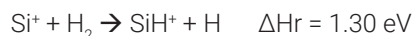
The mass-shift method using O<sub>2</sub> worked well for P and S measurement in NMP. The reactions of P and S with O<sub>2</sub> are exothermic, indicated by the negative value for ΔH, as shown below; therefore P<sup>+</sup> and S<sup>+</sup> are efficiently converted to their oxide ions, PO<sup>+</sup> and SO<sup>+</sup>. P and S can be measured as the product ions, avoiding the original spectroscopic interferences on their elemental masses, *m/z* 31 and *m/z* 32.



In MS/MS mode, Q1 rejects <sup>36</sup>ArC<sup>+</sup> before it can enter the cell, preventing it from overlapping SO<sup>+</sup>. This allows ICP-QQQ to control the reaction chemistry pathways and reaction product ions, ensuring that the analyte product ion is measured free from overlap, regardless of the levels of other co-existing analyte (or matrix) elements. MS/MS mode with the O<sub>2</sub> mass-shift method achieved BECs of 0.55 ppb and 5.5 ppb for P and S respectively in NMP. The low BECs and linear calibration plots achieved in MS/MS mode also prove that the matrix-based interferences do not react with O<sub>2</sub>, allowing the analytes to be separated from the interferences.

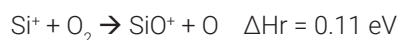
### Si measurement in NMP

H<sub>2</sub> cell gas was applied to the measurement of Si in NMP. The reaction kinetics for Si and its major interferences with H<sub>2</sub> cell gas are shown below. The reaction rate data suggests that Si does not react with H<sub>2</sub> cell gas (endothermic reaction indicated by the positive value for ΔH), and so could be measured in NMP using the direct, on-mass method. While the reaction of Si<sup>+</sup> with H<sub>2</sub> is endothermic, the reactions of the major interfering ions on Si at mass 28 (N<sub>2</sub><sup>+</sup> and CO<sup>+</sup>) are exothermic, and these interferences are therefore neutralized or reacted away.



The results obtained are shown in Figure 2 (top). The H<sub>2</sub> on-mass method achieved a BEC of 15.8 ppb for Si in NMP.

Oxygen cell gas was also tested of the measurement of Si in NMP. As shown below, the reaction of Si<sup>+</sup> with O<sub>2</sub> to form SiO<sup>+</sup> is endothermic. However, collisional processes in the cell provide additional energy which promotes the reaction, enabling the O<sub>2</sub> mass-shift method to be applied.



Unfortunately, a major interference on Si at *m/z* 28 (CO<sup>+</sup>) also reacts with O<sub>2</sub>, so the BEC achieved using the O<sub>2</sub> mass-shift method to measure Si as SiO<sup>+</sup> (Q1 = 28, Q2 = 44) was not satisfactory. Fortunately, another Si reaction product ion (SiO<sub>2</sub><sup>+</sup>) also forms and this can be measured at *m/z* 60 (Q1 = 28, Q2 = 60) giving a BEC of 11.9 ppb for Si in NMP (Figure 2, bottom).

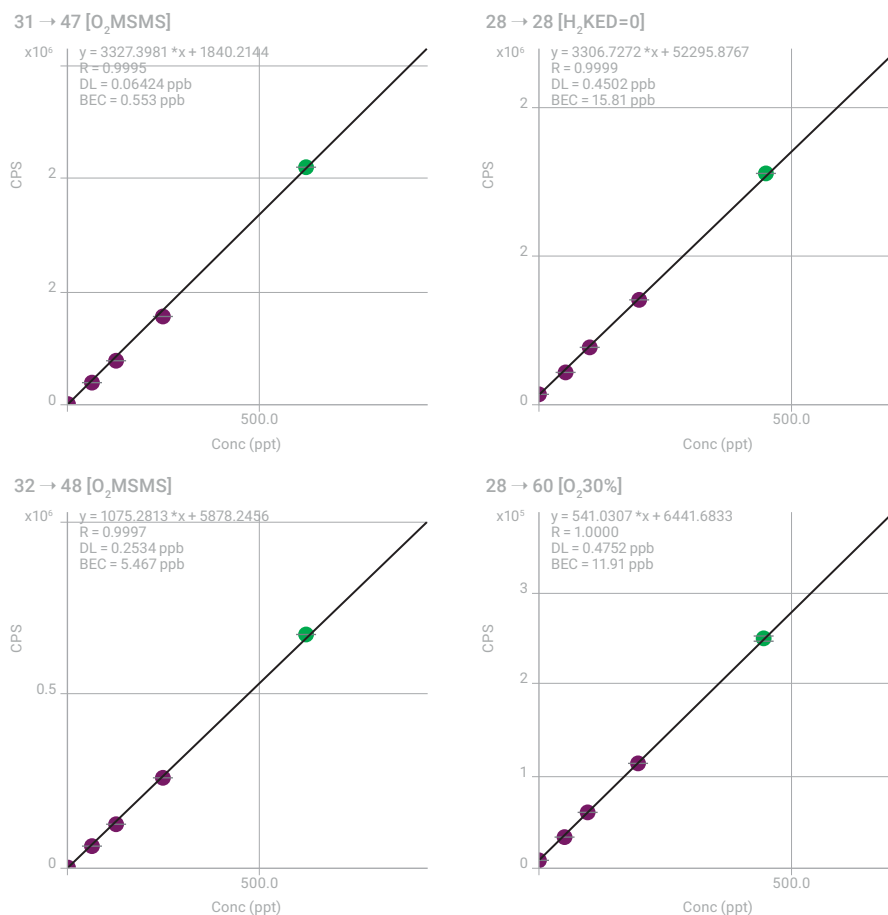


**Figure 1.** Calibration curve using MS/MS with O<sub>2</sub> mass-shift for P (top) and S (bottom) in NMP.

**Figure 2.** Calibration plots for Si in NMP. Top: H<sub>2</sub> on-mass method (Q1=Q2=28). Bottom: O<sub>2</sub> mass-shift method (Q1=28, Q2=60).



## Cl in NMP

Cl<sup>+</sup> reacts exothermically with H<sub>2</sub> to form ClH<sup>+</sup> as shown below. ClH<sup>+</sup> continues to react via a chain reaction to form ClH<sub>2</sub><sup>+</sup>.

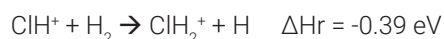
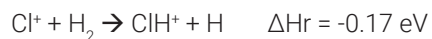
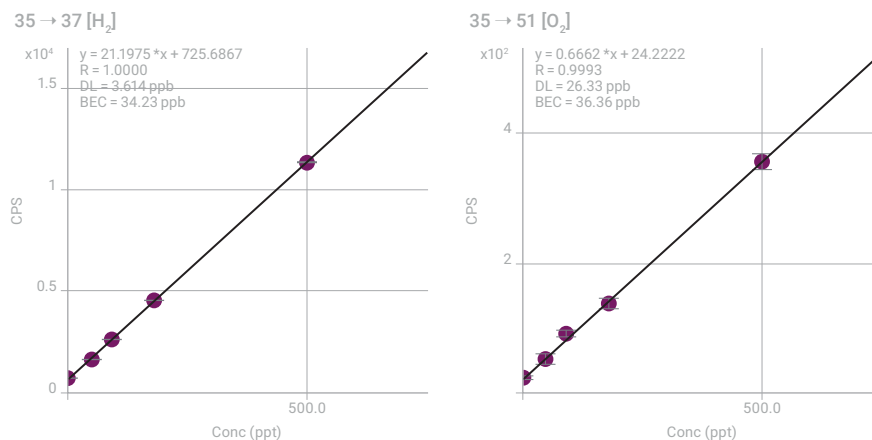


Figure 3 (left) shows calibration plots obtained for Cl in NMP using the H<sub>2</sub> mass-shift method. The plot obtained using the O<sub>2</sub> mass-shift method (Figure 3, below) is also shown for comparison. A slightly better BEC of 34.2 ppb was achieved with much higher sensitivity for Cl in NMP using the H<sub>2</sub> mass-shift method.



**Figure 3.** Calibration plots for Cl in NMP. Left: H<sub>2</sub> mass-shift method (Q1 = 35, Q2 = 37). Right: O<sub>2</sub> mass-shift method (Q1=35, Q2=51).

## More information

Trace level analysis of sulfur, phosphorus, silicon and chlorine in NMP using the Agilent 8800 Triple Quadrupole ICP-MS, 2013, Agilent publication, [5991-2303EN](#)

# Analysis of Silicon, Phosphorus, and Sulfur in 20% Methanol

## Authors

Emmett Soffey, Bert Woods and Steve Wilbur  
Agilent Technologies, Japan

## Keywords

organic solvents, methanol, silicon, phosphorus, sulfur, hydrogen on-mass, oxygen mass-shift

## Introduction

Analysis of organic solvents for trace metals presents a number of challenges to ICP-MS, many of which have been overcome to varying degrees on Agilent's 7700 Series quadrupole ICP-MS systems. However, even with these advances, several elements remain challenging in organic solvents, particularly silicon, phosphorus and sulfur. All three elements are subject to intense interferences from polyatomic ions based on carbon, nitrogen and oxygen, which are difficult to completely remove using conventional quadrupole ICP-MS (ICP-QMS). Examples include  $\text{CO}^+$ ,  $\text{COH}^+$ ,  $\text{N}_2^+$  and  $\text{NO}^+$  on silicon 28, 29 and 30;  $\text{COH}^+$ ,  $\text{NOH}^+$ ,  $\text{N}_2\text{H}^+$ ,  $\text{NO}^+$  and  $\text{CO}^+$  on phosphorus 31 and  $\text{O}_2^+$ ,  $\text{NO}^+$ ,  $\text{NOH}^+$  and  $\text{NOH}_2^+$  on sulfur 32 and 34. Additionally, phosphorus and sulfur have high first ionization potentials (IP) of 10.5 eV and 10.4 eV respectively, resulting in relatively poor sensitivity compared to more typical elements whose IPs are in the range of ~6 – 8 eV.

## Experimental

**Instrumentation:** Agilent 8800 #200.

**Plasma conditions and ion lens tune:** RF power = 1550 W, Sampling depth = 8.0 mm and Carrier gas flow rate = 1.05 L/min were used with soft extraction tune, Extract 1 = 0 V and Extract 2 = -190 V.

Ultra pure methanol was spiked with silicon (Si), phosphorus (P) and sulfur (S) at 1, 5, 10 and 50 ppb and measured using the ICP-QQQ in several operational modes in order to evaluate the optimum conditions for the simultaneous analysis of all three analytes. Hydrogen and oxygen reaction gases were evaluated, with  $\text{H}_2$  cell gas used in both Single Quad (SQ) and MS/MS modes. In addition, helium collision gas was investigated in both SQ and MS/MS mode to determine the effects of using MS/MS with a non-reactive cell gas.

The CRC conditions are outlined in Table 1, which includes the five analysis modes evaluated. Two Single Quad modes were tested, using both He and  $\text{H}_2$  in the cell, to simulate the capability of a single quadrupole ICP-MS. In addition, three conditions using MS/MS mode were tested using  $\text{H}_2$ , He and  $\text{O}_2$  as cell gases.

**Table 1.** 8800 ICP-QQQ acquisition conditions tested, including five operational modes.

Parameter	Unit	He SQ	$\text{H}_2$ SQ	$\text{H}_2$ MS/MS	He MS/MS	$\text{O}_2$ MS/MS
Acquisition mode		SQ	SQ	MS/MS	MS/MS	MS/MS
Cell gas		He	$\text{H}_2$	$\text{H}_2$	He	$\text{O}_2$
Cell gas flow rate	mL/min	5.0	7.0	7.0	7.0	0.40
KED	V	5	0	0	5	-7

## Results and discussion

The BECs and DLs results are summarized in Tables 2–4, for silicon, phosphorus and sulfur respectively, for all 5 analysis modes tested. SQ and optimum MS/MS results are in bold type for comparison. A few mass-pairs were measured in each mode as shown. For example, Table 2 shows silicon monitored in MS/MS mode with O<sub>2</sub> cell gas, using a mass-pair of Q1 = 28 and Q2 = 44. With Q1 set to *m/z* 28, only silicon 28 and any on-mass interferences are allowed to enter the ORS cell. The silicon 28 in the cell reacts with the oxygen cell gas to form SiO<sup>+</sup>, and Q2 is set to measure at Q1 + 16 (*m/z* = 44), ensuring that only the M + <sup>16</sup>O reaction transition is measured.

**Table 2.** DLs and BECs for silicon. Silicon was not measurable at the spiked concentrations in helium mode.

Mode	Mass or mass pair	BEC (ppb)	DL (ppb)
H <sub>2</sub> SQ	Q2=28	25.46	0.12
H <sub>2</sub> MS/MS	Q1=28, Q2=28	2.17	0.03
O <sub>2</sub> MS/MS	Q1=28, Q2=44	85.54	28.21
O <sub>2</sub> MS/MS	Q1=29, Q2=45	N/A	N/A
O <sub>2</sub> MS/MS	Q1=30, Q2=46	99.09	21.26

**Table 3.** DLs and BECs for phosphorus. Phosphorus was not measurable at the spiked concentrations in H<sub>2</sub> Single Quad mode.

Mode	Mass or mass pair	BEC (ppb)	DL (ppb)
He SQ	Q2=31	3.81	0.63
He MS/MS	Q1=31, Q2=31	2.99	0.72
H <sub>2</sub> MS/MS	Q1=31, Q2=33	0.56	0.07
H <sub>2</sub> MS/MS	Q1=31, Q2=34	0.58	0.67
O <sub>2</sub> MS/MS	Q1=31, Q2=47	0.40	0.05
O <sub>2</sub> MS/MS	Q1=31, Q2=63	0.41	0.02

**Table 4.** DLs and BECs for sulfur using MS/MS mode with O<sub>2</sub> cell gas. Sulfur was not measurable at the spiked concentrations in helium or hydrogen mode.

Mode (cell gas)	Mass or mass pair	BEC (ppb)	DL (ppb)
MS/MS (O <sub>2</sub> )	Q1 = 34, Q2 = 34	51.17	4.37
MS/MS (O <sub>2</sub> )	Q1 = 32, Q2 = 48	3.13	0.10
MS/MS (O <sub>2</sub> )	Q1 = 34, Q2 = 50	3.11	0.20

Sample calibration plots are displayed in Figure 1. They are displayed in pairs showing the results obtained using SQ mode with a typical cell gas (upper calibration), compared to MS/MS mode using the optimum conditions (lower calibration).

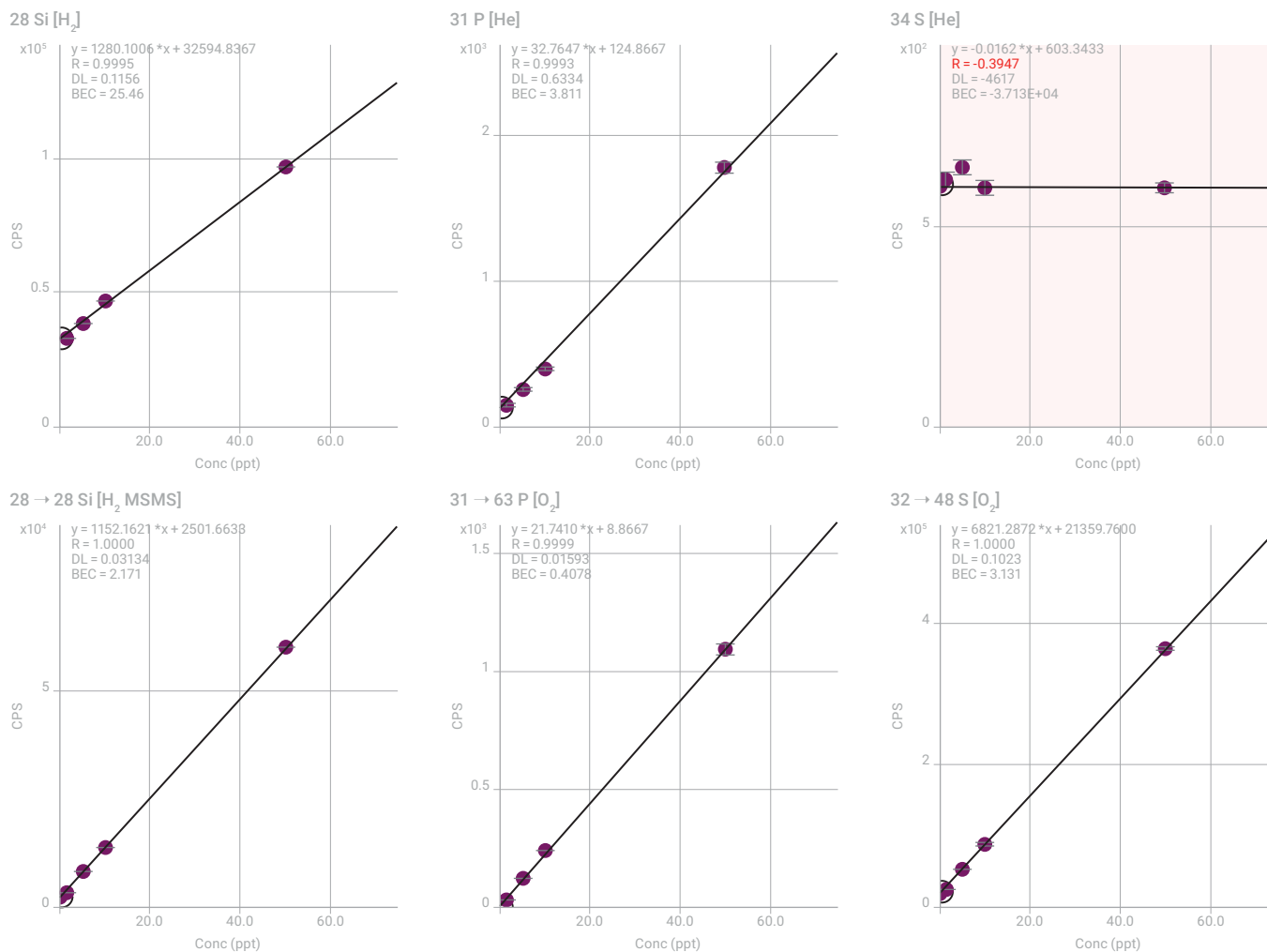


**Figure 1.** Calibration curves for Si, P and S showing SQ results (upper) compared with MS/MS results (lower). <sup>32</sup>S was not measurable at the spiked concentrations in methanol in SQ mode due to the intense <sup>16</sup>O<sub>2</sub><sup>+</sup> polyatomic interference.

## Conclusion

It can be seen that in all cases the use of MS/MS mode significantly improves both the BEC and instrument detection limit when compared to Single Quad mode. The most notable improvement was for sulfur which cannot be measured at the spiked concentrations (1, 5, 10, 50 ppb) in SQ He mode due to the intense polyatomic background resulting from the methanol matrix. By contrast, on the 8800 ICP-QQQ using MS/MS mode with O<sub>2</sub> mass-shift, S can be measured with a DL of 0.1 ppb.

## More information

Analysis of silicon, phosphorus and sulfur in 20% methanol using the Agilent 8800 Triple Quadrupole ICP-MS, Agilent publication, [5991-0320EN](#)

# Automated ultratrace element analysis of isopropyl alcohol with the Agilent 8900 ICP-QQQ

## Authors

Kazuhiro Sakai and Katsuo Mizobuchi  
Agilent Technologies, Japan

Riro Kobayashi  
IAS Inc, Japan

Online calibration using the IAS Automated Standard Addition System (ASAS)

## Introduction

Contamination control is critical in the semiconductor industry. Inorganic impurities are of particular concern, as they affect the electrical properties of the insulating and conducting layers from which semiconductor devices are made. Trace element contamination during wafer fabrication can therefore reduce the manufacturing yield and operational reliability of semiconductor devices. To minimize contamination, process chemicals must be monitored for ultratrace (ng/L; ppt) levels of elemental impurities.

Isopropyl alcohol (IPA) is an important organic solvent used in semiconductor manufacturing to remove organic and metallic residues and impurities from the surface of silicon wafers. Since IPA comes into direct contact with the wafer surface, the concentration of trace metals present in the solvent should be extremely low. For high purity Grade 4 IPA, SEMI standard C41-0705 specifies a maximum contaminant level of 100 ppt for each element (1). Delivering accurate analysis at these low concentrations requires a highly sensitive analytical instrument, together with a suitable clean laboratory environment, and advanced sample handling skills. Modern ICP-MS systems include predefined settings and auto-optimization routines to simplify operation. But the sample preparation, sample processing, and calibration steps still require a highly skilled analyst. Automating these steps would simplify the method, reducing the level of skill required for analysts to reliably perform the analysis.

Agilent ICP-MS systems can be integrated with various automated sample introduction systems, depending on a laboratory's requirements. Systems are available that automate a range of sample handling steps such as dilution, acidification, spiking, and calibration. One of the simplest, easiest-to-use and most cost-effective systems for automating semiconductor sample handling is the Automated Standard Addition System (ASAS) from IAS Inc. The ASAS can automatically add online spikes to generate a method of standard additions (MSA) or external calibration curve. In addition to simplifying the analysis, the automated sample introduction system decreases manual sample handling, reducing errors, and lowering the potential for sample contamination.

In this study, trace element impurities in IPA were quantified by online MSA using an IAS ASAS (Tokyo, Japan) and Agilent 8900 Triple Quadrupole ICP-MS (ICP-QQQ). The method allows the accurate and reliable quantification of ultratrace level impurities in IPA without requiring a highly skilled analyst.

## Experimental

### Reagents and samples

High purity IPA was prepared for analysis by distilling electronic-grade IPA in the lab. The IPA samples were introduced into the ICP-QQQ undiluted, to minimize the risk of contamination and to achieve the lowest possible detection limits (DLs).

A 1 µg/L (ppb) mixed multi-element standard solution was used to create the MSA calibration spikes. The working standard solution was prepared by diluting a 10 ppm mixed multi-element standard (SPEX CertiPrep, Metuchen, NJ, US) with distilled IPA. To stabilize the spiked elements, nitric acid (68% ultrapure HNO<sub>3</sub>) was added to the IPA samples at a final acid concentration of 1%.

The 1 ppb working standard solution was placed into a clean sample bottle and connected to the standard line of the ASAS. All MSA calibration (spike) solutions required for the analysis were automatically prepared and added online by the ASAS. Spike concentrations of 0, 5, 10, 20, and 50 ppt were added to the IPA sample. The sample preparation and analysis steps were performed in a Class 10,000 clean-room.

### **Instrumentation**

An Agilent 8900 Semiconductor configuration ICP-QQQ instrument was used. The instrument was fitted with a glass concentric nebulizer (G1820-65138) self-aspirating with PFA sample tubing (G1820-65478; 0.3 mm id, 1.6 mm od).

A Peltier-cooled quartz spray chamber, quartz torch, platinum-tipped sampling and skimmer cones, and s-lens were used.

When organic solvents are analyzed, carbon in the sample aerosol can be deposited on the sampling cone, causing instability and signal drift. To prevent carbon deposition during the analysis of solvents such as IPA, oxygen is added to the carrier gas to oxidize the carbon in the plasma. Volatile organic solvents also cause a very high solvent vapor pressure in the spray chamber, leading to plasma instability. To reduce solvent vapor pressure and ensure reliable plasma ignition and operation, the spray chamber temperature is reduced to below zero degrees. In this work, the spray chamber was cooled to -5 °C using the Peltier device that is standard on all Agilent ICP-MS systems. For stable operation of the plasma, a torch with a narrow (1.5 mm) injector replaced the standard 2.5 mm injector torch.

Combining cool plasma with collision/reaction cell (CRC) operation has been shown to be a powerful mode for interference removal in ICP-MS (2). These conditions can also be used for the analysis of organic solvent samples, but such samples require more plasma energy to decompose the organic matrix. The analyst must balance reducing the plasma temperature enough to control the ionization of interfering species, while maintaining sufficient energy to decompose the matrix. With Agilent ICP-MS systems, the ShieldTorch System provides effective reduction of the plasma potential, so ionization of polyatomic ions is minimized, even at higher forward power. "Cool plasma" conditions provide better robustness and matrix tolerance on Agilent ICP-MS systems than on systems that do not have such effective control of plasma potential.

Furthermore, all Agilent ICP-MS systems have two separate gas controls contributing to the total "carrier" gas flow passing through the central, injector tube. The nebulizer gas flow (the flow that passes through the nebulizer and aspirates the sample) is adjusted to give optimum sample aspiration. The make-up gas flow is then optimized to control the total carrier gas flow that transports the sample aerosol through the central channel of the plasma. This total carrier flow, combined with the plasma power and sampling depth, determines the "coolness" of the plasma conditions.

In advanced semiconductor applications, the key requirement is to deliver the absolute lowest possible detection limits for each analyte. Laboratories measuring ultratrace levels of contaminant metals often use a multitune method, where several tuning steps are applied sequentially during the measurement of each solution. This approach allows the tuning conditions to be optimized for the removal of different types of interferences, while maintaining sensitivity for each analyte. In this work, several reaction cell gases (He, H<sub>2</sub>, O<sub>2</sub>, and NH<sub>3</sub>) were used for the analytes being measured.

Instrument tuning conditions are shown in Table 1 and other acquisition parameters are shown in Table 2.

**Table 1.** Agilent 8900 ICP-QQQ operating conditions.

	H <sub>2</sub> (cool plasma*)	NH <sub>3</sub> (cool plasma*)	O <sub>2</sub> He	H <sub>2</sub>	He	No gas
Scan type	MS/MS					
RF power (W)	1500					
Sampling depth (mm)	18.0					
Nebulizer gas flow rate (L/min)	0.70					
20% O <sub>2</sub> Ar balance gas flow rate (L/min)	0.30 (30%)**					
Spray chamber temp (°C)	-5.0					
Make-up gas flow rate (L/min)	0.80	0.70	0.50			
Extract 1 (V)	-100					
Extract 2 (V)	-10.0					
Omega bias (V)	-70.0					
Omega lens (V)	4.0					
Q1 entrance (V)	-50.0					
He cell gas flow rate (mL/min)	-	1.0	12.0	-	5.0	-
H <sub>2</sub> cell gas flow rate (mL/min)	5.0	-	-	10.0	-	-
NH <sub>3</sub> cell gas flow rate (mL/min)***	-	2 (20%)**	-	-	-	-
O <sub>2</sub> cell gas flow rate (mL/min)	-	-	0.075 (5%)**	-	-	-
OctP bias (V)	-18	-5	-3	-30	-20	-10
Axial acceleration (V)	1.0			0		
Energy discrimination (V)	0	-10			3	

**Table 2.** Acquisition parameters.

Parameter	Setting
Q2 peak pattern	1 point
Replicates	3 (spiked samples) 10 (unspiked sample)
Sweeps/replicate	10
Integration time (s)	1 (all elements except phosphorus) 10 (phosphorus)

\* Optimum cool plasma conditions were achieved by adjusting the make-up gas flow while maintaining a high forward power setting.

\*\* Values in parentheses are % of the maximum flow of the gas controller, as displayed in the tuning pane of ICP-MS MassHunter.

\*\*\* 10% NH<sub>3</sub> balanced with 90% He.

### Automated Standard Addition System (ASAS)

The IAS ASAS is an automated online sample processing device. It uses a precise, microflow syringe pump to add specific volumes of spike solutions or diluent to the sample flow as it passes to the ICP-MS nebulizer. The small footprint of the ASAS allows it to be easily positioned between the autosampler and ICP-MS, as shown in Figure 1. This arrangement is beneficial in the small workspace typically available in semiconductor clean-rooms. Once connected in line, the ASAS can be used to automatically generate a calibration curve using either external standards or MSA.

MSA calibrations have the advantage of exact matrix matching, since the calibration is created in the actual sample matrix. However, conventional manual MSA spiking is often regarded as complicated and time-consuming. With automatic spike additions using ASAS, the complexity is eliminated. Also, the Agilent ICP-MS MassHunter software allows an MSA calibration in one sample to be automatically converted to an external calibration. This function allows other samples of the same type to be run against the MSA calibration, without requiring the subsequent samples to be spiked individually. With these two improvements, MSA can be as fast and easy to run as conventional external calibration.

Spike recoveries are typically carried out as a routine performance check during semiconductor chemical analysis. This can be automated to simplify and speed up the analysis. The ASAS microvolume syringe pump adds the spike to the continuously flowing sample stream, so the risk of sample contamination and errors is minimized.

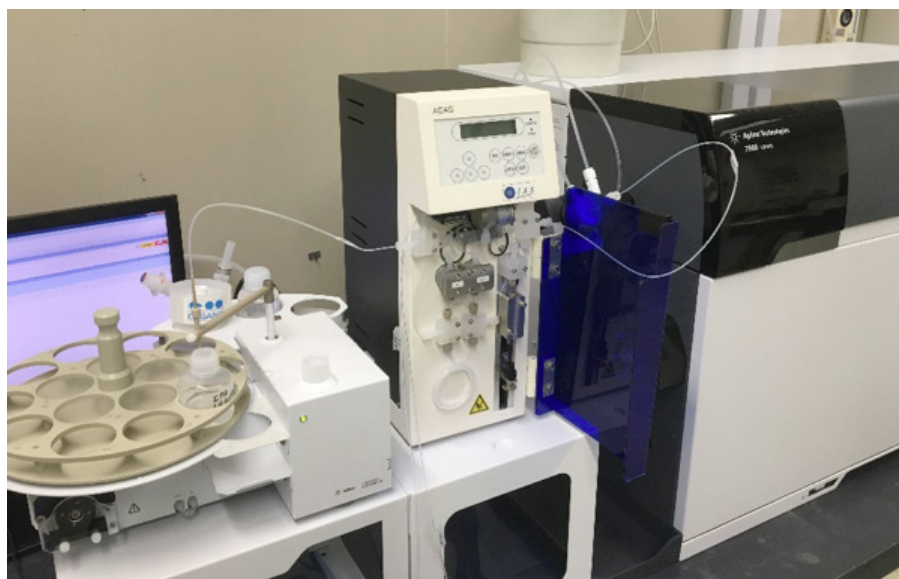


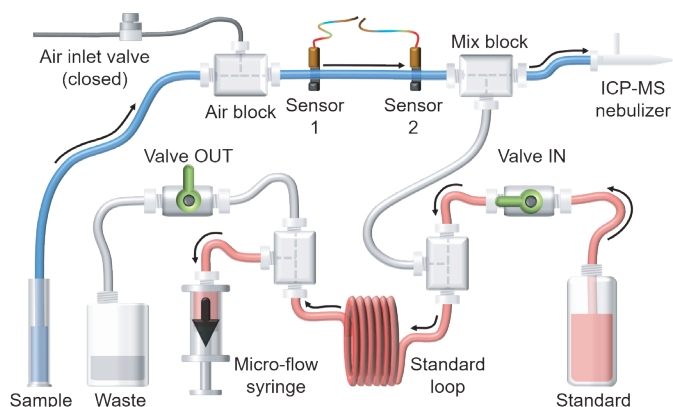
**Figure 1.** An Agilent ICP-MS fitted with an IAS ASAS automated standard addition system and the Agilent I-AS integrated autosampler.



ASAS operation consists of the following four steps:

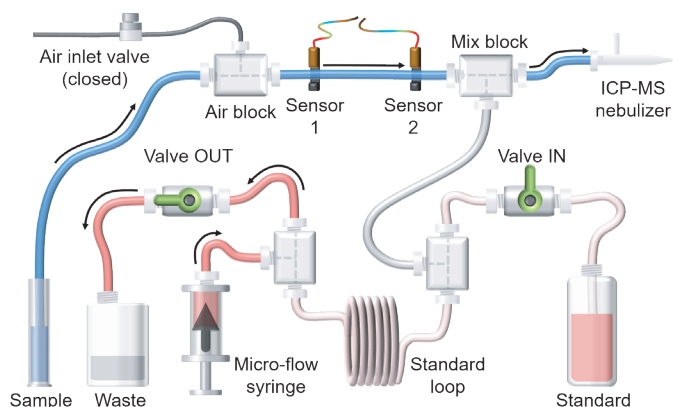
**Step 1: Loop is filled with the standard solution.**

“Valve IN” in the standard line opens and the syringe pump activates. This loads the standard solution along a dedicated uptake line from the standard bottle to the loop.



**Step 2: Excess standard solution is pumped to waste.**

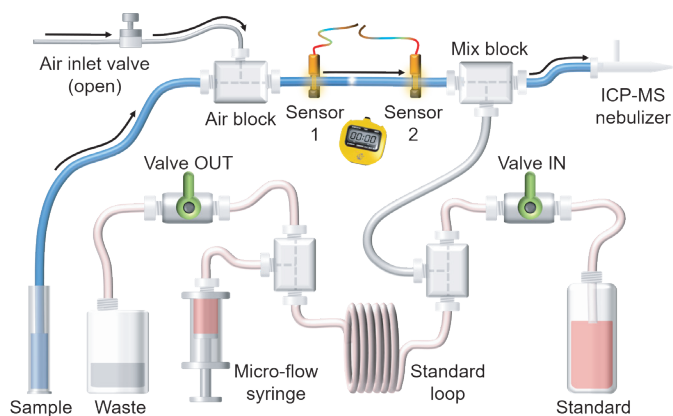
“Valve OUT” in the standard line opens, “Valve IN” closes, and the syringe pump discharges, pumping the remaining standard solution to the waste bottle—bypassing the loop.



**Step 3: Sample flow rate is measured to allow calculation of MSA spike volumes.**

To minimize the potential for contamination from peristaltic pump tubing, high-purity samples are usually introduced using self aspiration. This means that the flow rate varies, depending on the sample viscosity and tubing length. To allow the MSA spike additions to be calculated accurately, the ASAS system first measures the sample flow rate, as follows:

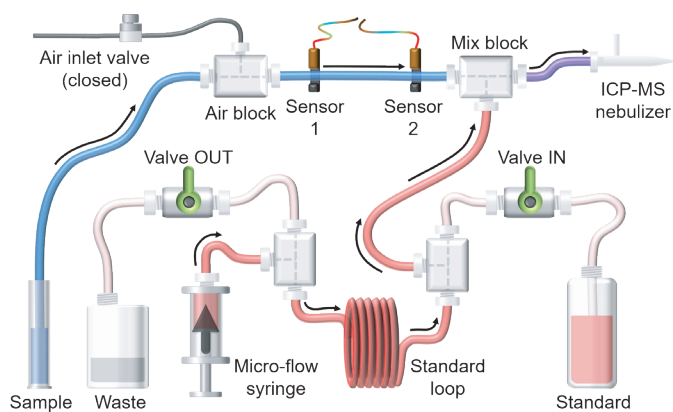
- When the autosampler probe moves to the sample vial, it triggers measurement of the sample uptake rate.
- An air bubble is introduced via the “Air inlet valve”.
- Optical fiber sensors measure the elapsed time between the air bubble passing Sensor 1 and Sensor 2. The elapsed time is inversely proportional to the sample flow rate, allowing the actual solution flow rate to be calculated.



#### Step 4: MSA spikes are added automatically.

The syringe pump delivers the standard solution from the loop into the sample line via the “Mix Block”. The standard solution flow rate needed to give each of the required MSA spike levels is calculated automatically, as explained later in the worked example.

The MSA spike solution is mixed with the sample online and the spiked sample is passed to the ICP-MS nebulizer.



*Worked example: Addition of a 50 ppt MSA spike to a sample flowing at 200  $\mu\text{L}/\text{min}$ .*

- A 1 ppb spike standard is prepared and placed in a sample bottle connected to the Standard line of the ASAS.
- The microflow syringe loads the spike standard into the ASAS loop via the dedicated uptake line.
- The autosampler moves to the next sample vial.
- The ASAS measures the sample uptake line flow rate (as previously outlined in Step 3). In this example, we will use a nominal flow rate of 200  $\mu\text{L}/\text{min}$ .
- Based on the measured sample flow rate, the ASAS software calculates the flow rate of the 1 ppb stock standard required to give a 50 ppt spike concentration. In this case, to achieve a spike level of 50 ppt in the sample flow of 200  $\mu\text{L}/\text{min}$ , the standard would need to be introduced at a flow rate of 10.0  $\mu\text{L}/\text{min}$  (20x dilution of the 1 ppb standard).
- The standard in the loop is added to the sample via the “Mix Block” at the calculated flow rate. The mixed, spiked sample then passes to the ICP-MS for analysis.

The ASAS can accurately add the standard solution at any flow rate between 0.10 and 99.99  $\mu\text{L}/\text{min}$ . However, to avoid over diluting the sample, the recommended standard flow rate is between 1.00 and 10.00  $\mu\text{L}/\text{min}$ . This assumes a typical nebulizer self-aspiration flow rate of 200  $\mu\text{L}/\text{min}$ .

The volume of the ASAS microflow syringe is about 800  $\mu\text{L}$ , and the loop volume is 700  $\mu\text{L}$ . When the volume of the standard solution remaining in the syringe falls below a set value, the syringe is automatically refilled. This happens after the current set of standard additions has completed.

If the total volume of standard solution required for the spike additions exceeds the loop volume, the syringe automatically refills the loop to ensure continuous operation.

Integrating the ASAS with the Agilent 8900 ICP-QQQ offers the following advantages for ultratrace elemental analysis of semiconductor samples:

- Compatibility with the Agilent I-AS autosampler and self-aspirating nebulizers
- Compact, easy-to-use, online system
- Automated creation of MSA or external calibrations
- Automated spike addition for spike recovery studies
- The ASAS can also be installed as part of the IAS Continuous Chemical Samples Inspection (CSI) system. This system provides online monitoring of multiple streams, baths, and containers of semiconductor process chemicals.

## Results and discussion

### DLs and BECs

In total, 47 elements—including all 22 elements specified in SEMI standard C41-0705—were measured using the 8900 ICP-QQQ. The instrument was operated in multiple tune modes, which were switched automatically during a single visit to each sample vial. Data for each of the modes was combined automatically into a single report for each sample. Detection Limits (DLs) and Background Equivalent Concentrations (BECs) in undiluted IPA are given in Table 3. The DLs were calculated from 3 x the standard deviation (SD) of 10 replicate measurements of the blank (unspiked) IPA sample. The DLs and BECs for all SEMI required elements (shown in bold) were all well below the grade 4 requirements of 100 ppt; many were below 0.1 ppt. These results illustrate how the 8900 ICP-QQQ provides performance that ensures compliance with higher chemical purities that will be required for semiconductor manufacturing in the future. DLs and BECs for Hf and Re could not be calculated, as the measured background signal was zero counts per second in all replicates of the blank IPA. The BEC for Cu reported using the normal, preferred isotope of Cu-63 was unexpectedly high, at 6.4 ppt. This result was compared to the BEC measured using the secondary isotope,  $^{65}\text{Cu}$ , and the two measured concentrations were in agreement. This suggests the high BEC observed using  $^{63}\text{Cu}$  was due to trace Cu contamination in the IPA sample rather than any interference on  $^{63}\text{Cu}$ .

The ASAS was used to perform an automatic spike recovery test. Ten separate IPA solutions were spiked at 20 ppt and measured against an external calibration that was created automatically by converting the MSA calibration. The spike recovery accuracy and repeatability (%RSD) results are also shown in Table 3. Excellent spike recoveries of between 91–108% were achieved for all elements at the 20 ppt level,

and RSDs (n=10) were between 1.6 and 8.9%. The results show the excellent reproducibility of the ASAS spike additions, as well as the good stability of the 8900 ICP-QQQ when aspirating organic solvents. This demonstrates the suitability of the ASAS-ICP-QQQ method for the routine analysis of ppt-level contaminant elements in IPA.

**Table 3.** DLs, BECs, and spike recoveries in IPA. Analytes shown in bold are SEMI grade 4 elements.

Analyte	Q1	Q2	Tune mode	DL (ng/L)	BEC (ng/L)	20 ng/L Recovery (%)	20 ng/L n=10 RSD (%)	SEMI standard C41-0705 Grade 4 (ng/L)
Li	7	7	*H <sub>2</sub>	0.010	0.040	99	2.4	< 100
Be	9	9	No gas	0.023	0.005	99	2.4	
B	11	11	No gas	1.2	12	96	8.0	< 100
Na	23	23	*NH <sub>3</sub>	0.060	0.97	109	5.7	< 100
Mg	24	24	*NH <sub>3</sub>	0.020	0.082	102	2.7	< 100
Al	27	27	*NH <sub>3</sub>	0.042	0.16	100	2.8	< 100
P	31	47	O <sub>2</sub> He	2.6	43	99	7.9	<16,000*
K	39	39	*NH <sub>3</sub>	0.64	1.1	107	4.9	< 100
Ca	40	40	*NH <sub>3</sub>	0.19	0.62	108	4.7	< 100
Ti	48	64	O <sub>2</sub> He	0.23	1.3	99	2.4	< 100
V	51	67	O <sub>2</sub> He	0.020	0.030	99	2.3	< 100
Cr	52	52	*NH <sub>3</sub>	0.16	0.48	92	1.7	< 100
Mn	55	55	*NH <sub>3</sub>	0.030	0.030	102	2.4	< 100
Fe	56	56	*NH <sub>3</sub>	0.16	0.72	101	2.5	< 100
Co	59	59	He	0.020	0.020	99	2.1	
Ni	60	60	He	0.43	0.80	101	2.0	<100
Cu	63	63	O <sub>2</sub> He	0.38	6.4	97	2.3	<100
Zn	64	64	He	0.71	0.72	98	6.9	<100
Ga	71	71	O <sub>2</sub> He	0.013	0.005	100	2.8	
Ge	74	74	He	0.30	0.070	96	8.1	
As	75	91	O <sub>2</sub> He	0.41	0.26	108	2.7	<100
Rb	85	85	H <sub>2</sub>	0.17	0.59	101	2.4	
Sr	88	88	O <sub>2</sub> He	0.005	0.002	98	2.4	
Zr	90	90	O <sub>2</sub> He	0.030	0.020	99	2.7	
Nb	93	93	H <sub>2</sub>	0.14	0.41	102	4.0	
Mo	98	130	O <sub>2</sub> He	0.17	0.11	103	4.1	
Ru	101	101	He	0.080	0.03	99	2.9	
Rh	103	103	O <sub>2</sub> He	0.070	0.18	99	2.1	
Pd	105	105	O <sub>2</sub> He	0.070	0.040	100	2.5	
Ag	107	107	O <sub>2</sub> He	0.014	0.006	97	2.6	
Cd	111	111	O <sub>2</sub> He	0.035	0.004	98	4.0	<100
In	115	115	O <sub>2</sub> He	0.012	0.008	99	1.8	
Sn	118	118	O <sub>2</sub> He	0.058	0.034	100	4.9	<100
Sb	121	121	O <sub>2</sub> He	0.056	0.009	103	2.3	<100
Te	125	125	O <sub>2</sub> He	0.78	0.29	97	8.9	
Cs	133	133	*H <sub>2</sub>	0.060	0.022	96	4.2	
Ba	138	138	O <sub>2</sub> He	0.009	0.004	99	2.4	<100

Analyte	Q1	Q2	Tune mode	DL (ng/L)	BEC (ng/L)	20 ng/L Recovery (%)	20 ng/L n=10 RSD (%)	SEMI standard C41-0705 Grade 4 (ng/L)
Hf	178	178	He	0.000	0.000	105	5.1	
W	182	214	O <sub>2</sub> He	0.21	0.049	97	5.7	
Re	185	185	O <sub>2</sub> He	0.000	0.000	96	3.0	
Ir	193	193	No gas	0.060	0.006	101	6.7	
Pt	195	195	O <sub>2</sub> He	0.51	0.45	100	3.0	
Tl	205	205	O <sub>2</sub> He	0.018	0.008	99	2.1	
Pb	208	208	O <sub>2</sub> He	0.047	0.042	100	2.7	<100
Bi	209	209	O <sub>2</sub> He	0.021	0.004	98	1.6	
Th	232	248	O <sub>2</sub> He	0.11	0.022	97	4.6	
U	238	254	O <sub>2</sub> He	0.18	0.048	91	6.6	

\* High-power cool plasma conditions: the temperature of the plasma was adjusted by changing the make-up gas flow rate.

\*\* < 16,000 ppt is the concentration limit for elemental P that is equivalent to the SEMI specified limit of 50 ppb (50,000 ppt) for PO<sub>4</sub>.

### Resolving polyatomic interferences on Mg, Al, and Cr

In this work, high-power cool plasma conditions were combined with reaction cell gases to provide the most effective control of intense background and matrix-based interferences. Cool plasma conditions were obtained by adjusting the make-up gas flow, while maintaining plasma energy with normal “hot plasma” RF power of 1500 W. These plasma conditions ensured sufficient plasma robustness to allow long-term analysis of the organic matrix, while providing effective control of carbon-based interferences on analytes such as Mg, Al, and Cr (Table 4).

**Table 4.** Main interferences arising from organic solvent matrix.

Analyte	Interferences	DL (ng/L)	BEC (ng/L)
<sup>24</sup> Mg	<sup>12</sup> C <sub>2</sub> <sup>+</sup>	0.020	0.082
<sup>27</sup> Al	<sup>12</sup> C <sup>15</sup> N <sup>+</sup> , <sup>13</sup> C <sup>14</sup> N <sup>+</sup> , <sup>12</sup> C <sup>14</sup> N <sup>1</sup> H <sup>+</sup>	0.042	0.16
<sup>31</sup> P	<sup>15</sup> N <sup>16</sup> O <sup>+</sup> , <sup>14</sup> N <sup>17</sup> O <sup>+</sup> , <sup>13</sup> C <sup>18</sup> O <sup>+</sup>	2.6	43
<sup>52</sup> Cr	<sup>40</sup> Ar <sup>12</sup> C <sup>+</sup>	0.16	0.48

The major isotope of magnesium, <sup>24</sup>Mg<sup>+</sup>, suffers an intense polyatomic interference from <sup>12</sup>C<sub>2</sub><sup>+</sup> in organic samples. Cool plasma conditions can suppress the ionization of C<sub>2</sub>, and CRC mode can also be employed successfully to resolve the interference. In this work, the lowest DLs for Mg were achieved using a combination of high-power cool plasma conditions and on-mass measurement in MS/MS mode with NH<sub>3</sub> cell gas. The calibration curve for <sup>24</sup>Mg shows that the <sup>12</sup>C<sub>2</sub><sup>+</sup> interference was removed successfully, achieving a BEC less than 0.1 ng/L (ppt), and a detection limit of 0.020 ppt (Figure 2).

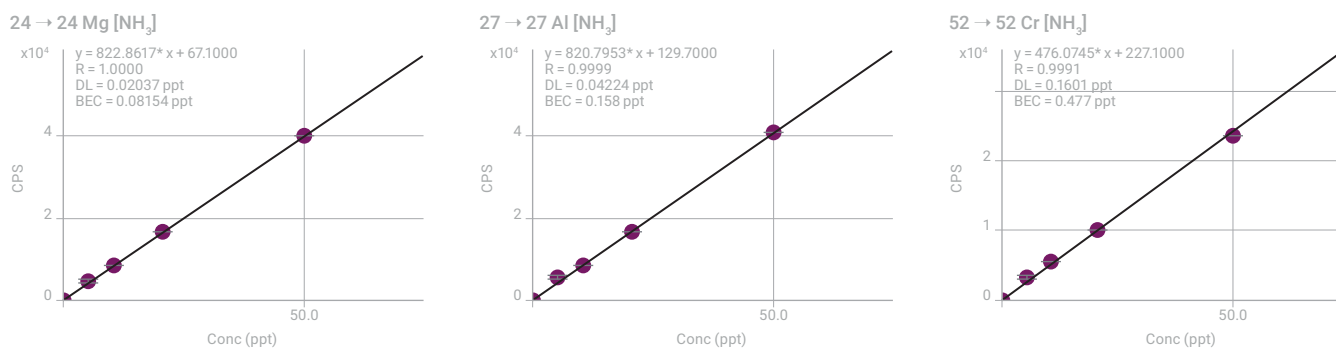


Figure 2. MSA calibration curves for  $^{24}\text{Mg}$ ,  $^{27}\text{Al}$ , and  $^{52}\text{Cr}$ .

The same approach was effective for the determination of other elements that suffer carbon-based polyatomic interference in organic solvents, such as  $^{27}\text{Al}$  and  $^{52}\text{Cr}$ . The calibrations shown in Figure 2 demonstrate that the interferences from  $^{12}\text{C}^{15}\text{N}^+$ ,  $^{13}\text{C}^{14}\text{N}^+$ ,  $^{12}\text{C}^{14}\text{NH}^+$  on  $^{27}\text{Al}^+$  and  $^{40}\text{Ar}^{12}\text{C}^+$  on  $^{52}\text{Cr}^+$  were minimized using high-power cool plasma conditions and  $\text{NH}_3$  cell gas. These conditions gave BECs and DLs of 0.16 and 0.042 ppt for Al, and 0.48 and 0.16 ppt for Cr, respectively (Table 4).

### P determination

SEMI Standard C41-0705 specifies the maximum concentration of phosphate allowed in high purity IPA, with a limit of 50  $\mu\text{g}/\text{L}$  (ppb) or 50,000 ppt. This limit equates to an elemental concentration of about 16,000 ppt for phosphorus (P).

The analysis of P in IPA needs an ORS cell mode that can resolve P from the normal plasma background polyatomic ions formed from N and O –  $^{14}\text{N}^{16}\text{O}^+\text{H}^+$ ,  $^{15}\text{N}^{16}\text{O}^+$ , and  $^{14}\text{N}^{17}\text{O}^+$ . In addition, potential carbon-based interferences that overlap  $\text{P}^+$  at  $m/z$  31 must also be resolved. MS/MS mass shift operation with oxygen reaction cell gas has been shown to be suitable for the analysis of P. Using this method, the  $\text{P}^+$  ions react with  $\text{O}_2$  cell gas to form a reaction product ion  $\text{PO}^+$  at  $m/z$  47, mass-shifted away from the original on-mass interferences.

A previous study (3) demonstrated that a relatively high octopole bias ( $-3$  V) with a mix of cell gases comprising 0.075 mL/min oxygen plus 12 mL/min helium could be used successfully for low-level analysis of P. The relative cell gas flow rates mean that the density of helium atoms in the cell is 160 (12/0.075) times greater than that of oxygen. Most of the ions entering the cell will therefore collide multiple times with helium atoms before they collide (and react) with an oxygen atom. Helium works as a buffer gas, reducing the kinetic energy of the ions before they react with the  $\text{O}_2$  cell gas. This low collision energy should reduce the in-cell formation of certain unwanted reaction product ions, for example,  $^{13}\text{C}^{18}\text{O}^+ + \text{O}_2 \rightarrow ^{13}\text{C}^{18}\text{O}^{16}\text{O}^+ + \text{O}$ . Suppressing these reactions reduces the formation of interfering product ions that could overlap the analyte product ion  $^{31}\text{P}^{16}\text{O}^+$  at  $m/z$  47. Using these mixed cell gas conditions, a minimum BEC for P of 27 ppt in IPA was reported (3).

The measurement conditions for P described in reference 3 were also used in this study. The calibration curve in Figure 3 shows good linearity from 5 to 50 ppt for P. The BEC was 43 ng/L (ppt) and the DL was 2.6 ppt (Table 3). Given the much higher typical contaminant levels for P compared to the other trace metals, it would be reasonable to calibrate P at a higher concentration level than the other elements. This modification could easily be applied to the ASAS methodology

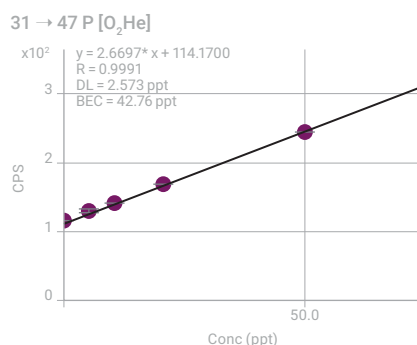


**Figure 3.** MSA calibration curve for <sup>31</sup>P.

described here, if a higher P concentration was added to the working stock standard solution. The ASAS would then prepare and inject the online MSA spikes from the mixed standard, including the higher P spike levels. The upper limit for P defined in SEMI Grade 4 purity chemicals is also much higher than for the other trace elements. The relatively high BEC of 43 ppt is still several orders of magnitude lower than the 16,000 ppt concentration limit specified for P.

## Conclusion

By automating the processes of sample preparation and standard spiking, the IAS ASAS automated-MSA system simplifies the elemental analysis of semiconductor process chemicals using the Agilent 8900 ICP-QQQ. The multi-element standard is prepared and connected to the ASAS, and the samples are loaded into the I-AS autosampler. The ASAS system then automatically performs all required steps, including online MSA spike additions and introduction of the sample to the ICP-QQQ.

Eliminating manual sample handling steps during ultratrace analysis lowers the risk of contamination. Limiting the handling of reagents and samples also reduces the likelihood of errors arising during the experimental procedure. Automating calibration and spike addition leads to increased consistency and higher confidence in the quality of the results.

The Agilent 8900 ICP-QQQ was operated using optimized plasma conditions and MS/MS mode to measure 47 elements in IPA. BECs at sub-ppt to ppt levels were acquired for all analytes – including all the elements specified in SEMI C41-0705. The results easily meet the current SEMI grade 4 specifications for all elements, including P, in IPA.

The excellent spike recovery and repeatability results for all elements at the 20 ppt level show the suitability of the automated ASAS method for the routine analysis of semiconductor process chemicals. The long-term robustness of this method is enhanced by using high-power cool plasma conditions. These conditions provide superior matrix decomposition and improved analyte ionization in the presence of the organic solvent matrix.

## References

1. SEMI C41-0705, Specifications and Guidelines for 2-Propanol, 2005.
2. J. Takahashi and K. Mizobuchi, Asia Pacific Winter Conference on Plasma Spectroscopy 2008.
3. K. Mizobuchi, N. Yamada and M. Yukinari, The Japan Society for Analytical Chemistry, 66th Nenkai, 2017.

# Analysis of Nanoparticles in Organic Reagents by Agilent 8900 ICP-QQQ in spICP-MS Mode

## Authors

Donna Hsu, Yoshinori Shimamura,  
Brian Liao, and Michiko Yamanaka<sup>1</sup>

Chun-Hua Chen and Chiu-Hun Su<sup>2</sup>

Ching Heng Hsu<sup>3</sup>

1 Agilent Technologies, Inc.

2 Industrial Technology Research  
Institute of Taiwan, Taiwan

3 BASF Taiwan Ltd., Taiwan

Determination of 25 and 30 nm Fe<sub>3</sub>O<sub>4</sub> NPs in low particle concentration solutions

## Introduction

Semiconductor device manufacturing involves several processes including lithography, etching, ion implantation, and peeling. Even small amounts of impurities present in processing reagents such as developer, rinse solution, and etching liquid can cause defects, resulting in a reduction of product yield and degradation of product reliability. Metallic nanoparticles (NPs), especially iron (Fe) NPs, can lead to the occurrence of 'cone defects' on the surface of wafers, which cause shorting of electrical signals (1). To prevent these problems from arising, an accurate analytical method is required to determine metallic NPs in semiconductor process chemicals.

Single particle ICP-MS (spICP-MS) is a powerful tool that is used increasingly to characterize the NP content of various types of samples (2–4). spICP-MS allows the simultaneous determination of the number, concentration, and size of particles, plus the dissolved element concentration. It can be applied to the measurement of semiconductor grade organic solvents such as isopropyl alcohol (IPA), propylene glycol methyl ether acetate (PGMEA), and butyl acetate (BuAc), as well as aqueous solutions (3). To detect very small-sized NPs using spICP-MS, an instrument with a low background and high sensitivity such as the Agilent 8900 Triple Quadrupole ICP-MS (ICP-QQQ) is needed. Also, since some metallic NPs suffer from spectral interferences, the advanced interference removal capability of the 8900 ICP-QQQ is advantageous for the application.

In this study, Fe NPs were measured in semiconductor grade IPA, PGMEA, and BuAc using the Agilent 8900 ICP-QQQ operating in spICP-MS mode.

## Experimental

### Sample preparation

Two kinds of Fe<sub>3</sub>O<sub>4</sub> NP (Fe NP) solutions, 25 nm (Sigma Aldrich, p/n 900027) and 30 nm (Sigma Aldrich, p/n 747408), were used as NP standards. The Fe NPs were spiked into IPA, PGMEA, and BuAc. These organic solvents were introduced directly to the ICP-QQQ. To measure the ionic sensitivity of Fe, an aqueous Fe standard (1000 ppm, Kanto Chemicals, Japan) was diluted with each organic solvent.

### Instrumentation

An Agilent 8900 ICP-QQQ (#200, Semiconductor configuration) and Agilent SPS 4 autosampler were used for all measurements. The sample introduction system comprised a quartz torch with a 1.5 mm i.d. injector, quartz spray chamber, and platinum-tipped interface cones. The SPS 4 autosampler was fitted with a sample rack (produced in Taiwan) designed to accommodate larger sample bottles (100 to 500 mL). Being able to load the same bottles used for sample preparation into



the SPS 4 rack reduces the risk of contamination as the samples don't need to be transferred to smaller bottles. Also, larger bottles are convenient for the long-term stability test. The samples were self-aspirated using an Agilent PFA nebulizer, which is part of the SPS 4 probe kit (p/n G3139-68000). Clean argon gas was purged into the cover of the autosampler and there was a constant flow of ultrapure water via a continuous flow rinse port fitted to the SPS 4.

The 8900 ICP-QQQ was operated in MS/MS mode for all Fe measurements. Both Q1 and Q2 (unit mass filters) were set to  $m/z$  56. Q1 selects which elements enter the ORS<sup>4</sup> collision/reaction cell (CRC), allowing controlled reaction chemistry to take place in the cell when a reactive cell gas is introduced. Ammonia cell gas was used to control the ArO and C<sub>2</sub>O<sub>2</sub> interferences that overlap Fe at  $m/z$  56.

The signal generated by a single NP lasts for about 1 ms, so Fast Time Resolved Analysis (TRA) mode of the 8900 ICP-QQQ was used to acquire the data. Fast TRA allows single element acquisition at a sampling rate of 100  $\mu$ s (10,000 measurements per second) and no settling time is needed between measurements. Data analysis was performed using the Single Nanoparticle Application Module of the Agilent ICP-MS MassHunter software.

The operating conditions of the Agilent 8900 ICP-QQQ are detailed in Table 1. As shown, slightly different parameters were used to achieve optimum sensitivity for the determination of Fe NPs in each solvent. To enable the direct injection of organic solvents to the ICP-QQQ without the deposition of carbon on the cones, oxygen gas (20%, Ar balanced) was added to the sample gas flow.

**Table 1.** ICP-QQQ operating conditions.

Parameter	Value		
	IPA	PGMEA	BuAc
RF power (W)	1400	1500	1500
Sampling depth (mm)	18.0		
Nebulizer gas (L/min)	0.70		
Makeup gas (L/min)	0.50	0.60	0.45
*Option gas (L/min)	0.40 (40%)	0.20 (20%)	0.40 (40%)
Spray chamber temp. (°C)	2		
Extraction lens 1 (V)	-150	-125	-125
Extraction lens 2 (V)	-10	-15	-15
Octopole bias (V)	-10	-3	-3
Axial acceleration (V)	1.5		
Energy discrimination (V)	-10	-7	-7
He flow rate (mL/min)	1		
**NH <sub>3</sub> flow rate (mL/min)	2 (20%)	3 (30%)	3 (30%)
Dwell time ( $\mu$ s)	100		
Masses monitored	Fe (Q1: 56, Q2: 56)		
Data acquisition time (s)	60		

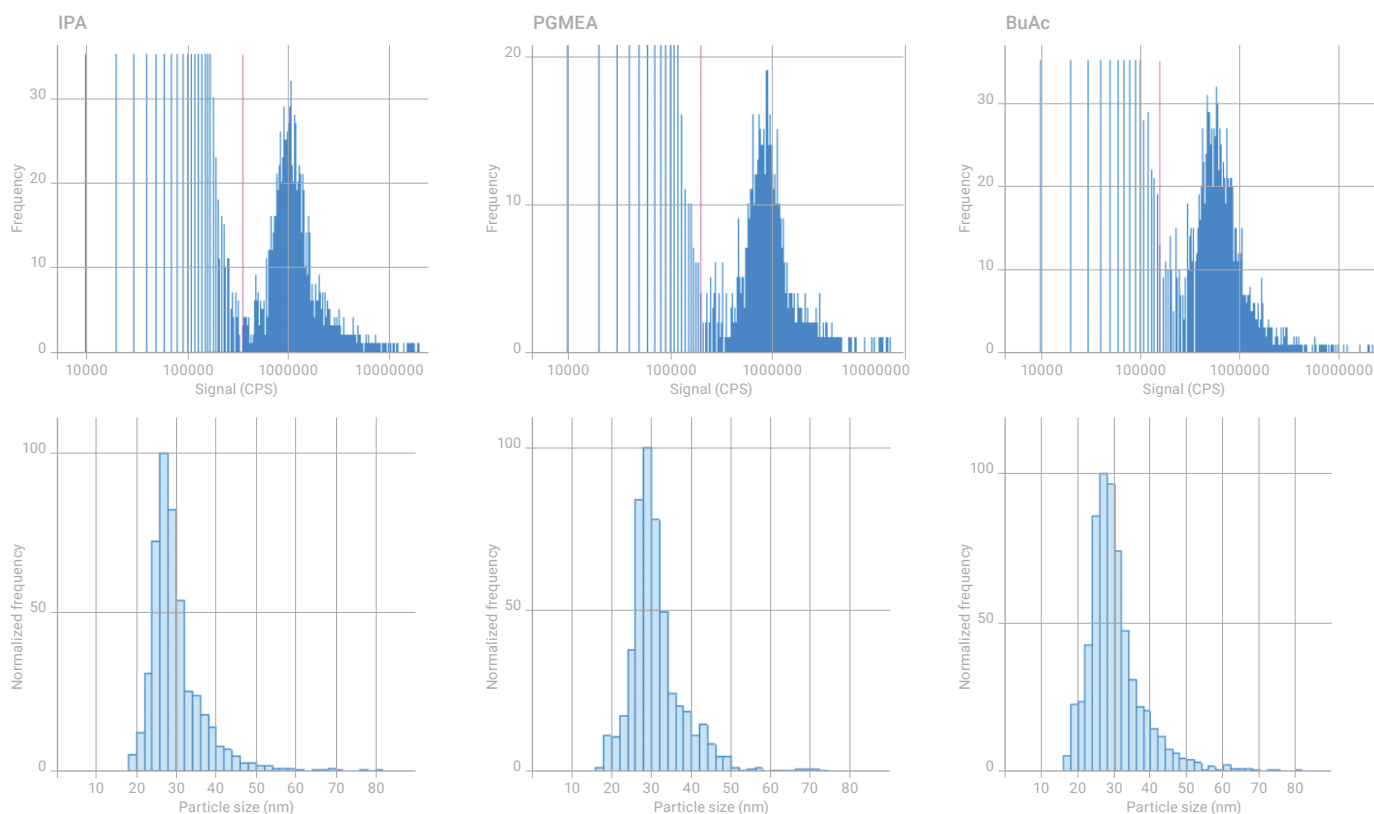
\*20% O<sub>2</sub> balanced with Ar added using the option gas mass flow controller, which is fitted as standard on the Agilent 8900 Semiconductor ICP-QQQ.

\*\*10% NH<sub>3</sub> balanced with He.

## Results and discussion

### Analysis of Fe NPs in IPA, PGMEA, and BuAc

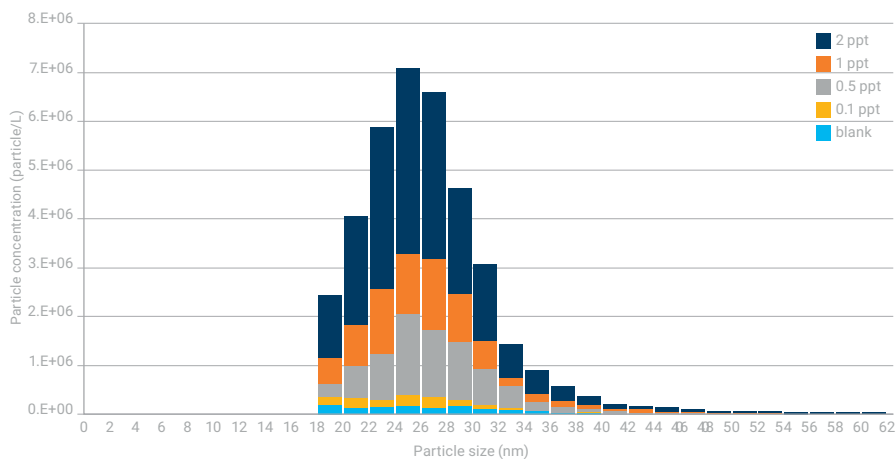
Solutions of IPA, PGMEA, and BuAc containing 30 nm Fe NPs spiked at 5 ppt were measured using the 8900 ICP-QQQ. The signal distribution and size distribution plots for Fe NPs in each of the samples are shown in Figure 1. The signals generated from the Fe NPs were clearly separated from the background signals. Also, the mean measured particle size was around 30 nm in all spiked solvents, which is consistent with the nominal Fe NP diameter (30 nm). The Single Nanoparticle Application Module software automatically sets the particle threshold, which is shown by the pink line in the signal distribution plots. The spICP-MS software automatically calculates the nebulization efficiency, which is the ratio of the amount of analyte entering the plasma to the amount of analyte delivered to the nebulizer. By measuring 30 nm Fe NP, the nebulization efficiency (calculated by size) was found to be around 0.30 (30%) for all three organic solvents. The sensitivity of ionic Fe ranged from 1500 cps/ppt to 2400 cps/ppt depending on the solvent. The background equivalent concentration (BED) of the blank reagents was around 6 nm.



**Figure 1.** Signal distribution (upper) and size distribution (lower) of 30 nm Fe NPs in solutions of IPA, PGMEA, and BuAc.

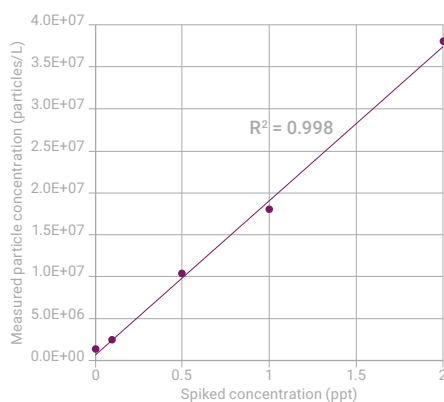
### Linearity of detected particle number concentration in terms of spiked concentration

Figure 2 shows the size distribution of 25 nm Fe NPs dispersed in IPA solution at several concentrations (0, 0.1, 0.5, 1, and 2 ppt). The graph clearly indicates a Gaussian distribution for 0.5, 1, and 2 ppt of Fe NPs. It wasn't possible to detect NPs smaller than 18 nm due to the background signal from the small amount of ionic Fe present in the sample (BEC = 0.6 ppt).



**Figure 2.** Size distribution data for 25 nm Fe NPs spiked at 0, 0.1, 0.5, 1, and 2 ppt in IPA. The vertical axis shows the particle number concentration for each range of particle sizes (each bar represents a size range of 2 nm).

Figure 3 shows the relationship of measured particle number concentration (particle/L) against the spiked concentration of Fe NPs in IPA. Almost perfect linearity ( $R^2 = 0.998$ ) was obtained across the concentration range of 0.1 to 2 ppt. These results show that 25 nm Fe NPs can be determined in IPA solutions containing very low concentrations of Fe NPs using the 8900 ICP-QQQ operating in spICP-MS mode.



**Figure 3.** Relationship between the spiked concentration of 25 nm Fe NPs and measured particle number concentration in IPA.

## Long-term stability test

Figure 4 shows the stability of detected particle number (representing particle number concentration) and particle size for 30 nm Fe NPs in the three solvents over 12 hours. Both the detected particle number and the size were constant over 12 hours, as indicated by the %RSDs. The stability of Fe NPs in each solvent means they can be measured accurately, even a long time after sample preparation.

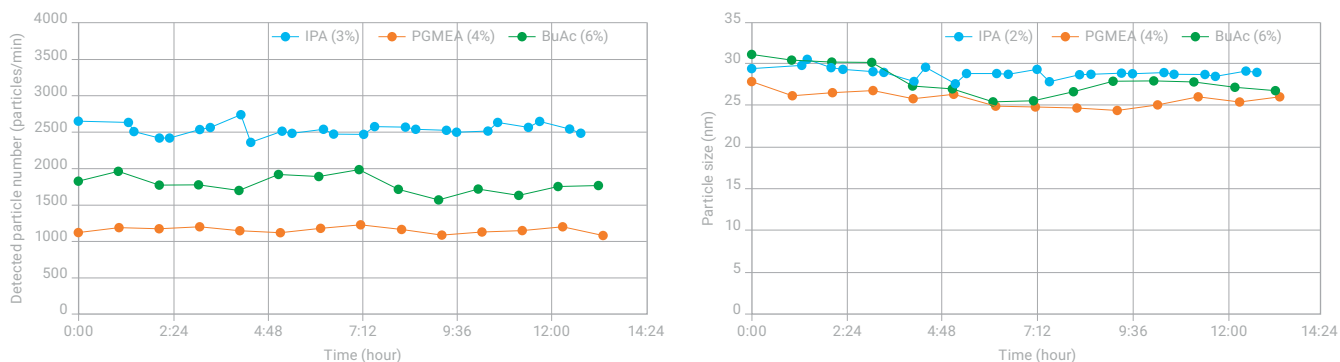


**Figure 4.** Long-term stability of 30 nm Fe NPs in IPA, PGMEA, and BuAc over 12 hours. The left graph shows the detected particle number and the right graph shows the average particle size. The numbers in parentheses are RSD%.

## Conclusion

Using an spICP-MS method, the Agilent 8900 ICP-QQQ operating in MS/MS mode was used for the determination and characterization of iron-based nanoparticles in IPA, PGMEA, and BuAc.

Standards containing 25 or 30 nm Fe<sub>3</sub>O<sub>4</sub> nanoparticles were spiked into the organic solvents and the particle size and the particle number concentration were determined using the spICP-MS method. The small-sized particles were successfully measured in solutions with a particle concentration ranging from 0.1 to 2 ppt. Also, the particle size and particle concentration of Fe NPs were stable in each of the three organic solvents over 12 hours.

Overall, the method delivered the low background, sensitivity, and spectral interference removal necessary for the analysis of small-sized NPs in semiconductor grade organic solvents.

## References

1. Takuya Hagiwara, Kentaro Saito, Hiraku Chakihara, Shuji Matsuo, Masao Inoue, Seiji Muranaka, Yuki Ota, Masazumi Matsuura, Study on Cone-defects during the Pattern Fabrication Process with Silicon Nitride, *J. Photopolym. Sci. Technol.*, 28, No.1, **2015**, 17–24
2. Michiko Yamanaka and Steve Wilbur, Measuring Multiple Elements in Nanoparticle using spICP-MS: Acquire NP data for up to 16 elements in Rapid Multi-Element Nanoparticle Analysis Mode, Agilent publication, [5994-0310EN](#)
3. Yoshinori Shimamura, Donna Hsu, and Michiko Yamanaka, Multielement Nanoparticle Analysis of Semiconductor Process Chemicals Using spICP-QQQ: Characterization of Ag, Fe<sub>3</sub>O<sub>4</sub>, Al<sub>2</sub>O<sub>3</sub>, Au, and SiO<sub>2</sub> NPs in TMAH in a single analytical run, Agilent publication, [5994-0987EN](#)
4. Michiko Yamanaka and Steve Wilbur, Accurate Determination of TiO<sub>2</sub> Nanoparticles in Complex Matrices using the Agilent 8900 ICP-QQQ, Agilent publication, [5991-8358EN](#)

# Analysis of 15 nm Iron Nanoparticles in Organic Solvents by spICP-MS

## Authors

Donna Hsu<sup>1</sup>

Yoshinori Shimamura<sup>1</sup>

Katsuo Mizobuchi<sup>1</sup>

Brian Liao<sup>1</sup>

Kuo-Lin Wang<sup>2</sup>

Chiu-Hun Su<sup>3</sup>

Ching Heng Hsu<sup>4</sup>

<sup>1</sup>Agilent Technologies, Inc.

<sup>2</sup>Shiny Chemical Industrial Co., Ltd.,  
Taiwan

<sup>3</sup>Industrial Technology Research  
Institute of Taiwan

<sup>4</sup>BASF Taiwan Ltd.

Using the exceptional sensitivity and low background of the Agilent 8900 ICP-QQQ

## Monitor metallic nanoparticles in process chemicals

In semiconductor device manufacturing, even small amounts of impurities present in processing reagents can affect product yield and reliability. There is growing awareness that metallic nanoparticles (NPs), especially Fe NPs, can lead to the occurrence of defects on the surface of wafers. Single particle ICP-MS (spICP-MS) is a powerful tool that is used increasingly to characterize the NP content of various types of samples, including semiconductor process chemicals.

## Measurement of 15 nm Fe NPs using spICP-MS

The Agilent 8900 ICP-QQQ (semiconductor configuration) was fitted with a quartz torch with a 1.5 mm i.d. injector. Interferences on <sup>56</sup>Fe from ArO and C<sub>2</sub>O<sub>2</sub> were resolved using oxygen as the cell gas. The Agilent SPS 4 autosampler was used, so large bottles (100 to 500 mL) could be used for long-term stability tests. The samples were self-aspirated using an Agilent PFA nebulizer with SPS 4 probe kit (G3139-68000). Data analysis was performed using the optional Single Nanoparticle Application module of Agilent ICP-MS MassHunter software.

**Table 1.** 8900 ICP-QQQ operating parameters used for spICP-MS method.

Parameter	Setting	Parameter	Setting
RF Power (W)	1200	Energy Discrimination (V)	-8.0
Sampling Depth (mm)	16	Cell gas (O <sub>2</sub> ) Flow (mL/min)	0.38 (25%)
Neb Gas Flow (L/min)	0.75	Dwell Time (us)	100
Makeup Gas Flow (L/min)	0.5	Scan Mode	Single quad mode
*Option Gas (O <sub>2</sub> ) Flow (L/min)	0.12 (12%)	Mass Monitored	56 (Fe)
Spray Chamber Temp (deg)	-2	Data Acquisition Time (s)	60
Axial Acceleration (V)	2		

*\*Direct injection of organic solvents was possible by adding oxygen (50% balanced with Ar) to prevent the deposition of carbon on the cones.*

The spICP-MS method was used to measure isopropyl alcohol (IPA), propylene glycol methyl ether acetate (PGMEA), and propylene glycol monomethyl ether (PGME) spiked with 15 nm Fe<sub>2</sub>O<sub>3</sub> NPs (Sigma Aldrich). Figure 1 shows the signal distribution (upper) and size distribution plots (lower) for Fe NPs in each of the samples. The NP signals were clearly separated from the background signals. Also, the mean measured particle size was around 15 nm in all spiked samples, which is consistent with the nominal Fe NP diameter of 15 nm.

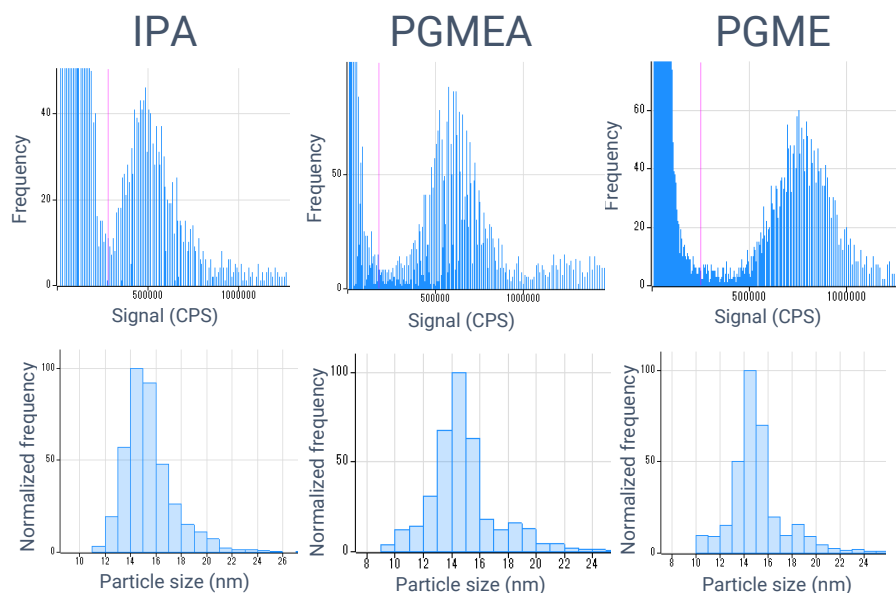


**Figure 1.** Signal distribution (upper) and size distribution (lower) of 15 nm Fe NPs in solution of IPA, PGMEA, and PGME.

### Size ratio of 15 and 30 nm particles

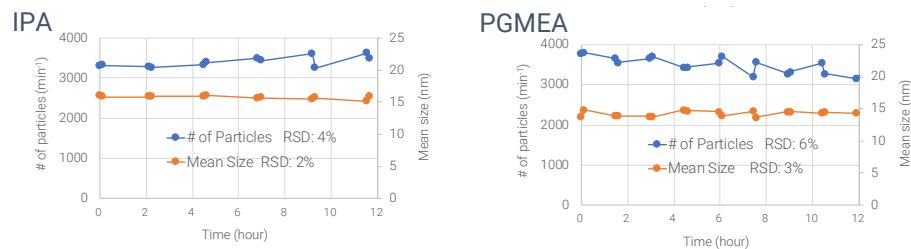
Table 2 shows the average signal intensities from one particle with a 30 nm diameter and one particle with a 15 nm diameter, and the ratio of these intensities (30 nm/15 nm). As the signal intensity is proportional to the cube of the diameter of the particle, the ratio of signal intensities from the 15 and 30 nm NPs should be 8. The measured ratio was 8.44, which is acceptable, considering the accuracy of the nominal diameters.

**Table 2.** Average particle signal intensities and ratio of the intensities.

Average signal intensity from one particle (cps)		Ratio (30 nm/15 nm)
30 nm	15 nm	
5,216,482	617,736	8.44

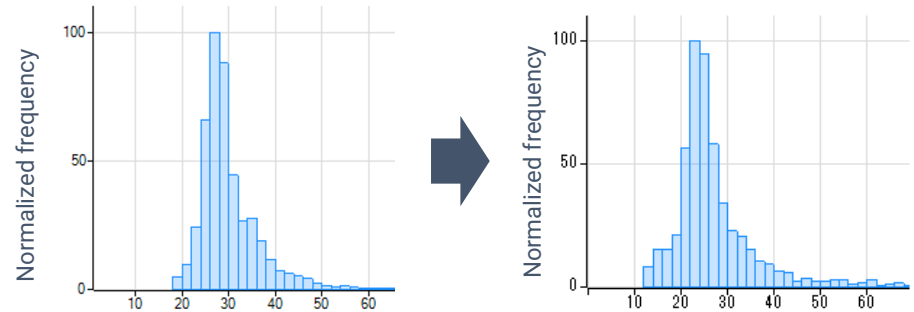
### Long-term stability tests

Figure 2 shows the stability of detected number (representing particle number concentration) and particle size for 15 nm Fe NPs in two of the solvents over 10 hours. Both the detected particle number and the size were constant over 10 hours, as indicated by the %RSDs.



**Figure 2.** Long-term stability of 15 nm Fe NPs in IPA and PGMEA over 10 hours.

Figure 3 shows the size distribution profiles of 30 nm Fe NPs in IPA on the day of sample preparation and six months later. After six months, the signals from 30 nm Fe NPs were clearly observed and the shape of the size distribution is almost the same as the one in the fresh solution. The results show that Fe NPs are stable in IPA for a long period, suggesting that they don't dissolve into or precipitate out of the solvent.



**Figure 3.** Size distribution of 30 nm Fe NPs in IPA on the day of preparation (left) and six months later (right).

### Single particles in high purity solvents

The 8900 spICP-MS method satisfies the emerging needs of the semiconductor industry to monitor low concentrations of small sized particles in high purity solvents.

# GC-ICP-QQQ Achieves Sub-ppb Detection Limits for Hydride Gas Contaminants

## Authors

William Geiger, ConSci Corporation,  
Pasadena, Texas, USA

Emmett Soffey, Steve Wilbur and Chris  
Scanlon, Agilent Technologies Inc.,  
USA

## Keywords

semiconductor, petrochemical,  
phosphine, arsine, hydrogen sulfide,  
carbonyl sulfide, germane, silane,  
oxygen mass-shift, hydrogen on-mass

## Introduction

Hydride gases, such as phosphine and arsine, are important contaminants in process chemicals used in both the petrochemical and semiconductor industries. The presence of phosphine, arsine, hydrogen sulfide, and carbonyl sulfide in polymer grade ethylene or propylene can have a deleterious effect on catalysts used in the production of polypropylene plastics. In the semiconductor industry, phosphine is used as a precursor for the deposition of group III-V compound semiconductors, and as a dopant in the manufacturing of semiconductor devices, such as diodes and transistors. The presence of unwanted hydride gas impurities can have a profound effect on the performance of the final device.

To date, measurement of these contaminants at ppb levels has been sufficient, but increasing competition within the industry and evolving performance criteria are pushing specifications ever lower. In addition, high purity gas manufacturers often require analytical detection limits 5-10 times lower than reported specifications. In anticipation of increasing industry demand for lower level detection, a new high sensitivity GC-ICP-QQQ method was developed for this application.

## Experimental

**Instrumentation:** An Agilent 7890 GC was coupled to an Agilent 8800 #200 using the Agilent GC-ICP-MS interface.

**Acquisition conditions:** MS/MS mass-shift mode using oxygen as the cell gas for the measurement of Ge, As, P and S. MS/MS mode with hydrogen cell gas was used for the on-mass measurement of the primary isotope of Si at  $m/z$  28.

**Table 1.** Agilent 8800 ICP-QQQ operating conditions.

	O <sub>2</sub> mode	H <sub>2</sub> mode
RF power (W)		1350
Sample depth (mm)		8.4
Argon carrier (make-up) gas flow (L/min)		0.85
Extract 1 (V)		-150
Extract 2 (V)		-190
Kinetic Energy Discrimination (V)	-4	0
Cell gas/flow (mL/min)	0.35	5.0

**Reagents and sample preparation:** Gas standards of silane, phosphine, germane, arsine (all balanced with H<sub>2</sub>), and hydrogen sulfide and carbonyl sulfide (balanced with Ar) were supplied by Custom Gas Solutions at a nominal value of 10 ppmv. These standards were dynamically diluted in helium using a pressure/flow restrictor based diluter supplied by Merlin MicroScience.



## Results and discussion

### Low level phosphine analysis

The purpose of this experiment was to establish a detection limit for phosphine ( $\text{PH}_3$ ) using GC-ICP-QQQ under ideal conditions. Q1 was set to  $m/z$  31 (the precursor ion  $^{31}\text{P}^+$ ) and Q2 was set to  $m/z$  47 to measure the product ion  $^{31}\text{P}^{16}\text{O}^+$ . Since the eluting peaks are relatively narrow, with duration of no more than  $\sim 12$  seconds, a maximum of 1 second was set for the total scan time. For the single element analysis of phosphine (measured as  $\text{PO}^+$ ), an integration time of 1.0 second was used. A multi-point calibration curve was generated for  $\text{PH}_3$  at concentrations of 8.2, 18.8 and 50.8 ppb. This covers the representative concentration range required for the measurement of this contaminant.

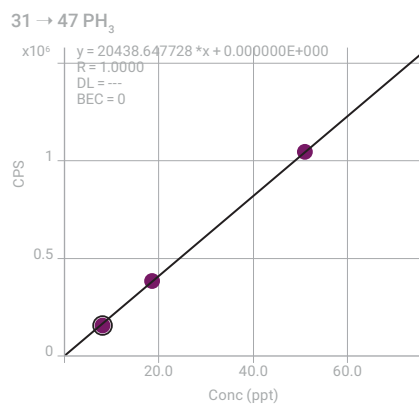


**Figure 1.** Phosphine calibration curve with an R value of 1.000 over the concentration range.

A low level phosphine standard ( $\sim 0.42$  ppb) was also prepared, to allow the detection limit (DL) to be calculated. Two different methods for DL calculation were used:

- Two times the signal to noise (S/N) of the phosphine peak in the low level standard based on "Peak to Peak" noise method
- The standard deviation of the concentrations measured in seven replicate analyses of the low level standard.

Full Time Range EIC (31  $\rightarrow$  47) : 030SMPL.d

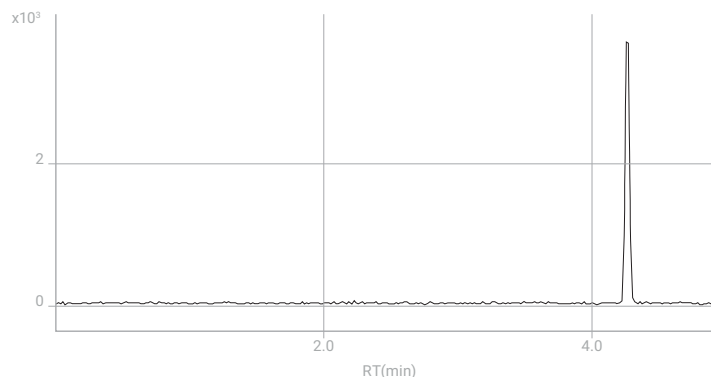


**Figure 2.** Chromatogram of 0.42 ppb  $\text{PH}_3$  standard. S/N: 96.9.

In the chromatogram shown in Figure 2, a S/N ratio of 96.9 was determined for the phosphine peak. Using the equation  $DL = 2 \times ((\text{concentration of standard}) / (S/N))$ , a detection limit approximation of 8.67 ppt was calculated based on  $2 \times ((0.42 \text{ ppb}) / (96.9))$ . Using the standard deviation method, where multiple replicates of the low level standard were analyzed, the detection limit was 19 ppt.

#### **Analysis of additional hydride gases**

The GC-ICP-QQQ method was applied to the multielement analysis of germane, arsine and phosphine within a single analysis. Ge and As were measured as their  $O_2$  reaction product ions,  $GeO^+$  and  $AsO^+$ , as was the case with P ( $PO^+$ ). Hydrogen sulfide ( $H_2S$ ) and carbonyl sulfide (COS) were also analyzed using  $O_2$  mass-shift mode, based on the ICP-QQQ measurement of sulfur as the  $^{32}S^{16}O^+$  reaction product ion at  $m/z$  48. For the analysis of silane, Si was measured directly (on-mass) at its major isotope  $^{28}Si$ , using  $H_2$  cell gas. The primary polyatomic interferences on  $^{28}Si^+$  are  $^{12}C^{16}O^+$  and  $^{14}N_2^+$ , due to the presence of  $CO_2$ ,  $N_2$  and  $O_2$  in the argon supply and from air entrainment into the plasma.  $H_2$  was selected as the reaction gas as both the  $CO^+$  and  $N_2^+$  interferences react readily with  $H_2$  cell gas.  $Si^+$  remains unreactive and so can be measured, free from interferences, at its original mass.

#### **Comparison of GC-ICP-QQQ and GC-ICP-MS DLs**

For comparison purposes,  $H_2S$ , COS,  $PH_3$ ,  $GeH_4$ ,  $AsH_3$ , and  $SiH_4$  were analyzed by both GC-ICP-QQQ with the 8800 ICP-QQQ, and GC-ICP-MS using the same GC method with an Agilent 7900 conventional quadrupole ICP-MS. A summary of the detection limits (DLs) for both techniques is given in Table 1. For analytes where the background noise is very low (Ge-74, As-75), single digit ppt level detection limits are easily achieved using either GC-ICP-MS or GC-ICP-QQQ. However, for analytes that are prone to higher backgrounds (P-31 and S-32), significantly lower detection limits can be achieved by using MS/MS with  $O_2$  cell gas and measuring the oxygen addition reaction product ions  $PO^+$  and  $SO^+$  in mass-shift mode. In addition, MS/MS mode with  $H_2$  cell gas provides effective removal of background interferences at mass 28, allowing on-mass measurement of Si at its primary isotope.

**Table 1.** Detection limit comparison between GC-ICP-QQQ and GC-ICP-MS.

Hydride gas	8800 ICP-QQQ		7900 ICP-MS	
		DL, ppb		DL, ppb
H <sub>2</sub> S	32 -> 48 (O <sub>2</sub> )		32 (No gas)	
	MDL 7 reps	0.21	MDL 7 reps	0.62
	MDL 2 X S/N	0.11	MDL 2 X S/N	0.22
COS	32->48 (O <sub>2</sub> )		32 (No gas)	
	MDL 7 reps	0.12	MDL 7 reps	0.51
	MDL 2 X S/N	0.11	MDL 2 X S/N	0.21
PH <sub>3</sub>	31->47 (O <sub>2</sub> )		31 (No gas)	
	MDL 7 reps	0.019	MDL 7 reps	0.139
	MDL 2 X S/N	0.009	MDL 2 X S/N	0.077
GeH <sub>4</sub>	74->90 (O <sub>2</sub> )		74 (No gas)	
	MDL 7 reps	NA	MDL 7 reps	0.013
	MDL 2 X S/N	0.0038	MDL 2 X S/N	0.0013
AsH <sub>3</sub>	75->91 (O <sub>2</sub> )		75 (No gas)	
	MDL 7 reps	NA	MDL 7 reps	0.016
	MDL 2 X S/N	0.0013	MDL 2 X S/N	0.006
SiH <sub>4</sub>	28->28 (H <sub>2</sub> )		28 (H <sub>2</sub> )	
	MDL 7 reps	0.14	MDL 7 reps	1.09
	MDL 2 X S/N	0.196	MDL 2 X S/N	1.18

NA = not available

**GC-ICP-QQQ sets benchmark detection limits**

The significantly lower background and higher sensitivity of the Agilent 8800 ICP-QQQ resulted in a GC-ICP-QQQ method that shows a clear advantage for the determination of a range of contaminants in high purity gases at the low detection levels demanded by the industry. Compared to GC-ICP-MS with conventional quadrupole ICP-MS, GC-ICP-QQQ DLs for silane, phosphine, hydrogen sulfide, and carbonyl sulfide were lower by a factor of 5 to 10, with silane detection limits in the ~200 ppt range and phosphine detection limits in the ~15 ppt range.

**More information**

Sub-ppb detection limits for hydride gas contaminants using GC-ICP-QQQ. Agilent Publication [5991-5849EN](#)

Find out more about CONSCI at [www.consci.com](http://www.consci.com) or contact William Geiger at [bill@conscicorp.com](mailto:bill@conscicorp.com)

# Determination of Trace Impurities in Electronic Grade Arsine by GC-ICP-QQQ

## Authors

William M. Geiger, Blake McElmurry,  
Jesus Anguiano<sup>1</sup>  
Mark Kelinske<sup>2</sup>

<sup>1</sup>CONSCI, Ltd., Pasadena, Texas, USA

<sup>2</sup>Agilent Technologies Inc., USA

Sub-ppb detection limits for hydride gas contaminants using a single column, single injection volume, and multi-tune method

## Introduction

Most electronic devices use silicon-based semiconductors. However certain applications can benefit from alternative semiconductor materials, such as III-V compound semiconductors. These compounds are made of elements from groups III and V of the periodic table, usually Al, Ga, or In combined with N, P, As, or Sb. The appeal of these compounds is that they have much higher “carrier mobility” than silicon, which means they offer high performance and greater chip density with lower power consumption and less heat generation. These are critical factors in microelectronics, leading to increased use of III-V compound semiconductors in high electron mobility transistors (HEMT) and field effect transistors (FET).

Unlike Si semiconductors, III-V compound semiconductors are also able to emit light, which makes them essential for the large and growing field of optoelectronics. Light emitting diodes (LED) are widely used in lighting, displays, illuminated switches, and infrared remote controls. Other III-V compound semiconductor devices include vertical-cavity surface-emitting lasers (VCSEL), which are used in optical fiber communications.

Among the most widely used III-V compounds are gallium arsenide (GaAs), aluminum gallium arsenide (AlGaAs), and indium gallium arsenide nitride (InGaAsN), all of which require arsine gas as a precursor for manufacture.

Dopants are added deliberately to modify the electrical properties of semiconductor materials, but incorporation of unwanted dopant elements into III-V compound semiconductor structures can be problematic, even at trace levels (1). The unwanted dopants will introduce energy levels in the energy gap of the semiconductor, altering the electrical and optical properties of the semiconductor substrate through an increase in electron mobility, leakage current, or photoluminescence.

For example, n-type dopants such as Ge, Si, P, and S increase leakage current and reduce the gain of transistors. Therefore, it is critical to determine the concentration of germane (GeH<sub>4</sub>), silane (SiH<sub>4</sub>), phosphine (PH<sub>3</sub>), and hydrogen sulfide (H<sub>2</sub>S) impurities in arsine to prevent them affecting the performance of the final device. There may be some slight variation in the gas purity levels required for the manufacture of each type of device, but, in general, process gases need to be free of dopant impurities. Because Ge is of particular concern in the manufacture of many devices, there is a need to measure GeH<sub>4</sub> impurities at or below single digit ppb levels in arsine. However, the ability to detect such low level impurities requires a highly sensitive analytical method.

Gas chromatography (GC) coupled with ICP-MS is currently the only technique capable of measuring germane in arsine at sub-ppb levels (2–4). The non-atmospheric molecular impurities typically determined by GC-ICP-MS are H<sub>2</sub>S, SiH<sub>4</sub>, PH<sub>3</sub>, and GeH<sub>4</sub>. Occasionally, stibine (SbH<sub>3</sub>), hydrogen selenide (H<sub>2</sub>Se), and stannane (SnH<sub>4</sub>) are also of interest.

The goal of this work was to measure as many of the critical hydride gas impurities as practically possible in arsine, using a single GC-ICP-MS injection and a multi-tune "time program" acquisition method. This approach avoids the need to use different detectors, columns, methods, and even instruments to cover the full range of impurities.

## Experimental

### Sample and standard preparation

Standards of SiH<sub>4</sub>, PH<sub>3</sub>, GeH<sub>4</sub>, and H<sub>2</sub>S were made using a 10 ppm standard mixture (Custom Gas Solutions, Durham, NC, USA) and dynamically diluting it to a value of 24 ppb using a UHP-MMSD dilution system (CONSCI, Pasadena, TX). Standards for H<sub>2</sub>Se, SbH<sub>3</sub>, and SnH<sub>4</sub> are difficult to obtain due to the labile nature of these compounds. Only qualitative retention time standards were made using hydride generation with sodium borohydride. Although H<sub>2</sub>Se, SbH<sub>3</sub>, and SnH<sub>4</sub> can be determined by GC-ICP-MS, they were not studied quantitatively in this investigation.

### Instrumentation

An Agilent 7890B GC was used for the separation of impurities in arsine and an Agilent 8900 Triple Quadrupole ICP-MS (ICP-QQQ) was used as the detector. The standard Agilent GC-ICP-MS interface was modified using a high flow Deans switch, as shown in Figure 1. This configuration allowed the arsine matrix to be vented at its elution time, preventing the matrix from entering the ICP-MS torch. The column was selected based on a previous study that used an Agilent 8800 ICP-QQQ (3). The GC operating parameters are given in Table 1.

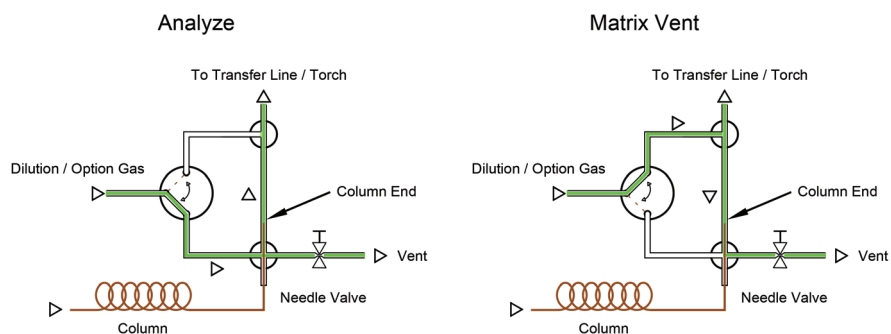


**Figure 1.** Schematic of the Deans switch used to vent arsine eluted by the GC column, preventing the matrix from being passed to the 8900 ICP-QQQ.

**Table 1.** GC operating parameters.

Parameter	Setting
Column	Two 100 m x 0.53 mm x 5.0 μm DB-1
Carrier Gas (psig Ar)	20
Oven Temperature (°C)	30 (isothermal)
Sample Size (μL)	60
Transfer Line Temperature (°C)	120

Standard instrument operating parameters for the ICP-MS recommended by Agilent were used. To optimize the ICP-QQQ, a standard containing 5 ppm sulfur hexafluoride, xenon, and krypton in argon (CSI Gas, Texas City, TX) was used. The standard was introduced into the argon dilution gas flow path at 2 mL/min and the signal at  $m/z$  32 was maximized. The S, Kr, and Xe peaks were used to optimize torch position and confirm mass calibration.

As described in a previous study (3), Agilent ICP-QQQ instruments feature two identical, full-sized quadrupole mass filters (Q1 and Q2), situated either side of the Octopole Reaction System (ORS) collision/reaction cell (CRC). This configuration enables double mass selection (MS/MS), which is vital for successful interference removal using reactive cell gases. Like Q2, Q1 operates in a high vacuum region, so it provides excellent resolution and abundance sensitivity while also maintaining high transmission. This allows precise selection of the ions that enter the cell, ensuring the reactions used to remove interferences on analyte ions are consistent and predictable. A reactive cell gas such as hydrogen, oxygen, or ammonia is used to react with either the interfering ion or the analyte ion ( $M^+$ ) to attain interference-free measurement. Analytes are measured in 'on-mass' or 'mass-shift' mode. When the cell gas reacts with the interferent, but not the analyte ion, the analyte is measured at its natural mass (on-mass) and the interference ions are removed by Q2. When the analyte ion reacts more readily with the cell gas than the interference ions do, the analyte forms a reaction product ion e.g.  $MH^+$  or  $MO^+$ . These product ions are then measured at a new mass, away from the interfering ion overlaps.

The ICP-QQQ can also be operated in no gas mode or the ORS cell can be pressurized with a collision gas, such as helium (He). He mode removes many common polyatomic ion interferences by kinetic energy discrimination (KED) or by collision-induced dissociation (CID).

Compared to the 8800 ICP-QQQ used in the previous study (3), the 8900 uses newer technology, such as an ORS<sup>4</sup> cell, which provides higher sensitivity and lower backgrounds. In addition, the 8900 #100 (Advanced Applications) model used in this work includes inert, low sulfur and silicon argon gas lines, which reduce instrumental backgrounds for these elements. To identify the best method conditions for the application, three different MS/MS tune modes were investigated: no gas, hydrogen, and oxygen with and without a mass-shift. Instrument operating conditions are listed in Table 2.

**Table 2.** ICP-QQQ operating parameters.

Parameter	No Gas	H <sub>2</sub>	O <sub>2</sub>
RF Power (W)	1450		
Sampling Depth (mm)	3		
Dilution Gas Flow (L/min)	0.7		
Extract 1 (V)	-20		
Extract 2 (V)	-250		
Kinetic Energy Discrimination (V)	5	2	-7
Cell Entrance (V)	-50		
Cell Exit (V)	-80	-70	
Cell Gas Flow Rate	NA	2 mL/min	0.6 mL/min (40% of full scale)

## Method development

The method conditions that provided the best detection limits (DLs) for each compound are summarized using bold text in Table 3. The DLs were calculated from signal-to-noise value multiplied by three (as described later). For analytes where the background noise is low due to the absence of interferences (e.g.  $^{74}\text{Ge}$ ), single digit ppt level DLs were easily achieved using GC-ICP-QQQ operating in no gas,  $\text{H}_2$ , or  $\text{O}_2$  mode. For analytes that are prone to higher backgrounds, such as  $^{31}\text{P}$ ,  $^{32}\text{S}$ , and  $^{28}\text{Si}$ , lower DLs were achieved using a reactive cell gas method. The presence of  $\text{CO}_2$ ,  $\text{N}_2$ , and  $\text{O}_2$  in the argon supply and from air entrainment into the plasma leads to the formation of spectral interferences. These interferences include  $^{12}\text{C}^{18}\text{OH}^+$ ,  $^{14}\text{N}^{16}\text{OH}^+$ ,  $^{15}\text{N}_2\text{H}^+$ ,  $^{15}\text{N}^{16}\text{O}^+$  and  $^{13}\text{C}^{18}\text{O}^+$  on  $^{31}\text{P}^+$ ,  $^{16}\text{O}_2^+$  and  $^{14}\text{N}^{18}\text{O}^+$  on  $^{32}\text{S}^+$ , and  $^{12}\text{C}^{16}\text{O}^+$  and  $^{14}\text{N}_2^+$  on  $^{28}\text{Si}^+$ . P and S react quickly with  $\text{O}_2$ , so both analytes were measured as reaction product ions,  $^{31}\text{P}^{16}\text{O}^+$  and  $^{32}\text{S}^{16}\text{O}^+$ , at  $m/z$  47 and 48, respectively, in mass-shift mode.  $\text{H}_2$  cell gas provided effective removal of the background interferences at mass 28, allowing on-mass measurement of  $^{28}\text{Si}^+$  at  $m/z$  28.

The measurement of different analytes in different reaction modes is simple to set up and run using a single multi-tune method on the 8900. In the acquisition method, the cell gases and measurement modes are switched automatically during the analysis, giving a fast and automated analysis using the optimum mode for each analyte. Switching conditions during the run allows the analyst to use the best cell conditions, as well as increase the analyte acquisition times to improve sensitivity.

Increasing the injection volume would provide even lower DLs for all compounds except for  $\text{H}_2\text{S}$ . A 60  $\mu\text{L}$  (or smaller) sample size is needed for the separation of  $\text{H}_2\text{S}$  from the arsine matrix.

**Table 3.** Comparison of GC-ICP-QQQ method conditions for each gas mode.

	No Gas				
	Mass	Integration Time (s)	Area of 24 ppb Standard	S/N	3 sigma DL, ppbv
Silane	28 > 28	0.2	165967	14	5
Germane	74 > 74	0.2	447435	8260	0.01
Phosphine	31 > 31	0.2	32118	870	0.08
Hydrogen sulfide	32 > 32	0.2	234053	175	0.41
	Hydrogen				
	Mass	Integration Time (s)	Area of 24 ppb Standard	S/N	3 sigma DL, ppbv
Silane	28 > 28	0.2	79068	42	1.7
Germane	74 > 74	0.2	272006	8300	0.01
Phosphine	31 > 31	0.2	17919	650	0.11
Hydrogen sulfide	32 > 32	0.2	145124	180	0.40
	Oxygen				
	Mass	Integration Time (s)	Area of 24 ppb Standard	S/N	3 sigma DL, ppbv
Silane	28 > 28	0.2	51499	34	2
Silane	28 > 44	0.2	34201	37	2
Germane	74 > 74	0.2	422359	8000	0.01
Germane	74 > 90	0.2	15577	1240	0.06
Phosphine	31 > 31	0.2	0	0	NA
Phosphine	31 > 47	0.2	29011	1500	0.05
Hydrogen sulfide	32 > 32	0.2	22579	13	6
Hydrogen sulfide	32 > 48	0.2	218640	290	0.24

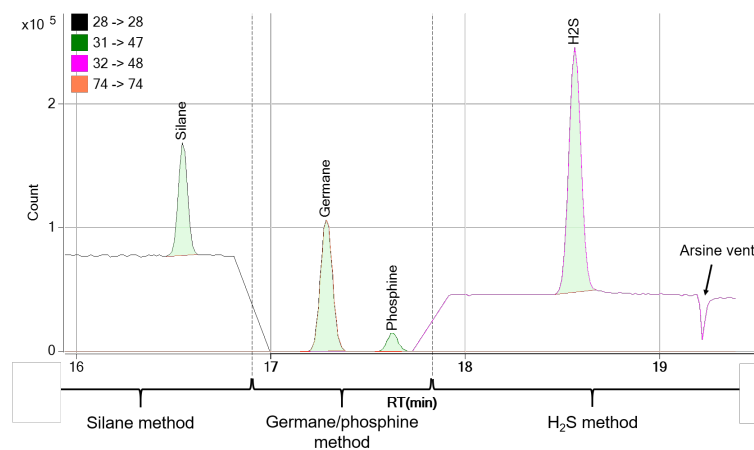


**Figure 2.** Overlaid chromatograms of  $\text{SiH}_4$ ,  $\text{PH}_3$ ,  $\text{H}_2\text{S}$ , and  $\text{GeH}_4$  in arsine by GC-ICP-QQQ obtained using a multi-tune method.

### Multi-element analysis of $\text{SiH}_4$ , $\text{PH}_3$ , $\text{H}_2\text{S}$ , and $\text{GeH}_4$

Since the best sensitivity (peak area) was obtained using different cell gas conditions for each analyte compound, a time program method was used where the acquisition conditions were changed during the run. The optimized single-method parameters are given in Table 4 and the chromatograms are shown in Figure 2. If analysts preferred to simplify the analysis and use a single cell gas,  $\text{O}_2$  would provide acceptable data, with some loss of sensitivity compared to the multi-tune method.

**Table 4.** Multi-tune method parameters.

	Acquisition Time (s)	Retention Time (s)	Gas Mode	Q1 -> Q2	Integration Time/Mass (s)
Silane	1008	992	$\text{H}_2$	28 -> 28	0.8
Germane	77	1037	$\text{O}_2$	74 -> 74	0.2
Phosphine		1057	$\text{O}_2$	31 -> 47	0.4
Hydrogen sulfide	89	1112	$\text{O}_2$	32 -> 48	0.8

**Table 5.** DLs for  $\text{SiH}_4$ ,  $\text{GeH}_4$ ,  $\text{PH}_3$ , and  $\text{H}_2\text{S}$ .

	Mass	Integration Time (s)	Gas Mode	Area of 24 ppb Standard	S/N	3 sigma DL, ppbv
Silane	28 > 28	0.8	$\text{H}_2$	308146	140	0.51
Germane	74 > 74	0.2	$\text{O}_2$	438374	8000	0.01
Phosphine	31 > 47	0.4	$\text{O}_2$	60451	4700	0.02
Hydrogen sulfide	32 > 48	0.8	$\text{O}_2$	883099	490	0.15

## Results and discussion

The DLs reported for  $\text{SiH}_4$ ,  $\text{GeH}_4$ ,  $\text{PH}_3$ , and  $\text{H}_2\text{S}$  (Table 5) were determined using the chromatograms (Figure 2) that were obtained using the parameters outlined in Table 4. The ICP-MS MassHunter software signal-to-noise (S/N) tool was used. The software divides the concentration of the analyte by the S/N value followed by multiplication by three to determine the DL. The EPA protocol MDL and a Student T-test could have been applied if a standard 10 times or less than the expected DL had been available (5). That level standard was not available for this work.



Other compounds of potential interest in the quality control testing of arsine including  $\text{H}_2\text{Se}$  and  $\text{SbH}_3$  eluted well beyond the arsine retention time (not shown in Figure 2). The relative retention time of  $\text{SnH}_4$  and arsine prevented  $\text{SnH}_4$  from being separated on a boiling point column, so an Agilent Select Low Sulfur column (p/n CP8575) was used instead. DLs for  $\text{SnH}_4$ ,  $\text{H}_2\text{Se}$ , and  $\text{SbH}_3$  were estimated at 1 ppb or lower, based on their relative response in aqueous samples and their first ionization potentials.

## Conclusion

GC-ICP-QQQ was used to separate and measure all hydride gas contaminants in arsine at or below single digit ppbv levels. Germane, which is probably the most critical contaminant in semiconductor-grade arsine, was determined at low ppt levels. Measurements of  $\text{SiH}_4$ ,  $\text{PH}_3$ ,  $\text{H}_2\text{S}$ ,  $\text{GeH}_4$ ,  $\text{H}_2\text{Se}$ , and  $\text{SbH}_3$  were performed using a single GC column and a single injection.

The best detection limits for all compounds were achieved by operating the 8900 ICP-QQQ in MS/MS mode with  $\text{H}_2$  and  $\text{O}_2$  cell gases. Using a single multi-tune method allowed us to maximize signal averaging, and therefore achieve low DLs with a single injection.

The determination of dopants/contaminants in arsine provides extra process control to aid in the quality of the manufacturing process, thus improving the yield and performance of micro-electronic and opto-electronic devices.

## References

1. J. Feng, R. Clement, M. Raynor, Characterization of high-purity arsine and gallium arsenide epilayers grown by MOCVD. *J. of Crystal Growth*, **2008**, 310, 23, 4780–4785
2. C. J. Meyer and W. M. Geiger, The Chromatographic Analysis of Trace Atmospheric Gases. In J. D. Hogan (Ed.), *Specialty Gas Analysis: A Practical Guidebook*. 1997, 76–77. New York: Wiley-VCH.
3. W. M. Geiger and E. Soffey, GC-ICP-QQQ Achieves Sub-ppb Detection Limits for Hydride Gas Contaminants. In *Agilent 8800 ICP-QQQ Application Handbook*, Fourth edition, **2020**, 37–40, Agilent publication [5991-2802EN](#)
4. D. Decker and L. M. Sidisky, Gas Chromatographic Column Considerations. In W. M. Geiger, & M. W. Raynor (Eds.), Geiger, W. M., and Raynor, M. W. (2013). *Trace analysis of specialty and electronic gases*. (pp. 251–274). Hoboken, N.J: John Wiley & Sons, Inc.
5. G. Wells, H. Prest, C. W. Russ IV, Signal, Noise, and Detection Limits in Mass Spectrometry, Agilent publication, [5990-7651EN](#)

# Materials

Title	Page
<b>Rare earth oxides</b>	
Direct measurement of trace rare earth elements in high purity REE oxides	123
Removal of $MH^+$ interferences in refined REE material analysis	126
Direct analysis of trace REEs in high purity $Nd_2O_3$	129
Direct determination of challenging trace rare earth elements in high purity lanthanide REE oxides	132
<b>Metals</b>	
Arsenic measurement in cobalt matrix using MS/MS mode with oxygen mass-shift	135
Analysis of ultratrace impurities in high purity copper using the Agilent 8900 ICP-QQQ	138
Determination of sulfur, phosphorus, and manganese in high purity iron	145
The benefits of improved abundance sensitivity with MS/MS for trace elemental analysis of high purity metals	148
Ultratrace copper analysis in a semiconductor grade organometallic titanium complex	152
<b>Nanomaterials</b>	
Analysis of 10 nm gold nanoparticles using the high sensitivity of the Agilent 8900 ICP-QQQ	155
High sensitivity analysis of $SiO_2$ nanoparticles using the Agilent 8900 ICP-QQQ	158
Accurate determination of $TiO_2$ nanoparticles in complex matrices using the Agilent 8900 ICP-QQQ	161

# Direct Measurement of Trace Rare Earth Elements in High Purity REE Oxides

## Author

Kazumi Nakano  
Agilent Technologies, Japan

## Keywords

Rare Earth Elements, REE, rare earth oxide, REO, samarium oxide, gadolinium oxide, oxygen mass-shift, ammonia on-mass

## Introduction

The rare earth elements (REEs) are widely used in advanced technologies including high-power permanent magnets, lasers, phosphors used in fluorescent lamps, radar screens and plasma displays. REEs are also used in petroleum refining, automobile catalytic converters and batteries, and in high-technology glasses. It is clear from these examples that REEs play a key role in many types of materials used in high-technology industries. However, the presence of other REEs as contaminants in a purified single-element REE material often impacts the functionality of the final product, so impurities in the REE oxide raw material must be carefully controlled.

ICP-MS is the most commonly used atomic spectrometry technique for the measurement of trace REEs due to its simple REE spectra – particularly when compared to emission techniques. The measurement of mid- and high-mass REEs in a low-mass REE matrix is, however, very challenging for ICP-MS because REEs have among the highest metal-oxide (M-O) bond strengths of any element, and the oxide ions of the low mass REE overlap the preferred isotopes of the mid-mass and high-mass REEs. Table 1 shows the interferences observed in the analysis of trace REEs in high-purity samarium (Sm) oxide and gadolinium (Gd) oxide.

Separation of the trace REE analytes from the REE matrix can be performed utilizing a chelating resin, but this technique is time-consuming and customization is needed according to the analyte and matrix element. The direct analysis of trace REEs in a variety of high-purity REE matrices is therefore desired. In this work, an Agilent 8800 Triple Quadrupole ICP-MS was used for the direct analysis of trace REE in two high-purity REE materials: Sm<sub>2</sub>O<sub>3</sub> and Gd<sub>2</sub>O<sub>3</sub>. Operating the ICP-MS in MS/MS mode effectively removes the challenging interferences, enabling the determination of REE impurities at trace levels in these two materials.

**Table 1.** Preferred isotope for ICP-MS analysis of each REE, and the potential interferences caused by Sm<sub>2</sub>O<sub>3</sub> and Gd<sub>2</sub>O<sub>3</sub> matrices.

Element	La	Ce	Pr	Nd	Sm	Eu	Gd	Tb	Dy	Ho	Er	Tm	Yb	Lu
Mass	139	140	141	146	147	153	157	159	163	165	166	169	172	175
Gd <sub>2</sub> O <sub>3</sub>							N/A	GdH <sup>+</sup>					GdO <sup>+</sup>	GdOH <sup>+</sup>
Sm <sub>2</sub> O <sub>3</sub>					N/A	SmH <sup>+</sup>			SmO <sup>+</sup>	SmO <sup>+</sup>	SmO <sup>+</sup>	SmO <sup>+</sup>	SmOH <sup>+</sup>	

## Experimental

**Instrumentation:** Agilent 8800 #100.

**Plasma conditions:** Preset plasma/General purpose.

**Ion lens tune:** Soft extraction tune: Extract 1 = 0 V, Extract 2 = -180 V.

**Acquisition parameters:** Three cell modes were used with MS/MS acquisition: No gas, O<sub>2</sub> mass-shift, and NH<sub>3</sub> on-mass mode. In MS/MS O<sub>2</sub> mass-shift mode, the REEs were determined as their oxide ions. REE ions react efficiently with the O<sub>2</sub> cell gas and are converted to the oxide ion REE-O<sup>+</sup>. For example, in the measurement of <sup>153</sup>Eu<sup>+</sup>, Q1 is set to *m/z* 153 (<sup>153</sup>Eu<sup>+</sup>) and Q2 is set to *m/z* 169 (<sup>153</sup>Eu<sup>16</sup>O<sup>+</sup>). Cell tuning parameters are summarized in Table 2.

**Table 2.** CRC tuning parameters.

Cell mode	Unit	No gas	O <sub>2</sub>	*NH <sub>3</sub>
Scan mode	MS/MS			
Cell gas		N/A	O <sub>2</sub>	NH <sub>3</sub>
Cell gas flow rate	mL/min	N/A	0.35	9.0
Octopole bias	V	-8	-5	-18
KED	V	5	-8	-8
Cell exit	V	-80	-90	-110
Deflect lens	V	20	10	-3
Plate	V	-80	-90	-110

\*10% NH<sub>3</sub> balanced in Ar

## Results and discussion

Two high purity REE oxide materials Gd<sub>2</sub>O<sub>3</sub> (5N) and Sm<sub>2</sub>O<sub>3</sub> (4N8) were gently dissolved in semiconductor grade HNO<sub>3</sub> and diluted to a concentration of 1 ppm (as the REE). The other (trace) REEs were measured in each matrix solution using the three cell modes. The results are given in Figure 1 and Figure 2. As expected, analysis of the 1 ppm Gd solution in no gas mode gave positive errors on some elements due to interferences from Gd polyatomic ions: GdH<sup>+</sup> interferes with <sup>159</sup>Tb<sup>+</sup>, GdO<sup>+</sup> interferes with <sup>172</sup>Yb<sup>+</sup> and GdOH<sup>+</sup> interferes with <sup>175</sup>Lu<sup>+</sup>.

Preliminary studies showed that NH<sub>3</sub> cell gas reacts with many of the polyatomic ions that interfere with the REE. However, NH<sub>3</sub> also reacts quickly with some of the REE ions, leading to reduced sensitivity of < 1 cps/ppt [1], so this mode is only suitable for the measurement of the less reactive analytes: Pr, Eu, Dy, Ho, Er, Tm and Yb. For these elements, NH<sub>3</sub> on-mass mode gave excellent results, including for Yb in the Gd matrix, where the measured Yb background concentration was reduced by four orders of magnitude (Figure 1) indicating effective removal of the GdO<sup>+</sup> overlap. Background signals for Dy, Ho, Er and Tm in the Sm matrix were also dramatically improved (Figure 2).

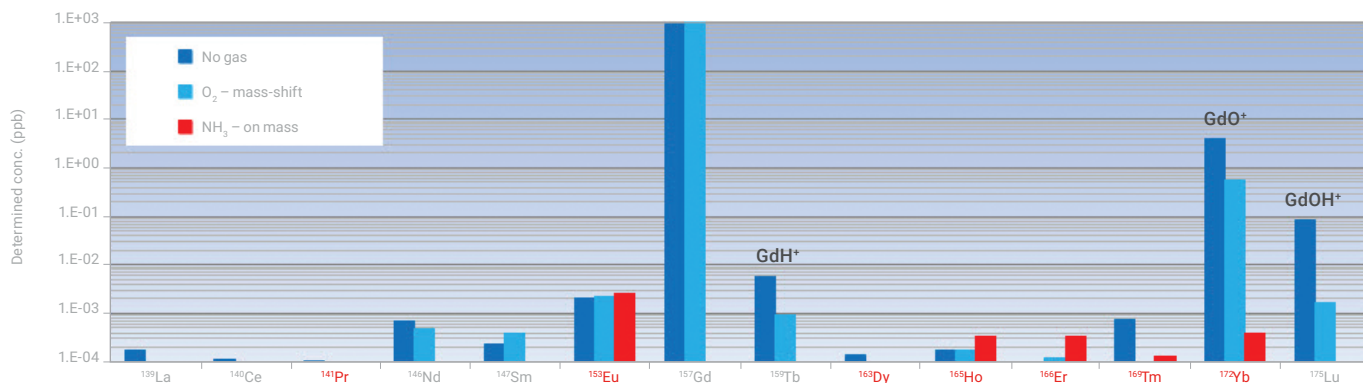


**Figure 1.** Measured concentration of REE impurities in 1 ppm Gd solution. Gd based interferences are observed on Tb, Yb and Lu. Only the elements in red were measured in  $\text{NH}_3$  on-mass mode.

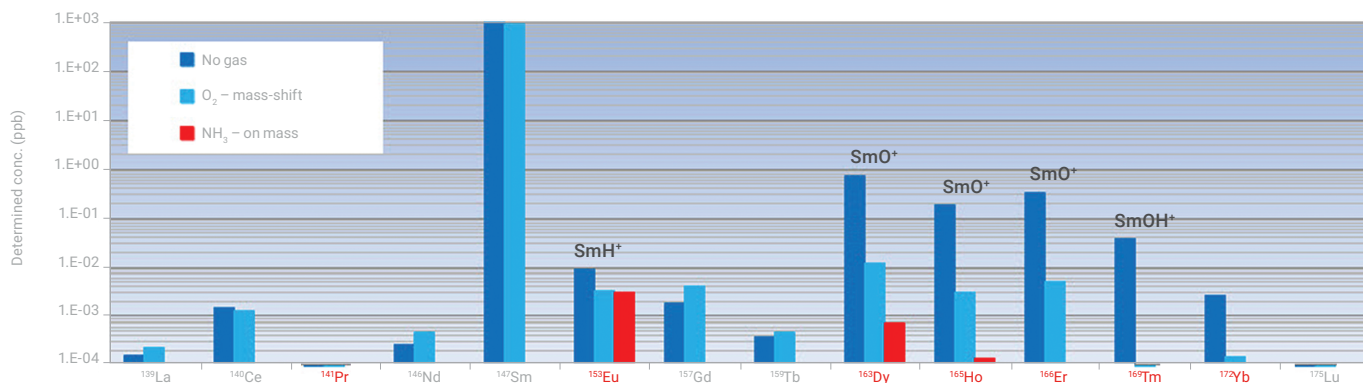


**Figure 2.** Measured concentration of REE impurities in 1 ppm Sm solution. Sm based interferences are observed on Eu, Dy, Ho, Er, Tm and Yb. Only the elements in red were measured in  $\text{NH}_3$  on-mass mode.

For the REEs that react with  $\text{NH}_3$  (La, Ce, Nd, Sm, Gd, Tb and Lu),  $\text{O}_2$  mass-shift mode and measurement of the target analyte as its  $\text{REE-O}^+$  ion is the preferred approach. Most REEs are effectively converted to the oxide ion via reaction with  $\text{O}_2$  cell gas [7], and this mode was applied to the measurement of Lu in the Gd matrix, avoiding the  $\text{GdOH}^+$  interference on the  $\text{Lu}^+$  isotope and giving a good improvement in the background signal. Compared to no gas mode,  $\text{O}_2$  mass-shift mode also gave a good improvement in the background signals for Dy, Ho, Er, Tm and Yb in the Sm matrix, but for all these analytes the backgrounds in  $\text{NH}_3$  mode were lower still.

## Reference

1. Direct measurement of trace rare earth elements (REEs) in high-purity REE oxide using the Agilent 8800 Triple Quadrupole ICP-MS with MS/MS mode, Agilent application note, [5991-0892EN](#).

# Removal of MH<sup>+</sup> Interferences in Refined REE Material Analysis

## Author

Naoki Sugiyama  
Agilent Technologies, Japan

## Keywords

Rare Earth Elements, REE, geochemistry, mining, material science, lanthanum, barium, cerium, method of standard additions, MSA, oxygen mass-shift

## Introduction

The measurement of Rare Earth Elements (REEs) is of great importance in geochemistry, mining and material science. Manufacturers of high purity REE materials need to quantify metal impurities, including trace levels of the other REEs, in the refined, single element REE matrix. ICP-MS is the technique of choice for the measurement of REEs, but most of the REE isotopes suffer from interference by polyatomic species (predominantly hydride ions, MH<sup>+</sup> and oxide ions, MO<sup>+</sup>) derived from other, lower-mass REE elements. While MH<sup>+</sup> interferences are lower in intensity than MO<sup>+</sup> interferences, they present a more challenging problem for REEs that have no isotope free from interference. For example, <sup>139</sup>La<sup>+</sup> is interfered by <sup>138</sup>BaH<sup>+</sup> and <sup>140</sup>Ce<sup>+</sup> by <sup>139</sup>LaH<sup>+</sup>. These interferences are too close in mass to be resolved by high-resolution (HR-)ICP-MS [1]. In this paper, we describe the removal of the MH<sup>+</sup> interferences using an Agilent 8800 ICP-QQQ in MS/MS mass-shift mode, with oxygen as the reaction gas.

## Experimental

**Instrumentation:** Agilent 8800 #100. The standard glass nebulizer was replaced with a C-flow nebulizer (G3285-80000) for optimal washout between the high matrix samples.

**Plasma conditions:** Preset plasma/General purpose.

**Ion lens tune:** Soft extraction tune: Extract 1 = 0 V, Extract 2 = -180 V.

**CRC conditions:** O<sub>2</sub> gas at 0.3 mL/min, Octopole bias = -5 V, KED = -5 V.

**Acquisition parameters:** MS/MS mode with O<sub>2</sub> mass-shift method.

Figure 1 illustrates the mechanism of MS/MS O<sub>2</sub> mass-shift mode used for measuring Ce in a La matrix sample. The major isotope of Ce at *m/z* 140 suffers an interference from <sup>139</sup>LaH<sup>+</sup>. Q1 is set to *m/z* 140, allowing only the analyte ion <sup>140</sup>Ce<sup>+</sup> and any other ions at *m/z* 140 to pass through to the cell. All other ions not at *m/z* 140 are rejected. In the cell, Ce reacts with oxygen to form CeO<sup>+</sup> at *m/z* 156. Q2 is set to *m/z* 156, allowing CeO<sup>+</sup> to pass to the detector. Since <sup>139</sup>LaH<sup>+</sup> does not react with O<sub>2</sub> to form <sup>139</sup>LaOH<sup>+</sup>, it remains as LaH<sup>+</sup> at *m/z* 140 and is rejected by Q2. The same principle is used for the separation of <sup>139</sup>La<sup>+</sup> from <sup>138</sup>BaH<sup>+</sup> in a Ba matrix.

## Results and discussion

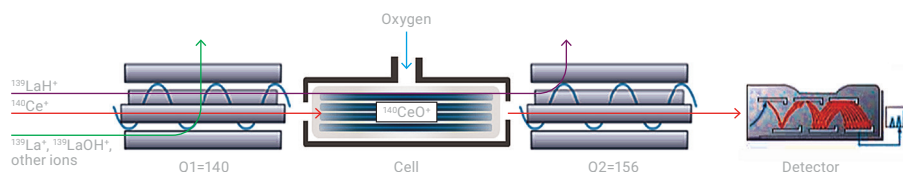


**Figure 1.** MS/MS mass-shift method with O<sub>2</sub> reaction gas; used for the measurement of Ce, as CeO at *m/z* 156, in a La matrix.

Using the Method of Standard Addition (MSA), the BECs and DLs of La in a matrix of 50 ppm Ba, and Ce in a matrix of 50 ppm La were determined. Data was acquired using MS/MS mode with O<sub>2</sub> mass-shift, and also using Single Quad (SQ) mode with O<sub>2</sub> reaction gas to emulate conventional quadrupole ICP-MS (ICP-QMS) for comparison.

As shown in Figures 2A and 2B, SQ mode with O<sub>2</sub> reaction gas suffers from interferences that prevent the measurement of La in the Ba matrix and Ce in the La matrix, respectively. In contrast, the calibration plots shown in Figures 2C and 2D demonstrate that MS/MS mode with O<sub>2</sub> mass-shift can successfully remove the matrix overlaps to permit the trace quantitation of La in a Ba matrix and Ce in a La matrix. The BECs and DLs achieved were 8.5 ppt and 2.5 ppt respectively for La in a 50 ppm Ba solution, and 10.6 ppt and 0.8 ppt respectively for Ce in a 50 ppm La solution.

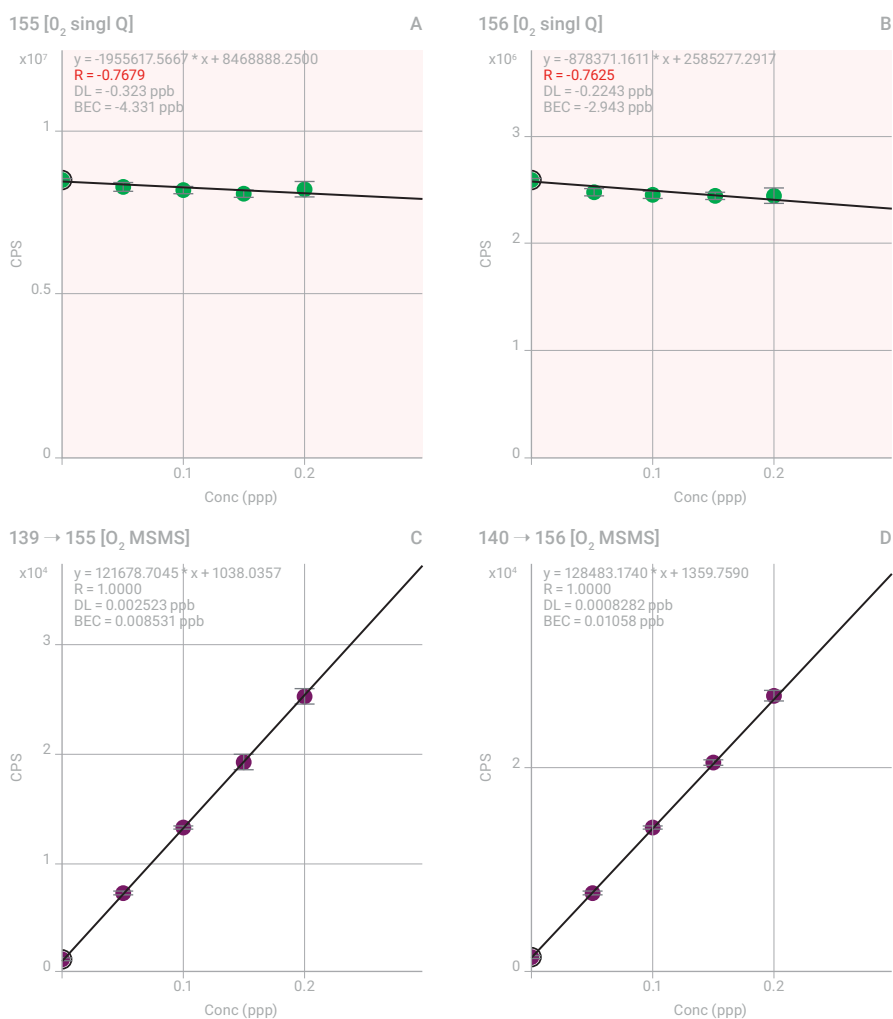


**Figure 2.** Top: Calibration plots up to 0.2 ppb for La in 50 ppm Ba matrix (A) and Ce in 50 ppm La matrix (B), acquired in SQ mode with oxygen reaction gas (emulating conventional quadrupole ICP-MS). Bottom: Calibration plots up to 0.2 ppb for La in 50 ppm Ba matrix (C) and Ce in 50 ppm La matrix (D) acquired in MS/MS mode with oxygen mass-shift.

## Investigation of unexpected product ion observed at $m/z$ 156 in the 50 ppm La matrix

The background signals that contributed to the poor result obtained for Ce in the La matrix using SQ mode with  $O_2$  reaction gas (Figure 2B) were investigated by carrying out a precursor ion scan for product ion mass 156. The precursor ion scan capability of the 8800 ICP-QQQ provides a uniquely powerful approach to identifying the source of potential polyatomic and reaction product interferences. Oxygen cell gas was introduced into the cell and a precursor ion spectrum was obtained by scanning Q1 from 2 to 260 u (Figure 3) with Q2 fixed at mass 156. From the spectrum, we can identify which precursor ions react with  $O_2$  to produce product ions at mass 156, overlapping  $^{140}\text{CeO}^+$  in SQ mode.

Figure 3 shows the precursor ion scan spectrum for product ion mass 156 for the 50 ppm La matrix, with intense peaks at  $m/z$  139 ( $^{139}\text{La}^+$ ) and 156 ( $^{139}\text{La}^{16}\text{OH}^+$ ). In SQ mode, as with conventional ICP-QMS, these ions all enter the cell, and with Q2 set to 156 u, the  $^{139}\text{La}^{16}\text{OH}^+$  polyatomic ions contribute to the signal measured at  $m/z$  156 ( $^{140}\text{Ce}$  measured as analyte product ion  $^{140}\text{CeO}^+$ ). These unwanted precursor ions cannot be rejected by a CRC operating as a bandpass filter in ICP-QMS, as they are too close in mass to the target analyte precursor ion. Only by using MS/MS mode on the 8800 ICP-QQQ, where Q1 operates as a unit mass filter, can non-target masses (like  $^{139}\text{La}^{16}\text{OH}^+$  in this example) be prevented from entering the cell.

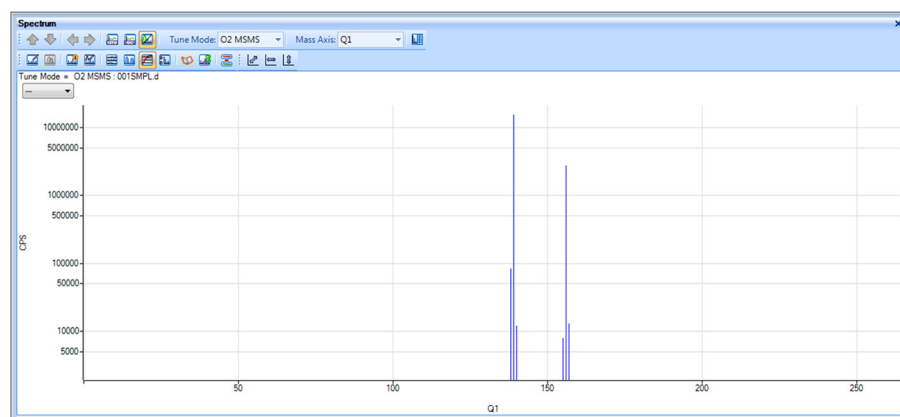


**Figure 3.** Precursor ion scan from 2-260 u for product ion mass 156, in a 50 ppm La matrix. Six peaks are seen at  $m/z$  = 138, 139, 140, 155, 156 and 157, with the intense peaks at  $m/z$  139 and  $m/z$  156 being due to  $^{139}\text{La}^+$  and  $^{139}\text{La}^{16}\text{OH}^+$  respectively.

## Reference

1. Sabine Becker and Hans Joachim Dietze, J. Anal. At. Spectrom., 1997, vol.12, p881.

## More information

Removal of hydride ion interferences ( $\text{MH}^+$ ) on Rare Earth Elements using the Agilent 8800 Triple Quadrupole ICP-MS, Agilent publication, [5991-1481EN](#)



# Direct Analysis of Trace REEs in High Purity Nd<sub>2</sub>O<sub>3</sub>

## Authors

Juane Song<sup>1</sup>, Xiang-Cheng Zeng<sup>1</sup>,  
Dong Yan<sup>1</sup> and Wei-ming Wu<sup>2</sup>

<sup>1</sup>Agilent Technologies, China,

<sup>2</sup>Jiangxi University of Science and  
Technology, Jiangxi, China

## Keywords

Rare earth elements (REE), high purity  
metals, neodymium, neodymium (III)  
oxide, oxygen mass-shift, ammonia  
on-mass, ammonia mass-shift,  
geochemistry, mining, materials  
science

## Introduction

Advanced technology products containing Rare Earth Elements (REEs) are increasing at a rapid rate. However, the presence of other REEs as contaminants in a purified single-element REE material may affect the functionality of the final product, so impurities in the REE oxide raw material must be carefully controlled.

The measurement of mid- and high-mass REEs in a low-mass REE matrix is challenging for ICP-MS because REEs have high metal-oxide (M-O) bond strengths, and the oxide ions of the low mass REEs overlap the preferred isotopes of the mid-mass and high-mass REEs. For example, in the analysis of trace REEs in high purity Nd<sub>2</sub>O<sub>3</sub>, <sup>145</sup>Nd<sup>16</sup>OH<sub>2</sub><sup>+</sup> and <sup>146</sup>Nd<sup>16</sup>OH<sup>+</sup> overlap the preferred isotope of dysprosium (<sup>163</sup>Dy<sup>+</sup>), <sup>143</sup>Nd<sup>16</sup>O<sup>+</sup> overlaps the only isotope of terbium (<sup>159</sup>Tb<sup>+</sup>) and <sup>148</sup>Nd<sup>16</sup>OH<sup>+</sup> overlaps the sole isotope of holmium (<sup>165</sup>Ho<sup>+</sup>). While separation of the trace REEs from the REE matrix can be performed using a chelating resin, this technique is time-consuming and needs to be customized to the particular analyte and matrix under investigation. Clearly there is a requirement for a method capable of the direct analysis of trace REEs in a variety of high purity REE matrices.

## Experimental

**Instrumentation:** Agilent 8800 #100.

**Plasma conditions:** Preset plasma/HMI-L.

**Acquisition parameters:**

Five operational modes were evaluated:

- No gas
- Helium mode, 5 mL/min
- O<sub>2</sub> mass-shift, 0.3 mL/min
- NH<sub>3</sub> on-mass, 8 mL/min (NH<sub>3</sub> as 10% NH<sub>3</sub> in He)
- NH<sub>3</sub> mass-shift, 3 mL/min, (NH<sub>3</sub> as 10% NH<sub>3</sub> in He).

**Sample and sample prep:** High purity Nd<sub>2</sub>O<sub>3</sub> (99.999%, purchased from the Baotou Research Institute of Rare Earths, China) was dissolved gently in semiconductor grade HNO<sub>3</sub>, and diluted to 500 ppm as Nd<sub>2</sub>O<sub>3</sub>.

## Results and discussion

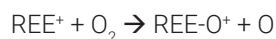
Thirteen trace REEs were measured in the Nd<sub>2</sub>O<sub>3</sub> sample using the five different cell modes, and the results are summarized in Table 1. As expected, the BEC of low- and mid-mass REEs, such as La, Ce, Pr, Sm, Eu and Gd (Pr and Sm were present as impurities) were comparable in all modes, as these elements are free from interferences due to Nd. In contrast, the BECs for high-mass REEs in He mode were lower in He mode than in no gas mode, suggesting that high mass REEs suffered interferences from Nd-derived polyatomic ions.

**Table 1.** BECs of 13 REEs in 500 ppm Nd<sub>2</sub>O<sub>3</sub>. All units ug/kg (ppb).

Element	Isotope	No gas	He	O <sub>2</sub> mass-shift	NH <sub>3</sub> on-mass	NH <sub>3</sub> mass-shift
La	139	0.143	0.127	0.143	-	-
Ce	140	0.018	0.012	0.011	-	-
Pr	141	1.376	1.202	1.056	-	-
Sm	152	1.061	0.950	0.999	-	-
Eu	153	0.032	0.026	0.028	-	-
Gd	155	0.035	0.046	0.033	-	-
Tb	159	442.6	74.6	1.258	-	0.022
Dy	163	250.3	196	1.161	0.040	-
Ho	165	20.43	16.2	0.101	0.004	-
Er	170	0.065	0.020	0.013	-	-
Tm	169	0.084	0.031	0.003	-	-
Yb	174	0.251	0.120	0.058	-	-
Lu	175	0.014	0.006	0.004	-	-

**O<sub>2</sub> mass-shift mode**

All 13 REEs react with O<sub>2</sub> efficiently to form REE-oxide ions, as shown below.



The MS/MS capability of the 8800 ICP-QQQ enables the removal of spectral interferences on each element using "mass-shift". For example in O<sub>2</sub> mass-shift mode, all 13 REEs can be detected as REE-O<sup>+</sup> ions at 16 u higher than the original elemental mass (M+16). From Table 1, it can be seen that O<sub>2</sub> reaction mode with mass-shift further reduced the BEC for Tb, Dy, Ho, Er, Tm, Yb, and Lu, compared to He mode.

While the improvement in O<sub>2</sub> mass-shift mode is significant for Tb, Dy and Ho that suffer intense interference from NdO<sup>+</sup>, the BECs of the other high-mass REEs such as Er, Tm, Yb and Lu were also improved in this mode, indicating that these elements also suffer interferences from Nd-based polyatomic ions: <sup>150</sup>NdOH<sub>3</sub><sup>+</sup> interferes with <sup>169</sup>Tm<sup>+</sup>, <sup>142</sup>NdN<sub>2</sub><sup>+</sup> (or <sup>142</sup>NdCO<sup>+</sup>) and <sup>144</sup>NdCN<sup>+</sup> with <sup>170</sup>Er<sup>+</sup>, <sup>142</sup>NdO<sub>2</sub><sup>+</sup> with <sup>174</sup>Yb<sup>+</sup>, <sup>143</sup>NdO<sub>2</sub><sup>+</sup> and <sup>144</sup>NdONH<sup>+</sup> (or <sup>144</sup>NdC<sub>2</sub>H<sup>+</sup>) with <sup>175</sup>Lu<sup>+</sup>. The contribution of the above mentioned interferences on Er, Tm, Yb and Lu are not overly significant. However, O<sub>2</sub> mass-shift mode was shown to be an effective approach for the removal of all polyatomic ion interferences, typically leading to a 5-10x lower BEC compared to no gas mode.

### **NH<sub>3</sub> on-mass mode for Dy and Ho**

A previous study showed that NH<sub>3</sub> cell gas reacts with many of the polyatomic ions that interfere with the REEs. However, NH<sub>3</sub> also reacts quickly with some of the REE ions, leading to reduced sensitivity of < 1 cps/ppt for La, Ce, Nd, Sm, Gd, Tb and Lu. NH<sub>3</sub> on-mass mode is valuable for the determination of a limited number of REEs; Pr, Eu, Dy, Ho, Er, Tm and Yb [1]. The results in Table 1 show that NH<sub>3</sub> on-mass mode gave excellent results for Dy and Ho in the Nd<sub>2</sub>O<sub>3</sub> matrix, with an improvement in BECs of 20x compared to O<sub>2</sub> mass-shift mode.

### **NH<sub>3</sub> mass-shift mode for Tb**

For the REEs that react efficiently with NH<sub>3</sub> (La, Ce, Nd, Sm, Gd, Tb and Lu), NH<sub>3</sub> mass-shift mode can be used. In this study, NH<sub>3</sub> mass-shift mode was investigated for the determination of Tb, and the reaction product ion TbNH<sup>+</sup> (*m/z* 174) was found to give the lowest BEC. A BEC of 22 ppt for Tb in a 500 ppm Nd<sub>2</sub>O<sub>3</sub> solution was achieved, which is 50x lower than the result achieved in O<sub>2</sub> mass-shift mode, indicating the effective removal of the NdO<sup>+</sup> overlap.

### **Conclusion**

The Agilent 8800 ICP-QQQ with MS/MS capability was used to successfully measure 13 REE impurities in a high-purity Nd<sub>2</sub>O<sub>3</sub> sample solution. Tandem MS with MS/MS mode is essential for accurate reaction mode analysis in a complex matrix. On conventional quadrupole ICP-MS, there is no additional quadrupole (Q1) to select which ions can enter the cell. As a result, all ions enter the cell so, when a reactive cell gas is used, a complex and variable population of reaction product ions is created, depending on the sample matrix and other analytes. With ICP-QQQ, the first quadrupole selects only the target mass to pass into the cell, so the reaction chemistry is controlled and consistent. With the combination of HMI and MS/MS reaction cell mode, the 8800 ICP-QQQ provided effective removal of the polyatomic interferences from the Nd matrix.

### **Reference**

1. Naoki Sugiyama and Glenn Woods, Direct measurement of trace rare earth elements (REEs) in high-purity REE oxide using the Agilent 8800 Triple Quadrupole ICP-MS with MS/MS mode, Agilent publication, 2012, [5991-0892EN](#).

### **More information**

Application note: Routine determination of trace rare earth elements in high purity Nd<sub>2</sub>O<sub>3</sub> using the Agilent 8800 ICP-QQQ. Agilent publication [5991-5400EN](#)

# Direct Determination of Challenging Trace Rare Earth Elements in High Purity Lanthanide REE Oxides

## Authors

Juan-e Song and Xiang-cheng Zeng  
Agilent Technologies, China

## Keywords

Rare Earth Elements, REE, rare earth oxides, REO, oxygen mass-shift, ammonia on-mass, ammonia mass-shift

## Introduction

ICP-MS is widely used for trace impurity analysis of high purity rare earth element (REE) oxide materials. But the analysis of trace REEs in high purity REE oxide materials remains challenging. Matrix-based polyatomic ions such as REEO<sup>+</sup>, REEOH<sup>+</sup>, and REEH<sup>+</sup> cause severe spectral interferences on some REE elements. Trace REE analytes can be separated from the REE matrix using a chelating resin, but this technique is time-consuming, and customization is needed per the analyte and matrix element.

In this study, trace REEs in lanthanide oxide materials were determined using an Agilent 8900 ICP-QQQ with O<sub>2</sub> and NH<sub>3</sub> reaction cell gases. Since the analysis of La<sub>2</sub>O<sub>3</sub>, Tm<sub>2</sub>O<sub>3</sub> and Lu<sub>2</sub>O<sub>3</sub> is relatively interference free, these matrices weren't included in the study.

## Experimental

**Instrumentation:** An Agilent 8900 Advanced Applications configuration ICP-QQQ was used without any modification. For the analysis of 500 ppm REE matrix samples, 'general-purpose plasma' conditions were selected in the MassHunter software. The preset plasma function automatically sets all plasma-related parameters, simplifying instrument set-up.

Five cell modes were investigated: no gas, helium (He), oxygen (O<sub>2</sub>), and ammonia (20% NH<sub>3</sub> in He). Tuning conditions are summarized in Table 1. In NH<sub>3</sub> mass-shift mode, a pre-study was done using 'product ion scan' to identify the most abundant NH<sub>3</sub> cluster ion. The masses of the cluster ions used for the analysis are given in Tables 2 and 3, together with the analytical results.

**Table 1.** Cell gas mode-related tuning parameters.

Cell gas mode	No gas	He	O <sub>2</sub> mass-shift	NH <sub>3</sub> on-mass	NH <sub>3</sub> mass-shift
Scan Mode	Single Quad		MS/MS		
Octopole bias (V)	-8	-18	-3	-5	-5
Octopole RF (V)	140	180	180	180	180
KED (V)	+5	+4	-7	-7	-7
Axial Acceleration (V)	0	1	1.5	0.5	0.5
He (mL/min)		5		1	1
O <sub>2</sub> (mL/min)			0.45		
NH <sub>3</sub> (mL/min)				4.0 ~ 6.0	1.0 ~ 8.0

## Results and discussion

Ten REE oxide materials of the highest-grade purity (5N) including Ce<sub>2</sub>O<sub>3</sub>, Pr<sub>6</sub>O<sub>11</sub>, Nd<sub>2</sub>O<sub>3</sub>, Gd<sub>2</sub>O<sub>3</sub>, Sm<sub>2</sub>O<sub>3</sub>, Eu<sub>2</sub>O<sub>3</sub>, Tb<sub>4</sub>O<sub>7</sub>, Dy<sub>2</sub>O<sub>3</sub>, Er<sub>2</sub>O<sub>3</sub>, and Yb<sub>2</sub>O<sub>3</sub> were dissolved in semiconductor grade HNO<sub>3</sub> and diluted to 500 ppm (as REE oxide). H<sub>2</sub>O<sub>2</sub> was added during the dissolution of Ce<sub>2</sub>O<sub>3</sub> and Tb<sub>4</sub>O<sub>7</sub>. REEs were measured in each matrix solution using the five cell modes specified in Table 1. The results are given in Tables 2 and 3.

As expected, in no gas mode, the BECs for the REEs were relatively high due to spectral interferences. He collision cell mode was able to alleviate some of the interferences, but not all. Previous studies have shown that both O<sub>2</sub> and NH<sub>3</sub> are effective for the removal of polyatomic ions that interfere with the REEs [1, 2]. A drawback of NH<sub>3</sub> mode has been low sensitivity. However, Axial Acceleration of cluster ions in the cell of the 8900 ICP-QQQ increases sensitivity. The results reported in Tables 2 and 3 show that the BECs for all REEs were dramatically improved using a reactive cell gas. The improvement factor data relates to the difference in BEC obtained in reaction mode compared to no gas mode.

**Table 2.** BECs of REE impurities in 500 ppm Ce, Pr, Nd, and Gd oxide solutions.

Sample		Ce <sub>2</sub> O <sub>3</sub>			PrO		Nd <sub>2</sub> O <sub>3</sub>		Gd <sub>2</sub> O <sub>3</sub>		
Analyte		Pr	Gd	Tb	Tb	Tb	Dy	Ho	Tb	Yb	Lu
Isotope		141	160	159	159	159	163	165	159	172	175
Interference		<sup>140</sup> CeH <sup>+</sup>	<sup>142</sup> Ce <sup>18</sup> O <sup>+</sup>	<sup>142</sup> Ce <sup>16</sup> OH <sup>+</sup>	<sup>141</sup> Pr <sup>18</sup> O <sup>+</sup>	<sup>142</sup> NdOH <sup>+</sup> , <sup>143</sup> NdO <sup>+</sup>	<sup>145</sup> Nd <sup>18</sup> O <sup>+</sup>	<sup>148</sup> NdOH <sup>+</sup>	<sup>158</sup> GdH <sup>+</sup>	<sup>156</sup> GdO <sup>+</sup>	<sup>159</sup> GdOH <sup>+</sup>
BEC (ppb)	No gas	6.17	3.36	29.2	10.3	721	163	13.4	2.23	3420	75.0
	He	3.79	11.9	0.725	2.50	234	36.6	3.06	2.16	1200	66.4
	O <sub>2</sub>	0.064	0.030	9.76	0.001	1.95	0.804	0.070	0.106	284	0.444
	NH <sub>3</sub>	BEC		0.284	0.055	0.039	0.255	0.021		0.030	7.16
		mass pair		(159/174)	(159/244)	(159/174)	(163/163)	(165/165)		(172/172)	(175/260)
Improvement factor		x100	x100	x100	x10,000	x20,000	x1000	x1000	x20	x100,000	x200

**Table 3.** BECs of REE impurities in 500 ppm Sm, Eu, Tb, Dy, Er, and Yb oxide solutions.

Sample		Sm <sub>2</sub> O <sub>3</sub>				Eu <sub>2</sub> O <sub>3</sub>	Tb <sub>4</sub> O <sub>7</sub>	Dy <sub>2</sub> O <sub>3</sub>	Er <sub>2</sub> O <sub>3</sub>	Yb <sub>2</sub> O <sub>3</sub>
Analyte		Dy	Ho	Er	Tm	Tm	Lu	Ho	Tm	Lu
Isotope		162	165	167	169	169	175	165	169	175
Interference		<sup>147</sup> SmO <sup>+</sup>	<sup>148</sup> SmOH <sup>+</sup> , <sup>149</sup> SmO <sup>+</sup>	<sup>150</sup> SmOH <sup>+</sup>	<sup>152</sup> SmOH <sup>+</sup>	<sup>141</sup> EuO <sup>+</sup>	<sup>159</sup> TbO <sup>+</sup>	<sup>164</sup> DyH <sup>+</sup>	<sup>168</sup> ErH <sup>+</sup>	<sup>174</sup> YbH <sup>+</sup>
BEC (ppb)	No gas	0.408	185	44.9	39.0	64.8	3270	2.13	1.26	0.97
	He	0.169	61.9	18.1	13.6	38.20	1670	1.28	1.57	1.38
	O <sub>2</sub>	0.083	0.158	0.916	0.240	2.73	26.1	0.057	0.025	0.195
	NH <sub>3</sub>	BEC		0.035	0.055	0.092	0.127	0.002	0.244	0.074
		mass pair		(162/162)	(165/165)	(167/167)	(169/169)	(169/169)	(175/260)	(165/165)
Improvement factor		x10	x3000	x500	x200	x30,000	x10,000	x50	x50	x5

## Conclusion

The Agilent 8900 ICP-QQQ method was used to measure REE impurities in high purity REE oxide materials. REE matrix-based hydride, oxide, and hydroxide polyatomic ion interferences were removed by operating the ICP-QQQ in MS/MS mode with O<sub>2</sub> and NH<sub>3</sub> reaction cell gases. The BECs were improved by one to four orders of magnitude using reactive cell gases compared to no gas mode. The method is suitable for the direct analysis of trace REEs in the presence of high concentration matrix-REEs.

## References

1. Direct measurement of trace rare earth elements (REEs) in high-purity REE oxide using the Agilent 8800 Triple Quadrupole ICP-MS with MS/MS mode, Agilent application note, 2012, [5991-0892EN](#)
2. Routine determination of trace rare earth elements in high purity Nd<sub>2</sub>O<sub>3</sub> using the Agilent 8800 ICP-QQQ, Agilent application note, 2015, [5991-5400EN](#)

# Arsenic Measurement in Cobalt Matrix using MS/MS Mode with Oxygen Mass-Shift

## Author

Katsuo Mizobuchi  
Agilent Technologies, Japan

## Keywords

arsenic, high purity metals, cobalt, zirconium, oxygen mass-shift

## Introduction

Measuring the purity of materials such as high purity metals is of interest across advanced technology industries, to support the development of new materials and/or improve the performance of existing products. ICP-MS is widely used for determining elemental impurities in these materials due to its unique features: High sensitivity, low DLs, multi element analysis capability, wide dynamic range, fast analysis and minimal sample preparation requirements.

For many applications, the errors caused by spectral interferences in quadrupole ICP-MS have been adequately addressed by the introduction of CRC technology. However, the analysis of trace contaminants in high purity materials presents a particular challenge due to the high matrix levels and the need to determine impurities at the trace level. For example, the determination of As in Co is difficult for quadrupole ICP-MS due to the signal from  $\text{CoO}^+$  that overlaps the only isotope of arsenic at  $m/z$  75. Although only about

0.01% of the Co ions in the plasma are present as  $\text{CoO}^+$  ions, the Co concentration in a 1000 ppm solution is 6 or 7 orders of magnitude higher than the trace levels of As that are of interest in this application. Consequently, the  $\text{CoO}^+$  interference is still very significant relative to the  $\text{As}^+$  signal. This note describes the measurement of trace As in a 1000 ppm Co solution using an Agilent 8800 ICP-QQQ in MS/MS mass-shift mode, using oxygen as the reaction gas.

## Experimental

**Instrumentation:** Agilent 8800 #100.

**Plasma conditions:** Preset plasma/HMI-mid.

**CRC conditions:**  $\text{O}_2$  gas at 0.3 mL/min,  
Octopole bias = -5 V, KED = -7 V.

**Acquisition conditions:** Three oxygen ( $\text{O}_2$ ) mass-shift operational modes were compared:

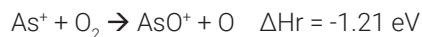
- Single Quad mode A with low mass cut off at  $m/z < 59$
- Single Quad mode B with low mass cut off at  $m/z = 59$
- MS/MS mode with Q1 as a 1 u mass filter, Q1 = 75 and Q2 = 91

**Sample:** SPEX CLCO2-2Y (SPEX CertiPrep Ltd., UK) was used as 1000 ppm Co solution.

## Results and discussion

### BEC of As in 1000 ppm Co solution using O<sub>2</sub> mass-shift method

From the equation and reaction enthalpy below, it can be seen that arsenic reacts readily with O<sub>2</sub> cell gas via an O-atom transfer reaction. This creates the reaction product ion AsO<sup>+</sup> at *m/z* 91, moving the analyte away from the CoO<sup>+</sup> interference on As<sup>+</sup> at *m/z* 75.



The reaction enthalpy for CoO<sup>+</sup> with the O<sub>2</sub> cell gas is much less favorable, so the overlap from the CoO<sup>+</sup> polyatomic interference is successfully avoided. To evaluate the effectiveness of MS/MS mode for this application, the 8800 ICP-QQQ was operated in three acquisition modes: MS/MS mode and two “Single Quad” modes, in which Q1 functions as a bandpass filter rather than a unit (1 u) mass filter. In Single Quad mode A, Q1 was set to allow most of the plasma-formed ions to enter the cell; in Single Quad mode B, Q1 was set with a low mass cutoff around *m/z* 59 to allow only ions with a mass greater than 59 to enter the cell (most <sup>59</sup>Co<sup>+</sup> ions are rejected); and finally in MS/MS mode Q1 was set to allow only ions at *m/z* 75 to enter the cell (all <sup>59</sup>Co<sup>+</sup> rejected).

The BECs for As obtained using the three acquisition modes are shown in Figure 1. MS/MS mode achieved the lowest BEC for As of 330 ppt in 1000 ppm Co. The BEC obtained by the Single Quad modes were orders of magnitude higher, which suggests the occurrence of the following undesired reactions in the cell and indicates the incomplete rejection of Co<sup>+</sup> by Single Quad mode B:



Note that this sequential reaction chemistry leads to a relatively intense signal for CoO<sub>2</sub><sup>+</sup>, because the number of precursor ions for the reaction (the Co<sup>+</sup> ions from the plasma) is so high (10000 times higher intensity than the CoO<sup>+</sup> signal in the plasma). Consequently, in Single Quad mode, the CoO<sup>+</sup> overlap cannot be successfully avoided by moving the As<sup>+</sup> to its AsO<sup>+</sup> product ion at *m/z* 91 using O<sub>2</sub> cell gas, because CoO<sub>2</sub><sup>+</sup> (also at *m/z* 91) is formed relatively easily when a large number of Co<sup>+</sup> ions are allowed to enter the cell.

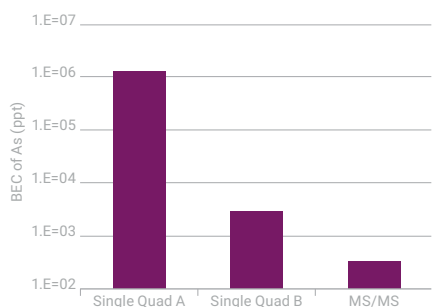


**Figure 1.** BEC of As in 1000 ppm Co solution with O<sub>2</sub> mass-shift method using three acquisition modes (note log intensity scale).



## AsO<sup>+</sup> in the presence of zirconium

To successfully avoid interferences using the mass-shift method, the mass of the analyte product ion must itself be free from interference. For example, in this application the AsO<sup>+</sup> product ion is measured at  $m/z$  91 where it could be overlapped by an isotope of zirconium ( $^{91}\text{Zr}^+$ ). The presence of Zr in a sample may therefore cause an error in the results for As measured as AsO<sup>+</sup> using O<sub>2</sub> reaction mode on ICP-QMS. The potential effect of co-existing Zr on AsO<sup>+</sup> measurement using ICP-QMS was investigated.

Figure 2 is a spectrum of 10 ppm Zr obtained using Single Quad mode A with O<sub>2</sub> mass-shift. Zr reacts with O<sub>2</sub> very efficiently ( $\Delta H_r = -3.84$ ) and is converted to ZrO<sup>+</sup>. However not all the Zr<sup>+</sup> ions are converted to ZrO<sup>+</sup> so some Zr<sup>+</sup> remains, interfering with the measurement of AsO<sup>+</sup> at  $m/z$  91. In contrast, in MS/MS mode the  $^{91}\text{Zr}^+$  ion is rejected by Q1, so the potential overlap on the AsO<sup>+</sup> product ion at  $m/z$  91 is removed.

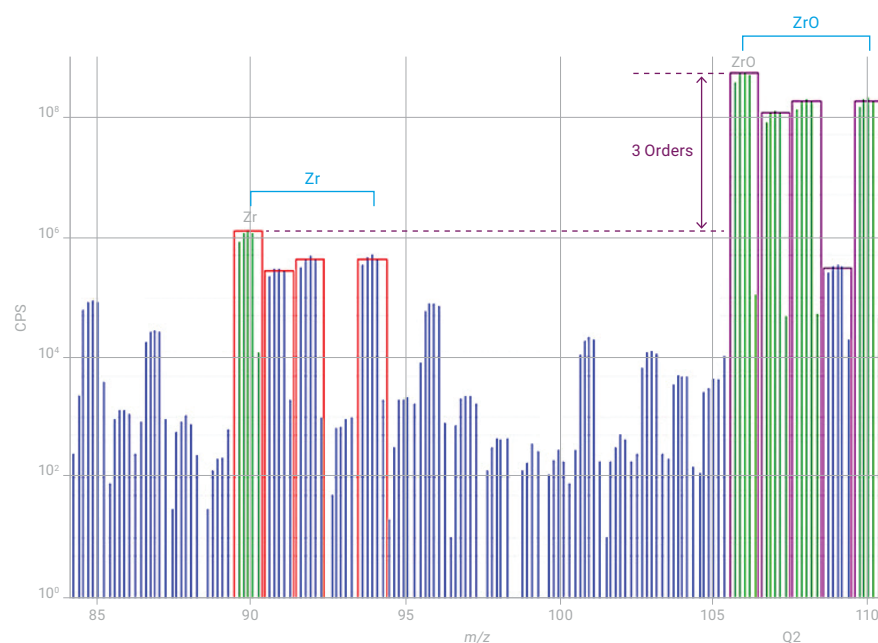


**Figure 2.** Spectrum of 10 ppm Zr obtained using Single Quad mode A with O<sub>2</sub> mass-shift-method.

## Conclusion

Trace levels of arsenic in a 1000 ppm cobalt matrix can be successfully measured (BEC of 330 ppt) using the 8800 ICP-QQQ operating in MS/MS mass-shift mode, with oxygen as the reaction gas. There are two main advantages of using MS/MS compared to ICP-QMS:

1. In MS/MS mode, Co<sup>+</sup> is prevented from entering the cell by Q1, which is set to  $m/z$  75. In ICP-QMS, CoO<sub>2</sub><sup>+</sup> is formed in the cell via a chain reaction and will interfere with AsO<sup>+</sup> at  $m/z$  91.
2. In MS/MS mode, the potential  $^{91}\text{Zr}^+$  overlap on the AsO<sup>+</sup> product ion at  $m/z$  91 is eliminated, as  $^{91}\text{Zr}^+$  ions (and all other ions apart from  $m/z$  75) are rejected by Q1.

# Analysis of ultratrace impurities in high purity copper using the Agilent 8900 ICP-QQQ

## Author

Naoki Sugiyama  
Agilent Technologies, Japan

Low-ppt determination of alkali metals in high matrix samples using the optional "m-lens"

## Introduction

Metals such as copper (Cu), aluminum (Al), tantalum (Ta), tungsten (W), and hafnium (Hf) are essential for the manufacture of semiconductor devices. Metal sputtering targets are used to form conducting or insulating (dielectric) layers by thin film deposition using chemical vapor deposition (CVD) or physical vapor deposition (PVD). Conducting metals, originally Al but now typically Cu, are used as interconnects within wiring levels and as "vias" between layers. A complex, large-scale integrated circuit (IC) microprocessor chip may contain tens of layers of interconnect "wires" with a total length up to about 100 km (1, 2). To ensure high performance and high production-yield of the final devices, very high purity metals are required for these components.

Semiconductor manufacturers may require high-purity, electronic-grade metals at grades of 5N (5 9s – 99.999% purity) up to 9N (99.9999999% purity) or above, depending on the proposed application. A 6N metal (99.9999% purity) contains a total of only 1 mg/kg (ppm) of the impurities of interest, so each individual impurity element would typically be certified as <0.01 or <0.005 ppm in the solid metal.

Determination of trace contaminants in high-purity metals is often performed using glow discharge mass spectrometry (GD-MS). However, GD-MS is expensive and requires the availability of solid metal calibration standards containing the trace elements of interest. GD-MS also has relatively slow speed of data acquisition leading to low sample throughput—around 10 minutes or more per sample—often longer when a cryo-cooled source is used. The fact that solid samples are analyzed also makes automation of sample changeover for unattended analysis more problematic than for liquid sample digests.

ICP-MS is widely used for quality-control of semiconductor materials, but some elements are difficult to measure at ultratrace levels in the presence of a high matrix. ICP-MS operating with a "cool" or reduced-energy plasma has been widely employed since the 1990s as a powerful mode for the analysis of high-purity chemicals and materials. Cool plasma suppresses the formation of intense argon-based interferences such as Ar<sup>+</sup> and ArO<sup>+</sup>, allowing low-level analysis of <sup>40</sup>Ca and <sup>56</sup>Fe, respectively. Cool plasma conditions are also beneficial in the analysis of the alkali metal elements, providing lower background equivalent concentrations (BECs) than hot plasma conditions. A lower-temperature plasma causes less re-ionization of traces of easily-ionized elements (EIEs) from the cones and ion lens, giving lower background signals for these elements. Cool plasma is not universally applicable, though, as the lower power plasma has less energy, which reduces its ability to decompose the sample matrix. Poor tolerance of high matrix levels is especially problematic for the analysis of high matrix, high-purity samples such as electronic-grade metals.

This note describes a new approach to the measurement of ultratrace impurities in high-purity copper using triple quadrupole ICP-MS (ICP-QQQ). An optional ion lens (called the "m-lens") has been developed for the Agilent 8900 ICP-QQQ to allow ultra-low-level measurement of alkali metals under matrix tolerant, high-power plasma conditions. The m-lens has an optimized geometry that minimizes background signals from EIEs deposited on the ICP-MS interface components. matrix samples using the optional "m-lens".

## Experimental

### Sample preparation

All samples and standards were prepared in 5% semiconductor grade TAMAPURE AA-100 nitric acid ( $\text{HNO}_3$ ) bought from Tama Chemicals Co. Ltd, Kanagawa, Japan. Solutions were prepared and analyzed in PFA vials, which were cleaned with diluted HCl and  $\text{HNO}_3$  and then rinsed using ultrapure water (UPW) before use.

A 0.1% copper (Cu) solution was prepared for analysis. A sample of 9N high purity copper was cleaned in diluted  $\text{HNO}_3$ , rinsed with UPW, weighed (about 0.05 g), and dissolved in 5 mL of 50%  $\text{HNO}_3$  (1:1 concentrated  $\text{HNO}_3$ :UPW). The solution was brought up to volume (50 mL) with UPW, giving a total dilution of 1000x, and a matrix level of 0.1%. The 8900 ICP-QQQ can tolerate % levels of dissolved solids, but higher dilutions allow non-matrix-matched calibrations to be used. This removes the need for certified metal standards containing every element of interest. The exceptionally low detection limits of the 8900 ICP-QQQ (sub-ppt for most elements) enable ultratrace analysis even in higher sample dilutions.

The 1000x dilution factor simplifies conversion of the measured concentrations in ng/L (ppt) in the digest solution to the concentrations in  $\mu\text{g}/\text{kg}$  (ppb) in the original solid.

Calibration standards for 49 elements were prepared from several mixed, multi-element stock standards (SPEX CertiPrep, NJ, USA). To minimize signal suppression due to physical sample transport and nebulization effects, the calibration standards were matrix matched to the  $\text{HNO}_3$  concentration (5%) of the Cu sample digest.

All samples and standards were spiked with a mix of three internal standard (ISTD) elements, Be, Sc, and In, at 5.0, 0.5, and 0.5 ppb, respectively. ISTDs were added to compensate for matrix differences between the standards (no Cu) and the 0.1% Cu solutions, and to correct for any long-term signal drift.

### Instrumentation

An Agilent 8900 Semiconductor configuration ICP-QQQ was used for all measurements. The standard PFA nebulizer was used in self-aspiration mode, connected to the standard quartz spray chamber and quartz torch with 2.5 mm i.d. injector. The 8900 ICP-QQQ was fitted with the standard Pt-tipped sampling cone, optional m-lens (part number G3666-67500), and optional Pt-tipped, Ni-based skimmer cone for m-lens (part number G3666-67501). The skimmer cone for m-lens also requires a non-standard skimmer cone base (part number G3666-60401).

## Tuning and method

Hot plasma conditions (1% CeO<sup>+</sup>/Ce<sup>+</sup>) were used to ensure good tolerance of the high concentration of Cu matrix. A single collision/reaction cell (CRC) tuning mode was used to measure all 49 analyte elements in the Cu samples. A cell gas mixture of oxygen (O<sub>2</sub>) and hydrogen (H<sub>2</sub>) was used to remove interferences using a combination of MS/MS on-mass and mass-shift modes. Operating conditions are summarized in Table 1, and acquisition parameters and given in Table 2.

**Table 1.** Agilent 8900 ICP-QQQ operating parameters.

Parameter	Setting
RF power (W)	1550
Sampling depth (mm)	8.0
Carrier gas flow rate (L/min)	0.70
Make-up gas flow rate (L/min)	0.46
Extract 1 (V)	0.0
Extract 2 (V)	-70
Omega bias (V)	-60
Omega lens (V)	8.0
Cell gas flow rate (mL/min)	O <sub>2</sub> = 0.2; H <sub>2</sub> = 7.0
Octopole bias (V)	-10
KED (V)	-10
Axial acceleration (V)	+2.0

**Table 2.** Acquisition parameters.

Element	Q1/Q2	Main interferences	Scan method	Measured ion	Integration time (s)	ISTD
Li	7/7		On-mass	Li <sup>+</sup>	0.5	Be
B	11/11		On-mass	B <sup>+</sup>	2.0	Be
Na	23/23		On-mass	Na <sup>+</sup>	0.5	Sc
Mg	24/24		On-mass	Mg <sup>+</sup>	0.5	Sc
Al	27/27		On-mass	Al <sup>+</sup>	0.3	Sc
Si	28/28	N <sub>2</sub> <sup>+</sup> , CO <sup>+</sup>	On-mass	Si <sup>+</sup>	0.5	Sc
P	31/47	NOH <sup>+</sup> , Cu <sup>++</sup>	Mass shift	PO <sup>+</sup>	2.0	Be
S	32/48	O <sub>2</sub> <sup>+</sup> , Cu <sup>++</sup>	Mass shift	SO <sup>+</sup>	2.0	Be
K	39/39	ArH <sup>+</sup>	On-mass	K <sup>+</sup>	0.5	Be
Ca	40/40	Ar <sup>+</sup>	On-mass	Ca <sup>+</sup>	0.3	Sc
Ti	48/48	SO <sup>+</sup>	On-mass	Ti <sup>+</sup>	0.5	Sc
V	51/51	(ClO <sup>+</sup> )	On-mass	V <sup>+</sup>	0.3	Sc
Cr	52/52	ArC <sup>+</sup>	On-mass	Cr <sup>+</sup>	0.3	Sc
Mn	55/55	ArNH <sup>+</sup>	On-mass	Mn <sup>+</sup>	0.3	Sc
Fe	56/56	ArO <sup>+</sup>	On-mass	Fe <sup>+</sup>	0.3	Sc
Co	59/59		On-mass	Co <sup>+</sup>	0.3	Sc
Ni	60/60		On-mass	Ni <sup>+</sup>	0.5	Sc
Zn	68/68	ArNN <sup>+</sup> , CuHHH <sup>+</sup>	On-mass	Zn <sup>+</sup>	2.0	Sc
Ga	71/71		On-mass	Ga <sup>+</sup>	0.5	In

Element	Q1/Q2	Main interferences	Scan method	Measured ion	Integration time (s)	ISTD
Ge	72/72	ArAr <sup>+</sup>	On-mass	Ge <sup>+</sup>	0.5	In
As	75/91	(ArCl <sup>+</sup> )	Mass shift	AsO <sup>+</sup>	1.0	In
Se	78/78	ArAr <sup>+</sup>	On-mass	Se <sup>+</sup>	3.0	In
Rb	85/85		On-mass	Rb <sup>+</sup>	0.3	In
Sr	88/88		On-mass	Sr <sup>+</sup>	0.5	In
Zr	90/106		Mass shift	ZrO <sup>+</sup>	0.5	In
Nb	93/125	CuNO <sup>+</sup>	Mass shift	NbOO <sup>+</sup>	0.3	In
Mo	95/127	CuOO <sup>+</sup>	Mass shift	MoOO <sup>+</sup>	0.5	In
Ru	99/99	ArCu <sup>+</sup>	On-mass	Ru <sup>+</sup>	0.5	In
Rh	103/103	ArCu <sup>+</sup>	On-mass	Rh <sup>+</sup>	0.3	In
Pd	105/105	ArCu <sup>+</sup>	On-mass	Pd <sup>+</sup>	0.5	In
Ag	107/107		On-mass	Ag <sup>+</sup>	0.3	In
Cd	111/111		On-mass	Cd <sup>+</sup>	1.0	In
Sn	118/118		On-mass	Sn <sup>+</sup>	0.5	In
Sb	121/121		On-mass	Sb <sup>+</sup>	0.5	In
Te	125/125		On-mass	Te <sup>+</sup>	3.0	In
Cs	133/133		On-mass	Cs <sup>+</sup>	0.5	In
Ba	137/137		On-mass	Ba <sup>+</sup>	0.5	In
Hf	178/194		Mass shift	HfO <sup>+</sup>	0.5	In
Ta	181/213		Mass shift	TaOO <sup>+</sup>	0.5	In
W	182/214		Mass shift	WOO <sup>+</sup>	0.5	In
Re	185/185		On-mass	Re <sup>+</sup>	0.5	In
Ir	193/193		On-mass	Ir <sup>+</sup>	0.5	In
Pt	195/195		On-mass	Pt <sup>+</sup>	0.5	In
Au	197/197		On-mass	Au <sup>+</sup>	0.5	In
Tl	205/205		On-mass	Tl <sup>+</sup>	0.3	In
Pb	208/208		On-mass	Pb <sup>+</sup>	0.3	In
Bi	209/209		On-mass	Bi <sup>+</sup>	0.3	In
Th	232/248		Mass shift	ThO <sup>+</sup>	0.3	In
U	238/270		Mass shift	UOO <sup>+</sup>	0.3	In

## Results and discussion

### BECs and DLs in 5% HNO<sub>3</sub> blank

Background equivalent concentrations (BECs) in 5% HNO<sub>3</sub> were obtained from the calibration plots for each analyte. Calibration plots for three alkaline elements (Li, Na, and K) are shown in Figure 1. The BECs for the three elements were 0.1, 6.1, and 5.4 ppt, respectively, indicating very low background signals obtained using the m-lens. Calibration plots for Si, P, and S are also given in Figure 1. The BECs for these challenging elements were 231, 7.2, and 84 ppt, respectively. P and S have relatively high first ionization potentials (IPs) and so are poorly ionized under cool plasma conditions. Using hot plasma conditions in this work, these poorly ionized elements – together with others such as B, Zn, As, Cd, Ir, Pt, and Au – were all measured at low ppt levels.

The BECs and  $3\sigma$  DLs for all 49 elements in the 5% HNO<sub>3</sub> blank are shown in Figure 2. The BECs for most elements were below 1 ng/L (ppt) in solution. This value is equivalent to <1 µg/kg (ppb) relative to the solid Cu, taking the 1000x dilution into account. This sensitivity indicates that the 8900 ICP-QQQ method is suitable for ultratrace analysis of these impurity elements in high-purity Cu. Low ppt BECs were also achieved for alkali elements, Li, Na, and K, under the hot plasma conditions used. BECs at the 10s to 100s ppt-level were achieved for the most challenging elements: S (84 ppt) and Si (231 ppt).

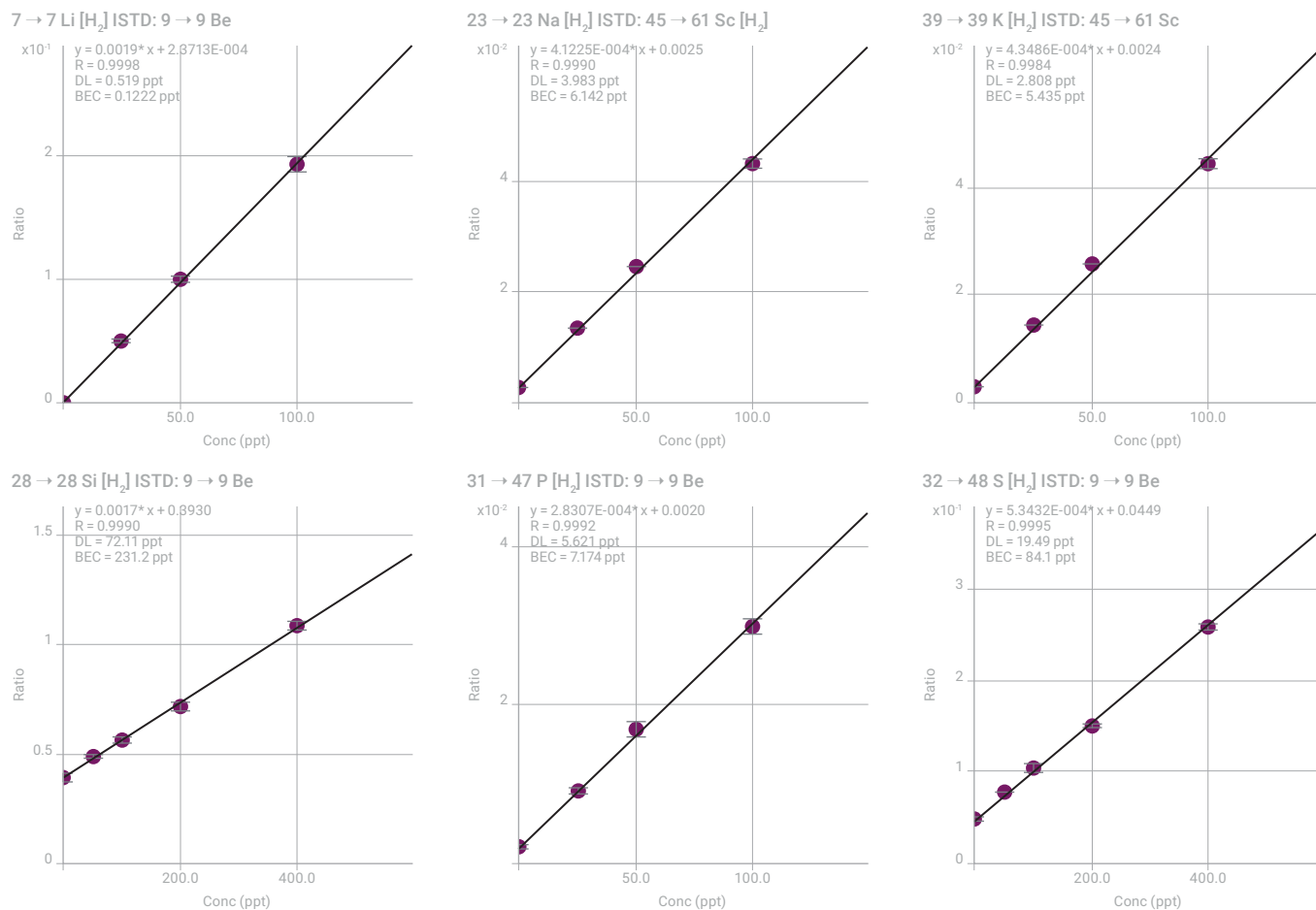
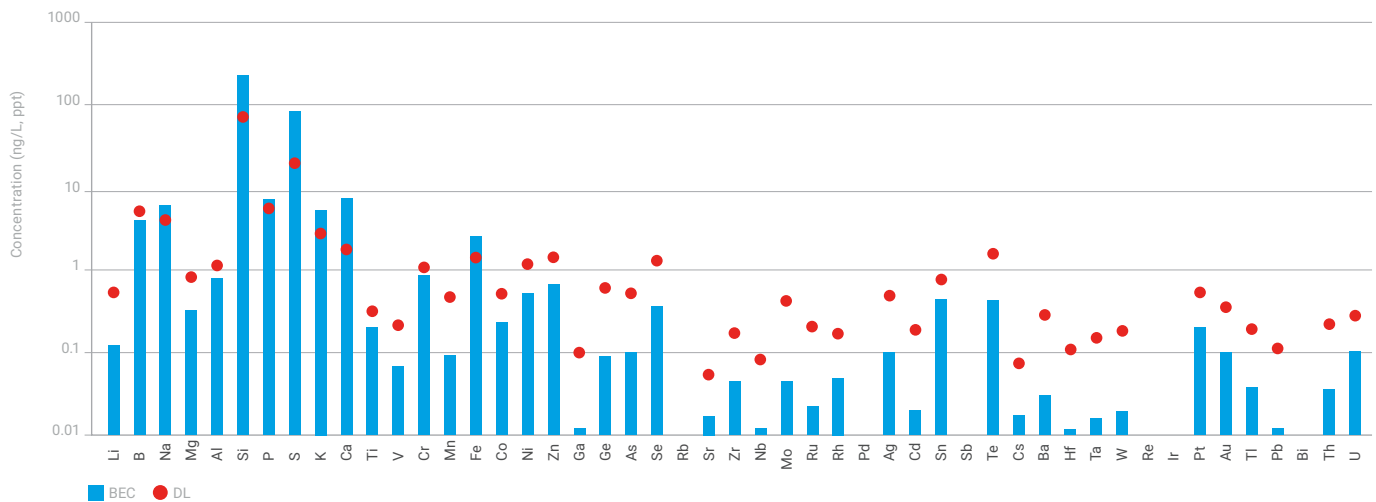


Figure 1. Calibrations for easily-ionized elements Li, Na, and K, and challenging elements Si, P, and S.



**Figure 2.** BECs and 3σ DLs for 49 elements in 5% HNO<sub>3</sub> blank. The BEC and DL for Rb, Pd, Sb, Re, Ir, and Bi could not be calculated, as the measured counts were zero in all replicates of the blank.

### Determination of impurities in 0.1% 9N high purity copper

The 8900 ICP-QQQ method was used to determine the concentration of 49 elements in the 0.1% high purity copper solutions. ISTD correction was applied to correct for signal differences between the synthetic standards (with no Cu matrix) and the 0.1% Cu samples. Signal differences were all less than 30% between the non-matrix and Cu-matrix samples, demonstrating the robustness of the hot plasma conditions used.

All elements measured—apart from Si, S, and Te—were <10 ppt in the digest, as shown in Figure 3. Most elements were measured at 1 ppt or below, which is equivalent to <1 g/kg (ppb) in the solid metal. The mixed O<sub>2</sub> + H<sub>2</sub> reaction cell gas removed the significant spectral interferences caused by ArCu<sup>+</sup> on Ru<sup>+</sup>, Rh<sup>+</sup>, and Pd<sup>+</sup> (see Table 2). Removing the interferences allowed the determination of these elements at single- or sub-ppt levels (equivalent to single- or sub-ppb in the solid metal).

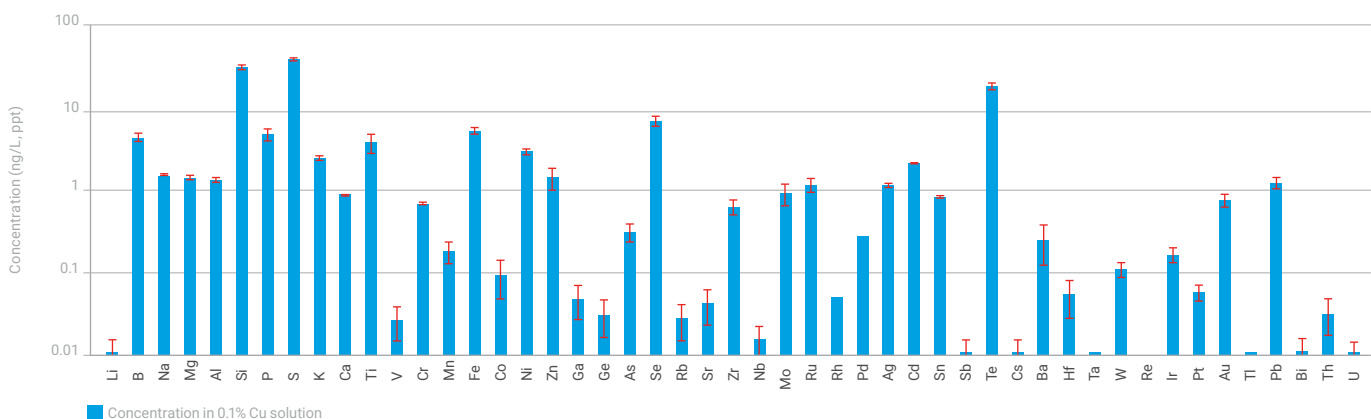


**Figure 3.** Measured concentrations of 49 elements in 0.1% 9N Cu sample (error bars = standard deviation for three samples). The values shown in ng/L (ppt) in solution) are equivalent to the values in μg/kg (ppb) in the original solid metal. The concentration reported for Re was 0.000 ppt. SDs were zero for Rh, Pd, Ta, Re, and Tl.

## Spike recovery

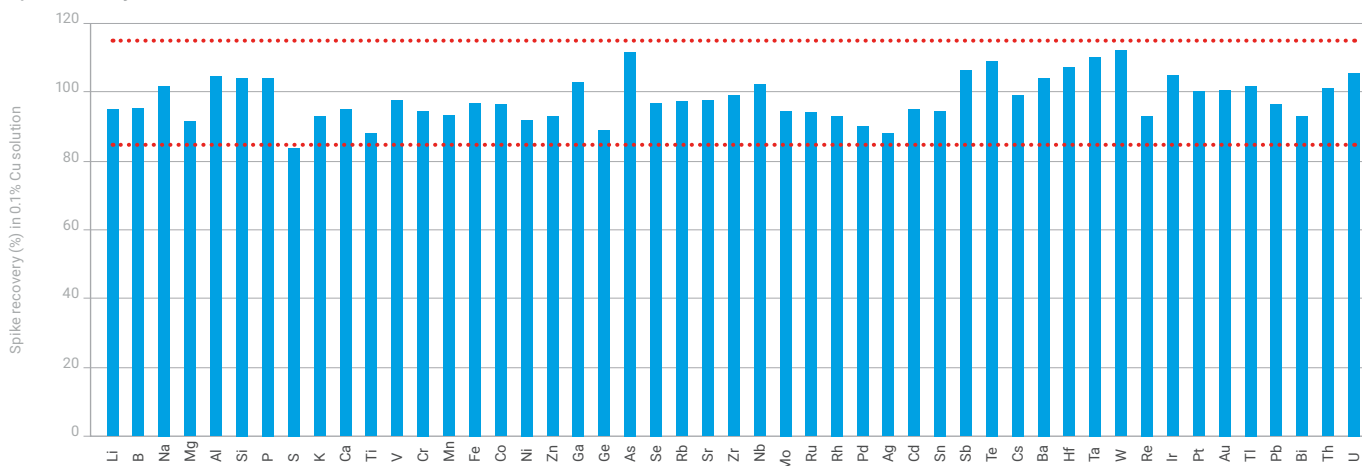


**Figure 4.** Spike recovery test at 50 ppt (200 ppt for S, P, and Si) in 0.1% Cu solution. Most elements were within 90–110% recovery. The red lines indicate upper and lower limits of 85 to 115% recovery.

To validate the method, a spike recovery test was carried out for all 49 impurity elements. A 0.1% 9N copper blank solution was spiked at 50 ppt (200 ppt for Si, P, and S). The recoveries were within 84–112% for all 49 elements, with most being within 90–110%, as shown in Figure 4.

## Conclusion

Ultratrace level impurities can be analyzed quickly and accurately in high purity copper metal digests using the Agilent 8900 ICP-QQQ. The optional m-lens ensures that the background signals for the alkali elements are minimized under hot plasma conditions. Using MS/MS mode with a mixed cell gas ( $O_2 + H_2$ ), the method delivered the following performance benefits:

- Low ppt level BECs were achieved for most impurities, including the alkali elements, using matrix-tolerant hot plasma conditions.
- Low-level BECs at the 10s to 100s ppt-level were obtained for sulfur and silicon—the most challenging elements to measure using ICP-MS.
- No matrix matching for Cu matrix was required, as ISTDs corrected for matrix differences between the standards (in 5%  $HNO_3$ ) and the samples (in 0.1% Cu).
- Using the fast and simple method with a single, mixed cell gas mode, a total of 49 elements were determined at ultralow levels in 0.1% high purity Cu sample.

## References

1. Larry Zhao, All About Interconnects, Semiconductor Engineering, 2017, accessed October 2018, <https://semiengineering.com/all-about-interconnects/>
2. Katherine Bourzac, Making Wiring that Doesn't Trip Up Computer Chips, MIT Technology Review, 2012, accessed October 2018, <https://www.technologyreview.com/s/428466/making-wiring-that-doesnt-trip-up-computer-chips/>



# Determination of Sulfur, Phosphorus, and Manganese in High Purity Iron

## Authors

Yasuyuki Shikamori and  
Kazumi Nakano  
Agilent Technologies, Japan

## Keywords

phosphorus, sulfur, manganese,  
iron, steel, JSS 001-6, JSS 003-6,  
abundance sensitivity, oxygen  
mass-shift

## Introduction

ICP-MS is the analytical technique of choice for the analysis of trace elements in iron and steel. However, the sensitivity and interference removal performance of quadrupole ICP-MS (ICP-QMS) is not sufficient for the determination of difficult analytes such as phosphorus (P) and sulfur (S) at the low levels required.

Furthermore, the determination of manganese (Mn) in an iron matrix is extremely challenging for ICP-QMS due to overlap (or tailing) from the very intense  $^{54}\text{Fe}$  and  $^{56}\text{Fe}$  peaks that occur either side of the single isotope of manganese at  $m/z$  55.

The Agilent 8800 Triple Quadrupole ICP-MS (ICP-QQQ) provides more effective and reliable removal of polyatomic interferences, such as  $^{14}\text{N}^{16}\text{OH}$  on  $^{31}\text{P}$  and  $^{16}\text{O}_2$  on  $^{32}\text{S}$ , using controlled chemical reaction in the CRC. This note describes the performance of the 8800 ICP-QQQ operating in MS/MS mode, for the determination of the trace elements S, P and Mn in two high purity iron CRMs (JSS 001-6 and 003-6).

## Experimental

**Instrumentation:** Agilent 8800 #100.

**Plasma condition:** Preset plasma/HMI-mid.

**Ion lens tune:** Soft extraction tune: Extract 1 = 0 V, Extract 2 = -175 V.

### CRC and acquisition conditions:

- MS/MS  $\text{O}_2$  mass-shift method to remove the  $^{14}\text{N}^{16}\text{OH}^+$  and  $^{16}\text{O}_2^+$  interferences on  $^{31}\text{P}^+$  and  $^{32}\text{S}^+$  respectively:  $\text{O}_2$  gas at 0.3 mL/min, Octopole bias = -5 V and KED = -7 V.
- MS/MS He on-mass mode to measure  $^{55}\text{Mn}^+$ :  
He gas at 5.0 mL/min, Octopole bias = -18 V and KED = 4 V.

All other parameters were optimized by Autotune in the MassHunter software. Figure 1 shows the mechanism used on the 8800 ICP-QQQ to avoid the  $^{14}\text{N}^{16}\text{OH}^+$  and  $^{16}\text{O}_2^+$  interferences on  $^{31}\text{P}^+$  and  $^{32}\text{S}^+$  by mass-shift mode ( $Q1 \neq Q2$ ) using  $\text{O}_2$  reaction gas.

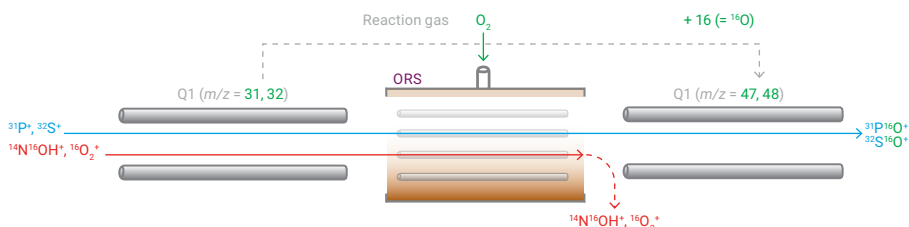


**Figure 1.** Mechanism of MS/MS mass-shift mode ( $Q2 = Q1+16$ ) using  $\text{O}_2$  reaction gas for the measurement of P as  $^{31}\text{P}^{16}\text{O}^+$  and S as  $^{32}\text{S}^{16}\text{O}^+$  at  $m/z$  47 and 48 respectively.

**Sample preparation:** Two Steel CRMs, JSS-001 and JSS-003 were purchased from The Japan Iron and Steel Federation (Tokyo, Japan). 0.1 g of each Steel CRM was digested in a mixture of 1 mL HCl and 2 mL HNO<sub>3</sub> and diluted to 100 mL with UPW. No further chemical matrix separation, e.g., solvent extraction, ion exchange, etc. was applied. The digested CRM samples containing 0.1% (1000 ppm) Fe were analyzed directly on the ICP-QQQ using the robust plasma conditions provided by Agilent's HMI aerosol dilution system.

## Results and discussion

### BEC and DL of P and S

The calibration plots shown in Figure 2 demonstrate that the 8800 ICP-QQQ with MS/MS mass-shift mode can successfully perform the trace level (single ppb) quantitation of P and S in 0.1% Fe solutions. The BEC and DL achieved for P were 0.14 ppb and 0.05 ppb respectively, and the BEC and DL for S were 6.45 ppb and 0.75 ppb respectively.

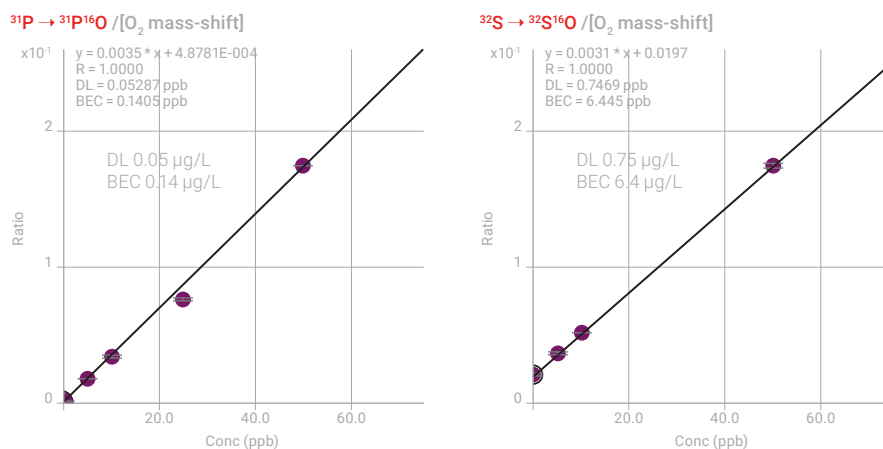


**Figure 2.** Calibration curve for P (left) and S (right) in 0.1% Fe matrix, obtained using O<sub>2</sub> mass-shift mode under robust plasma conditions.

### Trace Mn analysis in Fe matrix

The abundance sensitivity (AS, a measure of peak separation) of ICP-QQQ in MS/MS mode is the product of the Q1 AS x Q2 AS. This means the AS of the 8800 ICP-QQQ is theoretically about 2x that achievable on ICP-QMS, and the ICP-QQQ is therefore able to successfully separate the <sup>55</sup>Mn peak from the very intense overlaps from <sup>54</sup>Fe and <sup>56</sup>Fe in a high iron matrix. This is demonstrated in Figure 3 which shows the spectra of 10 ppb Mn in a 0.1% Fe matrix sample solution measured in Single Quad mode (left) and MS/MS mode on the ICP-QQQ (right). Helium was used as the cell gas in both cases to remove <sup>54</sup>FeH<sup>+</sup> and ArNH<sup>+</sup> interferences by KED.

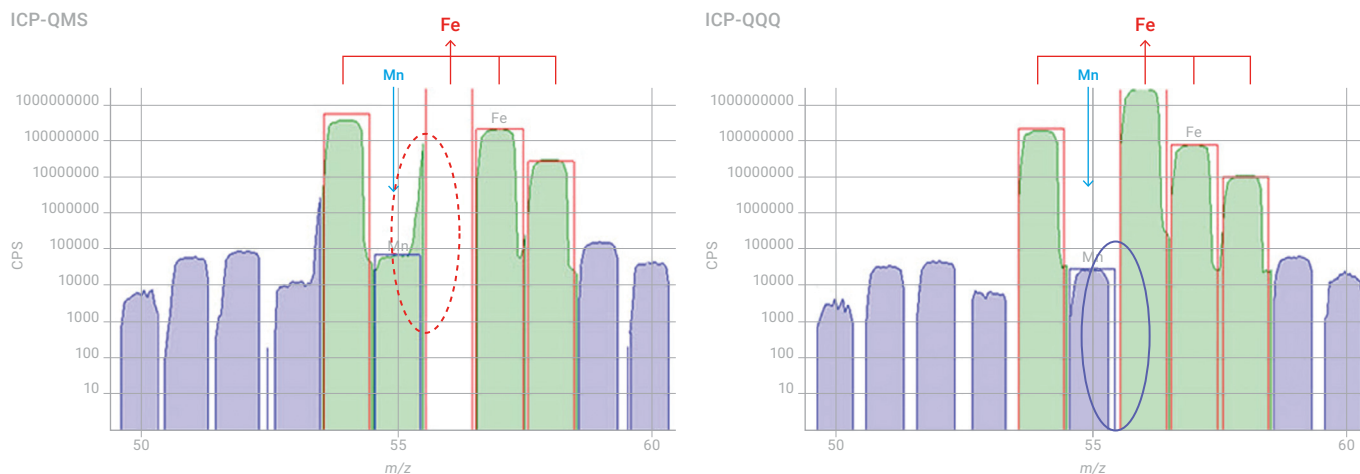


**Figure 3.** Spectra of 10 ppb Mn in a 0.1% Fe matrix sample solution obtained in Single Quad mode (left) and ICP-QQQ in MS/MS mode (right).

### Determination of P, S and Mn in high purity iron CRMs

Trace elements including P, S and Mn were determined by ICP-QQQ in high purity iron CRMs: JSS 001-6 and 003-6, using O<sub>2</sub> mass-shift mode (for P and S) and He mode (for Mn). As summarized in Table 1, excellent agreement was obtained between the measured (found) and certified values for all three elements, indicating the effective interference removal offered by the 8800 ICP-QQQ in MS/MS mode. Excellent spike recovery at the 50 ppb level was also confirmed with JSS 003.

**Table 1.** Analytical results for P, S and Mn in two high purity iron CRMs.

Element	Q1	Q2	ORS	JSS 001-6			JSS 003-6			50 ppb spike recovery %
				Certified value [mg/kg]	Uncertainty	Found [mg/kg]	Certified value [mg/kg]	Uncertainty	Found [mg/kg]	
P	31	47	O <sub>2</sub>	0.5*		0.458	3.5	0.7	3.170	103
S	32	48	O <sub>2</sub>	1.5	0.3	1.512	1.3	0.5	1.287	92
Mn	55	55	He	0.03*		0.036	3.2	0.2	3.432	101

# The Benefits of Improved Abundance Sensitivity with MS/MS for Trace Elemental Analysis of High Purity Metals

## Author

Fred Fryer  
Agilent Technologies, Australia

## Keywords

quadrupole, resolution, hyperbolic, abundance sensitivity, copper, high purity zinc

## Introduction

The use of a quadrupole mass filter for the separation of compounds in mass spectrometry is well established. Initially used for organic mass spectrometry and residual gas analysis, the quadrupole spectrometer was adopted for the earliest ICP-MS systems, and has remained the default choice throughout the history of ICP-MS. However, the performance characteristics of the quadrupole mass filter do impose several limitations on quadrupole ICP-MS (ICP-QMS).

The resolution ( $R$ ) of a mass filter (meaning its ability to separate adjacent masses) is defined as  $M/\Delta M$ , the mass of the target peak/the mass difference to nearest adjacent peak that can be distinguished (separated). However, for practical specifications, the resolution is often simply quoted as the width of the peak at a given peak height. The quadrupole mass filter used in an ICP-QMS instrument is typically operated with a nominal peak width of about 0.75 u at 10% peak height, illustrated in Figure 1.

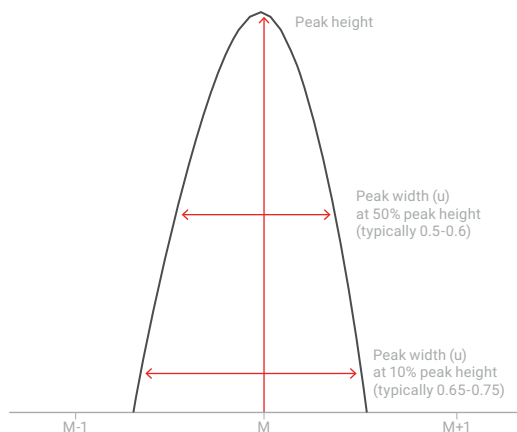


**Figure 1.** Illustration of resolution calculation for a mass spectrometer.

For two peaks within the normal signal range of the instrument, this allows the complete, baseline separation of masses 1 u apart, within the elemental mass range from Li (7 u) to U (238 u) and beyond. Higher resolution of 0.4 u peak width is possible by adjusting the quadrupole voltages, but the signal is reduced (less ion transmission) due to rejection of a higher proportion of the ions that are nominally “on-mass”. Typically, the signal loss at higher resolution is around 10-50%, depending on the design and operating characteristics of the quadrupole.

Both the efficiency of transmission of ions at the set-mass (i.e., the sensitivity) and the rejection of ions at other masses (i.e., the resolution of adjacent peaks) are affected by the shape of the field within the quadrupole, and the frequency of the alternating RF fields.

A hyperbolic field (generated by rods with a hyperbolic profile) alternating at high frequency gives more effective filtering of the ion beam than a lower frequency field generated by round quadrupole rods. The practical benefit of hyperbolic rods and high frequency RF voltage is therefore better ion transmission at higher resolution. Some of the many real-world applications where the combination of high sensitivity and good peak separation is required for adjacent low/high concentration elements measured by ICP-MS are shown in Table 1.

**Table 1.** Elements that require improved separation of adjacent peaks for low level analysis.

Low concentration	High signal	Example matrix
<sup>31</sup> P	<sup>16</sup> O <sub>2</sub> , <sup>32</sup> S	Soil, plants
<sup>55</sup> Mn	<sup>56</sup> Fe, <sup>40</sup> Ar <sup>16</sup> O	Iron and steel, soil
<sup>63</sup> Cu, <sup>65</sup> Cu	<sup>64</sup> Zn, <sup>66</sup> Zn	Metal refining
<sup>11</sup> B	<sup>12</sup> C	Soils, solvents, petrochem
<sup>13</sup> C	<sup>14</sup> N	Laser imaging

Due to the ion transmission characteristics of a quadrupole, the peak that is generated from the ion signals at each mass forms a non-symmetric Gaussian distribution with a negative skew; i.e., the peak has a longer tail on the leading edge (low mass side) than the trailing edge (high mass side). These “tails” may extend significantly beyond the limits of the nominal 0.75 u peak width, but since they are at intensities far below 10% of the peak height, they cannot be measured using the simple resolution figure quoted above. The contribution that a peak at mass M makes to its neighbors at M-1 u and M+1 u can be quantified, however, and this figure is referred to as the abundance sensitivity (AS) of the quadrupole, illustrated in Figure 2.

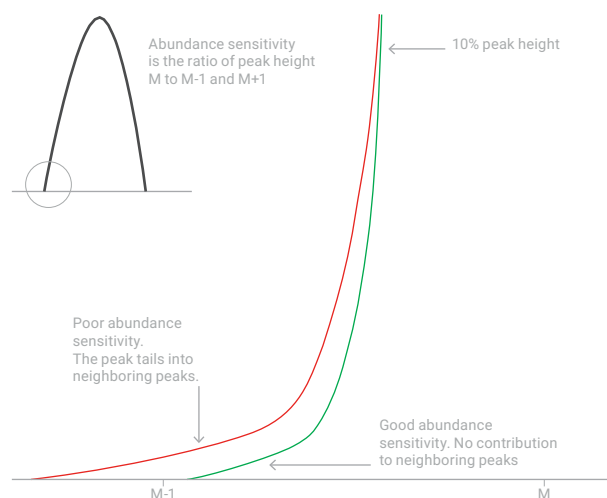


**Figure 2.** Illustration of abundance sensitivity calculation for a mass spectrometer.

For a good quadrupole mass spectrometer in ICP-QMS, the AS would typically be of the order of  $10^{-7}$ , meaning that for an on-mass signal of  $10^7$  counts, there is a contribution of one count at the adjacent mass ( $M\pm 1$  u).

In applications where the trace analyte must be separated from a very intense matrix peak at the adjacent  $M+1$  mass, such as the examples shown in Table 1, the matrix peak may be at an intensity greater than  $10^9$  or  $10^{10}$ , and the AS of a quadrupole mass spectrometer is insufficient for accurate trace measurement of an adjacent overlapped analyte at low/sub ppb levels.

The problem of adjacent mass overlaps now has an elegant solution in the Agilent 8800 Triple Quadrupole ICP-MS (ICP-QQQ). The 8800 ICP-QQQ uses a tandem mass spectrometer configuration with two quadrupole mass filters (Q1 and Q2) separated by a collision/reaction cell. In MS/MS mode, both quadrupoles are operated as unit mass filters, so the overall AS of the instrument is the product of the Q1 AS x the Q2 AS. With two research-grade, high frequency, hyperbolic quadrupoles, each operating with AS of  $10^{-7}$ , the combined AS of the 8800 ICP-QQQ is theoretically  $10^{-14}$ , although this cannot be verified experimentally as the magnitude of the signal difference exceeds the dynamic range of the detector.

## Experimental

### Trace copper in high purity zinc

Major uses of Zn include galvanized coating to protect steel, die castings, and solder. Impurities in the metal cause Zn plating to lift, die casts to crack, or solder to 'de-wet', hence high purity zinc (>99.995 %) is a preferred commodity. Common impurities are Cu, Au and Sb, but may also include Cd, Al, Fe, Ag, Bi, As, In, Ni, P, and S.

**Instrumentation:** Agilent 8800 #100.

**Plasma conditions:** Preset plasma/Low matrix.

**Ion lens tune:** Auto tune was used for optimization.

**CRC conditions:** Helium cell gas at 4.8 mL/min with KED of 4 V.

## Results and discussion

Analysis was performed on high purity Zn, dissolved to give a 0.1% (1000 mg/L) Zn solution in a final acid concentration of 2%  $\text{HNO}_3$ . The sensitivity of the 8800 ICP-QQQ was reduced to bring the signal for the major Zn isotopes (64, 66) within the detector's upper limit of dynamic range ( $\sim 10^{10}$  cps). The intense Zn signals were measured automatically in analog detector mode, while the Cu isotopes were measured in pulse mode. It can clearly be seen in Figure 3 that the intense Zn peaks at  $m/z$  64 and 66 made no contribution to the signal at the two adjacent trace Cu isotopes at  $m/z$  63 and 65. The Cu isotope ratio matched the theoretical abundances ( $^{63}\text{Cu}/^{65}\text{Cu}$  natural ratio of 69.17/30.83), at 1  $\mu\text{g/L}$  concentration. If there was a contribution from an adjacent Zn mass, then the isotope ratio would be biased.

From the  $^{63}\text{Cu}$  calibration (Figure 4), the BEC and DL measured for Cu in the 0.1% Zn matrix were 1.7 ppb and 0.01 ppb respectively, indicating a low and stable background signal. The sensitivity of Cu was 7700 cps/ppb in 1000  $\mu\text{g}/\text{L}$  Zn, under the “de-tuned” conditions used to bring the Zn peaks within the detector range. This represents about a 2x reduction in the signal that would be obtained under normal tuning conditions for this type of matrix, if measurement of the matrix element peaks was not required.

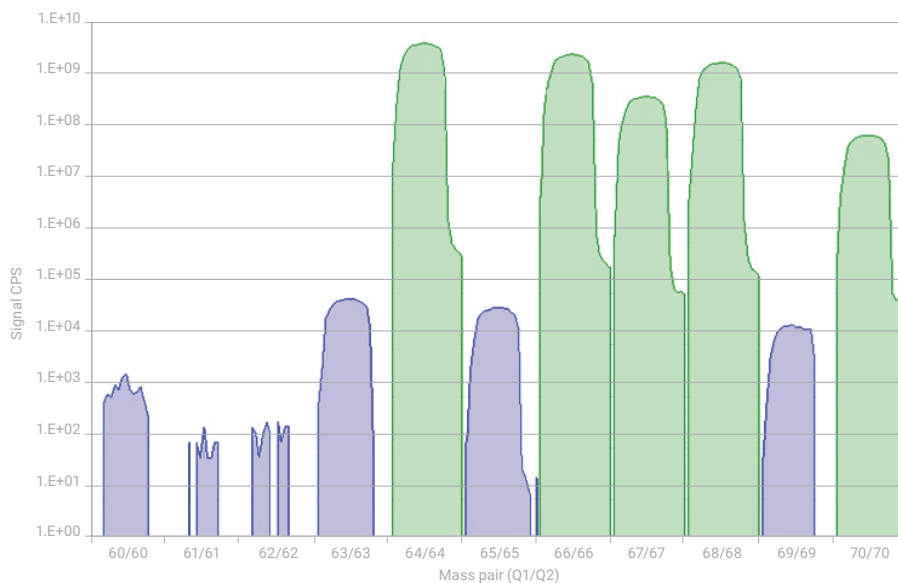


**Figure 3.** 1000 mg/L Zn spiked with 1  $\mu\text{g}/\text{L}$  Cu. (1 ppb: 63/total = 0.667, 65/total = 0.333, no mass bias correction performed. If there was some contribution from Zn it would influence  $m/z$  63 differently from  $m/z$  65, because of the different abundance of the Zn isotopes).

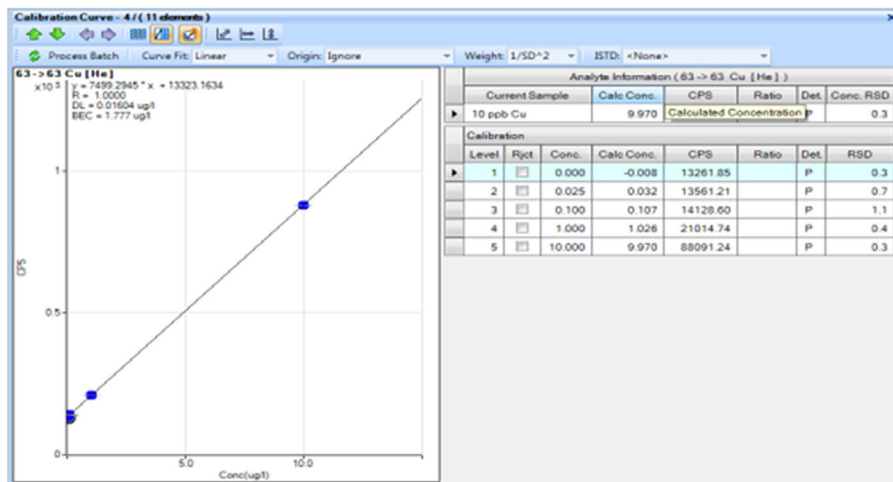


**Figure 4.** Standard addition calibration of  $^{63}\text{Cu}$  in 1000 mg/L Zn.

# Ultratrace Copper Analysis in a Semiconductor Grade Organometallic Titanium Complex

## Authors

Akio Hashizume, Toshiya Shingen,  
ADEKA Corporation, Japan

Katsuo Mizobuchi,  
Agilent Technologies, Japan

## Keywords

semiconductor, organometallic,  
copper, titanium, ammonia mass-shift

## Introduction

Most quadrupole ICP-MS (ICP-QMS) instruments use CRC technology to resolve spectroscopic interferences. Helium collision mode is widely accepted due to its versatility and ease of use for multi-element analysis of complex and variable samples. While the performance achievable with He mode meets the requirements for most applications, there are some applications, for example impurity analysis of semiconductor materials, that require improved interference removal capability. For these applications, a reactive cell gas (reaction mode) may be used, but the use of highly reactive cell gases in quadrupole ICP-MS is prone to unexpected interferences and overlaps, especially when the matrix is complex, or other analytes are present at varying concentrations. The new Agilent 8800 Triple Quadrupole ICP-MS (ICP-QQQ) eliminates the variability associated with reactive cell gases in ICP-QMS, by using the first quadrupole (Q1) to control the ions that enter the CRC. This ensures that the reactions are predictable and the product ion spectrum is simple and consistent.

This report describes the measurement of trace Cu in a semiconductor grade organometallic Ti complex used in advanced semiconductor processing. It is a challenging application for quadrupole ICP-MS since both isotopes of copper,  $^{63}\text{Cu}$  and  $^{65}\text{Cu}$ , suffer interference from TiO and TiOH ions, and the use of reactive cell gases to avoid the overlap leads to a very complex product ion spectrum, particularly for organic samples. We demonstrate that the Agilent 8800 ICP-QQQ, operating in MS/MS mass-shift mode using ammonia as a reaction gas, was able to separate  $\text{Cu}^+$  from the Ti-based interferences and measure Cu at low ppt levels in a matrix of 500 ppm Ti. Results were also acquired using MS/MS He collision mode, for comparison.

## Experimental

**Instrumentation:** Agilent 8800 #200 with narrow injector (id = 1.5 mm) torch (G3280-80080) used for organic solvent analysis. A low flow PFA nebulizer (G3285-80002) was used in self-aspiration mode. An option gas flow of 20%  $\text{O}_2$  balanced in Ar was added to the carrier gas via the standard option-gas line to prevent carbon build up on the interface cones.

**Operating conditions:** Table 1 summarizes plasma, ion lens and cell tuning conditions.

**Acquisition conditions:** MS/MS mode was used; cell gas was either  $\text{NH}_3$  or He.

**Sample and sample preparation:** Semiconductor grade organometallic Ti complex (ADEKA Corp., Japan) was diluted with high purity IPA (Tokuyama Corp., Japan) to 500 ppm Ti solution. A spiked standard was prepared from the multi-element standard, xstc-331, purchased from SPEX CertiPrep Ltd. (UK).



**Table 1.** Experimental conditions.

		Units	He collision cell mode	NH <sub>3</sub> reaction cell mode
Cell conditions	Cell gas		He	NH <sub>3</sub> (10% NH <sub>3</sub> in He)
	Cell gas flow rate	mL/min	8.0	6.5
	Octopole bias	V	-18	-18
	KED	V	4	-10
	Cell exit	V	-100	-70
	Deflect	V	-3	-12
	Plate	V	-70	-60
Plasma conditions	RF	W	1600	
	SD	mm	12.0	
	Carrier gas	L/min	0.70	
	Make-up gas	L/min	0.20	
	Opt gas flow rate	L/min	0.20	
Ion lens	Extract 1	V	-60	
	Extract 2	V	-10	

## Results and discussion

### He collision mode

The He cell gas flow rate was optimized for the lowest BEC of Cu in a 500 ppm Ti solution. As the BEC for <sup>63</sup>Cu was lower than the BEC for <sup>65</sup>Cu due to the higher abundance of the 63 isotope and the more significant interference from TiO<sup>+</sup> at *m/z* 65, Cu was determined on-mass at *m/z* 63. In MS/MS mode, this is achieved by the acquisition conditions: Q1 = 63; Q2 = 63 (63, 63).

Two solutions were analyzed: 500 ppm Ti solution and 500 ppm Ti + 1 ppb Cu spike. Figure 1 (left) shows the signal at *m/z* 63 obtained from the analysis of the two solutions, plotted as a function of He flow rate. The BEC calculated from these signals is also given in the figure. It shows that the lowest Cu BEC in He mode was 46 ppt, achieved at a flow rate of 8.0 mL/min He.

### NH<sub>3</sub> reaction cell mode

Cu<sup>+</sup> reacts efficiently with NH<sub>3</sub> to form NH<sub>3</sub> cluster ions with the general form Cu(NH<sub>3</sub>)<sub>*n*</sub><sup>+</sup>. TiO<sup>+</sup> does not follow the same reaction pathway as Cu<sup>+</sup>, so the Cu product ion can be measured free from Ti overlap. Based on a preliminary study, one of the intense product ions, Cu(NH<sub>3</sub>)<sub>2</sub><sup>+</sup>, was selected to measure Cu separated from the original TiO<sup>+</sup> interference. A mass pair of Q1 = 63, Q2 = 97 was used with NH<sub>3</sub> as the reaction gas. Figure 1 (right) shows the result. A BEC of 11 ppt for Cu in 500 ppm Ti solution was achieved in NH<sub>3</sub> mode (10% NH<sub>3</sub>/He mixed gas), at a flow rate of 6.5 mL/min NH<sub>3</sub>.

## Conclusion

Table 2 summarizes the analytical performance achieved by the 8800 ICP-QQQ operating in MS/MS mode with He collision and  $\text{NH}_3$  reaction gas. As can be seen,  $\text{NH}_3$  reaction mode is more effective than He collision mode for the removal of the  $\text{TiO}^+$  interference on Cu. The BEC obtained for Cu in a Ti matrix by  $\text{NH}_3$  reaction mode is four times lower than He mode, with seven times higher sensitivity.

**Table 2.** Summary of Cu measurement in Ti matrix.

	Flow rate (mL/min)	BEC (ppt) of Cu in 500 ppm Ti	Sensitivity (cps/ppb)
<b>He collision mode</b>	<b>8.0</b>	<b>45.5</b>	<b>810</b>
<b><math>\text{NH}_3</math> reaction mode</b>	<b>6.5</b>	<b>10.9</b>	<b>5900</b>

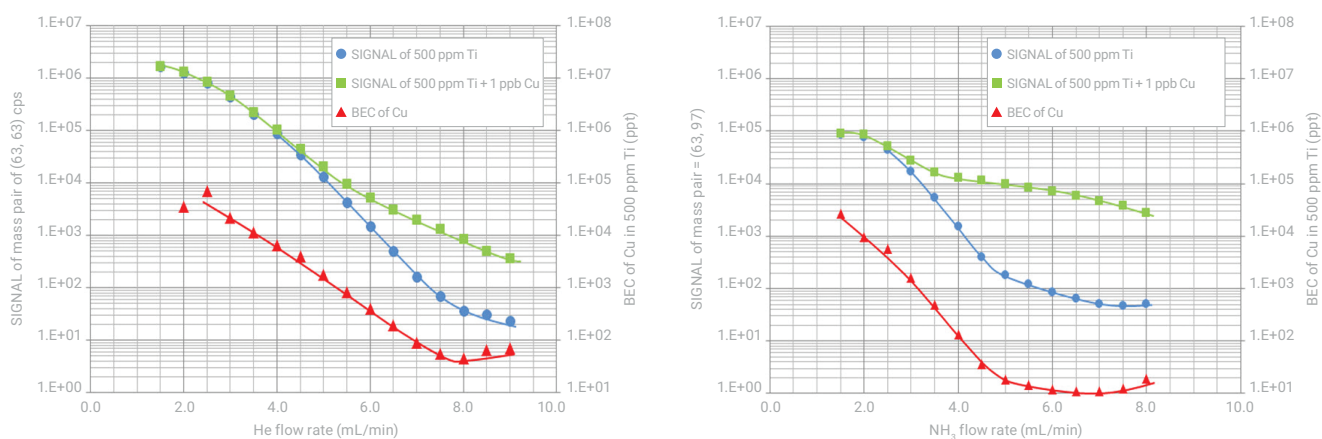


**Figure 1.** (Left) Cu signal (mass pair 63, 63) vs. He cell gas flow rate, for 500 ppm Ti matrix unspiked and with 1 ppb Cu spike, and calculated BEC. (Right) Cu signal (mass pair 63, 97) vs.  $\text{NH}_3$  cell gas flow rate, for 500 ppm Ti matrix unspiked and with 1 ppb Cu spike, and calculated BEC.

# Analysis of 10 nm Gold Nanoparticles using the High Sensitivity of the Agilent 8900 ICP-QQQ

## Authors

Susana Nunez and Heidi Goenaga Infante, LGC Limited, UK  
Michiko Yamanaka, Takayuki Itagaki, and Steve Wilbur, Agilent Technologies

## Keywords

nanoparticles, single nanoparticle analysis, TRA, dwell time, gold nanoparticles

## Introduction

The measurement of nanoparticles (NPs) is of public and scientific interest. More information is needed to understand the fate of NPs in the environment and the potential toxic effects once absorbed into the body. Gold (Au) NPs have a broad range of uses in medical, industrial, and technology applications. Au is a relatively easy element to measure by ICP-MS, as it is not affected by common spectral interferences. However, the detection of very small particles (<20 nm) remains challenging for ICP-MS, due to the low signal generated from such particles. The Agilent 8900 ICP-QQQ has a low background (<0.2 cps) and sensitivity up to Gcps/ppm, making it suited to small particle detection.

## Experimental

**Instrumentation:** Agilent 8900 Advanced Applications configuration ICP-QQQ with 1-mm i.d. injector torch and standard sample introduction system.

**Method:** All aspects of method setup and data analysis were carried out using the fully integrated Single Nanoparticle Application Module option for ICP-MS MassHunter. The “Batch at a Glance” data table shown in Figure 1 summarizes the sample results for an entire batch. Detailed graphical results are displayed for each selected sample, allowing results to be viewed and compared, or method settings to be optimized if necessary. Reference [1] gives details of the particle size calculation used in the module.

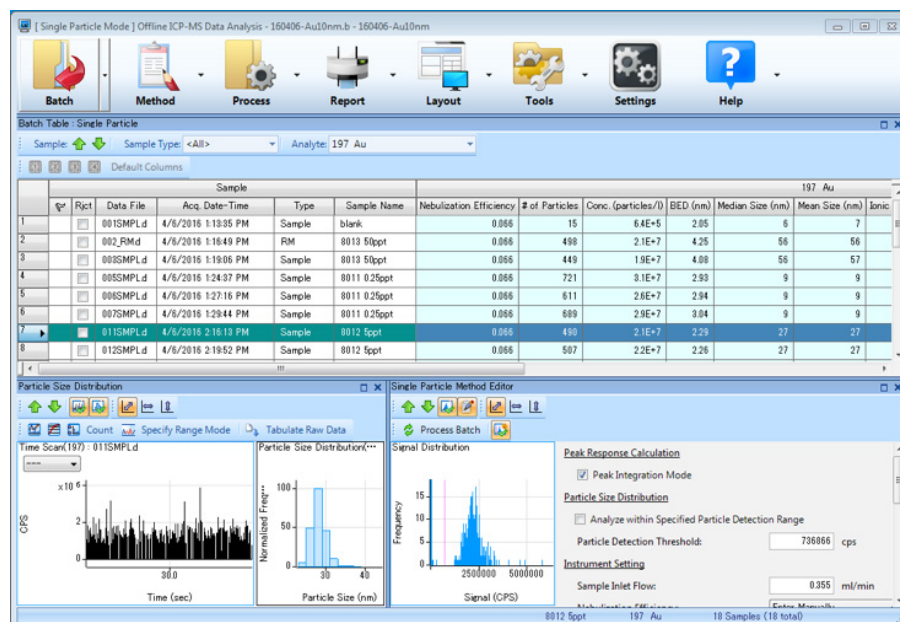


Figure 1. Data analysis view of the Single Nanoparticle Application software module.

**Tuning conditions:** For highest sensitivity,  $^{197}\text{Au}$  was measured in single quad mode with no cell gas.

**Plasma parameters:** RF power = 1550 W, sampling depth = 7.0 mm, and carrier gas flow rate = 0.78 L/min.

**Data acquisition:** TRA analysis with a dwell time of 0.1 ms. Data acquisition time was 60 s.

**Reference materials and sample preparation:**

Three Au NP reference materials (RMs) were used in the study: NIST 8011 with a nominal diameter of 10 nm ( $8.9 \pm 0.1$  nm determined by Transmission Electron Microscopy (TEM)); NIST 8012 with a nominal diameter of 30 nm ( $27.6 \pm 2.1$  nm determined by TEM); and NIST 8013 with a nominal diameter of 60 nm ( $56.0 \pm 0.5$  nm determined by TEM). All final solutions containing Au nanoparticles or ionic Au standards were prepared in 0.01% L-cysteine for stabilization.

**Results and discussion**

**Analysis of Au NP samples**

Solutions containing gold NPs with particle sizes of 10 nm, 30 nm, and 60 nm were prepared at concentrations of 0.25 ng/L, 5 ng/L and 50 ng/L, respectively. The solutions were measured using fast TRA acquisition. Figure 2 shows the measured raw signal event frequency and the calculated size distribution for a solution containing 10 nm particles. From the results, the practical detection limit of the particle diameter was estimated to be around 30,000 cps (equivalent to ~6.5 nm) and the background equivalent diameter (BED) was 3 nm.

The 30 nm and 60 nm particles were also measured, and the results are summarized in Table 1. The results for the median, mode, and mean particle sizes for all three standards agreed well with the reference sizes obtained by TEM.

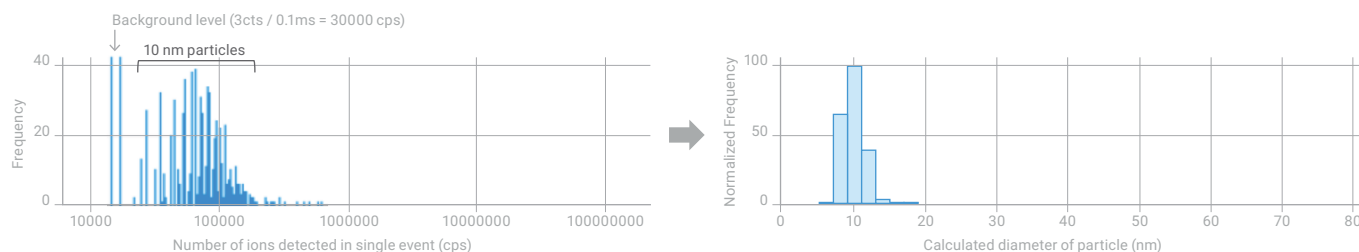


**Figure 2.** Raw signal event frequency (left) and calculated size distribution of 10 nm particles (right).

**Table 1.** Measured particle size for Au NPs in three NIST RMs.

Nominal size (nm)	Particle size (nm) by TEM		Measured particle size ( n = 10 )					
			Median		Mode		Mean	
			size (nm)	RSD (%)	size (nm)	RSD (%)	size (nm)	RSD (%)
10	8.9	$\pm 0.1$	9.0	3.3	10	0.0	9.2	3.3
30	27.6	$\pm 2.1$	26.9	0.3	28	0.0	27.0	0.3
60	56.0	$\pm 0.5$	56.1	0.3	56	1.8	57.2	0.4

## Conclusion

The low background and high sensitivity of the Agilent 8900 ICP-QQQ make it suitable for single particle analysis of solutions containing the smallest-sized nanoparticles. The size and composition of gold NP solutions were characterized from 10 nm up to 60 nm, with good accuracy. The practical detection limit of the particle diameter was estimated to be 6.5 nm and the BED was 3 nm.

## Reference

1. H. E. Pace, N. J. Rogers, C. Jarolimek, V.A. Coleman, C.P. Higgins, and J. F. Ranville, *Anal. Chem.*, **2011**, 83, 9361-9369

## More information

Analysis of 10 nm gold nanoparticles using the high sensitivity of the Agilent 8900 ICP-QQQ, Agilent publication, [5991-6944EN](#)

# High Sensitivity Analysis of SiO<sub>2</sub> Nanoparticles using the Agilent 8900 ICP-QQQ

## Authors

Michiko Yamanaka, Takayuki Itagaki,  
and Steve Wilbur,  
Agilent Technologies

## Keywords

nanoparticles, single nanoparticle  
analysis, TRA, dwell time, silicon  
dioxide NPs

## Introduction

ICP-MS is a well-established technique for measuring the elemental content of materials. With the recent development of Single Particle ICP-MS (spICP-MS) acquisition mode, ICP-MS can also be used to characterize the nanoparticle (NP) content of a sample.

Silicon dioxide (SiO<sub>2</sub>) NPs are used for many applications including paints, coatings, adhesives, food additives, polishing micro-electronic devices etc. Given their wide spread use, there is a clear requirement for SiO<sub>2</sub> NPs to be monitored. Si measurement by ICP-MS is not easy since the major isotope of Si, <sup>28</sup>Si (92.23% abundance), is interfered by the background polyatomic ions CO<sup>+</sup> and N<sub>2</sub><sup>+</sup>. The interferences can be addressed using reaction chemistry in the collision/reaction cell of an ICP-MS. However, for controlled and consistent reaction processes, a tandem mass spectrometer instrument such as the Agilent 8900 Triple Quadrupole ICP-MS (ICP-QQQ) is required.

## Experimental

**Instrumentation:** Agilent 8900 Advanced Applications configuration ICP-QQQ fitted with a 1 mm i.d. injector torch and standard sample introduction system.

**Method:** All aspects of the method setup and data analysis were carried out using the fully integrated Single Nanoparticle Application Module option of the ICP-MS MassHunter software. The “Batch at a Glance” data table summarizes the sample results for an entire batch. The detailed graphical results are displayed for each selected sample, allowing results to be viewed and compared, or method settings to be optimized if necessary. References [1 and 2] provide details of the particle size calculation used in the module.

**Tuning conditions:** H<sub>2</sub> on-mass mode was used to remove potential interferences by CO<sup>+</sup> and N<sub>2</sub><sup>+</sup> on <sup>28</sup>Si<sup>+</sup>. H<sub>2</sub> cell gas flow = 3 mL/min.

**Plasma parameters:** RF power =1550 W, sampling depth of 7.0 mm and carrier gas flow rate of 0.76 L/min.

**Data acquisition:** TRA analysis with dwell time of 0.1 ms.

**Reference materials and sample preparation:** SiO<sub>2</sub> NP reference materials (RMs) with nominal diameters of 50 nm, 60 nm, 100 nm, and 200 nm were bought from nanoComposix (San Diego, USA). They were diluted to a particle concentration of between 40 and 1000 ng/L with de-ionized (DI) water and sonicated for 5 min to ensure sample homogeneity. A Si ionic standard of 5 µg/L was prepared with DI water and used to measure the elemental response factor.

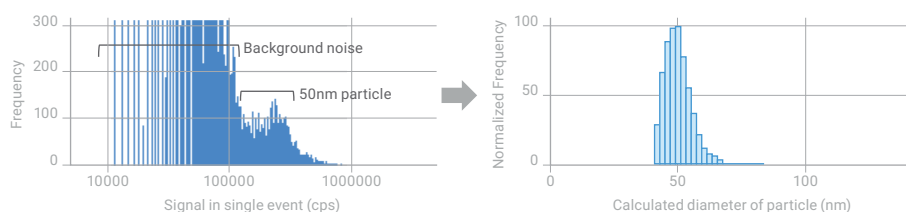


**Figure 1.** Raw signal event frequency (left) and calculated size distribution of 50 nm particles (right).

## Results and discussion

### Analysis of SiO<sub>2</sub> NPs in UPW

The frequency distribution plots of the signals obtained from 50 nm SiO<sub>2</sub> NPs are shown in Figure 1. The particle signals were clearly distinguished from the background (dissolved, ionic component). From the results, we can estimate that the practical detection limit for the particle diameter was below 50 nm and the background equivalent diameter (BED) was 22 nm.

The results for the size analysis of different SiO<sub>2</sub> NP solutions are summarized in Table 1. The results for median, mode, and mean particle sizes agreed well with the reference sizes obtained by TEM.

**Table 1.** Measured particle size for SiO<sub>2</sub> NPs in four RMs.

Nominal size (nm)	Particle size (nm) by TEM	Prepared particle concentration (ng/L)	Measured particle size (n = 10)		
			Median size (nm)	Mode size (nm)	Mean size (nm)
50	46.3 ± 3.1	40	49	50	50
60	57.8 ± 3.5	40	61	62	62
100	97.0 ± 4.8	100	99	100	102
200	198.5 ± 10	1000	200	204	200

### Analysis of SiO<sub>2</sub> NPs in a high-level carbon matrix

Real samples such as biological samples, food matrices, pharmaceutical ingredients, and organic solvents contain carbon matrices that give rise to a <sup>12</sup>C<sup>16</sup>O<sup>+</sup> polyatomic ion interference on <sup>28</sup>Si<sup>+</sup>. Figure 2 shows the particle size distribution for a mixed solution of the 100 and 200 nm SiO<sub>2</sub> measured in a sample containing 1% ethanol. Despite the high concentration of carbon, the size distribution for each group of particle sizes was consistent with the results obtained by TEM. The 8900 ICP-QQQ in MS/MS mode with hydrogen cell gas was able to eliminate the <sup>12</sup>C<sup>16</sup>O<sup>+</sup> interference effectively.

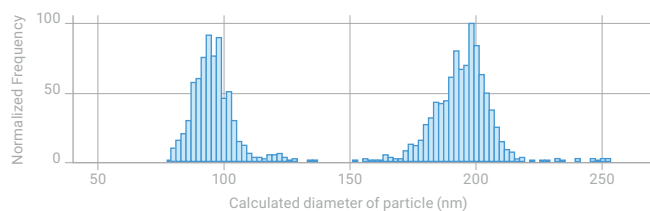


**Figure 2.** Size distribution result of 100 and 200 nm SiO<sub>2</sub> NPs in 1% ethanol.

## Conclusion

SiO<sub>2</sub> NPs can be determined and characterized successfully using the Agilent 8900 ICP-QQQ operating in MS/MS mode with H<sub>2</sub> cell gas. Even in the presence of a high level of carbon matrix. The Single Nanoparticle Application Module for ICP-MS MassHunter was used to calculate the particle sizes. The spICP-QQQ method provides fast analysis times, excellent detection limits for particle size and concentration, and accurate results for SiO<sub>2</sub> particles less than 100 nm.

## References

1. H. E. Pace, N. J. Rogers, C. Jarolimek, V.A. Coleman, C.P. Higgins, and J. F. Ranville, *Anal. Chem.*, **2011**, 83, 9361-9369
2. M. Yamanaka, T. Itagaki and S. Wilbur, Agilent publication, 2016, [5991-6596EN](#)

## More information

High sensitivity analysis of SiO<sub>2</sub> nanoparticles using the Agilent 8900 ICP-QQQ in MS/MS mode, Agilent publication [5991-6596EN](#)



# Accurate determination of TiO<sub>2</sub> nanoparticles in complex matrices using the Agilent 8900 ICP-QQQ

## Authors

Michiko Yamanaka  
Agilent Technologies, Japan  
Steve Wilbur  
Agilent Technologies, USA

## Introduction

Titanium dioxide (TiO<sub>2</sub>) nanoparticles (NPs) are widely used in paints, food colorants, cosmetics, pharmaceuticals, and many other applications. Due to their high refractive index, TiO<sub>2</sub> NPs are common ingredients in sun protection products used to guard against UV exposure. However, the fate of NPs in the environment and the potential for toxic effects once absorbed into the body remain largely unknown. Many researchers have investigated different methodologies to measure TiO<sub>2</sub> NPs in cosmetic or food samples [1, 2, 3, 4].

TiO<sub>2</sub> NPs have three principal levels of structure, beginning with nanoscale crystallites. These crystals fuse to form 'hard' nanoscale aggregates, which in turn associate to form microscale agglomerates [5]. When aqueous dispersions of TiO<sub>2</sub> NPs are prepared, the particle sizes observed are the aggregation or agglomeration sizes, which are usually different from (larger than) the primary (crystal) particle sizes [5, 6]. Typically, the primary size is measured by transmission electron microscopy (TEM) or X-ray diffraction (XRD), and the dispersion size is measured by laser diffraction spectrometry (LDS) or dynamic light scattering (DLS).

The relatively recent development of Single Particle ICP-MS (spICP-MS) now provides a powerful tool to characterize the NP content of dispersed samples. spICP-MS is used to measure the target element signals generated from individual NPs in the solution analyzed. This approach allows the simultaneous determination of the number, concentration, and size of particles present, as well as the dissolved element concentration.

In practice, however, there are some challenges for the measurement of TiO<sub>2</sub> NPs using conventional single quadrupole ICP-MS (ICP-QMS). Many real samples may contain P, S, Ca, Si and C, and all these elements cause interferences that hinder the measurement of Ti. Also, the most abundant isotope of Ti, <sup>48</sup>Ti (73.7% abundance), suffers an isobaric interference from <sup>48</sup>Ca; therefore, the less interfered isotopes <sup>47</sup>Ti or <sup>49</sup>Ti are typically measured. However, the less abundant isotopes provide lower sensitivity, which limits the detection of smaller-sized TiO<sub>2</sub> NPs by ICP-QMS.

The Agilent 8900 Triple Quadrupole ICP-MS (ICP-QQQ) can operate in MS/MS mode to resolve the spectral interferences on Ti, including the isobaric interference from <sup>48</sup>Ca on <sup>48</sup>Ti. The 8900 ICP-QQQ is a tandem mass spectrometer, meaning that it has an additional mass spectrometer with unit (1 u) resolution, positioned before the collision/reaction cell. This extra mass filter selects the ions that can enter the cell, providing control of the reaction chemistry when reactive cell gases are used. ICP-QQQ with MS/MS provides an elegant and effective approach for solving the most challenging spectral overlaps [7].

In this study, TiO<sub>2</sub> NPs in sunscreen were measured in spICP-MS mode using the Agilent 8900 ICP-QQQ in MS/MS mode. The optional Single Nanoparticle Application Module software for ICP-MS MassHunter was used for method setup and data processing.

### **Current regulations**

The methodologies used to evaluate the properties of nanomaterials are not yet considered to be finalized and approved, which may be impeding the introduction of specific regulations relating to NPs. In June 2014, the USA Food and Drug Administration (FDA) issued guidance on the safety assessment of nanomaterials in cosmetic products [8]. As part of the FDA, the Center for Drug Evaluation and Research (CDER) is responsible for ensuring the safety of titanium dioxide (and zinc oxide) nanomaterials for use in over-the-counter (OTC) sunscreen products.

Currently, the European Union Scientific Committee on Consumer Safety (SCCS) considers that it is safe to use TiO<sub>2</sub> NPs as a UV filter at a concentration up to 25% in sunscreens. Manufacturers must respect this limit according to European legislation (annex VI list of UV filters) of the EU regulation on cosmetic products; regulation EC 1223/2009 [9]. The regulation was amended in 2016 to state that in the case of combined use of titanium dioxide and titanium dioxide (nano), the sum shall not exceed 25% [10].

In 2016, following a request from the European Commission to the European Food Safety Authority (EFSA), the Scientific Panel on Food Additives and Nutrient Sources added to Food (ANS) considered the safety of titanium dioxide (TiO<sub>2</sub>, E 171) when used as a food additive [11]. The Panel will establish a health-based guidance value for acceptable daily intake (ADI) once more data is available on the reproductive toxicity of E 171.

## **Experimental**

### **Reference materials and calibration solutions**

The TiO<sub>2</sub> standard reference material (SRM) NIST 1898 Titanium Dioxide (Maryland, US) was used. The SRM contains crystal or primary sized particles <50 nm, but the size of particles dispersed in the aqueous phase range from 71 to 112 nm due to nanoscale aggregation [5]. The SRM was diluted with de-ionized water to a particle concentration that was calculated to give 500 – 2000 particle counts per minute, and sonicated to ensure sample homogeneity. A 1 ppb Ti ionic standard prepared in 1 % nitric acid was used to measure the elemental response factor for Ti. A gold NP RM with a nominal particle size of 60 nm (NIST 8013 Gold Nanoparticles) was used to measure the nebulization efficiency of the ICP-QQQ.

### **Sunscreen samples**

Sunscreen products were bought in a local store in Tokyo, Japan. The samples were diluted with de-ionized water plus 0.1 % Triton™ X-100. The results obtained from an initial screening analysis using the spICP-MS method, showed the size-range of TiO<sub>2</sub> particles present in the different sunscreen samples varied. One of the samples contained particles <30 nm, while another product contained particles sized 30 to 200 nm. A sunscreen that contained TiO<sub>2</sub> NPs sized 30 to 100 nm was selected for further investigation. The selected sunscreen was prepared in various diluent matrices: de-ionized water; tap water; and a “matrix

mixture” containing 100 ppm of P and S, 50 ppm of Ca and Si, and 0.1 % of ethanol. The matrix mixture was used to check the impact of matrix-based interferences on the measurement of Ti.

### Instrumentation

An Agilent 8900 Advanced Applications configuration ICP-QQQ was used throughout. The instrument was equipped with the standard glass concentric nebulizer and quartz spray chamber, optional quartz torch with 1.0 mm i.d. injector, and standard nickel sampling and skimmer cones. Samples were introduced directly into the ICP-QQQ using the standard peristaltic pump and 1.02 mm i.d. pump tubing. Analyses were performed in fast Time Resolved Analysis (fast TRA) mode, using a dwell time of 0.1 ms (100  $\mu$ s) per point, with no settling time between measurements. The major titanium isotope,  $^{48}\text{Ti}$ , was measured in MS/MS mass-shift mode, using a mixed cell gas containing oxygen and hydrogen to resolve all the polyatomic and isobaric interferences. Q1 was set to  $m/z$  48 (the mass of the precursor  $^{48}\text{Ti}$  ion) and Q2 was set to  $m/z$  64 (the mass of the target product ion  $^{48}\text{Ti}^{16}\text{O}$ ).  $\text{O}_2$  and  $\text{H}_2$  cell gases were used to promote the formation of the  $\text{TiO}^+$  product ion, avoiding the on-mass interference from  $^{48}\text{Ca}$  and matrix-based polyatomic ions that overlap  $^{48}\text{Ti}$ . The operating conditions of the Agilent 8900 ICP-QQQ are detailed in Table 1.

**Table 1.** ICP-QQQ operating conditions.

Parameter	Value
RF power	1550 W
Sampling depth	8.0 mm
Carrier gas	0.70 L/min
Sample uptake rate	0.35 L/min
Spray chamber temp.	2 °C
Dwell time	0.1 ms
Settling time	None
Acquisition mode	MS/MS (Q1: $m/z$ 48, Q2: $m/z$ 64)
Oxygen flow rate	0.15 mL/min (10% of full scale)
Hydrogen flow rate	7.0 mL/min
Axial Acceleration	1.0 V
Octopole bias voltage	-6 V
Energy discrimination	-15 V

The Single Nanoparticle Application Module of the ICP-MS MassHunter software was used for method setup and data analysis. Sample results for an entire batch are summarized in the interactive ‘Batch at a Glance’ table. Detailed graphical results are displayed for selected samples, permitting visual confirmation and optimization of parameters if needed.

## Results and discussion

### Optimization of cell gas conditions using ionic Ti solution

Before measurement of the NPs, cell gas conditions were investigated. Ti reacts readily with oxygen, so can be measured as  $\text{TiO}^+$  in oxygen mass-shift mode. The first quadrupole (Q1) was set to pass only  $m/z$  48, to allow  $^{48}\text{Ti}^+$  (and any on-mass interferences) to enter the cell. The second quadrupole (Q2), which is located after the collision/reaction cell, was set to  $m/z$  64 to pass the target product ion ( $^{48}\text{Ti}^{16}\text{O}^+$ ) to the detector. Any potential native ion overlaps at  $m/z$  64 (e.g.  $^{64}\text{Zn}$  and  $^{64}\text{Ni}$ ) are rejected by Q1. Most of the primary interferences at  $m/z$  48, such as  $^{32}\text{S}^{16}\text{O}^+$ ,  $^{30}\text{Si}^{18}\text{O}^+$ ,  $^{31}\text{P}^{16}\text{OH}^+$ ,  $^{12}\text{C}^{18}\text{O}_2^+$ , can be avoided by measuring Ti as  $\text{TiO}^+$  in oxygen cell gas mode. However, some of the  $^{48}\text{Ca}$  ions also react with oxygen to form  $^{48}\text{CaO}^+$ , which interferes with the  $^{48}\text{TiO}^+$  product ions at  $m/z$  64. Adding hydrogen gas can eliminate the Ca interference by converting  $\text{CaO}^+$  to  $\text{CaOH}^+$ .  $\text{TiO}^+$  does not react in the same way with  $\text{H}_2$  cell gas, so remains as the  $\text{TiO}^+$  product ion at  $m/z$  64. Inter-isotope overlaps (such as  $^{46}\text{Ti}^{18}\text{O}$  and  $^{46}\text{Ca}^{18}\text{O}$ ) can affect the  $^{48}\text{Ti}^{16}\text{O}$  measurement at  $m/z$  64 when a single quadrupole or bandpass MS system is used. With MS/MS, however, these overlaps are avoided as the precursor ions ( $^{46}\text{Ti}$  and  $^{46}\text{Ca}$ ) are rejected by Q1 and so do not enter the cell to react.

Table 2 shows the quantitative results for Ti (measured as  $^{48}\text{Ti}^+$  in no gas mode and  $^{48}\text{TiO}^+$  in  $\text{O}_2/\text{H}_2$  mode) in various matrices. The quantitative results obtained in no gas mode show a large positive error due to the interferences on  $^{48}\text{Ti}$ . In contrast,  $\text{O}_2/\text{H}_2$  cell gas mode effectively reduces the interferences including the potential  $\text{CaO}^+$  product ion overlap formed from  $^{48}\text{Ca}$ . This method enables the  $\text{TiO}^+$  product ion from the most abundant isotope of Ti (mass 48; 73.7% relative abundance) to be measured, providing the sensitivity required for detection of small particles.

**Table 2.** Interference check results for  $^{48}\text{Ti}$  in various matrices, with and without cell gas.

Cell gas mode	Sensitivity (cps/ppb)	Apparent concentration of Ti, measured as $^{48}\text{Ti}^+$ or $^{48}\text{TiO}^+$ (ppb)					
		100 ppm P	100 ppm S	50 ppm Ca	50 ppm Si	0.1% ethanol	Matrix mixture*
No gas	155,000	1.7	6.0	225	0.39	0.14	261
$\text{O}_2 + \text{H}_2$	79,000	0.010	0.001	0.18	0.054	0.001	0.23

\*Includes all the matrices (100 ppm of P and S, 50 ppm of Ca and Si, and 0.1% ethanol).

### Measurement of a $\text{TiO}_2$ NP reference material

NIST 1898  $\text{TiO}_2$  NP reference material was measured by ICP-QQQ in MS/MS mass-shift mode with  $\text{O}_2/\text{H}_2$  reaction gas. The time resolved signal chart for NIST 1898 (Figure 1) shows clear NP peaks with a wide variation in intensity (peak heights). In single particle ICP-MS, the peak height for each particle signal “plume” is representative of the particle mass (size). Figure 2 shows the signal frequency distribution for NIST 1898 (upper), and the calculated particle size distribution (lower). The mean size of 71 nm agrees well with the results by LDS ( $71 \pm 4$  nm), X-Ray Disc Centrifugation ( $77 \pm 7$  nm), and DLS ( $112 \pm 4$  nm) according to the NIST certificate [5]. Note that DLS measures the hydrodynamic particle size, which includes the layer where the particle surface interacts with the solvent. Consequently, DLS has been reported to give particle sizes that are larger than the value measured by other techniques [12].

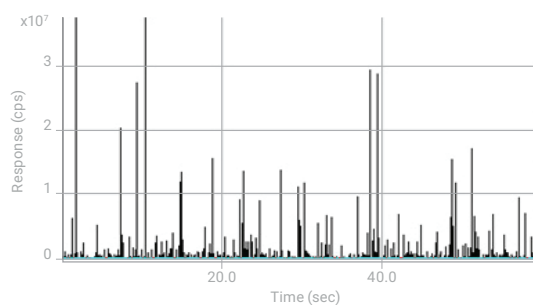


**Figure 1.** Time resolved signal for NIST 1898 TiO<sub>2</sub> NP reference material. The blue line represents a baseline automatically set by the MassHunter software function.

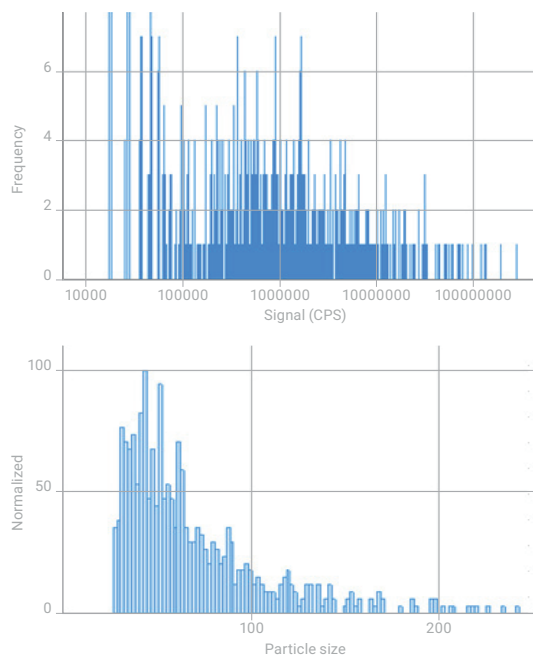


**Figure 2.** Signal frequency distribution (upper) and particle size distribution (lower) for NIST 1898 TiO<sub>2</sub> NP reference material.

### Analysis of TiO<sub>2</sub> NPs in sunscreens

TiO<sub>2</sub> NPs were measured in a commercial sunscreen prepared (dispersed) in several different solutions and the results are presented in Figure 3. Figure 3-A shows the TiO<sub>2</sub> signal distribution and Figure 3-B shows the particle size distribution for the sunscreen dispersed in de-ionized water (plus Triton X-100). The mean particle size of TiO<sub>2</sub> was calculated as 77 nm. The same sunscreen was dispersed in tap water (Figures 3-C and 3-D), and a synthetic matrix mixture comprising 100 ppm of P and S, 50 ppm of Ca and Si, 0.1 % of ethanol (Figures 3-E and 3-F). These results show signal distributions that are almost the same as the ones obtained for the sunscreen dispersed in de-ionized water. The mean particle sizes (79 nm for tap water and 84 nm for the matrix mixture) are similar. The particle size detection limit (the threshold between the baseline noise and particle signals) was about 30 nm for the dispersed sunscreens in all the matrices. The synthetic high matrix (Figure 3-E and 3-F) did not affect the size-DL or the accuracy of the particle size measurement.

The results show that TiO<sub>2</sub> NPs <100 nm diameter can easily be measured using the MS/MS capability of the 8900 ICP-QQQ, even in a high concentration matrix.

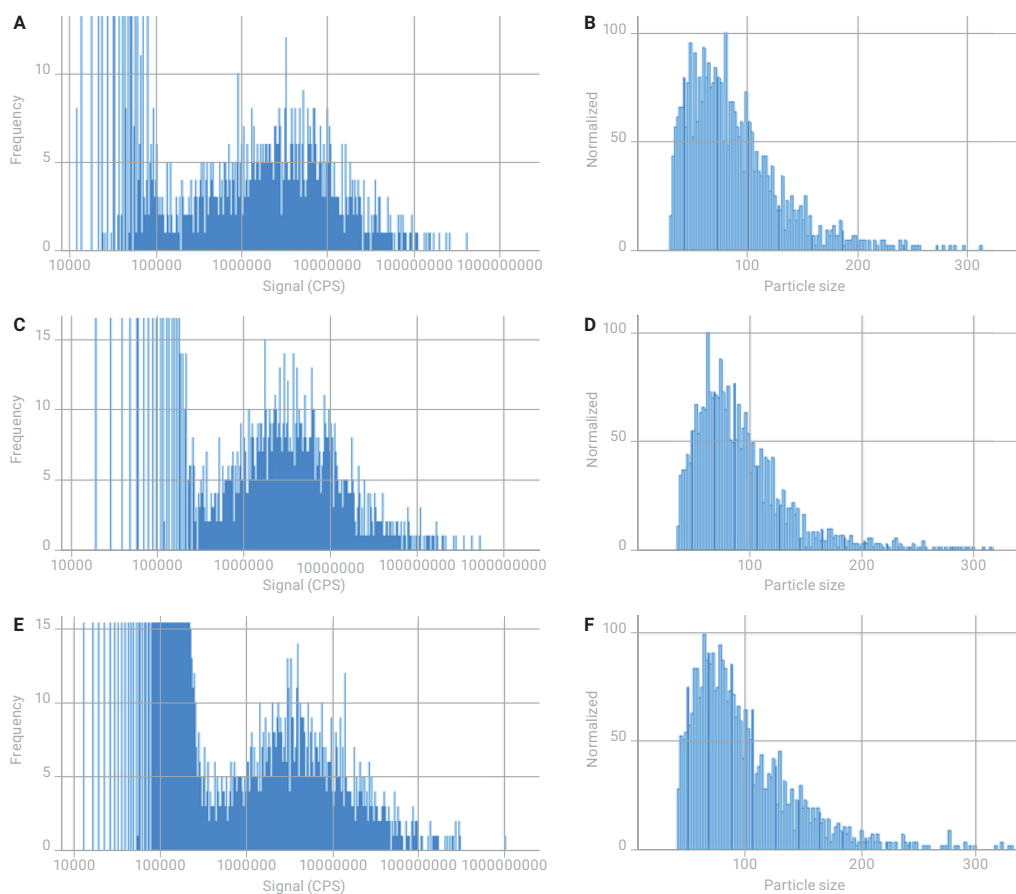


**Figure 3.** TiO<sub>2</sub> NP measurement of commercial sunscreen using ICP-QQQ. Signal distribution A) and particle distribution B) of sunscreen dispersed in de-ionized water. Signal distribution C) and particle distribution D) of sunscreen dispersed in tap water. Signal distribution E) and particle distribution F) of sunscreen dispersed in the matrix mixture.

## Conclusion

The Agilent 8900 ICP-QQQ operating in MS/MS mode with O<sub>2</sub>/H<sub>2</sub> cell gas was used for the successful determination and characterization of TiO<sub>2</sub> nanoparticles in various sample matrices. MS/MS mass-shift mode effectively resolved the polyatomic and isobaric ions that interfere with the measurement of Ti at its most abundant isotope. This unique MS/MS capability provided a particle size detection limit of ~30 nm.

Overall, the method delivered low background signals and excellent sensitivity, even in the presence of a high level of P, S, Ca, Si, and C matrix.

## References

1. V. Nischwitz and H. Goenaga-Infante, *J. Anal. At. Spectrom.*, **2012**, 27(7), 1084–1092.
2. C. Contado and A. Pagnoni, *Anal. Methods*, **2010**, 2, 1112–1124.
3. I. López-Heras, Y. Madrid, C. Cámara, *Talanta*, **2014**, 124, 71–78.
4. P. Lu, S. Huang, Y. Chen, L. Chiueh and D. Y. Shih, *J. Food and Drug Anal.*, **2015**, 23, 587–594.
5. Standard Reference Material 1898 (Titanium Dioxide Nanomaterial) Certificate of Analysis, 2012.
6. Z. Magdolenova, D. Bilaničová, G. Pojana, L. M. Fjellsbø, A. Hudecova, K. Hasplova, A. Marcomini and M. Dusinska, *J. Environ. Monit.*, **2012**, 14, 455–464.
7. G. Woods and E. McCurdy, *Spectroscopy*, **2015**, 30 (11), 18–25.
8. Guidance for Industry: Safety of Nanomaterials in Cosmetic Products, U.S. Department of Health and Human Services Food and Drug Administration Center for Food Safety and Applied Nutrition, June 2014, <https://www.fda.gov/Cosmetics/GuidanceRegulation/GuidanceDocuments/ucm300886.htm#introduction> (accessed July, 2017).
9. Regulation (EC) No 1223/2009 of the European Parliament and of the Council of 30 November 2009 on cosmetic products, <http://eur-lex.europa.eu/legal-content/EN/ALL/?uri=CELEX%3A32009R1223> (accessed July, 2017).
10. Commission Regulation (EU) 2016/1143 of 13 July 2016 amending Annex VI to Regulation (EC) No 1223/2009 of the European Parliament and of the Council on cosmetic products, <http://eur-lex.europa.eu/legal-content/EN/TXT/?uri=CELEX:32016R1143> (accessed July, 2017).
11. Re-evaluation of titanium dioxide (E 171) as a food additive, EFSA Journal 2016; 14 (9):4545, [www.efsa.europa.eu/efsajournal](http://www.efsa.europa.eu/efsajournal), (accessed July 2017).
12. A. Dhawan and V. Sharma, *Anal. Bioanal. Chem.*, **2010**, 398 (2), 589–605.

# Environmental

Title	Page
Routine soil analysis using the Agilent 8800 ICP-QQQ	169
The accurate measurement of selenium in reference materials using online isotope dilution	172
ICP-QQQ with oxygen reaction mode for accurate trace-level arsenic analysis in complex samples	176
Avoidance of spectral overlaps on reaction product ions with O <sub>2</sub> cell gas: comparison of quadrupole ICP-MS and ICP-QQQ	181
Removal of complex spectral interferences on noble metal isotopes	184
Analysis of platinum group elements (PGEs), silver, and gold in roadside dust using triple quadrupole ICP-MS	190
Direct analysis of ultratrace rare earth elements in environmental waters by ICP-QQQ	199
Solving doubly charged ion interferences using an Agilent 8900 ICP-QQQ	205
Removal of REE <sup>++</sup> interference on arsenic and selenium	211
Removal of molybdenum oxide interference on cadmium	215
Rapid analysis of radium-226 in water samples by ICP-QQQ	218
Feasibility study of fluorine detection by ICP-QQQ	222
HPLC-ICP-MS/MS: fluorine speciation analysis	225



# Routine Soil Analysis using the Agilent 8800 ICP-QQQ

## Author

Kazuhiro Sakai  
Agilent Technologies, Japan

## Keywords

soil, sediment, routine analysis, As, Se, HMI, matrix tolerance, robustness

## Introduction

Quadrupole ICP-MS is widely used in inorganic testing laboratories, due to its high sensitivity, low detection limits, wide dynamic range, and high speed multi-element analysis. The technique is well suited to the analysis of elemental contaminants present in soil and sediment samples. Helium (He) collision cell technology can be used successfully to remove many common matrix-based polyatomic interferences. He mode is less effective for the removal of interferences caused by doubly charged ions though. For example, interferences on arsenic (As) and selenium (Se) by doubly charged ions of rare earth elements (REEs). Typically, the REE content of environmental samples is low. However, all interferences, including the doubly charged ions of REEs on As and Se, can be removed using oxygen mass-shift mode of Agilent's ICP-QQQ. This approach provides a high level of confidence in the analysis of unknown samples. Agilent's ICP-QQQ instruments also offer the same robustness and matrix tolerance of Agilent's single-quadrupole ICP-MS systems.

This study demonstrates the robustness of the Agilent 8800 ICP-QQQ for routine soil analysis.

## Experimental

**Instrumentation:** Agilent 8800 #100.

**Plasma conditions:** Preset plasma/HMI-4. The ICP-MS MassHunter software automatically sets robust plasma tuning conditions that are suitable for soil/sediment analysis.

**Method:** the method was based on a preset method for soil (EPA 6020). It was modified to include O<sub>2</sub> mass-shift mode for sulfur (S), As, and Se. All other elements were measured in He mode. After the calibration standards and initial QC samples had been analyzed, 13 sample blocks were analyzed. Each block consisted of 10 samples (two each of Soil A, Soil B, Estuarine Sediment, River Sediment A, River Sediment B). A Periodic Block consisting of Continuing Calibration Blank (CCB) and Continuing Calibration Verification (CCV) samples was automatically inserted into the sequence after each set of 10 samples.

**Samples:** Five soil and sediment CRMs bought from High-Purity Standards Inc. (Charleston, SC, USA) were analyzed in this study. These included CRM River Sediment A, CRM River Sediment B, CRM Estuarine Sediment, CRM Soil A, and CRM Soil B.

## Results and discussion

The total number of analyses of calibration standards, QC samples, and soil samples was 177 over ~12 hours. The internal standard (ISTD) stability plot, shown in Figure 1, met EPA 6020 requirements of between 70 and 120% of the value of the initial calibration standard.

The accuracy of the method was evaluated by analyzing the soil and sediment CRMs as unknown samples. Each CRM was measured 26 times in the batch. The mean concentrations and relative standard deviations (%RSD) were calculated and compared to the certified value, as shown in Table 1. The mean concentration for all elements was in good agreement with the certified value, with most RSDs well below 5% over the 12-hour analysis.

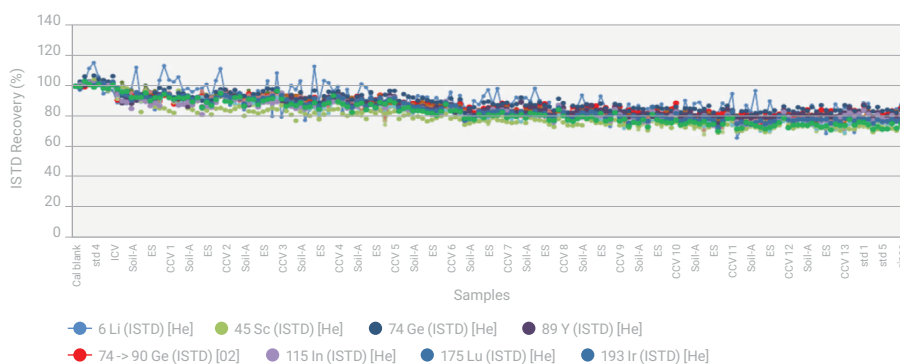


Figure 1. ISTD signal stability plot over 12 hours.

## Conclusion

The Agilent 8800 ICP-QQQ with HMI offers the robustness and matrix tolerance required for the routine analysis of the widest range of trace and major elements in high matrix samples, such as soil and sediments. Doubly charged REE interferences that can affect arsenic and selenium measurement at trace levels were avoided using MS/MS mass-shift mode with O<sub>2</sub> cell gas. Most other elements were measured in He mode, proven to remove common matrix-based polyatomic interferences in complex and variable matrices. Not all soils, sediments, and food products contain significant concentrations of REEs. However, the presence of REEs in samples that are analyzed using single quadrupole ICP-MS can lead to false positive results for As and Se. The use of the ICP-QQQ with MS/MS improves confidence in the results for these two important elements. Furthermore, method development is simplified with the use of preset methods and autotuning, ensuring reproducible performance from day-to-day and irrespective of operator experience.

## More information

Routine soil analysis using an Agilent 8800 ICP-QQQ, Agilent publication [5991-6409EN](#)

Table 1. Mean recovery % of three soil/sediment CRMs.

Element	Integration time (s)	MDL (ppb)	River Sediment A			Estuarine Sediment A			Soil A		
			Mean conc. (ppb)	RSD (%)	Mean recovery (%)	Mean conc. (ppb)	RSD (%)	Mean recovery (%)	Mean conc. (ppb)	RSD (%)	Mean recovery (%)
<sup>9</sup> Be	3	0.06	< MDL			2.1	5.5	106	< MDL		
<sup>23</sup> Na	0.1	0.98	5191	2.6	104	20862	2.4	104	7292	2.6	104
<sup>24</sup> Mg	0.1	0.73	7292	2.6	104	10553	2.7	106	7341	2.6	105
<sup>27</sup> Al	0.1	1.00	25862	2.4	103	70884	2.7	101	51034	2.5	102
<sup>31</sup> P	1	3.20	< MDL			520	2.4	104	1042	2.0	104
<sup>32</sup> S	1	4.10	< MDL			< MDL			< MDL		
<sup>39</sup> K	0.1	7.50	15623	2.2	104	15568	2.7	104	20678	2.3	103
<sup>44</sup> Ca	0.1	2.70	28860	2.1	96	7760	3.2	97	33670	1.8	96
<sup>51</sup> V	0.3	0.021	26	2.6	105	103	2.9	103	10.4	3.4	104
<sup>52</sup> Cr	0.3	0.04	29792	2.7	99	83	3.0	104	< MDL		
<sup>55</sup> Mn	0.3	0.062	809	2.2	101	399	2.9	100	10.9	3.0	109
<sup>56</sup> Fe	0.1	0.45	120085	2.7	100	35335	3.3	101	20215	2.2	101
<sup>59</sup> Co	0.3	0.017	11	2.9	106	10.8	2.8	108	0.33	3.1	
<sup>60</sup> Ni	0.3	0.049	52	2.8	103	30.7	3.2	102	30.2	2.6	101
<sup>63</sup> Cu	0.3	0.021	102	2.9	102	20.2	3.1	101	30.2	2.4	101
<sup>66</sup> Zn	0.3	0.063	1499	2.5	100	151	2.9	101	101	2.3	101
<sup>75</sup> As	1	0.024	60	3.6	100	10.5	3.6	105	20.4	3.0	102
<sup>78</sup> Se	3	0.049	2.0	3.6	101	4.9	3.0	99	1.0	6.2	99
<sup>95</sup> Mo	0.3	0.022	0.19	10.5		< MDL			< MDL		
<sup>107</sup> Ag	0.3	0.015	0.15	9.0		0.015	16.4		0.038	17.3	
<sup>111</sup> Cd	3	0.012	10.3	2.0	103	0.11	4.5		0.37	2.9	125
<sup>121</sup> Sb	0.3	0.011	50.8	2.1	102	0.58	4.4		3.2	3.5	106
<sup>135</sup> Ba	0.3	0.055	50.9	2.1	102	1.5	5.4		513	2.6	103
<sup>201</sup> Hg	1	0.003	< MDL			< MDL			0.018		
<sup>205</sup> Tl	0.3	0.008	0.97	2.0	97	< MDL			< MDL		
<sup>208</sup> Pb	0.3	0.009	719	2.1	103	30.7	2.6	102	41	2.4	101
<sup>232</sup> Th	0.3	0.007	2.1	3.1	106	10.4	2.5	104	10	2.2	103
<sup>238</sup> U	0.3	0.09	1.0	2.4	104	< MDL			1.0	2.5	102

# The Accurate Measurement of Selenium in Reference Materials using Online Isotope Dilution

## Author

Naoki Sugiyama  
Agilent Technologies, Japan

## Keywords

selenium, environmental, agricultural, online isotope dilution analysis, OIDA, oxygen mass-shift

## Introduction

Selenium (Se) is an important element in environmental and agricultural studies. It is an essential trace nutrient but is toxic in excess. ICP-MS is the analytical method of choice for both total and speciated Se measurements, but Se is a difficult element to quantify accurately at trace levels by ICP-MS for several reasons:

- The signal for Se is low, since it is poorly ionized in the plasma due to its high Ionization Potential (IP) of 9.75 eV.
- Because Se is poorly ionized, it suffers signal suppression in high matrix samples – an issue that is further compounded by the lack of a suitable internal standard element with a similar mass and IP.
- All the analytically useful Se isotopes suffer from multiple spectral interferences, as summarized in Table 1.
- The resolution required to separate all of the spectral interferences is beyond the capabilities of sector-type high resolution (HR-)ICP-MS.

The Agilent 8800 ICP-QQQ in MS/MS mode is able to remove the complex spectral interferences from all the Se isotopes shown in Table 1, allowing the use of Isotope Dilution (ID) analysis, which requires at least two interference-free isotopes. ID is the most accurate quantification technique as it is based on direct measurement of isotopic abundances in each sample, rather than a relative measurement of analyte response compared to a standard. As a result, it offers better traceability and improved correction of non-spectroscopic interferences encountered in high matrix sample analysis. This note describes the application of the Agilent 8800 ICP-QQQ using ID for the accurate quantification of Se in a range of certified reference materials (CRMs).

**Table 1.** Spectral interferences on Se isotopes.

Mass	Se isotope			Interference				
	Abundance %	Isobaric	Argide	Oxides	Hydride	Chloride	Doubly charged	Dimer
77	7.63		<sup>39</sup> K <sup>38</sup> Ar <sup>+</sup>	<sup>61</sup> Ni <sup>16</sup> O <sup>+</sup> , <sup>59</sup> Co <sup>18</sup> O <sup>+</sup>	<sup>76</sup> GeH <sup>+</sup> , <sup>76</sup> SeH <sup>+</sup>	<sup>40</sup> Ar <sup>37</sup> Cl <sup>+</sup> , <sup>40</sup> Ca <sup>37</sup> Cl <sup>+</sup>	<sup>154</sup> Sm <sup>++</sup> , <sup>154</sup> Gd <sup>++</sup>	
78	23.77	<sup>78</sup> Kr <sup>+</sup>	<sup>40</sup> Ca <sup>38</sup> Ar <sup>+</sup>	<sup>62</sup> Ni <sup>16</sup> O <sup>+</sup>	<sup>77</sup> SeH <sup>+</sup>	<sup>41</sup> K <sup>37</sup> Cl <sup>+</sup>	<sup>156</sup> Gd <sup>++</sup> , <sup>156</sup> Dy <sup>++</sup>	<sup>38</sup> Ar <sup>40</sup> Ar <sup>+</sup> , <sup>39</sup> K <sup>39</sup> K <sup>+</sup>
80	49.61	<sup>80</sup> Kr <sup>+</sup>	<sup>40</sup> Ca <sup>40</sup> Ar <sup>+</sup>	<sup>64</sup> Ni <sup>16</sup> O <sup>+</sup> , <sup>64</sup> Zn <sup>16</sup> O <sup>+</sup> , <sup>32</sup> S <sub>2</sub> <sup>16</sup> O <sup>+</sup> , <sup>32</sup> S <sup>16</sup> O <sub>3</sub> <sup>+</sup>	<sup>79</sup> BrH <sup>+</sup>	<sup>45</sup> Sc <sup>35</sup> Cl <sup>+</sup>	<sup>160</sup> Gd <sup>++</sup> , <sup>160</sup> Dy <sup>++</sup>	<sup>40</sup> Ar <sup>40</sup> Ar <sup>+</sup> , <sup>40</sup> Ca <sup>40</sup> Ca <sup>+</sup>
82	8.73	<sup>82</sup> Kr <sup>+</sup>	<sup>42</sup> Ca <sup>40</sup> Ar <sup>+</sup>	<sup>66</sup> Zn <sup>16</sup> O <sup>+</sup>	<sup>81</sup> BrH <sup>+</sup>	<sup>45</sup> Sc <sup>37</sup> Cl <sup>+</sup>	<sup>164</sup> Dy <sup>++</sup> , <sup>164</sup> Er <sup>++</sup>	

## Experimental

**Instrumentation:** Agilent 8800 #100.

**Plasma conditions:** Preset plasma/General purpose.

**Ion lens tune:** Soft extraction tune: Extract 1 = 0 V,  
Extract 2 = -180 V.

**CRC conditions:** O<sub>2</sub> gas at 0.4 mL/min plus H<sub>2</sub> gas at  
2.0 mL/min, Octopole bias = -18 V and KED = -6 V.

**Acquisition parameters:** MS/MS O<sub>2</sub> mass-shift method. The reaction of Se<sup>+</sup> with O<sub>2</sub> to form SeO<sup>+</sup> is endothermic ( $\Delta H_r = 0.71$  eV), but the reaction is efficiently promoted using high collision energy using a low octopole bias voltage setting [1]. Preliminary studies have shown that low BEC for Se isotopes can be achieved via the addition of a small amount of H<sub>2</sub> in MS/MS O<sub>2</sub> mass-shift method.

**Method:** Online isotope dilution analysis (OIDA) [2] was used. OIDA is a useful development of traditional isotope dilution, as it removes the time consuming step of spiking enriched-isotope standards into each individual sample. A <sup>82</sup>Se enriched standard purchased from Oak Ridge National Laboratory (USA) was prepared at the appropriate concentration and added via the standard online ISTD mixing kit to the samples. Product ions derived from the <sup>16</sup>O-atom addition transition were measured for the three most analytically useful isotopes of Se. On the 8800 ICP-QQQ, this is simply achieved by defining the acquisition method with Q1/Q2 settings: Q1=78/Q2=94, Q1=80/Q2=96 and Q1=82/Q2=98 for the Se isotopes at *m/z* 78, 80 and 82 respectively.

It should be noted that the use of MS/MS (where Q1 acts as a 1 u mass filter) is essential for this measurement, as it ensures that only one Se isotope enters the cell for any given mass pair measurement, and only the <sup>16</sup>O atom addition is measured because the mass difference between Q1 and Q2 is 16 u. This ensures that there is no overlap due to the precursor ions from different Se<sup>+</sup> isotopes giving SeO<sup>+</sup> product ions at the same mass, such as the <sup>80</sup>Se<sup>18</sup>O<sup>+</sup> product ion overlap on <sup>82</sup>Se<sup>16</sup>O<sup>+</sup>, both of which appear at *m/z* 98. ICP-QQQ in MS/MS mode thereby removes one of the critical limitations of reaction chemistry with ICP-QMS, where all the sample ions enter the cell together so no specific reaction transition can be defined. Each Se isotope mass pair was measured with an integration time of 1 s and three replicates.

**Sample preparation:** The CRMs were microwave digested using a Milestone ETHOS closed vessel microwave digestion system (Milestone, Sorisole, Italy) and following the manufacturer's recommended procedures. The final dilution factor of the samples varied from 250 to 500x.

## Results and discussion

### Study of cell gases for spectroscopic interference removal

Figure 1 shows the result of a preliminary study of the effects of the choice of cell gas on interference removal. The findings of the study showed that  $O_2/H_2$  mass-shift (Figure 1) enables the measurement of  $^{78}\text{Se}$ ,  $^{80}\text{Se}$  and  $^{82}\text{Se}$  relatively free from interferences in the range of synthetic matrices tested.

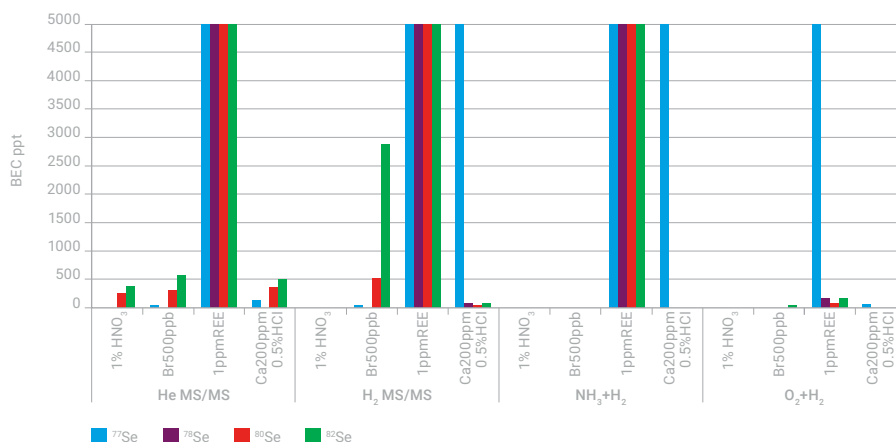


**Figure 1.** Preliminary study of the effectiveness of different cell gases for interference removal. Four synthetic matrices likely to give rise to interferences on the Se isotopes were measured using each of the 4 different cell gas modes.

### Measurement of Se in CRMs

The concentration of Se was determined in 12 different CRMs using the OIDA method. The CRMs were obtained from NIST (Gaithersburg MD, USA), GSJ Geochemical Reference Samples (Tokyo, Japan), Japan Society for Analytical Chemistry (Tokyo, Japan), and National Institute of Metrology (Beijing, China). The matrices included environmental waters (NIST 1643e and JASC 0302-3 River Water), rock (JB-3 basalt), sedimentary rock (JSI-1 and NIST 1646a Estuarine Sediment), soil (JSAC0411 Volcanic Ash Soil), biological samples (NIST 1566a Oyster Tissue, NIST 2976 Mussel Tissue), and plant materials (NIST 1575a Pine Needles, NIST 1515 Apple Leaves, NIST1573a Tomato Leaves).

Figure 2 shows the Se results for each CRM expressed as % recovery relative to the certified value. The measured results for Se were in good agreement with the CRM values (90%-112%), using two Se isotope pairs: 78/82 and 80/82. This demonstrates the effectiveness of the Agilent 8800 ICP-QQQ in MS/MS mode for the removal of multiple interferences on  $^{78}\text{Se}$ ,  $^{80}\text{Se}$  and  $^{82}\text{Se}$ .

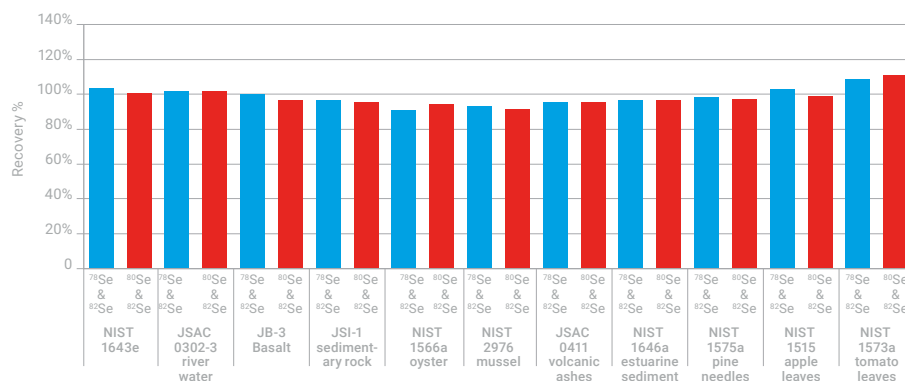


Figure 2. Result of Se quantification using OIDA in various CRMs.

## References

Agilent 8800 Triple Quadrupole ICP-MS: Understanding oxygen reaction mode in ICP-MS/MS, 2012, Agilent technical overview, [5991-1708EN](#)

On-line isotope dilution analysis with the 7700 Series ICP-MS: Analysis of trace elements in high matrix samples, Giuseppe Centineo, Jose Angel Rodriguez Castrillon and Esther Munoz Agudo, 2011, Agilent application note, [5990-9171EN](#)

## More information

The accurate measurement of selenium in twelve diverse reference materials using on-line isotope dilution with the 8800 Triple Quadrupole ICP-MS in MS/MS mode, Agilent publication [5991-0259EN](#)

# ICP-QQQ with Oxygen Reaction Mode for Accurate Trace-Level Arsenic Analysis in Complex Samples

## Authors

Ed McCurdy and Glenn Woods  
Agilent Technologies (UK) Ltd.

## Keywords

arsenic, zirconium, doubly-charged ion interferences, oxygen mass-shift

## Introduction

Arsenic (As), with its high first ionization potential and single isotope at mass 75, is one of the most difficult elements to measure accurately by ICP-MS, particularly in complex matrices. The polyatomic interferences from  $\text{ArCl}^+$  and  $\text{CaCl}^+$  that overlap  $\text{As}^+$  at mass 75 can be removed effectively using quadrupole ICP-MS (ICP-QMS) in helium collision mode, but collision mode cannot resolve the doubly-charged ion interferences from  $^{150}\text{Nd}^{++}$  and  $^{150}\text{Sm}^{++}$ . A quadrupole mass spectrometer separates ions based on their mass to charge ratio ( $m/z$ ), so doubly-charged ions appear at half their true mass;  $^{150}\text{Nd}^{++}$  and  $^{150}\text{Sm}^{++}$  therefore give an apparent overlap on As at mass 75.

Oxygen reaction mode ( $\text{O}_2$  mode) offers a solution to these doubly-charged ion overlaps, since As can be converted to a reaction product ion  $^{75}\text{As}^{16}\text{O}^+$ , measured at  $m/z$  91, where it is separated from the doubly charged Nd and Sm, which do not form such product ions. However, the new mass of the  $\text{AsO}^+$  product ion is also overlapped by an isotope of zirconium ( $^{91}\text{Zr}^+$ ). The presence of Zr in a sample may therefore cause an error in the results for As measured as  $\text{AsO}^+$  using  $\text{O}_2$  reaction mode on ICP-QMS.

ICP-QQQ solves this problem, as MS/MS mode allows all masses apart from  $m/z$  75 (including the  $^{91}\text{Zr}^+$  ions) to be rejected by the first quadrupole (Q1), ensuring that the  $\text{AsO}^+$  product ions can be measured free from overlap. ICP-QQQ with MS/MS therefore allows the accurate determination of As in complex samples that contain any combination of Cl, Ca, Nd, Sm and Zr.



## Experimental

**Reagents and sample preparation:** All of the sample matrices used for this work were prepared using single-element stock solutions (Spex CertiPrep, Claritas grade). The acid matrix and elemental standard concentrations are shown in the caption for each spectrum and are representative of the acid matrix (dilute  $\text{HNO}_3/\text{HCl}$ ) and matrix levels commonly found in ICP-MS samples.

The sample matrices investigated were:

- Dilute nitric acid (1%  $\text{HNO}_3$ )
- Dilute hydrochloric acid (5%  $\text{HCl}$ )
- Calcium (100 ppm)
- Neodymium and samarium (1 ppm each element)
- Zirconium (0.5 ppm)

**Instrumentation:** Agilent 8800 #100.

**Plasma conditions and ion lens tune:** Preset plasma/General purpose, Soft extraction tune: Extract 1 = 0 V, Extract 2 = -170 V.

**Acquisition conditions:** Four operational modes were used, to investigate the different interference removal performance provided by the different cell modes:

- Single Quad (SQ); no gas
- Single Quad (SQ); collision mode (using helium ( $\text{He}$ ) cell gas at a flow rate of 4 mL/min)
- Single Quad (SQ); reaction mode (using oxygen ( $\text{O}_2$ ) cell gas at a flow rate of 0.2 mL/min).
- MS/MS; reaction mode (using  $\text{O}_2$  cell gas at a flow rate of 0.2 mL/min)

KED bias voltage was +5 V in no gas and He mode, and -8 V in  $\text{O}_2$  mode.

The three "Single Quad" modes represent the performance available on conventional ICP-QMS operating in collision or reaction mode. MS/MS mode is unique to the tandem mass spectrometer configuration of the 8800 ICP-QQQ.

## Results and discussion

Figures 1a, 1b and 1c illustrate how Single Quad mode with He cell gas is effective at removing the common  $\text{ArCl}^+$  and  $\text{CaCl}^+$  polyatomic interferences on  $\text{As}^+$  at  $m/z$  75, but is ineffective against the  $\text{Nd}^{++}/\text{Sm}^{++}$  interferences.



**Figure 1. a)**  $\text{As}^+$  ( $m/z$  75) in no gas mode, showing polyatomic interferences from  $\text{ArCl}^+$  and  $\text{CaCl}^+$ ; **b)**  $\text{ArCl}^+$  and  $\text{CaCl}^+$  polyatomics are removed in He collision mode; **c)** He collision mode fails to remove  $\text{Nd}^{++}$  and  $\text{Sm}^{++}$  interferences at  $m/z$  75.

Figures 2a and 2b show how Single Quad mode with O<sub>2</sub> reaction gas successfully avoids the doubly-charged Nd and Sm interferences by mass-shifting the As to the new AsO<sup>+</sup> product ion mass at *m/z* 91; but O<sub>2</sub> reaction mode on ICP-QMS cannot remove the <sup>91</sup>Zr<sup>+</sup> overlap on the AsO<sup>+</sup> product ion.

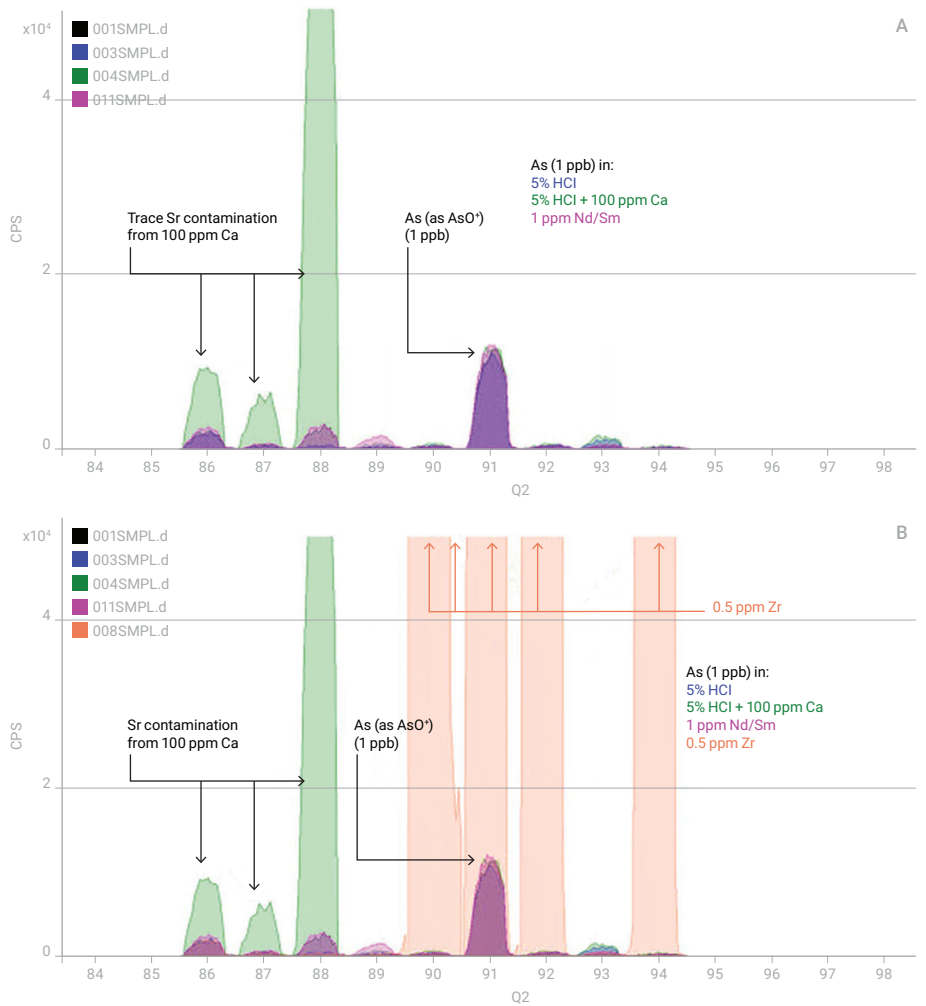


**Figure 2. a)** Nd<sup>++</sup> and Sm<sup>++</sup> interferences at *m/z* 75 are avoided in SQ O<sub>2</sub> reaction mode, by measuring As as the AsO<sup>+</sup> product ion at *m/z* 91; **b)** SQ O<sub>2</sub> reaction mode fails to remove <sup>91</sup>Zr<sup>+</sup> overlap on the AsO<sup>+</sup> product ion.

Figure 3 shows that the 8800 ICP-QQQ in MS/MS mode with O<sub>2</sub> reaction gas provides reliable and consistent measurement of As (as AsO<sup>+</sup>) in all matrices. All the original polyatomic and doubly-charged interferences at *m/z* 75 are avoided by mass-shifting the As to *m/z* 91; and in MS/MS mode the <sup>91</sup>Zr<sup>+</sup> ion is removed by Q1, so the potential overlap on the AsO<sup>+</sup> product ion at *m/z* 91 is also removed.

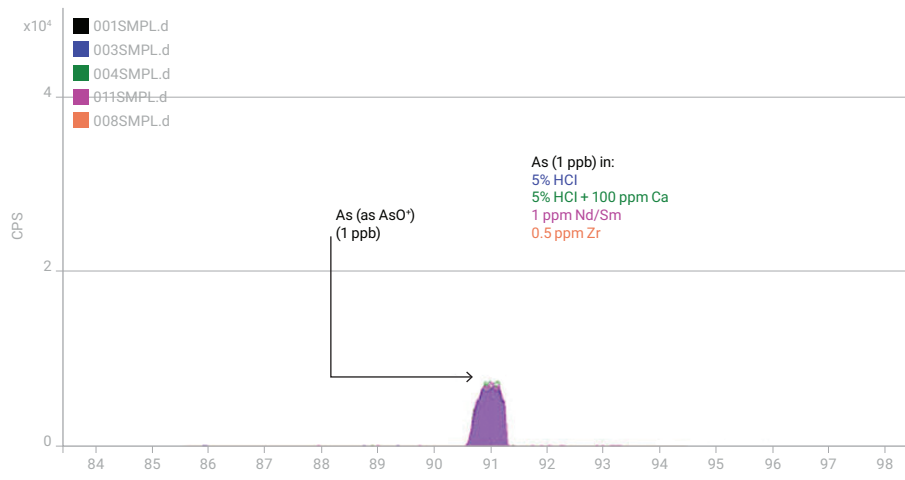


**Figure 3.** MS/MS mass-shift with O<sub>2</sub> reaction mode provides consistent, interference-free measurement of As as AsO in all the matrices.

## Conclusion

With the combination of O<sub>2</sub> reaction mode and MS/MS operation, the 8800 ICP-QQQ provides a reliable approach to the accurate measurement of As in complex samples. All the polyatomic and doubly-charged interferences that affect As measurement at its native mass (*m/z* 75) are avoided by using O<sub>2</sub> mode to mass-shift the As to its AsO<sup>+</sup> product ion, measured at *m/z* 91. Furthermore, MS/MS mode on the 8800 ICP-QQQ also eliminates potential native ion overlaps at *m/z* 91, as they are rejected by Q1 that is set to *m/z* 75 when measuring As.

# Avoidance of Spectral Overlaps on Reaction Product Ions with O<sub>2</sub> Cell Gas: Comparison of Quadrupole ICP-MS and ICP-QQQ

## Author

Ed McCurdy  
 Agilent Technologies (UK) Ltd.

## Keywords

titanium, reaction chemistry, oxygen mass-shift

## Introduction

The 8800 ICP-QQQ opens up many new analytical possibilities and novel methodologies for interference removal based on reaction chemistry. The major benefit provided by the 8800 ICP-QQQ is its unique tandem mass spectrometer configuration, which permits operation in MS/MS mode. In MS/MS, the first quadrupole (Q1) operates as a 1 u mass filter, providing precise selection of the ions that can enter the reaction cell, and therefore control of the reaction processes that occur. This level of reaction process control is fundamentally different to the operation of conventional quadrupole ICP-MS (ICP-QMS) when using these same reaction chemistries, as ICP-QMS has no way to reject ions before they enter the cell, and so cannot select which ions are involved in the reactions.

This difference is apparent in many reaction chemistries, including both on-mass measurements (where the interfering ions are reactive and are moved away from the analyte ions, which are then measured at the natural mass), and mass-shift methods (where the analyte ions are reactive and are moved to a new product ion mass that is free from the original overlap). Overlaps on analyte product ions commonly occur in ICP-QMS and can give severe errors in results, especially in cases where the sample matrix or co-existing analyte levels vary from sample to sample.

In this note, we compare the performance of ICP-QMS (the 8800 ICP-QQQ operated in Single Quad mode with Q1 as a bandpass filter) and ICP-QQQ (the 8800 ICP-QQQ operated in MS/MS mode) for the measurement of titanium (Ti) as TiO<sup>+</sup> product ions, using oxygen reaction mode (O<sub>2</sub> mode).

The native ion overlaps that could affect the measurement of TiO<sup>+</sup> product ions with oxygen reaction gas are shown in Table 1. It should be noted that these native ion overlaps cannot be rejected by the cell bandpass settings of a conventional quadrupole ICP-MS, because they occur at the same mass as the analyte product ion being measured.

**Table 1.** Potential native ion overlaps on TiO<sup>+</sup> product ions in O<sub>2</sub> reaction mode.

Precursor ion (Q1)	Product ion (Q2)	Potential overlaps from other analytes		
		Ni	Cu	Zn
46	62	<sup>62</sup> Ni	–	–
47	63	–	<sup>63</sup> Cu	–
48	64	–	–	<sup>64</sup> Zn
49	65	–	<sup>65</sup> Cu	–
50	66	–	–	<sup>66</sup> Zn

## Experimental

For the spectral comparison, scan data were collected for the mass range from  $m/z$  60 to 69, covering the  $\text{TiO}^+$  product ions formed from Ti in  $\text{O}_2$  reaction mode.

**Instrumentation:** Agilent 8800 #100.

**Plasma conditions and ion lens tune:** Preset plasma/General purpose,  
Soft extraction tune: Extract 1 = 0 V, Extract 2 = -180 V.

**CRC conditions:** Cell gas =  $\text{O}_2$  gas at 0.3 mL/min, Octopole bias = -5 V, KED = -7 V.

**Acquisition parameters:** Scan range =  $m/z$  60 to 69; points per peak = 20;  
integration time per mass = 1 sec.

## Results and discussion

The comparative results for  $\text{TiO}^+$  measured in Single Quad (SQ) mode and MS/MS mode are shown in the overlaid spectra in Figures 1 and 2. In both cases, the  $\text{TiO}^+$  ions at mass 62, 63, 64, 65 and 66 (from the 5 isotopes of Ti at 46, 47, 48, 49 and 50, respectively) are shown, measured using the same  $\text{O}_2$  reaction mode conditions for both modes. The four solutions measured for the overlaid spectra are:

- 1 ppb Ti in 1%  $\text{HNO}_3$
- 1 ppb Ti + 10 ppb Ni in 1%  $\text{HNO}_3$
- 1 ppb Ti + 10 ppb Cu in 1%  $\text{HNO}_3$
- 1 ppb Ti + 10 ppb Zn in 1%  $\text{HNO}_3$

The overlaid spectra in Single Quad mode, shown in Figure 1, show that the peaks for the five  $\text{TiO}^+$  isotopes match the theoretical isotopic template in the 1 ppb Ti sample. However, in the other samples containing the elements Ni, Cu and Zn, all of the  $\text{TiO}^+$  product ions suffer significant overlap from the native Ni ( $m/z$  62), Cu ( $m/z$  63 and 65) and Zn ( $m/z$  64 and 66) ions. Unexpected or variable levels of these common elements would lead to an error in the reported results for Ti measured as  $\text{TiO}^+$  using quadrupole ICP-MS in  $\text{O}_2$  reaction mode.

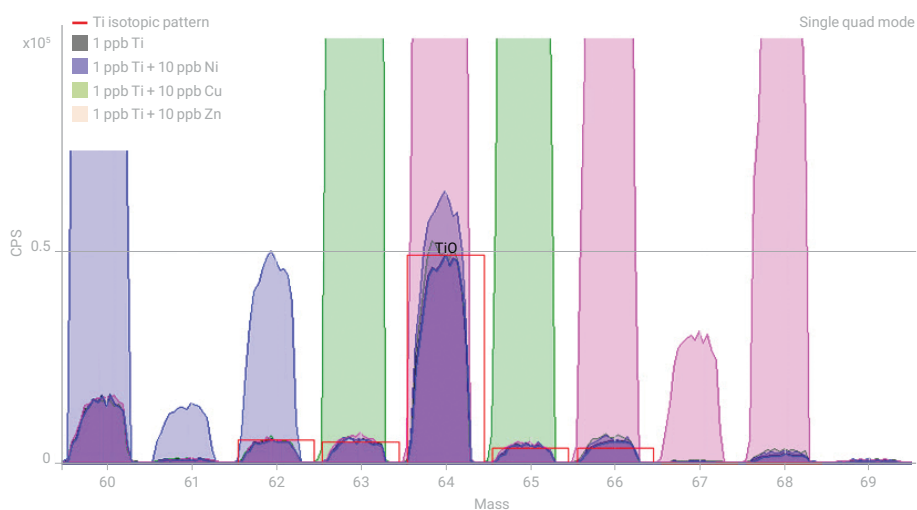


**Figure 1.** Overlaid spectra for  $\text{TiO}^+$  product ions in variable samples measured using SQ mode (see text for sample composition).

In contrast, the overlaid spectra for MS/MS mode, shown in Figure 2, demonstrate consistent measurement of all five  $\text{TiO}^+$  product ions in all four solutions. The presence of the other elements Ni, Cu and Zn has no impact on the  $\text{TiO}^+$  peaks and all five  $\text{TiO}^+$  product ion isotopes could be used to give reliable results for Ti in these variable samples. This illustrates how MS/MS mode on the 8800 ICP-QQQ can simplify method development, because consistent cell conditions, acquisition parameters and isotope selection can be used for a range of variable sample types. A further benefit is that interferences are removed from all isotopes under the same cell conditions, so secondary (or qualifier) isotopes become available for data confirmation or isotope analysis.

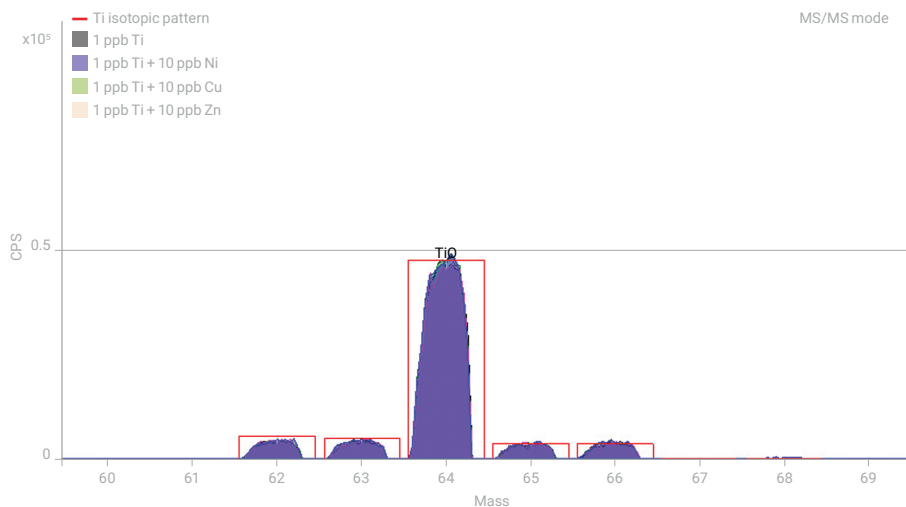


**Figure 2.** Overlaid spectra for  $\text{TiO}^+$  product ions in variable samples measured using MS/MS mode (see text for sample composition).

## Conclusion

The comparative spectra presented in this note illustrate the improved accuracy and consistency delivered by ICP-QQQ operating in MS/MS mode, compared to a conventional quadrupole ICP-MS using a reaction cell with bandpass filter. By rejecting non-target native ions that would occur at the same mass as analyte product ions, potential interferences can be eliminated by MS/MS. This allows simpler, more consistent method development, as well as improving accuracy for interfered elements in complex and variable samples.

# Removal of Complex Spectral Interferences on Noble Metal Isotopes

## Author

Naoki Sugiyama  
Agilent Technologies, Japan

## Keywords

Platinum Group Elements, gold, silver, ore exploration, geochemical, environmental, catalytic converter, ammonia

## Introduction

The precise determination of the noble metals, comprising the Platinum Group Elements (PGEs: Ru, Rh, Pd, Os, Ir and Pt), Au and Ag, is of great interest in areas such as ore exploration and geochemical studies, and these metals are increasingly used for industrial applications including advanced materials and alloys, medical devices, and catalysts for pharmaceutical manufacturing.

Environmental monitoring is also required as some of these elements are used in automobile catalytic converters. ICP-MS is widely used for these applications due to its high sensitivity and multi-element capability. However, the analysis is challenging because the metal concentrations are often low and they are subject to severe spectral overlaps.

Table 1 summarizes the interferences and abundance (%) of each isotope of the elements (the isotopes highlighted in yellow represent the recommended isotope for determination by ICP-MS). Several methods have been developed to resolve the interferences, such as mathematical correction, matrix removal and high-resolution magnetic sector (HR-)ICP-MS. However, the mass resolution required to separate some of the interferences is beyond the capability of current commercial HR-ICP-MS. For example, separation of  $^{103}\text{Rh}^+$  from  $^{87}\text{Sr}^{16}\text{O}^+$ ,  $^{105}\text{Pd}^+$  from  $^{89}\text{Y}^{16}\text{O}^+$ , and  $^{109}\text{Ag}^+$  from  $^{93}\text{Nb}^{16}\text{O}^+$  requires mass resolution ( $M/\Delta M$ ) of 102900, 27600 and 31500, respectively; commercial HR-ICP-MS instruments are limited to a maximum resolution of 10,000. To remove the multiple, complex interferences on noble elements, the Agilent 8800 ICP-QQQ was used in MS/MS mode, using ammonia as the reaction gas.

## Experimental

**Instrumentation:** Agilent 8800 #100.

**Plasma conditions:** Preset plasma/Low matrix.

**Ion lens tune: Soft extraction tune:** Extract 1 = -3 V, Extract 2 = -200 V.

**CRC conditions:**  $\text{NH}_3$  (10%  $\text{NH}_3$  in He) was used as CRC gas in MS/MS mode.

Following a preliminary optimization study, three different  $\text{NH}_3$  gas flow rates (low (L), medium (M) and high (H)) were used. Cell conditions are given in Table 2. No gas mode was also applied for comparison purposes.



**Table 1.** Abundance (%) of each isotope of noble metals and the interference on each isotope.

m		96	97	98	99	100	101	102	103	104	105	106	107	108	109	110
Element	Ru	5.54		1.87	12.76	12.6	17.06	31.55		8.62						
	Rh								100							
	Pd							1.02		11.14	22.33	27.33		26.46		11.72
	Ag												51.84		48.16	
Interference	Atomic	Zr, Nb, Mo		Mo		Mo						Cd		Cd		Cd
	MH			MoH	MoH		MoH									
	MO, MOH	SeO, BrOH		SeO		SrO	RbO	SrO	SrO, RbO	SrO	YO, SrOH	YOH, ZrO	ZrO	ZrO, MoO	NbO	ZrO, MoO
	Argide			NiAr		NiAr	NiAr	NiAr	CuAr	ZnAr	CuAr	ZnAr	ZnAr	ZnAr		
	Others			CuCl	ZnCl	CuCl	ZnCl	CuCl, ZnCl	ZnCl, Pb <sup>++</sup>	ZnCl	ZnCl					
m		184	185	186	187	188	189	190	191	192	193	194	195	196	197	198
Element	Os	0.02		1.59	1.96	13.24	16.15	26.26		40.78						
	Ir								37.3		62.7					
	Pt							0.014		0.782		32.97	33.83	25.24		7.163
	Au														100	
Interference	Atomic	W		W	Re									Hg		Hg
	MH				WH											
	MO, MOH			YbO	YbO	YbO	YbO	YbO	LuO	YbO, LuD, HfO	HfO	HfO	HfO	HfO	TaO, HfOH	Wo, TaOH
	Argide	NdAr	NdAr	NdAr	SmAr	SmAr, NdAr	SmAr	SmAr, NdAr	EuAr	SmAr	EuAr	SmAr, GdAr	GdAr	GdAr	GdAr	GdAr
Others																

**Table 2.** CRC conditions.

	No gas	NH <sub>3</sub> -L	NH <sub>3</sub> -M	NH <sub>3</sub> -H
Cell gas	na	NH <sub>3</sub>	NH <sub>3</sub>	NH <sub>3</sub>
Gas flow rate (mL/min)	na	2.0	3.0	5.0
Octopole bias (V)	-8	-5	-10	-12
KED (V)	+5		-8	
Cell exit (V)			-90	
Deflect lens (V)	20	10	6	2
Plate lens (V)			-110	

## Method

The BECs of the noble metals were determined in a series of synthetic-matrix samples, using an external calibration method. Indium (In) internal standard (ISTD) was mixed online with the sample via the standard ISTD mixing T-connector. An integration time of 1 s per isotope was used with 3 replicates (7 replicates for blank).

## Samples and sample preparation

Standards and matrix samples were prepared from single element stock solutions purchased from Kanto Chemical Co., Inc. (Saitama, Japan) and a REE mixture standard, XSTC-1 purchased from Spex certiPrep. All solutions were diluted into a final acid mix of 1% HNO<sub>3</sub> and 3% HCl.

## Results and discussion

### Matrix interference study

Tables 3 and 4 summarize the results of the spectral interference study obtained by analyzing individual synthetic matrix blank solutions. Table 3 shows the observed interferences, expressed as BEC (ppb), in each matrix blank measured using no gas mode. As expected from Table 1, the synthetic matrices caused significantly elevated BECs (>> 1 ppb) on all the primary and secondary isotopes of all the analytes except for Ru; Rh suffered a relatively minor increase in BEC of ~0.5 ppb in the 10 ppm Pb/1 ppm Hg matrix.

Table 4 shows the results obtained using NH<sub>3</sub> reaction mode. The optimum gas flow rate for NH<sub>3</sub> for each element was investigated and three gas flow rates (Low: 2.0, Medium: 3.0, and High: 5.0 mL/min) were used. The best isotope and method is highlighted in bold in the Table. It can clearly be seen that NH<sub>3</sub> reaction mode effectively removes the interferences on all the analytes, giving BECs of << 0.1 ppb for the preferred isotope/cell mode in all the matrices. The mechanism for the removal of each interference using the MS/MS capability of the 8800 ICP-QQQ is as follows:

- Ru: slight interferences from Zn and Mo were resolved using on-mass method with NH<sub>3</sub>-M.
- Rh: Pb<sup>++</sup> interference was resolved using on-mass method with NH<sub>3</sub>-M.
- Pd: significant interferences from SrOH<sup>+</sup> and YO<sup>+</sup> were seen on <sup>105</sup>Pd, the only isotope free from atomic isobar. On-mass method with NH<sub>3</sub>-H removed the interferences.
- Ag: significant ZrO<sup>+</sup> interference on both <sup>107</sup>Ag and <sup>109</sup>Ag was resolved using on-mass method with NH<sub>3</sub>-H.

- Os: YbO<sup>+</sup> interference was observed on both <sup>188</sup>Os<sup>+</sup> and <sup>189</sup>Os<sup>+</sup>. Since Os<sup>+</sup> sensitivity in NH<sub>3</sub> mode is low, but Os<sup>+</sup> forms a product ion of OsNH<sup>+</sup>, NH<sub>3</sub>-L with mass-shift gave the best result.
- Ir: LuO<sup>+</sup> and HfO<sup>+</sup> interfere with <sup>191</sup>Ir<sup>+</sup> and <sup>193</sup>Ir<sup>+</sup> respectively. NH<sub>3</sub>-M with mass-shift method worked for <sup>191</sup>Ir<sup>+</sup> as Ir<sup>+</sup> forms a product ion of IrNH<sup>+</sup>.
- Pt: <sup>195</sup>Pt<sup>+</sup> suffers a significant interference from HfO<sup>+</sup>. While the overlap is less significant on <sup>198</sup>Pt<sup>+</sup>, <sup>198</sup>Pt<sup>+</sup> suffers an atomic isobar interference from <sup>198</sup>Hg<sup>+</sup>. However, Hg<sup>+</sup> is effectively neutralized by NH<sub>3</sub> so <sup>198</sup>Pt<sup>+</sup> can be measured free from interference.
- Au: significant interferences by TaO<sup>+</sup> and HfOH<sup>+</sup> are resolved by mass-shift method with NH<sub>3</sub>-M. Au<sup>+</sup> forms a product ion of Au(NH<sub>3</sub>)<sub>2</sub><sup>+</sup>.

**Table 3.** Summary of spectral interferences in no gas mode, showing analyte BECs (ppb) in each matrix blank. Matrix overlaps that made a significant contribution to the analyte BECs are indicated in red (BEC > 10 ppb) and orange (BEC > 1 ppb).

	Ru		Rh	Pd	Ag		Os	
Isotope	99	101	103	105	107	109	188	189
NH <sub>3</sub> flow rate mL/min	NA							
Method	on-mass		on-mass	on-mass	on-mass	on-mass	on-mass	on-mass
Mass pair	99-99	101-101	103-103	105-105	107-107	109-109	188-188	189-189
10 ppm Cu Zn	0.058	0.041	0.138	0.328	0.064	0.061	0.000	0.000
10 ppm Sr Rb	0.000	0.034	0.150	4.39	0.005	0.001	0.000	0.000
10 ppm Ni	0.007	0.019	0.000	0.022	0.012	0.016	0.000	0.000
10 ppm Mo	0.059	0.018	0.000	0.004	0.000	0.018	0.000	0.000
10 ppm Pb, 1 ppm Hg	0.000	0.000	0.472	0.002	0.033	0.034	0.000	0.000
10 ppm Zr Nb	0.000	0.000	0.000	0.022	21.9	1.59	0.000	0.000
10 ppm REE	0.004	0.000	0.009	165	0.147	0.005	2.78	2.99
10 ppm Ta	0.008	0.000	0.000	0.004	0.003	0.000	0.000	0.000
10 ppm Hf	0.000	0.000	0.000	0.004	0.312	0.026	0.000	0.000
10 ppm W	0.000	0.000	0.000	0.003	0.001	0.001	0.000	0.000

	Ir		Pt	Au	
Isotope	191	193	195	198	197
NH <sub>3</sub> flow rate mL/min	NA				
Method	on-mass		on-mass	on-mass	on-mass
Mass pair	191-191	193-193	195-195	198-198	197-197
10 ppm Cu Zn	0.003	0.002	0.000	0.279	0.001
10 ppm Sr Rb	0.002	0.000	0.001	0.310	0.004
10 ppm Ni	0.009	0.004	0.002	0.444	0.011
10 ppm Mo	0.000	0.000	0.000	0.295	0.000
10 ppm Pb, 1 ppm Hg	0.002	0.002	0.000	1293	0.000
10 ppm Zr Nb	0.002	0.775	1.98	3.17	0.417
10 ppm REE	123	0.712	0.788	2.17	0.138
10 ppm Ta	0.000	0.000	0.244	114	284
10 ppm Hf	0.071	28.1	70.9	2.34	14.1
10 ppm W	0.001	0.000	0.000	19.6	0.002

**Table 4.** Summary of spectral interferences in MS/MS NH<sub>3</sub> reaction cell mode, showing analyte BECs (ppb) in each matrix blank. Matrix overlaps that made a significant contribution to the analyte BECs are indicated in red (> 10 ppb) and orange (> 1 ppb).

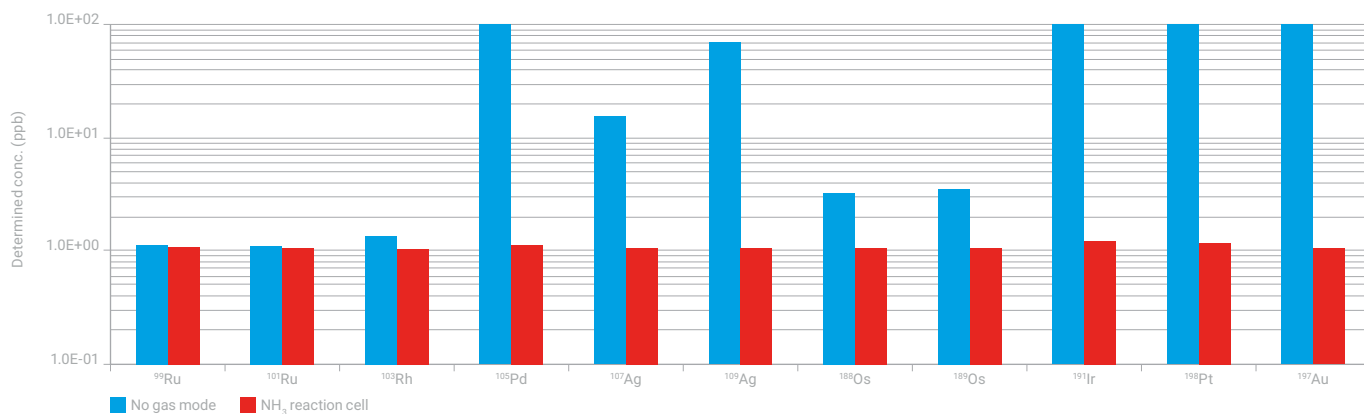
t	Ru		Rh	Pd	Ag		Os			
Isotope	99	101	103	105	107	109	188	189		
NH <sub>3</sub> flow rate mL/min	3.0		3.0	5.0	5.0	2.0				
Method	on-mass	on-mass	on-mass	on-mass	on-mass	on-mass	on-mass	mass-shift	on-mass	mass-shift
Mass pair	99-99	101-101	103-103	105-105	107-107	109-109	188-188	188-203	189-189	189-204
10 ppm Cu Zn	0.000	0.000	0.000	0.001	0.061	0.057	0.000	0.000	0.001	0.002
10 ppm Sr Rb	0.000	0.005	0.016	0.033	0.000	0.000	0.000	0.000	0.002	0.000
10 ppm Ni	0.000	0.000	0.000	0.000	0.010	0.009	0.000	0.000	0.000	0.000
10 ppm Mo	0.005	0.001	0.000	0.000	0.001	0.000	0.000	0.000	0.001	0.000
10 ppm Pb, 1 ppm Hg	0.000	0.000	0.000	0.001	0.033	0.035	0.000	0.000	0.001	0.000
10 ppm Zr Nb	0.000	0.000	0.000	0.000	0.003	0.000	0.000	0.000	0.002	0.001
10 ppm REE	0.000	0.000	0.000	0.014	0.004	0.004	2.79	0.003	5.85	0.010
10 ppm Ta	0.000	0.000	0.000	0.000	0.000	0.000	0.000	0.001	0.003	0.000
10 ppm Hf	0.000	0.000	0.000	0.000	0.000	0.000	0.000	0.001	0.058	0.000
10 ppm W	0.000	0.000	0.000	0.001	0.001	0.001	0.000	0.000	0.000	0.000

	Ir		Pt				Au			
Isotope	191		193		195		198		197	
NH <sub>3</sub> flow rate mL/min	3.0		5.0				3.0		3.0	
Method	on-mass	mass-shift	on-mass	mass-shift	on-mass	mass-shift	on-mass	mass-shift	on-mass	mass-shift
Mass pair	191-191	191-206	193-193	193-208	195-195	195-229	198-198	198-232	197-197	197-231
10 ppm Cu Zn	0.004	0.000	0.003	0.004	0.003	0.000	0.002	0.000	0.000	0.000
10 ppm Sr Rb	0.002	0.000	0.001	0.001	0.000	0.000	0.000	0.000	0.000	0.000
10 ppm Ni	0.004	0.000	0.001	0.004	0.000	0.000	0.000	0.002	0.000	0.000
10 ppm Mo	0.000	0.000	0.000	0.000	0.000	0.000	0.003	0.000	0.000	0.000
10 ppm Pb, 1 ppm Hg	0.002	0.001	0.000	0.000	0.000	0.000	0.005	0.001	0.000	0.000
10 ppm Zr Nb	0.017	0.000	0.679	0.066	0.031	0.009	0.003	0.001	0.000	0.000
10 ppm REE	44.3	0.019	1.56	0.019	0.031	0.002	0.000	0.000	0.044	0.003
10 ppm Ta	0.000	0.000	0.000	0.000	0.004	0.000	0.261	0.009	4.11	0.046
10 ppm Hf	0.690	0.095	21.4	2.40	0.904	0.115	0.141	0.070	0.070	0.003
10 ppm W	0.001	0.000	0.000	0.000	0.001	0.000	0.479	0.000	0.001	0.000

### Analysis of complex synthetic matrix sample using optimized NH<sub>3</sub> reaction mode

A complex synthetic matrix sample containing 10 ppm each of Cu, Zn, Sr, Rb, Ni, Mo, Pb, Zr, Nb, REEs, Ta, Hf, W and 1 ppm Hg was prepared, and this matrix was spiked with 1 ppb each of Ru, Rh, Pd, Ag, Os, Ir, Pt and Au as analytes. The concentration of the noble metals was determined in two modes: No gas mode and NH<sub>3</sub> reaction cell mode, and the spike recovery results are displayed in Figure 1 for each mode. The results demonstrate that MS/MS mode with NH<sub>3</sub> reaction cell gas successfully removes multiple interferences on all the noble metals, providing accurate results for these analytes even in a complex and challenging matrix.



**Figure 1.** Result of synthetic matrix sample test. 1 ppb noble metals were measured in a multi-matrix sample containing 10 ppm of each Cu, Zn, Sr, Rb, Ni, Mo, Pb, Zr, Nb, REEs, Ta, Hf, W and 1 ppm Hg.

# Analysis of Platinum Group Elements (PGEs), Silver, and Gold in Roadside Dust using Triple Quadrupole ICP-MS

## Authors

Dominique Demare and  
Liliane Jean-Soro,  
Université Gustave Eiffel (IFSTTAR),  
Nantes, France

Alain Desprez,  
Agilent Technologies Ltd, France

Glenn Woods and Ed McCurdy,  
Agilent Technologies LDA (UK) Ltd

Accurate, interference-free measurement of sub-ppb levels of the PGEs using the Agilent 8900 ICP-QQQ

## Introduction

There is increasing interest in monitoring the noble metals—that is the Platinum Group Elements (PGEs), Ru, Rh, Pd, Os, Ir, and Pt, together with Ag and Au—in the environment. The levels of these elements have increased due to deposition arising from automobile catalytic converters (1, 2). Precious metals are also used in healthcare and pharmaceuticals and in advanced technologies such as industrial catalysts, fuel cells, and electrodes, capacitors, and magnetic storage for consumer electronics. Production, use, and disposal of these products leads to wider release of the PGEs into the environment, which increases the need for routine monitoring of the metals in environmental samples. ICP-MS is widely used for analysis of trace levels of metals and metalloids, due to the technique's high sensitivity and multi-element capability. However, determination of the PGEs in samples such as soil and roadside dust is challenging for conventional single quadrupole ICP-MS because of the low concentration of the elements. Also, there is the potential for intense spectral overlaps from several common matrix elements, as shown in Table 1.

Many different approaches have been employed in an attempt to avoid, correct, or resolve matrix-based spectral overlaps in ICP-MS, including mathematical correction, matrix removal, and magnetic sector High-Resolution (HR)-ICP-MS. However, mathematical corrections are often unreliable, and matrix elimination is time-consuming, expensive, and prone to errors and contamination. HR-ICP-MS seems an attractive option, as it should give certainty that the analyte has been resolved from the overlapping ion on the mass scale. But many common spectral interferences require mass resolution far beyond the capability of commercial HR-ICP-MS instruments. For example, resolving  $^{103}\text{Rh}^+$  from  $^{87}\text{Sr}^{16}\text{O}^+$  requires mass resolution ( $M/\Delta M$ ) of 102,900; resolving  $^{105}\text{Pd}^+$  from  $^{89}\text{Y}^{16}\text{O}^+$ , requires resolution of 27,600; and resolving  $^{109}\text{Ag}^+$  from  $^{93}\text{Nb}^{16}\text{O}^+$  requires resolution of 31,500. Current HR-ICP-MS instruments have a maximum mass resolution of 10,000, so are unable to separate any of these spectral overlaps.

The most widely used approach to resolve the common polyatomic ion overlaps that occur in quadrupole ICP-MS is to use a Collision/Reaction Cell (CRC) pressurized with helium (He) cell gas. He mode enables selective attenuation of polyatomic ions using a process called kinetic energy discrimination (KED). However, some of the matrix-based interferences on the trace PGEs are at too high intensity to be completely removed using He KED mode. Also, some interferences, such as  $^{206}\text{Pb}^{++}$  on Rh at mass 103, are caused by spectral overlaps that are not polyatomic ions, so He mode cannot remove them effectively.

**Table 1.** Noble metal isotopic abundances (%) and potential spectral interferences on each isotope. Preferred isotopes for ICP-MS analysis are highlighted in yellow, secondary isotopes may be useful for data confirmation.

Mass	Analyte Isotope Abundance (%)				Potential Spectral Interferences				
	Ru	Rh	Pd	Ag	Isobaric	Hydride	Oxide/ Hydroxide	Argide	Other
96	5.54				Zr, Nb, Mo		SeO, BrOH		
98	1.87				Mo	MoH	SeO	NiAr	CuCl
99	12.76					MoH			ZnCl
100	12.6				Mo		SrO	NiAr	CuCl
101	17.06					MoH	RbO	NiAr	ZnCl
102	31.55		1.02				SrO	NiAr	CuCl, ZnCl
103		100					SrO, RbO	CuAr	ZnCl, Pb <sup>++</sup>
104	8.62		11.14				SrO	ZnAr	ZnCl, Pb <sup>++</sup>
105			22.33				YO, SrOH	CuAr	ZnCl
106			27.33		Cd		YOH, ZrO	ZnAr	
107				51.84			ZrO	ZnAr	
108			26.46		Cd		ZrO, MoO	ZnAr	
109				48.16			NbO		
110			11.72		Cd		ZrO, MoO		
	Os	Ir	Pt	Au					
184	0.02				W			NdAr	
186	1.59				W		YbO	NdAr	
187	1.96				Re	WH	YbO	SmAr	
188	13.24						YbO	SmAr, NdAr	
189	16.15						YbO	SmAr	
190	26.26		0.014				YbO	SmAr, NdAr	
191		37.3					LuO	EuAr	
192	40.78		0.782				YbO, LuO, HfO	SmAr	
193		62.7					HfO	EuAr	
194			32.97				HfO	SmAr, GdAr	
195			33.83				HfO	GdAr	
196			25.24		Hg		HfO	GdAr	
197				100			TaO, HfOH	GdAr	
198			7.163		Hg		WO, TaOH	GdAr	

In this work, an alternative approach to He KED was investigated, using an Agilent 8900 Triple Quadrupole ICP-MS (ICP-QQQ) to resolve the multiple, matrix-based interferences that affect analysis of the PGEs (7). The 8900 ICP-QQQ is a tandem mass spectrometer with two high performance, hyperbolic, quadrupole mass filters, one before (Q1) and one after (Q2) the ORS<sup>4</sup> CRC. The tandem (MS/MS) configuration gives the possibility to use the additional quadrupole—Q1, before the CRC—to select the ions that can enter the cell. This allows the ion/molecule reaction chemistry to be precisely controlled, even when highly reactive cell gases such as ammonia (NH<sub>3</sub>) are used in the CRC. Reaction chemistry processes happen much faster than He KED, so can provide more effective separation of trace analytes that are overlapped by intense spectral interferences.

The 8900 ICP-QQQ includes UHMI (Ultra High Matrix Introduction) aerosol dilution technology, which increases plasma robustness and allows samples with higher Total Dissolved Solids (TDS) to be analyzed routinely. The 8900 with UHMI improves trace level analysis, as samples can be analyzed with minimal dilution, which reduces the risk of errors and contamination from the dilution step. Use of a more robust (hotter) plasma also increases ionization, improving sensitivity for poorly ionized noble metals such as Ir, Pt, and Au.

A series of synthetic matrix element mixes and a certified reference material (CRM) of road dust were used to evaluate the effectiveness and accuracy of the 8900 ICP-MS/MS method.

This work was performed in collaboration with the Université Gustave Eiffel, formerly IFSTTAR, Institut Français des Sciences et Technologies des Transports, de l'Aménagement et des Réseaux (the French Institute of Science and Technology for Transport, Development and Networks).

## Experimental

### Instrumentation

An Agilent 8800 ICP-QQQ was used for initial measurements, with later work being performed using an Agilent 8900 ICP-QQQ model. Both instruments were operated in the standard configuration, which includes Ni interface cones and standard "x" type ion lens. The standard sample introduction system was used, consisting of a MicroMist nebulizer, Peltier-cooled quartz double-pass Scott-type spray chamber, and quartz torch with 2.5 mm injector. Preset plasma condition UHMI-4 (aerosol dilution factor of approximately 4) was selected for the analysis.

The interference removal capability of NH<sub>3</sub> reaction gas in MS/MS mode (both quadrupoles functioning as true mass filters) was assessed. Results acquired with NH<sub>3</sub> in MS/MS mode were compared to the data collected with no cell gas and in He KED mode, as typically used on single quadrupole ICP-MS. Three different NH<sub>3</sub> gas flow rates (Low (NH<sub>3</sub>-L), Medium (NH<sub>3</sub>-M), and High (NH<sub>3</sub>-H)) were used. The NH<sub>3</sub> cell modes used a cell gas of 10% NH<sub>3</sub> in He buffer gas, which controls the in-cell formation of unwanted reaction gas product ions. Details of all the cell gas modes and other acquisition conditions are given in Table 2.

**Table 2.** Agilent 8900 ICP-QQQ acquisition and CRC conditions.

	No Gas	He	NH <sub>3</sub> -L	NH <sub>3</sub> -M	NH <sub>3</sub> -H
Acquisition Mode	SQ	SQ	MS/MS	MS/MS	MS/MS
Cell Gas	N/A	He	NH <sub>3</sub>	NH <sub>3</sub>	NH <sub>3</sub>
Gas Flow (mL/min)	N/A	5.0	2.0	3.0	5.0
Octopole Bias (V)	-8	-18	-5	-10	-12
KED (V)	+5		-8		
Cell Exit (V)	-90				
Deflect Lens (V)	20	0	10	6	2
Integration Time/Mass (s)	0.2	0.3	1	1	1



## Method

The Background Equivalent Concentrations (BECs) of the PGEs were quantified in a series of synthetic interference solutions containing several potentially interfering matrix elements, either individually or in various combinations. The BECs for the PGEs were calibrated against simple, synthetic, non-matrix-matched calibration standards.

Spike recoveries were measured for a spike containing 1 µg/L (ppb) of each of the PGEs, Ag, and Au in the highest, most complex synthetic matrix (all individual matrix components in one solution). To check the accuracy of the method for real sample analysis, the PGEs were also quantified in a digested CRM (BCR 723 Road Dust, IRMM, Geel, Belgium). The CRM has certified values for Rh, Pd, and Pt.

Data was acquired for all three cell gas modes during one visit to the sample vial, and three replicate measurements were acquired for each sample. The no gas and He mode conditions used Single Quad (SQ) mode (Q1 not operating as a mass filter) to replicate the interference removal performance achievable with single quadrupole ICP-MS. The NH<sub>3</sub> cell gas conditions used MS/MS mode with either on-mass measurement of the analyte ion, or mass-shift measurement where an analyte reaction product ion is measured. The indium (In) internal standard (ISTD) was added to the sample solutions online via the standard ISTD mixing T-connector.

## Standards and sample preparation

Standards and interference matrices—most elements at 10 mg/L (ppm)—were prepared from single element 1000 or 10,000 mg/L stock solutions. The single and multiple matrix element mixes analyzed are shown in Table 3. All synthetic solutions were acidified to 4% HNO<sub>3</sub> and 12% HCl. This matrix is typical of the final acid concentration resulting from digestion of soil, dust, and mineral ore samples using aqua regia (a 1:3 mix of concentrated HNO<sub>3</sub>/HCl).

The acid concentration in the synthetic samples matched the acid mix in the digested CRM. The CRM was prepared by mineralization of 0.5084 g of BCR 723 in 2 mL of concentrated HNO<sub>3</sub> and 6 mL of concentrated HCl. The volume was then brought up to 50 mL by addition of ultrapure water, giving a final matrix containing approximately 1% TDS in 16% aqua regia.

## Results and discussion

### Interference removal in complex synthetic matrices

The BEC results obtained in the study of matrix-based spectral interferences in the synthetic matrix solutions are shown in Table 3. The BECs for the PGEs in each of the matrix solutions are compared for no gas, He, and the optimum NH<sub>3</sub> mode (low, medium, or high NH<sub>3</sub> flow). The colored cells in Table 3 indicate the level of contribution that the matrix interferences made to the PGE BEC. For example, a matrix interference contribution causing a BEC of between 0.1 ppb and 1 ppb is indicated by the yellow shading. As can be seen from Table 3, Ru did not suffer significant interference in any of the synthetic matrices, even when measured in no gas mode. However, the other PGEs all suffered moderate or severe interference (up to 996 ppb BEC) in no gas mode. Interference contributions were higher than 10 ppb for Pd, Ag, Ir, Pt, and Au. The BECs for Rh and Os were lower, but still in the 100s of ng/L (ppt) or low ppb range.

The He mode data in Table 3 was evaluated to assess the relative performance of the standard single quadrupole ICP-MS approach to controlling polyatomic ions. Compared to no gas mode, He KED mode gave lower BECs for many of the PGEs, some improved by several orders of magnitude. But He mode was not able to completely resolve all the overlaps to a low enough level for trace analysis of all the PGEs. In He mode, the contribution of the spectral interferences from some of the matrix combinations was still in the ppb range for Pd, Ag, and Os and above 10 ppb for Ir, Pt, and Au.

By contrast, the optimum NH<sub>3</sub> mode significantly reduced the interference contributions on the PGEs in all the matrix solutions, including the most complex interference mix. BECs were lower than single or low 10s ppt for all the PGEs except Ir and Pt-195. The BECs for Ir and Pt in NH<sub>3</sub> mode remained a little higher at 0.1 to 0.2 ppb. But these BECs are still around 100x lower than was achieved in He mode and up to 1000x lower than in no gas mode. The improved interference removal capability provided by NH<sub>3</sub> in MS/MS mode allows the reliable quantitation of PGEs at ultra-trace levels in a complex environmental matrix such as roadside dust.

### Spike recoveries, detection limits (DLs) and BECs in a complex matrix mix

To evaluate more specifically the accuracy of the ICP-MS/MS method, a 1 µg/L (ppb) PGE spike was measured in the highest and most complex synthetic interference solution. The mix contained 10 ppm of all interfering elements (listed in Table 3) except for Hg, which was present at 1 ppm. The PGE spike concentrations were quantified in no gas, He, and the optimum NH<sub>3</sub> cell gas mode. As shown in Figure 1, the PGE spike concentrations measured in no gas mode were strongly affected by spectral overlaps formed from the matrix elements. The matrix interferences in He mode were lower, but several of the measured results were still far above the true spike concentrations. The NH<sub>3</sub> mode results are all free from significant overlap, with measured PGE spike concentrations close to the true value of 1 ppb.

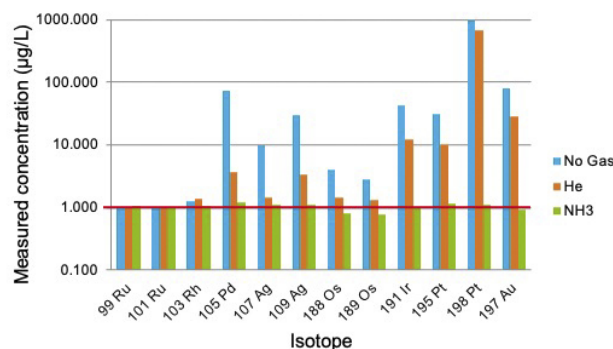


**Figure 1.** Reported concentrations of the PGEs spiked at 1 ppb in the most complex mixed matrix, measured in three different gas modes.

Table 4 shows the DL and BEC for each PGE in the optimum NH<sub>3</sub> cell gas mode. The DLs were calculated from three times the standard deviation of a low standard (10 ppt) divided by the slope of the calibration. The BECs were calculated from the blank intensity divided by the sensitivity. The DLs and BECs for the PGEs measured in NH<sub>3</sub> mode were all in the low or sub-ppt range despite the reduction in sensitivity that occurs due to the use of aerosol dilution with UHMI. The low DLs and BECs indicate that the 8900 ICP-QQQ can achieve excellent detection capability, even when combined with the very robust plasma conditions needed for routine analysis of high matrix sample digests.

**Table 3.** PGE Background Equivalent Concentrations (BECs) in µg/L (ppb) due to matrix-based spectral overlaps measured in no gas, He, and NH<sub>3</sub> cell gas modes. Significant matrix interferences are indicated by colored cells: Yellow (BEC >0.1 ppb), orange (BEC >1 ppb), and red (BEC >10 ppb). MS/MS mode with NH<sub>3</sub> cell gas resolves interferences on all analytes. Note, some PGEs have two usable isotopes.

No cell gas, SQ mode BEC results (µg/L)												
Element	Ruthenium		Rhodium	Palladium	Silver		Osmium		Iridium	Platinum		Gold
Isotope	99	101	103	105	107	109	188	189	191	195	198	197
10 ppm Cu Zn	0.035	0.028	0.036	0.069	0.014	0.004	0.001	0.002	0.005	0.000	0.000	0.002
10 ppm Sr Rb	0.001	0.021	0.096	2.957	0.004	0.001	0.001	0.001	0.002	0.000	0.000	0.002
10 ppm Ni	0.001	0.004	0.002	0.020	0.007	0.008	0.001	0.003	0.005	0.000	0.000	0.001
10 ppm Mo	0.016	0.005	0.001	0.006	0.001	0.006	0.004	0.005	0.001	0.000	0.000	0.001
10 ppm Pb, 1 ppm Hg	0.000	0.000	0.254	0.004	0.002	0.004	0.011	0.012	0.006	0.000	666.924	0.001
10 ppm Zr Nb	0.000	0.000	0.001	0.829	10.436	34.858	0.018	0.018	0.004	0.005	5.270	0.127
10 ppm REE, Sc, Y	0.012	0.030	0.014	78.040	0.098	0.008	3.793	2.229	45.307	1.004	4.540	0.390
10 ppm Ta	0.000	0.001	0.000	0.004	0.001	0.001	0.001	0.001	0.001	0.090	45.386	62.760
10 ppm Hf	0.000	0.000	0.000	0.001	0.001	0.002	0.001	0.016	0.325	29.337	1.062	5.095
10 ppm W	0.001	0.000	0.000	0.001	0.000	0.002	0.004	0.001	0.001	0.005	104.237	0.614
10 ppm all, 1 ppm Hg	0.081	0.078	0.347	75.342	9.210	30.395	3.314	1.936	43.256	31.971	996.057	81.912

He cell gas, SQ mode BEC results (µg/L)												
Element	Ruthenium		Rhodium	Palladium	Silver		Osmium		Iridium	Platinum		Gold
Isotope	99	101	103	105	107	109	188	189	191	195	198	197
10 ppm Cu Zn	0.001	0.001	0.001	0.001	0.005	0.004	0.004	0.002	0.005	0.001	0.000	0.002
10 ppm Sr Rb	0.000	0.001	0.002	0.058	0.001	0.001	0.003	0.002	0.001	0.001	0.000	0.001
10 ppm Ni	0.001	0.000	0.000	0.004	0.005	0.007	0.004	0.003	0.004	0.000	0.000	0.000
10 ppm Mo	0.005	0.001	0.000	0.001	0.000	0.001	0.008	0.005	0.001	0.000	0.000	0.001
10 ppm Pb, 1 ppm Hg	0.000	0.000	0.468	0.001	0.004	0.003	0.016	0.013	0.007	0.000	602.063	0.000
10 ppm Zr Nb	0.000	0.000	0.000	0.038	0.479	0.155	0.023	0.019	0.002	0.004	3.969	0.041
10 ppm REE, Sc, Y	0.000	0.001	0.010	2.692	0.010	0.005	0.543	0.366	11.157	0.064	1.578	0.020
10 ppm Ta	0.002	0.000	0.000	0.002	0.001	0.000	0.002	0.002	0.001	0.055	16.102	25.002
10 ppm Hf	0.000	0.000	0.000	0.001	0.001	0.000	0.004	0.006	0.082	8.937	0.627	1.122
10 ppm W	0.001	0.000	0.000	0.000	0.001	0.001	0.007	0.003	0.001	0.002	36.586	0.199
10 ppm all, 1 ppm Hg	0.016	0.003	0.399	2.748	0.510	0.169	0.489	0.320	11.158	9.264	669.894	27.554

NH <sub>3</sub> cell gas, MS/MS mode BEC results (µg/L)												
Element	Ruthenium		Rhodium	Palladium	Silver		Osmium		Iridium	Platinum		Gold
Isotope	99	101	103	105	107	109	188	189	191	195	198	197
NH <sub>3</sub> flow rate (mL/min)	3.0	3.0	3.0	5.0	5.0	5.0	2.0	2.0	3.0	5.0	5.0	5.0
MS/MS mode	On-mass	On-mass	On-mass	On-mass	On-mass	On-mass	Mass-shift	Mass-shift	Mass-shift	Mass-shift	Mass-shift	Mass-shift
Mass Pair (Q1 - Q2)	99 - 99	101 - 101	103 - 103	105 - 105	107 - 107	109 - 109	188 - 203	189 - 204	191 - 206	195 - 229	198 - 232	197 - 231
10 ppm Cu Zn	0.002	0.001	0.000	0.000	0.004	0.004	0.002	0.004	0.003	0.000	0.000	0.001
10 ppm Sr Rb	0.000	0.003	0.009	0.012	0.000	0.001	0.002	0.003	0.003	0.000	0.000	0.000
10 ppm Ni	0.001	0.001	0.000	0.003	0.005	0.008	0.004	0.003	0.005	0.000	0.000	0.000
10 ppm Mo	0.001	0.001	0.000	0.001	0.000	0.001	0.004	0.008	0.003	0.001	0.003	0.000
10 ppm Pb, 1 ppm Hg	0.000	0.000	0.000	0.001	0.002	0.003	0.010	0.011	0.010	0.000	0.004	0.001
10 ppm Zr Nb	0.000	0.000	0.000	0.002	0.004	0.006	0.020	0.018	0.005	0.001	0.002	0.000
10 ppm REE, Sc, Y	0.000	0.001	0.009	0.017	0.002	0.006	0.050	0.046	0.105	0.008	0.031	0.001
10 ppm Ta	0.000	0.000	0.000	0.000	0.000	0.002	0.004	0.007	0.003	0.001	0.000	0.000
10 ppm Hf	0.001	0.000	0.000	0.000	0.000	0.001	0.007	0.009	0.036	0.113	0.003	0.000
10 ppm W	0.000	0.000	0.000	0.000	0.000	0.002	0.009	0.007	0.006	0.000	0.000	0.000
10 ppm all, 1 ppm Hg	0.002	0.004	0.020	0.044	0.022	0.023	0.030	0.017	0.183	0.137	0.023	0.002

The low DLs and BEC are partly due to the optimized configuration of the 8900 ICP-QQQ, which gives extremely low background signals. For example, 0 cps were measured in the calibration blank for Os, Ir, and Au in NH<sub>3</sub> mode. A second factor is the highly selective reaction chemistry in the CRC when the 8900 is operated in MS/MS mode with NH<sub>3</sub> cell gas. The MS/MS configuration uses Q1 to select the specific mass of ions that are allowed to enter the CRC and react. Q1 ensures that only the selected analyte ions and on-mass interfering ions enter the CRC, so the reactions are controlled and predictable, leading to very effective resolution of the interfering ions. No new potentially overlapping product ions can form from ions at other masses, because all other masses are excluded from the CRC when Q1 is operating as a true mass filter.

Table 4 also shows the percent recoveries for the 1 ppb PGE spike in the highest, most complex mixed matrix solution. All recoveries in NH<sub>3</sub> mode were within 10% of the target value, with the exception of Os, which suffers from chemical instability in the presence of HNO<sub>3</sub>. Osmium stability can be improved by reducing the HNO<sub>3</sub> concentration in the solutions and increasing the HCl concentration.

**Table 4.** PGE DLs, BECs, and recoveries of a 1 ppb spike in a complex synthetic interference matrix.

Element	Mass Pair (Q1 - Q2)	DL (ng/L)	BEC (ng/L)	1 ppb Spike Recovery (%)
Ru	99 - 99	1.691	1.123	104
Ru	101 - 101	0.67	0.129	101
Rh	103 - 103	0.653	0.126	101
Pd	105 - 105	5.541	2.133	108
Ag	107 - 107	3.78	5.288	106
Ag	109 - 109	0.849	0.327	107
Os	188 - 203	6.245	3.704	81
Os	189 - 204	6.558	3.571	78
Ir	191 - 206	8.566	5.882	103
Pt	195 - 229	6.247	1.202	102
Pt	198 - 232	2.232	0.918	109
Au	197 - 231	7.592	4.348	91

### Recovery of PGEs in CRM BCR 723 Road Dust

The aqua regia digestion of CRM BCR 723 Road Dust was analyzed to evaluate the accuracy of the ICP-MS/MS method for quantitative analysis of the PGEs in a representative complex sample matrix. BCR 723 Road Dust has certified values for Rh, Pd, and Pt, and the recoveries for these elements in NH<sub>3</sub> mode on the 8900 ICP-QQQ are shown in Figure 2.

For all three certified elements, the values measured using the 8900 ICP-QQQ in NH<sub>3</sub> mode were in good agreement with the certified values. For Rh and Pt, the 8900 mean measured concentrations were almost identical to the certified mean values, and the measured precision (n=3) was less than 2% RSD. For Pd, the 8900 result was a little higher than the certified mean value, but still within the 95% confidence limits. The Pd result measured by the 8900 method is close to the limit of quantification (LOQ), as indicated by the relatively high RSD of 7%. However, note that the uncertainty of the certified value is also high at 31% (6.1 ± 1.9 µg/kg), due to the low concentration of the element. The certified value for Pd is also based on results from only 8 of the 20 labs that participated in the CRM certification exercise, further illustrating the difficulty of measuring this element at the low levels present in BCR 723.

## Conclusion

A method has been developed for the routine analysis of the PGEs and other noble metals in high and complex matrices using the Agilent 8900 ICP-QQQ in MS/MS mode with NH<sub>3</sub> cell gas. Using the UHMI aerosol dilution system, the ICP-MS was able to tolerate the high levels of TDS (~10 g/L, 1%) in an aqua regia digest of a Road Dust CRM sample. UHMI enables high matrix sample digests such as soil, roadside dust, and mining samples to be analyzed with minimal dilution, avoiding potential problems of dilution errors or contamination from the diluent.

The 8900 ICP-QQQ method used MS/MS mode with NH<sub>3</sub> cell gas to resolve matrix-based interferences on the noble metals. The ability of ICP-MS/MS to resolve severe spectral interferences on the PGEs was shown by the low BECs obtained in a range of complex synthetic matrices. The method was further validated by demonstrating accurate spike recovery of the PGEs in the most complex matrix mix and accurate recovery of the certified elements in a Road Dust CRM sample. Potential matrix-based spectral interferences that cannot be addressed either by He KED mode on single quadrupole ICP-MS or by High Resolution ICP-MS were resolved successfully using the ICP-MS/MS method with NH<sub>3</sub> cell gas.

The 8900 ICP-QQQ offers a unique combination of exceptional matrix tolerance due to the robust UHMI plasma conditions, together with the low background and effective control of NH<sub>3</sub> reactions due to the MS/MS configuration. This combination allowed the development of a method that enables the accurate, interference-free measurement of sub-ppb levels of the PGEs with good precision in complex sample matrices.

The method is suitable for routine environmental monitoring of trace PGEs, as well as other applications such as mineral prospecting, extraction, and processing/reprocessing of the PGEs.

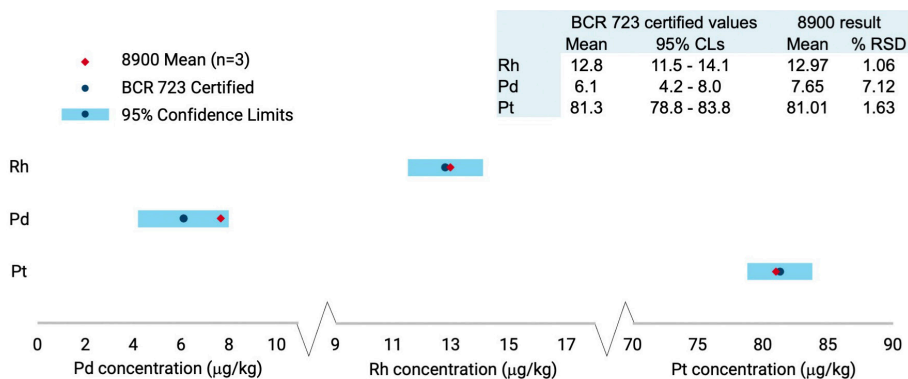


Figure 2. Agilent 8900 ICP-MS/MS measured results compared to certified mean values and uncertainly ranges (95% confidence limits) for Rh, Pd, and Pt in CRM BCR 723 Road Dust.

## References

1. M. Omrani, M. Goriaux, Y. Liu, S. Martinet, L. Jean-Soro, V. Ruban, *Environ. Pollut.*, 257 (2020) 113477
2. M. Omrani, M. Goriaux, L. Jean-Soro, V. Ruban, *Environ. Sci. Pollut. Res.* 28 (2021) 33231–33240
3. Handbook of ICP-QQQ Applications using the Agilent 8800 and 8900, 4th Edition, Agilent publication [5991-2802EN](#), 2020

# Direct Analysis of Ultratrace Rare Earth Elements in Environmental Waters by ICP-QQQ

## Author

Naoki Sugiyama,  
Agilent Technologies Inc.

Measure emerging pollutants in river water using the Agilent 8900 ICP-QQQ in MS/MS mass-shift mode

## Introduction

The Rare Earth Elements (REEs)—also known as the lanthanides—range from lanthanum to lutetium. Scandium and yttrium are also commonly considered to be REEs. REEs are used in a wide range of applications from the glass industry, phosphors, permanent magnets, and lasers to clean energy, defense technologies, and batteries (1–3). With their increasing importance in high tech applications, there is growing concern about the migration of REEs into the environment during mining, processing, use, discarding, or recycling. More evidence is required to understand the effects of REEs on the environment, ecosystems, and from dietary intake. Depending on the findings that emerge from the research, regulations may be introduced to limit the disposal of REEs into water courses. In support of both research and routine monitoring purposes, quick, reliable, and sensitive analytical methods are needed to measure these emerging pollutants at low concentrations in a range of sample-types.

While ICP-MS is suited to the measurement of REEs at trace levels, the direct measurement of REEs in waste and natural waters remains challenging for two main reasons. Typically, the natural background concentration of the REEs is very low in environmental waters, often at or below the detection capabilities of conventional single quadrupole ICP-MS. Also, the analysis may be hindered by spectral interferences such as  $\text{BaO}^+$  on  $\text{Eu}^+$ ,  $\text{BaH}^+$  on  $\text{La}^+$ , or low mass REE-oxide ions overlapping high mass REEs. A chelating resin can be used to preconcentrate the REEs and separate them from Ba, which is usually present at a much higher concentration. But this approach must be optimized for each sample matrix, requiring time, skill, and resources that may not be available in routine labs.

Triple quadrupole ICP-MS (ICP-QQQ) is a simpler, faster, direct method for the analysis of REEs in environmental waters at the ultratrace level. Compared to single quadrupole ICP-MS, ICP-QQQ offers greater sensitivity and advanced interference removal using controlled reaction chemistry in the collision/reaction cell (CRC). Agilent ICP-QQQ instruments feature two quadrupoles (Q1 and Q2), one either side of the CRC, enabling double mass selection (MS/MS). Q1 rejects all nontarget ions before they enter the cell, allowing only analyte ions and on-mass interference ions to pass to the cell. These ions can then be separated using predictable, consistent, and reproducible reaction chemistry (4). Q2 then ensures that only the analyte ions (on mass mode) or analyte-product ions (mass-shift mode) pass to the detector, free of interferences.

In this study, an Agilent 8900 ICP-QQQ was used for the direct analysis of REEs in water that was collected at four different points along a Japanese river. Using an MS/MS mass-shift method with nitrous oxide ( $\text{N}_2\text{O}$ ) as a reaction cell gas, any interferences were resolved quickly and effectively.

## Experimental

### Instrumentation

An Agilent 8900 ICP-QQQ (model #100 for advanced applications) was used in this study. The instrument was fitted with a quartz double-pass spray chamber, quartz torch with 2.5 mm id injector, and Ni interface cones. Sample delivery was via a peristaltic pump and PFA microflow nebulizer (G3139-65100 nebulizer) with a small dead volume. The samples were clean, natural waters, so 'low-matrix' preset plasma conditions were selected in the Agilent ICP-MS MassHunter software. The preset plasma setting automatically optimizes the plasma conditions for the routine analysis of samples with total dissolved solids < 0.1%.

### Selection of reactive cell gas

Oxygen (O<sub>2</sub>) and N<sub>2</sub>O were investigated as reaction cell gases to remove spectral interferences on REEs using a MS/MS mass-shift method. The potential spectral interferences include BaO<sup>+</sup> on Eu<sup>+</sup>, BaH<sup>+</sup> on La<sup>+</sup>, or low mass REE-oxide ions on high mass REE ions.

Since the O atom transfer reaction of REE<sup>+</sup> with N<sub>2</sub>O (REE<sup>+</sup> + N<sub>2</sub>O → REEO<sup>+</sup> + N<sub>2</sub>) is exothermic for all REEs, good sensitivity was expected with N<sub>2</sub>O. As shown in Figure 1, comparable or greater sensitivity was achieved for all REEs using N<sub>2</sub>O compared to O<sub>2</sub> cell gas. Based on these results, N<sub>2</sub>O was used as the reaction cell gas in this study.

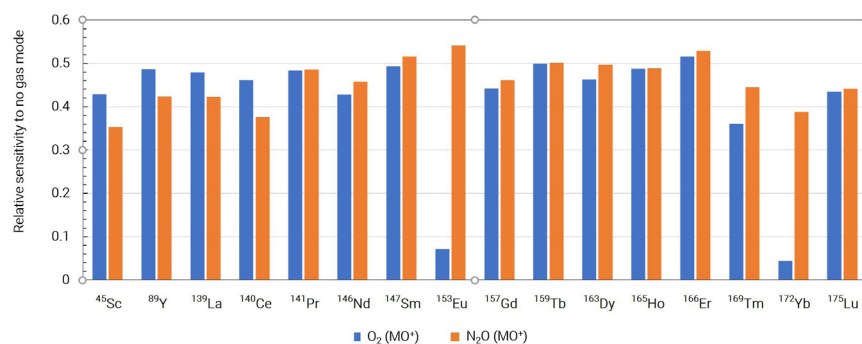


**Figure 1.** Comparison of the sensitivity of ICP-QQQ MS/MS mass-shift method with O<sub>2</sub> and N<sub>2</sub>O cell gas.

All 8900 ICP-QQQ operating and tuning conditions are summarized in Table 1.

**Table 1.** ICP-QQQ tuning and operating conditions.

Parameter	Setting
RF Power (W)	1550
Sampling Depth (mm)	8.0
Nebulizer Gas Flow Rate (mL/min)	1.05
Makeup Gas Flow Rate (mL/min)	0.0
Extraction 1 Lens (V)	-5.0
Extraction 2 Lens (V)	-200
Omega Lens (V)	7.0
Omega Bias Lens (V)	-110
Octopole Bias (V)	-3.0
Cell Gas Flow Rate (% of full scale)	20
Axial Acceleration (V)	1.0



### Method detection limits (MDLs)

MDLs for the REEs were calculated from three times the standard deviation of nine replicate measurements of a low-level standard (0.3 ppt each REE in 1% HNO<sub>3</sub>). The results are summarized in Table 2. All the MDLs are sub ppt, confirming the suitability of the method for the determination of REEs at background levels in environmental waters.

### Certified reference material analysis

A river water certified reference material (CRM), SLRS-6 (NRC-CNRC, Ottawa, Canada) was analyzed using the ICP-QQQ in MS/MS mode with N<sub>2</sub>O. All REEs were measured as oxide ions, with a mass-shift of 16 u, as indicated in the Q1/Q2 settings provided in Table 2.

There is good agreement between the CRM reported values (5) and measured concentrations for all elements except for Sc (Table 2). To investigate the discrepancy, Sc was analyzed in the CRM using no gas and helium (He) collision (kinetic energy discrimination) mode. The measured concentrations were 367 and 33.3 ppt, respectively. No detailed information is given for the reported value for Sc on the CRM certificate. Since the reported concentration (333.0 ppt) agrees with the measured value obtained in no gas mode (367 ppt), the author suspects the CRM reported value provided for Sc is not correct. Because the CRM contains Si at the ppm level, a spectral interference on Sc<sup>+</sup> by SiO<sup>+</sup> or SiOH<sup>+</sup> may account for the high reported value.

Using the ICP-QQQ method, any Si-based interferences on Sc<sup>+</sup> would be avoided. In MS/MS mode, Q1 operates as a single (1 u) mass filter so that only ions with the targeted *m/z* enter the CRC and react with the cell gas. Q1 rejects all other masses (including Si ions), avoiding any subsequent interferences by SiO<sup>+</sup> or SiOH<sup>+</sup> on Sc<sup>+</sup>.

### River water analysis

River water samples were collected at four points (A to D) of the Tama River, Japan. Two of the samples were collected at wastewater treatment plant (WWTP) discharge points (C and D), as shown in Figure 2. Three samples were collected from each sampling point, then filtered through a 0.45 μm filter, and acidified to 1% HNO<sub>3</sub>.

**Table 2.** MDLs and SLRS-6 river water CRM reported values (5) and ICP-QQQ measured results.

Element	Q1/Q2	Integration Time (s)	MDL (ppt)	SLRS-6 Reported (ppt)	SLRS-6 This Study (ppt)
Sc	45/61	1.0	0.127	333.0	16.3
Y	89/105	1.0	0.053	128.0	125.7
La	139/155	1.0	0.062	248.3	241.3
Ce	140/156	1.0	0.061	292.7	288.5
Pr	141/157	1.0	0.057	59.1	57.3
Nd	146/162	3.0	0.066	227.8	221.3
Sm	147/163	3.0	0.096	39.5	37.8
Eu	153/169	1.0	0.082	7.26	6.50
Gd	157/173	3.0	0.078	31.6	29.9
Tb	159/175	1.0	0.059	4.07	3.75
Dy	163/179	3.0	0.073	21.9	21.1
Ho	165/181	1.0	0.100	4.30	4.14
Er	166/182	1.0	0.092	12.4	11.7
Tm	169/185	1.0	0.079	1.79	1.63
Yb	172/188	3.0	0.096	11.2	10.7
Lu	175/191	1.0	0.052	1.91	1.74

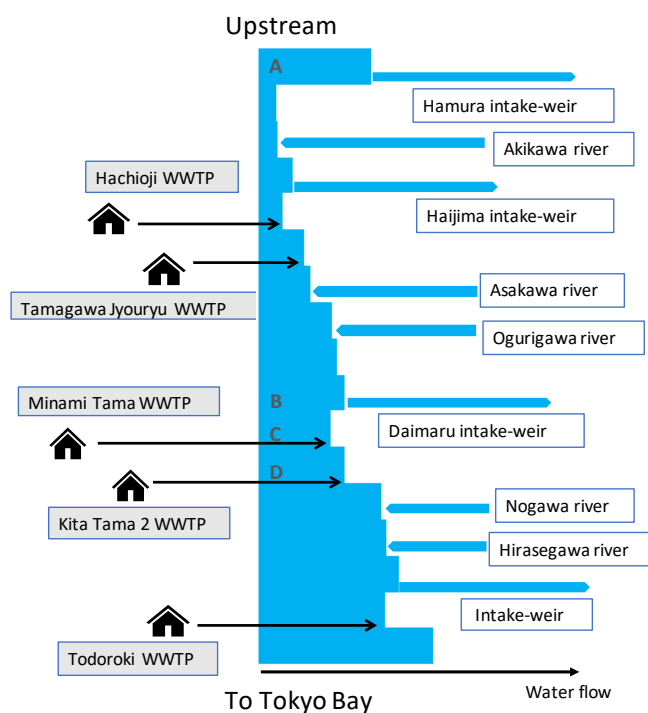


**Figure 2.** Tama River water flow balance and sample collection points A to D. The water flow balance is based on data provided by the Japanese Ministry of Land, Infrastructure, Transport, and Tourism, 1999.

## Results and discussion

Each water sample was analyzed in triplicate using the 8900 ICP-QQQ method, and the average REE concentration for each site is shown in Figure 3 (left). The REEs are a chemically similar group of elements, so tend to behave consistently. However, in most natural materials, the REEs alternate between high and low concentrations, giving a saw-tooth profile which makes it difficult to see anomalies. For this reason, geochemists often normalize REE data by dividing the concentration of each REE measured in the sample by that element's value in a reference material. In this case, the reference material used was Post-Archean Australian Shales (PAAS) (6), as shown in Figure 3 (right).

Apart from gadolinium (Gd), the normalized REE results for waters from different points on the river gave consistent, smooth profiles, despite the low concentrations. Gd was consistent with the other REEs in the river water collected at the upstream location (Mitake). But there was a spike in the Gd concentration in the samples taken at the other three sites. The results indicate contamination by Gd compounds, which were not removed by WWTP and so were discharged into the river. A possible source is widely used Gd-based magnetic resonance imaging (MRI) contrast agents.

The plots in Figure 3 also suggest that the light REEs were depleted in the WWTP effluents, but the higher mass REEs were somewhat enriched. There is also a suggestion that Ce might be anomalously high in the water from the Kita Tama WWTP, as this element lies above the smooth line formed by the other light REEs.

These patterns may indicate other sources of REE contamination from local industry, although most REE concentrations apart from Gd were at the single ppt level or below.

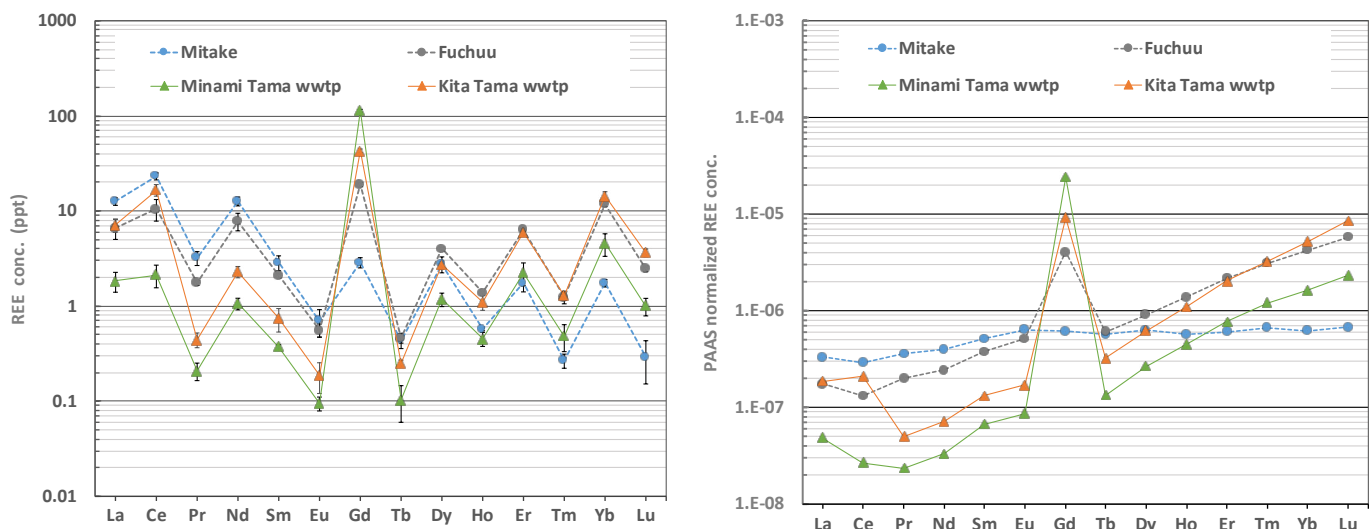


**Figure 3.** Concentrations of REEs in Tama River water samples by ICP-QQQ. Left: Average of three samples from each site with error bars showing two times the standard deviation. Right: Same REE results normalized to PAAS values.

### Conclusion

The study demonstrates the suitability of the Agilent 8900 ICP-QQQ with MS/MS mode for the direct measurement of 16 REEs in river water. All potential polyatomic interferences arising from Ba oxide or low mass REE-based hydride, oxide, and hydroxide polyatomic interferences were resolved using the N<sub>2</sub>O mass-shift method.

Sub ppt MDLs were achieved for all the REEs using the MS/MS method.

The high sensitivity and low background provided by the 8900 are needed for the determination of emerging pollutants in environmental samples, which are typically present at ultratrace concentrations.

The results from the analysis of the Japanese river water samples collected at different points along the river highlighted an interesting finding for Gd. While all the other REEs were measured below 50 ppt in all samples, there was a spike in the Gd concentration in samples collected at or near to wastewater discharge points. Gd MRI reagents may be the source of the contamination.

## References

1. US Geological Survey Mineral Resources Program  
The Rare-Earth Elements—Vital to Modern Technologies and Lifestyles,  
Fact Sheet 2014–3078, November 2014
2. Naoki Sugiyama and Glenn Woods, Direct measurement of trace rare earth elements (REEs) in high-purity REE oxide using the Agilent 8800 Triple Quadrupole ICP-MS with MS/MS mode, Agilent publication, [5991-0892EN](#)
3. Juane Song, Xiang-Cheng Zeng, Dong Yan, and Wei-ming Wu, Routine determination of trace rare earth elements in high purity Nd<sub>2</sub>O<sub>3</sub> using the Agilent 8800 ICP-QQQ, Agilent publication, [5991-5400EN](#)
4. Reaction data for 70 elements using O<sub>2</sub>, NH<sub>3</sub> and H<sub>2</sub> with the Agilent 8800 Triple Quadrupole ICP-MS, Agilent publication, [5991-4585EN](#)
5. Delphine Yeghicheyan et al, A New Interlaboratory Characterisation of Silicon, Rare Earth Elements and Twenty-Two Other Trace Element Concentrations in the Natural River Water Certified Reference Material SLRS-6 (NRC-CNRC), *Geostandards and Geoanalytical Research*, Vol. 43 issue 3, **2019**, 475–4
6. W.B Nance and S.R Taylor, Rare earth element patterns and crustal evolution—I. Australian post-Archean sedimentary rocks, *Geochimica et Cosmochimica Acta*, Vol. 40, issue 12, **1976**, 1539-1551

# Solving Doubly Charged Ion Interferences using an Agilent 8900 ICP-QQQ

## Author

Naoki Sugiyama,  
Agilent Technologies Inc.

Improved data quality using MS/MS oxygen mass-shift method to resolve common  $M^{++}$  ion interferences

## Introduction

Most ICP-MS instruments use collision/reaction cell (CRC) technology to control spectral interferences, greatly improving data accuracy for many elements in routine applications. Helium collision cell mode (He mode) is the most widely used CRC technique for the trace element analysis of many commonly analyzed samples. It is especially effective at resolving spectral interferences that arise from overlapping matrix or plasma-based ions such as metal oxide ions or argide ions. He mode uses Kinetic Energy Discrimination (KED) to reduce the transmission of all common matrix-based polyatomic interferences under a single set of cell conditions.

A different approach is needed to remove doubly charged ion interferences ( $M^{++}$ ) though, since He mode enhances the interference. While  $M^{++}$  interferences are not as common as polyatomic ion interferences in most general applications, it is useful for analysts to be aware of the potential for their formation. It is also useful for analysts to have a method to correct for  $M^{++}$  interferences should they arise. A quadrupole mass spectrometer separates ions based on their mass-to-charge ratio ( $m/z$ ), so  $M^{++}$  ions appear at half their true mass, overlapping any singly charged analyte ions with the same  $m/z$ .  $M^{++}$  interferences can be corrected using mathematical interference correction equations. This approach is often used to compensate for doubly charged ion interferences from rare earth elements ( $REE^{++}$ ) on arsenic (As) and selenium (Se). But accurate results can only be obtained using correction equations when the interference and analyte signal are of the same order of magnitude. Otherwise, the correction provides an inaccurate value. With the development of samples with more complex matrices, there is an increasing need for more reliable, reproducible, and higher-quality data.

Triple quadrupole ICP-MS (ICP-QQQ) with its double mass selection (MS/MS) can remove  $M^{++}$  interferences using controlled reaction chemistry in the CRC. ICP-MS/MS methods enable reactive cell gases such as hydrogen, oxygen, and ammonia to be used effectively (1, 2).

In this study, an ICP-MS/MS reaction cell method using  $O_2$  was used to remove  $M^{++}$  interferences on various analytes. Many elemental ions react with  $O_2$  to form an oxide ion while the  $M^{++}$  interference remains unreactive or is much less reactive. This allows the element of interest to be quantified by measuring the oxide ion at + 16 u, away from the spectral interference (1, 2). This "mass-shift" methodology was used to remove doubly charged ion interferences on Ca, Sc, Zn, As, and Se.

## Experimental

### Instrumentation

An Agilent 8900 Triple Quadrupole ICP-MS (ICP-QQQ #100 for Advanced applications) was used. The instrument was fitted with the standard sample introduction system comprising a glass concentric nebulizer, quartz double-pass spray chamber, quartz torch with 2.5 mm id injector, and Ni interface cones. The ICP-QQQ was operated in single quadrupole (SQ) no gas mode, in SQ He mode, and with O<sub>2</sub> cell gas in MS/MS mass-shift mode. The 8900 is fitted with a four cell gas channels, allowing different cell gases to be used in the same method if needed. Robust “general purpose” plasma conditions were set automatically using the ICP-MS MassHunter software. The main operating conditions and tuning parameters are shown in Table 1.

### Calibration standards and sample preparation

Calibration standards were prepared from Agilent Environmental Calibration Standards (p/n 5183-4688) via sequential dilution using de-ionized water. Fe, Sc, and Sr calibration standards were prepared separately from single elements standards (Kanto Chemical Co Inc., Japan). A Rare Earth Element (REE) mixed solution was bought from SPEX CertiPrep Inc. National Institute of Standards and Technology (NIST) 1640a Trace Elements in Natural Water Standard Reference Material (Gaithersburg MD, USA) was used to evaluate the method. The SRM was also spiked with 1 ppm of each of Sr, Zr, Ba, Sm, Gd, Nd, and Dy to simulate a more challenging sample matrix for the evaluation. Also, since no Sc is present in NIST 1640a, a 10 ppb spike was added to the SRM to represent the analyte.

**Table 1.** ICP-QQQ operating conditions and tuning parameters.

	No Gas	He	O <sub>2</sub>
Acquisition mode	Single quad	Single quad	MS/MS
RF power (W)	1550		
Sampling depth (mm)	10		
Nebulizer gas flow rate (mL/min)	1.05		
Make up gas flow rate	0.0		
Octopole bias (V)	-8	-18	-10
Axial acceleration (V)	2		
KED (V)	5		-8
Cell gas flow rate (mL/min)	-	4.5	0.6 (40% full scale)
Deflection lens (V)	20	4	2

*Shaded parameters are predefined by selecting general-purpose plasma settings.*

## Results and discussion

### Attenuation of doubly charged ion interferences

To study the effectiveness of the method for the removal of  $M^{++}$  interferences,  $Sr^{++}$  interference on  $Ca^+$ ,  $Zr^{++}$  on  $Sc$ ,  $Ba^{++}$  on  $Zn^+$ , and  $REE^{++}$  interferences on  $As^+$  and  $Se^+$  were investigated. The background equivalent concentrations (BECs) of  $Ca$ ,  $Sc$ , and  $Zn$  were determined in a solution containing 10 ppm of  $Sr$ ,  $Zr$ , and  $Ba$ .  $As$  and  $Se$  were measured in a solution containing 10 ppm each of 16 REEs.

The results, which were obtained using no gas mode, He mode, and  $O_2$  mass-shift mode, are shown in Figure 1. The graphs show that the lowest BECs for all elements were obtained using  $O_2$  mass-shift mode. The higher results obtained in no gas mode highlight the effect of the doubly charged ion spectral interferences that arise from the matrix elements on all five analytes. The results also show that He mode is ineffective for the removal of  $M^{++}$  ion interferences, even enhancing the interference slightly compared to no gas mode.

### Natural water SRM analysis

Matrix spiked and unspiked samples of the NIST 1640a natural water SRM were analyzed using ICP-QQQ. All elements were measured in He mode. For comparison purposes, the five analyte elements ( $Ca$ ,  $Sc$ ,  $Zn$ ,  $As$ , and  $Se$ ) that potentially suffer  $M^{++}$  interferences arising from the  $Sr$ ,  $Zr$ ,  $Ba$ ,  $Sm$ ,  $Gd$ ,  $Nd$ , and  $Dy$  matrix spikes were also measured in MS/MS mass-shift mode with  $O_2$  cell gas. Quantitative results are given in Tables 2 and 3.

As can be seen in Table 2, He mode provided accurate results for all elements in the non-matrix spiked SRM sample. All isotopes were within  $\pm 10\%$  of the certified values apart from  $^{43}Ca$  (111%), which suffered interference from a  $Sr^{++}$  overlap (the SRM contains 126 ppb  $Sr$ ).

There was a large deviation from the certified concentrations for some isotopes of  $Ca$ ,  $Sc$ ,  $Zn$ ,  $As$ , and  $Se$  in the 1 ppm matrix spiked SRM due to  $M^{++}$  ion interferences, as indicated by the shaded cells in Table 2.

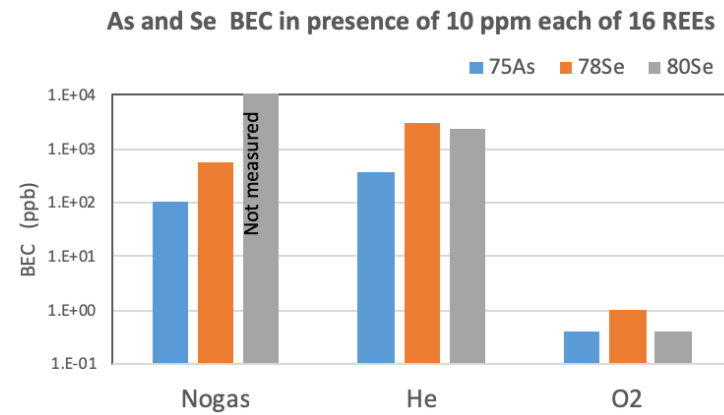
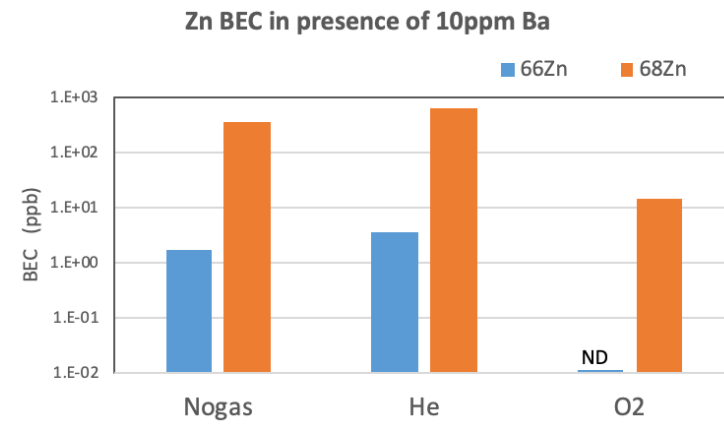
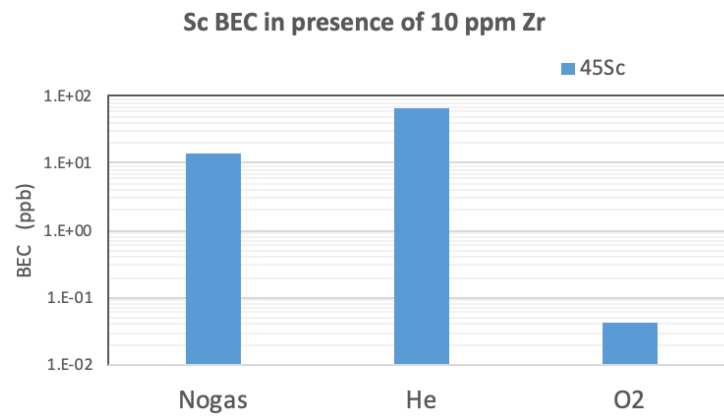
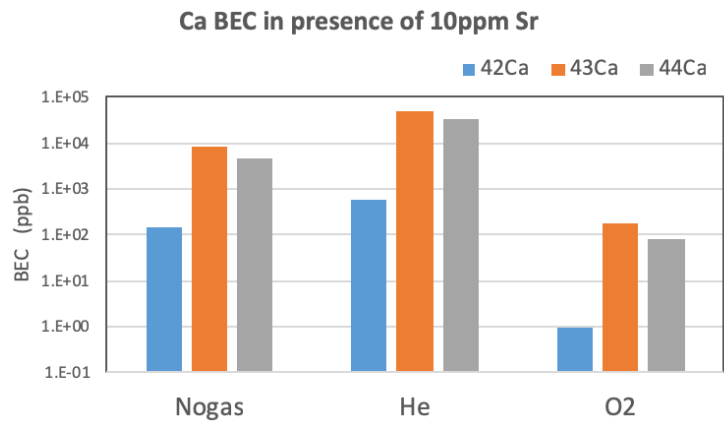


Figure 1. BEC results of the matrix spectroscopic interference study.



**Table 2.** Analytical results for NIST 1640a Trace Elements in Natural Water SRM with and without matrix element spikes. All data was acquired using the 8900 ICP-QQQ operating in He mode.

Element	Integration Time (s)	MDL** n=9 (µg/L)	SRM 1640a	SRM 1640a		SRM 1640a + 1 ppm Matrix	
			Certified (µg/L)	Average n=3 (µg/L)	Recovery (%)	Average n=3 (µg/L)	Recovery (%)
<sup>9</sup> Be	0.5	0.06	3.026	3.15	104	3.15	104
<sup>23</sup> Na	0.5	0.54	3137	3195	102	3200	102
<sup>24</sup> Mg	0.5	0.35	1058.6	1056	100	1028	97
<sup>27</sup> Al	0.5	0.07	53.0	54.2	102	52.0	98
<sup>39</sup> K	0.5	2.8	579.9	595	103	568	98
<sup>42</sup> Ca	0.5	58	5615	5598	100	5376	96
<sup>43</sup> Ca	0.5	5.8	5615	6257	111	11120	198
<sup>44</sup> Ca	0.5	1.0	5615	5767	103	9085	162
<sup>45</sup> Sc	0.5	0.02	10*	10.6	106	13.7	137
<sup>51</sup> V	0.5	0.01	15.05	14.9	99	14.3	95
<sup>52</sup> Cr	0.5	0.01	40.54	40.4	100	38.9	96
<sup>53</sup> Cr	0.5	0.02	40.54	41.3	102	39.8	98
<sup>55</sup> Mn	0.5	0.01	40.39	39.9	99	38.1	94
<sup>56</sup> Fe	0.5	0.03	36.8	34.7	94	33.4	91
<sup>59</sup> Co	0.5	0.01	20.24	20.9	103	20.2	100
<sup>60</sup> Ni	0.5	0.02	25.32	26.3	104	25.4	101
<sup>66</sup> Zn	1.0	0.01	55.64	55.6	100	54.0	97
<sup>68</sup> Zn	1.0	0.01	55.64	59.3	107	107	192
<sup>75</sup> As	1.0	0.02	8.075	8.1	100	40.9	506
<sup>78</sup> Se	1.0	0.14	20.13	19.7	98	320	1588
<sup>80</sup> Se	1.0	8.6	20.13	19.3	96	165	819
<sup>88</sup> Sr	0.5	0.01	126	127.1	101	1130.2	100
<sup>95</sup> Mo	0.5	0.01	45.6	44.8	98	43.3	95
<sup>107</sup> Ag	0.5	0.01	8.081	8.47	105	8.52	105
<sup>111</sup> Cd	0.5	0.01	3.992	4.03	101	4.01	101
<sup>121</sup> Sb	0.5	0.01	5.105	4.99	98	4.77	93
<sup>137</sup> Ba	0.5	0.02	151.8	151	100	1165	101
<sup>205</sup> Tl	0.5	0.00	1.619	1.51	93	1.47	91
<sup>208</sup> Pb	0.5	0.01	12.101	11.5	95	11.1	92
<sup>238</sup> U	0.5	0.00	25.35	27.1	107	26.5	104

\*SRM was spiked with 10 ppb Sc analyte

\*\* MDL was calculated as 3 sigma of quantified value of 9 replicates of the solution which contains 1/10 of the concentration of the lowest level of calibration standards ; 1 ppb for Na, Mg, Ca, K and 0.1 ppb for other elements.

In contrast to the He mode data, accurate results were obtained for Ca, Sc, Zn, As, and Se in both the matrix spiked and matrix unspiked SRM using O<sub>2</sub> mass-shift mode (Table 3). The results demonstrate the effective interference removal capability of O<sub>2</sub> reaction cell mode to handle M<sup>++</sup> ion overlaps.

**Table 3.** Analytical results for NIST 1640a Trace Elements in Natural Water SRM with and without matrix element spikes. All data was acquired using the 8900 ICP-QQQ operating in MS/MS mass-shift mode with O<sub>2</sub> cell gas.

Element	Integration Time (s)	MDL** n=9 (µg/L)	SRM 1640a	SRM 1640a		SRM 1640a + 1 ppm Matrix	
			Certified (µg/L)	Average n=3 (µg/L)	Recovery (%)	Average n=3 (µg/L)	Recovery (%)
<sup>42</sup> Ca	0.5	2.48	5615	5671.2	101	5739.5	102
<sup>43</sup> Ca	0.5	9.72	5615	5731.7	102	5839.4	104
<sup>44</sup> Ca	0.5	1.36	5615	5721.5	102	5774.5	103
<sup>45</sup> Sc	0.5	0.001	10*	10.4	104	10.5	105
<sup>66</sup> Zn	1.0	0.09	55.64	54.2	97	52.8	95
<sup>68</sup> Zn	1.0	0.07	55.64	54.9	99	53.9	97
<sup>75</sup> As	1.0	0.01	8.075	8.4	104	8.6	106
<sup>78</sup> Se	1.0	0.05	20.13	20.4	101	20.7	103
<sup>80</sup> Se	1.0	0.03	20.13	20.4	101	20.8	103

\*SRM was spiked with 10 ppb Sc analyte

\*\* MDL was calculated as 3 sigma of quantified value of 9 replicates of the solution which contains 1/10 of the concentration of the lowest level of calibration standards; 1 ppb for Na, Mg, Ca, K and 0.1 ppb for other elements.

## Conclusion

The Agilent 8900 ICP-QQQ operating in MS/MS mode with O<sub>2</sub> cell gas is highly effective for the removal of doubly charged ion interferences on different isotopes.

A natural water SRM was spiked with Sr, Zr, Ba, and REEs to cause M<sup>++</sup> interferences on Ca, Sc, Zn, As, and Se. Accurate results were obtained for all elements in the SRM apart from Ca, Sc, Zn, As, and Se using helium mode. Although He mode is a proven approach used to reduce common polyatomic interferences in ICP-MS, it isn't effective for the removal of M<sup>++</sup> interferences – as confirmed by the results in this study. However, M<sup>++</sup> interferences were successfully resolved using a MS/MS mass-shift method with O<sub>2</sub> cell gas, providing accurate results for Ca, Sc, Zn, As, and Se.

Agilent ICP-QQQ instruments combine the versatile, almost universal He mode (using KED) with controlled reactive cell gas modes (using MS/MS). This combination of methods enables ICP-QQQ to generate the most accurate results for environmental and food sample analysis, without sacrificing instrument ease-of-use. It also allows the analytical results to be checked across multiple isotopes, providing extra confidence in the final data.

## References

1. Reaction data for 70 elements using O<sub>2</sub>, NH<sub>3</sub> and H<sub>2</sub> with the Agilent 8800 Triple Quadrupole ICP-MS, Agilent publication, [5991-4585EN](#)
2. Agilent 8800 Triple Quadrupole ICP-MS: Understanding oxygen reaction mode in ICP-MS/MS, Agilent publication, [5991-1708EN](#)

# Removal of REE<sup>++</sup> Interference on Arsenic and Selenium

## Authors

Kazumi Nakano and  
Yasuyuki Shikamori  
Agilent Technologies, Japan

## Keywords

Rare Earth Elements, REE, arsenic, selenium, environmental, food, CRMs, oxygen mass-shift

## Introduction

Trace analysis of arsenic (As) and selenium (Se) in environmental and food samples is of a great interest, since both elements can be toxic even at quite low levels. It is difficult to quantify As and Se accurately at trace levels in some matrices by quadrupole ICP-MS as all the analytically useful isotopes can suffer from multiple spectral interferences, as summarized in Table 1. This application investigates ICP-QQQ in MS/MS reaction mode to remove interferences on As and Se, with an emphasis on the removal of the doubly-charged ions arising from Rare Earth Elements (REE<sup>++</sup>). While the concentration of REEs in environmental and food samples is usually low, some plants will accumulate REEs from the soil, and a high concentration will lead to false positive results for As and Se.

**Table 1.** Spectroscopic interferences on As and Se isotopes.

Element	As and Se isotope			Interference	
	Mass	Abundance %	Doubly charged	Matrix	Dimer
As	75	100	<sup>150</sup> Sm <sup>++</sup> , <sup>150</sup> Nd <sup>++</sup>	<sup>40</sup> Ar <sup>37</sup> Cl <sup>+</sup> , <sup>40</sup> Ca <sup>37</sup> Cl <sup>+</sup>	
Se	77	7.63	<sup>154</sup> Sm <sup>++</sup> , <sup>154</sup> Gd <sup>++</sup>	<sup>40</sup> Ar <sup>37</sup> Cl <sup>+</sup> , <sup>40</sup> Ca <sup>37</sup> Cl <sup>+</sup>	
	78	23.77	<sup>156</sup> Gd <sup>++</sup> , <sup>156</sup> Dy <sup>++</sup>	<sup>41</sup> K <sup>37</sup> Cl <sup>+</sup>	<sup>38</sup> Ar <sup>40</sup> Ar <sup>+</sup> , <sup>39</sup> K <sup>39</sup> K <sup>+</sup>
	80	49.61	<sup>160</sup> Gd <sup>++</sup> , <sup>160</sup> Gd <sup>++</sup>	<sup>45</sup> Sc <sup>35</sup> Cl <sup>+</sup>	<sup>40</sup> Ar <sup>40</sup> Ar <sup>+</sup> , <sup>40</sup> Ca <sup>40</sup> Ca <sup>+</sup>
	82	8.73	<sup>164</sup> Dy <sup>++</sup> , <sup>164</sup> Er <sup>++</sup>	<sup>45</sup> Sc <sup>37</sup> Cl <sup>+</sup>	

## Experimental

**Instrumentation:** Agilent 8800 #100.

**Plasma conditions:** Preset plasma/Low matrix.

**Ion lens tune:** Soft extraction tune: Extract 1 = 0 V, Extract 2 = -180 V.

**CRC conditions:** O<sub>2</sub> gas flow rate of 0.2 mL/min, Octopole bias = -8 V and KED = -6 V.

**Acquisition parameters:** MS/MS O<sub>2</sub> mass-shift method to measure As<sup>+</sup> (as AsO<sup>+</sup>) and Se<sup>+</sup> (as SeO<sup>+</sup>), as illustrated in Figure 1. Unlike conventional quadrupole ICP-MS, the 8800 ICP-QQQ mass-shift method can be applied to complex matrix samples that may contain Zr and/or Mo. The MS/MS configuration prevents undesired ions such as <sup>91</sup>Zr<sup>+</sup> and <sup>94</sup>Mo<sup>+</sup> from overlapping the MO<sup>+</sup> product ions, as they are rejected by Q1.

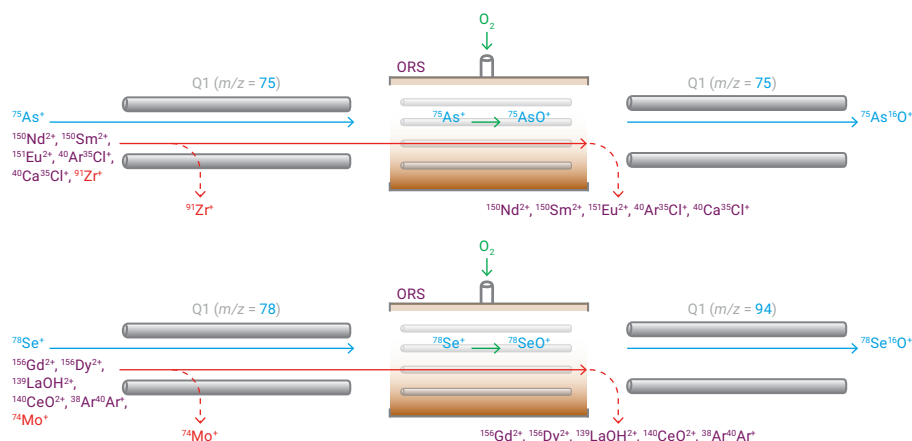


Figure 1. ICP-MS/MS  $O_2$  mass-shift method for measuring  $^{75}\text{As}$  (top) and  $^{78}\text{Se}$  (bottom).

**Samples and sample preparation:** SPEX XSTC-1 (a mixture of 10 ppm each of Ce, Dy, Er, Eu, Gd, Ho, La, Lu, Nd, Pr, Sm, Sc, Tb, Tm, Yb and Y) purchased from SPEX CertiPrep Ltd. (UK) was used. Four certified reference materials (CRMs): NIST 1515 Apple Leaves, NIST 1573a Tomato Leaves, NIST 1575a Pine Needles and NMIJ 7531a Brown Rice, were used for the method validation. It should be noted that NIST 1515 contains 3 mg/kg Sm and Gd, and 0.2 mg/kg Eu. NIST 1573a contains 0.19 mg/kg Sm, 0.17 mg/kg Gd, 5% Ca and 2.7% K, a combination of matrix elements that might be expected to cause severe interferences on As and Se. All CRMs were microwave-digested in  $\text{HNO}_3$  and  $\text{H}_2\text{O}_2$ , diluted and analyzed.

## Results and discussion

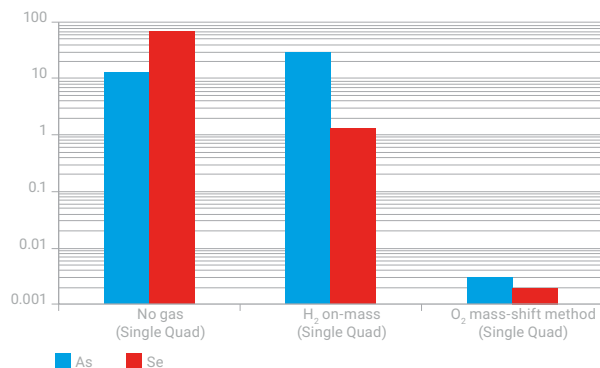
### Effectiveness of $O_2$ mass-shift method for removing REE<sup>++</sup> interferences

To investigate the effectiveness of interference removal modes on the 8800 ICP-MS/MS, As and Se were measured in a mixed REE solution containing 1 ppm each of Ce, Dy, Er, Eu, Gd, Ho, La, Lu, Nd, Pr, Sm, Sc, Tb, Tm, Yb and Y. Three different 8800 ICP-MS/MS cell modes were used:

- Single Quad (SQ); no gas
- Single Quad (SQ); reaction mode using hydrogen ( $\text{H}_2$ ) cell gas
- MS/MS; reaction mode using  $O_2$  cell gas with + 16 u mass-shift

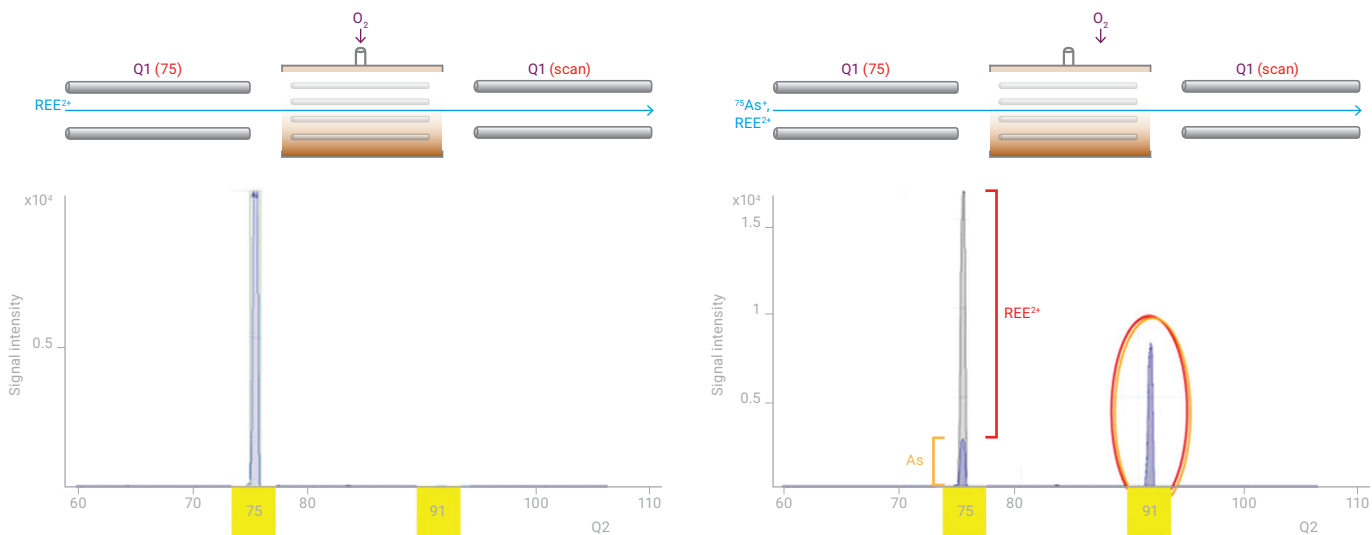
“Single Quad” represents the performance of conventional ICP-QMS while MS/MS mode is unique to ICP-MS/MS.

Figure 2 shows the BECs of As and Se in each of the measurement modes. The results in Figure 2 illustrate the excellent interference removal performance of the O<sub>2</sub> mass-shift method for the detection of As and Se in a matrix containing REEs.



**Figure 2.** BEC of As and Se in 1 ppm REE mixed solution with three measurement modes: no gas, H<sub>2</sub> on-mass and O<sub>2</sub> mass-shift mode.

Figure 3 shows the product ion scan spectra obtained using O<sub>2</sub> mass-shift mode for a solution containing 1 ppm REEs without (left) and with (right) a 1 ppb As spike. As illustrated in the schematic, Q1 was fixed at  $m/z = 75$  and Q2 was scanned across the selected mass range to monitor all existing and cell-formed ions derived from precursor ions at  $m/z = 75$ . Figure 3 (left) shows the product ions from  $m/z = 75$  in the blank REE matrix; the signal at Q2  $m/z = 75$  (mass of As) is due to REE<sup>2+</sup>. The absence of a signal at  $m/z = 91$  (the mass of AsO<sup>+</sup>) in the blank REE matrix, indicates that the REEs do not react with O<sub>2</sub> in the cell to give rise to product ions (such as REEO<sub>2</sub><sup>++</sup>) that overlap AsO<sup>+</sup> at  $m/z = 91$ . Consequently, As can be successfully measured as AsO<sup>+</sup> at  $m/z = 91$  as shown in Figure 3 (right).



**Figure 3.** Product ion scan spectrum of O<sub>2</sub> mass-shift method. (Left) 1 ppm mixed-REE solution and (right) 1 ppm mixed-REE plus 1 ppb As spike.

### Method validation with CRMs

The ICP-QQQ method was applied to the measurement of As and Se in four CRMs. Table 2 summarizes the results. The measured concentrations of As and Se in the CRMs were all in good agreement with the certified values.

**Table 2.** Results of the determination of As and Se in four CRMs using MS/MS O<sub>2</sub> mass-shift mode on the 8800 ICP-QQQ.

	As (as AsO <sup>+</sup> at m/z 91)			Se (as SeO <sup>+</sup> at m/z 94)		
	Certified mg/kg	Found average mg/kg	Recovery %	Certified mg/kg	Found average mg/kg	Recovery %
NIST1515 Apple Leaves	0.038±0.007	0.037	97	0.050±0.009	0.050	100
NIST1575a Pine Needles	0.039±0.002	0.038	97	0.099±0.004	0.099	100
NIST1573a Tomato Leaves	0.112±0.004	0.113	101	0.054±0.003	0.058	107
NMIJ 7531a Brown Rice	0.280±0.009	0.258	92	NA	0.032	NA

# Removal of Molybdenum Oxide Interference on Cadmium

## Authors

Michiko Yamanaka  
Agilent Technologies, Japan

## Keywords

cadmium, molybdenum oxide,  
environmental, food, CRMs, hydrogen  
on-mass

## Introduction

Cadmium (Cd) is a well-known toxic element along with As, Hg and Pb. The maximum contamination level of these elements in food, pharmaceuticals, drinking water, wastewater and other matrices is strictly controlled under national and international legislation. Out of the eight natural isotopes of Cd, only  $^{111}\text{Cd}$  is free from direct overlap by an atomic isobar (an isotope of a different element at the same mass as the Cd isotope), and even  $^{111}\text{Cd}$  is potentially subject to spectroscopic interference by  $^{95}\text{MoO}^+$ . Fortunately, the concentration of Mo is low in most samples, and quadrupole ICP-MS (ICP-QMS) operating in helium collision mode can remove the interference, allowing the accurate measurement of Cd. However, there are some cases where the Mo concentration is high and a better interference removal technique is required in order to accurately determine Cd. This paper describes the application of MS/MS  $\text{H}_2$  reaction mode on the Agilent 8800 ICP-QQQ for the determination of trace Cd in the presence of a high concentration of Mo.

## Experimental

**Instrumentation:** Agilent 8800 #100. Indium (In) was introduced as the internal standard using the on-line ISTD kit.

**Plasma conditions and ion lens tune:** RF power = 1550 W; sampling depth = 8.0 mm; carrier gas = 1.01 L/min; make-up gas/dilution gas = 0.0 L/min; Soft extraction tune: Extract 1 = 0 V, Extract 2 = -165 V, Omega bias = -100 V, Omega = 11.4 V.

**CRC conditions:**  $\text{H}_2$  flow rate 9.0 mL/min, Octopole bias = -22 V, KED = +5 V.

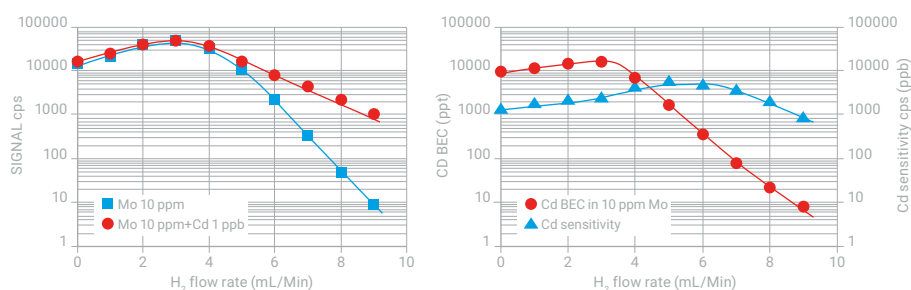
**Acquisition parameters:** MS/MS  $\text{H}_2$  on-mass method i.e.  $^{111}\text{Cd}$  was measured at  $m/z$  111 using quadrupole settings of (Q1 = 111, Q2 = 111).

## Results and discussion

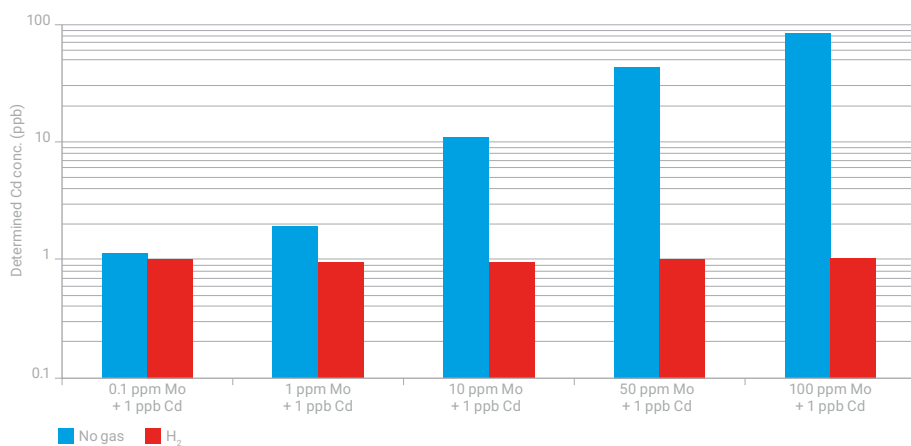
### Optimization of H<sub>2</sub> flow rate

Figure 1 (left) shows the signal at  $m/z$  111 for a 10 ppm Mo solution and a 10 ppm Mo + 1 ppm Cd solution, plotted as a function of H<sub>2</sub> flow rate. Figure 1 (right) shows the calculated BEC of Cd in the presence of 10 ppm Mo. The optimum cell gas flow rate of 9.0 mL/min was used for subsequent experiments.

In order to test the effectiveness of MS/MS mode with H<sub>2</sub> cell gas in comparison to no gas mode, a spike recovery test of 1 ppb Cd in a series of Mo matrix solutions ranging from 0.1 to 100 ppm was conducted. Figure 2 summarizes the results. In no gas mode, the error in quantification of the 1 ppb Cd spike dramatically increases with the concentration of Mo; in contrast, H<sub>2</sub> reaction mode delivers a consistent and accurate result for Cd even in the presence of 100 ppm Mo.



**Figure 1.** (Left): Signal for  $m/z$  111 with 10 ppm Mo and 10 ppm Mo + 1 ppb Cd, plotted as a function of H<sub>2</sub> flow rate. (Right): Estimated Cd BEC in the presence of 10 ppm Mo as a function of H<sub>2</sub> flow rate.



**Figure 2.** 1 ppb Cd spike recovery in a series of Mo matrix solutions using no gas mode and MS/MS H<sub>2</sub> mode.



### Method validation: Analysis of Cd in CRMs

The concentration of Cd was determined in four different CRMs: NIST 1515 Apple Leaves, NIST 1573a Tomato Leaves, NIST 1575a Pine Needles and NMIJ 7531a Brown Rice Flour (National Metrology Institute of Japan). Each sample was microwave digested following the manufacturer's recommended procedures, then diluted and analyzed by ICP-QQQ; the final dilution factor was around 100–200. For each CRM, the digested sample was analyzed using the developed method. A second sample of each CRM was prepared and analyzed after the addition of a 10 ppm Mo spike. As summarized in Table 1, good recoveries were obtained for all four references materials both for the unspiked samples and the duplicates with the high added Mo concentration, demonstrating the validity of the method for real sample analysis.

**Table 1.** Measurement of Cd in four CRMs using the 8800 ICP-QQQ in MS/MS mode with H<sub>2</sub> reaction gas.

CRMs	Without Mo addition			With 10 ppm Mo addition	
	Certified mg/kg	Determined mg/kg	Recovery %	Determined mg/kg	Recovery %
NIST1515 Apple Leaves	0.014	0.013	93	0.016	100
NIST1573a Tomato Leaves	1.52	1.496	98	1.475	100
NIST1575a Pine Needles	0.223	0.220	99	0.224	107
NMIJ 7531a Brown Rice Flour	0.308	0.298	97	0.293	NA

# Rapid Analysis of Radium-226 in Water Samples by ICP-QQQ

## Authors

Ben Russell<sup>1</sup>, Elsje May van Es<sup>1,2</sup>,  
Glenn Woods<sup>3</sup>, David Read<sup>1,2</sup>

1. National Physical Laboratory,  
Teddington, UK

2. Chemistry Department, University of  
Surrey, Guildford, Surrey, UK

3. Agilent Technologies UK Limited,  
Lakeside, Stockport, UK

## Introduction

Radium-226 is a radionuclide that occurs naturally as part of the uranium-238 decay series. <sup>226</sup>Ra decays with a half-life of 1,600 years to radon-222 with the emission of alpha and gamma radiation. The element is known for its historical use in the luminescent paint used in clocks, watches, and other instruments. These uses led to severe health problems for the so-called Radium Girls who painted the watch and clock dials. <sup>226</sup>Ra has a long half-life compared to the other Ra isotopes and is considered a significant contributor to occupational radiological dose with regards to industrial sources of naturally occurring radioactive materials (NORM).

<sup>226</sup>Ra occurs naturally in waters through interaction with uranium-bearing minerals [1]. It is also present as a result of waste from the industrial exploitation of mineral resources (including uranium mining and processing sites, and produced waters following hydraulic fracturing). Radium waste producers are required to comply with stringent limits when discharging to watercourses. Analytical methods must therefore be capable of detecting <sup>226</sup>Ra at values ranging from 0.01 Bq/L to 1 Bq/L (equivalent to 0.3 – 30 pg/L (ppq) or 0.0003 – 0.03 ppt) [2,3,4].

<sup>226</sup>Ra analysis is typically performed by alpha spectrometry, which requires time-consuming and labor-intensive separation before measurement, followed by count times of several days per sample to reach the target detection limits.

This study outlines a new method developed by the National Physical Laboratory (NPL) Nuclear Metrology Group for the rapid analysis of <sup>226</sup>Ra in water samples. The new method uses a preconcentration step prior to measurement of <sup>226</sup>Ra using triple quadrupole ICP-MS (ICP-QQQ)[5]. The procedural time is significantly reduced compared to decay counting techniques, and <sup>226</sup>Ra is measurable at concentrations required to meet the regulatory detection limits.

## Experimental

### Sample preparation

Radium-226 calibration standards were prepared from an in-house standard solution in a dedicated facility used for the preparation of aqueous radioactive sources for decay counting or mass spectrometry measurement. The calibration standards were diluted in 2% (v/v) HNO<sub>3</sub>.

Groundwater samples were also investigated to assess the impact of a more complex sample matrix. Samples were evaporated to dryness and redissolved in 2% (v/v) HNO<sub>3</sub>. The solutions were then spiked with <sup>226</sup>Ra over a concentration range of 0.03 – 30 ppt to represent the concentrations expected following preconcentration.

High volume water samples (1 L) were spiked over the same concentration range as the groundwater samples to represent samples close to, and higher than, the regulatory discharge limits. Samples were acidified to pH 2 and passed through a chromatographic column to trap <sup>226</sup>Ra [6]. The <sup>226</sup>Ra was then eluted, evaporated to

incipient dryness and then made up in 5 mL 2% HNO<sub>3</sub>, representing a concentration factor of ~200. Unspiked water samples were run through the same preconcentration procedure, and then measured to establish the elemental composition and confirm no contribution of polyatomic interferences to the background at  $m/z = 226$ . Matrix matched calibration standards were prepared by spiking water samples following preconcentration, which also enabled the recovery to be calculated ( $\geq 70\%$  over the concentration range studied).

### Instrumentation

An Agilent 8800 Triple Quadrupole ICP-MS (ICP-QQQ) was used throughout. The standard sample introduction system was used, comprising a quartz torch with 2.5 mm i.d. injector, a quartz spray chamber, glass concentric nebulizer, and nickel-tipped interface cones. The instrument operating conditions are summarized in Table 1.

**Table 1.** ICP-QQQ operating conditions; low matrix tuning is appropriate for samples where most of the matrix has been removed during analyte preconcentration.

Parameter	Setting	
Scan mode	Single Quad	
Plasma conditions	Low matrix (optimized for high sensitivity)	HMI
RF power (W)	1550	
Carrier gas (L/min)	1.07	0.60
Dilution gas (L/min)	0	0.35
Extract 1	0.0	
Extract 2	-200.0	
Omega Bias (V)	-100.0	
Omega lens (V)	13.6	
Octopole bias (V)	-8.0	
He cell gas (mL/min)	0 – 1.0	0.5 – 1.0

## Results and discussion

### Sensitivity of ICP-QQQ for <sup>226</sup>Ra

The half-life of <sup>226</sup>Ra is relatively short with regards to ICP-MS measurements (1 Bq/kg is equivalent to 27.3 ppq, compared to long-lived <sup>238</sup>U (half-life 4.5×10<sup>9</sup> years), where 1 Bq/kg is equivalent to 8.0×10<sup>7</sup> ppq). In practice, this means that calibration should be performed using standards prepared for the radioisotope of interest, rather than calibrating using a long-lived or stable isotope as an analog. The instrument detection limits (IDLs) for several operating conditions (Q1 modes and cell gas flows), were calculated from a calibration curve prepared by spiking 2% (v/v) HNO<sub>3</sub> with <sup>226</sup>Ra at concentrations of 0.01–30 ppt (Table 2).

**Table 2.** Limit of detection for different instrument conditions and cell gas flow rates.

Instrument mode	Single Quad			MS/MS		
He flow rate (mL/min)	0.0	0.5	1.0	0.0	0.5	1.0
Limit of detection (ppt)	0.08	0.10	0.02	0.04	0.04	0.07

The IDLs in Table 2 are close to the higher end of the regulatory limits quoted (0.03 ppt), and orders of magnitude higher than the lowest values (0.3 ppq). Measurement of  $^{226}\text{Ra}$  at environmentally relevant levels therefore requires an effective preconcentration step prior to ICP-QQQ analysis, to rival the detection limits of traditional alpha spectrometry measurement.

### Interference removal by ICP-QQQ

Multiple potential interferences from polyatomic ions including  $^{88}\text{Sr}^{138}\text{Ba}^+$ ,  $^{87}\text{Sr}^{139}\text{La}^+$ ,  $^{86}\text{Sr}^{140}\text{Ce}^+$ ,  $^{208}\text{Pb}^{18}\text{O}^+$ ,  $^{186}\text{W}^{40}\text{Ar}^+$ , and  $^{97}\text{Mo}^{129}\text{Xe}^+$  can potentially affect ICP-MS measurement of  $^{226}\text{Ra}$ . Multiple separation stages prior to sample introduction are often required to remove the interferences. As an alternative approach, helium (He) collision mode was investigated for the removal of polyatomic interferences, initially by introducing up to 100 ppm Sr + Ba, Sr + La, Ce, W, and Pb standards. The background at  $m/z = 226$  was 0 cps in single quad mode when using 0.5–1.0 mL/min He cell gas, confirming the ability of He mode to attenuate all the polyatomic ions. Given that the on-mass polyatomic interferences are formed during sample introduction and not in the collision/reaction cell (CRC), MS/MS was not required, so the instrument was operated in single quad mode throughout.

Groundwater samples from different locations in North West England were then analyzed to determine the impact of a more complex sample matrix on instrument performance. The samples were spiked with  $^{226}\text{Ra}$  and measured at varying He gas flow rates together with unspiked samples and blank solutions. Bismuth-209 was used as an internal standard. The impact of matrix suppression was overcome using robust plasma conditions and aerosol dilution with the High Matrix Introduction (HMI) system of the 8800. HMI allows higher matrix levels to be analyzed directly without requiring chemical separation prior to measurement, further reducing the total procedural time. The reduction in sensitivity when operating with 0.5 mL/min He cell gas was offset by the lower background, giving comparable or improved background equivalent concentrations (BECs) at  $m/z = 226$  compared to no gas mode (Table 3). The sensitivity at 0.5 mL/min He cell gas is illustrated in the calibration plot shown in Figure 1.

**Table 3.** BECs of  $^{226}\text{Ra}$  using no gas and He gas mode.

He flow rate (mL/min)	BEC (ppt)		
	Sample 1	Sample 2	Sample 3
0	0.015	0.017	0.0085
0.5	0.0083	0.0089	0.0092
1.0	0.011	0.0092	0.013

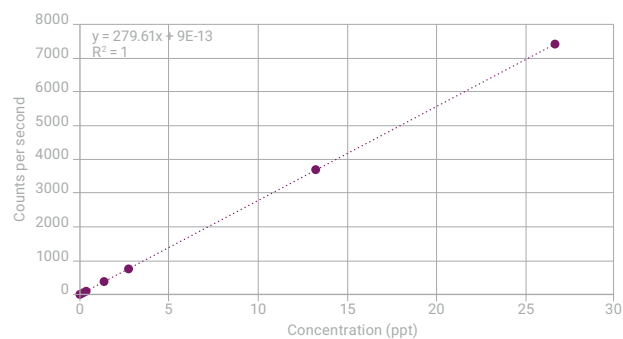


Figure 1. Calibration plot for  $^{226}\text{Ra}$  standards in single quad mode with 0.5 mL/min He.

### Measurement of high volume water samples

In water samples,  $^{226}\text{Ra}$  was detected down to 0.03 ppt (1 Bq/L), which is equivalent to 5 mBq/L in the original sample, assuming a preconcentration factor of 200. The RSD was <10% at concentrations above 1.4 ppt (50 Bq/L), equivalent to 250 mBq/L in the original sample. The results demonstrate that ICP-QQQ combined with preconcentration from high volume water samples is capable of measuring  $^{226}\text{Ra}$  at concentrations relevant to regulatory discharge limits. Improved accuracy at the lower limits is potentially achievable through higher preconcentration factors.

### Conclusion

A method is presented that demonstrates the capabilities of ICP-QQQ for the measurement of the naturally occurring radionuclide  $^{226}\text{Ra}$ . The use of He collision gas effectively removes potential polyatomic interferences, while operating with HMI reduces the impact of matrix suppression. When combined with preconcentration using chromatographic separation techniques, the detection limits achievable are applicable to the regulatory limits for water. The measurement time of several minutes per sample represents a significant improvement compared to several days using traditional alpha spectrometry. The increase in sample throughput is potentially beneficial for routine monitoring of water supplies, as well as routine environmental monitoring at nuclear and industrial sites.

### References

1. P.L. Smedley, A survey of the inorganic chemistry of bottled mineral waters from the British Isles. *Applied Geochem.* **2010**, 25, 1872–1888
2. Environmental Permitting Guidance: Radioactive Substances Regulation, Environment Agency, London, 2010,
3. Guidelines for Drinking-water Quality (Fourth Edition), World Health Organisation, 2011, ISBN 978 92 4 154815 1
4. National Primary Drinking Water Regulations; Radionuclides; Final Rule (Part II), 40 CFR Parts 9, 141, and 142, Environment Protection Agency, 2011
5. E.M. van Es, B.C. Russell, P. Ivanov, D. Read, Development of a method for rapid analysis of Ra-226 in groundwater and discharge water samples by ICP-QQQ-MS. *App. Rad. & Isotopes*, 126, **2017**, 31-34
6. E.M. van Es, B.C. Russell, P. Ivanov, M. Garcia Miranda, D. Read, The behaviour of  $^{226}\text{Ra}$  in high volume environmental water samples on TK100 resin. *J. Radioanal. Nucl. Chem.*, **2017**, 312: 10

# Feasibility Study of Fluorine Detection by ICP-QQQ

## Author

Noriyuki Yamada  
Agilent Technologies, Japan

## Keywords

fluorine-containing polyatomic ions, barium, oxygen on-mass, ammonia mass-shift

## Introduction

Fluorine ( $^{19}\text{F}$ ) cannot be directly detected by conventional quadrupole ICP-MS (ICP-QMS) because of severe water-derived interferences at  $m/z$  19 from  $^1\text{H}_3^{16}\text{O}^+$  and  $^1\text{H}^{18}\text{O}^+$ , and extremely low sensitivity due to the fact that it is very difficult to convert fluorine atoms to the positive ions that are measured in ICP-MS. The interference problem can be resolved by high resolution ICP-MS, but the sensitivity issue remains a challenge because almost no F atoms are ionized in an argon plasma due to F having an ionization potential (17.423 eV) that is higher than that of Ar (15.760 eV).

However, fluorine-containing polyatomic ions ( $\text{XF}^+$ ) can be formed in the plasma and they may be used to determine fluorine. Candidate ions are those with a high bond-dissociation energy for the  $\text{X}^+\text{-F}$  bond and low ionization potential of X or XF. Since oxygen is present in the plasma (from the water matrix or from air entrainment), the formation of  $\text{XO}^+$  or  $\text{XO}$  often competes against that of  $\text{XF}^+$ . Therefore, a low bond-dissociation energy for  $\text{X}^+\text{-O}$  and  $\text{X-O}$  bonds (low affinity of  $\text{X}^+$  and X for O) is also desirable for the efficient formation of  $\text{XF}^+$ . Barium was selected as "X" for this feasibility study, based on its thermochemical properties (Table 1).

**Table 1.** Gas phase thermochemical properties of elements having an affinity for fluorine\*.

Element X	$D_0(\text{X}^+\text{-F})$	IP (X)	$D_0(\text{X-F})$	IP (XF)	$D_0(\text{X}^+\text{-O})$	$D_0(\text{X-O})$
C	7.77	11.27	5.60	9.11	8.35	11.15
Al	3.16	5.99	6.99	9.73	1.81	5.31
Si	7.01	8.15	5.69	7.54	4.99	11.49
Ba	6.39	5.21	5.98	4.70	5.60	5.80
La	6.83	5.61	6.86	5.56	8.73	8.50
Eu	6.05	5.67	5.59	5.90	4.00	5.90

\*Unit: eV.  $D_0(\text{A-F})$  is the bond-dissociation energy for A-F bond (affinity of A for F) and  $\text{IP}(\text{B})$  is the ionization potential of B.

## Experimental

**Instrumentation:** Agilent 8800 #200 with a Micromist nebulizer.

**Plasma conditions and ion lens tune:** RF power = 1500 W; Sampling depth = 8 mm; Carrier gas flow rate = 1.00 L/min; sample uptake rate 0.33 mL/min; 100 ppm Ba uptake rate = 0.03 mL/min; Make-up gas flow rate = 0.32 L/min; Extract 1 = -150 V, Extract 2 = -4 V.

**CRC conditions:**  $\text{O}_2$  gas at 1 mL/min (100%), Octopole bias = -60 V, Energy discrimination = -10 V in  $\text{O}_2$  mode; 10%  $\text{NH}_3$ /90% He flow rate 8.5 mL/min (85%), Octopole bias = -20 V, Energy discrimination = -10 V in  $\text{NH}_3$  mode.

**Acquisition parameters:** MS/MS O<sub>2</sub> on-mass and MS/MS NH<sub>3</sub> mass-shift. Integration time per mass for BaF and BaF(NH<sub>3</sub>)<sub>3</sub> = 1 sec; integration time per mass for BaF(NH<sub>3</sub>)<sub>4</sub> = 10 sec.

In order to produce BaF<sup>+</sup> in the plasma, Ba solution was mixed online with fluorine standards per a fixed mixing ratio of 1:10. The mixing occurred just before the nebulizer. BaF<sup>+</sup> was efficiently formed under general plasma conditions with the BaO<sup>+</sup>/Ba<sup>+</sup> ratio at about 11%. Under hotter plasma conditions, the formation of BaF<sup>+</sup> decreases because it tends to break apart. Under cooler plasma conditions, the formation of BaF<sup>+</sup> also decreases because of the formation of BaO<sup>+</sup> or, possibly, BaO. The signal intensity of BaF<sup>+</sup> was proportional to the concentration of Ba, which was fixed at about 10 ppm (after mixing).

### Interference removal using MS/MS mode

<sup>138</sup>Ba<sup>19</sup>F<sup>+</sup> (*m/z*=157) suffers an interference from <sup>138</sup>Ba<sup>18</sup>O<sup>1</sup>H<sup>+</sup>. O<sub>2</sub> and NH<sub>3</sub> were tested as reaction gases to reduce the interference. It was found that O<sub>2</sub> reacts with BaOH<sup>+</sup> more efficiently than it reacts with BaF<sup>+</sup> in high energy reaction mode (octopole bias < -50 V). Therefore, using MS/MS mode, a mass pair (Q1 → Q2) = (157 → 157) was selected to detect BaF<sup>+</sup> in O<sub>2</sub> mode. With Q1 set to 157 u, <sup>138</sup>Ba<sup>+</sup> was prevented from entering the cell and forming new interferences through unwanted reactions.

NH<sub>3</sub> was found to react with BaF<sup>+</sup> at a high NH<sub>3</sub> flow rate to form BaF(NH<sub>3</sub>)<sub>n</sub><sup>+</sup>, where n = 2, 3, 4. The most abundant complex ion was BaF(NH<sub>3</sub>)<sub>3</sub><sup>+</sup> at *m/z* = 208, but BaF(NH<sub>3</sub>)<sub>4</sub><sup>+</sup> at *m/z* = 225 was preferable in terms of signal to background ratio or BEC. Mass pairs (Q1 → Q2) = (157 → 208) and (157 → 225) were selected in NH<sub>3</sub> mode.

### Results and discussion

Figures 1 and 2 show calibration curves up to 2 mg/L (ppm) for fluorine in deionized water. The lowest detection limit (27 ppb) was obtained in O<sub>2</sub> mode. The lowest BEC (87 ppb) was obtained by measuring BaF(NH<sub>3</sub>)<sub>4</sub><sup>+</sup> in NH<sub>3</sub> mode. Table 2 shows the BEC and DL results for F obtained from this study in comparison with the literature values.

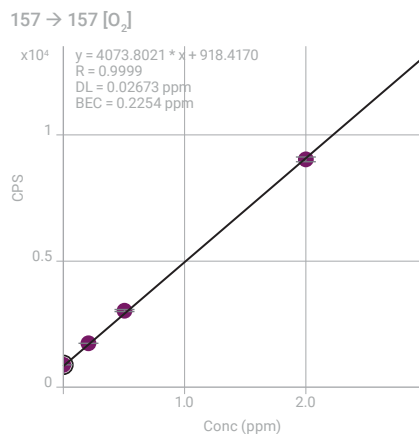


**Figure 1.** Calibration curve for F measured as BaF<sup>+</sup> in O<sub>2</sub> mode.

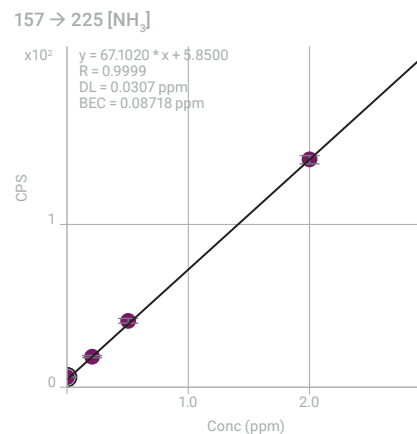


**Figure 2.** Calibration curve for F measured as BaF(NH<sub>3</sub>)<sub>4</sub><sup>+</sup> in NH<sub>3</sub> mode.

**Table 2.** Analytical performance for fluorine detection by ICP-MS.

Analyte ion	Sensitivity [cps/ppm]	BEC [ppm]	DL [ppm]	Technique, reference
F <sup>-</sup>	60,000	NA	0.11	Negative ion mode ICP-MS, Appl. Spectrosc, 42, 425 (1988)
F <sup>+</sup>	3,000	NA	0.023	He-ICP-MS, Japan analyst 52(4), 275-278, 2003
Al <sup>+</sup> (AlF <sup>2+</sup> complex)	NA	0.0033	0.0001	IC-ICP-MS (indirect determination), Analyst. 1999 Jan;124(1):27-31
F <sup>+</sup>	26	2.05	5.07	HR-ICP-MS, J. Anal. At. Spectrom, 18, 1443, 2003
BaF <sup>+</sup>	4,073	0.23	0.027	ICP-QQQ, O <sub>2</sub> mode, this work
BaF(NH <sub>3</sub> ) <sub>3</sub> <sup>+</sup>	929	0.17	0.043	ICP-QQQ, NH <sub>3</sub> mode, this work
BaF(NH <sub>3</sub> ) <sub>4</sub> <sup>+</sup>	67	0.087	0.031	ICP-QQQ, NH <sub>3</sub> mode, this work

## Conclusion

Based on this preliminary study, it is clear that the controlled reaction chemistry that is possible with MS/MS mode on the 8800 ICP-QQQ can provide a novel approach to the measurement of F by ICP-MS. In addition to demonstrating detection limits that are comparable with published data measured using conventional quadrupole ICP-MS or high-resolution ICP-MS, the 8800 ICP-QQQ also allows unprecedented flexibility to monitor specific reaction transitions, making it invaluable for method development.



# HPLC-ICP-MS/MS: Fluorine Speciation Analysis

## Authors

Nor Laili Azua Jamari, Jan Frederik Dohmann, Andrea Raab, Eva M. Krupp, and Jörg Feldmann  
Trace Element Speciation Laboratory (TESLA), University of Aberdeen, Scotland, UK

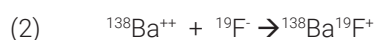
## Keywords

BaF<sup>+</sup>, fluorine speciation analysis, fluoride, fluoroacetate, trifluoroacetate, HPLC-ICP-QQQ

## Introduction

Fluorine is often used in the form of organofluorine compounds in applications such as pharmaceuticals, agrochemicals, and materials. This usage has resulted in the accumulation of large quantities of unknown organofluorine compounds in the environment [1, 2]. Fluorine is a difficult element to determine by ICP-MS. Its high ionization potential (17.423 eV) results in a low yield of F<sup>+</sup> ions in the plasma, leading to low sensitivity.

Fluorine can be determined, however, by mixing barium and fluorine solutions and measuring the polyatomic ion BaF<sup>+</sup> by triple quadrupole ICP-MS (ICP-QQQ) [3]. Because <sup>138</sup>Ba is the most abundant isotope, the highest sensitivity would be achieved for <sup>138</sup>Ba<sup>19</sup>F<sup>+</sup> at *m/z* 157. Mechanisms for the formation of BaF<sup>+</sup> are shown in equations 1 and 2.



While this approach resolves the low ionization yield issue for F, the formation of potential interfering ions at *m/z* 157 from <sup>138</sup>Ba<sup>18</sup>O<sup>1</sup>H<sup>+</sup>, <sup>138</sup>Ba<sup>16</sup>O<sup>1</sup>H<sub>3</sub><sup>+</sup>, and <sup>138</sup>Ba<sup>17</sup>O<sub>2</sub>H<sup>+</sup> also needs to be considered. These interferences can be reduced by operating the ICP-QQQ in MS/MS mode, using oxygen as the reaction gas. This approach was used for development of an online HPLC-ICP-QQQ speciation method for the determination of F.

## Experimental

**Instrumentation:** Agilent 8800 ICP-QQQ with Micromist nebulizer and s-lens.

**Operating conditions:** Table 1 summarizes the plasma, ion lens, and cell tuning conditions.

**Acquisition parameters:** MS/MS mode with O<sub>2</sub> on-mass. Integration time per *m/z* for BaF<sup>+</sup> = 1 sec.

**HPLC system:** Agilent 1290 with Metrosep A Supp 5 (150 mm x 4.0 mm) separation column and Metrosep RP Guard/3.5 column. Buffer = 3.2 mM sodium carbonate and 1.0 mM sodium bicarbonate (pH 10); flow rate = isocratic 0.7 mL/min of 70% buffer solution; sample injection = 100 μL.

A transfer capillary was used to connect the chromatographic column to the nebulizer of the ICP-QQQ system via a T-pin, which allowed the mixing of Ba with F solution. The parameters were optimized in a previous study [4].

**Table 1.** ICP-QQQ operating conditions.

Parameter	Unit	Value
<b>Plasma</b>		
RF power	W	1500
Sampling depth	mm	8.0
Carrier gas flow rate	L/min	1.00
Make-up gas flow rate	L/min	0.36
<b>Lenses</b>		
Extract 1	V	-150.0
Extract 2	V	5.0
Deflect	V	-48.0
<b>Cell</b>		
Oxygen flow rate	mL/min	0.75
Octopole Bias	V	-60.0
Octopole RF	V	200
Energy discrimination	V	-10.0
Wait time offset	msec	2
Sample uptake rate	mL/min	0.33
32 mg/L Ba uptake rate	mL/min	0.22

## Results and discussion

Figures 1 and 2 show the chromatograms and calibration curves for fluorine speciation analysis of three different fluorine compounds: fluoride, fluoroacetate (FAA), and trifluoroacetate (TFA). All compounds were baseline separated within 10 minutes. The sensitivity of F is similar for each sample, indicating the method is compound independent and fluorine specific.

The limits of detection (LOD) of the HPLC-ICP-QQQ method were 0.012 mg/L, 0.073 mg/L, and 0.12 mg/L for fluoride, FAA, and TFA, respectively. Table 2 shows the LOD results for F from this study compared to data reported in the literature.

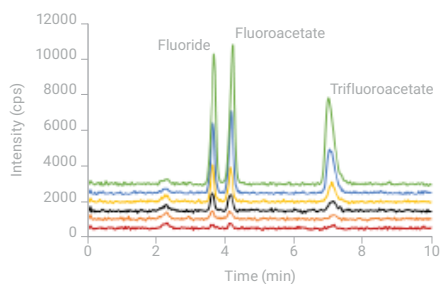


**Figure 1.** HPLC-ICP-QQQ chromatogram of fluoride, fluoroacetate, and trifluoroacetate at different F concentrations: 0.1, 0.25, 0.5, 1.0, 2.5, and 5.0 mg/L (as indicated by red to green colored lines).

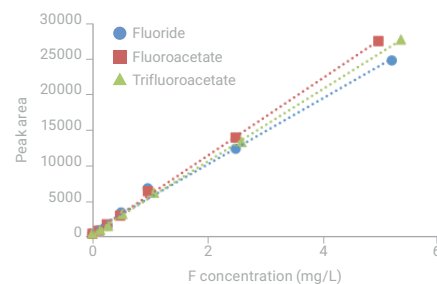


**Figure 2.** HPLC-ICP-QQQ calibration curves of fluorine compounds: fluoride, fluoroacetate, and trifluoroacetate.

**Table 2.** Limit of detection (LOD) of F analysis obtained by different methods.

Method	Analyte ion	LOD (mg/L)	Reference
IC-ICP-MS (indirect determination)	Al <sup>+</sup> (AlF <sup>+</sup> complex)	0.0001	Analyst, 1999, 124, 27–31
HR-ICP-MS	F <sup>+</sup>	5.1	J. Anal. At. Spectrom., 2003, 18, 1443–1451
ETV-ICP-MS	F <sup>+</sup>	3.2	J. Anal. At. Spectrom., 2001, 16, 539–541
ICP-MS/MS	BaF <sup>+</sup>	0.027	Agilent, 2015, 5991-2802EN
		0.043	J. Anal., At. Spectrom., 2017, 32, 942-950
HPLC-ICP-MS/MS	BaF <sup>+</sup> for fluoride	0.012	This work
	BaF <sup>+</sup> for fluoroacetate	0.073	This work
	BaF <sup>+</sup> for trifluoroacetate	0.12	This work

## Conclusion

For the first time, coupling an HPLC directly to an ICP-QQQ enabled the speciation analysis of fluorine-containing compounds through the formation of the polyatomic ion BaF<sup>+</sup> [4]. The method was not only able to detect fluorine specifically but also has a comparable low LOD, which opens up possibilities for future non-targeted fluorine speciation analysis in environmental samples.

## References

1. L. Ahrens, Polyfluoroalkyl compounds in the aquatic environment: A review of their occurrence and fate. *J. Environ. Monit.*, **2011**, 13, 20–31.
2. A. Harsanyi, G. Sandford, Organofluorine chemistry: applications, sources, and sustainability. *Green Chem.*, **2015**, 17: 2081–2086.
3. N. Yamada, Feasibility study of fluorine detection by ICP-QQQ, Agilent Applications Handbook, 2015, [5991-2802EN](#).
4. N. L. A. Jamari, J. F. Dohmann, A. Raab, E. M. Krupp, J. Feldmann, Novel non-target analysis of fluorine compounds using ICP-MS/MS and HPLC-ICP-MS/MS. *J. Anal., At. Spectrom.*, **2017**, 32, 942-950.

# Foods and Consumer Products

<b>Title</b>	<b>Page</b>
<b>Elemental analysis</b>	
Benefits of the Agilent 8900 ICP-QQQ with MS/MS operation for routine food analysis	229
Routine elemental analysis of dietary supplements using an Agilent 8900 ICP-QQQ	241
Accurate and sensitive analysis of arsenic and selenium in foods using ICP-QQQ to remove doubly-charged REE interferences	250
Analysis of TiO <sub>2</sub> nanoparticles in foods and personal care products by single particle ICP-QQQ	254
Accurate analysis of trace mercury in cosmetics using the Agilent 8900 ICP-QQQ	263
Sulfur isotope fractionation analysis in mineral waters using an Agilent 8900 ICP-QQQ	269
<b>Speciation</b>	
Fast analysis of arsenic species in infant rice cereals using LC-ICP-QQQ	275
High throughput determination of inorganic arsenic in rice using hydride generation-ICP-QQQ	282
Fast determination of inorganic arsenic (iAs) in food and animal feed by HPLC-ICP-MS	286
Multielement analysis and selenium speciation in cattle and fish feed using LC-ICP-QQQ	295
Arsenic speciation analysis in apple juice using HPLC-ICP-MS with the Agilent 8800 ICP-QQQ	304
Speciated arsenic analysis in wine using HPLC-ICP-QQQ	312
Fast analysis of arsenic species in wines using LC-ICP-QQQ	319
Simultaneous iodine and bromine speciation analysis of infant formula by HPLC-ICP-MS	326
Determination of pesticides using phosphorus and sulfur detection by GC-ICP-QQQ	333

# Benefits of the Agilent 8900 ICP-QQQ with MS/MS operation for routine food analysis

## Authors

Kazuhiro Sakai,  
Agilent Technologies, Japan

## Introduction

Growing awareness of and concern about the issue of food safety is reflected in the tightening of regulations governing toxic elements and compounds in food. Many toxic elements such as As, Hg, Cd, Pb etc. are routinely monitored to ensure food safety, while minerals that are beneficial/essential to human health such as Se, Na, Mg, K, Ca, etc., are also measured. As a fast, high throughput, multi-element technique, with a wide dynamic range and high sensitivity, ICP-MS is increasingly used for routine food analysis. Recent improvements in matrix tolerance with Agilent's High Matrix Introduction (HMI/UHMI) technology is a further benefit for the application as food matrices are varied and can be complex. UHMI uses aerosol dilution to reduce the sample matrix load on the plasma, allowing matrix levels up to several percent total dissolved solids (TDS) to be analyzed routinely. This is much higher than the limit of 0.2% (2000 ppm) which has traditionally applied to samples intended for ICP-MS analysis.

Control of polyatomic ion interferences in quadrupole ICP-MS has also improved significantly with the development of collision/reaction cells (CRCs), which use kinetic energy discrimination (KED) to attenuate polyatomic ions in helium (He) collision mode. Agilent's octopole-based CRC, the ORS<sup>4</sup>, is routinely used to suppress a wide range of matrix-based polyatomic ion interferences under one set of cell conditions [1]. Hence, reliable and accurate quantification of all required elements at regulated levels in a variety of sample matrices is now possible using conventional quadrupole ICP-MS (ICP-QMS).

However, some food-analysis applications require greater sensitivity for specific elements, while some complex sample matrices may cause spectral interferences that remain a challenge for ICP-QMS. For example, doubly charged ions of some rare earth elements (REEs) appear at the same mass as key analytes, hindering accurate low-level measurement of arsenic (As) and selenium (Se) in some sample types [2, 3].

### Improved interference removal with ICP-QQQ

The Agilent 8900 Triple Quadrupole ICP-MS (ICP-QQQ) has a unique tandem MS configuration, comprising two scanning quadrupole mass analyzers either side of an octopole-based ORS<sup>4</sup> collision reaction cell. As a result, the 8900 ICP-QQQ is able to utilize reactive cell gases and ion/molecule reaction chemistry in combination with MS/MS mode to resolve difficult spectral interferences [4]. The superior interference removal offered by reaction chemistry with MS/MS led to the previous generation Agilent 8800 ICP-QQQ being widely accepted in industry and research labs in fields such as semiconductor device and high purity chemical/material manufacturing, life-science, geoscience, radionuclides and many others [5-8]. MS/MS mode is also beneficial for the analysis of certain elements which are subject to problematic interferences in routine applications, such as the analysis of food samples, soils, waste water and groundwater.

Since the matrix tolerance and robustness of the Agilent 8900 ICP-QQQ is comparable to Agilent's market-leading single quadrupole ICP-MS systems, the 8900 ICP-QQQ can be used to analyze these high-matrix samples routinely.

### **Solving problems associated with As and Se analysis**

Arsenic is a well-known toxic element, while Se is an essential element that can be toxic in excess. Consequently, many countries regulate the permitted concentrations of As and Se in food, animal feed, drinking water, surface water and soils. However, As and Se can suffer spectral interferences from polyatomic ions including  $\text{ArCl}^+$ ,  $\text{CaCl}^+$ ,  $\text{ArAr}^+$ ,  $\text{S}_2\text{O}^+$ ,  $\text{SO}_3^+$ ,  $\text{GeH}^+$ , and  $\text{BrH}^+$ . These interferences can be reduced using ICP-QMS operating in helium (He) cell mode, allowing the accurate and precise measurement of As and Se at the concentration levels required to meet typical regulatory demands.

However, He mode is not effective against doubly-charged ion overlaps. The lanthanides or rare earth elements (REE) can form doubly charged ions ( $\text{REE}^{++}$ ) which overlap As and Se. These doubly-charged overlaps can be avoided using mass-shift mode with  $\text{O}_2$  as the reaction cell gas. In this mode, the analytes are measured as reaction product ions  $^{75}\text{As}^{16}\text{O}^+$  and  $^{78}\text{Se}^{16}\text{O}^+$ , mass-shifted to  $m/z$  91 and 94 respectively, where they are free from the original  $\text{REE}^{++}$  overlaps. This reaction chemistry can be used in the CRC of an ICP-QMS, but existing ions from the plasma may overlap the newly-formed product ions; e.g.  $^{91}\text{Zr}^+$  on  $^{75}\text{As}^{16}\text{O}^+$ , and  $^{94}\text{Mo}^+$  on  $^{78}\text{Se}^{16}\text{O}^+$ . To ensure controlled and consistent reaction chemistry, MS/MS mode on an ICP-QQQ is required, where the first quadrupole (Q1) operates as a mass filter set to the appropriate  $\text{As}^+$  or  $\text{Se}^+$  precursor ion mass. Q1 rejects all other masses, thereby removing the existing  $\text{Zr}^+$  and  $\text{Mo}^+$  ions and preventing them from overlapping the new analyte product ions.

Typically, the REE content of food and other natural samples is low, but crops grown in REE-enriched soils can take up high concentrations of these elements. The use of MS/MS mode with  $\text{O}_2$  reaction cell gas avoids the potential risk of reporting incorrect results for As and Se in the case of an unexpectedly high level of REEs.

In this study, the Agilent 8900 ICP-QQQ was evaluated as a routine tool for the analysis of 30 elements, including As and Se, in food sample digests.

## **Experimental**

### **Certified Reference Materials (CRMs)**

Five food CRMs purchased from National Institute of Standards and Technology (NIST) and High-Purity Standards Inc. (Charleston, SC, USA) were analyzed in this study. The CRMs used were NIST 1567b Wheat Flour, NIST 1568b Rice Flour, NIST 1515 Apple Leaves, NIST 1573a Tomato Leaves and High Purity Standards Mixed Food Diet Solution.

### **Sample preparation**

Due to the requirement to measure several volatile elements, including Hg, closed vessel microwave digestion using a Milestone ETHOS 1 Advanced Microwave Digestion System was used to digest the food CRMs. Sample weights of approximately 1.0 g for each of the flour CRMs (NIST 1567b, NIST 1568b) and 0.5 g for each of the other sample types (NIST 1515, NIST 1573a) were accurately weighed into closed microwave vessels. 6 mL of  $\text{HNO}_3$  and 1 mL of HCl

(electronics (EL) grade acids, Kanto Chemicals) were added to the microwave vessels. After 15 minutes held at room temperature, microwave heating was applied, using the heating program shown in Table 1. All CRMs were completely dissolved, resulting in clear solutions which were diluted to a final volume of 100 mL with ultrapure water (Merck, Darmstadt, Germany).

**Table 1.** Microwave digestion heating programs for four CRM food samples.

Power (W)	Temp (°C)	Ramp (min)	Hold (min)
500	70	2	3
1000	140	5	5
100	200	5	15
Ventilation			30

It is well known that carbon present in the sample solution enhances the ICP-MS signal of some elements, notably As, Se and P, although the precise mechanism of the enhancement is not clearly understood [9, 10]. With the high digestion temperature used in this work (200 °C), the carbon matrix was effectively decomposed during digestion. If any residual carbon did remain its effect could be mitigated by adding 2% butan-1-ol online with the internal standard solution.

### Instrumentation

An Agilent 8900 ICP-QQQ (Standard configuration) with the standard sample introduction system consisting of a glass concentric nebulizer, quartz spray chamber, and Ni interface cones was used. UHMI technology is included on the 8900 ICP-QQQ Standard configuration, allowing matrices as high as 25% NaCl solution to be analyzed [11]. The plasma conditions were selected according to the sample type and expected matrix level using the “Preset plasma” function of the MassHunter software.

### Acquisition conditions

For the multi-element analysis of the food samples, a multi-tune method was used so all elements could be acquired in the optimum cell gas mode. Multi-tune permits samples to be automatically analyzed using the optimum tune and cell conditions for each analyte element. He mode was used for all elements except P, S, As and Se which were determined in mass-shift mode using O<sub>2</sub> cell gas. The method was based on an appropriate preset method for food samples, which was modified to include O<sub>2</sub> cell gas mode. Preset plasma condition “UHMI-4” was selected, where the number 4 represents the approximate aerosol dilution factor. The UHMI setting automatically applies the predefined and calibrated parameters for RF power, sampling depth, carrier gas flow rate and dilution gas flow rate, giving precise and reproducible plasma conditions for the target sample types. The lens voltages were auto-tuned for maximum sensitivity. Table 2 summarizes the instrument operating parameters.

**Table 2.** Agilent 8900 ICP-QQQ operating conditions.

Parameter	Setting	
Cell mode	He mode	O <sub>2</sub> mode
Scan type	Single Quad	MS/MS
Plasma conditions	UHMI-4	
RF power (W)	1600	
Sampling depth (mm)	10	
Carrier gas flow rate (L/min)	0.77	
Dilution gas flow rate (L/min)	0.15	
Extract 1 (V)	0	
Extract 2 (V)	-250	
Omega Bias (V)	-140	
Omega lens (V)	8.8	
Cell gas flow (mL/min)	5.5	0.3 (20% of full scale)
KED (V)	5	-7

Bold parameters are predefined by selecting preset plasma condition UHMI-4.

### Calibration standards and internal standards

Calibration standards were prepared from an Agilent multi-element environmental calibration standard (p/n 5183-4688) which contains 1000 ppm each of Fe, K, Ca, Na, Mg and 10 ppm each of Ag, Al, As, Ba, Be, Cd, Co, Cr, Cu, Mn, Mo, Ni, Pb, Sb, Se, Th, Tl, U, V, and Zn. Standards for B, Rb, Sr, Sn and Hg were prepared from 1000 ppm Atomic-Absorption grade single element standards from Kanto Chemicals (Tokyo, Japan). S and P were prepared from 10,000 ppm Spex single element standards (SPEX CertiPrep, NJ, USA). The internal standard (ISTD) solution was prepared from an Agilent internal standard stock solution for ICP-MS systems (p/n 5188-6525) containing 6-Li, Sc, Ge, Rh, In, Tb, Lu, and Bi. Ir was added from an Atomic-Absorption grade single element standard purchased from Kanto Chemicals. The ISTD was added to the sample using the standard online ISTD kit.

Calibration standards were prepared in 6% HNO<sub>3</sub> and 1% HCl to match the acid content of the sample solutions. The ISTDs were prepared in 1% HNO<sub>3</sub> and 0.5% HCl. The calibration ranges were as follows: major elements: 0-100 ppm, trace elements: 0-500 ppb, B: 0-200 ppb, Hg: 0-1 ppb and Sn: 0-2 ppb.



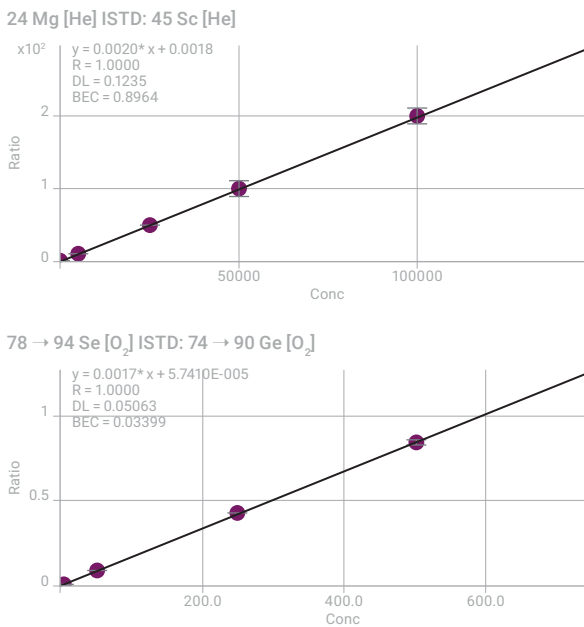


Figure 1. Representative calibration curves for a major element (Mg) and a trace element (Se).

### Sequence of calibrants, samples, and QC solutions

The sequence consisted of an initial multi-level calibration, covering the typical range for the target analytes, followed by a QC block containing an Initial Calibration Blank (ICB) check and Initial Calibration Verification (ICV) solution. After calibration and initial QC check, twelve sample blocks were analyzed per the flow chart shown in Figure 2; each block consisted of 2 preparation blanks and 10 samples (2 each of Wheat Flour, Rice Flour, Apple Leaves, Tomato Leaves and Mixed Food Diet). A Periodic Block consisting of Continuing Calibration Blank (CCB) and Continuing Calibration Verification (CCV) samples was automatically inserted into the sequence after each sample block.

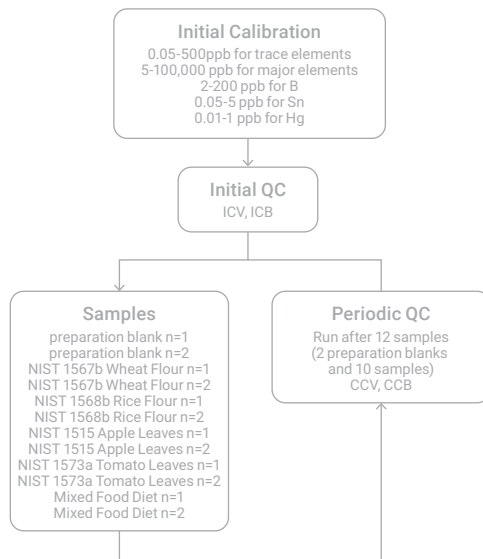
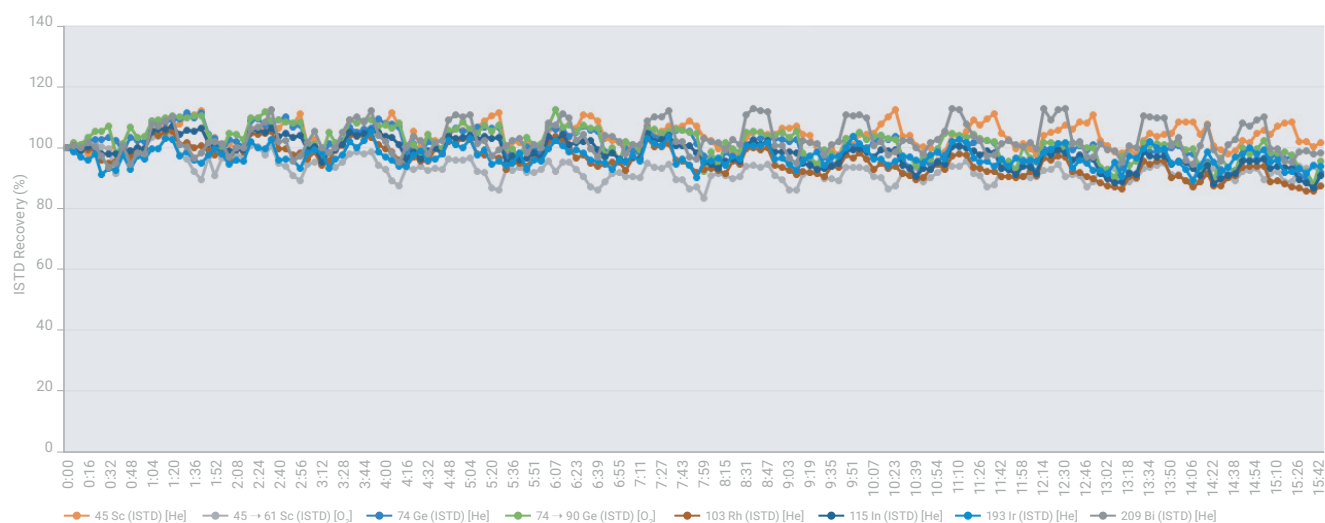


Figure 2. Sequence of calibrants, samples, and QC solutions analyzed in a single 15-hour sequence. Sample Block was repeated continuously with automatic insertion of Periodic QC Block after each Sample Block.

The total number of analyses of calibration standards, QC samples and food digest samples was 183 over ~15 hours. The sample-to-sample run time was about 5 minutes, which included a 10 s probe rinse and 60 s sample introduction system rinse at 0.3 rps peristaltic pump rate. Table 3 shows the detection limits (DL) obtained using this method.

**Table 3.** Method detection limits.

Element	Scan Mode	Q1	Q2	DI (ppb)
B	Single Quad		11	0.3653
Na	Single Quad		23	0.1945
Mg	Single Quad		24	0.1235
Al	Single Quad		27	0.1847
P	MS/MS	31	47	0.0919
S	MS/MS	32	48	0.4367
K	Single Quad		39	7.0656
Ca	Single Quad		44	8.7579
V	Single Quad		51	0.0079
Cr	Single Quad		52	0.0880
Mn	Single Quad		55	0.0099
Fe	Single Quad		56	0.1595
Co	Single Quad		59	0.0009
Ni	Single Quad		60	0.0484
Cu	Single Quad		63	0.0102
Zn	Single Quad		66	0.0308
As	Single Quad		75	0.0044
As	MS/MS	75	91	0.0040
Se	Single Quad		78	0.3158
Se	MS/MS	78	94	0.0506
Rb	Single Quad		85	0.0115
Sr	Single Quad		88	0.0006
Mo	Single Quad		95	0.0090
Ag	Single Quad		107	0.0063
Cd	Single Quad		111	0.0018
Sn	Single Quad		118	0.0074
Sb	Single Quad		121	0.0026
Ba	Single Quad		138	0.0008
Hg	Single Quad		202	0.0005
Tl	Single Quad		205	0.0104
Pb	Single Quad		208	0.0016
Th	Single Quad		232	0.0018
U	Single Quad		238	0.0009



**Figure 3.** ISTD signal stability for the sequence of 183 samples analyzed over 15 hours.

## Results and discussion

### ISTD and CCV stability

Figure 3 shows the ISTD signal stability for the sequence of 183 samples analyzed over 15 hours. The ISTD recoveries for all samples were well within  $\pm 20\%$  of the value in the initial calibration standard. These ISTD recoveries are comparable to the results obtained routinely using ICP-QMS, demonstrating the equivalent robustness of the 8900 ICP-QQQ.

The midpoint of the calibration standards was used as the CCV solution. CCV recovery over the 15-hour analysis was stable and within  $\pm 10\%$  for all elements, as shown in Figure 4, again demonstrating that the 8900 ICP-QQQ has the high matrix tolerance required for routine food digest analysis.

### CRM recovery results

The accuracy of the method was evaluated by analyzing the five food CRMs as unknown samples. Each CRM was measured 24 times in the batch. The mean concentration and relative standard deviation (%RSD) were calculated for each element and compared to the certified value, as shown in Tables 4 to 8. Using the preferred measurement mode, the results for all elements were in good agreement with the certified and reference values. Results are shown for both He mode and O<sub>2</sub> mass-shift mode for As and Se, to compare the results for samples where a sample might contain an unexpected high level of REEs. NIST 1515 Apple Leaves CRM contains low  $\mu\text{g}/\text{kg}$  concentrations of As and Se (Table 6) and high concentrations of REEs. Reference (non-certified) values for Nd, Sm, and Gd are 17, 3, and 3 mg/kg, respectively. In the case of Apple Leaves and, to a lesser extent, Tomato Leaves, more accurate recovery was obtained for As and Se using O<sub>2</sub> mass-shift mode, illustrating the potential error that can be caused by the relatively high level of REE in these two reference materials.



Figure 4. CCV recovery for all elements over the 15-hour analysis.

Table 4. Results for NIST 1567b Wheat Flour, n = 24.

Element	Measured Solution Concentration (µg/L)	RSD (%)	Calculated Sample Concentration (mg/kg)		Certified Concentration (mg/kg)		Recovery (%)
23 Na	65.2	2.3	6.50	± 0.15	6.71	± 0.21	97
24 Mg	3842	1.6	383	± 6	398	± 12	96
27 Al	39	2.8	3.9	± 0.1	4.4	± 1.2	88
31 → 47 P	12936	2.0	1291	± 26	1333	± 36	97
32 → 48 S	15496	2.2	1546	± 34	1645	± 25	94
39 K	12700	2.3	1267	± 29	1325	± 20	96
44 Ca	1871	1.8	186.7	± 3.4	191.4	± 3.3	98
51 V	0.10	8.1	0.010	± 0.001		0.01*	100
55 Mn	86	1.7	8.54	± 0.14	9.00	± 0.78	95
56 Fe	142	1.6	14.20	± 0.22	14.11	± 0.33	101
63 Cu	19	1.6	1.94	± 0.03	2.03	± 0.14	96
66 Zn	112	1.9	11.17	± 0.21	11.61	± 0.26	96
75 As	0.047	16.5	0.0046	± 0.001	0.0048	± 0.0003	97
75 → 91 As	0.049	19.4	0.0049	± 0.001	0.0048	± 0.0003	101
78 Se	11.5	4.2	1.15	± 0.05	1.14	± 0.10	101
78 → 94 Se	11.8	1.9	1.17	± 0.02	1.14	± 0.10	103
85 Rb	6.54	1.8	0.652	± 0.012	0.671	± 0.012	97
95 Mo	4.60	2.1	0.459	± 0.009	0.464	± 0.034	99
111 Cd	0.239	5.7	0.0238	± 0.0014	0.0254	± 0.0009	94
118 Sn	0.0355	12.8	0.0035	± 0.0005		0.003*	118
202 Hg	0.0066	11.3	0.0007	± 0.0001		0.0005*	131
208 Pb	0.0937	4.4	0.0094	± 0.0004	0.0104	± 0.0024	90

\* Reference value

**Table 5.** Results for NIST 1568b Rice Flour, n = 24.

Element	Measured Solution Concentration (µg/L)	RSD (%)	Calculated Sample Concentration (mg/kg)		Certified Concentration (mg/kg)			Recovery (%)
23 Na	65.6	3.2	6.54	± 0.28	6.74	± 0.19	97	
24 Mg	5454	1.5	543	± 8	559	± 10	97	
27 Al	40.3	3.3	4.01	± 0.13	4.21	± 0.34	95	
31 -> 47 P	15162	2.8	1510	± 43	1530	± 40	99	
32 -> 48 S	11369	2.5	1133	± 28	1200	± 10	94	
39 K	12371	2.0	1233	± 24	1282	± 11	96	
44 Ca	1158	2.1	115.3	± 2.5	118.4	± 3.1	97	
51 V	182.3	1.0	18.2	± 0.2	19.2	± 1.8	95	
55 Mn	75.4	1.0	7.51	± 0.08	7.42	± 0.44	101	
56 Fe	0.173	1.7	0.0173	± 0.0003	0.0177	± 0.0005*	98	
63 Cu	22.7	1.0	2.26	± 0.02	2.35	± 0.16	96	
66 Zn	191.7	1.4	19.10	± 0.26	19.42	± 0.26	98	
75 As	2.97	1.4	0.296	± 0.004	0.285	± 0.014	104	
75 -> 91 As	3.01	1.7	0.300	± 0.005	0.285	± 0.014	105	
78 Se	3.4	8.9	0.341	± 0.030	0.365	± 0.029	93	
78 -> 94 Se	3.5	3.8	0.352	± 0.013	0.365	± 0.029	96	
85 Rb	61.1	1.1	6.088	± 0.069	6.198	± 0.026	98	
95 Mo	13.96	1.2	1.391	± 0.017	1.451	± 0.048	96	
111 Cd	0.201	4.9	0.0201	± 0.0010	0.0224	± 0.0013	90	
118 Sn	0.060	7.4	0.0060	± 0.0004	0.005	± 0.001*	121	
202 Hg	0.0529	2.1	0.0053	± 0.0001	0.0059	± 0.0004	89	
208 Pb	0.068	3.0	0.0068	± 0.0002	0.008	± 0.003*	85	

\* Reference value

**Table 6.** Results for NIST 1515 Apple Leaves, n = 24.

Element	Measured Solution Concentration (µg/L)	RSD (%)	Calculated Sample Concentration (mg/kg)		Certified Concentration (mg/kg)			Recovery (%)
11 B	141	2.9	28	± 0.8	27	± 2	104	
23 Na	196	1.6	39.1	± 0.6	24.4	± 1.2	160*1	
24 Mg	14083	1.3	2812	± 36	2710	± 80	104	
27 Al	1458	1.6	291	± 5	286	± 9	102	
31 -> 47 P	8088	2.2	1615	± 35	1590*		102	
32 -> 48 S	9211	1.4	1839	± 26	1800*		102	
39 K	80429	2.2	16057	± 361	16100	± 200	100	
44 Ca	74060	1.2	14786	± 172	15260	± 1500	97	
51 V	1.20	2.8	0.24	± 0.01	0.26	± 0.03	92	
52 Cr	1.3	1.4	0.25	± 0.00	0.3*		85	
55 Mn	265	1.0	53	± 1	54	± 3	98	
56 Fe	379	0.8	76	± 1	80*		95	
59 Co	0.44	1.5	0.088	± 0.001	0.09*		98	
60 Ni	4.4	1.7	0.88	± 0.02	0.91	± 0.12	97	
63 Cu	28.2	1.0	5.62	± 0.06	5.64	± 0.24	100	
66 Zn	60.3	0.9	12.0	± 0.1	12.5	± 0.3	96	
75 As	2.0	1.2	0.395	± 0.005	0.038	± 0.007	1040	
75 -> 91 As	0.2	3.7	0.036	± 0.001	0.038	± 0.007	94	
78 Se	13.43	5.8	2.7	± 0.2	0.050	± 0.009	5364	
78 -> 94 Se	0.271	13.8	0.054	± 0.008	0.050	± 0.009	108	
85 Rb	46.3	0.9	9.2	± 0.1	9*		103	
88 Sr	123.0	1.0	25	± 0	25	± 2	98	

Element	Measured Solution Concentration (µg/L)	RSD (%)	Calculated Sample Concentration (mg/kg)			Certified Concentration (mg/kg)			Recovery (%)
95 Mo	0.44	5.3	0.088	±	0.005	0.094	±	0.013	94
111 Cd	0.06	7.0	0.013	±	0.001	0.014*			91
121 Sb	0.06	4.6	0.011	±	0.001	0.013*			85
138 Ba	245	1.9	49	±	1	49	±	2	100
202 Hg	0.21	2.0	0.041	±	0.001	0.044	±	0.004	93
208 Pb	2.3	1.3	0.452	±	0.006	0.470	±	0.024	96
232 Th	0.14	2.2	0.028	±	0.001	0.03*			93
238 U	0.034	3.7	0.0068	±	0.0003	0.006*			113

\*Reference value.

Bold values for As and Se were obtained in single quad mode with He cell gas. The accurate results obtained using MS/MS mode with O<sub>2</sub> mass-shift are shown in the lines below.

\*1 The measured Na result was high compared to the reference value; the same result was obtained from a repeated analysis of the same solution, so a spike recovery test was performed for confirmation. The spike recovery result was good (recovery: 99%), suggesting that the original sample had suffered Na contamination.

**Table 7.** Results for NIST 1573a Tomato Leaves, n = 24.

Element	Measured Solution Concentration (µg/L)	RSD (%)	Calculated Sample Concentration (mg/kg)			Certified Concentration (mg/kg)			Recovery (%)
11 B	167	1.9	33.3	±	0.6	33.3	±	0.7	10
23 Na	613	2.5	122	±	3	136	±	4	90
24 Mg	57311	2.0	11412	±	225	12000*			95
27 Al	2573	2.4	512	±	12	598	±	12	86
31 -> 47 P	10928	2.7	2176	±	59	2160	±	40	101
32 -> 48 S	48387	1.4	9635	±	131	9600*			100
39 K	134250	2.2	26732	±	591	27000	±	500	99
44 Ca	243939	1.4	48574	±	671	50500	±	900	96
51 V	4.0	2.2	0.792	±	0.017	0.835	±	0.010	95
52 Cr	9.3	1.6	1.85	±	0.03	1.99	±	0.06	93
55 Mn	1236.5	1.5	246	±	4	246	±	8	100
56 Fe	1843.3	1.7	367	±	6	368	±	7	100
59 Co	2.8	1.4	0.55	±	0.01	0.57	±	0.02	96
60 Ni	7.9	1.9	1.56	±	0.03	1.59	±	0.07	98
63 Cu	23.7	1.5	4.71	±	0.07	4.70	±	0.14	100
66 Zn	149.4	1.5	29.8	±	0.5	30.9	±	0.7	96
75 As	0.7	2.3	0.141	±	0.003	0.112	±	0.004	126
75 -> 91 As	0.6	1.7	0.112	±	0.002	0.112	±	0.004	100
78 Se	1.03	15.6	0.205	±	0.032	0.054	±	0.003	380
78 -> 94 Se	0.31	11.2	0.061	±	0.007	0.054	±	0.003	113
85 Rb	69.7	1.2	13.88	±	0.16	14.89	±	0.27	93
88 Sr	421.0	1.3	84	±	1	85*			99
95 Mo	2.1	2.8	0.42	±	0.01	0.46*			91
107 Ag	0.09	9.1	0.018	±	0.002	0.017*			104
111 Cd	7.4	1.4	1.47	±	0.02	1.52	±	0.04	97
121 Sb	0.28	3.4	0.055	±	0.002	0.063	±	0.006	88
138 Ba	302.8	2.1	60.3	±	1.3	63*			96
202 Hg	0.15	2.4	0.030	±	0.001	0.034	±	0.004	88
232 Th	0.52	2.1	0.104	±	0.002	0.12*			87
238 U	0.14	2.3	0.029	±	0.001	0.035*			81

\* Reference value

Bold values for As and Se were obtained in single quad mode with He cell gas. The accurate results obtained using MS/MS mode with O<sub>2</sub> mass-shift are shown in the lines below.

**Table 8.** Results for the High Purity Standard Mixed Food Diet Solution, n = 24.

Element	Measured Solution Concentration (µg/L)	RSD (%)	Calculated Sample Concentration (mg/kg)		Certified Concentration (mg/kg)			Recovery (%)
23 Na	15808	2.9	61.8	± 1.8	60.0	± 0.6	105	
24 Mg	3300	2.3	12.9	± 0.3	12.0	± 0.1	108	
27 Al	26	4.5	0.100	± 0.005	0.100	± 0.002	100	
31 -> 47 P	15543	3.3	60.8	± 2.0	60.0	± 0.6	101	
39 K	41898	2.2	164	± 4	160	± 2	102	
44 Ca	9800	2.7	38.3	± 1.0	40.0	± 0.4	96	
52 Cr	0.55	10.4	0.0021	± 0.0002	0.002*		107	
55 Mn	49.2	1.7	0.192	± 0.003	0.200	± 0.004	96	
56 Fe	204.5	1.8	0.80	± 0.01	0.80	± 0.01	100	
59 Co	0.2	2.4	0.0008	± 0.0000	0.0008*		98	
60 Ni	5.1	2.5	0.020	± 0.001	0.020	± 0.001	99	
63 Cu	15.3	1.7	0.060	± 0.001	0.060	± 0.006	100	
66 Zn	74.5	2.0	0.29	± 0.01	0.30	± 0.01	97	
75 As	5.1	2.0	0.020	± 0.000	0.020	± 0.001	99	
75 -> 91 As	5.2	2.6	0.020	± 0.001	0.020	± 0.001	102	
78 Se	1.26	14.8	0.0049	± 0.0007	0.005*		99	
78 -> 94 Se	1.31	6.6	0.0051	± 0.0003	0.005*		102	
95 Mo	1.5	3.1	0.0059	± 0.0002	0.006*		98	
111 Cd	2.0	2.1	0.0078	± 0.0002	0.0080	± 0.0008	98	

\* Reference value

Bold values for As and Se were obtained in single quad mode with He cell gas. The accurate results obtained using MS/MS mode with O<sub>2</sub> mass-shift are shown in the lines below.

## Conclusion

The Agilent 8900 Standard configuration ICP-QQQ with UHMI offers the robustness and matrix tolerance required for the routine analysis of the widest range of trace and major elements in high matrix samples, such as food digest samples. Doubly-charged REE interferences that can affect the accurate measurement of arsenic and selenium at trace levels were avoided using O<sub>2</sub> cell gas with MS/MS mass-shift mode. Most other elements were measured in He mode; a field-proven method that is widely used to remove common matrix-based polyatomic interferences in complex and variable matrices.

While not all food products, soils and sediments contain significant concentrations of REEs, the use of ICP-QQQ with MS/MS improves the accuracy and confidence in the results for As and Se measured in food and environmental samples that often contain complex, variable, high TDS matrices.

Method development was greatly simplified with the use of Pre-set Methods and auto tuning, which ensures reproducible performance irrespective of operator experience.

## References

1. Ed McCurdy and Glenn Woods, *J. Anal. At. Spectrom.*, **2004**, 19, 607-615
2. Brian P Jackson et al, *J. Anal. At. Spectrom.*, **2015**, 30, 1179-1183
3. Kazuhiro Sakai, Agilent Application Note, 2015, 5991-6409EN
4. Agilent 8800 ICP-QQQ Application Handbook, Second Edition, 2015, 5991-2802EN
5. Lieve Balcaen et al, *Anal. Chim. Acta*, **2014**, 809, 1-8
6. S.D. Fernandez et al, *Geochem Geophy Geosy*, **2015**, 16, 2005 - 2014
7. Takeshi Ohno and Yasuyuki Muramatsu, *J. Anal. At. Spectrom.*, **2014**, 29, 347-351
8. Clarice D. B. Amaral et al, *Anal. Methods*, **2015**, 7, 1215-1220.
9. Erik H. Larsen, Stefan Sturup, *J. Anal. At. Spectrom.*, **1994**, 9, 1099-1105
10. Maurizio Pettine, Barbara Casentini, Domenico Mastroianni, Silvio Capri, *Anal. Chim. Acta*, **2007**, 599, 2, 191-198
11. Wim Proper, Ed McCurdy and Junichi Takahashi, Agilent Application Note, 2014, 5991-4257EN



# Routine Elemental Analysis of Dietary Supplements using an Agilent 8900 ICP-QQQ

## Authors

Kazuhiro Sakai,  
Agilent Technologies Inc.

Effective removal of doubly charged and oxide ion interferences ensures accurate measurement of As and Cd

## Introduction

Global consumer demand for dietary supplements is expected to increase steadily over the next few years (1). Dietary supplements contain ingredients such as nutrients, vitamins, and minerals that may be lacking in the consumer's normal diet. Supplements are marketed as supporting a balanced diet as part of a healthy lifestyle, and therefore differ from drugs that are intended to treat or prevent an illness. Supplements may be consumed in forms such as tablets, capsules, softgels, gelcaps, powders, and liquids (2). In the European Union, the term food supplement is usually applied to products that are called dietary supplements in the US (3).

As with any food product, dietary supplements may be subject to contamination. For example, trace metals can be introduced from raw materials, during manufacturing/processing, or from packaging materials. Therefore, the responsibility for a product's quality and safety lies mainly with manufacturers and distributors. In the European Union, manufacturers must adhere to regulations on labeling, contents, claims, and dosage recommendations (3). The U.S. Food and Drug Administration (FDA) also requires accurate labeling according to current Good Manufacturing Practice (cGMP) and labeling regulations (2). Since any unsafe or mislabeled products can be taken off the market, manufacturers are increasingly testing their products for potential contaminants including trace elements.

To assist manufacturers with quality assuring their products, the United States Pharmacopeia (USP) issued General Chapter <2232>, which deals with the regulation of Elemental Contaminants in Dietary Supplements (4). While <2332> is intended for products labeled as conforming to USP or National Formulary (NF) standards, it contains useful guidance for analysts.

In this study, triple quadrupole ICP-MS (ICP-QQQ) was used for the routine analysis of the four most toxic elements—arsenic, cadmium, lead, and mercury—in dietary supplements.

### Improved interference removal with ICP-QQQ

The Agilent 8900 ICP-QQQ features a unique tandem MS configuration, comprising a scanning quadrupole mass analyzer either side of an octopole-based collision/reaction cell (CRC). This configuration enables the 8900 ICP-QQQ to use MS/MS mode to resolve difficult spectral interferences using reactive cell gases in a wide range of sample types (5 to 9). MS/MS mode is also beneficial for the more difficult elements and problematic interferences sometimes encountered in routine applications, such as the analysis of food samples, soils, wastewater, and groundwater (5).

### Solving doubly charged and oxide interferences

Due to their toxicity, many countries regulate the permitted concentrations of As and Cd in drinking water, surface water, soils, foodstuffs, and drugs. The only isotope of As ( $m/z$  75) can suffer spectral interferences from polyatomic ions including  $\text{ArCl}^+$  and  $\text{CaCl}^+$ . These interferences can be reduced using single quadrupole ICP-QMS operating in helium collision mode (He mode), allowing the accurate measurement of As at the concentration levels required to meet typical regulatory demands. While He mode can be considered a universal cell gas for reducing polyatomic interferences using kinetic energy discrimination (KED), KED is not effective against doubly charged ( $M^{++}$ ) ion overlaps. The lanthanides or rare earth elements (REE) can form doubly charged ions ( $\text{REE}^{++}$ ) which overlap As (and Se) (10, 11). Also, KED does not eliminate oxide interferences well (5). For example,  $^{59}\text{Co}^{16}\text{O}^+$  interference on  $^{75}\text{As}^+$ ,  $^{95}\text{Mo}^{16}\text{O}^+$  on  $^{111}\text{Cd}^+$ , and  $^{98}\text{Mo}^{16}\text{O}^+$  on  $^{114}\text{Cd}^+$ . Vitamin B 12 is rich in Co as cyanocobalamin, and multimineral supplements are rich in Mo, included as an essential nutrient (12).

ICP-QQQ has been shown to be effective for the removal of  $M^{++}$  and oxide interferences on various analytes using a reactive cell gas (11). Many elemental ions react with  $\text{O}_2$  to form an oxide ion, while the  $M^{++}$  interference remains unreactive or is much less reactive. This allows the element of interest to be quantified by measuring the oxide ion at + 16 u, free from the spectral interference.

$\text{CoO}^+$  does not react with  $\text{O}_2$ , while  $\text{As}^+$  reacts with  $\text{O}_2$  to form  $\text{AsO}$ , allowing AsO and Co to be separated.  $\text{MoO}^+$  reacts with  $\text{O}_2$  to form  $\text{MoO}_2^+$ , while  $\text{Cd}^+$  does not react with  $\text{O}_2$ , allowing MoO and Cd to be separated. To test the method, 1 ppb As was determined in a series of solutions containing 0 to 100 ppm Co, and 1 ppb Cd was determined in solutions containing 0 to 10 ppm Mo. All solutions were analyzed in He mode (to represent conventional ICP-QMS) and MS/MS mode using  $\text{O}_2$  cell gas (only available with ICP-QQQ).

As shown in Figure 1, He mode is suitable for the analysis of As and Cd in matrices that contain Co and Mo at low ppm concentrations. However, poor recoveries were achieved for As in the presence of 100 ppm Co and Cd in a 10 ppm Mo matrix. In contrast, ICP-QQQ operating in MS/MS mode with  $\text{O}_2$  cell gas avoided the oxide ion interferences on As and Cd, respectively, at all matrix concentrations. The method allows consistent, low-level determination of As, measured as  $^{75}\text{AsO}^+$  at  $m/z$  91, and  $^{111}\text{Cd}^+$  at  $m/z$  111.

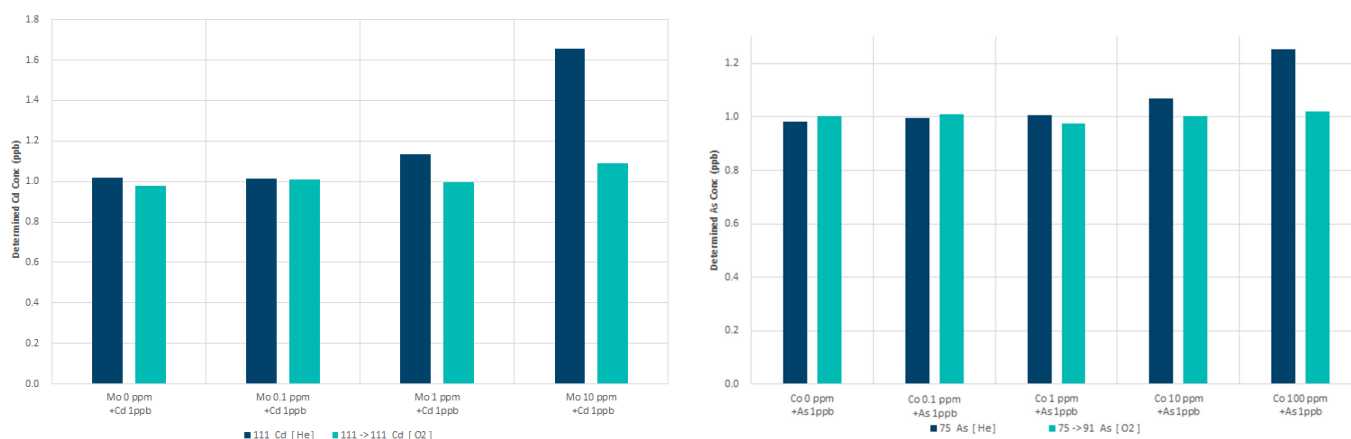


**Figure 1.** Left: Recoveries of 1 ppb As spikes in a series of Co matrix solutions. Right: Recoveries of 1 ppb Cd spikes in a series of Mo matrix solutions. He mode results (blue bars) and MS/MS O<sub>2</sub> mode results (green bars).

## Experimental

### Standard reference materials

Three National Institute of Standards and Technology (NIST) standard reference materials (SRMs) were analyzed in this study, including 1515 Apple Leaves, 1573a Tomato Leaves, and 3280 Multivitamin/Multielement tablets (Gaithersburg MD, USA). The Apple Leaves SRM contains low  $\mu\text{g}/\text{kg}$  levels of As in the presence of  $\text{mg}/\text{kg}$  levels of REEs.

### Samples and sample preparation

Three vitamin supplements and two multimineral supplements were bought in a local store in Tokyo, Japan. All SRMs and samples were prepared using a single microwave digestion method. A subsample of 0.20 g was accurately weighed and placed in a PTFE microwave vessel and 6.0 mL of 61% Electronic grade nitric acid and 1.0 mL of 36% Electronic grade hydrochloric acid (Kanto Chemical Co., Inc, Japan) were added. The samples were left for 20 minutes before being placed into a microwave (Mars 6, CEM) and digested using the program given in Table 1. The fully digested samples were then diluted to 50 mL with de-ionized water (DIW). The final digests of the multimineral supplements were further diluted two-fold with acid diluent (total of 12.0 mL HNO<sub>3</sub>, 2 mL HCl, and 86 mL DIW) to match the acid concentration of the other samples.

Although vitamins are water soluble, they were acid-digested because the carbon concentration was expected to be high. Carbon present in the sample solution enhances the ICP-MS signal of some elements, notably As, Se, and P, although the precise mechanism of the enhancement is not clearly understood (13, 14). With the high temperature used in this work (210 °C), the carbon in the samples converts to CO<sub>2</sub> through acid digestion, so the carbon concentration in the sample solution decreases. If any residual carbon did remain, its effect could be mitigated by adding 2% butan-1-ol online with the internal standard (ISTD) solution.

**Table 1.** Microwave digestion program.

Temperature (°C)	Ramp Time (min)	Hold Time (min)
210	15	15
Ventilation		30

### Calibration standards and internal standards

Calibration standards for As, Cd, Hg, and Pb were prepared from 1000 ppm single element standards (Kanto Chemicals, Tokyo, Japan). The ISTD solution containing Ge, In, Tl, and Bi was also prepared from single element standard (Kanto Chemicals). Calibration standards and ISTDs were prepared to match the acid content of the sample solutions. The ISTD was added to the sample using the standard online ISTD kit.

### Instrumentation

An Agilent 8900 Triple Quadrupole ICP-MS (ICP-QQQ, Standard configuration) with UHMI technology was used. The ICP-QQQ was fitted with the standard sample introduction system consisting of a glass concentric nebulizer, quartz spray chamber, and Ni interface cones. The plasma conditions were selected according to the sample type and expected matrix level using the “preset plasma” function of the Agilent ICP-MS MassHunter software. UHMI allows matrices as high as 25% NaCl solution to be analyzed (15).

### Acquisition conditions

The method was based on an appropriate preset method for food samples, which was modified to include O<sub>2</sub> cell gas mode. Preset plasma conditions “HMI-4” were selected, where the number 4 represents the approximate aerosol dilution factor. The HMI setting automatically applies the predefined and calibrated parameters for RF power, sampling depth, nebulizer gas flow rate, and dilution gas flow rate. Automating these settings speeds up and simplifies instrument set up as well as ensuring precise and reproducible plasma conditions for the target sample types. The lens voltages were autotuned for maximum sensitivity. Table 2 summarizes the instrument operating parameters.

**Table 2.** ICP-QQQ operating conditions.

Parameter	Setting	
	He mode	O <sub>2</sub> mode
Cell mode	He mode	O <sub>2</sub> mode
Scan type	Single Quad	MS/MS
Plasma conditions	HMI-4	
RF power (W)	1600	
Sampling depth (mm)	10	
Nebulizer gas flow rate (L/min)	0.82	
Dilution gas flow rate (L/min)	0.15	
Extract 1 (V)	0	
Extract 2 (V)	-250	
Omega bias (V)	-130	
Omega lens (V)	8.6	
Cell gas flow (mL/min)	5.5	0.45 30% of full scale
Energy Discrimination (V)	5	-7

*Shaded parameters are predefined by selecting HMI-4 preset plasma conditions.*

## Results and discussion

Calibration curves for As and Cd acquired in He mode and MS/MS mode with O<sub>2</sub> cell gas are shown in Figure 2.

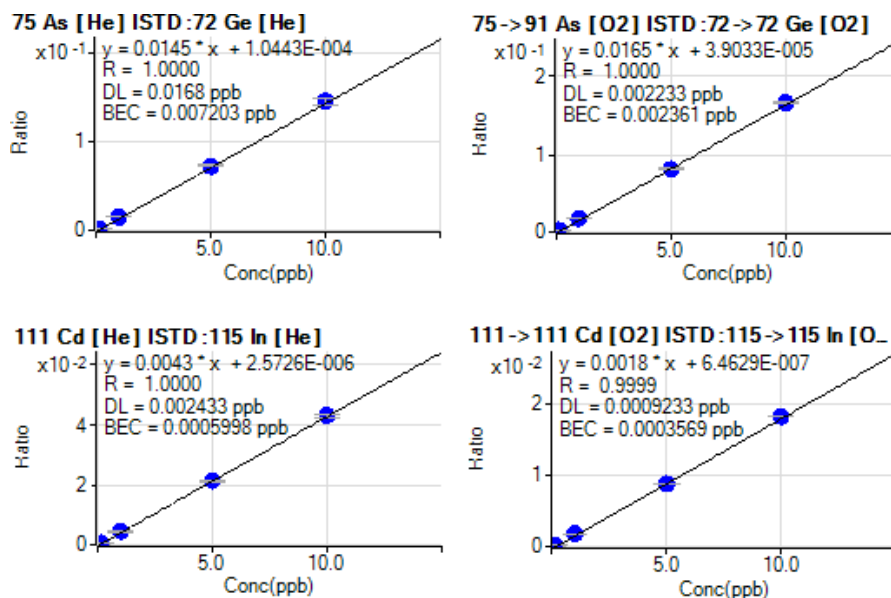


Figure 2. Calibration curves for As (top) and Cd (bottom).

All analytes were measured in He mode, and As and Cd were also analyzed in MS/MS O<sub>2</sub> mode. Three sigma method detection limits (MDLs) and 10 sigma Limit of Quantitation (MLOQs) were calculated from 10 measurements of the preparation blank (Table 3).

### SRM recovery

The accuracy of the method was evaluated by analyzing the three SRMs as unknown samples. Each SRM was measured nine times in the batch. The mean concentrations and relative standard deviation (%RSD) were calculated and compared to the certified value, as shown in Tables 4 to 6. The results for all elements were in good agreement with the certified and reference values. The results for the Apple Leaves SRM and, to a lesser extent Tomato Leaves, show that more accurate recoveries were obtained for As using O<sub>2</sub> mass shift mode compared to He mode. The results illustrate the potential error that can be caused by the relatively high level of REEs in these two reference materials.

### Quantitative analysis of bought products and spike recoveries

The 8900 ICP-QQQ was used to analyze three vitamin supplements (Samples 1 to 3) and two multimineral supplements (Samples 4 and 5). The quantitative results and spike recovery results are shown in Tables 7 and 8, respectively. The spikes were added to the microwave vessels before microwave digestion. The spike recoveries for all elements were  $\pm 10\%$  of the expected values.

Table 4. Results for NIST 1515 Apple Leaves. The shaded value for As was obtained in single quad mode with He cell gas. The unshaded (accurate) result was obtained using MS/MS mass-shift mode with O<sub>2</sub>.

**Table 3.** Method Detection Limits and Method Limits of Quantification.

Analyte	Q1	Q2	Cell Mode	Integration Time (sec)	ISTD	In Solution Prep Blank (n=10)		In Sample Multimineral		In Sample Other Samples	
						MDL µg/L	MLOQ µg/L	MDL µg/g	MLOQ µg/g	MDL µg/g	MLOQ µg/g
As		75	He	1	<sup>72</sup> Ge	0.0067	0.022	0.0033	0.011	0.0017	0.0055
As	75	91	O <sub>2</sub>	1	<sup>72</sup> Ge	0.0015	0.0050	0.0008	0.0025	0.0004	0.0013
Cd		111	He	1	<sup>115</sup> In	0.0019	0.0062	0.0009	0.0031	0.0005	0.0016
Cd	111	111	O <sub>2</sub>	1	<sup>115</sup> In	0.0005	0.0018	0.0003	0.0009	0.0001	0.0004
Hg		202	He	3	<sup>205</sup> Tl	0.0004	0.0014	0.0002	0.0007	0.0001	0.0004
Pb		208	He	1	<sup>209</sup> Bi	0.0027	0.0089	0.0013	0.0044	0.0007	0.0022

**Table 4.** Results for NIST 1515 Apple Leaves. The shaded value for As was obtained in single quad mode with He cell gas. The unshaded (accurate) result was obtained using MS/MS mass-shift mode with O<sub>2</sub>.

	Q1	Q2	Cell Mode	Measured Solution Concentration (µg/L)	RSD % (n=9)	Calculated Sample Concentration (mg/kg)	Certified Concentration (mg/kg)	Recovery (%)
As		75	He	1.6	1.1	0.406 ± 0.004	0.038 ± 0.007	1069
As	75	91	O <sub>2</sub>	0.14	2.1	0.035 ± 0.001		91
Cd		111	He	0.057	13	0.014 ± 0.002	0.014 *	102
Cd	111	111	O <sub>2</sub>	0.059	4.3	0.015 ± 0.001		105
Hg		202	He	0.18	4.6	0.045 ± 0.002	0.044 ± 0.004	102
Pb		208	He	2.0	2.4	0.49 ± 0.012	0.47 ± 0.024	104

\*Reference value

**Table 5.** Results for NIST 1573a Tomato Leaves. The shaded value for As was obtained in single quad mode with He cell gas. The unshaded (accurate) result was obtained using MS/MS mass-shift mode with O<sub>2</sub>.

	Q1	Q2	Cell Mode	Measured Solution Concentration (µg/L)	RSD % (n=9)	Calculated Sample Concentration (mg/kg)	Certified Concentration (mg/kg)	Recovery (%)
As		75	He	0.56	6.7	0.139 ± 0.009	0.112 ± 0.004	124
As	75	91	O <sub>2</sub>	0.45	2.6	0.113 ± 0.001		101
Cd		111	He	6.1	7.8	1.53 ± 0.12	1.52 ± 0.04	101
Cd	111	111	O <sub>2</sub>	6.4	6.7	1.60 ± 0.11		105
Hg		202	He	0.12	8.2	0.031 ± 0.003	0.034 ± 0.004	91
Pb		208	He	2.6	9.1	0.64 ± 0.058	-	-

**Table 6.** Results for NIST 3280 Multivitamin/Multielement Tablets.

	Q1	Q2	Cell Mode	Measured Solution Concentration (µg/L)	RSD % (n=9)	Calculated Sample Concentration (mg/kg)	Certified Concentration (mg/kg)	Recovery (%)
As		75	He	0.25	2.7	0.127 ± 0.003	0.132 ± 0.044	96
As	75	91	O <sub>2</sub>	0.24	2.2	0.119 ± 0.003		90
Cd		111	He	0.17	4.4	0.0851 ± 0.0037	0.08015 ± 0.00086	106
Cd	111	111	O <sub>2</sub>	0.16	6.5	0.0802 ± 0.0052		100
Hg		202	He	< 0.0004	-	< 0.0002	-	-
Pb		208	He	0.53	4.1	0.266 ± 0.011	0.2727 ± 0.0024	97

**Table 7.** Quantitative results for vitamin supplements.

				Sample 1				Sample 2				Sample 3			
	Q1	Q2	Cell Mode	Unspiked (µg/L)	Spiked (µg/L)	Spike Recovery (%)	Calculated Sample Concentration (µg/g)	Unspiked (µg/L)	Spiked (µg/L)	Spike Recovery (%)	Calculated Sample Concentration (µg/g)	Unspiked (µg/L)	Spiked (µg/L)	Spike Recovery (%)	Calculated Sample Concentration (µg/g)
As		75	He	0.035	1.10	106	0.0086	<0.0067	1.10	110	<0.0017	0.024	1.08	105	0.006
As	75	91	O <sub>2</sub>	0.038	1.08	104	0.0093	<0.0015	1.04	104	<0.0004	0.021	1.07	105	0.005
Cd		111	He	0.013	1.05	103	0.0031	<0.0019	1.02	102	<0.0005	<0.0019	1.01	101	<0.0005
Cd	111	111	O <sub>2</sub>	0.014	1.10	109	0.0034	0.0008	1.07	106	0.0002	0.0009	1.05	105	0.0002
Hg		202	He	<0.0004	0.098	98	<0.0001	<0.0004	0.098	98	<0.0001	<0.0004	0.098	98	<0.0001
Pb		208	He	0.029	1.07	104	0.0069	0.011	1.04	103	0.0026	0.007	1.03	102	0.0018

**Table 8.** Quantitative results for multiminerals supplements.

				Sample 4				Sample 5			
	Q1	Q2	Cell Mode	Unspiked (µg/L)	Spiked (µg/L)	Spike Recovery (%)	Calculated Sample Concentration (µg/g)	Unspiked (µg/L)	Spiked (µg/L)	Spike Recovery (%)	Calculated Sample Concentration (µg/g)
As		75	He	0.38	1.37	100	0.18	0.47	1.46	99	0.23
As	75	91	O <sub>2</sub>	0.33	1.35	102	0.16	0.45	1.38	92	0.23
Cd		111	He	0.21	1.17	97	0.10	0.29	1.21	92	0.14
Cd	111	111	O <sub>2</sub>	0.21	1.21	101	0.10	0.29	1.26	97	0.14
Hg		202	He	0.0019	0.098	97	0.0009	0.0015	0.094	92	0.0007
Pb		208	He	0.29	1.29	100	0.14	0.12	1.06	94	0.060

### Correction techniques using single quadrupole ICP-MS

All five samples could be measured in He mode using a single quadrupole ICP-QMS. However, if the ratio of Co/As and/or Mo/Cd is high, there would be interference from <sup>59</sup>Co<sup>16</sup>O<sup>+</sup> on <sup>75</sup>As<sup>+</sup> and <sup>95</sup>Mo<sup>16</sup>O<sup>+</sup> on <sup>111</sup>Cd<sup>+</sup>. Because it is difficult for the analyst to be aware of oxide interferences, the Quick Scan function can be used to identify all elements present in the sample. As shown in Figure 3, by checking the Quick Scan data, potential interferences can be identified, such as CoO<sup>+</sup> based on the high concentration of Co in one of the samples.

Once any potential interferences have been identified using Quick Scan, interference correction equations can be applied to compensate for doubly charged and oxide interferences.

Alternatively, it is possible to perform routine analysis without prior knowledge of potential interferences using an 8900 ICP-QQQ operating in MS/MS mode.

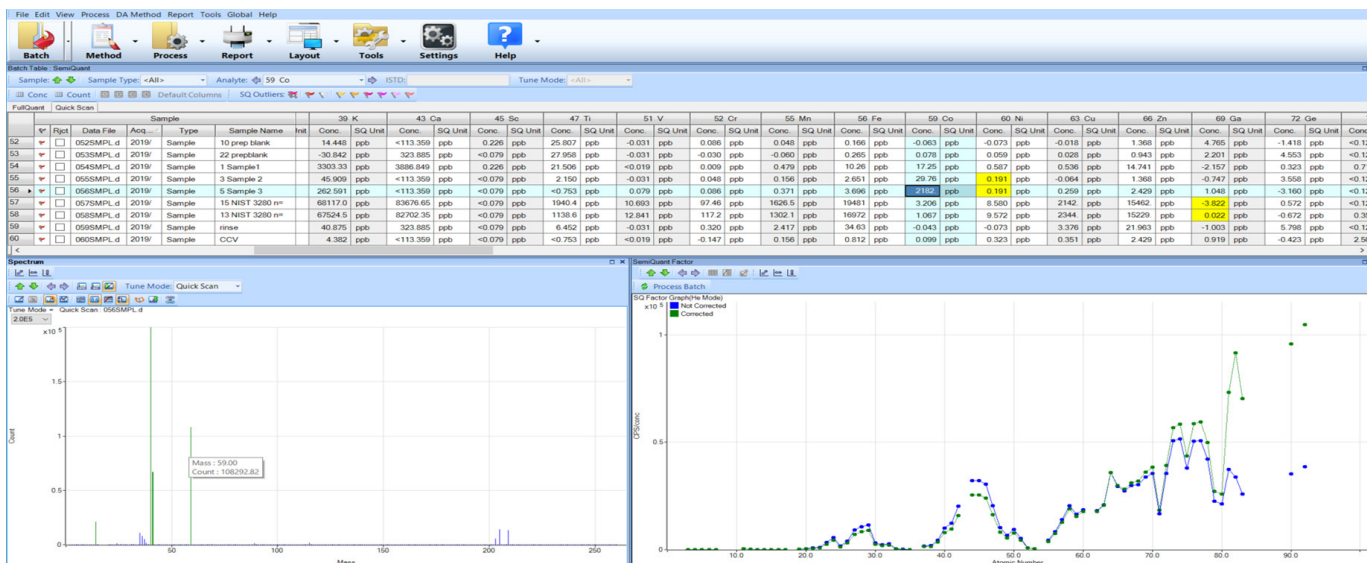


Figure 3. ICP-MS MassHunter Quick Scan qualitative results showing a high concentration of Co in one of the samples.

### Conclusion

The Agilent 8900 ICP-QQQ with UHMI effectively removes challenging spectral interferences making it suitable for the routine analysis of the trace elements in high matrix samples such as multiminerals supplements.

Doubly charged REE interferences that can affect As measurement at trace levels were avoided using O<sub>2</sub> cell gas and MS/MS mass-shift mode, as shown by the recoveries for the Apple Leaves SRM. Also, oxide interferences that can affect As and Cd measurement at trace levels were avoided using the same MS/MS method. Excellent recoveries were achieved for Hg and Pb using He mode – a proven technique for the removal of common matrix-based polyatomic interferences in complex and variable matrices. Therefore, it is possible to perform routine analysis of all elements without prior knowledge of potential interferences using an 8900 ICP-QQQ operating in He mode and MS/MS mode.

For laboratories without access to ICP-QQQ, only ICP-QMS, the Quick Scan function of ICP-MS MassHunter can be used to identify potential interferences from M<sup>++</sup> and oxide ion interferences. These interferences can then be corrected using interference correction equations.



## References

1. GVR, Dietary Supplements Market Worth \$194.63 Billion By 2025, May 2019, accessed July 2019, <https://www.grandviewresearch.com/press-release/global-dietary-supplements-market>
2. US FDA, What You Need to Know about Dietary Supplements, accessed July 2019, <https://www.fda.gov/food/buy-store-serve-safe-food/what-you-need-know-about-dietary-supplements>
3. European Food Safety Authority (EFSA), Food Supplements, accessed July 2019, <http://www.efsa.europa.eu/en/topics/topic/food-supplements>
4. USP Elemental Impurities—Dietary Supplements, (Pharm. Forum, 2010) 36(1), Chapter <2232>, accessed July 2019, <https://www.uspnf.com/notices/general-chapter-elemental-contaminants-dietary-supplements>
5. Handbook of ICP-QQQ Applications, Agilent publication, [5991-2802EN](#)
6. M. A. Amr, N. D. A. Dawood, A. I. Helal and B. Russell, Rare earth elements and  $^{143}\text{Nd}/^{144}\text{Nd}$  isotope ratio measurements using tandem ICP-CRC-MS/MS: characterization of date palm (*Phoenix dactylifera* L.), *J. Anal. At. Spectrom.*, **2017**, 32, 1554–1565
7. Silvia Diez Fernández, Jorge Ruiz Encinar, Alfredo Sanz-Medel, Kirsten Isensee, Heather M. Stoll, Determination of low B/Ca ratios in carbonates using ICP-QQQ, *Geochem Geophys Geosy*, **2015**, 16, 2005–2014
8. Takeshi Ohno and Yasuyuki Muramatsu, Determination of radioactive cesium isotope ratios by triple quadrupole ICP-MS and its application to rainwater following the Fukushima Daiichi Nuclear Power Plant accident, *J. Anal. At. Spectrom.*, **2014**, 29, 347–351
9. Clarice D. B. Amaral et al. A novel strategy to determine As, Cr, Hg and V in drinking water by ICP-MS/MS, *Anal. Methods*, **2015**, 7, 1215–1220
10. Kazuhiro Sakai, Routine soil analysis using an Agilent 8800 ICP-QQQ, Agilent publication, [5991-6409EN](#)
11. Naoki Sugiyama, Solving Doubly Charged Ion Interferences using an Agilent 8900 ICP-QQQ, Agilent publication, [5994-1155EN](#)
12. Alexandra Rowles, Why Molybdenum Is an Essential Nutrient, Healthline, 2017, accessed July 2019, <https://www.healthline.com/nutrition/molybdenum>
13. Erik H. Larsen, Stefan Sturup, Carbon-enhanced inductively coupled plasma mass spectrometric detection of arsenic and selenium and its application to arsenic speciation, *J. Anal. At. Spectrom.*, **1994**, 9, 1099–1105
14. Maurizio Pettine, Barbara Casentini, Domenico Mastroianni, Silvio Capri, Dissolved inorganic carbon effect in the determination of arsenic and chromium in mineral waters by ICP-MS, *Anal. Chim. Acta*, **2007**, 599, 2, 191–198
15. Wim Proper, Ed McCurdy, Junichi Takahashi, Performance of the Agilent 7900 ICP-MS with UHMI for high salt matrix analysis, Agilent publication, [5991-4257EN](#)

# Accurate and Sensitive Analysis of Arsenic and Selenium in Foods using ICP-QQQ to Remove Doubly-Charged REE Interferences

## Authors

Brian Jackson, Dartmouth College,  
Hanover, New Hampshire, USA

Amir Liba, Jenny Nelson,  
Agilent Technologies, USA

## Keywords

arsenic, selenium, rare earth elements, environmental, agricultural, human health, NIST 1547 Peach Leaves, NIST 1515 Apple Leaves, oxygen mass-shift

## Introduction

Concern about the impact on public health from potentially toxic elements and compounds present in everyday foodstuffs has led to new legislative guidance [1, 2]. The inorganic forms of arsenic (As) are known to be toxic and carcinogenic to humans, and food and drinks are a potential source of exposure [3]. Selenium (Se) is an essential micro-nutrient that can be deficient in the diet as Se-poor soils yield Se-poor food crops. Accurate quantification of Se in food is necessary to assess nutrient status.

As and Se can be difficult to quantify accurately at trace levels by conventional quadrupole ICP-MS (ICP-QMS), as all the analytically useful isotopes can suffer from multiple spectral interferences, as shown in Table 1. Potential interferences on As and Se include the doubly-charged ions of the Rare Earth Elements (REE<sup>++</sup>) and matrix and plasma-born polyatomic ions. The quadrupole mass spectrometer separates ions based on mass to charge ratio ( $m/z$ ), so the REE<sup>++</sup> ions appear at half their true mass, overlapping the singly-charged analyte ions of As and Se. Typically the REE content in food samples is low, but crops grown in REE-enriched soils may take up higher concentrations of these elements [4, 5] leading to false positive results for As and Se. In this study, we evaluated the capability of the Agilent 8800 ICP-QQQ in MS/MS reaction mode to remove interferences, including REE<sup>++</sup>, on As and Se.

**Table 1.** Spectroscopic interferences on As and Se isotopes.

As and Se isotope			Interference		
Element	Mass	Abundance %	Doubly charged	Matrix	Dimer
As	75	100	<sup>150</sup> Sm <sup>++</sup> , <sup>150</sup> Nd <sup>++</sup>	<sup>40</sup> Ar <sup>35</sup> Cl <sup>+</sup> , <sup>40</sup> Ca <sup>35</sup> Cl <sup>+</sup>	
Se	77	7.63	<sup>154</sup> Sm <sup>++</sup> , <sup>154</sup> Gd <sup>++</sup>	<sup>40</sup> Ar <sup>35</sup> Cl <sup>+</sup> , <sup>40</sup> Ca <sup>35</sup> Cl <sup>+</sup>	
	78	23.77	<sup>156</sup> Gd <sup>++</sup> , <sup>156</sup> Dy <sup>++</sup>	<sup>41</sup> K <sup>37</sup> C <sup>+</sup>	<sup>38</sup> Ar <sup>40</sup> Ar <sup>+</sup> , <sup>39</sup> K <sup>39</sup> K <sup>+</sup>
	80	49.61	<sup>160</sup> Gd <sup>++</sup> , <sup>160</sup> Dy <sup>++</sup>	<sup>32</sup> S <sub>2</sub> <sup>16</sup> O <sup>+</sup> , <sup>32</sup> S <sup>16</sup> O <sub>3</sub> <sup>+</sup> , <sup>40</sup> Ca <sup>40</sup> Ar <sup>+</sup> , <sup>45</sup> Sc <sup>35</sup> Cl <sup>+</sup>	<sup>40</sup> Ar <sup>40</sup> Ar <sup>+</sup> , <sup>40</sup> Ca <sup>40</sup> Ca <sup>+</sup>
	82	8.73	<sup>164</sup> Dy <sup>++</sup> , <sup>164</sup> Er <sup>++</sup>	<sup>45</sup> Sc <sup>37</sup> Cl <sup>+</sup>	

## Experimental

**Instrumentation:** Agilent 8800 #100.

**Plasma conditions:** Preset plasma/General purpose.

**Acquisition parameters:** MS/MS mass-shift mode using O<sub>2</sub>/H<sub>2</sub> at a gas flow of 0.6 mL/min and 1.0 mL/min respectively. As was measured as the reaction product ion AsO<sup>+</sup> at *m/z* 91, and Se was measured as SeO<sup>+</sup> at *m/z* 96.

**Reagents:** Two National Institute of Standards and Technology (NIST) standard reference materials (SRMs), NIST 1547 Peach Leaves and NIST 1515 Apple Leaves, were studied. These SRMs contain low µg/kg levels of As and Se in the presence of mg/kg levels of REEs.

**Sample prep:** All samples were acid digested using a closed vessel microwave digestion system. The SRMs were prepared in triplicate. First, 0.25 g sample was digested in 2.5 mL of 9:1 HNO<sub>3</sub>:HCl acid mix, and the digest was then diluted to a final weight of 25 g with ultra-pure water. 5% butanol was added to the internal standard mixture to equalize the organic plasma load between samples and standards. NIST 1547 and 1515 contain low µg/kg concentrations of As and Se (Table 2) and high concentrations of REEs. Reference (non-certified) values for Nd, Sm and Gd are 7, 1, and 1 mg/kg in NIST 1547, and 17, 3, and 3 mg/kg in NIST 1515, respectively.

## Results and discussion

Both SRM digests were analyzed using the 8800 ICP-QQQ with O<sub>2</sub>/H<sub>2</sub> as the reaction gas (Table 2). A previous study showed that the presence of H<sub>2</sub> in the cell further improved Se detection capability [6]. The measured values for As and Se in NIST 1547 and 1515 were well within the certified range for both SRMs, demonstrating the successful elimination of the REE<sup>++</sup> interferences in O<sub>2</sub>/H<sub>2</sub> MS/MS mode on the 8800. These results were obtained without the need for correction equations (i.e. uncorrected).

**Table 2.** Analysis of As and Se in NIST 1547 and 1515 in He mode and H<sub>2</sub> mode using ICP-QMS (both uncorrected and corrected data is given) and by ICP-QQQ in MS/MS mode. All concentrations are in mg/kg, and are averages of 3 replicate sample digests expressed as mean ± standard deviation.

SRM	ICP-QMS He mode			ICP-QMS H <sub>2</sub> mode		ICP-QQQ O <sub>2</sub> /H <sub>2</sub> mass-shift
	Certified	Uncorrected	Corrected	Uncorrected	Corrected	Uncorrected
<b>As (mg/kg)</b>						
NIST 1547	0.060±0.018	0.170±0.016	0.068±0.003*	0.113±0.004	0.079±0.004*	0.065±0.002*
NIST 1515	0.038±0.007	0.250±0.016	0.026±0.021*	0.126±0.005	0.047±0.004*	0.032±0.002*
<b>Se (mg/kg)</b>						
NIST 1547	0.120±0.009	0.394±0.04	0.113±0.02*	0.119±0.009*	0.119±0.009*	0.127±0.006*
NIST 1515	0.050±0.009	0.808±0.04	0.013±0.04*	0.050±0.003*	0.050±0.003*	0.047±0.006*

\*95% confidence interval overlaps with the certified range

Results obtained using ICP-QMS are included for comparison purposes. "Corrected" refers to the use of correction equations. ICP-QMS operating in helium mode is suitable for the analysis of As and Se in general routine sample types that might contain a small amount of REEs, and H<sub>2</sub> mode has been shown to be effective at reducing doubly charged species. Compared to these conventional methods, ICP-QQQ had 10-fold lower detection limits, which makes it particularly suited to low level determination of As and Se in complex sample matrices.

ICP-QMS can also use O<sub>2</sub> mass-shift mode but, with ICP-QMS, all matrix and analyte ions enter the cell, so the analyte reaction product ions measured (<sup>75</sup>As<sup>16</sup>O<sup>+</sup> at *m/z* 91, and <sup>78</sup>Se<sup>16</sup>O<sup>+</sup> at *m/z* 94), could suffer overlap from existing analyte or matrix ions at the product ion mass (e.g. <sup>91/94</sup>Zr<sup>+</sup> and <sup>94</sup>Mo<sup>+</sup>). To confirm that the ICP-QQQ MS/MS method can be applied to samples that contain high concentrations of Zr and Mo, an aliquot of NIST 1547 was spiked with 1 mg/L (1000 ppm) Zr and Mo, and the results are shown in Table 3. The measured values for As (as AsO<sup>+</sup>) and Se (as SeO<sup>+</sup>) in the spiked sample are the same as for the unspiked samples, demonstrating that MS/MS mode is effective at rejecting existing overlapping ions present at the mass of the cell-formed analyte product ions. This capability is unique to the tandem mass spectrometer configuration of the 8800 ICP-QQQ, where the ions that enter the cell are controlled by an additional mass filter, Q1, positioned in front of the collision/reaction cell.

**Table 3.** ICP-QQQ measured results for As and Se in NIST 1547 unspiked and spiked with 1 mg/L Zr and Mo. No correction equations were applied.

SRM NIST 1547	Certified	ICP-QQQ O <sub>2</sub> /H <sub>2</sub> mass-shift	
		Unspiked (n=3)	Spiked with 1 mg/L Zr & Mo (n=1)
As (mg/kg)	0.060±0.018	0.065±0.002	0.063
Se (mg/kg)	0.120±0.009	0.127±0.006	0.13

## Conclusion

The Agilent 8800 ICP-QQQ with MS/MS capability has been shown to be the optimum method to successfully measure trace levels of As and Se in the presence of high concentration of REEs in NIST 1547 Peach Leaves and NIST 1515 Apple Leaves. All REE doubly-charged and matrix-based polyatomic interferences that affect As and Se measurement at *m/z* 75 and *m/z* 78 are avoided using O<sub>2</sub>/H<sub>2</sub> cell gas and MS/MS mass-shift mode. Arsenic is shifted to its product ion AsO<sup>+</sup> which is measured at *m/z* 91, and Se is shifted to SeO<sup>+</sup>, measured at *m/z* 94. Importantly, MS/MS mode also eliminates potential ion overlaps at *m/z* 91 and *m/z* 94 from <sup>91/94</sup>Zr<sup>+</sup> and <sup>94</sup>Mo<sup>+</sup>, as these ions are rejected by Q1. The extent and concentration of REEs in food products is not well studied. However, monitoring for the presence of Nd<sup>++</sup>, Sm<sup>++</sup>, and Gd<sup>++</sup> at *m/z* 150 and 156 during an analysis would identify samples where doubly charged REE formation might be problematic.

## More information

For a full account of this application see publication: Advantages of reaction cell ICP-MS on doubly charged interferences for arsenic and selenium analysis in foods, Brian P. Jackson, Amir Liba and Jenny Nelson, *J. Anal. At. Spectrom.*, **2015**, Advance Article. DOI: 10.1039/C4JA00310A.

## Acknowledgements

Brian Jackson acknowledges the support of NIEHS P42 ES007373, NIEHS P01 ES022832, EPA RD83544201 for the work presented herein.

## References

1. U.S.FDA. 2013. Guidance for Industry. Arsenic in apple juice: Action level.
2. COMMISSION CA. 2014. Report of the eighth session of the codex committee on contaminants in foods. CL2014/11-CF. Geneva, Switzerland.
3. Agency for Toxic Substances and Disease Registry (ATSDR), 2007, Toxicological Profile for Arsenic, U.S. Department of Health and Human Services, Public Health Service
4. Sucharova J. 2011. Optimisation of drc icp-ms for determining selenium in plants. *J. Anal. At. Spectrom.*, **2011**,26, 1756-1762
5. Wang R-Y, Hsu Y-L, Chang L-F, Jiang S-J. 2007. Speciation analysis of arsenic and selenium compounds in environmental and biological samples by ion chromatography-inductively coupled plasma dynamic reaction cell mass spectrometer. *Anal Chim Acta* **2007**; 590: 23
6. Sugiyama N. The accurate measurement of selenium in twelve diverse reference materials using on-line isotope dilution with the 8800 Triple Quadrupole ICP-MS in MS/MS mode, Agilent publication 2012, [5991-0259EN](#)

# Analysis of TiO<sub>2</sub> Nanoparticles in Foods and Personal Care Products by Single Particle ICP-QQQ

## Authors

Janja Vidmar<sup>1</sup>

Katrin Loeschner<sup>1</sup>

Raquel Larios<sup>2</sup>

<sup>1</sup>National Food Institute, Technical University of Denmark (DTU Food), Denmark

<sup>2</sup>Agilent Technologies, Spain

Using the 8900 ICP-QQQ in MS/MS mass-shift mode to resolve <sup>48</sup>Ca<sup>+</sup> isobaric interference on <sup>48</sup>Ti<sup>+</sup>

## Introduction

Titanium dioxide (TiO<sub>2</sub>) is classified as a food additive within the European Union (E171) and in the USA (INS171), where it is widely used as whitening and brightening agent. In the EU, E171 can be used in several food categories with no maximum upper limit (*quantum satis*) (1). E171 mainly consists of larger TiO<sub>2</sub> particles, but it also contains a fraction of nanoparticles (NPs), which are defined as particles with one or more dimensions less than 100 nm (2). TiO<sub>2</sub> is also used in food contact materials, cosmetics, and personal care products, such as toothpaste.

With increasing production and use of TiO<sub>2</sub> based additives, there is concern among regulatory authorities and consumers about the potential impact of human exposure to TiO<sub>2</sub> NPs. Several toxicological studies on TiO<sub>2</sub> NPs have been carried out (3–5), but no general agreement on the effects of TiO<sub>2</sub> NPs on biological systems has been reached. The European Food Safety Authority (EFSA) has released several scientific opinions (6, 7). EFSA concluded that the use of TiO<sub>2</sub> as a food additive does not raise a genotoxic concern and established a No Observed Adverse Effect Levels (NOAEL) of 2.250 mg/TiO<sub>2</sub> kg/bw per day. However, when the French food safety agency, ANSES, reviewed recent studies on TiO<sub>2</sub>, they found a lack of conclusive results on the safety of the E171 additive. Following the appraisal, the French government announced that the sale of food products containing TiO<sub>2</sub> (E171) will be banned from January 1, 2020 (8). EFSA recently released a scientific opinion stating the need for further research on the particle size distribution of E171 in food (9).

European regulations state that all ingredients present in the form of engineered nanomaterials shall be clearly indicated in the list of ingredients. The names of such ingredients shall be followed by the word 'nano' in brackets (10). In 2011, the European Commission published a recommendation for the definition of a nanomaterial suggesting that for regulatory purposes, the size distribution and number concentration of nanomaterials should be known (11). To keep pace with evolving regulations, effective analytical methods are needed for the characterization of TiO<sub>2</sub> NPs in a range of sample types.

ICP-MS is a powerful tool for the characterization of NPs, providing composition information that complements established techniques such as transmission and scanning electron microscopy (TEM/SEM), and dynamic light scattering (DLS). When used in single particle (sp) mode, spICP-MS provides simultaneous determination of the particle number and size distribution (assuming spherical particles). In addition, spICP-MS provides the concentrations of both the particles and the dissolved content of the element or elements of interest. The ease-of-use of modern ICP-MS instruments makes it the technique of choice for regulatory purposes, while its flexibility ensures that the same instrument can be used for multi-element analysis and speciation studies.

Titanium is a challenging element to measure by conventional single quadrupole ICP-QMS. The isobaric interference on the most abundant isotope,  $^{48}\text{Ti}$ , by  $^{48}\text{Ca}$  cannot be mass resolved by ICP-QMS. At its highest resolution setting, High Resolution (HR) ICP-MS can theoretically resolve  $^{48}\text{Ca}$  from  $^{48}\text{Ti}$ , as the required resolution ( $M/\Delta M$ ) is 10,458. However,  $^{48}\text{Ca}$  is present at high concentrations in many food samples, such as milk, making separation of the adjacent peaks more difficult. Also, the combination of low sensitivity at high resolution, and peak tailing due to the poor abundance sensitivity of HR-ICP-MS means that this measurement is often not practical. Other elements such as sulfur, phosphorus, silicon, and carbon, which are also present in many foods at significant concentrations, form polyatomic interferences that hinder the accurate measurement of  $^{48}\text{Ti}$ . Typically, the less interfered isotopes  $^{47}\text{Ti}$  or  $^{49}\text{Ti}$  are measured by ICP-QMS. However, these less abundant isotopes provide lower sensitivity, which limits the detection of smaller-sized  $\text{TiO}_2$  NPs by ICP-QMS, leading to biased size distribution results.

The Agilent 8900 Triple Quadrupole ICP-MS (ICP-QQQ) can operate in MS/MS mode with reactive cell gases to resolve the spectral interferences on  $^{48}\text{Ti}$ , including the isobaric interference from  $^{48}\text{Ca}$ . The first quadrupole, Q1, positioned before the collision/reaction cell (CRC), operates as a unit mass filter, allowing only the ions with target  $m/z$  to enter the cell and rejecting all ions of different masses. Analyte-ion selection by Q1 enables excellent control of the reaction chemistry in the cell. Also, the low background, high sensitivity, and very short dwell times (100  $\mu\text{s}$ ) of the 8900 enable the ICP-QQQ to detect small-sized particles.

In this study,  $\text{TiO}_2$  NPs present in different food samples and toothpaste were characterized by sICP-MS using an Agilent 8900 ICP-QQQ. The results show the benefits of triple quadrupole (MS/MS mode) technology with  $\text{O}_2/\text{H}_2$  cell gases to resolve polyatomic and isobaric interferences on  $^{48}\text{Ti}$ .

## Experimental

### Standards and reference materials (RM)

NIST 8012 gold NPs RM (Gaithersburg, MD, USA) and ionic gold standards (PlasmaCAL standard, SCP Science, Baie D'Urfé, QC, Canada) were used. The gold NP RM, with a known average particle diameter of 27.6 nm as determined by TEM, and the ionic gold standard were analyzed to calculate the nebulization efficiency.

To determine the response factor for titanium, ionic titanium standard (PlasmaCAL standard, SCP Science) was used. Solutions of 5 to 200 ng Ti/mL in 100 times diluted milk (for milk samples) or 0.1% nitric acid (for  $\text{TiO}_2$  NPs in water and food samples) were analyzed.

Anatase and rutile are two naturally occurring mineral forms of  $\text{TiO}_2$ . Two  $\text{TiO}_2$  nanomaterials with different size distributions were used to spike milk samples and check the performance of the method. The nanomaterials included a  $\text{TiO}_2$  representative test material, JRCNM 10200a (referred to as JRC NPs), from the Joint Research Centre's Nanomaterial Repository. The JRC NPs material contains primary particles of 115 nm and consists of anatase. NIST 1898  $\text{TiO}_2$  NPs SRM (referred to as NIST NPs) was also used. The NIST NPs SRM has a primary size < 50 nm and consists of 76% anatase and 24% rutile.

### **Samples and sample preparation**

The concentrations of Ca, S, and P in cow's milk are in the range of 1070–1330  $\mu\text{g/mL}$ , 320  $\mu\text{g/mL}$ , and 630–1020  $\mu\text{g/mL}$ , respectively (12). A matrix mimicking a diluted (100 times) milk matrix was prepared by diluting ionic Ca, S, and P standards (PlasmaCAL standards, SCP Science) in water. The final concentrations were 10  $\mu\text{g/mL}$  for Ca, 3  $\mu\text{g/mL}$  for S, and 10  $\mu\text{g/mL}$  for P (individually and as a mix). In addition, 10 ng/mL of ionic Ti was spiked into the 100-fold diluted simulated milk matrix, and in 0.1% nitric acid ( $\text{HNO}_3$ ).

Different food samples were bought from local stores in Denmark. The foods included skimmed milk with 0.1% fat content, salad dressing, and cake decorations (edible gold stars). A commercial toothpaste from a Dutch supermarket, which was extensively studied in the EU FP7 Project "NanoDefine" (13), was also analyzed. Details of the sample preparation for each sample type were as follows:

- Milk spiked with  $\text{TiO}_2$  NPs: Stock suspensions of 1 mg  $\text{TiO}_2/\text{mL}$  were prepared. After appropriate dilution,  $\text{TiO}_2$  was spiked into undiluted skimmed milk at 200 and 400 ng  $\text{TiO}_2/\text{mL}$  for JRC NPs, and 15 and 30 ng  $\text{TiO}_2/\text{mL}$  for NIST NPs.
- Toothpaste: The sample preparation protocol was adopted from Correia et al. (14). 100 mg of toothpaste was dispersed in 10 mL of ultrapure water (UPW) by vortexing. The solution was further diluted 10 times in 0.1% sodium dodecyl sulfate (SDS, Sigma-Aldrich, St. Louis, MO, USA), followed by vortexing.
- Salad dressing: 100 mg of salad dressing was dispersed in 5 mL of 0.1% SDS placed in a high intensity cup horn (Branson Digital Sonifier SFX 550). The solution was further diluted 10 times in 0.1% SDS, followed by vortexing.
- Cake decorations: One golden star was added to 5 mL of UPW and dissolved, with assistance from a high intensity cup horn. The solution was further diluted 10 times in UPW, followed by vortexing.
- Before analysis, all samples were diluted with UPW (milk 100x, toothpaste 2500x, salad dressing 500x, and cake decoration 250x).



## Instrumentation

An Agilent 8900 ICP-QQQ (#100, Advanced Applications configuration) was used with an SPS 4 autosampler. The instrument was equipped with a MicroMist concentric nebulizer, Scott type double-pass quartz spray chamber, a quartz torch with a small internal diameter (1.0 mm) injector, and standard nickel cones. Samples were introduced directly into the ICP-QQQ via the standard peristaltic pump and tubing. The operating conditions of the Agilent 8900 ICP-QQQ are detailed in Table 1.

**Table 1.** ICP-MS operating conditions.

Parameter	Value
RF Power (W)	1550
Sampling Depth (mm)	8
Nebulizer Gas (L/min)	0.70
Sample Inlet Flow (mL/min)	~ 0.35
Spray Chamber Temperature (°C)	2
Dwell Time (ms)	0.1
Settling Time (ms)	0
Acquisition Mode	MS/MS (Q1: $m/z$ 48, Q2: $m/z$ 64)
Gas Flow Rates (mL/min)	O <sub>2</sub> : 0.15 (10% of full scale) H <sub>2</sub> : 7.0
Axial Acceleration (V)	1.0
Octopole Bias Voltage (V)	-6.0
Energy Discrimination (V)	-15.0
Acquisition Time (s)	60

Data was acquired for 60 s with a dwell time of 0.1 ms for each sample. The major titanium isotope, <sup>48</sup>Ti, was measured in MS/MS mass-shift mode, using a mixed cell gas containing oxygen and hydrogen. The method was used to resolve all the isobaric interferences—mainly arising from <sup>48</sup>Ca—and the matrix-based polyatomic interferences, such as those derived from C, S, and P. Q1 was set to  $m/z$  48 (the mass of the precursor <sup>48</sup>Ti ion) and Q2 was set to  $m/z$  64 (the mass of the target product ion <sup>48</sup>Ti<sup>16</sup>O<sup>+</sup>). O<sub>2</sub> promoted the formation of the <sup>48</sup>Ti<sup>16</sup>O<sup>+</sup> product ion, and H<sub>2</sub> helped with the formation of <sup>48</sup>Ca<sup>16</sup>O<sup>1</sup>H<sup>+</sup>, avoiding interference on <sup>48</sup>Ti<sup>16</sup>O<sup>+</sup> by <sup>48</sup>Ca<sup>16</sup>O<sup>+</sup> (Figure 1). The instrument operating parameters were also used in a previous study (15). After each run, the sample introduction system was rinsed using UPW, diluted acids, and Triton X-100.

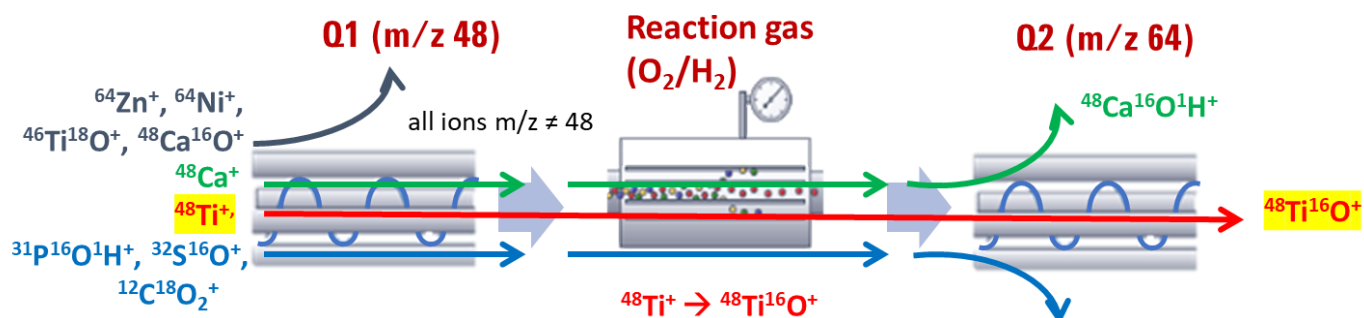


**Figure 1.** Determination of <sup>48</sup>Ti<sup>+</sup> as <sup>48</sup>Ti<sup>16</sup>O<sup>+</sup> product ion using the 8900 ICP-QQQ operating in MS/MS mass-shift mode with O<sub>2</sub>/H<sub>2</sub> as the reaction cell gases.

The Single Nanoparticle Application Module of the Agilent ICP-MS MassHunter software was used for method setup and data analysis. Analysis was performed in peak integration mode. The particle baseline was determined automatically by the software. The particle detection threshold was adjusted manually, and the same value was used for samples of the same type. The application of the same threshold ensured that a direct comparison of particle mass concentrations and median particle diameters between samples was possible. A particle density of 3.9 g/cm<sup>3</sup> and an analyte mass fraction (the value of molecular mass divided by analyte mass) of 1.67 was used for the calculations. The sample inlet flow was determined gravimetrically.

## Results and discussion

### Interference check in relevant matrices containing ionic Ti

To check the effectiveness of the MS/MS mass-shift mode to remove potential interferences on Ti, solutions containing single interfering elements and a mixture simulating 100 times diluted milk were analyzed (Table 2). The apparent Ti concentration was measured in all the solutions, as <sup>48</sup>TiO<sup>+</sup> in MS/MS mode with O<sub>2</sub>/H<sub>2</sub>, and as <sup>48</sup>Ti<sup>+</sup> without any reaction gas (in Single Quad and MS/MS modes).

The results in no gas mode (SQ and MS/MS) show a large positive error in all matrices containing interfering elements, with the most pronounced errors in the presence of Ca. In contrast, O<sub>2</sub>/H<sub>2</sub> in MS/MS mode effectively reduced all interferences, allowing the accurate measurement of Ti, even in the presence of Ca and in the simulated milk matrix. The highest Ti sensitivity and the lowest detection limit (DL) were also achieved in O<sub>2</sub>/H<sub>2</sub> MS/MS mode. The results suggest that the 8900 ICP-QQQ operating in MS/MS mass-shift mode with O<sub>2</sub>/H<sub>2</sub> would detect smaller sized particles compared to the two no gas modes.

### Analysis of TiO<sub>2</sub> NPs spiked into milk samples

TiO<sub>2</sub> has been considered as a whitener for low-fat milk (16), although its addition to milk is currently not permitted in Europe. To check the effectiveness of the method to accurately measure TiO<sub>2</sub> NPs of different size distributions and concentrations, two different TiO<sub>2</sub> NPs (JRC and NIST) were spiked into the milk samples. JRC NPs, which contain larger sized particles with a broader size distribution than NIST NPs, resemble E171, which consists primarily of anatase. The fraction of NPs in E171 ranges between 17 and 36% and the mean diameters of the primary particles range between 115 to 145 nm (17).

**Table 2.** Interference check results for <sup>48</sup>Ti in various matrices, with and without cell gas.

Matrix	Ca 10 µg/mL	S 3 µg/mL	P 10 µg/mL	Mix Ca+S+P	10 ng/mL Ti in Mix Ca+S+P	10 ng/mL Ti in 0.1% HNO <sub>3</sub>		
Cell Mode	Apparent Ti Measured Concentration, ng/mL						Sensitivity <sup>1</sup> (cps/ ng/mL)	DL <sup>2</sup> (ng/mL)
No gas MS/MS	35.6	0.395	0.264	36.3	41.7	9.58	207,044	4.1
No gas SQ	35.0	0.341	0.224	34.2	45.8	11.1	294,872	8.2
O <sub>2</sub> /H <sub>2</sub> MS/MS	0.017	0.004	0.012	0.031	10.0	10.2	399,949	0.0075

1. Based on calibration curve of six ionic standards from 0.1 to 50 ng/mL ionic Ti in 0.1% HNO<sub>3</sub>

2. DL calculated as three times the standard deviation of four blanks (mix Ca + S + P)

Figure 2 shows the comparison of the measurement of the same TiO<sub>2</sub> NPs spiked at the same concentration into diluted milk or UPW and analyzed in MS/MS mode with O<sub>2</sub>/H<sub>2</sub> reaction gas. The particle size distributions were similar in UPW and in the milk matrix for both particle types. In water and the milk-matrix, the mean particle diameters were 226 ± 7 and 223 ± 2 nm (JRC NPs), and 78 ± 1 and 72 ± 2 nm (NIST NPs), respectively. The similarity of the results shows that interferences from Ca, S, or P in the milk matrix were resolved.

The particle size data agreed with existing data for the two particle types. According to the certificate of analysis for the NIST NPs, the stable nanoscale species is a monomodal aggregate of fused crystallites with a modal size of 70 nm. The JRC NPs are similar to NM-100 (18), which contain primary particles ranging from 20 up to 300 nm and aggregates ranging from 30 up to 700 nm. The mean diameter obtained by TEM was 190 nm (18).

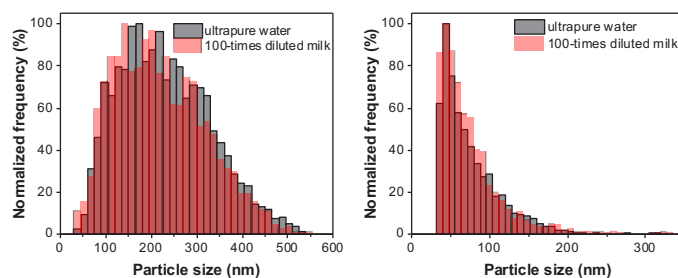


**Figure 2.** Particle size distributions for 4 ng/mL JRC NPs (left) and 0.15 ng/mL NIST NPs (right) in UPW and 100 times diluted milk measured in MS/MS mass-shift mode.

Similar particle size results were obtained by comparing the two spiked levels for both NP types (Table 3). The average mass recoveries, which were in the range of 71 to 85%, were considered satisfactory.

**Table 3.** spICP-MS results for measuring JRC and NIST NPs in 100 times diluted milk at two different concentration levels (n=3 for each spike level).

	JRC NPs 2 ng/mL	JRC NPs 4 ng/mL	NIST NPs 0.15 ng/mL	NIST NPs 0.30 ng/mL
Number of Detected Particles (particles/min)	917 ± 135	1624 ± 113	1648 ± 199	2988 ± 90
Particle Number Conc (E+07 particles/L)	4.40 ± 0.55	7.80 ± 0.54	7.60 ± 0.92	13.80 ± 0.42
Particle Mass Conc (ng/mL)	1.55 ± 0.26	2.91 ± 0.11	0.13 ± 0.01	0.25 ± 0.02
Mass Recovery (%)	76 ± 13	71 ± 6	85 ± 7	81 ± 4
Median Particle Size (nm)	204 ± 3	210 ± 2	60 ± 2	62 ± 1
Mean Particle Size (nm)	216 ± 0	223 ± 2	72 ± 2	74 ± 0

### Effects of interferences on measurement of <sup>47</sup>Ti and <sup>48</sup>Ti in no gas mode

To show the interference removal benefits of MS/MS mass-shift mode compared to SQ or MS/MS in no gas mode, <sup>47</sup>Ti and <sup>48</sup>Ti were measured without cell gas in the same spiked diluted milk samples. NIST NPs were not detectable due to the high background on <sup>47</sup>Ti and <sup>48</sup>Ti. The larger JRC NPs were detectable (Figure 3), but the minimum detectable size increased from 40 nm (MS/MS mass-shift mode) to 213 nm (<sup>47</sup>Ti) and 160 nm (<sup>48</sup>Ti) in no gas mode. There was also an increase in the median diameters from 210 nm (MS/MS mass-shift mode) to 292 nm, and 210 nm (MS/MS mass-shift mode) to 260 nm, respectively.

The high (ionic) background on  $^{48}\text{Ti}$  could be attributed to the isobaric interference of  $^{48}\text{Ca}$ , as shown in Table 2. For  $^{47}\text{Ti}$ , a high particle background was observed in both the spiked and non-spiked milk matrix. As no particles were detected in the non-spiked milk sample in MS/MS mass-shift mode, it could be concluded that these were not Ti-containing particles, but likely caused by polyatomic interferences.

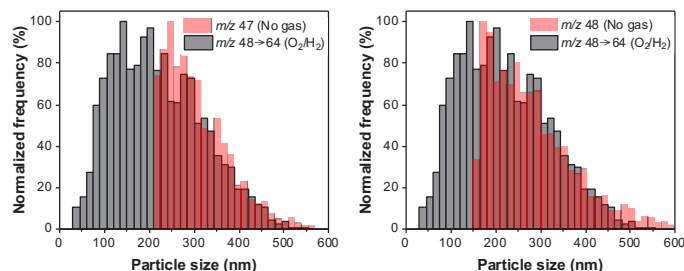


**Figure 3.** Particle size distributions for 4 ng/mL JRC NPs in 100 times diluted milk determined by analyzing  $^{47}\text{Ti}$  in no gas mode (left) and  $^{48}\text{Ti}$  in no gas mode (right). For comparison purposes, the size distribution obtained in MS/MS mode with  $\text{O}_2/\text{H}_2$  gas is shown in grey in both graphs.

### Analysis of $\text{TiO}_2$ NPs in toothpaste, salad dressing, and cake decorations

Other products that include  $\text{TiO}_2$  in the list of ingredients were analyzed. Toothpaste, salad dressing, and a cake decoration (edible golden star) were selected as examples. The particle size distribution results, which are presented in Figure 4, show that each of the samples contains  $\text{TiO}_2$  NPs with different size ranges. The cake decoration contained the smallest sized NPs (median size of 54 nm), while the salad dressing contained the largest particles (median size of 334 nm). The particle sizes determined in toothpaste (median size 155 nm) agreed with previously published results (14). The fraction of particles < 100 nm was 22, 3, and 70% for toothpaste, salad dressing, and the cake decoration, respectively. The average  $\text{TiO}_2$  mass concentrations were in the mg/g sample range.

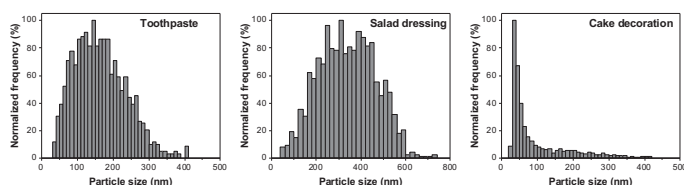


**Figure 4.** Particle size distributions for  $\text{TiO}_2$  NPs in toothpaste (left), salad dressing (middle), and a cake decoration (right).

## Conclusion

A single particle ICP-MS method was developed for the determination and characterization of  $\text{TiO}_2$  NPs in foods and personal care products. An Agilent 8900 ICP-QQQ was used in the study, since its high sensitivity and short dwell times provide fast analysis times and excellent detection limits for the determination of small-sized particles. Also, the advanced interference-removal capabilities of ICP-QQQ using MS/MS allowed the analysis of the most abundant titanium isotope,  $^{48}\text{Ti}$ , enabling the accurate analysis of small-sized  $\text{TiO}_2$  NPs.

Operating the ICP-QQQ in MS/MS mode with  $\text{O}_2/\text{H}_2$  cell gas, isobaric ( $^{48}\text{Ca}$ ) and polyatomic interferences on  $^{48}\text{Ti}$  were successfully resolved in matrices containing high concentrations of P, S, and Ca. By measuring  $^{48}\text{Ti}$  rather than the less abundant Ti isotopes, a particle size detection limit of 30 nm was achieved for  $\text{TiO}_2$  NPs.

The method was used for the characterization of TiO<sub>2</sub> NPs in foods that are known to contain the food additive E171, including toothpaste, salad dressing, and a cake decoration. spICP-MS can be used to indicate the elemental composition and size of particles in a sample, complementing the information on particle size and shape provided by electron microscopy.

Having access to reliable analytical methods for the characterization of NPs is important, as France will ban the sale of food products containing E171 from January 1, 2020. EFSA has also identified the need for further research on the particle size distribution of TiO<sub>2</sub> NPs in food.

### Acknowledgments

We thank Luisa Hässmann for her contribution to the experimental work and Michiko Yamanaka (Agilent) for her technical support.

### References

1. Regulation (EC) No 1333/2008 of the European Parliament and of the Council of 16, December **2008** on food additives, Official Journal of the European Union, 2008, L354, 16–33
2. Y. Yang, K. Doudrick, X. Bi, K. Hristovski, P. Herckes, P. Westerhoff, R. Kaegi, Characterization of food-grade titanium dioxide: the presence of nanosized particles. *Environ. Sci. Technol*, **2014**, 3; 48 (11): 6391-40
3. S. Bettini, E. Boutet-Robinet, C. Cartier, C. Coméra, E. Gaultier, J. Dupuy, N. Naud, S. Taché, P. Grysan, S. Reguer, N. Thieriet, M. Réfrégiers, D. Thiaudière, J. -P. Cravedi, M. Carrière, J. N. Audinot, F. H. Pierre, L. Guzylack-Piriou, E. Houdeau, Food-grade TiO<sub>2</sub> impairs intestinal and systemic immune homeostasis, initiates preneoplastic lesions and promotes aberrant crypt development in the rat colon. *Sci Rep*, **2017**, 7: 40373
4. Z. Chen, Y. Wang, T. Ba, Y. Li, J. Pu, T. Chen, Y. Song, Y. Gu, Q. Qian, J. Yang, G. Jia, Genotoxic evaluation of titanium dioxide nanoparticles in vivo and in vitro. *Toxicol. Letter*, **2014**, 3, 314–319
5. R. Liu, X. Zhang, Y. Pu, L. Yin, Y. Li, Small-sized TiO<sub>2</sub> nanoparticles mediate immune toxicity in rat pulmonary alveolar macrophages in vivo. *J. Nanosci. Nanotechnol*, **2010**, 10, 5161–5169
6. Re-evaluation of titanium dioxide (E 171) as a food additive, *EFSA Journal*, **2016**; 14 (9): 4545
7. Evaluation of four new studies on the potential toxicity of titanium dioxide used as a food additive (E 171), *EFSA Journal*, **2018**; 16 (7): 5366
8. Sybille de La Hamaide, France to ban titanium dioxide whitener in food from 2020, Reuters, April 2017, accessed November 2019, <https://www.reuters.com/article/us-france-food-additive/france-to-ban-titanium-dioxide-whitener-in-food-from-2020-idUSKCN1RT23D>
9. Scientific opinion on the proposed amendment of the EU specifications for titanium dioxide (E 171) with respect to the inclusion of additional parameters related to its particle size distribution, *EFSA Journal*, **2019**; 17 (7): 5760

10. Regulation (EU) No 1169/2011 of the European Parliament and of the Council of 25, October 2011 on the provision of food information to consumers, *Official Journal of the European Union*, **2011**, L304, 16–63
11. Commission Recommendation of 18 October 2011 on the definition of nanomaterial, *Official Journal of the European Union*, **2011**, L275, 38–40
12. Š. Zamberlin, N. Antunac, J. Havranek, D. Samaržija. Mineral elements in milk and dairy products. *Mljekarstvo*, **2012**, 62 (2), 111–125
13. NanoDefine Project Development of Methods and Standards Supporting the Implementation of the Commission Recommendation for a Definition of Nanomaterial (FP7-NMP-2013-LARGE-7, no. 604347). Available online: <http://www.nanodefine.eu> (accessed October 2019)
14. M. Correia, T. Uusimäki, A. Philippe, K. Löschner, Challenges in Determining the Size Distribution of Nanoparticles in Consumer Products by Asymmetric Flow Field-Flow Fractionation Coupled to Inductively Coupled Plasma-Mass Spectrometry: The Example of Al<sub>2</sub>O<sub>3</sub>, TiO<sub>2</sub>, and SiO<sub>2</sub> Nanoparticles in Toothpaste. *Separations*, **2018**, 5 (4), 56
15. M. Yamanaka, S. Wilbur, Accurate determination of TiO<sub>2</sub> nanoparticles in complex matrices using the Agilent 8900 ICP-QQQ, Agilent publication, [5991-8358EN](#)
16. M. B. Frøst, G. Dijksterhuis, M. Martens, Sensory perception of fat in milk. *Food Quality and Preference*, **2001**, 12, 327–336
17. W. Dufou, H. Terrisse, M. Richard-Plouet, E. Gautron, F. Popa, B. Humbert, M.-H. Ropers, Criteria to define a more relevant reference sample of titanium dioxide in the context of food: a multiscale approach. *Food Additives and Contaminants Part A*, **2017**, 34, 653–665
18. K. Rasmussen et al. *Titanium dioxide*, NM-100, NM-101, NM-102, NM-103, NM-104, NM-105 Characterisation and Physico-Chemical properties. *EUR - Scientific and Technical Research Series* (Publications Office of the European Union, 2014)

# Accurate Analysis of Trace Mercury in Cosmetics using the Agilent 8900 ICP-QQQ

## Authors

Xin-mei Wang and Ke Wang<sup>1</sup>.  
Xiang-cheng Zeng, Donna Hsu,  
and Juan-e Song<sup>2</sup>.

1 Shanghai Institute for Food and  
Drug Control, China

2 Agilent Technologies Co. Ltd,  
China

Effective removal of tungsten-based interferences on  
five Hg isotopes using MS/MS

## Introduction

Many mercury (Hg) compounds are toxic, causing symptoms ranging from skin irritation, headaches, and tremors, through to nervous system damage, renal failure, and heart disease (1). Because Hg compounds are easily absorbed through the skin, their use in cosmetics is controlled. For example, the US Food and Drug Administration (FDA) does not allow Hg in cosmetics, except under specific conditions where there are no other safe and effective preservatives available (2). Increasingly, however, Hg has been found in cosmetic products such as skin creams, soap, and lotions sold as “anti-aging” or “skin lightening”.

Mercury is a challenging element to determine at low levels by ICP-MS. It has a high first ionization potential (10.44 eV), so is relatively poorly ionized in the plasma, leading to low sensitivity. Also, Hg has seven naturally occurring isotopes, each with relatively low % abundance, further reducing sensitivity. Many forms of Hg are also volatile, and the element’s chemistry means that it can be difficult to stabilize in solution. To address these issues, analysts must control the acid mix used for sample preservation and rinse solutions, to avoid problems with poor linearity and long washout times. Despite these difficulties, ICP-MS can still be used successfully to perform trace-level analysis of Hg, if appropriate sample stabilization—for example with the addition of HCl—is used.

Trace-level mercury analysis is even more difficult in samples—including some cosmetics—that contain a high concentration of tungsten (W). The W matrix forms polyatomic ions  $WO^+$  and  $WOH^+$  that overlap all the Hg isotopes, making Hg measurement even more challenging. For example, the most abundant Hg isotopes,  $^{200}Hg$  and  $^{202}Hg$ , suffer interferences from  $^{184}W^{16}O^+$  and  $^{186}W^{16}O^+$ , respectively. Collision/reaction cells (CRCs) are used successfully to control many common polyatomic interferences in conventional single quadrupole ICP-MS (ICP-QMS). However, even with CRC operation, ICP-QMS cannot reduce the  $WO^+$  and  $WOH^+$  interferences sufficiently to allow the accurate determination of Hg at trace levels in samples that contain a high level of W.

The superior interference removal capability of triple quadrupole ICP-MS (ICP-QQQ) was investigated for this application. ICP-QQQ has dramatically improved the performance of reaction cell methods by using two mass-selection steps (MS/MS), one before and one after the CRC. In MS/MS, reaction chemistry in the CRC is controlled and consistent because only the target analyte mass enters the CRC. This capability offers a much more predictable and reliable approach to resolving interferences on a wide range of elements, particularly in complex and variable samples (3–5).

In this study, an Agilent 8900 ICP-QQQ was used for the measurement of Hg in a tungsten-rich cosmetic sample.

## Experimental

### Standards and samples

Mercury standards were prepared in 0.5 % high purity hydrochloric acid (TAMA-Pure-AA-100, Kanagawa, Japan).

A tungsten-rich cosmetic toning lotion was bought from a local store in Shanghai. The liquid sample was weighed to the nearest 0.100 g, and then diluted 100-fold with de-ionized water acidified with 0.5 % HCl to ensure Hg stability. The sample was shaken for a couple of minutes to ensure it was fully homogenized.

The concentration of W in the original cosmetic sample was about 4000 mg/kg (ppm), as determined by ICP-QQQ in a diluted sample. Therefore, the W matrix in the sample as analyzed was about 40 mg/L (ppm) after the 100x dilution.

### Instrumentation

An Agilent 8900 Standard configuration ICP-QQQ was used. The instrument was fitted with the standard sample introduction system comprising a glass concentric nebulizer, quartz double-pass spray chamber, quartz torch with 2.5 mm id injector, and Ni interface cones. The ICP-QQQ was operated in no gas mode, with He cell gas, and with O<sub>2</sub> cell gas in both single quad (SQ) and MS/MS modes. The main operating conditions are shown in Table 1.

**Table 1.** 8900 ICP-QQQ operating conditions.

Parameter	No gas	He	O <sub>2</sub>	O <sub>2</sub>
Acquisition mode		Single Quad		MS/MS
RF power (W)		1550		
Sampling depth (mm)		8.0		
Carrier gas flow rate (L/min)		0.8		
Make-up gas flow rate (L/min)		0.4		
Spray chamber temp. (°C)		2		
He cell gas flow rate (mL/min)	–	5.0		–
O <sub>2</sub> cell gas flow rate (mL/min)		–		0.9

## Results and discussion

As the most abundant isotope, <sup>202</sup>Hg is selected as the preferred isotope for ICP-MS measurements. However, some analysts select <sup>201</sup>Hg instead (or as well), as the <sup>201</sup> isotope has proportionally lower W-based interference. The Hg calibration was prepared in a matrix of dilute (0.5 to 1.0%)

HCl to ensure that the Hg remained stable in solution as a Cl-complex.

The calibration plots for <sup>201</sup>Hg and <sup>202</sup>Hg are shown in Figure 1. The figures of merit—linearity, detection limit (DL), and background equivalent concentration (BEC)—taken from the <sup>202</sup>Hg calibration are presented in Table 2.

**Table 2.** DL, BEC, and R value of the calibration curve of <sup>202</sup>Hg in dilute HCl determined in four different cell modes.

	8900 calibration performance figures of merit for <sup>202</sup> Hg			
	No gas	He	O <sub>2</sub> Single Quad	O <sub>2</sub> MS/MS
R	0.997	0.999	0.999	0.999
DL (µg/L)	0.002	0.001	0.002	0.002
BEC (µg/L)	0.011	0.008	0.003	0.003



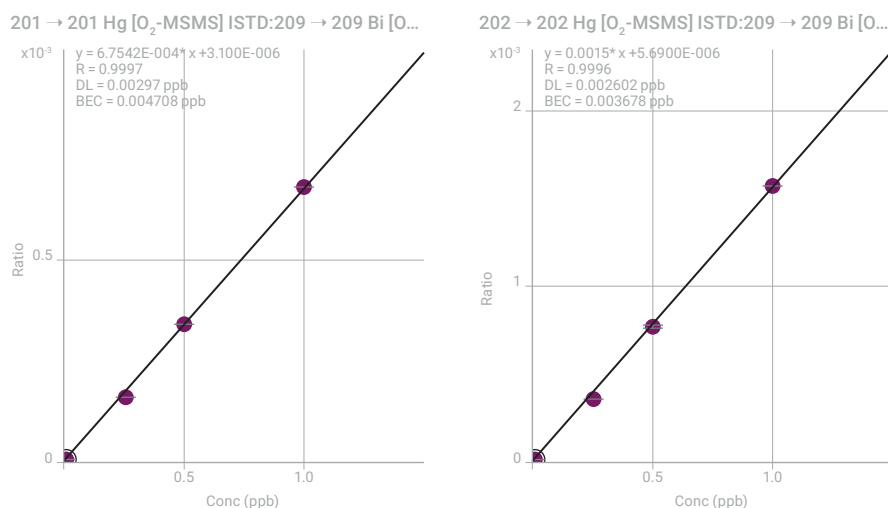


**Figure 1.** Calibration plots for  $^{201}\text{Hg}$  and  $^{202}\text{Hg}$ , demonstrating good sensitivity and linearity due to effective stabilization of Hg by the addition of HCl.

### ICP-MS/MS reaction mechanism used to resolve W-based interferences on Hg

The general reaction mechanism using MS/MS mode with  $\text{O}_2$  cell gas to resolve the  $\text{WO}^+$  and  $\text{WOH}^+$  interferences on Hg is shown in Figure 2. Since  $^{200}\text{Hg}$  suffers the most serious polyatomic ion overlaps, the reaction mechanism is illustrated using the example of the  $^{184}\text{W}^{16}\text{O}^+$  overlap on  $^{200}\text{Hg}^+$ . Q1 is set to  $m/z$  200, so  $^{200}\text{Hg}^+$  and  $\text{WO}^+$  ions at  $m/z$  200 pass through Q1 and enter the CRC.  $\text{WO}^+$  reacts with the  $\text{O}_2$  cell gas to form  $\text{WO}_2^+$  and  $\text{WO}_3^+$ , shifting to higher masses. The  $^{200}\text{Hg}^+$  ions do not react with the  $\text{O}_2$  cell gas and so remain at  $m/z$  200. By setting Q2 to  $m/z$  200,  $^{200}\text{Hg}^+$  ions pass to the detector free of interference. The same reaction mechanism is effective at resolving the  $\text{WOH}^+$  interferences, as  $\text{WOH}^+$  also reacts with the  $\text{O}_2$  cell gas to form higher-order product ions.

### Multiple isotope analysis study

To investigate the effectiveness of interference removal in the different cell gas modes, a  $1 \mu\text{g/L}$  (ppb) Hg spike was added to the diluted W-rich cosmetic lotion sample. The five most abundant Hg isotopes were measured in the four different cell gas modes, and the isotopic ratios calculated. Comparing the measured isotope ratios with the theoretical natural ratios gives an excellent indication of the effectiveness of the interference-removal on each isotope. This capability is important for many ICP-MS applications, where the results calculated from a second isotope can be used to confirm the concentration reported using the primary or preferred isotope. Performing “confirmatory measurements” is recommended or required in several regulated methods across the environmental, food, and pharmaceutical industries. This approach is analogous to the use of “qualifier ions” in organic mass spectrometry.

The isotope ratios for several Hg isotope pairs measured in the W-rich cosmetic sample using the four cell gas modes are presented in Table 3. These results show that MS/MS mode with  $\text{O}_2$  cell gas gives measured Hg ratios that are virtually identical to the theoretical natural ratios.  $\text{O}_2$  in MS/MS mode is much more effective than the other modes for the removal of the tungsten oxide and hydroxide polyatomic interferences. The effective removal of the  $\text{WOH}^+$  overlap on  $^{201}\text{Hg}$  is illustrated by the accurate ratios obtained for the  $^{200}\text{Hg}/^{201}\text{Hg}$  ratio in MS/MS mode using  $\text{O}_2$  cell gas.

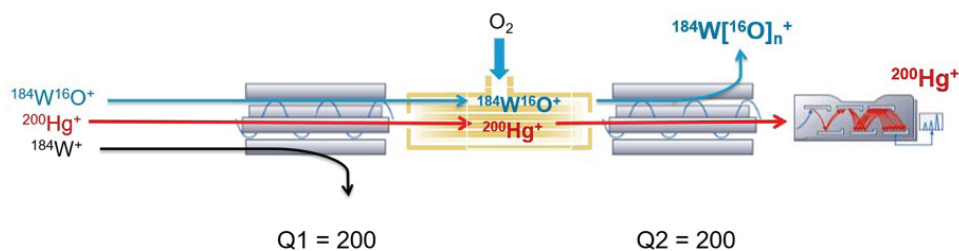


**Figure 2.** Reaction mechanism in MS/MS mode with O<sub>2</sub> cell gas for removal of WO<sup>+</sup> overlap to allow on-mass detection of Hg in a tungsten matrix. The same mechanism is also effective at resolving WOH<sup>+</sup> overlaps.

**Table 3.** Hg isotope ratios in tungsten-rich sample measured in different cell modes.

Hg ratio	Natural value	8900 measured results			
		No gas	He	O <sub>2</sub> Single Quad	O <sub>2</sub> MS/MS
198/199	0.591	1.738	1.769	1.435	0.598
198/200	0.432	0.831	0.823	0.739	0.43
200/201	1.75	49.4	61.4	7.75	1.76
201/202	0.441	0.022	0.017	0.126	0.445

As a further illustration of the ability of MS/MS to resolve interferences on multiple Hg isotopes, a scan spectrum comparison was made using on-mass measurement (Q1 = Q2). The mass range of the Hg isotopes was acquired for a simple Hg standard (1 µg/L) and a solution containing the same concentration of Hg spiked into a high W matrix (10 mg/L). The overlaid spectra are shown in Figure 3, together with the template indicating the natural abundance of the Hg isotopes. The spectra show that the measured isotopic abundances match the natural Hg isotope pattern in both samples. This confirms the ability of MS/MS mode with O<sub>2</sub> cell gas to remove the W-based overlaps caused by the high W matrix in the second sample.

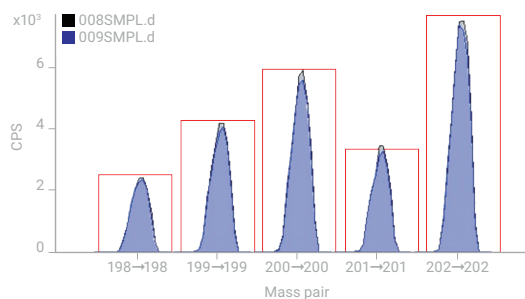


**Figure 3.** Hg isotopes with W matrix (blue shading) and without W matrix (gray shading), confirming accurate Hg isotope abundances and effective removal of W-based interferences on all Hg isotopes by ICP-QQQ with MS/MS.

### Hg in tungsten-rich samples

Hg was measured in a tungsten-rich cosmetic sample using four different cell gas modes. The five most abundant isotopes of Hg (198, 199, 200, 201, and 202) were used for quantitation, giving five independently calibrated results for total Hg. The results for Hg in the original cosmetic sample, corrected for the 100 times dilution, are shown in Table 4.

**Table 4.** Apparent Hg concentration ( $\mu\text{g}/\text{kg}$ ) in tungsten-rich cosmetic sample, quantitated independently using five isotopes. The data shows errors due to the contribution from  $\text{WO}^+$  and  $\text{WOH}^+$  overlaps in no gas, He, and  $\text{O}_2$  (SQ) cell modes.

8900 measured results					
Cell mode	198	199	200	201	202
No gas	267000	872000	126400	4770	98700
He	173200	57700	90700	2460	66500
$\text{O}_2$ Single Quad	772	249	399	2.8	288
$\text{O}_2$ MS/MS	2.1	1.8	2.4	1.5	1.7

Matrix-based interferences affect different isotopes of an analyte to different degrees, so giving different errors in the quantitative results calculated from each isotope.

Comparing the elemental concentrations calculated from the different isotopes of an element can therefore be used to identify whether the reported concentrations were affected by interferences. The reported Hg concentrations in MS/MS mode with  $\text{O}_2$  ( $\sim 2 \mu\text{g}/\text{kg}$  in the original sample, or  $0.02 \mu\text{g}/\text{L}$  in the 100x diluted solution) are much lower than the results reported using the other cell modes. Also, the good agreement between the results obtained for the five isotopes in  $\text{O}_2$  (MS/MS) mode shows that this mode can simultaneously remove polyatomic interferences from all five Hg isotopes. These results contrast with the other modes, where incomplete removal of interferences from most of the isotopes led to erroneously high values and large differences between the results calculated using the different isotopes. The reported concentration of  $2.8 \mu\text{g}/\text{kg}$  obtained for  $^{201}\text{Hg}$  using  $\text{O}_2$  cell gas in single-quad mode shows that the  $\text{WOH}^+$  interference could be reduced reasonably effectively. However, the other isotopes gave variable results in  $\text{O}_2$ (SQ) mode, so the  $^{201}\text{Hg}$  result could not be verified by comparing it with a second, qualifier isotope. The data in Table 4 shows that, even when a suitable reaction gas is identified, MS/MS is essential for full control of the reaction chemistry.

#### Spike recovery test

A spike recovery test was carried out to further evaluate the interference removal capability and matrix tolerance of the method. Since  $^{200}\text{Hg}$  suffers the most serious polyatomic ion overlaps, it was selected as the target mass for the spike recovery test.

A 30 ppt spike of Hg was added to the diluted cosmetic lotion sample. The spike recovery in  $\text{O}_2$  (MS/MS) mode was 104%, confirming the interference removal capability and matrix tolerance of the method (Table 5).

**Table 5.** 30 ppt Hg spike recovery results in different cell gas modes.

	Mode	Sample ( $\mu\text{g}/\text{L}$ )	Spike recovery (%)
200 Hg	No gas SQ	1364	6635
200 Hg	He SQ	906	879
200 Hg	$\text{O}_2$ SQ	3.99	216
200 Hg	$\text{O}_2$ MS/MS	0.024	104

## Conclusion

The Agilent 8900 ICP-QQQ operating in MS/MS mode with O<sub>2</sub> cell gas is highly effective for the removal of tungsten oxide/hydroxide polyatomic interferences on the five major Hg isotopes.

- Hg was measured accurately and consistently at trace levels in the presence of W using an MS/MS on-mass method with O<sub>2</sub> reaction cell gas.
- Compared to conventional single quadrupole ICP-MS, ICP-MS/MS reduced interferences by more than two orders of magnitude.
- The ICP-MS/MS method easily meets the requirements of trace level Hg analysis in tungsten-rich cosmetic samples.

## References

1. G. Genchi, M. S. Sinicropi, A. Carocci, G. Lauria, and A. Catalano, Mercury Exposure and Heart Diseases, *Int. J. Environ. Res. Public Health*, **2017**, 14(1), 74, <https://doi.org/10.3390/ijerph14010074>
2. Federal Food, Drug, and Cosmetic Act (FD&C Act), Cosmetics and U.S. Law, accessed October 2018, <https://www.fda.gov/Cosmetics/GuidanceRegulation/LawsRegulations/ucm2005209.htm>
3. E. Bolea-Fernandez, L. Balcaen, M. Resano, and F. Vanhaecke, Overcoming spectral overlap via inductively coupled plasma-tandem mass spectrometry (ICPMS/MS). A tutorial review, *J Anal. At. Spectrom.*, **2017**, 32, 1660-1679
4. L. Fu, S. Shi, and X. Chen, Accurate quantification of toxic elements in medicine food homologous plants using ICP-MS/MS, *Food Chemistry*, 245, **2018**, 692-697
5. L. Whitty-Léveillé, K. Turgeon, C. Bazin, and D. Larivière, A comparative study of sample dissolution techniques and plasma-based instruments for the precise and accurate quantification of REEs in mineral matrices, *Anal Chim Acta*, 961, **2017**, 33–41

# Sulfur isotope fractionation analysis in mineral waters using an Agilent 8900 ICP-QQQ

## Authors

Naoki Sugiyama  
Agilent Technologies, Tokyo, Japan

## Introduction

Stable isotope geochemistry is a branch of geology that investigates the age of natural materials, their origin and the processes they have undergone since formation [1]. Stable isotope analysis is also used in biogeochemical studies to monitor element cycling in ecosystems [2] and to identify geographical/regional differences for food provenance and archaeology. Of the elements of interest in stable isotope studies (hydrogen, carbon, nitrogen, oxygen and sulfur), only sulfur is accessible using aqueous solution analysis by ICP-MS, and even sulfur is difficult to measure by conventional quadrupole ICP-MS.

The relative abundance of the two major stable isotopes of sulfur,  $^{32}\text{S}$  (94.99% abundance) and  $^{34}\text{S}$  (4.25%), varies significantly in nature, so the  $^{34}\text{S}/^{32}\text{S}$  ratio can be used to characterize a sample. In sulfur stable isotope analysis, the variation in the  $^{34}\text{S}/^{32}\text{S}$  isotope ratio is calculated and reported as a deviation or delta ( $\delta$ ) in  $^{34}\text{S}$  abundance relative to a standard material, the troilite (iron sulfide) mineral from the Canyon Diablo meteorite, referred to as  $\delta\text{VCDT}$  (Vienna Canyon Diablo Troilite). Natural variations in  $^{34}\text{S}$  abundance, expressed in parts per thousand or “per mil” (‰), can be of the order of -50‰ to +40‰ (and occasionally much greater), due to redox reaction. Examples of some values for natural S isotope fractionation are given in Table 1 [3].

**Table 1.** Sulfur isotope distribution in nature.

Source	$\delta^{34}\text{S}$ (‰) relative to VCDT
Igneous rocks	0
Sedimentary rocks	-40 to +40
Seawater $\text{SO}_4$	+21
Atmospheric $\text{SO}_4$	-30 to +30
Surface water/groundwater $\text{SO}_4$	-22 to +135
Soil (organic sulfur)	-30 to +30
Vegetation (organic sulfur)	-34 to +32
Animals (organic sulfur)	-10 to +22
Fossil fuels (organic sulfur)	-11 to +28

Sulfur isotope ratio (IR) analysis has been mostly done by gas phase isotope ratio mass spectrometry (IRMS) but recent developments in ICP-MS technology have vastly improved its ability to measure sulfur accurately at low levels. In this work, we investigated the performance of a new, high sensitivity ICP-MS instrument, the Agilent 8900 Triple Quadrupole ICP-MS (ICP-QQQ), for low level S IR analysis of mineral waters. Spectral interferences on S arising from  $\text{O}_2^+$  can be removed by operating the ICP-QQQ in MS/MS mode, allowing both sulfur isotopes to be measured and potentially offering a faster and simpler S isotope analysis technique.

## Experimental

### Sulfur IR analysis method: mass-bias correction, matrix effects and background control

For accurate and precise IR analysis by ICP-MS, the instrumental mass bias must be corrected, and the effect of the sample matrix must be controlled.

As is typical for isotope ratio analysis by ICP-MS, instrumental mass-bias was corrected using sample-standard bracketing. A standard solution of known S isotope composition was measured before and after each sample, and the sample IR was corrected by the average IR of the two standard measurements. A 0.5 ppm solution of IAEA-S-1 was used as the mass bias correction standard [4].

The sample matrix can also affect the relative transmission of different mass ions in ICP-MS, and consequently the mass bias and the measured IR. To overcome this effect, a chelation technique can be used to remove the sample matrix before analysis [5]. Alternatively, the variation in sample matrix composition can be reduced by diluting all samples and standards in a consistent matrix. In this work, the mass bias standard and samples were diluted using a solution which contained 50 ppm calcium (Ca) and 100 ppm sodium chloride (NaCl). Use of this diluent reduced the matrix variation that could otherwise have caused fluctuations in the mass bias. The S concentration in the matrix blank was around 0.7 ppb which was low enough not to affect the accuracy of the IR analysis.

Sample dilution in a consistent matrix avoided the necessity for time consuming matrix removal. The matrix dilution approach was made possible by the high sensitivity and low S background of the 8900 ICP-QQQ. Sulfur is ubiquitous in laboratory consumables, supplies, and many of the materials used in instrument components, typically leading to a high elemental background signal. To minimize the contribution from the ICP-MS hardware, key components of the argon gas flow path of the 8900 #100 (Advanced Applications configuration) ICP-QQQ have been replaced using more inert materials. This has successfully reduced the background signal for S (and Si), allowing a detection limit specification of < 50 ppt for S, Si (and P) to be quoted<sup>1</sup>. In a recent study, S was measured with a sensitivity of 10<sup>4</sup> cps/ppb using the 8900 #100 ICP-QQQ to achieve a background equivalent concentration (BEC) of less than 100 ppt S in ultrapure water [6].

### Instrumentation

An Agilent 8900 ICP-QQQ (#100, Advanced Applications configuration) equipped with the standard Ni cones and x-lens was used. The standard glass concentric nebulizer was replaced with a PFA nebulizer, run using self-aspiration for better signal precision.

The two most abundant isotopes of S, <sup>34</sup>S and <sup>32</sup>S, were measured using the Agilent 8900 #100 in MS/MS mass-shift mode with O<sub>2</sub> cell gas [6]. The polyatomic interference from <sup>16</sup>O<sub>2</sub><sup>+</sup> on the primary isotope of S, <sup>32</sup>S<sup>+</sup> at *m/z* 32, and from <sup>16</sup>O<sup>18</sup>O<sup>+</sup> on the minor <sup>34</sup>S isotope at *m/z* 34 were avoided by shifting S<sup>+</sup> to a new mass. S<sup>+</sup> reacts readily with O<sub>2</sub> cell gas to form the product ion SO<sup>+</sup>, while the O<sub>2</sub><sup>+</sup> interference does not react in the same way with the O<sub>2</sub> cell gas. Consequently, the SO<sup>+</sup> product ions can be measured free of interference at M + 16 u (*m/z* 48 for the primary <sup>32</sup>S<sup>16</sup>O<sup>+</sup> isotope product ion and *m/z* 50 for <sup>34</sup>S<sup>16</sup>O<sup>+</sup>). Tuning conditions and method parameters are summarized in Table 2.

1. This specification is verified on every Agilent 8900 Advanced Applications and Semiconductor configuration instrument during factory testing

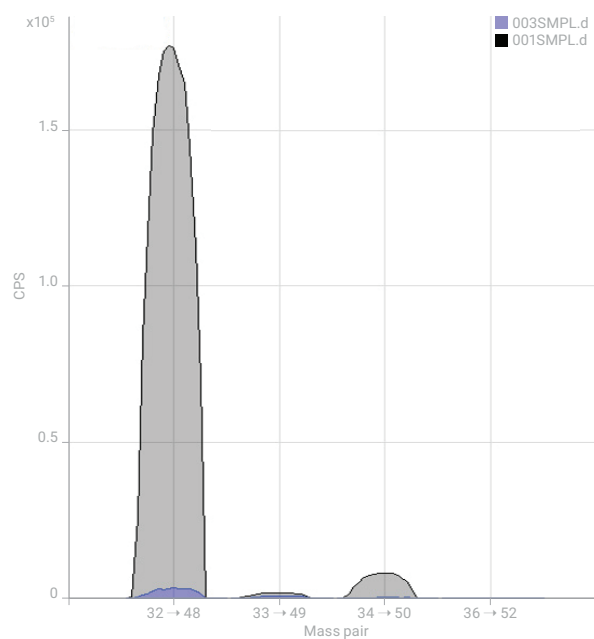
**Table 2.** Agilent 8900 ICP-QQQ tuning and method conditions.

	Tuning parameter	Value
Plasma	RF power (W)	1550
	Sampling depth (mm)	8.0
	Nebulizer gas flow rate (L/min)	0.90
	Make up gas flow rate (L/min)	0.30
Lens	Extract 1 (V)	-80
	Extract 2 (V)	-150
	Omega (V)	10.0
	Omega bias (V)	-120
Cell	Octp Bias (V)	-5.0
	Axial Acceleration (V)	2.0
	KED (V)	-8.0
	Cell gas	Oxygen
	Cell gas flow rate (mL/min)	0.45

	Method parameter	Value
Data Acquisition	Integration time (s)	1 and 5 for <sup>32</sup> S and <sup>34</sup> S
	Number of sweeps	1000
	Number of replicates	10
Rinse	1% HNO <sub>3</sub> rinse (s)	20
	50 ppm Ca/100 ppm NaCl rinse (s)	30
Peripump	Uptake time (s)	30
	Stabilization time (s)	30

The high sensitivity and low background of <sup>32</sup>S and <sup>34</sup>S can be clearly seen in Figure 1, which shows a spectrum of sulfur obtained using the MS/MS method.

**Figure 1.** MS/MS spectrum of 10 ppb sulfur solution (grey) and blank (blue).

## Sample and sample preparation

Sulfur isotope certified reference materials (CRMs) IAEA-S-1 ( $^{34}\delta_{\text{VCDT}} = -0.3\text{‰}$ ) and IAEA-S-2 ( $^{34}\delta_{\text{VCDT}} = +22.7\text{‰}$ ) were purchased from National Institute of Standards and Technology (NIST), Gaithersburg, MD, USA. Each CRM was gently dissolved in diluted nitric acid and diluted to the appropriate concentration. A matrix blank was prepared with 50 ppm Ca (SPEX Certiprep, US) and 100 ppm NaCl (Wako Pure Chemical Industries Ltd, Japan) in 1% nitric acid (Tmapure 100: Tama Chemicals Co. Ltd, Japan). This solution was also used to dilute the standards and samples.

The seawater and mineral water samples were diluted between 10 and 2000 times to give a S concentration in the range 0.2 to 0.8 ppm. Concentration matching contributed to accurate isotope ratio analysis because, at these levels,  $^{32}\text{S}$  is measured in analogue mode and  $^{34}\text{S}$  in pulse counting mode. Concentration matching also removes any potential errors caused by detector dead time (the instrument default dead time was 36.3 ns for mass 32).

## Results and discussion

### Synthetic sample analysis

Sulfur isotope CRMs IAEA-S-1 and IAEA-S-2 and two mixes of the two CRMs were prepared to give four samples with theoretical  $^{34}\delta_{\text{VCDT}}$  values of -0.3, 5.4, 11.2 and 22.6. Each blend was prepared at a S concentration of 0.5 ppm. The S IRs were measured six times (standard corrected as described previously).

Figure 2 shows the raw IR data for the IAEA-S-1 mass bias standard and the corrected IR data for the CRM blend samples. The average  $^{34}\delta$  values and errors (two times the standard deviation) were determined for the four CRM mixes, and these measured values were plotted against the theoretical values for each mixed standard. The results can be seen in Figure 3, demonstrating the good linearity obtained.

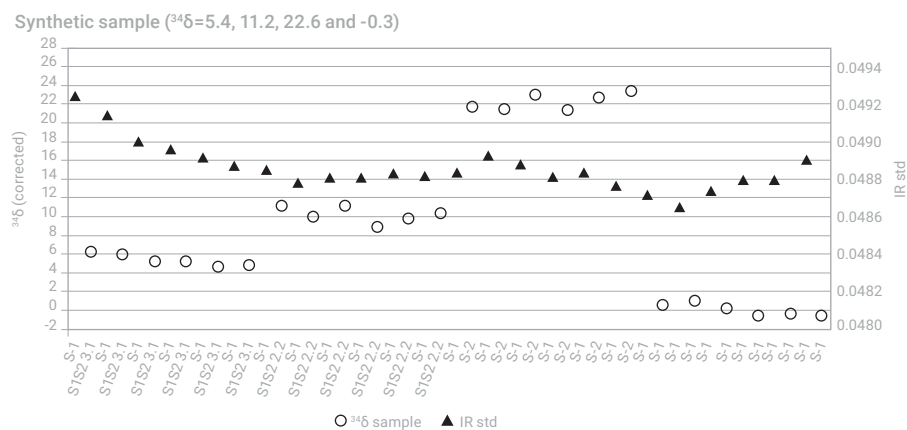


**Figure 2.** Raw IR analysis of bracketing mass bias standard IAEA-S-1 (triangles) and corrected S IRs of six separate measurements of each of four isotope CRM blends (points).



### Synthetic samples IR analysis

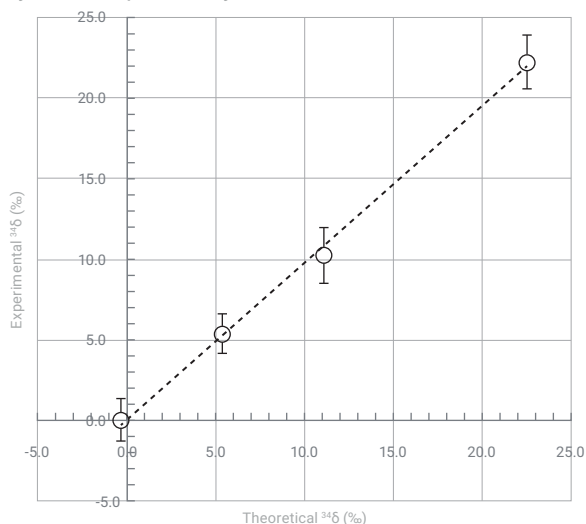


**Figure 3.** Average of Sulfur IR analysis of the four IAEA CRM blends.

### Water sample analysis

Three different brands of mineral water were purchased at a local store in Tokyo, Japan. The mineral water samples were prepared for analysis, together with samples of; JSAC 0301, a Japanese river water CRM (from the Japan Society for Analytical Chemistry); a spring water collected from the IKAHO hot spring in the north of Japan; a NASS 5 seawater CRM (National Research Council, Canada); and Tamapure-AA 100 high purity sulfuric acid (Tama Chemicals Co., Ltd.).

Before the IR measurements were undertaken, the sulfur concentration of each sample was checked to determine the appropriate dilution factor. The dilution factors applied to the samples are given in Table 3. Each sample was measured 10 times and the average and the standard deviation were calculated. Figure 4 shows the average IR and the error (as two times standard deviation) of the IR.

**Table 3.** Dilution factors.

Sample	Dilution factor
Mineral water A	10
Mineral water B	10
Mineral water C	1000
JSAC 0301: Japanese river water CRM	10
IKAHO hot spring water	1000
NASS 5	2000
High purity sulfuric acid	50000

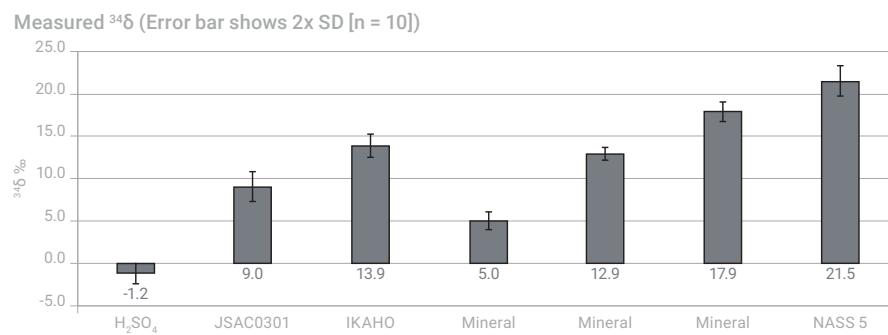


**Figure 4.** Measured sulfur IR for sulfuric acid, river water CRM, spring water, 3 commercial mineral waters (brands A, B and C) and seawater CRM.

The results show a clear difference in the S IRs for all of the samples, including between the 3 brands of mineral water. The  $^{34}\delta$  value of +21.5‰ determined in the seawater reference material agrees well with the global average oceanic seawater value of +21‰ for seawater sulfate (see Table 1 and reference 3).

The new, fast ICP-QQQ method for sulfur isotope analysis could be useful in identifying the natural characteristics of a water-source, monitoring seasonal and biogeochemical variations, and also for determining the impact of man-made sources of sulfur on the environment.

## Conclusion

The Agilent 8900 Advanced Applications configuration ICP-QQQ is ideally suited to  $^{34}\text{S}/^{32}\text{S}$  isotope ratio analysis, which can provide valuable information for sample characterization in natural systems or to monitor anthropogenic impact. The 8900 ICP-QQQ provides a low background and high sensitivity for sulfur, which enabled a method to be developed that simply required the sample to be diluted with the matrix blank before analysis. Sample/standard bracketing was used to correct for any instrumental mass-bias or drift.

By operating the 8900 ICP-QQQ in MS/MS mode with O<sub>2</sub> cell gas, problematic spectral interferences due to O<sub>2</sub><sup>+</sup> overlaps on  $^{32}\text{S}^+$  and  $^{34}\text{S}^+$  were successfully avoided. The S IR analysis method was applied to various samples including three mineral waters, a river CRM, a seawater CRM, a hot spring water, and high purity sulfuric acid. The precision of the IRs achieved was excellent at 1-1.5 ‰ (as two times the standard deviation).

## References

1. J. Ryu, R.A. Zierenberg, R.A. Dahlgren et al, **2006**, *Chemical Geology* 229 : 257-272 [2]
2. R. Tostevin, A. V. Turchyn, J. Farquhar, D. T. Johnston, D. L. Eldridge, J. K. B. Bishop and M. McIlvin, **2014**, *Earth and Planetary Science Letters*, 396, 14-21.
3. T.B. Coplen et. Al., **2002**, *Pure and Applied Chemistry*, 74 (10), 1987-2017.
4. National Institute of Standards and Technology certificate sheet for Reference Material 8554 - IAEA-S-1 (Sulfur Isotopes in Silver Sulfide), [https://www-s.nist.gov/srmors/view\\_msds.cfm?srm=8554](https://www-s.nist.gov/srmors/view_msds.cfm?srm=8554)
5. X. K. Zhu, A Makishima, Y. Guo et al, *Int. J. Mass Spectrom.*, 2002, 220, 21-29
6. K. Nakano, Ultra-low level determination of phosphorus, sulfur, silicon and chlorine using the Agilent 8900 ICP-QQQ, Agilent publication, 2016, [5991-6852EN](#)

# Fast Analysis of Arsenic Species in Infant Rice Cereals using LC-ICP-QQQ

## Authors

Courtney K. Tanabe<sup>1,2</sup>, Susan E. Ebeler<sup>1,2</sup>, Jenny Nelson<sup>1,3</sup>

1. Food Safety and Measurement Facility, University of California, Davis, USA

2. Department of Viticulture and Enology, University of California, Davis, USA

3. Agilent Technologies, Inc., USA

## Introduction

Arsenic contamination of food can be harmful to human health. To assess the risk, several speciation methods have been developed to separate the toxic inorganic forms of As (iAs)—a class 1 carcinogen—from less toxic or non-toxic forms.

In a previous study (1), a speciation method specified in US FDA EAM: Section 4.11 (2) was used to separate four arsenic species in 31 baby rice cereals. The arsenic species included the inorganic forms; As(III) (arsenite) and As(V) (arsenate), and two organic forms; monomethylarsonic acid (MMA), and dimethylarsinic acid (DMA). The four species were separated using isocratic anion-exchange HPLC, and ICP-MS was used to detect arsenic-containing chromatographic peaks.

This study aimed to develop a rapid and reliable screening method for inorganic arsenic (iAs) analysis, to assist the food industry in meeting existing and future regulations. As shown in Table 1, the FDA has proposed an action limit of 100 ppb for iAs in infant rice cereals. This limit is in line with the European Union's limit for rice used for the production of food for infants and young children.

**Table 1.** Example regulatory maximum concentrations governing iAs in rice and rice-based products.

Regulating body	Action or Maximum Concentration for iAs (ppb)	Rice Type or Rice Product
US FDA (3)	100 (proposed)	Infant rice cereals
Codex Alimentarius Commission (4, 5)	200	Polished (white) rice
	350	Husked (brown) rice
European Union (6)	200	Polished rice
	250	Parboiled and husked rice
	300	Rice waffles, wafers, crackers, and cakes
	100	Rice used for the production of food for infants and young children
China (7)	150	Rice grains

The methodology described in this application note is based on a previous method developed by Jackson (8), where As species were determined using HPLC coupled to a triple quadrupole ICP-MS (ICP-QQQ). HPLC-ICP-QQQ was also used in this study, but instead of analyzing the iAs species separately, As(III) was intentionally oxidized to As(V) with hydrogen peroxide before analysis (9, 10). By converting As(III) and analyzing all inorganic species as As(V), this method was able to separate MMA and DMA from iAs (as As(V)) in less than 2 minutes. The analysis time is 10 times faster than the current FDA methods used for As speciation (2). The same fast HPLC-ICP-QQQ approach has also been applied to As speciation in wine (11).

Oxygen was used as a reaction gas in the collision/reaction cell (CRC) of the ICP-QQQ to resolve the Cl-based spectral interferences on As-75 for total As measurements. For the speciation measurements, the potential Cl-based interferences are resolved chromatographically, so ICP-QQQ with MS/MS is not essential. While this analysis could be done on a single quadrupole ICP-MS such as the Agilent 7800 or 7900 ICP-MS, ICP-QQQ offers higher sensitivity and lower detection limits where both As speciation and total As analysis is required. Results are presented that demonstrate the accuracy and reproducibility of the new method. The method was further validated by analyzing four rice standard and certified reference materials.

## Experimental

### Standards

The As(III) and As(V) standards were bought from Spex Certiprep (Metuchen, NJ, USA). The MMA and DMA standards were bought from Chem Service (West Chester, PA, USA). An arsenobetaine (AB) standard was also purchased from Chem Service to be used as a flow injection marker (internal standard) for post-column injection. Calibration standards were prepared at 0.1, 0.5, 1.0, 5.0, 10, and 20 µg/L (ppb) for each of DMA, MMA, and total iAs (sum of As(III) and As(V)).

### Standard/certified reference materials

Four SRM/CRMs were used as quality control materials for the As speciation measurements and total As measurements (without HPLC separation). The SRM used was the National Institute of Standards and Technology (NIST) 1568a Rice Flour. The three CRMs were the National Metrology Institute of Japan (NMIJ) 7503a White Rice Flour, the NMIJ 7532a Brown Rice Flour, and the Joint Research Centre (JRC) ERM-BC211 - Arsenic in Rice.

### Samples and sample preparation

Six baby rice cereals were purchased from a local store in Berkeley, CA, USA. Each cereal was produced by a different manufacturer.

Arsenic was extracted from the rice matrix according to FDA method EAM 4.11 (2). Infant rice cereal (1 g) was weighed into a centrifuge tube and 10 mL of 0.28 mol/L HNO<sub>3</sub> was added. The capped tube was placed in a preheated block digestion system at 95 °C for 90 minutes. The mixture was then diluted with 6.6 mL H<sub>2</sub>O, centrifuged, and filtered. Equal 0.5 mL portions of rice extract, H<sub>2</sub>O<sub>2</sub>, and mobile phase were pipetted into a 2 mL plastic HPLC vial as the test solution. Each sample was prepared in duplicate.

### Instrumentation

An Agilent 1260 HPLC fitted with a Hamilton PRP-X100 5 µm 50 x 2.1 mm column was coupled to an Agilent 8800\* Triple Quadrupole ICP-MS (ICP-QQQ). The mobile phase was 40 mM ammonium carbonate ((NH<sub>4</sub>)<sub>2</sub>CO<sub>3</sub>, trace metal grade 99.999%, Sigma Aldrich) with 3% v/v methanol (Optima LC/MS grade, Fisher Chemical) adjusted to a pH of 9.0 with ammonium hydroxide (Optima Grade, Fisher Scientific). The ICP-QQQ was equipped with a standard sample introduction system comprising a glass concentric nebulizer, quartz spray chamber, quartz torch with 2.5 mm i.d. injector, and nickel-tipped interface cones. Peak integration was carried out according to FDA EAM §4.10 (12) and 4.11.15 (2). The instrument operating conditions are summarized in Table 2.

**Table 2.** HPLC-ICP-QQQ operating conditions.

ICP-QQQ	
Forward power	1550 W
Sampling depth	8.0 mm
Spray chamber temp.	2 °C
Carrier gas	0.95 L/min
Make-up gas	0.20 L/min
Extract 1	0 V
Octopole bias	-5.0 V
Energy discrimination	-7 V
O <sub>2</sub> cell gas flow rate	0.31 mL/min
Scan mode	MS/MS
Q1/Q2 mass	75/91 u
HPLC	
Mobile phase flow	0.5 mL/min
Injection volume	5 µL
Sample temperature	4 °C
ISTD injection volume	5 µL

## Results and discussion

### Development of a fast method

The focus of the method was to reduce the analysis time per sample compared to the current FDA method for As speciation. In common with Jackson's method (8), a small injection volume, short ion-exchange column, high mobile phase linear velocity, and oxygen cell gas mode were used.

Figure 1 shows overlaid chromatograms for a representative calibration set of 0.5, 1.0, 5.0, and 20 µg/kg standards. All As species are baseline separated in less than two minutes. Simply by oxidizing As(III) to As(V) and analyzing all iAs in the form of As(V), the analysis time was reduced significantly compared to approximately 20 minutes for the current FDA regulatory method (2).

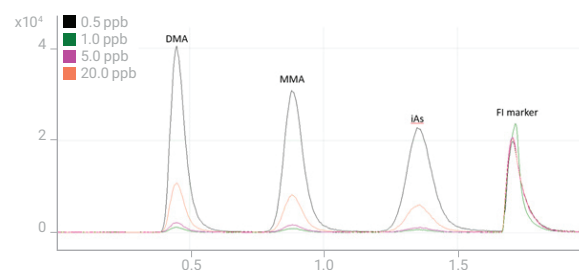


**Figure 1.** Overlay of the 0.5, 1.0, 5.0, and 20.0 µg/kg As species calibration standards. An AB internal standard (flow injection marker; fourth peak) was added post column via an external switching valve.

## Linear calibrations

The calibration curves for DMA, MMA, and iAs showed good linearity (Figure 2). All As concentrations in the rice samples were within the linear range except iAs, which was measured at a maximum concentration of 150% of the highest calibration standard.

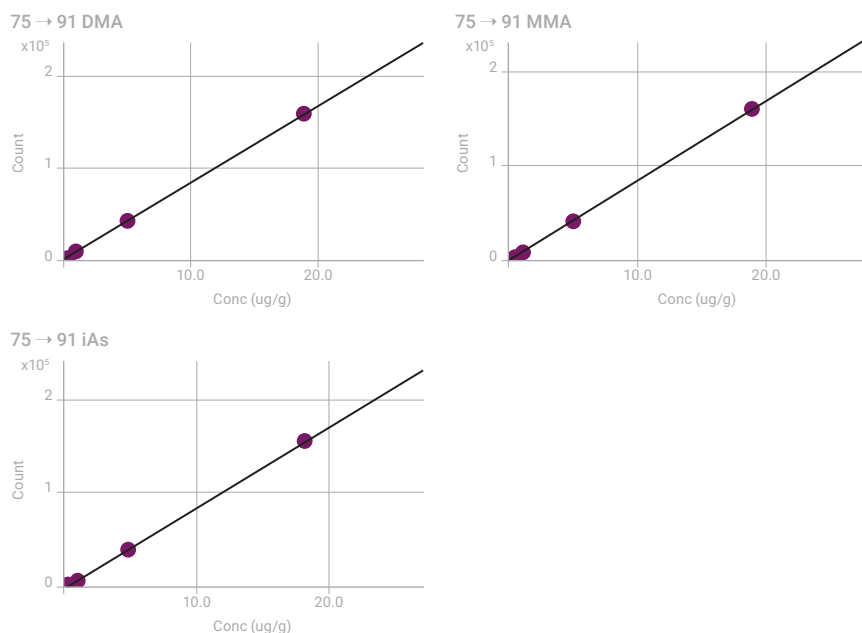


**Figure 2.** Calibration curves for DMA, MMA, and total iAs (sum of converted As(III) and As(V)).

## Detection limits

The limits of detection (LOD) and limits of quantitation (LOQ) given in Table 3 are based on repeated measurements of the 0.05  $\mu\text{g}/\text{kg}$  (ppb) mixed standard,  $n=15$ .

**Table 3.** LOD (3 sigma), LOQ (30 sigma), and estimated LOQ in rice for each As species.

	LOD, $\mu\text{g}/\text{kg}$	LOQ, $\mu\text{g}/\text{kg}$	Estimated wine LOQ, (50 x dilution) $\mu\text{g}/\text{kg}$
DMA	0.018	0.175	8.8
MMA	0.026	0.258	12.9
iAs	0.022	0.221	11.0

Reproduced by permission of The Royal Society of Chemistry. P. J. Gray et al, *J. Anal. At. Spectrom.*, 2017, 32, 1031 Analysis of rice RMs

Arsenic species were determined in four rice reference materials using the new HPLC-ICP-QQQ method. The total As concentration in each sample was also determined by direct ICP-QQQ analysis (no HPLC separation). Table 4 lists the reference and measured concentrations for DMA, MMA, iAs, and total As. Only one of the reference materials—NIST 1568b—had a reference value for MMA. The HPLC-ICP-QQQ measured concentrations were compared to the reference values, where available. Species recoveries ranged from 93 to 123% of their certified values when concentrations were above the LOQ. The recoveries for total As were also acceptable, ranging from 92 to 112%.

**Table 4.** Quantitative results for As species and total As in rice reference materials.

Rice RM	DMA (mg/kg)		MMA (mg/kg)		iAs (mg/kg)		Total As (mg/kg)	
	Reference	Measured	Reference	Measured	Reference	Measured	Reference	Measured
NIST 1568b	180 ± 12	195 ± 4 (109%)	11.6 ± 3.5	14.9 ± 0.9 (128%)	92 ± 10	105 ± 1 (114%)	285 ± 14	315 ± 3 (110%)
NMIJ 7503a	13.3 ± 0.9	15.4 ± 0.1 (116%)	None reported	<LOD	84.1 ± 3a	79 ± 4 (94%)	98 ± 7	94 ± 4 (96%)
NMIJ 7532a	18.6 ± 0.8	18.7 ± 1.3 (101%)	None reported	2.2 ± 1.9	298 ± 8	277 ± 12 (93%)	320 ± 10	297 ± 12 (93%)
ERM BC-211	119 ± 13	146 ± 3 (123%)	None reported	19.9 ± 0.6	124 ± 11	124 ± 2 (100%)	260 ± 13	290 ± 5 (112%)

a. NMIJ 7503a iAs uncertainty estimated as the square root of the sum of squares of the AsIII and AsV uncertainties. Reproduced with permission of The Royal Society of Chemistry. P. J. Gray et al, J. Anal. At. Spectrom., 2017, 32, 1031.

To check the quality of the data, z-scores were also calculated. Z-scores are the number of standard deviations from the mean, with values between -3 and +3 being sufficient for regulatory purposes. The percent recovery for DMA in ERM BC211 RM was biased high, but the z-score was 2.1. The recovery for MMA in NIST 1568b RM was 128% but the reference concentration was below the method's LOQ. The z-score was 0.94.

### Quantitative results in infant rice products

Six baby rice cereal samples were measured in duplicate using the HPLC-ICP-QQQ speciation method. Table 5 lists the measured concentrations for DMA and iAs; MMA was only present above the LOQ (0.026 ppb) in two of the rice samples (E and F). There was no significant difference between the two duplicates run for each cereal sample, showing the reproducibility of the method.

The concentration of iAs in four of the six rice samples was below the US FDA's proposed action limit and the EU's maximum limit of 100 ppb for iAs in infant rice cereals. Samples C and D exceeded the regulatory limit.

**Table 5.** Quantitative results in µg/kg (ppb) for As species in six infant rice market basket samples measured in duplicate.

Sample Name	DMA	MMA	iAs	Proposed US FDA limit of 100 ppb for iAs
Baby rice cereal A_1	11.4	N/D	63.3	Pass
Baby rice cereal A_2	11.2	N/D	62.3	
Baby rice cereal B_1	12.5	N/D	53.6	Pass
Baby rice cereal B_2	14.9	N/D	56.4	
Baby rice cereal C_1	33.9	N/D	106.4	Fail
Baby rice cereal C_2	36.0	N/D	113.5	
Baby rice cereal D_1	15.4	N/D	102.6	Fail
Baby rice cereal D_2	15.1	N/D	103.6	
Baby rice cereal E_1	41.9	2.2	87.9	Pass
Baby rice cereal E_2	39.0	2.3	89.4	
Baby rice cereal F_1	46.4	8.7	89.4	Pass
Baby rice cereal F_2	46.7	9.0	90.4	

N/D = Not detected

## Conclusion

A fast and fit-for-purpose HPLC-ICP-QQQ method is described for the measurement of inorganic As and two organic As species in baby rice cereal. A full speciation analysis can be completed in under two minutes.

- By oxidizing As(III) to As(V) with H<sub>2</sub>O<sub>2</sub> during sample preparation, total iAs was determined as As(V).
- The narrow bore column and 0.5 mL/min HPLC flow rate provided excellent sensitivity, which allowed low volume injections to be used.
- Sample run times were 10x faster than the current FDA 4.11 method for the determination of As in rice.
- The HPLC-ICP-QQQ method delivered improved sensitivity, limits of detection and limits of quantification compared to the FDA 4.11 method.

The reproducibility of the method was demonstrated by the good agreement between the quantitative results for duplicate measurements of six rice cereal samples. The results showed that two of the samples contained iAs above 100 ppb.

This method provides valuable information for the safety of rice and rice-based infant cereals, as well as allowing food producers to meet regulatory requirements.

## References

1. Rima Juskelis, Wanxing Li, Jenny Nelson, and Jack C. Cappozzo, Arsenic Speciation in Rice Cereals for Infants, *J. Agric. Food Chem.*, **2013**, 61, 45, 10670-10676
2. K. M. Kubachka, N. V. Shockey, T. A. Hanley, S. D. Conklin and D. T. Heitkemper, Arsenic Speciation in Rice and Rice Products Using High Performance Liquid Chromatography - Inductively Coupled Plasma-Mass Spectrometric Determination draft 1.1, Nov 2012, accessed May 2018, <https://www.fda.gov/downloads/Food/FoodScienceResearch/LaboratoryMethods/UCM479987.pdf>
3. Codex Alimentarius Commission, Report from the Thirty-Seventh Session, Geneva, Switzerland, 2014
4. Codex Alimentarius Commission, Report from the Thirty-Ninth Session, Rome, Italy, 2016
5. European Union Commission, 2015, Regulation (EC) No. 1881/2006
6. Y. G. Zhu, G. X. Sun, M. Lei, M. Teng, Y. X. Liu, N. C. Chen, L. H. Wang, A. M. Carey, C. Deacon, A. Raab, A. A. Meharg and P. N. Williams, High Percentage Inorganic Arsenic Content of Mining Impacted and Nonimpacted Chinese Rice, *Environ. Sci. Technol.*, **2008**, 42, 5008–5013
7. B. Sadee, M. E. Foulkes, S. J. Hill, Coupled techniques for arsenic speciation in food and drinking water: a review, *J. Anal. At. Spectrom.*, **2015**, 30, 102–118
8. B. P. Jackson, Fast ion chromatography-ICP-QQQ for arsenic speciation, *J. Anal. At. Spectrom.*, **2015**, 30, 1405–1407



9. S. Musil, Á. H. Pétursdóttir, A. Raab, H. Gunnlaugsdóttir, E. Krupp, J. Feldmann, Speciation without chromatography using selective hydride generation: inorganic arsenic in rice and samples of marine origin, *Anal. Chem.*, **2014**, 86 (2), 993–999
10. H. R. Hansen, A. Raab, A. H. Price, G. Duan, Y. Zhu, G. J. Norton, J. Feldmann, A. A. Meharg, Identification of tetramethylarsonium in rice grains with elevated arsenic content, *J. Environ. Monit.*, **2011**, 13, 32–34
11. C. K. Tanabe, H. Hopfer, S. E. Ebeler, J. Nelson, Fast Analysis of Arsenic Species in Wines using LC-ICP-QQQ, Agilent publication, 2017, [5991-8454EN](#)
12. S. D. Conklin, K. Kubachka, N. Shockey, Elemental Analysis Manual for Food and Related Products, §4.10 HPLC-ICP-MS As Species in Fruit Juice (Ver. 1; 2013), accessed May 2018, <http://www.fda.gov/EAM>

### More information

For a full account of this study, see Patrick J. Gray, Courtney K. Tanabe, Susan E. Ebeler, and Jenny Nelson, A fast and fit-for-purpose arsenic speciation method for wine and rice, *J. Anal. At. Spectrom.*, **2017**, 32, 1031–1034; DOI: 10.1039/C7JA00041C

### Acknowledgement

The Food Safety and Measurement Facility is supported by donations and gifts from Agilent Technologies, Gerstel US, and Constellation Brands.

# High Throughput Determination of Inorganic Arsenic in Rice using Hydride Generation-ICP-QQQ

## Authors

Ásta H. Pétursdóttir, Stanislav Musil, Nils Friedrich, Eva M. Krupp and Jörg Feldmann. University of Aberdeen, Scotland, UK

Helga Gunnlaugsdóttir Matis, Environment and Genetics Department, Reykjavik, Iceland

## Keywords

arsenic, arsenite, arsenate, IMEP-7 rice, NIST 1568a Rice Flour, oxygen mass-shift

## Introduction

The concentration of potentially toxic chemicals such as arsenic in rice is closely monitored to ensure food safety. However, the toxicity of arsenic depends on the chemical form or “species” of the element that is present rather than total concentration. Inorganic arsenic (iAs) species, arsenite (As(III)) and arsenate (As(V)), are known to be carcinogenic and highly toxic, whereas the common organoarsenic species monomethylarsonic acid (MMA) and dimethylarsinic acid (DMA) are less toxic [1].

Rice is an important food source for a large percentage of the world's population, but it does contain relatively high concentrations of iAs due to the uptake of As from the soil and water in which the rice plants are grown. Available As from soils can be both naturally occurring and due to anthropogenic sources such as As-based pesticides that were widely used until the 1970s. Clearly there is an urgent food-safety requirement for a simple and quick analytical method to screen large numbers of rice and other food samples for iAs. In this study, a fast and sensitive method using hydride generation (HG) with ICP-QQQ is described for the separation and detection of iAs in commercial rice samples.

## Experimental

**Instrumentation:** A Hydride Generation (HG) accessory for Agilent's ICP-MS Integrated Sample Introduction System (ISIS) was used with an Agilent 8800 #100 ICP-QQQ. When treated with  $\text{NaBH}_4$  under acidic conditions, iAs is very efficiently converted into volatile arsine ( $\text{AsH}_3$ ), whereas organically bound As compounds are not converted, or form only less volatile arsine species such as dimethylarsine ( $\text{CH}_3)_2\text{AsH}$ , which has a boiling point of  $35^\circ\text{C}$ . Adding high concentrations of HCl further reduces the production of the less volatile arsines, and iAs is almost entirely converted to arsine, enabling the measurement of iAs without species separation using chromatography.

**Plasma conditions and ion lens tune:** RF power = 1550 W, Sampling depth = 8.0 mm and Carrier gas flow rate = 0.93 L/min were used with soft extraction tune, Extract 1 = 0.5 V and Extract 2 = -170 V.

**Acquisition parameters:** MS/MS mass-shift mode using  $\text{O}_2$  cell gas at a flow rate of 2.0 mL/min. As was measured as the reaction product ion  $\text{AsO}^+$  at  $m/z$  91.

**Samples:** Samples included 31 different rice products purchased from local stores. Sub-samples (30g) of the commercially sourced rice samples were ground to a fine homogeneous powder using a coffee grinder. Two rice reference materials IMEP-107 rice (Institute for Reference Materials and Measurements Geel, Belgium) and rice SRM NIST 1568a Rice Flour were used as quality control for iAs concentration measurements.

**Sample prep:** 0.15g of each rice sample was digested in 1 mL concentrated HNO<sub>3</sub> and 2 mL H<sub>2</sub>O<sub>2</sub> (30 % w/w) using open vessel digestion in a CEM Mars microwave system. All samples were diluted to a final volume of 30 mL using deionized water.

**Table 1.** Cool plasma operating conditions.

Sample flow rate (mL/min)	0.5
HCl flow rate (mL/min)	2.5
NaBH <sub>4</sub> flow rate (mL/min)	0.5
Reaction coil volume (mL)	0.23
Ar flow rate (for HG) (L/min)	0.3
Ar flow rate (for nebulization of IS) (L/min)	0.85-0.95

## Results and discussion

The speciation results for iAs in IMEP-7 rice and NIST 1568a Rice Flour obtained using HG-ICP-QQQ were in good agreement with the values obtained using HPLC-ICP-QQQ and with the reported values (Table 2).

**Table 2.** iAs results obtained using HG-ICP-QQQ and HPLC-ICP-QQQ.

Inorganic As			
	HG-ICP-QQQ (µg/kg)	HPLC-ICP-QQQ (µg/kg)	Reported value (µg/kg)
IMEP-7 rice	100 ± 11 (n=15)	110 ± 12 (n=15)	107 ± 14 [2]
NIST 1568a	94 ± 8 (n=3)	105 ± 4 (n=3)	94 ± 12

A summary of the values for iAs, DMA and total As determined in the commercial rice samples is given in Table 3. The dominant arsenic species found in rice are iAs and dimethylarsinic acid (DMA), with only trace amounts of methylarsonic acid (MA). The method uses HCl (5 M) and NaBH<sub>4</sub> for the selective generation of arsines where iAs and DMA are converted almost exclusively to AsH<sub>3</sub>, with only minor (2-4%) conversion of DMA to dimethylarsine. MA forms methylarsine at approximately 40% efficiency with the method; however, since MA is generally absent from rice – or only present in trace amounts – this should not affect the quantification of iAs.

**Table 3.** Speciation results of iAs in 31 rice products determined by HG-ICP-QQQ and HPLC-ICP-QQQ. Results are also given for DMA and MMA, and the total As concentration determined by ICP-QQQ. All data  $\pm$  SD, with n=3 for speciation and n=2 or 3 for total As.

Rice product	HG iAs ( $\mu\text{g}/\text{kg}$ )	HPLC iAs ( $\mu\text{g}/\text{kg}$ )	HPLC DMA ( $\mu\text{g}/\text{kg}$ )	HPLC MMA ( $\mu\text{g}/\text{kg}$ )	Total As ( $\mu\text{g}/\text{kg}$ )
Arborio Risotto	113 $\pm$ 13	120 $\pm$ 18	63 $\pm$ 7	<LOQ	236 $\pm$ 15
Organic ArbRis	109 $\pm$ 12	119 $\pm$ 13	60 $\pm$ 8	<LOD	150 $\pm$ 7
Basmati, 1	41 $\pm$ 4	53 $\pm$ 7	8 $\pm$ 1	<LOD	100 $\pm$ 12
Basmati, 2	76 $\pm$ 6	88 $\pm$ 6	28 $\pm$ 4	<LOD	91 $\pm$ 8
Basmati (white)	72 $\pm$ 11	69 $\pm$ 9	24 $\pm$ 1	<LOD	240 $\pm$ 5
Organic Basmati (white)	95 $\pm$ 3	104 $\pm$ 3	21 $\pm$ 2	<LOD	117 $\pm$ 13
Brown Rice	127 $\pm$ 6	137 $\pm$ 5	35 $\pm$ 2	<LOD	205 $\pm$ 2
Japanese Rice	101 $\pm$ 5	99 $\pm$ 5	123 $\pm$ 1	<LOQ	252 $\pm$ 10
Long Grain (white)	89 $\pm$ 2	85 $\pm$ 1	16 $\pm$ 1	<LOD	121 $\pm$ 11
Long Grain Rice, 1	103 $\pm$ 2	94 $\pm$ 1	218 $\pm$ 9	<LOQ	392 $\pm$ 23
Long Grain Rice, 2	40 $\pm$ 2	52 $\pm$ 10	39 $\pm$ 3	<LOQ	111 $\pm$ 8
Long Grain white	47 $\pm$ 2	61 $\pm$ 4	19 $\pm$ 4	<LOD	102 $\pm$ 9
Organic Long Grain (brown)	111 $\pm$ 7	131 $\pm$ 14	54 $\pm$ 7	<LOQ	207 $\pm$ 15
Organic (white)	65 $\pm$ 4	65 $\pm$ 2	11 $\pm$ 1	<LOD	92 $\pm$ 4
Paella, 1	60 $\pm$ 5	65 $\pm$ 2	38 $\pm$ 1	1.2 $\pm$ 0.1	136 $\pm$ 1
Paella, 2	66 $\pm$ 4	70 $\pm$ 3	17 $\pm$ 1	<LOD	121 $\pm$ 6
Spanish Paella	67 $\pm$ 2	67 $\pm$ 3	13 $\pm$ 1	<LOD	109 $\pm$ 7
Pudding Rice	124 $\pm$ 9	125 $\pm$ 11	44 $\pm$ 5	<LOD	202 $\pm$ 4
Rice Flour	40 $\pm$ 1	46 $\pm$ 5	19 $\pm$ 2	<LOD	102 $\pm$ 6
Carnaroli Risotto Rice	81 $\pm$ 2	82 $\pm$ 4	84 $\pm$ 2	<LOD	210 $\pm$ 15
Risotto Rice	97 $\pm$ 11	114 $\pm$ 10	72 $\pm$ 9	<LOQ	221 $\pm$ 17
FLG Thai (white)	88 $\pm$ 3	102 $\pm$ 3	52 $\pm$ 5	<LOD	197 $\pm$ 9
Thai Jasmine	61 $\pm$ 4	64 $\pm$ 3	49 $\pm$ 5	<LOD	143 $\pm$ 3
Thai Jasmine (white)	62 $\pm$ 4	62 $\pm$ 3	49 $\pm$ 2	<LOD	171 $\pm$ 5
Vietnamese Rice Paper	21 $\pm$ 2	28 $\pm$ 1	<LOQ	<LOD	58 $\pm$ 10
White Rice	71 $\pm$ 5	76 $\pm$ 5	14 $\pm$ 4	<LOQ	124 $\pm$ 1
Whole Grain	133 $\pm$ 2	127 $\pm$ 2	151 $\pm$ 12	7.2 $\pm$ 0.3	370 $\pm$ 19

LOQ HG-ICP-QQQ: 5  $\mu\text{g}/\text{kg}$ , HPLC-ICP-QQQ: 1.1  $\mu\text{g}/\text{kg}$

## Conclusion

Inorganic arsenic (iAs) was quantified at low ppb levels in extracts of 31 rice samples using an Agilent Hydride Generator/ISIS coupled to an Agilent 8800 ICP-QQQ. Results obtained using HG-ICP-QQQ were in good agreement with HPLC-ICP-QQQ values across a wide linear range, with comparable limits of detection.

Following a simple sample preparation using microwave extraction, quick separation of iAs and DMA by HG-ICP-QQQ was performed online. A previous study has shown that HG-ICP-QQQ requires only 4 minutes total run time per sample (5 replicate measurements) compared to speciation with HPLC which commonly takes between 5 and 10 minutes for each sample replicate [3]. Data handling for the HG method is also straightforward as no peak-integration is necessary.

The new HG-ICP-MS method offers fast analysis time, high throughput, and simple, reliable operation. This makes it ideally suited to screening large numbers of food samples to meet the increasing demand for the routine determination of iAs in food, especially rice-based products.

## References

1. European Food Safety Authority, Scientific Opinion on Arsenic in Food. *EFSA Journal*, **2009**, 7(10):1351.
2. de la Calle, M. B.; Emteborg, H.; Linsinger, T. P. J.; Montoro, R.; Sloth, J. J.; Rubio, R.; Baxter, M. J.; Feldmann, J.; Vermaercke, P.; Raber, G., Does the determination of inorganic arsenic in rice depend on the method? *Trac-Trends Anal. Chem.* **2011**, 30, (4), 641-651.
3. Stanislav Musil, Ásta H. Pétursdóttir, Andrea Raab, Helga Gunnlaugsdóttir, Eva Krupp, and Jörg Feldmann, Speciation without Chromatography Using Selective Hydride Generation: Inorganic Arsenic in Rice and Samples of Marine Origin, *Anal. Chem.* **2014**, 86, 993–999.

## More information

For a full account of this application see publication: Ásta H. Pétursdóttir *et al.*, Hydride generation ICP-MS as a simple method for determination of inorganic arsenic in rice for routine biomonitoring, *Anal. Methods*, **2014**, 6, 5392-5396.

# Fast Determination of Inorganic Arsenic (iAs) in Food and Animal Feed by HPLC-ICP-MS

## Authors

Ana Jerše, Julie Storm Høgsbro,  
and Jens J. Sloth<sup>1</sup>

Raquel Larios<sup>2</sup>

<sup>1</sup>National Food Institute, Technical  
University of Denmark (DTU Food)\*,  
Denmark

<sup>2</sup>Agilent Technologies, Madrid, Spain

Method compliant with EU regulations and in accordance with two CEN standards on the analysis of iAs

## Introduction

It is well known that the two inorganic forms of arsenic (iAs), arsenite, As(III), and arsenate, As(V), are more toxic than the organo-arsenic species (1).

The difference in the toxicity of As species is why regulations in many countries specify the need to determine the iAs content of food and feedstuffs.

For example, European (EU) regulation 1881/2006 (2) includes maximum levels of iAs in rice and rice products—between 0.1 and 0.3 mg/kg. EU directive 2002/32/EC (3) states that the iAs content must be lower than 2 mg/kg in certain feedstuffs, such as feeds that contain seaweed. The European Commission is expected to establish maximum levels for iAs in other food commodities, especially foods that are widely consumed such as drinking water, milk, and dairy products. These foods have the potential to contribute more to the total dietary uptake of iAs.

HPLC-ICP-MS is widely used for As speciation studies. However, the separation of As species typically requires a long column, resulting in measurement times greater than 10 minutes. To shorten the measurement time significantly, a fast HPLC-ICP-MS method was developed by Jackson (4) and further modified by Gray *et al* (5). These methods have been used successfully for the analysis of iAs in rice (6) and wine samples (7).

To optimize a routine method that is suitable for official control of iAs in food and feedstuffs, we based this work on those previous studies. The method also needed to be compliant with current European regulations and meet the analytical requirements of two CEN standards on the determination of iAs in food and feed. The two CEN standards are EN16802:2016 (food) (8) and prEN17374:2019 (animal feed) (9). The sample preparation guidelines stated in the two CEN standards specify oxidation of As(III) to As(V) during the extraction procedure, which simplifies the determination of iAs in foods and animal feeds.

In this study, the chromatographic conditions were optimized to separate iAs (as As(V)) from dimethylarsinic acid (DMA), and monomethylarsonic acid (MA) in under two minutes. Method optimization and evaluation were performed using an Agilent 1260 HPLC coupled to an Agilent 8900 Triple Quadrupole ICP-MS (ICP-QQQ). The method can also be run using a single quadrupole ICP-MS, as the ICP-QQQ was operated in single quadrupole mode with helium (He) as a collision gas. The analytical performance of the method was tested, including limits of detection (LOD) and quantification (LOQ), linearity, spike recoveries, precision, and accuracy. The method was validated with suitable beverage, food, and animal feed reference materials (RMs).

## Experimental

### Reagents and standards

The As(V) standard solution for ICP-MS was bought from SCP Science (Canada). The As(III) solution and DMA salt were bought from Sigma Aldrich (USA), and MA was bought from Santa Cruz Biotechnology (USA). The arsenobetaine (AB) was a certified reference material (ERM-AC626) that was bought from the Institute for Reference Materials and Measurements (IRMM, Belgium). For the mobile phase, ammonium carbonate  $((\text{NH}_4)_2\text{CO}_3)$ , trace metal grade 99.999%, Alfa Aesar, USA), and methanol (HPLC grade from VWR Chemicals, USA) were used.

As(V) calibration standards (representing iAs) were prepared in duplicate between 0.05 and 50  $\mu\text{g/L}$  using the mobile phase as the diluent. MA and DMA were also added to the calibration standards to check the separation of the iAs peak from the organic compounds. The separation of the peak of the AB standard from the iAs peak was also tested. The As(III) standard was used to demonstrate the quantitative oxidation to As(V) during the sample preparation step (data not shown).

### Reference materials and samples

A list of samples and RMs used in this study is given in Table 1. Some of the iAs concentrations in the RMs were certified, reference values, or values established by collaborative trials and proficiency tests.

**Table 1.** Overview of samples and reference materials used in the study.

Sample/RM (Full name)	Sample/RM (Short name <sup>a</sup> )	iAs Conc (mg/kg)	Comments
Water from Plastic Bottle (Commercial Sample)	Bottled water	-	-
Apple Juice (Commercial Sample)	Apple juice	-	-
Rice (ERM-BC211)	Rice	0.124 ± 0.011 <sup>b</sup>	Certified value
White Rice Flour (NMIJ CRM 7503-b)	White rice flour	0.153 ± 0.010 <sup>b</sup>	Certified value
Brown Rice Flour (NMIJ CRM 7533-a)	Brown rice flour	0.530 ± 0.016 <sup>b</sup>	Certified value
Leek (DTU Food)	Leek	0.086 ± 0.012 <sup>c</sup>	Collaborative trial
Chili Powder (FAPAS T07288QC)	Chili powder	0.775 ± 0.024 <sup>d</sup>	Proficiency test
Bovine Liver (ERM-BB185)	Bovine liver	-	-
Fish Protein (NRCC-DORM-4)	Fish protein	0.27 ± 0.038 <sup>c</sup>	Collaborative trial
Blue Mussels (DTU Food)	Blue mussels	0.33 ± 0.049 <sup>c</sup>	Collaborative trial
Complete Marine Based Feed (DTU Food)	Marine based feed	0.802 ± 0.122 <sup>c</sup>	Collaborative trial
Mixed Corn Poultry Feed (FAPAS)	Mixed corn poultry feed	0.299 ± 0.010 <sup>d</sup>	Proficiency test
Kelp Powder (NIST SRM 3232)	Kelp powder	0.247 ± 0.019 <sup>e</sup>	Reference value
Hijiki (NMIJ 7405a)	Hijiki	10.1 ± 0.5 <sup>b</sup>	Certified value

<sup>a</sup> ... Short names of samples and RMs are used in the document

<sup>b</sup> ... Expanded uncertainty with the coverage factor  $k = 2$  (level of confidence of approx. 95%)

<sup>c</sup> ... Standard deviation of all the results from collaborative trial (duplicates from different laboratories)

<sup>d</sup> ... Uncertainty determined in proficiency test based on standard deviation of all the results and number of participants

<sup>e</sup> ... Expanded uncertainty with the coverage factor  $k = 2.36$

## Sample preparation

The sample preparation guidelines stated in the two CEN standards were followed (8, 9). For all solid samples, 0.1 M HNO<sub>3</sub> in 3% (v/v) H<sub>2</sub>O<sub>2</sub> was used as the extraction solution. Approx. 0.2 g of solid sample was mixed with 10 mL of the extraction solution. To obtain the same acid concentration after mixing with the sample at a ratio of 1:1, a more concentrated extraction solution was prepared for liquid samples. 5 mL of liquid sample was mixed with 5 mL of the more concentrated extraction solution (0.2 M HNO<sub>3</sub> in 6% (v/v) H<sub>2</sub>O<sub>2</sub>). Samples were heated in a water bath at 90 °C for 60 min. The extracts were then centrifuged for 10 min at 4000 rpm. The supernatants were transferred into filter vials (0.45 µm pore size). The vials containing the extracts were refrigerated at 4 °C before analysis. Because the Hijiki sample had a high iAs content (10.1 ± 0.5 mg/kg), the extract was further diluted 20-fold with the extraction solution and filtered, before analysis.

## Instrumentation

An Agilent 1260 HPLC with a binary pump was coupled to an Agilent 8900 ICP-QQQ. The HPLC was fitted with a PRP-X100 (5 µm, 50 x 2.1 mm) column and matching PRP-X100 analytical guard column (Hamilton Company, USA). The 8900 ICP-QQQ was equipped with a standard sample introduction system comprising a glass concentric nebulizer, quartz spray chamber, quartz torch with 2.5 mm i.d. injector, and nickel-tipped interface cones. The ICP-QQQ was operated in single quadrupole mode. Helium was used as a collision gas in the ORS<sup>4</sup> collision/reaction cell (CRC) to remove the potential interference from <sup>40</sup>Ar <sup>35</sup>Cl on <sup>75</sup>As. Although the 8900 offers higher sensitivity and lower detection limits than single quadrupole ICP-MS, the method could be run on the Agilent 7800 or 7900 ICP-MS, which are also fitted with an ORS<sup>4</sup>. The instrument operating conditions are summarized in Table 2.

**Table 2.** HPLC-ICP-MS operating conditions.

ICP-MS	
RF Power (W)	1550
Nebulizer Gas (L/min)	1.06
Sampling Depth (mm)	8
Spray Chamber Temperature (°C)	2
Peristaltic Pump Speed (rps)	0.5 <sup>a</sup>
Scan Mode	Single Quad
He Cell Gas Flow (mL/min)	3.5
Monitored <i>m/z</i>	<sup>75</sup> As, <sup>35</sup> Cl
HPLC	
Column Temperature	Ambient
Injection Volume (µL)	5
Mobile Phase	40 mM ammonium carbonate in 3% methanol, pH 9
Elution	Isocratic
Mobile Phase Flow (mL/min)	0.65
Run Time (min)	5 <sup>b</sup>

<sup>a</sup> ... Used for drain only

<sup>b</sup> ... Run time was set to 5 min to make sure that no other compounds eluted after the iAs peak.  
Figures 1 and 2 do not show the entire chromatogram



## Results and discussion

### Optimization of a fast method

The method was based on the approach used in two previous studies (4, 5). The relatively short anion exchange column was packed with small sized particles, allowing the use of a higher mobile phase flow rate and low volume injections.

Different mobile phase flow rates of 0.45, 0.5, 0.55, and 0.65 mL/min were tested. The fastest elution of arsenic compounds was achieved at 0.65 mL/min, without compromising the separation of the peaks. Higher flow rates were not tested since leaks were observed, due to the high backpressure. Since As(III) was oxidized to As(V), fewer As species were determined, allowing a stronger mobile phase to be used.

The chromatographic method achieved baseline separation of iAs from other arsenic species in less than two minutes, without compromising resolution, as shown in Figures 1 and 2. Figure 1 shows overlaid chromatograms of the individual arsenic species standards and Figure 2 shows overlaid chromatograms for a representative calibration set of standards from 0.05 to 50 µg/L. As shown, iAs (as As(V)) was well separated from the other As species.

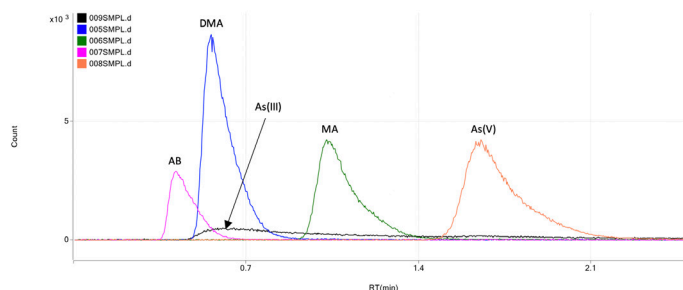


**Figure 1.** Overlaid chromatograms of individual As species standards.

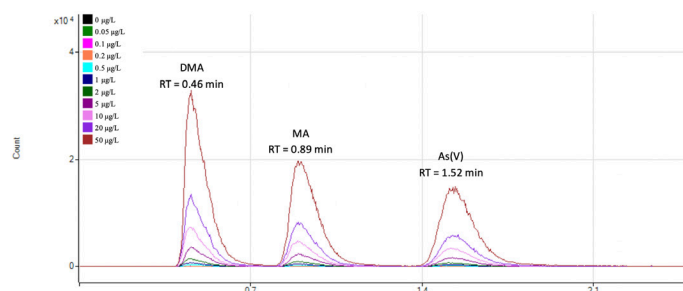


**Figure 2.** Overlaid chromatograms of calibration standards between 0.05 and 50 µg/L prepared in the mobile phase.

Helium was used as a collision gas in the ICP-MS to remove the potential interference from  $^{40}\text{Ar}^{35}\text{Cl}^+$  on  $^{75}\text{As}^+$ . To check the retention times (RT) of  $\text{Cl}^+$  and  $\text{As}^+$ , both ions were monitored at  $m/z$  35 and  $m/z$  75, respectively. Figure 3 shows that the RT of the chloride peak (black chromatogram) is distinct from the As(V) peak (green chromatogram), which complies with one of the requirements listed in EN16802:2016 and prEN17374:2019. The absence of a peak at the RT of Cl in the green chromatogram (although MA partly overlaps the Cl peak) suggests that  $^{35}\text{Cl}^{40}\text{Ar}^+$  was removed in He mode.

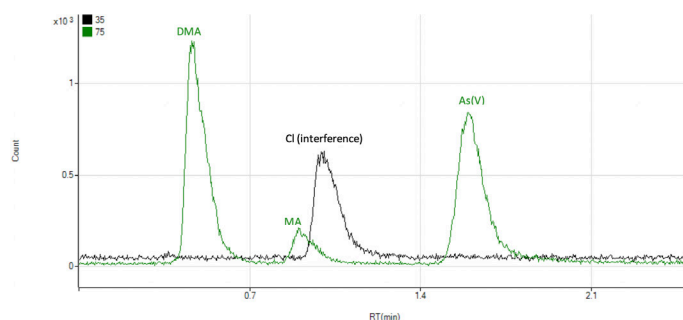


**Figure 3.** Chromatogram of Rice ERM-BC211 showing the RT of As species (green chromatogram) and the chloride peak (black chromatogram).

### Linear calibration

The calibration curve for iAs (as As (V)) showed good linearity, as shown in Figure 4.

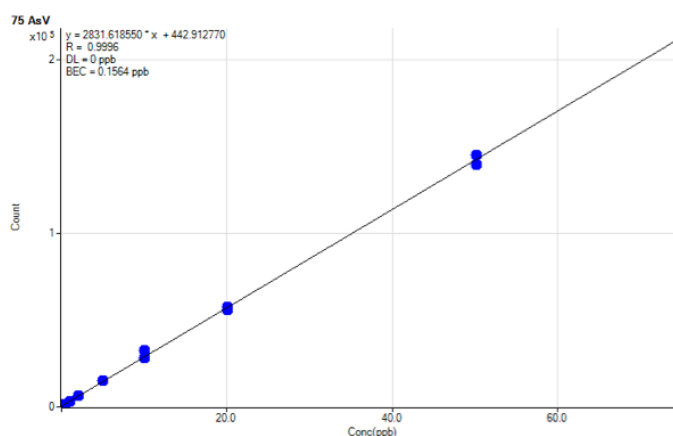


**Figure 4.** Calibration curve for iAs (represented by As(V)).

### Limits of detection and quantification

To evaluate the LOD and LOQ, 10 blank samples of the extraction solution were analyzed. The iAs peak of the As contaminant in the blank samples was integrated and the LOD and LOQ in solution were calculated using a 3-fold and 10-fold standard deviation, respectively. The LODs and LOQs in the samples were also calculated. The values for the solid samples are based on a test portion size of 0.2 g extracted with 10 mL of the extraction solution. The values for the liquid samples are based on 5 mL of sample diluted to 10 mL with the extraction solution. All LODs and LOQs are given in Table 3.

**Table 3.** LODs and LOQs for iAs calculated in solution, and in the solid and liquid samples.

	iAs in Solution ( $\mu\text{g/L}$ )	iAs in Solid Sample ( $\mu\text{g/kg}$ )	iAs in Liquid Sample ( $\mu\text{g/L}$ )
LOD	0.040	1.99	0.08
LOQ	0.133	6.64	0.27

The LOQ value for solid samples of 6.64  $\mu\text{g/kg}$  (0.0066 mg/kg) satisfies the European legislation for iAs determination in food (rice) of < 0.04 mg/kg (10). The LOQ is also well below the maximum iAs value of 2 mg/kg specified in European regulations for animal feed (3). The sensitivity of the method is sufficient for official control of iAs in food and feedstuffs.

## Spike recoveries and evaluation of matrix effects

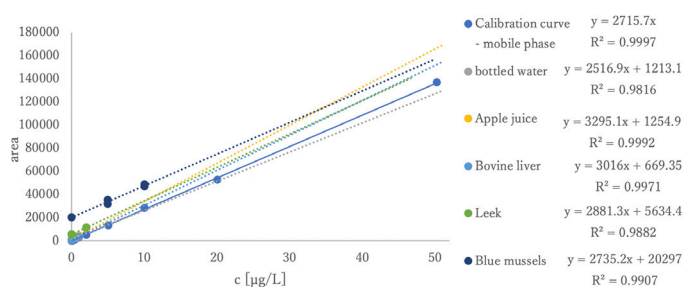
Several samples were spiked with iAs at two different concentration levels to evaluate potential matrix effects. Bottled water, apple juice, and bovine liver were selected as “unknown” samples, since no prior information on the iAs content was available for these samples. The iAs concentration of the two other spiked samples (leek and blue mussels) was obtained from collaborative trials.

Table 4 shows the spike recoveries were within  $100 \pm 10\%$  range for all samples apart from apple juice. The recoveries for apple juice were outside the  $100 \pm 10\%$  range for both the low and high concentration spike levels, indicating matrix effects.

**Table 4.** Spike recoveries of iAs in selected samples.

Sample	Low Spike Concentration ( $\mu\text{g/L}$ )	Spike Recovery (%)	High Spike Concentration ( $\mu\text{g/L}$ )	Spike Recovery (%)
Bottled Water	0.5	$109 \pm 9$	1	$90.0 \pm 0.6$
Apple Juice	0.5	$119 \pm 1$	1	$111 \pm 1$
Bovine Liver	0.5	$110 \pm 3$	1	$104 \pm 5$
Leek	2	$102 \pm 10$	5	$106.7 \pm 0.7$
Blue Mussels	5	$95 \pm 16$	10	$96 \pm 4$

The slope of the external calibration curve (solid line) was compared with the slopes of the standard addition curves (dotted lines; Figure 5). The trend lines for the standard addition curves are shown to help the comparison. For most of the samples, the difference in the slope between the external calibration curve and the standard addition curve was lower than 10%. The small difference suggests only minor matrix effects for these matrices, so external calibration can be used for the quantification of iAs in these samples. However, the difference in the two slopes for apple juice was higher than 20%, so standard addition is required for the quantification of iAs in apple juice.



**Figure 5.** Comparison of the slope of the external calibration curve with the slope of the standard addition curve.

## Precision and accuracy

All samples and RMs were prepared in triplicate and analyzed on the same day. The results of the three replicates were used to evaluate the precision of the method, which is reported as relative standard deviation (RSD). To evaluate the accuracy of the method, the average of the three replicates was compared to an RM target value. The results are reported as recovery.

The measured results for iAs in different samples are shown in Table 5. Recoveries were calculated using external calibration curves prepared in the mobile phase, as well as with the standard addition curves generated for selected samples. The original calibration for iAs was updated periodically through the sequence by running a QC check standard.

Precision of the measurements ranged from 0.3 to 9.4% RSD and iAs recoveries ranged from 81.8 to 110.7% of their certified, reference, or informative values. The results show that the method is suitable for the analysis of the different drinks, food, and feed samples analyzed in this study.

**Table 5.** Quantitative results for iAs content in samples and RMs with %RSD and recoveries.

Sample/RM	Target Value ( $\mu\text{g}/\text{kg}$ )	External Calibration Curve			Standard Addition	
		Measured Conc ( $\mu\text{g}/\text{kg}$ )	RSD (%)	Recovery (%)	Measured Conc ( $\mu\text{g}/\text{kg}$ )	Recovery (%)
Bottled Water <sup>a</sup>	-	0.81 $\pm$ 0.08 <sup>b</sup>	9.4	-	0.96 <sup>b</sup>	-
Apple Juice <sup>a</sup>	-	0.85 $\pm$ 0.06 <sup>b</sup>	6.8	-	0.76 <sup>b</sup>	-
Rice	124 $\pm$ 11	119 $\pm$ 3	2.1	96 $\pm$ 2	-	-
White Rice Flour	153 $\pm$ 10	151 $\pm$ 2	1.0	99 $\pm$ 1	-	-
Brown Rice Flour	530 $\pm$ 16	496 $\pm$ 9	1.8	94 $\pm$ 2	-	-
Leek	86 $\pm$ 12	95 $\pm$ 2	1.8	111 $\pm$ 2	87	101.6
Chilli Powder <sup>a</sup>	775 $\pm$ 24	860 $\pm$ 30	3.6	111 $\pm$ 4	-	-
Bovine Liver	-	12.5 $\pm$ 0.8	6.5	-	12	-
Fish Protein	270 $\pm$ 38	272.4 $\pm$ 0.8	0.3	100.9 $\pm$ 0.3	-	-
Blue Mussels	330 $\pm$ 49	337 $\pm$ 4	1.3	102 $\pm$ 1	350	106.1
Marine Based Feed <sup>a</sup>	802 $\pm$ 122	650 $\pm$ 30	4.1	82 $\pm$ 3	-	-
Mixed Corn Poultry Feed <sup>a</sup>	299 $\pm$ 10	293 $\pm$ 5	1.7	98 $\pm$ 2	-	-
Kelp Powder	247 $\pm$ 19	230 $\pm$ 20	7.5	94 $\pm$ 7	-	-
Hijiki	10100 $\pm$ 500	8800 $\pm$ 600	7.0	88 $\pm$ 6	-	-

<sup>a</sup> ... no dry matter correction

<sup>b</sup> ... in  $\mu\text{g}/\text{L}$

Figure 6 shows chromatograms of several of the sample matrices. Each chromatogram meets the requirements listed in the EN16802:2016 and prEN17374:2019 standard methods, which state that the chromatograms must show:

1. Selective separation of arsenate (As(V)) from the other arsenic compounds.
2. As(V) is separated from the nearest peak by a full peak width at 10% peak height.
3. As(V) is separated from the chloride peak (as shown in Figure 3).

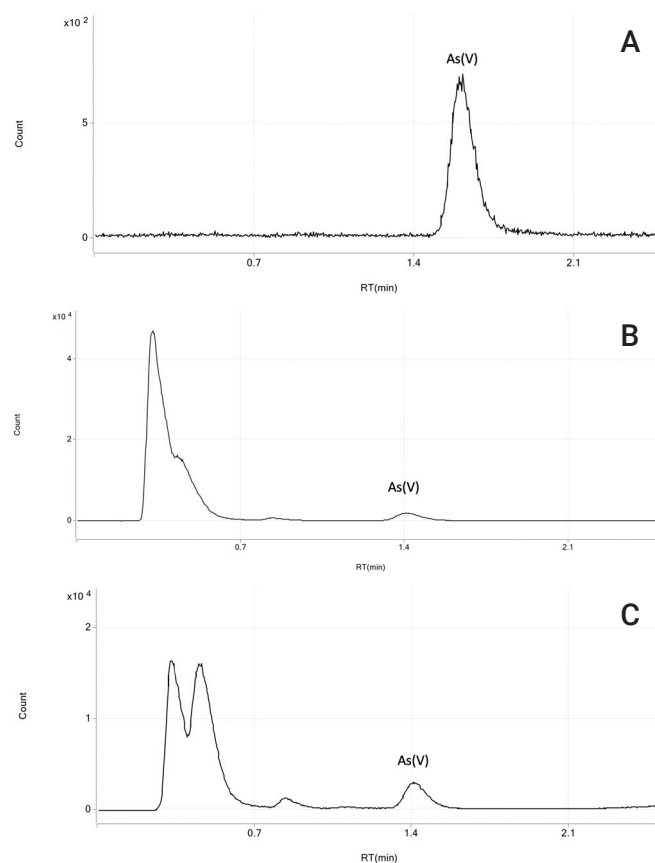


**Figure 6.** Chromatograms of several sample matrices. A: Chromatogram of Leek (DTU Food). B: Chromatogram of Fish Protein (NRCC-DORM-4). C: Chromatogram of Blue Mussels (DTU Food).

The data presented in this note was run over several days, and minor differences in the mobile phase composition and column conditioning led to some variation in the RTs between sequences. However, RT stability within each sample sequence was excellent, as shown in Table 6.

**Table 6.** Retention time stability for iAs peak in all standards and samples for three separate sample sequences.

	Average RT (min)	RSD (%)
Sequence 1 (n = 45)	1.61	1.24
Sequence 2 (n = 61)	1.41	1.28
Sequence 3 (n = 82)	1.85	1.73

## Conclusion

A fast HPLC-ICP-MS method was optimized for the analysis of iAs in beverages, food, and animal feed matrices. Using a small injection volume, short ion-exchange column, high strength mobile phase, and oxidizing As(III) to As(V) with H<sub>2</sub>O<sub>2</sub> during sample preparation, iAs could be determined in less than two minutes. The fast analysis time significantly increased sample throughput compared to methods that use a conventional ion-exchange column.

Following clear separation of As(V) from the organic As species and detection using an Agilent 8900 ICP-QQQ, LODs of 1.99 µg/kg (solid samples) and 0.08 µg/L (liquid samples) were obtained for iAs. The LOQs were lower than the LOQs established by European legislation for the analysis of iAs in food and feed samples. Several reference materials of different matrices with certified, reference, or informative values of iAs were analyzed with good accuracy (81.8 to 110.7%) and precision (0.3 to 9.4% RSD).

The HPLC-ICP-MS method is suitable for official control of iAs in food and feedstuffs as it complies with European regulations and meets the CEN standards' analytical requirements (8, 9). Given the toxicity of iAs, this fast, routine method provides valuable information on the safety of products that are widely consumed. It also enables food and feed producers to meet regulatory requirements for the analysis of iAs in their products.

## References

1. European Food Safety Authority, Scientific opinion on arsenic in food, EFSA Journal, 2009, 7, 1351
2. European Union Commission, 2006, Regulation (EC) No. 1881/2006 and later amendments
3. European Union Commission, 2002, Directive 2002/32/EC and later amendments
4. B. P. Jackson, Fast ion chromatography-ICP-QQQ for arsenic speciation, *J. Anal. At. Spectrom.*, **2015**, 30, 1405–1407
5. P. J. Gray, C. K. Tanabe, S. E. Ebeler, J. Nelson, A fast and fit-for-purpose arsenic speciation method for wine and rice, *J. Anal. At. Spectrom.*, **2017**, 32, 1031–1034
6. C. K. Tanabe, S. E. Ebeler, J. Nelson, Fast Analysis of Arsenic Species in Infant Rice Cereals using LC-ICP-QQQ, Agilent publication, [5991-9488EN](#)
7. C. K. Tanabe, H. Hopfer, S. E. Ebeler, J. Nelson, Fast Analysis of Arsenic Species in Wines using LC-ICP-QQQ, Agilent publication, [5991-8454EN](#)
8. EN 16802:2016: Determination of inorganic arsenic in foodstuffs of marine and plant origin by anion-exchange HPLC-ICP-MS
9. PrEN 17374:2019: Determination of inorganic arsenic in animal feed by anion-exchange HPLC-ICP-MS
10. European Union Commission, 2007, Regulation (EC) No. 333/2007 and later amendments

## Acknowledgment

Thanks to Michiko Yamanaka (Agilent) for her technical support.

# Multielement Analysis and Selenium Speciation in Cattle and Fish Feed using LC-ICP-QQQ

## Authors

Skyler W. Smith<sup>1</sup>, A. F. Oliveira<sup>1,2,3</sup>,  
J. Landero<sup>1</sup>, A. R. A. Nogueira<sup>2</sup>,  
M. A. Zanetti<sup>4</sup>, Jenny Nelson<sup>5</sup>

1. McMicken College of Arts and Sciences, Cincinnati, USA

2. Embrapa Southeast Livestock São Carlos, Brazil

3. University of São Carlos, Group of Applied Instrumental Analysis, Brazil

4. University of São Paulo, Faculty of Animal Science and Food Engineering, Brazil

5. Agilent Technologies, Inc., Santa Clara, CA, USA

## Validation of an extended FDA Elemental Analysis Manual method

### Introduction

In the USA, animal feed is subject to regulation under the Federal Food, Drug, and Cosmetic Act (FFDCA), which defines food as “articles used for food or drink for man or other animals”. The US Food and Drug Administration’s (FDA) Center for Veterinary Medicine (CVM) is responsible for regulations relating to the safety of feed intended for animals (including but not limited to horses, cattle, swine, poultry, and fish), under the Animal Feed Safety System (AFSS). The regulations control many aspects of the production, storage, and labeling of animal feed, and the permitted levels of additives and contaminants, such as potentially toxic heavy metals.

Selenium (Se) has been approved by the FDA as a supplement for animal feed since the 1970s. The FDA’s current method for Se quantification uses ICP-MS with helium collision/reaction cell (CRC) for control of interferences [1], but the sensitivity of this method is affected when high levels of interferences are present.

Selenium is an essential trace nutrient for vertebrates and is involved in several vital metabolic processes. The recommended human dietary intake is approximately 55 µg Se per day, which most people acquire through the consumption of plant-based foods, such as cereals. However, Se in the soil is not evenly distributed geographically, so dietary supplementation is commonplace in some parts of the world. This approach requires caution though, as Se is toxic in excess, with a tolerable upper intake level of about 200 µg/day depending on gender and age [2].

Animal feeds including cattle feed and fish feed are often supplemented with selenium. Supplementation may be in the form of sodium selenite/selenate, which is approved by the European Food Safety Authority (EFSA) as a food additive for all animal species [3]. Selenized yeast is also commonly used as an additive; if properly produced, the fortified yeast should contain primarily selenomethionine (SeMet). It is noted that the US regulations for supplemented selenium applicable for cattle feed and other livestock do not apply to fish feed.

### Total and speciation analysis of selenium

Determination of total Se concentration is commonly carried out as part of a multielement analysis using ICP-MS. More recently, Se analysis has benefited from the lower detection limits and greater freedom from spectral interferences provided by triple quadrupole ICP-MS (ICP-QQQ) [4, 5]. However, the toxicity of Se depends on the chemical form or species in which the Se occurs, so total elemental concentrations do not provide a complete picture of the element’s potential toxicity. As a result, separation and detection of the individual species (speciation) is required. The major Se species that occur naturally in the types of crop plant used to produce animal feed include two inorganic species, selenite

(Se(IV)) and selenate (Se(VI)), and some selenoamino acids: selenocystine (SeCys<sub>2</sub>), selenomethionine (SeMet), and Se-methyl selenocysteine (MeSeCys). Selenoamino acids are considered to be less toxic than the inorganic forms, with Se(IV) being the most toxic species [6]. In addition to the naturally occurring selenium species, animal feeds may contain various selenium compounds added during production to raise the level of total selenium in the animals' diet.

Se speciation analysis typically uses the well-established analytical method of HPLC (to separate the various Se-containing species) coupled to ICP-MS (to identify and quantify the individual Se species). HPLC-ICP-MS has been widely employed for analyzing various sample types [7] but there are few studies on selenium speciation in animal feed [8].

In this study, we developed an extraction and analytical method for the measurement of total Se using ICP-QQQ, and for Se speciation using LC-ICP-QQQ. The method provides low background and high sensitivity enabling low detection limits for total Se and Se compounds to be achieved. We then applied the speciation method to evaluate the selenium content and species distribution in cattle feed and fish feed.

## Experimental

### Samples and sample preparation

Two commercial cattle feeds and four commercial aquaculture feeds were bought from local stores.

#### *Total Se (and multi-element) analysis of feeds*

Cattle and fish feed samples were weighed to approximately 100 mg dry mass and microwave digested in a 1:1 mix of trace metal grade HNO<sub>3</sub> and distilled de-ionized (DDI) H<sub>2</sub>O. A solution containing various internal standards was added before digestion, giving an internal standard concentration of 5 ng/g in the final diluted solutions as analyzed. The microwave program consisted of a first step at 300 W with a 10 min ramp to 95 °C and a second step at 300 W including a 10 min ramp to 200 °C, followed by a 20 min hold time. After cooling, 1 mL of 30% H<sub>2</sub>O<sub>2</sub> was added and a second digestion was performed using the same heating program. The sample digests were diluted with DDI water to give a final acid concentration of approximately 2% HNO<sub>3</sub>. Two certified reference materials (CRMs) NIST 1547 Peach Leaves (NIST, Gaithersburg, MD USA) and SELM-1 Selenium Enriched Yeast (National Research Council of Canada) were prepared as quality control samples.

#### *Enzymatic extraction procedure for Se speciation in feeds*

An extraction solution containing 50 mM ammonium phosphate monobasic was prepared and the pH was adjusted to 7.5. Feed samples were weighed to approximately 200 mg with 3 mL of the extraction solution [9]. Samples were sonicated using QSonica sonication probe. The sonication program consisted of a 2 second pulse, followed by a 3 second rest at 60% amplitude for 2 minutes. Following sonication, approximately 20 mg of protease type XIV (from *Streptomyces griseus*, Sigma-Aldrich) and 10 mg of lipase (from *Candida rugose*, Sigma-Aldrich) dissolved in buffer solution were added to each sample and placed on a hot block for 12 hours at 37 °C. After 12 hours, the samples were sonicated again at 30% amplitude for 30 seconds and placed on the hot block for a further 12 hours.



The “enzyme extract” was filtered with a 0.45 m Spin-X Centrifuge Tube Filter (Costar, USA). The resulting sample was then diluted 1:1 with mobile phase 1 ready for analysis by reversed phase ion pairing LC-ICP-QQQ.

### Instrumentation

An Agilent 8800 Triple Quadrupole ICP-MS (ICP-QQQ) equipped with an Agilent SPS4 autosampler was used for analysis of total selenium and other elements in cattle and fish feed samples. Instrument operating conditions are given in Table 1.

**Table 1.** ICP-QQQ operating conditions.

Parameter	No gas	He	O <sub>2</sub>
Spray chamber temp (°C)	2		
RF power (W)	1550	1600	
Sampling depth (mm)	8.5	8	
Carrier gas (L/min)	1.00		
Make up gas (mL/min)	0.10	0.15	
Cell gas (mL/min)	0.0	3.4	0.5 (30%*)

\* Indicates % of full scale flow rate, as displayed in the ICP-MS MassHunter Tune screen

Agilent ICP-MS MassHunter software was used for the setup and operation of the ICP-QQQ for total Se and multielement data analysis. ICP-MS MassHunter with the optional Chromatographic Analysis module was used for combined instrument control and sequencing of the LC-ICP-QQQ Se-speciation study.

For the speciation studies in cattle and fish feed, an Agilent 1100 Series HPLC was coupled to the ICP-QQQ. Chromatographic separations were performed using an Agilent ZORBAX Extend column (80 Å C18, 4.6 x 250 mm, 5 µm). Details of the HPLC method used for Se speciation analysis of cattle and fish feed are given in Table 2.

The six Se species of interest, Se(IV), Se(VI), selenocystine (SeCys<sub>2</sub>), selenomethionine (SeMet), methyl selenocysteine (MeSeCys), and selenomethionine-Se-oxide (SeOMet), were calibrated using mixed standard solutions containing each of the Se species at levels from 1 to 50 ng/g.

In common with any ion pairing method, column equilibration is crucial to ensuring long-term reproducibility when using this LC-ICP-QQQ method. Equilibration is important after cleaning or when the column has been stored for a long time. To prevent deterioration of the column, 2 mM TBAH was added to the 65% acetonitrile storage solution. Following storage or cleaning, the column was equilibrated for 20 mins with 3x75 µL injections of 25 mM TBAH dissolved in the mobile phase.

**Table 2.** HPLC method used for the analysis of cattle and fish feed sample extracts.

Method	Salt gradient; reverse-phase ion-pairing		
Injection volume	25 $\mu$ L		
Mobile phase 1	5 mM ammonium acetate, 2 mM ammonium phosphate, 2 mM TBAH, 2% MeOH, pH 6.5		
Mobile phase 1	15 mM ammonium acetate, 5 mM ammonium phosphate, 2 mM TBAH, 2% MeOH, pH 6.5		
Method	Minute	% Mobile phase 2	Flow rate (mL/min)
	5	0	1
	10	100	1
	16	100	1
	20	0	1
	21	0	1.5
	40	0	1.5
	45	0	1

### Interference removal

Routine determination of total selenium concentrations or analysis of Se species using LC-ICP-MS does not necessarily require the use of ICP-QQQ. Conventional quadrupole ICP-MS (ICP-QMS) fitted with a CRC is able to resolve the  $^{40}\text{Ar}^{38}\text{Ar}^+$  dimer interference on  $^{78}\text{Se}$  sufficiently well to give acceptable results for Se speciation analysis in many sample types [7]. However, doubly-charged ion interferences such as  $^{156/160}\text{Gd}^{++}$  and  $^{156/160}\text{Dy}^{++}$  on  $^{78/80}\text{Se}$  can lead to positive bias in samples containing relatively high levels of the rare earth elements (REEs) [5]. In these sample types, ICP-QQQ is able to completely resolve the doubly charged REE interferences along with other spectral interferences, giving lower detection limits and better accuracy than ICP-QMS for Se (and As).

## Results and discussion

### Multielement analysis

The multielement analysis results including total Se content of the feed and CRM samples are summarized in Table 3. The measured value for total Se in Se-yeast SELM-1 CRM was in good agreement with the certified value at 94% recovery. The results validate the sample preparation method and the accuracy of the ICP-QQQ results. Accurate recovery of Se in NIST 1547 Peach Leaves was also obtained (102%, relative to the original 1991 certified value). This indicates the effective control of interferences including doubly charged rare earth elements, as NIST Peach Leaves contains up to 10 mg/kg (ppm) of the light rare earth elements. Table 3 also includes instrument detection limits (IDLs) demonstrating low ng/L (ppt) detection limits for most analytes.

**Table 3.** Total selenium dry weight concentration (mg/kg) determined in cattle feed, fish feed, and CRMs analyzed by ICP-QQQ.

Element	Tune	Q1 → Q2 Set Mass	Cattle Feed 1	Cattle Feed 2	Fish Feed 1	Fish Feed 2
Mg	He	24→24	2,278 ± 49	2,762 ± 26	1,873 ± 37	2,419 ± 17
K	He	39→39	8,771 ± 77	9,556 ± 60	7,064 ± 129	10,080 ± 196
V	He	51→51	1.37 ± 0.05	0.28 ± 0.01	0.30 ± 0.03	0.36 ± 0.02
Cr	He	52→52	1.79 ± 0.07	0.90 ± 0.03	1.16 ± 0.06	0.74 ± 0.06
Fe	He	56→56	392 ± 21	166 ± 25	432 ± 10	255 ± 3
Co	He	59→59	0.66 ± 0.02	1.3 ± 0.1	0.127 ± 0.001	0.67 ± 0.04
Cu	He	63→63	31.1 ± 0.8	26 ± 2	8.68 ± 0.08	66 ± 2
As	O2	75→91	0.21 ± 0.02	0.11 ± 0.01	1.14 ± 0.09	0.30 ± 0.05
Se	O2	78→94	0.86 ± 0.04	0.69 ± 0.03	1.07 ± 0.08	0.98 ± 0.05
Sr	He	88→88	11 ± 2	11.4 ± 0.5	49 ± 1	16.4 ± 0.6
Mo	He	95→95	1.35 ± 0.03	2.17 ± 0.01	0.77 ± 0.01	1.52 ± 0.02
Cd	He	111→111	0.094 ± 0.004	0.072 ± 0.003	0.40 ± 0.02	0.049 ± 0.002
Pb	No gas	208→208	0.24 ± 0.03	0.12 ± 0.01	0.38 ± 0.06	0.23 ± 0.09

Element	Tune	Fish Feed 3	Fish Feed 4	NIST 1547 <sup>a</sup>	ELM-1 <sup>a</sup>	IDL, ppb
Mg	He	2,152 ± 29	1,586 ± 56	4,406 ± 72 (98)		0.2116
K	He	11,298 ± 110	7,520 ± 66	22,167 ± 364 (91)		7.16
V	He	0.42 ± 0.01	1.14 ± 0.08	0.341 ± 0.006 (93)		0.0123
Cr	He	2.37 ± 0.01	1.10 ± 0.05	1.067 ± 0.009 (107b)		0.0044
Fe	He	204 ± 15	642 ± 50	225 ± 3 (102)		0.1027
Co	He	0.146 ± 0.002	0.20 ± 0.01	0.068 ± 0.002 (97b)		0.0005
Cu	He	16.2 ± 0.3	10.42 ± 0.08	3.8 ± 0.2 (101)		0.027
As	O2	0.171 ± 0.009	0.81 ± 0.03	0.08 ± 0.02 (133c)		0.0035
Se	O2	0.55 ± 0.02	1.05 ± 0.04	0.122 ± 0.003 (102c)	1911 ± 97 (94)	0.0031
Sr	He	40 ± 2	32 ± 2	62 ± 1 (117)		0.018
Mo	He	1.67 ± 0.03	1.11 ± 0.03	0.063 ± 0.006 (104)		0.002
Cd	He	0.074 ± 0.004	0.056 ± 0.006	0.028 ± 0.001 (107)		0.0039
Pb	No gas	0.25 ± 0.04	0.41 ± 0.03	0.82 ± 0.03 (94)		0.1946

a. Values enclosed in parenthesis are recoveries of the certified value of reference material.

b. Recovery determined relative to a non-certified, information value.

c. Recoveries for As and Se are calculated relative to the original certified values (1991 revision). These certified values have subsequently been removed from the certificate (2017 revision) so may not be reliable.

In the United States, the Association of American Feed Control Officials (AAFCO) 2011 Guidelines [10] and the US FDA's 21 CFR Part 573, Section 573.920 (Selenium) [11] state animal feeds intended for chickens, turkeys, swine, beef cattle, dairy cattle (and in the AAFCO Guidelines, bison, sheep, goats, llamas, alpacas, and horses) may contain selenium yeast at a level not to exceed 0.3 ppm (mg/kg) of selenium based on the complete feed [10]. Furthermore, the level of inorganic species should not exceed 2% of the total Se content in the final yeast product. Our results show that the two cattle feeds contained Se significantly above the 0.3 mg/kg limit, at 0.86 and 0.69 mg/kg Se. Similar results were found in the four fish feeds tested, which contained concentrations between 0.55 and 1.07 mg/kg Se.

All feeds contained at least twice the maximum Se concentration of 0.3 ppm (mg/kg) in selenium supplemented feeds. The feeds were likely supplemented by the addition of “antioxidants” including Se-yeast to increase the selenium content. To further investigate the Se content of the feeds, speciation analysis was performed to separate and quantify the individual Se species present in the feed samples.

### Selenium speciation analysis

Selenium speciation analysis was performed using LC coupled to ICP-QQQ. Se was measured using the oxygen cell gas tune mode as for Se in the multielement analysis. The selenium species concentrations were calibrated using mixed standard solutions containing each of the Se species at levels from 1 to 50 ng/g. The integrated peak areas for each species were plotted versus the standard concentrations to generate calibration curves covering the required calibration range.

The chromatogram shown in Figure 1 was obtained from the analysis of a mixed standard containing each Se species at 25 ng/g. The chromatogram demonstrates good sensitivity and peak separation for all species. Peak identities were confirmed by retention time (RT) matching and/or the use of standard spikes added to the extracts.

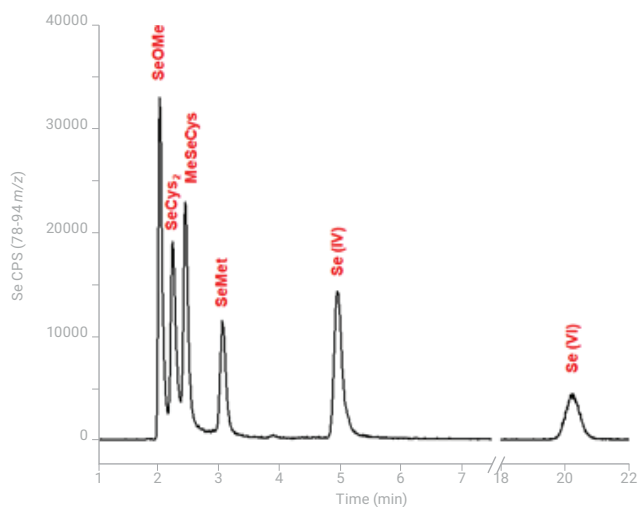


**Figure 1.** LC-ICP-QQQ chromatogram of standard containing six selenium species at 25 ng/g.

### Se species in cattle feed samples

The two cattle feed samples were analyzed using LC-ICP-QQQ. The overlaid chromatograms in Figure 2 show that both samples contained primarily SeMet, while cattle feed 2 also contained significant levels of Se(VI). Other species were present at trace levels. The source of SeMet was likely to be selenized yeast, which is often added intentionally to enrich the feeds. However, natural sources, such as grains and soybeans, are common additives that have been found to accumulate SeMet when supplied with inorganic Se sources [12–14]. Plants naturally uptake Se from soils, and inorganic Se species tend to be more mobile, which leads to increased plant uptake compared with organic forms. Depending on soil conditions, either Se (IV) or Se (VI) may be the major Se source for plants [15]. When Se (IV) is the main source of selenium, it gets metabolized to organic Se compounds; while Se (VI) uptake generally results in higher accumulation

without transformation [12, 14]. It can be concluded that the Se (VI) found in the cattle feeds for this study likely originated from the addition of high-selenium plant additives often used in feed production.

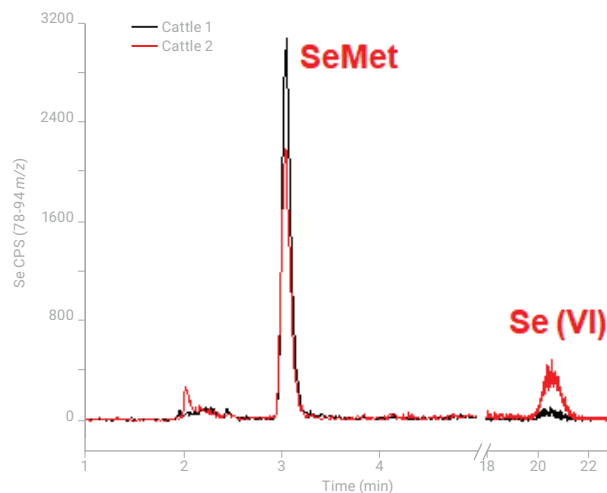


Figure 2. LC-ICP-QQQ speciation analysis of two cattle feed samples.

### Se species in fish feed samples

Figure 3 shows chromatograms for the four fish feed samples. As with the cattle feeds, a variety of Se species were observed in these samples. SeMet was the primary species in all feeds, but inorganic forms such as Se(IV) and Se(VI) were also present. The quantitative results in Table 4 show that Se(IV) was considerably higher in fish feed 1 compared to the other samples, while Se(VI) was higher in the cattle feeds than the fish feeds.

Selenium supplementation has been shown to improve growth and antioxidant status for fish reared in the crowded conditions that are typical of mass production methods [16]. Previous aquaculture studies have shown supplementation with inorganic forms of Se, mainly Se(IV), leads to inferior bioavailability compared to SeMet or seleno yeast [17, 18]. Due to greater accumulation of Se in fillets and whole body, many studies currently use organic Se for aquaculture and supplementation research [19, 20].

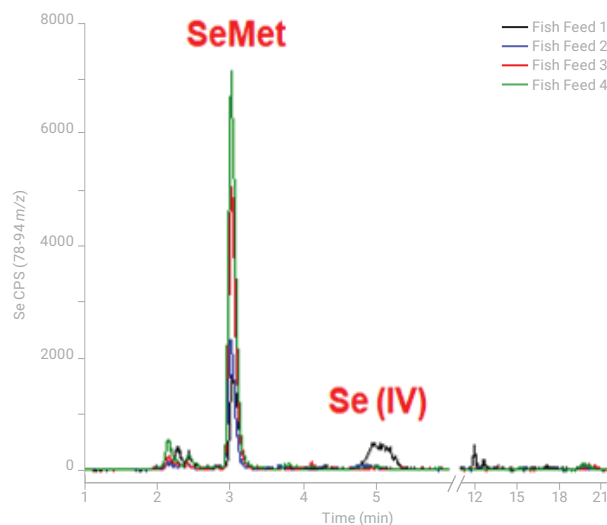


Figure 3. LC-ICP-QQQ speciation analysis of four fish feed samples.

**Table 4.** Enzymatic extraction and quantification of Se species for cattle and fish feeds using LC-ICP-QQQ.

Sample	Extraction total (µg/kg, ppb)	Extraction efficiency (%) <sup>*</sup>	Quantification of known species (µg/kg, ppb)					
			SeOMet	SeOMet	MeSeCys	SeMet	Se (IV)	Se (VI)
Cattle feed 1	386 ± 3	45 ± 1	2 ± 1	44 ± 41	5 ± 1	112 ± 8	0 ± 0	72 ± 3
Cattle feed 2	346 ± 14	50 ± 2	6 ± 3	4 ± 2	3 ± 1	97 ± 3	24 ± 27	128 ± 15
Fish feed 1	648 ± 32	61 ± 3	5 ± 2	19 ± 3	12 ± 1	79 ± 11	61 ± 8	23 ± 3
Fish feed 2	484 ± 90	49 ± 9	2 ± 1	14 ± 6	9 ± 1	117 ± 11	10 ± 3	22 ± 4
Fish feed 3	363 ± 103	66 ± 19	4 ± 2	17 ± 3	8 ± 2	222 ± 8	3 ± 5	30 ± 7
Fish feed 4	710 ± 43	68 ± 4	2 ± 1	27 ± 1	14 ± 1	293 ± 39	14 ± 3	31 ± 1

\* Compared to total Se concentration (shown in Table 3).

## Conclusion

Total concentrations of several elements, including selenium, were determined in cattle and fish feed sample-extracts, using the Agilent 8800 ICP-QQQ. In all samples, the concentration of Se was above the maximum of 0.3 ppm (µg/kg) Se recommended in the AAFCO and FDA guidelines for selenium supplemented feeds.

Reversed phase ion pairing LC-ICP-QQQ was then used successfully to separate and detect the selenium species at low mg/kg levels in the feed samples (low µg/L in the solutions analyzed). The method provided valuable information on the Se species present in the feeds. SeMet was found to be the predominant species, although the toxicologically relevant inorganic forms of Se (Se(IV) and Se(VI)) were also found to be present in most of the samples.

## More information

For a full account of part of this application, see A. F. Oliveira, J. Landero, K. Kubachka, A. R. A. Nogueira, M. A. Zanetti and J. Caruso, Development and application of a selenium speciation method in cattle feed and beef samples using HPLC-ICP-MS: evaluating the selenium metabolic process in cattle. *J. Anal. At. Spectrom.*, **2016**, 31, 1034. DOI: 10.1039/c5ja00330j

## References

1. Overview of FDA's Animal Feed Safety System, accessed August 2017, <http://www.fda.gov/downloads/AnimalVeterinary/SafetyHealth/AnimalFeedSafetySystemAFSS/UCM277673.pdf>
2. Selenium in Dietary Reference Intakes for Vitamin C, Vitamin E, Selenium and Carotenoids, Institute of Medicine, Washington, DC, 2000
3. EFSA Panel on Additives and Products or Substances used in Animal Feed (FEEDAP), Safety and efficacy of selenium compounds (E8) as feed additives for all animal species: sodium selenite, EFSA Journal 2016; 14 (2): 4398, [www.efsa.europa.eu/efsajournal](http://www.efsa.europa.eu/efsajournal)
4. B.P. Jackson, A. Liba, and J. Nelson, Advantages of reaction cell ICP-MS on doubly charged interferences for arsenic and selenium analysis in foods. *J. Anal. At. Spectrom.* **2015**, 30, 1179–1183
5. N. Sugiyama, The accurate measurement of selenium in twelve diverse reference materials using on-line isotope dilution with the 8800 Triple Quadrupole ICP-MS in MS/MS mode, Agilent publication, 2012, [5991-0259EN](https://www.agilent.com/chem/8800/8800-0259EN)

6. C. B'Hymer and J. A. Caruso, *J. Chromatogr. A*, 2006, 1114, 1–20.
7. *Handbook of ICP-MS Hyphenated Techniques*, 2nd Edition, Agilent publication, 2015, 5990-9473EN
8. M. Stadlover, M. Sager and K. Irgolic, *Die Bodenkultur*, 2001, 52, 233–241
9. L. H. Reyes, J. L. Guzmán Mar, G.M. Mizanur Rahman, B. Seybert, T. Fahrenholz, H.M. Skip Kingston, *Talanta* 78, 3, 2009, 983–990
10. Association of American Feed Control Officials: Official Publication, ed. M. K. Walsh, 2011, ch. 5, pp.216–353.
11. Code of Federal Regulations Title 21, Volume 6 [Revised as of April 1, 2017] 21CFR573.920
12. H.F. Li, S. P. McGrath, and F. J. Zhao. Selenium uptake, translocation and speciation in wheat supplied with selenate or selenite, *New Phytologist* 178.1, 2008, 92-102.
13. Q. Chan, S. E. Afton, and J. A. Caruso. Selenium speciation profiles in selenite-enriched soybean (*Glycine Max*) by HPLC-ICPMS and ESI-ITMS. *Metallomics* 2.2, 2010, 147-153.
14. P. D Whanger, Selenocompounds in plants and animals and their biological significance. *Journal of the American College of Nutrition*, 2002, 21(3), pp.223-232.
15. S. Eich-Greatorex et al. Plant availability of inorganic and organic selenium fertiliser as influenced by soil organic matter content and pH. *Nutrient Cycling in Agroecosystems*, 79.3, 2007, 221-231.
16. F. Z. Küçükbay et al. The effects of dietary organic or inorganic selenium in rainbow trout (*Oncorhynchus mykiss*) under crowding conditions. *Aquaculture Nutrition*, 15.6, 2009, 569-576.
17. C. Wang and R. T. Lovell. Organic selenium sources, selenomethionine and selenoyeast, have higher bioavailability than an inorganic selenium source, sodium selenite, in diets for channel catfish (*Ictalurus punctatus*). *Aquaculture* 152.1-4, 1997, 223-234.
18. M. Lorentzen, A. Maage, and K. Julshamn. Effects of dietary selenite or selenomethionine on tissue selenium levels of Atlantic salmon (*Salmo salar*). *Aquaculture* 121.4, 1994, 359-367.
19. M. Abdel-Tawwab, M.A.A Mousa and F.E. Abbass. Growth performance and physiological response of African catfish, *Clarias gariepinus* (B.) fed organic selenium prior to the exposure to environmental copper toxicity. *Aquaculture* 272.1, 2007, 335-345.
20. S. Lee et al. Dietary selenium requirement and toxicity levels in juvenile Nile tilapia, *Oreochromis niloticus*. *Aquaculture* 464, 2016, 153-158.

# Arsenic speciation analysis in apple juice using HPLC-ICP-MS with the Agilent 8800 ICP-QQQ

## Authors

Mina Tanoshima\*, Tetsushi Sakai\*  
and Ed McCurdy†

Agilent Technologies

\* Tokyo, Japan

† Stockport, UK

## Introduction

The presence of potentially toxic elements and compounds in foodstuffs is of intense public interest, and so food producers as well as regulators require rapid, reliable screening methods to accurately determine the levels of such contaminants in food and drink. In the case of arsenic (As), concentration levels in foods may be increased through the historical use of As-containing agrochemicals such as lead hydrogen arsenate (lead arsenate) or calcium arsenate. These compounds were used for much of the 20th century as a pre-harvest pesticide to control pests of fruit crops (primarily apples), such as codling moth, apple maggots, and fruit fly. While widespread use of these pesticides ceased in 1970, lead and calcium arsenate are stable and persist in soil, so may still affect crops grown in contaminated soil long after application has ceased.

As speciation is important in food safety because the toxicity of the element is strongly dependent on the chemical form or species in which it occurs. Inorganic arsenic species, arsenite (As(III)) and arsenate (As(V)) are known to be highly toxic and carcinogenic, whereas the organic As species monomethylarsonic acid (MMA) and dimethylarsinic acid (DMA) are less toxic, and arsenobetaine (AB) is considered to be non-toxic. Levels of inorganic As are therefore routinely monitored in many sample types including drinking water, food and beverages, pharmaceuticals, and petrochemicals.

Separation of the various As-containing species by HPLC followed by detection using ICP-MS is well established as the analytical method of choice for many sample types, including drinking water and urine [1].

In this study, a novel sample preparation method involving simple filtration and dilution in deionized water was developed for fast, routine measurement of low levels of As species in apple juice. The established and proven method from Reference 1 was used to separate and quantify the five As species discussed above in six commercial apple juices, to determine whether this commonly consumed fruit juice contains arsenic species at potentially harmful levels.

The maximum contaminant level (MCL) for total As in drinking water has been established at 10 µg/L by the US Environmental Protection Agency (USEPA). But As in food must be considered as part of the total dietary intake, which is recommended by the USEPA and European Food Safety Authority to be between 0.8 and 8 µg/kg body weight per day. Other dietary sources of arsenic (in a normal diet) include seafood, rice and other sources.



## Experimental

### Sample preparation

Six different apple juice samples (Apple Juice #1 to #6) were purchased in a Japanese supermarket. The apple juice samples were filtered using two disposable filters (Millex-LH, Millipore, USA, followed by TOYOPAK ODS M, TOSHO, Japan). The Millex-LH filter was used to remove the solid materials contained in the apple juice, and the TOYOPAK ODS M filter was then used to remove non-polar compounds, to avoid overloading the HPLC column. Both filters were washed and activated according to the manufacturers' instructions. After filtration, the apple juice samples were diluted by a factor of two with ultrapure water. Aggressive sample digestion and large dilution factors were avoided in order to minimize species inter-conversion and ensure the lowest possible detection limits in the original samples.

In order to assess the method capability for accurate low-level measurement of As species, the potential for As species contamination during sample preparation was evaluated. Preparation blank samples were prepared as follows to identify any possible contamination arising from the different sample preparation steps:

1. Deionized water blank
2. Millex membrane filter blank
3. TOYOPAK ODS filter blank
4. Method blank (de-ionized water filtered twice as for samples).

All four preparation blank samples were measured using the established chromatography column, mobile phase and HPLC method from Reference 1, and the chromatograms obtained are shown in Figure 1. The chromatograms for the four preparation blanks are shown overlaid with a mixed As species standard (50 ng/L (ppt) each species), confirming that no detectable levels of As were present in the preparation blanks.

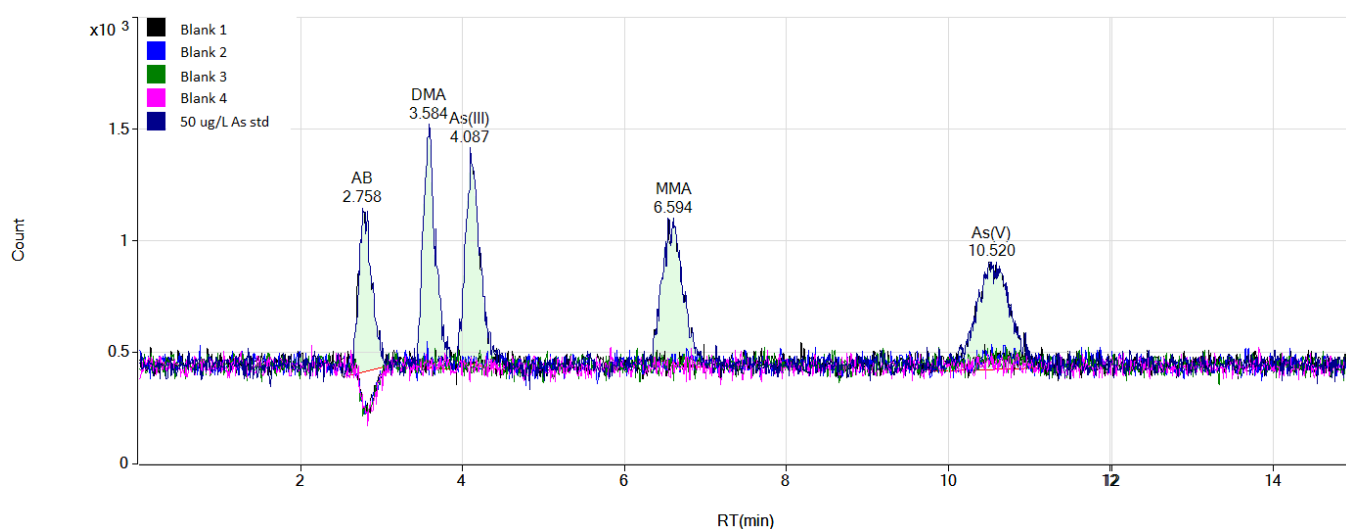


**Figure 1.** Evaluation of preparation blanks, confirming undetectable levels of As species contamination from the reagents and sample preparation filters. All four blanks are shown, overlaid with 50 ng/L (ppt) mixed As species standard.

It should be noted that the first peak that elutes is arsenobetaine (AB), which is not retained on the column and so elutes in the void volume, where it might also co-elute with other neutral or cationic species that are not retained on the column. While AB can be measured using the LC-ICP-MS method described, the results may be biased if other co-eluting species are present in the sample; but this limitation is not a problem for food safety applications, since AB is considered to be non-toxic even at very high concentrations.

For the purposes of food safety, the critical species that must be separated and quantified accurately and at low level are As(III) and As(V), the sum of which can be reported as 'total inorganic arsenic'.

## Instrumentation

An Agilent 1290 Infinity LC system comprising a binary pump, autosampler and vacuum degasser was coupled to an Agilent 8800 Triple Quadrupole ICP-MS (ICP-QQQ). An anion exchange guard column (Agilent part number G3154-65002, 4.6 mm id x 10 mm polymethacrylate) followed by As speciation column (Agilent part number G3288-80000, 4.6 mm id x 250 mm polymethacrylate) were used for separation. The columns were maintained at ambient temperature for all experiments. HPLC and ICP-MS parameters are shown in Table 1.

**Table 1.** Operating conditions and parameters of the Agilent 1290 LC and 8800 ICP Triple Quad

1290 Infinity LC	
Condition	Value
Column	G3154-65002 (guard column), G3288-80000, 4.6 x 250 mm (analytical column)
Mobile phase	2.0 mM PBS / 0.2 mM EDTA/10 mM CH <sub>3</sub> COONa / 3.0 mM NaNO <sub>3</sub> / 2% EtOH pH 11.00 adjusted with NaOH
Flow rate	1.0 mL/min
Temperature	Ambient
Injection volume	100 µL
8800 ICP Triple Quad	
Parameter	Value
RF power	1550 W
Carrier gas flow rate	1.05 L/min
Spray chamber temperature	2 °C
Sampling depth	10 mm
Exact 1 lens	0 V
Quadrupole mode	Single quad mode
Cell gas mode	No gas

The routine separation and analysis of As species does not require the use of ICP-QQQ to resolve interferences, as potential polyatomic overlaps on As (m/z 75) are resolved by the chromatography. As previously reported in Reference 1, the inorganic chloride elutes between the As(III) and MMA peaks and so the ArCl<sup>+</sup> polyatomic ion formed from the chloride does not affect any of the As compounds of interest.

However, the interest in As speciation in food and beverages extends to the measurement of the toxic inorganic compounds at extremely low concentrations (low ng/L or ppt levels) and the enhanced sensitivity and very low background of the Agilent 8800 ICP-QQQ compared to conventional quadrupole ICP-MS may therefore be beneficial. If slightly higher detection limits are acceptable within the method requirements, the sample preparation and HPLC method described here is completely transferable without any modification to the Agilent 7700 Series ICP-MS, which offers around 2x lower sensitivity, but detection limits still in the low tens ng/L (ppt) range.

## Results and discussion

Detection limits for each arsenic species were calculated as three times the chromatographic peak-to-peak signal-to-noise (S/N) ratio, alternatively sometimes expressed as the analyte concentration that would give a S/N of 3. The detection limits of all five As species were between 10 ng/L and 22 ng/L as summarized in Table 2. Figure 2 shows the 500 ng/L As species standard used for the S/N and LOD calculation, illustrating the good sensitivity and peak separation of the five As species studied.

The calibration concentration range was from 10 ng/L to 500 ng/L, showing linear response for each As species, as illustrated in Figure 3.

**Table 2.** 3x S/N detection limits for arsenobetaine (AB), dimethylarsinic acid (DMA), As(III) (arsenite), monomethylarsonic acid (MMA), and As(V) (arsenate). \* Arsenobetaine (AB) elutes in the void volume and cannot be reliably quantified in the presence of some other co-eluting species.

Compound	RT (min)	Height	Area	Noise	S/N	LOD (ng/L)	Noise type
AB*	2.823	19584	249584	153	127.99	11.72	Peak-to-peak
DMA	3.602	22117	277103	153	144.54	10.38	Peak-to-peak
As(III)	4.128	18022	265346	153	117.78	12.74	Peak-to-peak
MMA	6.566	14421	299863	153	94.24	15.92	Peak-to-peak
As(V)	10.431	10265	329325	153	67.08	22.36	Peak-to-peak

Full Time Range EIC(75) : 008CAL.S.d

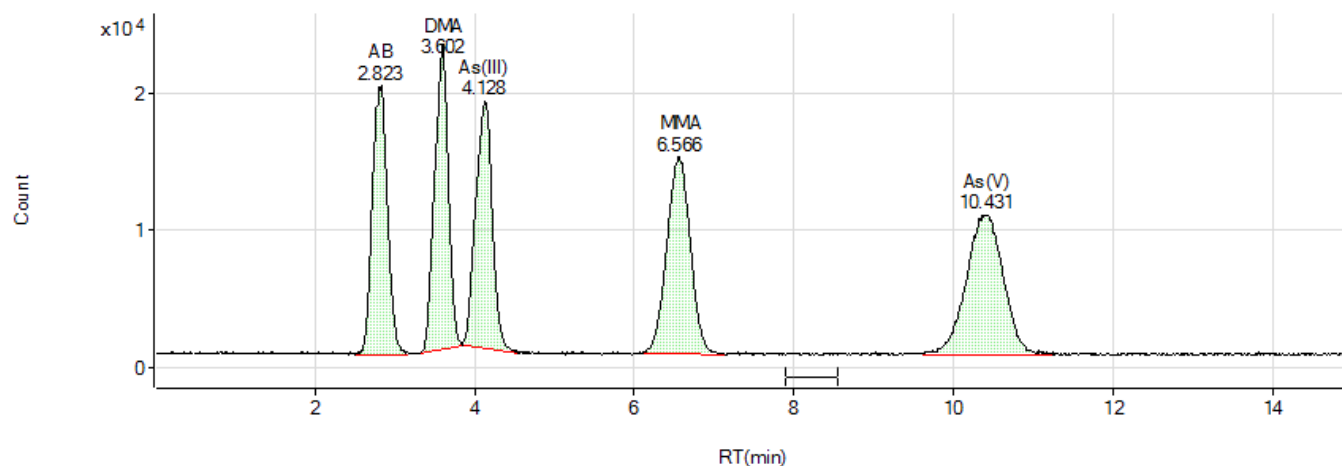


**Figure 2.** Chromatogram of 500 ng/L (ppt) mixed As species standard showing good sensitivity and peak separation, and noise region used for S/N and LOD calculation.

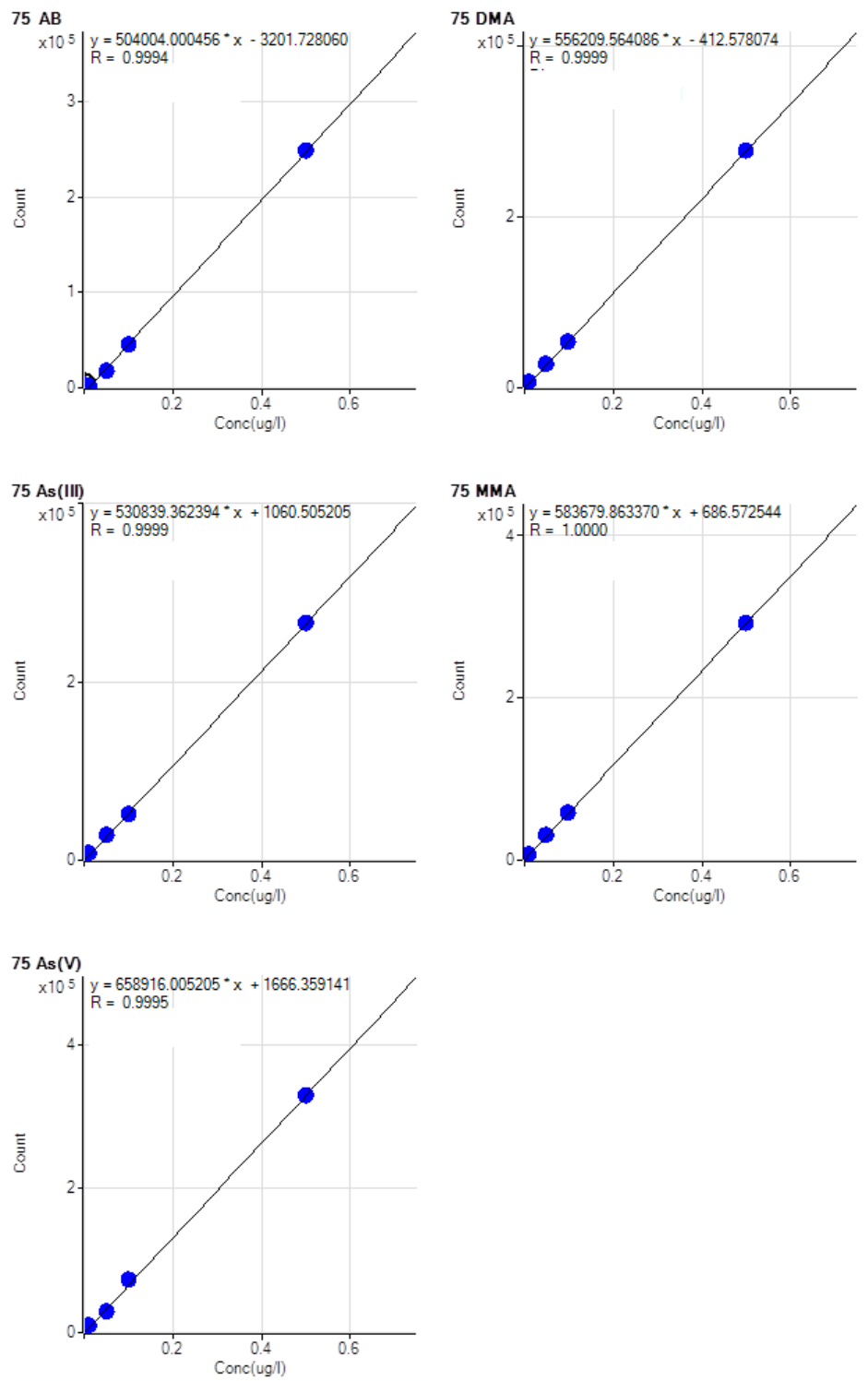


Figure 3. Calibration graphs for AB, DMA, As(III), MMA, and As(V).

## Results of apple juice analysis

The As concentrations determined in the six different apple juices are summarized in Table 3 (the 2x dilution factor has been applied to the results), and the chromatograms are displayed in Figure 4. From the concentration results it is clear that, while the majority of the As was in the toxic inorganic forms, all of the apple juice samples contained much lower levels of total As than the USEPA drinking water limit of 10 µg/L. The chromatograms in Figure 4 are all shown on the same intensity scale, to highlight the different relative concentrations of each species.

Although As species were found in all six apple juices, both the total As concentration and the relative concentrations of the different species varied among them. However the total concentration of arsenic (sum of all species) was below 5 µg/L in all tested juice samples, a level less than half the USEPA maximum contaminant level for drinking water (10 µg/L). The total inorganic As (sum of As(III) and As(V)) was less than 3 µg/L in all samples, and below 2 µg/L in five of the six apple juice samples measured.

## Spike recovery test and reproducibility

In order to validate the method performance in real samples, a spike recovery test was performed using the mixed As species standard solution. Apple juice sample #1 was spiked with the As species standard at a level of 500 ng/L in the 2x diluted sample. The spiked sample was analyzed repeatedly as an unknown, with seven separate injections being measured in total. Table 4 shows the retention time (RT) and concentration results for all the As species, indicating the excellent reproducibility of both the RT and concentration for the seven separate analyses. The %RSDs for all As species were less than 0.5% for retention time and less than 1.6% for concentration. The overlaid chromatograms of all seven injections are shown in Figure 5.

## Conclusions

Five arsenic species including the toxicologically relevant inorganic forms As(III) and As(V) were determined at low- and sub-µg/L concentrations in commercially available apple juice, using an Agilent 1290 Infinity LC coupled to an Agilent 8800 ICP-QQQ. Detection limits of between 10 and 20 ng/L (ppt) were obtained for all As species following a simple filtration and 2x dilution of the apple juice samples. Arsenic (As) species were detected in all of the apple juice samples measured, although the concentrations of the different species varied among the brands. None of the samples analyzed in this study contained more than 5 µg/L total As, and the level of inorganic As (sum of the As(III) and As(V) species) was below 3 µg/L in all samples and below 2 µg/L in five of the six brands analyzed.

On the basis of this small sample size of apple juice brands available in Japan, our data supports the current US Food and Drug Administration (FDA) advice that commercial apple juice does not pose a significant risk to health from raised levels of inorganic As. Our results for apple juice available in Japan confirm the findings of the FDA's monitoring program in the US, that the level of inorganic As is below the 10 µg/L drinking water limit in all apple juice samples tested.

## Reference

1. Tetsushi Sakai and Steve Wilbur, Routine Analysis of Toxic Arsenic Species in Urine Using HPLC with ICP-MS, Agilent publication 5989-5505EN.

**Table 3.** Quantitative results (µg/L) for all five As species in six commercial brands of apple juice measured by LC-ICP-QQQ

Sample name	Dilution	Concentration µg/L						Total As
		AB	DMA	As(III)	MMA	As(V)	Inorganic As	
Apple Juice 1	2	0.069	0.196	0.704	0.033	0.631	1.335	1.600
Apple Juice 2	2	0.066	0.037	0.062	0.006	0.008	0.070	0.173
Apple Juice 3	2	0.063	0.292	0.847	1.633	0.827	1.674	3.662
Apple Juice 4	2	0.052	0.276	1.014	1.475	1.977	2.991	4.794
Apple Juice 5	2	0.067	0.225	1.196	0.795	0.724	1.920	3.007
Apple Juice 6	2	0.043	0.254	1.218	0.005	0.095	1.313	1.610

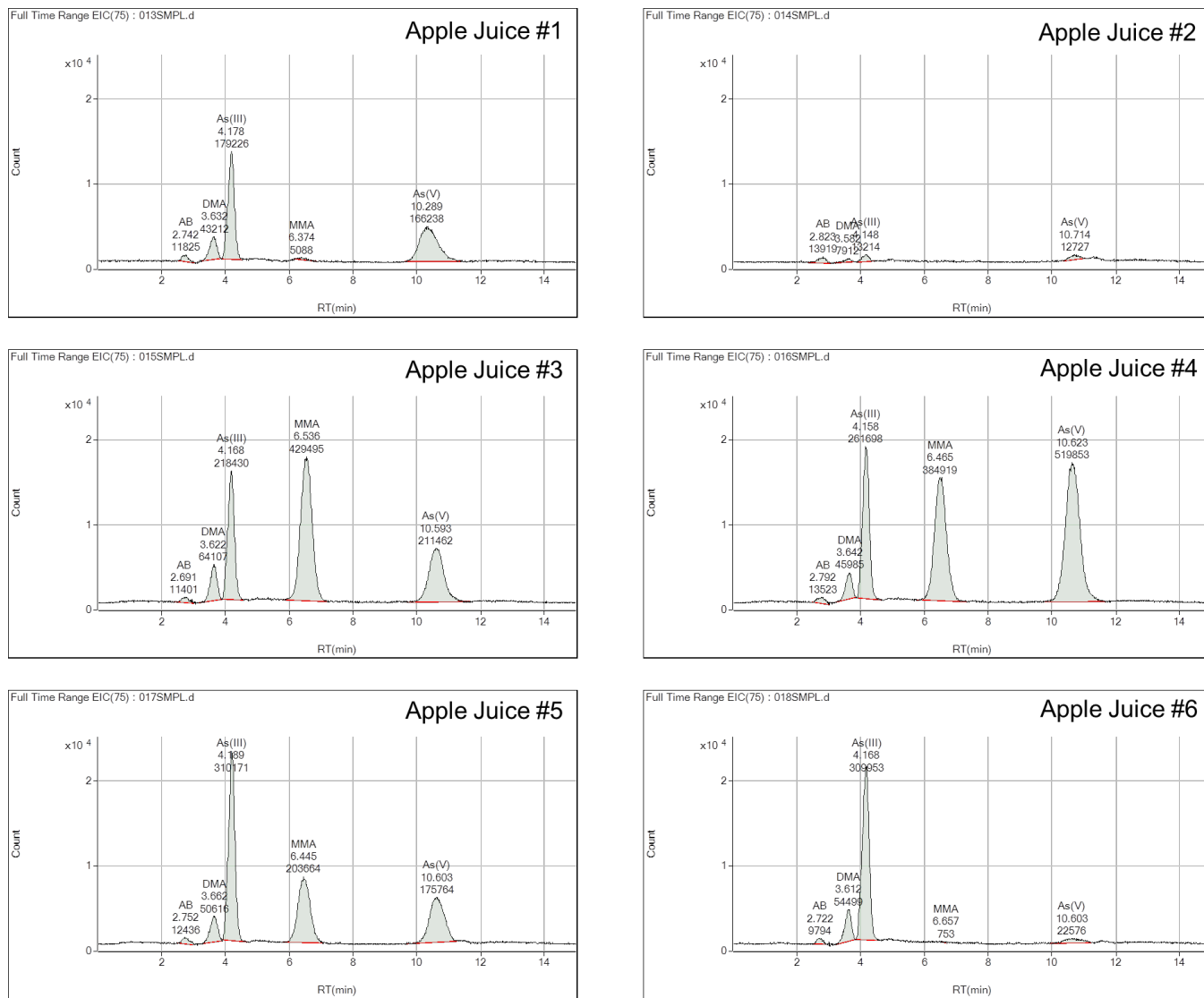


**Figure 4.** Chromatograms of As species in six apple juice samples.

**Table 4.** Results of spike recovery (n = 7) of 1 µg/L standard added to the Apple Juice #1

Sample name	AB RT (min)	Conc. (µg/L)	DMA RT (min)	Conc. (µg/L)	As(III) RT (min)	Conc. (µg/L)	MMA RT (min)	Conc. (µg/L)	As(V) RT (min)	Conc. (µg/L)
Apple Juice 1 Spike 1	2.77	0.848	3.62	1.112	4.19	1.606	6.43	0.980	10.62	1.524
Apple Juice 1 Spike 2	2.76	0.862	3.61	1.116	4.19	1.632	6.43	0.996	10.63	1.560
Apple Juice 1 Spike 3	2.77	0.872	3.61	1.125	4.19	1.621	6.41	1.007	10.62	1.551
Apple Juice 1 Spike 4	2.77	0.886	3.61	1.122	4.18	1.632	6.41	1.003	10.63	1.554
Apple Juice 1 Spike 5	2.78	0.882	3.61	1.134	4.19	1.643	6.41	1.008	10.65	1.561
Apple Juice 1 Spike 6	2.78	0.873	3.61	1.146	4.17	1.637	6.37	1.016	10.68	1.597
Apple Juice 1 Spike 7	2.78	0.881	3.60	1.145	4.17	1.651	6.35	1.018	10.69	1.588
Average	2.78	0.872	3.61	1.128	4.18	1.632	6.41	1.004	10.65	1.562
Standard deviation	0.0076	0.0133	0.0058	0.0135	0.0096	0.0148	0.0306	0.0130	0.0291	0.0242
%RSD	0.28	1.53	0.16	1.20	0.23	0.91	0.48	1.29	0.27	1.55

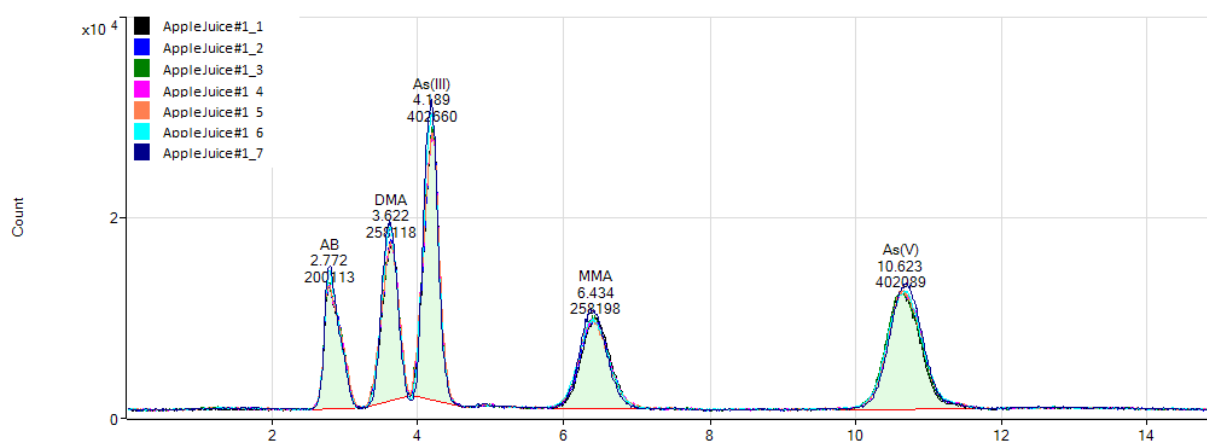


**Figure 5.** Seven overlaid chromatograms of Apple Juice #1, spiked with 500 ng/L As standard.

# Speciated Arsenic Analysis in Wine Using HPLC-ICP-QQQ

## Authors

C. K. Tanabe<sup>1</sup>, H. Hopper<sup>1,2,3</sup>,  
S. E. Ebeler<sup>1,2</sup>, J. Nelson<sup>1,2,4</sup>

1. Dept. Viticulture & Enology,  
University of California (Davis), USA

2. Food Safety & Measurement Facility,  
University of California, (Davis), USA

3. Depart. of Food Science, The  
Pennsylvania State University,  
Pennsylvania, USA

4. Agilent Technologies, USA

## Validation of an extended FDA Elemental Analysis Manual method

### Introduction

In 2013, the US Food and Drug Administration (FDA) released Elemental Analysis Manual (EAM) Method §4.10. The method describes the Determination of Four Arsenic Species in Fruit Juice using High-Performance Liquid Chromatography-Inductively Coupled Plasma-Mass Spectrometry [1]. To extend the method to include wine, a multi-laboratory validation (MLV) of the method was carried out with three US-based laboratories sharing their data [2]. The data shown in this application note is supplementary to the published data. In addition to the paper, this note includes long term stability of the method, and extended quantitative analysis of five commercially available wines. The method required separation and analysis of all target species. This approach differs from another Agilent application note, which focused on the development of a fast method for inorganic arsenic (iAs) [3].

The US Environmental Protection Agency (EPA) set a maximum threshold of total As in drinking water of 10 µg/kg [4]. There is no equivalent US regulation for As in wine. Studies have shown that As in wine can be the result of an accumulation of As in the grapes from the environment [5] or introduced during the wine making process [6].

Regulations in Canada (Vintners Quality Alliance VQA, Ontario) and Europe (International Organisation of Vine and Wine, OIV) specify limits for total As of 100 µg/L and 200 µg/L, respectively [7, 8]. However, the toxicity of As is determined by its chemical form. Because the inorganic forms of As (iAs) are the most carcinogenic, the FDA has established an action limit for iAs in apple juice of 10 µg/kg in 2013 [9]. FDA EAM Method §4.10 details a relatively simple and robust method for the determination of As species in fruit juice using HPLC-ICP-MS [1]. The method describes a procedure to determine iAs (the sum of arsenite, As(III), and arsenate, As(V)); dimethylarsinic acid (DMA); and monomethylarsonic acid (MMA). The method also states that a solution containing arsenobetaine (AB) and As(III) is analyzed to demonstrate adequate separation between unretained arsenic-containing species and As(III).

Due to recent media attention on As levels in wine, and the lack of published research on As speciation in wine, extension of EAM §4.10 to include wine is a logical next step.



In this study, EAM §4.10 was modified for the determination of the main organic arsenic species (DMA and MMA) and the more toxic inorganic forms (As(V) and As(III)) in wine using HPLC coupled to a triple quadrupole ICP-MS (ICP-QQQ). The ICP-QQQ was utilized to provide the highest possible sensitivity of all the instruments available in the lab at UC Davis. ICP-QQQ also provides superior resolution of potential spectral interferences, but the potential CI-based interferences on  $^{75}\text{As}$  are resolved chromatographically, so QQQ with MS/MS is not essential. This application could also be done on a single quadrupole ICP-MS such as the Agilent 7800 or 7900.

## Experimental

### Reagents

Arsenite (As(III)) and arsenate (As(V)) were bought as 1000 mg/L standard solutions from Spex Certiprep (Metuchen, NJ, USA). Monomethylarsonic acid (MMA, 98.5% purity) and dimethylarsinic acid (DMA, 98.9% purity) were bought from Chem Service (West Chester, PA, USA). Arsenobetaine (AB, purum p.a.,  $\geq 95.0\%$ ) was bought from Fluka Analytical (Morris Plains, NJ, USA).

### Samples and sample preparation

Five commercially available wine samples were bought from a local store in Davis, California. The wines were selected to represent the main types (and styles) of wine: red (Cabernet Sauvignon), white (Sauvignon blanc), rosé (Zinfandel), sparkling (sparkling white) and fortified (Port-style). To investigate the range of ethanol content that could be analyzed using the method, the alcohol concentrations of the wines selected ranged from 9.5–20% (v/v).

The sample preparation and analysis details were carried out according to the EAM §4.10 method. Each wine sample was diluted five times with de-ionized water and then filtered separately using syringe-filtration (0.45  $\mu\text{m}$  PVDF membrane).

Per EAM §4.10, calibration curves were prepared at nominal concentrations of 0.4, 0.5, 1, 5, 10, 20, 40  $\mu\text{g}/\text{kg}$  for the four arsenic species: As(III), DMA, MMA, and As(V). However, for this method, a fifth, low-level calibration point was also prepared at 0.1  $\mu\text{g}/\text{kg}$ . NIST 1643e Trace Elements in Water standard reference material (SRM), used to assess recovery and stability, was prepared using a 15-fold dilution. All calibration standards and the SRM were prepared in a 3% ethanol solution to approximately match the level of alcohol (carbon matrix) in the diluted wine samples. In addition to the effect that a change in sample viscosity has on sample transport and nebulization, the level of carbon also affects (increases) the degree of ionization of some elements in the ICP, including arsenic. Therefore, sample preparation for carbon-containing matrices should ensure a reasonably consistent level of carbon across all samples and standards, to avoid errors due to variable carbon enhancement in different sample solutions.

## Instrumentation

An Agilent 1260 Infinity LC comprising a binary pump, autosampler, and vacuum degasser was coupled to an Agilent 8800 Triple Quadrupole ICP-MS (ICP-QQQ). HPLC and ICP-QQQ parameters are shown in Table 1.

**Table 1.** HPLC-ICP-QQQ hardware system and operating conditions.

LC conditions	Value
Column	Hamilton PRP-X100 anion exchange (4.1 x 250 mm) column with a matching Hamilton PRP-X100 guard column
Mobile phase	Mobile phase, aqueous 10 mM ammonium phosphate dibasic, 1% ethanol, pH 8.25 ( $\pm 0.05$ )
Flow rate (mL/min)	1.0
Temperature	Ambient
Injection volume ( $\mu\text{L}$ )	100
Column compartment time table for introduction of ISTD	0.1 min, column position 1, 1.0 min; switch to column position 2, 2.0 min; switch back to column position 1
ICP-QQQ parameters	Value
RF power (W)	1550
Carrier gas flow (L/min)	1.0
Spray chamber temperature ( $^{\circ}\text{C}$ )	2
Sample depth (mm)	8.5
Peristaltic pump speed (rps)	0.3 (~1.2 mL/min)
Scan mode	MS/MS
Helium cell gas flow (mL/min)	~2.0

## Results and discussion

Method blanks (3% ethanol) spiked with low levels of As(III), DMA, MMA, and As(V) were prepared and analyzed for the determination of the detection limits.

Figure 1 shows overlaid chromatograms obtained for the mixed As species standards, demonstrating excellent peak separation of the As species of interest. The calibration curves in Figure 2 show a linear response for each As species across the concentration range from 0.1 to 40  $\mu\text{g}/\text{kg}$ .

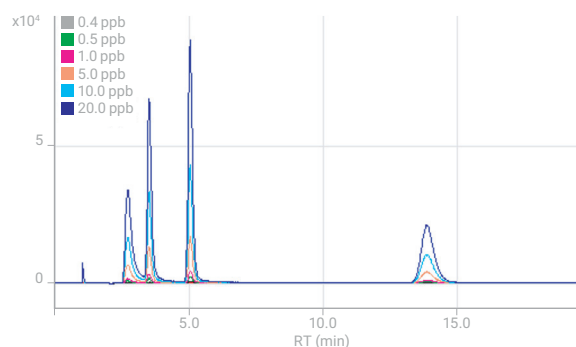


**Figure 1.** Overlaid chromatograms of As species standards at nominal concentrations of 0.4, 0.5, 1, 5, 10, 20  $\mu\text{g}/\text{kg}$  showing good peak separation. The 40  $\mu\text{g}/\text{kg}$  standard is not shown, to allow the lower concentration levels to be seen.

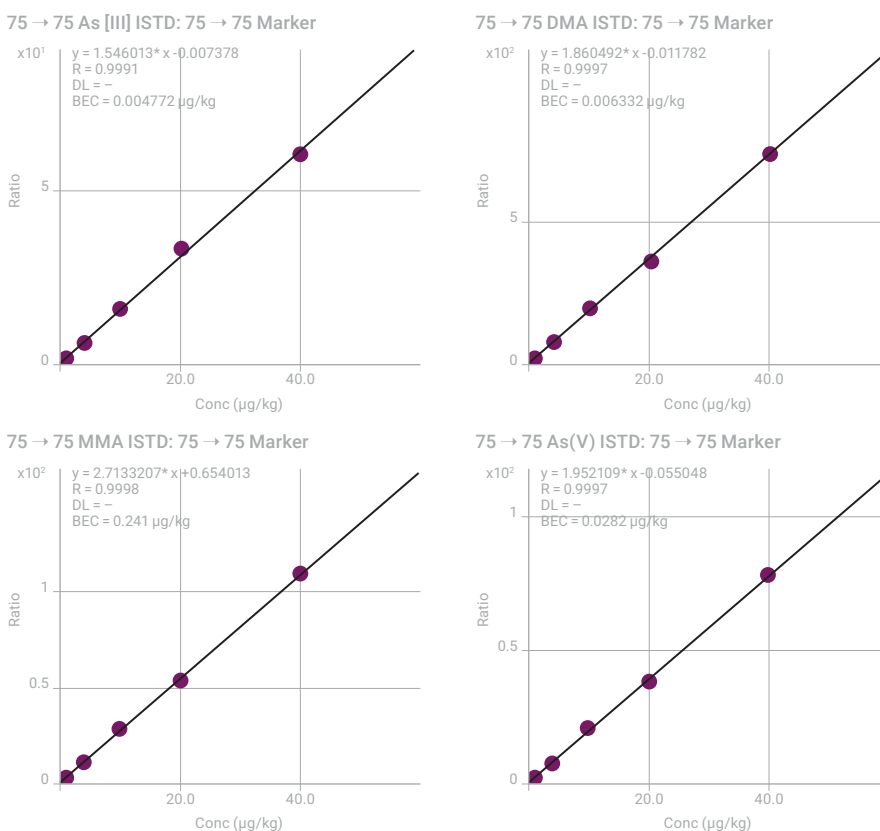


**Figure 2.** Calibration graphs for As(III), DMA, MMA, and As(V).

The limits of detection (LOD) for the As species in wine were calculated as described in the FDA's Elemental Analysis Manual Section 3.2 [1]. The limits of quantification (LOQ) for each species were calculated as  $LOQ = \text{Dilution Factor (DF)} \times 30 \times \sigma$ . The LOQs for As(III) and As(V) were 1.18 and 1.35  $\mu\text{g/kg}$ , respectively. The LOQ for total inorganic arsenic (calculated from the SD of the sum of the integrated peak areas for As(III) and As(V) in each repeat of the low standard) was 2.53  $\mu\text{g/kg}$ . The LODs and LOQs determined for the species DMA, MMA, and total iAs (sum of As(III) and As(V)) using the optimized method are given in Table 2. Results are reported for iAs since the current regulations only specify iAs, and not the individual species As(III) and As(V).

**Table 2.** LODs and LOQs for DMA, MMA, and iAs.

	LOD, $\mu\text{g/kg}$	LOQ, $\mu\text{g/kg}$
DMA	0.17	1.3
MMA	0.15	1.2
iAs	0.17	1.4

The iAs LOQ is well within the FDA's 10  $\mu\text{g/L}$  level of concern for iAs in juice samples. The sensitivity of the method is therefore sufficient to determine iAs in solution following a five-fold dilution of the samples.

### Quantitative results

The five wines included in the MLV were analyzed in the lab at UC Davis using LC-ICP-QQQ and the results are shown in Table 3. The average percent recovery of the sum of the species compared to the total As present in the samples (determined using direct analysis without HPLC separation) was calculated using the mass balance approach. The percent recovery for all samples was between 91–107%. The results were found to be in good agreement with the results obtained from the other laboratories taking part in the MLV study [2].

**Table 3.** Quantitative results for the five wines analyzed at UC Davis as part of the MLV study. Average  $\pm 1\sigma$ , n=3 for the individual species

Wine sample	% Ethanol (v/v)	DMA $\mu\text{g}/\text{kg}$	MMA $\mu\text{g}/\text{kg}$	iAs $\mu\text{g}/\text{kg}$	Sum of species $\mu\text{g}/\text{kg}$	Total As $\mu\text{g}/\text{kg}$	Mass balance %
Red (Cabernet)	9.5	0.81 $\pm$ 0.1*	<LOD	14.4 $\pm$ 1.0	15.2 $\pm$ 1.1	15.3 $\pm$ 1.2	99
White (Chardonnay)	13	0.74 $\pm$ 0.04*	<LOD	10.7 $\pm$ 0.2	11.4 $\pm$ 0.2	11.1 $\pm$ 0.8	103
Rosé (Zinfandel)	12	0.75 $\pm$ 0.1*	<LOD	9.2 $\pm$ 0.4	9.9 $\pm$ 0.4	9.3 $\pm$ 1.1	107
Sparkling wine	20	1.7 $\pm$ 0.1	<LOD	2.1 $\pm$ 0.3	3.8 $\pm$ 0.3	3.6 $\pm$ 0.3	105
Port-style wine	14.5	0.45 $\pm$ 0.01*	<LOD	1.5 $\pm$ 0.3	2.0 $\pm$ 0.3	2.2 $\pm$ 0.1	91

\* Value between LOD and LOQ

Reprinted with permission from Courtney K. Tanabe et al., J. Agric. Food Chem., 2017, 65 (20), 4193–4199. Copyright 2017. American Chemical Society.

### Long-term stability

To test the stability of the ICP-QQQ over an extended sampling period of 96 hours (four days), the wine samples were measured repeatedly in a continuous sequence. Two quality control (QC) samples—a 2-ppb mixed As species standard solution and NIST 1643e spiked with 3% ethanol— were analyzed after every 10 wine samples. The instrument was not recalibrated during the continuous analytical run. The plots shown in Figures 3 and 4 show exceptional stability was achieved over the course of the validation stability test.

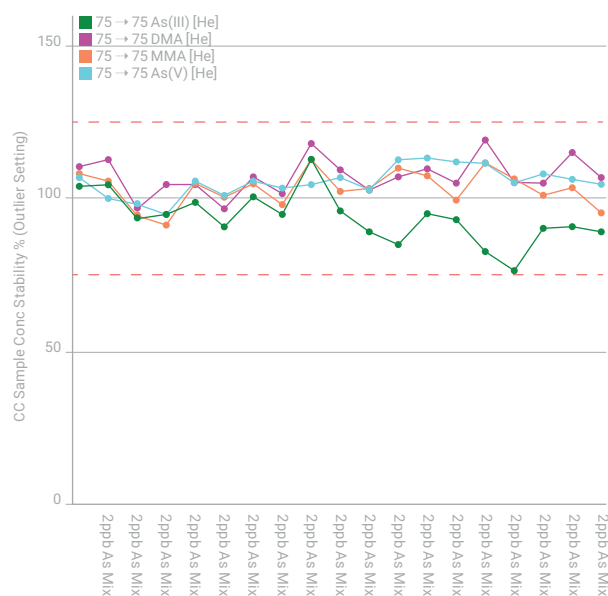


**Figure 3.** Stability plot of the 2-ppb mixed As species standard solution, analyzed over 96 hours (four days).

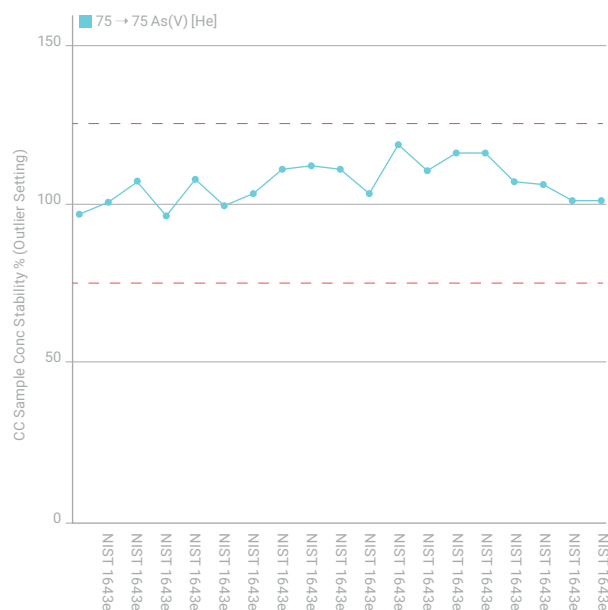


**Figure 4.** Stability plot of As in NIST 1643e spiked with ethanol and analyzed over four days.

### Results of additional market basket wine analysis

In addition to the five wines used in the MLV study, an extra 60 wines were analyzed as part of the method validation [2]. In this study, a selection of previously untested wines (S1 to S5) were analyzed. The results shown in Table 4 are consistent with the published data from the reference paper [2]. Most of the As was in the more toxic, inorganic forms. While four of the five wine samples contained levels of total As higher than the EPA drinking water limit of 10 µg/L, the levels in all five wines were below the 100 and 200 µg/kg limits for total As in wine set in Canada and Europe, respectively. However, the measured concentrations for iAs in four out of five of the wines exceeded the FDA’s action limit of 10 µg/kg for iAs in apple juice.

**Table 4.** Quantitative results (µg/kg) for As species in five commercially available wines measured by LC-ICP-QQQ.

Wine Sample	iAs	DMA	MMA	Sum of Species
S1	17.13 ± 0.22	0.83 ± 0.03	<LOD	17.96 ± 0.13
S2	7.49 ± 0.15	0.30 ± 0.06	0.77 ± 0.32	8.56 ± 0.17
S3	14.63 ± 0.40	0.80 ± 0.08	<LOD	15.43 ± 0.24
S4	25.03 ± 0.89	0.69 ± 0.26	0.47 ± 0.12	26.19 ± 0.42
S5	23.45 ± 1.12	0.32 ± 0.05	<LOD	23.77 ± 0.59

### Spike recovery test

Table 5 shows the spike recoveries for the MLV samples fortified at levels of approximately 5, 10, and 30 µg/kg for DMA, MMA, and iAs (the iAs spike concentration was the sum of As(III) and As(V) each spiked at 50% of the levels shown). The average recoveries of DMA, MMA, and iAs measured using LC-ICP-QQQ were 99, 92, and 104%, respectively. All the recoveries are within the FDA’s EAM acceptability criteria of 100 ± 20% for iAs, DMA, and MMA [1].

**Table 5.** Average spike recovery results for duplicate analyses of five samples spiked at 5, 10, and 30 µg/kg with DMA, MMA, and iAs. n=30.

	DMA	MMA	iAs
Average spike recovery, %	99	92	104
Recovery range	93 – 107	72 – 119	97 – 114

## Conclusion

The As speciation results obtained using an Agilent 1260 Infinity LC coupled to an Agilent 8800 ICP-QQQ were used as part of an MLV to validate the extension of Elemental Analysis Manual Method §4.10 to include wine. The method was optimized for the analysis of four arsenic species including the toxicologically relevant inorganic forms, As(III) and As(V).

In addition to the data published as part of the MLV, five more wines were analyzed. The total As levels of the five wines were between 8.56 and 26.19 µg/L. These levels are below the Canadian and European regulatory limits for total As in wine of 100 and 200 µg/kg, respectively. The average percentage of As found in the form of iAs in the five wine samples was 95%.

## References

1. S. D. Conklin, K. Kubachka, N. Shockey, Elemental Analysis Manual for Food and Related Products, 4.10 HPLC-ICP-MS As Species in Fruit Juice (Ver. 1; 2013), <http://www.fda.gov/EAM> (accessed September 2017)
2. C. K. Tanabe, H. Hopfer, S. E. Ebeler, J. Nelson, S. D. Conklin, K. M. Kubachka, and R. A. Wilson, *J. Agric. Food Chem.*, **2017**, 65 (20), pp 4193–4199
3. C. K. Tanabe, S. E. Ebeler, J. Nelson, Fast Analysis of Arsenic Species in Wines using LC-ICP-QQQ, Agilent publication, 2017, [5991-8454EN](#)
4. National Primary Drinking Water Regulations. US E.P.A, In Title 40, EPA, Ed. 2014; Vol. AE 2. 106/3:40/
5. D. Bertoldi, R. Larcher, M. Bertamini, S. Otto, G. Concheri, G. Nicolini, *J. of Agri and Food Chem.*, **2011**, 59, 7224–7236.
6. M. V. Aguilar, M.C. Martinez, T.A. Masoud, Z. Lebensm-Unters-Forsch., 1987, 185, 185–187.
7. Canada Ontario, V. Q. A., Wine Standards. 1999 <http://www.vqaontario.ca/Regulations/Standards> (accessed August 2017)
8. OIV–Compendium of International Methods of Analysis. Maximum acceptable limits of various substances contained in wine, 2011 issue. Europe
9. US Department of Health and Human Services Food and Drug Administration Center for Food Safety and Applied Nutrition, Guidance for Industry Arsenic in Apple Juice: Action Level (draft), 2013. <https://www.fda.gov/RegulatoryInformation/Guidances/ucm360020.htm> (accessed September 2017)

## More information

For a full account of this study, see Courtney K. Tanabe, Helene Hopfer, Susan E. Ebeler, Jenny Nelson, Sean D. Conklin, Kevin M. Kubachka, and Robert A. Wilson, Matrix Extension and Multilaboratory Validation of Arsenic Speciation Method EAM §4.10 to Include Wine, *J. Agric. Food Chem.*, **2017**, 65 (20), pp 4193–4199, DOI: 10.1021/acs.jafc.7b00855

# Fast Analysis of Arsenic Species in Wines using LC-ICP-QQQ

## Authors

Courtney Tanabe<sup>1,2</sup>, Susan E. Ebeler<sup>1,2</sup>,  
Jenny Nelson<sup>1,3</sup>

1 Food Safety and Measurement  
Facility, University of California,  
Davis, USA

2 Department of Viticulture and  
Enology, University of California,  
Davis, USA

3 Agilent Technologies, Inc.,  
Santa Clara, USA

## Introduction

Arsenic (As) occurs naturally in the environment but human activity has contributed to the levels found in some locations. Man-made sources of As include industrial processes such as mining, smelting and power generation, as well as agricultural pesticides and timber preservatives [1]. Once contamination has occurred, As persists in the environment for decades. For example, the widespread use of As-containing agrochemicals ceased in the 1970s, but lead and calcium arsenate levels remain high in some soils. As can be absorbed from soil and water into crops. In the case of wine, the As content can also be affected by the wine making processes.

Arsenic exists in multiple forms in foods and beverages and not all forms have the same toxicity. The inorganic forms of As (iAs), comprising As(III) (arsenite) and As(V) (arsenate), are the most toxic, and are categorized as class 1 carcinogens. In contrast, arsenobetaine (AB), the most abundant form of As in fresh seafood, is essentially non-toxic to humans. Due to the high variability in the toxicity of the different species of As, and the potential health threat of iAs, it is important to determine the levels of the individual species in foodstuffs – and not just the total As concentration. The US Food and Drug Administration (FDA) has established an action limit for iAs in apple juice of 10 µg/kg (ppb) [2] but there are currently no regulations in the US controlling the As content of wine. Canada (Vintners Quality Alliance VQA, Ontario) and Europe (International Organisation of Vine and Wine, OIV) have set maximum acceptable limits for total As in wine of 100 and 200 µg/L (ppb), respectively [3, 4].

Arsenic contamination of food is of great public interest. There is a clear demand for rapid and reliable screening methods to accurately determine the levels of iAs in food and drink to support existing and future regulations. One of the most useful and reliable approaches uses high performance liquid chromatography (HPLC) to separate the species, which are then quantified by inductively coupled plasma mass spectrometry (ICP-MS) [5].

The methodology described here is based on a previous As speciation method developed by Jackson, who coupled HPLC to a triple quadrupole ICP-MS (ICP-QQQ) [6]. HPLC-ICP-QQQ was also used in this study. However, instead of analyzing the iAs species separately, As(III) was intentionally oxidized to As(V) with hydrogen peroxide before analysis [7, 8]. By converting As(III) and analyzing all inorganic species as As(V), this method was able to separate monomethylarsonic acid (MMA) and dimethylarsinic acid (DMA) from iAs (as As(V)) in less than 2 minutes. The analysis time is 10 times faster than the current FDA methods used for the speciation of As [9].

In this work, oxygen reaction gas was used in the collision/reaction cell (CRC) of the ICP-QQQ to resolve the spectral interferences on <sup>75</sup>As, while maintaining excellent sensitivity. Results are presented that demonstrate the accuracy and reproducibility of the new method. The method was further validated using a wine matrix that was analyzed by two participating laboratories.

## Experimental

### Standards

The As(III) and As(V) standards were purchased from Spex Certiprep (Christiansburg, VA; Metuchen, NJ, USA). The MMA and DMA standards were purchased from Chem Service (West Chester, PA, USA). An AB standard was also purchased from Chem Service to be used as a flow injection marker (internal standard) for post-column injection. Calibration standards were prepared at 0.1, 0.5, 1.0, 5.0, 10 and 20 µg/L (ppb) for each of DMA, MMA, and total iAs (sum of As(III) and As(V)).

### Samples

Five different California wines were used for the validation (V) study. Each wine represented one of the five main styles of wine: red, white, rosé, sparkling, dessert. Five additional California wines were analyzed for a commercial market basket (MB) study. Details of the wine style, cultivar, growing region, vintage, and alcohol content for all samples are given in Table 1.

**Table 1.** Wine style, cultivar, regional origin, vintage, and alcohol content of the wine samples for the validation and commercial market basket studies.

Sample	Style	Cultivar	Region	Vintage	Alcohol (%v/v)
V-1	Rosé	Zinfandel	Napa and Lodi	NA	9.5
V-2	White	Sauvignon blanc	Oakville/Napa County	2013	13.0
V-3	Sparkling	Sparkling white blend	County	NA	12.0
V-4	Dessert	Petite Sirah Port-style	Clarksburg/Yolo County	2012	20.0
V-5	Red	Cabernet Sauvignon	Monterey County	2013	14.5
MB-1	Red	Cabernet Sauvignon	North Coast	2009	13.5
MB-2	Red	Pinot noir	Appellation Central Coast	2004	13.8
MB-3	White	Chardonnay	Santa Barbara County	2013	13.5
MB-4	Rosé	Zinfandel	Napa and Sonoma	2013	10.5
MB-5	White	Chardonnay	Central Coast	2013	13.5

### Sample preparation

H<sub>2</sub>O<sub>2</sub> was added to all samples at a 1:1 ratio to oxidize As(III) to As(V). Each sample was further diluted with de-ionized water to give a total dilution factor of 5 or 6 (there were no differences in results between the two dilution factors). Each sample was then passed through a 0.45 µm syringe filter to remove any particulates. Samples V-1, V-4, V-5 were spiked in duplicate with all As species at three concentration levels: 5, 10, and 30 µg/kg.

### Instrumentation

An Agilent 1260 HPLC fitted with a Hamilton PRP-X100 5 µm 50 x 2.1 mm column was coupled to an Agilent 8800 Triple Quadrupole ICP-MS (ICP-QQQ). The mobile phase was 40 mM ammonium carbonate ((NH<sub>4</sub>)<sub>2</sub>CO<sub>3</sub>, trace metal grade 99.999% from Sigma Aldrich) with 3% v/v methanol (Optima LC/MS grade, Fisher Chemical) adjusted to a pH of 9.0 with ammonium hydroxide (Optima Grade, Fisher Scientific). The ICP-QQQ was equipped with a standard sample introduction system comprising a quartz torch with 2.5 mm i.d. injector, a quartz spray chamber, glass concentric nebulizer, and nickel-tipped interface cones. Peak integration was carried out according to FDA EAM §4.10 and 4.11.15 [9]. The instrument operating conditions are summarized in Table 2.



**Table 2.** HPLC-ICP-QQQ operating conditions.

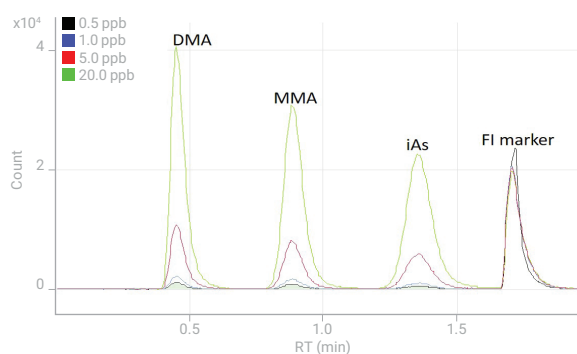
ICP-QQQ	
Forward power	1550 W
Sampling depth	8.0 mm
Spray chamber temp.	2 °C
Carrier gas	0.95 L/min
Make-up gas	0.20 L/min
Extract 1	0 V
Octopole bias	-5.0 V
Energy discrimination	-7 V
Cell gas (O <sub>2</sub> ) flow rate	0.31 mL/min
Scan mode	MS/MS
Q1/Q2 mass	75/91 u
HPLC	
Mobile phase flow rate	0.5 mL/min
Injection volume	5 µL
Sample temperature	4 °C
ISTD injection volume	5 µL

## Results and discussion

### Development of a fast method

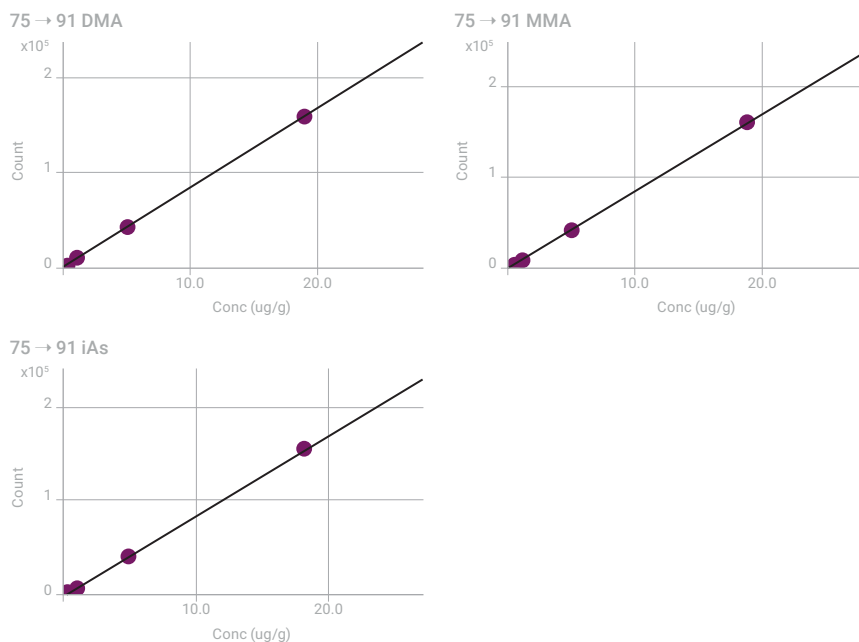
For this study, the focus of the method development was to reduce the analysis time per sample. In the development of this method, we followed Jackson's use of a small injection volume, short ion-exchange column, oxygen cell gas, and a high mobile phase linear velocity [6].

Figure 1 shows overlaid chromatograms for a representative calibration set of 0.5, 1.0, 5.0, and 20 µg/kg standards. All As species are clearly separated in less than two minutes. Simply by oxidizing As(III) to As(V) and analyzing all iAs in the form of As(V), the analysis time was reduced significantly compared to the current FDA regulatory method [9].

**Figure 1.** Overlay of the 0.5, 1.0, 5.0, and 20.0 µg/kg calibration standards. An AB internal standard (flow injection marker; fourth peak) was added post column via an external switching valve.

## Linear calibrations

The calibration curves for DMA, MMA, and iAs show good linearity (Figure 2). All As concentrations in the wine samples were within the linear range except iAs, which was measured at a maximum concentration of 150% of the highest calibration standard.



**Figure 2.** Calibration curves for DMA, MMA, and total iAs (sum of converted As(III) and As(V)).

## Detection limits

The limits of detection (LOD) and limits of quantitation (LOQ) given in Table 3 are based on repeated measurements of the 0.05  $\mu\text{g}/\text{kg}$  (ppb) mixed standard,  $n=15$ .

**Table 3.** LODs (3 sigma), LOQs (30 sigma), and estimated wine LOQ.

	LOD, $\mu\text{g}/\text{kg}$	LOQ, $\mu\text{g}/\text{kg}$	Estimated wine LOQ, (6 x dilution) $\mu\text{g}/\text{kg}$
DMA	0.018	0.175	1.1
MMA	0.026	0.258	1.5
iAs	0.022	0.221	1.3

## Spike recoveries

Samples V-1, V-4, V-5 were spiked in duplicate with each species (DMA, MMA, and total iAs as As(V)) at 5, 10, and 30  $\mu\text{g}/\text{kg}$ . The averaged recoveries for all As species at the three different fortification levels were  $100 \pm 3\%$  (Table 4).

**Table 4.** Percent recovery (mean and range) for three spiking levels of DMA, MMA and iAs in wines V-1, V-4 and V-5.

	DMA	MMA	iAs
Average, %	102	97	99
Range, %	97 – 107	91 – 102	95 – 103

## Quantitative results

All 10 wines were analyzed using the new HPLC-ICP-QQQ method. Table 5 lists the measured concentrations for DMA and iAs. All MMA values were below the calculated LOD (0.026 µg/kg) and could not be quantified. The measured concentrations using the new method were compared to the values obtained using the FDA EAM §4.10 extension method [10]. The agreement between the measurements was mostly within ±10%. iAs represented the majority of As in all wines, while only one wine sample (MB-3) contained DMA levels significantly above the LOQ of 1.1 µg/kg. A chromatogram of V-1 is shown in Figure 3.

Overall, the concentration of iAs ranged from  $1.7 \pm 0.3$  to  $32.9 \pm 0.8$  µg/kg (the latter being above the FDA's action limit for iAs in apple juice of 10 µg/kg). The sum of all As species (Table 5) ranged from a low of  $2.2 \pm 0.3$  µg/kg to a high of  $32.9 \pm 0.8$  µg/kg, which is under the Canadian limit of 100 µg/L and OIV limit of 200 µg/L.

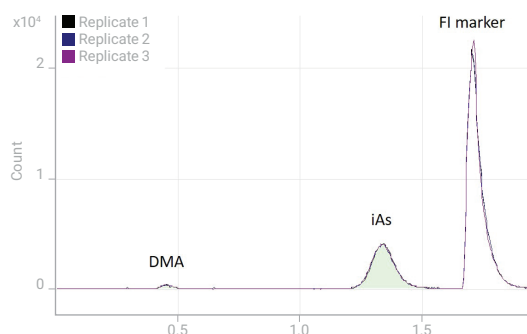


**Figure 3.** Chromatogram showing the overlay of the three replicates of wine sample V-1.

**Table 5.** Results from the fast and fit-for-purpose analysis method (measured at two different labs) compared to the FDA EAM §4.10 extension results for the five validation (V) and five market basket (MB) wines. % Recovery (shown in parentheses) calculated as “Measured” divided by “EAM §4.10” and “Sum of Species” divided by “Total”.

Sample	DMA (µg/kg)		iAs (µg/kg)		Total As (µg/kg)	
	EAM §4.10	Measured	EAM §4.10	Measured	Total	Sum of Species
V-1	0.81 ± 0.1*	0.72 ± 0.04 (89%)	14.4 ± 1.0	16.0 ± 0.5 (111%)	16.5 ± 0.02	16.7 ± 0.5 (101%)
V-2	0.74 ± 0.04*	0.72 ± 0.06 (98%)	10.7 ± 0.2	11.4 ± 0.4 (107%)	12.6 ± 0.16	12.1 ± 0.3 (96%)
V-3	0.75 ± 0.1*	0.83 ± 0.04 (111%)	9.2 ± 0.4	9.5 ± 0.6 (103%)	10.4 ± 0.11	10.3 ± 0.5 (99%)
V-4	1.70 ± 0.1	1.86 ± 0.06 (109%)	2.1 ± 0.3	2.3 ± 0.4 (109%)	4.5 ± 0.01	4.1 ± 0.4 (92%)
V-5	0.45 ± 0.01*	0.47 ± 0.04 (105%)	1.5 ± 0.3	1.7 ± 0.3 (113%)	2.4 ± 0.03	2.2 ± 0.3 (90%)
MB-1	<LOD	<LOD	30.2 ± 1.3	32.9 ± 0.8 (109%)	34.4 ± 0.4	32.9 ± 0.8 (96%)
MB-2	0.33 ± 0.04*	<LOD	7.57 ± 0.49	9.1 ± 0.4 (120%)	9.1 ± 0.3	9.1 ± 0.4 (100%)
MB-3	0.71 ± 0.08*	1.1 ± 0.0 (155%)	24.64 ± 0.40	27.6 ± 0.7 (112%)	28.9 ± 0.9	28.6 ± 0.7 (99%)
MB-4	1.16 ± 0.09*	1.0 ± 0.1 (86%)	26.3 ± 0.89	27.5 ± 0.9 (105%)	27.9 ± 0.9	28.5 ± 0.9 (102%)
MB-5	<LOD	<LOD	3.5 ± 0.25	4.5 ± 0.1 (129%)	4.7 ± 0.1	4.5 ± 0.1 (96%)

Average ± 1σ, n=3. \*Indicates value between LOD (0.17 µg/kg) and LOQ (1.3 µg/kg) for EAM §4.10 method. Refer to Table 3 for Measured LODs and LOQs

## Conclusion

This note describes a simple, robust, and fast HPLC-ICP-QQQ method to measure the sum of the most toxic inorganic As species (As(III) and As(V)) and two organic As species in under two minutes. By oxidizing As(III) to As(V) with H<sub>2</sub>O<sub>2</sub> during sample preparation, total iAs can be determined as As(V), leading to a much faster separation of the species of interest in wine samples. The narrow bore column and 0.5 mL/min flow rate provided excellent sensitivity which allowed low volume injections to be used. Compared to the current FDA method for the determination of As in wines, sample run times were 10x faster with improved limits of detection and quantification.

In this study, total As concentrations ranged from 2.2 to 32.9 µg/kg, which is well below the limit defined in regulations set in Ontario, Canada (100 µg/kg) and the maximum level established by the International Organisation of Vine and Wine in Europe (200 µg/kg). However, iAs was the predominant species present in the wines, and five of the wines tested contained iAs at concentrations that exceeded 10 µg/kg, which is the FDA's action limit for iAs in apple juice.

The results obtained using the new fast and fit-for-purpose method were in good agreement with data obtained using the FDA's EAM §4.10.

## References

1. H. Garelick, H. Jones, A. Dybowska, E. Valsami-Jones, Arsenic pollution sources, *Rev Environ Contam Toxicol.* **2008**, 197, 17–60
2. U.S. Department of Health and Human Services Food and Drug Administration Center for Food Safety and Applied Nutrition, Guidance for Industry Arsenic in Apple Juice: Action Level (draft), 2013, accessed August 2017: <https://www.fda.gov/RegulatoryInformation/Guidances/ucm360020.htm>
3. Canada Ontario, V. Q. A., Wine Standards. 1999, accessed August 2017: <http://www.vqaontario.ca/Regulations/Standards>
4. OIV–Compendium of International Methods of Analysis. Maximum acceptable limits of various substances contained in wine, 2011 issue. Europe
5. B. Sadee, M. E. Foulkes, S. J. Hill, *J. Anal. At. Spectrom.*, **2015**, 30, 102–118
6. B. P. Jackson, *J. Anal. At. Spectrom.*, **2015**, 30, 1405–1407
7. S. Musil, Á. H. Pétursdóttir, A. Raab, H. Gunnlaugsdóttir, E. Krupp, J. Feldmann, *Anal. Chem.*, **2014**, 86 (2), 993–999
8. H. R. Hansen, A. Raab, A. H. Price, G. Duan, Y. Zhu, G. J. Norton, J. Feldmann, A. A. Meharg, *J. Environ. Monit.*, **2011**, 13, 32–34
9. K. M. Kubachka, N. V. Shockey, T. A. Hanley, S. D. Conklin and D. T. Heitkemper, Arsenic Speciation in Rice and Rice Products Using High Performance Liquid Chromatography - Inductively Coupled Plasma-Mass Spectrometric Determination version 1.1, accessed August 2017, <https://www.fda.gov/downloads/Food/FoodScienceResearch/LaboratoryMethods/UCM479987.pdf>
10. C. K. Tanabe, H. Hopfer, S. E. Ebeler, J. Nelson, S. D. Conklin, K. M. Kubachka, and R. A. Wilson, Matrix Extension and Multilaboratory Validation of Arsenic Speciation Method EAM §4.10 to Include Wine, *J. Agric. Food Chem.*, **2017**, 65 (20), 4193–4199

### More information

For a full account of this study, see Patrick J. Gray, Courtney K. Tanabe, Susan E. Ebeler, and Jenny Nelson, A fast and fit-for purpose arsenic speciation method for wine and rice, *J. Anal. At. Spectrom.*, **2017**, 32, 1031–1034; DOI: 10.1039/C7JA00041C

### Acknowledgement

The Food Safety and Measurement Facility at the University of California, Davis, USA is supported by donations and gifts from Agilent Technologies, Gerstel US, and Constellation Brands.

# Simultaneous Iodine and Bromine Speciation Analysis of Infant Formula by HPLC-ICP-MS

## Authors

Lawrence Pacquette  
Abbott Nutrition,  
Columbus, Ohio, USA  
Jenny Nelson, Shuofei  
Dong, Michiko Yamanaka  
Agilent Technologies. Inc.

Determination of four halogen species in less than 6.5 minutes

## Introduction

Babies and young children often rely on infant formula for their nutritional requirements during early development, so regulators set high standards for the safety and nutritional value of these products. Most countries specify minimum levels for essential minerals in infant formulas, including iodine, to meet the nutritional needs of infants. If too little or too much iodine is consumed, babies and young infants are susceptible to developing thyroid problems (1, 2).

Regulatory values for iodine in infant formula manufactured from cow's milk or goat's milk proteins or protein hydrolysates relate to total iodine (Table 1). But the bio-availability of iodine depends on the chemical species present in a sample. Iodide ( $I^-$ ) has a higher bio-availability compared to iodate ( $IO_3^-$ ), which affects the nutritional status of iodine in food. For more information about the toxicity and health benefits of a food, elemental speciation is required to separate iodide and iodate from iodine ( $I_2$ ) and organic forms of iodine.

In the case of bromine, its toxicity is species-dependent. Bromide ( $Br^-$ ) has low toxicity compared to bromate ( $BrO_3^-$ ) which is possibly carcinogenic to humans (3).

**Table 1.** Regulatory levels for iodine in infant formula.

Regulatory body	Minimum concentration $\mu\text{g}/100 \text{ kcal}$	Maximum concentration $\mu\text{g}/100 \text{ kcal}$	Reference
US FDA	5	75	(4)
European Union	15	29	(5)
China	10.5	58.6	(6)

In this study, four species, iodide ( $I^-$ ), iodate ( $IO_3^-$ ), bromide ( $Br^-$ ), and bromate ( $BrO_3^-$ ), were determined in four commercially available milk-based infant formulas using HPLC coupled to a triple quadrupole ICP-MS (ICP-QQQ). HPLC-ICP-MS methodology is a well-established analytical technique that has been used for the speciation analysis of arsenic in various food matrixes, including infant formula (7, 8). This application could also be done using a single quadrupole ICP-MS such as the Agilent 7800 or 7900 ICP-MS as the elemental detector.

## Experimental

### Reagents and Standards

Standards for bromide, bromate, iodide, and iodate were prepared from 1000 ppm stock solutions. The bromide ion standard solution was bought from Kanto Chemical Co., Inc., Tokyo. A 1000 ppm stock solution of bromate was made by dissolving  $\text{NaBrO}_3$  (Wako Pure Chemical Corporation, Osaka) in water. Iodide and iodate stock solutions were prepared at 1000 ppm by dissolving KI and  $\text{KIO}_3$  (Wako Pure Chemical Corporation, Osaka), respectively.

### Standard reference material and samples

A milk-based standard reference material (SRM) NIST 1849a - Infant/Adult Nutritional Formula I (Gaithersburg, MD, USA) was used to validate the analytical method for the determination of total iodine.

Two of the four market basket infant formula samples were bought in Berkeley California, USA, and two were bought in Beijing, China. All four samples were in powder form.

Nitric acid ( $\text{HNO}_3$ ,  $\geq 65\%$ , Sigma-Aldrich) was used for microwave digestion and standard/sample preparation. All dilutions were done using 18.2 M $\Omega$ ·cm (Millipore, Bedford, MA, USA) de-ionized water (DIW).

### Sample preparation

For total bromine determinations about 0.2 g of NIST 1849a and each sample were weighed and digested in 5 mL of  $\text{HNO}_3$  by microwave digestion (Mars 6, CEM) using the program outlined in Table 2. The fully digested samples were then diluted to 40 mL with DIW. All samples and SRM were prepared in triplicate.

**Table 2.** Microwave digestion program.

Stages	Temp (°C)	Ramp (min)	Hold (min)
1	30	5	30
2	210	20	30
3	30	30	-

For I and Br speciation and total iodine determinations, about 0.2 g of each sample was weighed into 20 mL DIW and then put in a water bath at 50 °C for 1 h. The samples were then filtered using a syringe filter (0.45  $\mu\text{m}$  pore size). Approximately 1 mL filtered solution was placed in 1 mL polypropylene HPLC vials (Agilent part number 5182-0567), ready for analysis.

### Instrumentation

An Agilent 1260 Infinity II LC system comprising a quaternary pump was coupled to an Agilent 8900 Triple Quadrupole ICP-MS (ICP-QQQ) using the Agilent LC connection kit (part number G1833-65200). The Agilent Chromium Speciation Column for Drinking Water (part number G3268-80001) anion exchange column (4.6 mm internal diameter  $\times$  30 mm polyhydroxymethacrylate base resin) was used for separation of the iodine and bromine species. Details of the operating conditions and mobile phase are given in Table 3.

The Agilent 8900 ICP-QQQ (Advanced Applications configuration, #100) was fitted with the standard sample introduction system comprising a glass concentric nebulizer, quartz double-pass spray chamber, 2.5 mm injector quartz torch, and Ni interface cones. The ICP-QQQ was operated in single quadrupole (SQ) mode using helium cell gas, so the application could also be done using an Agilent 7800 or 7900 ICP-MS.

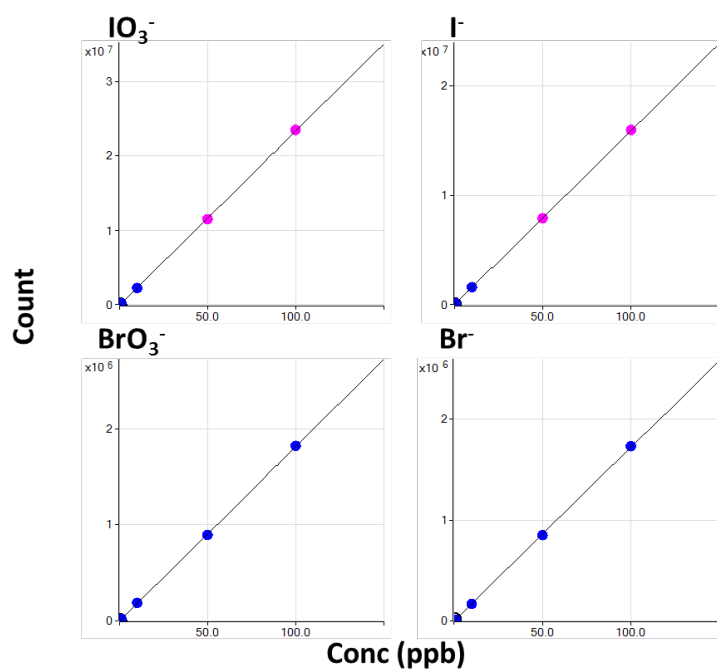
**Table 3.** HPLC and ICP-QQQ instrument operating conditions.

HPLC parameter	Setting
Mobile phase	5.0 mM NaH <sub>2</sub> PO <sub>4</sub> / 15.0 mM Na <sub>2</sub> SO <sub>4</sub> / 5.0 mM EDTA (pH 7.0)
Column	Agilent column for Cr speciation (part number G3268-80001)
Mobile phase flow (mL/min)	1.0
Injection volume (μL)	100
Temperature	Ambient
Run time (min)	8
ICP-QQQ parameter	Setting
Scan mode	Single quad mode
Sampling depth (mm)	8.0
Nebulizer gas flow (L/min)	1.10
Spray chamber temp. (°C)	2
Extract 1 (V)	0.0
Extract 2 (V)	-250
Octopole bias (V)	-20.0
Helium cell gas flow rate (mL/min)	2.0
Axial acceleration (V)	1.0
Energy discrimination (V)	3.0
Mass ( <i>m/z</i> )	79 for Br, 127 for I
Integration time (sec/mass)	0.5

## Results and discussion

### Calibration

Calibration was carried out by analyzing solutions of iodide, iodate, bromide, and bromate, between 0 and 100 ppb. Figure 1 demonstrates calibration curves with excellent linearity over the calibration range, with calibration linearity equal to or better than 0.9999.

**Figure 1.** Calibration curves of IO<sub>3</sub><sup>-</sup> (top left), I<sup>-</sup> (top right), BrO<sub>3</sub><sup>-</sup> (bottom left), and Br<sup>-</sup> (bottom right).



A chromatogram of the 5 ppb iodine and bromine standard is shown in Figure 2. All four species,  $\text{IO}_3^-$ ,  $\text{I}^-$ ,  $\text{BrO}_3^-$ , and  $\text{Br}^-$ , were separated and baseline-resolved in less than 6.5 minutes, all in the same run.

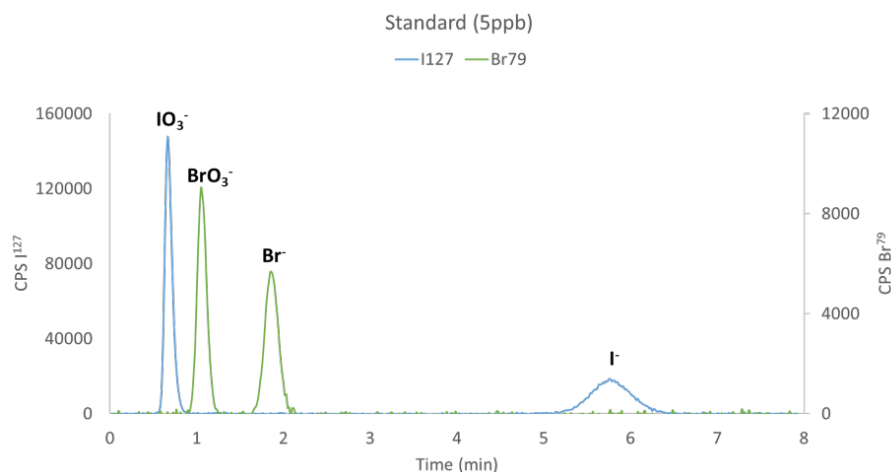


**Figure 2.** Chromatogram of 5 ppb standard showing  $\text{IO}_3^-$ ,  $\text{I}^-$ ,  $\text{BrO}_3^-$ , and  $\text{Br}^-$  in the same run.

### Detection limits

Signal-to-noise (S/N) detection limits (DLs) were calculated from 3x the background noise divided by the signal for each peak of interest. The DLs of the four species were between 0.072 and 0.667 ppb as shown in Table 4.

**Table 4.** S/N DLs for iodate, bromate, bromide, and iodide.

Species	Standard concentration (ppb)	Signal	Noise	S/N	DL in solution (ppb)
$\text{IO}_3^-$	0.98	27781	676.6	41.06	0.072
$\text{BrO}_3^-$	1.07	1979	320.2	6.18	0.519
$\text{Br}^-$	0.9	1296	320.0	4.05	0.667
$\text{I}^-$	0.78	3379	677.2	4.99	0.469

### Analysis of SRM

The four species were determined in the Infant/Adult Nutritional Formula SRM using LC-ICP-QQQ (seven sample preparation replicates, run in triplicate; n=21). The total iodine concentration was measured using the 8900 ICP-QQQ (without HPLC separation). The results for the four species, total iodine, and total bromine are shown in Table 5. No iodate or bromate was detected in the SRM. The measured concentrations for  $^{127}\text{I}$ , total iodine, and the certified concentration for total iodine are all in good agreement, suggesting a good level of method accuracy. Bromine isn't certified in the SRM.

**Table 5.** Results for the analysis of NIST 1849a Infant/Adult Nutritional Formula SRM\*. n=21. Units: mg/kg.

$^{127}\text{IO}_3^-$	$^{127}\text{I}^-$	$^{79}\text{BrO}_3^-$	$^{79}\text{Br}^-$	Total I*		Total Br**
Measured				Reference	Measured	Measured
ND	1.31 ± 0.04	ND	0.74 ± 0.12	1.29 ± 0.11	1.33 ± 0.37 (103%)	0.77 ± 0.07 (96%)***

ND = not detected. \*Prepared using water bath extraction. \*\*No certified value given for bromine. \*\*\* $^{79}\text{Br}$ /Total bromine.

## Quantitative analysis of infant formula products

Extracts of the four powder infant formula samples were prepared in duplicate and analyzed in duplicate (n=4) using LC-ICP-QQQ. As shown in Table 6, no iodate or bromate was detected in any of the samples. The recoveries of iodide compared to the total iodine results range from 87 to 102%, suggesting the iodine present in the samples was in the form of iodide. The recoveries of bromine to the total bromine results ranged from 85 to 100%, suggesting the bromine present in the samples was in the form of bromide.

The total iodine measured in the four infant formula samples ranged from 1232 to 2592  $\mu\text{g}/\text{kg}$ , which is equivalent to 25.9 to 54.5  $\mu\text{g}/100$  kcal. These concentrations are within the United States and China national standards for total iodine; however, some results fall outside the EU maximum limit for iodine of 29  $\mu\text{g}/100$  kcal.

**Table 6.** Infant formula sample analysis results. Units:  $\mu\text{g}/\text{kg}$ . The percentages are the recoveries of iodide and bromide compared to total iodine and bromine, respectively.

Sample ID	$^{127}\text{IO}_3^-$	$^{127}\text{I}^-$	$^{79}\text{BrO}_3^-$	$^{79}\text{Br}^-$	Total I*	Total Br**
1-USA	ND	1157 $\pm$ 11	ND	2993 $\pm$ 27	1333 $\pm$ 16 (87%)	3112 $\pm$ 151 (96%)
2-USA	ND	1455 $\pm$ 29	ND	10826 $\pm$ 141	1426 $\pm$ 50 (102%)	10815 $\pm$ 478 (100%)
3-China	ND	1240 $\pm$ 15	ND	25660 $\pm$ 230	1232 $\pm$ 23 (101%)	29850 $\pm$ 2392 (86%)
4-China	ND	2372 $\pm$ 24	ND	8529 $\pm$ 64	2592 $\pm$ 44 (92%)	9997 $\pm$ 389 (85%)

\*Sample preparation with the water extraction method

\*\* Sample preparation with microwave digestion method

## Spike recovery test

A spike recovery test was performed by spiking two infant formula samples with  $\text{IO}_3^-$ ,  $\text{BrO}_3^-$ ,  $\text{Br}^-$ , and  $\text{I}^-$  at 20 and 40 ppb, before extraction. Each spiked sample was prepared in triplicate and analyzed twice. Good recoveries for each of the four species in actual samples at 20 ppb and 40 ppb-level were achieved over the course of multiple 100  $\mu\text{L}$  injections (Table 7). The results indicate that the method could be used for the accurate determination of the four-halogen species in infant formula.

**Table 7.** Average spike recovery results for two infant formula samples spiked at 20 and 40 ppb with  $\text{IO}_3^-$ ,  $\text{BrO}_3^-$ ,  $\text{Br}^-$ , and  $\text{I}^-$ , n=12.

	$^{127}\text{IO}_3^-$	$^{79}\text{BrO}_3^-$	$^{127}\text{I}^-$	$^{79}\text{Br}^-$
Average recovery, %	96 $\pm$ 4	97 $\pm$ 5	98 $\pm$ 7	100 $\pm$ 5
Recovery range, %	90–100	89–101	88–104	94–105

Figure 3 shows the overlay of  $^{79}\text{Br}$  and  $^{127}\text{I}$  from the two infant formulas analyzed per Table 7. The infant formulas from the US and China were spiked at two levels ( $\sim 20$  and  $40$  ppb) and each level prepared in triplicate. The chromatograms show good repeatability for multiple  $100\ \mu\text{L}$  injections.

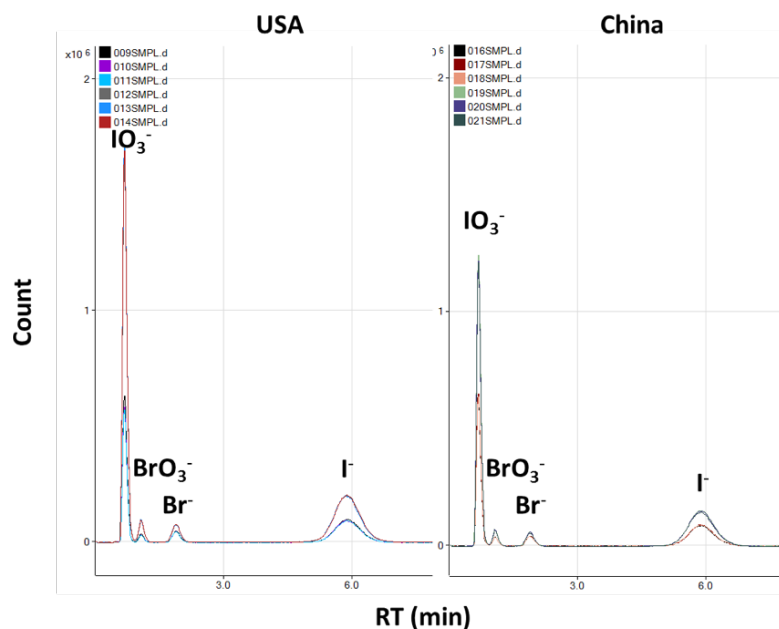


**Figure 3.** Overlay of  $^{79}\text{Br}$  and  $^{127}\text{I}$  spiked at two levels ( $\sim 20$  and  $40$  ppb) in the USA infant formula (chromatogram on the right) and a Chinese infant formula (chromatogram on the left).  $n=6$  for each chromatogram.

## Conclusion

For the first time, four halogen species were measured in the same run in infant formula samples using an Agilent 1260 Infinity II LC system coupled to an Agilent 8900 ICP-QQQ. Using an anion exchange column, baseline separations were achieved in around 6.5 minutes with detection limits for  $\text{I}^-$ ,  $\text{IO}_3^-$ ,  $\text{Br}^-$ , and  $\text{BrO}_3^-$  all less than or equal to  $0.67$  ppb.

Speciation analysis of infant formula provides valuable information on iodine bio-availability and the potential risk from bromate. Total elemental determinations of iodine and bromine were also performed using the 8900 ICP-QQQ. The measured value for iodine in an infant formula SRM was in good agreement with the certified value at 103% recovery. There was also good agreement between the measured concentration of  $^{127}\text{I}^-$  with the certified value at 101% recovery. No certified value was provided with the SRM for bromine.

None of the four commercially available infant formula samples that were analyzed in the study contained iodate or bromate, only iodide and bromide. The total iodine content in the samples ranged from  $25.9$  to  $54.5\ \mu\text{g}/100$  kcal. This range is within the US and China national standards for iodine in infant formula, but outside the EU maximum limit of  $29\ \mu\text{g}/100$  kcal.

To test the suitability of the method for the accurate determination of low concentrations of the four species in infant formula samples, a spike recovery test was carried out at  $20$  and  $40$  ppb. Baseline separations were achieved, with good repeatability over the course of multiple  $100\ \mu\text{L}$  injections.

## References

- A. Milanesi, and G. A. Brent, Molecular, Genetic, and Nutritional Aspects of Major and Trace Minerals, J.F. Collins (Ed.), 2017, Elsevier, London, UK, 143–150
- P. Ghirri, S. Lunardi, A. Boldrini, Iodine Supplementation in the Newborn, *Nutrients*, **2014**, 6(1), 382–390
- World Health Organization, International Agency of Research on Cancer, IARC Monographs on the Evaluation of Carcinogenic Risks to Humans, <https://monographs.iarc.fr/wp-content/uploads/2018/07/ClassificationsAlphaOrder.pdf>, (accessed February 2019)
- CFR Chapter I: Food and Drug Administration, in Title 21: Food and Drugs, Ch. 1, Part 107, Infant Formula, Code of Federal Regulations, U.S. Food and Drug Administration, Silver Spring, MD
- Commission Delegated Regulation No. 2016/127/EU (**2015**) Off. J. Eur. Union L25, 1–29
- GB 10765-2010: National Food Safety Standard Infant Formula, The Ministry of Health of the People's Republic of China, Beijing, China
- Standard Method Performance Requirements (SMPRs) for Quantitation of Arsenic Species in Selected Foods and Beverages, *AOAC Int*, **2015**, Gaithersburg, MD, Method 2015.006
- B. P. Jackson, V. F. Taylor, T. Punshon, K. L. Cottingham, Arsenic concentration and speciation in infant formulas and first foods, *Pure Appl. Chem.*, **2012**, 84, 215–223

## More Information

For a full account of this study, see Jennifer Nelson, Lawrence Pacquette, Shuofei Dong and Michiko Yamanaka, Simultaneous Analysis of Iodine and Bromine Species in Infant Formula using HPLC-ICP-MS, *JAOAC Int.*, 102, **2019**, DOI: 10.5740/jaoacint.18-0352

# Determination of Pesticides using Phosphorus and Sulfur Detection by GC-ICP-QQQ

## Authors

Jenny Nelson, Fabio Silva,  
Steve Wilbur, Jianmin Chen,  
Shiota Ozawa, and Philip L. Wylie,  
Agilent Technologies  
Helene Hopfer, Food Safety and  
Measurement Facility, University of  
California Davis

## Keywords

pesticides, GC-ICP-MS, GC-ICP-MS/  
MS, GC-ICP-QQQ, sulfur, phosphorus

## Introduction

The determination of pesticide residues in food products is important. Most pesticide residue laboratories use some variation of the QuEChERS (Quick, Easy, Cheap, Effective, Rugged, and Safe) extraction methods. Typically, the extracted material is analyzed using GC/MS/MS the thermally stable, less polar pesticides, or LC-MS/MS for the less volatile and/or more polar ones. A more recently developed alternative technique involves coupling GC to triple quadrupole ICP-MS (GC-ICP-QQQ). Pesticides can be quantified using GC-ICP-QQQ by measuring the heteroatoms P and S (also Cl and Br) contained in most pesticides. GC-ICP-QQQ offers good selectivity, specificity, and sensitivity that can be greater than the established methods.

## Experimental

**Instrumentation:** An Agilent 7890 GC was coupled to an Agilent 8800 #100 ICP-QQQ using an Agilent GC-ICP-MS interface (G3158D).

**GC:** Two Agilent columns were used in series. The first column was a 5 m length cut from a 20 m x 0.18 mm x 0.18  $\mu\text{m}$  film thickness DB-35ms Ultra Inert (UI) capillary column (p/n 121-3822UI). This column was installed between the inlet and one end of the purged union. It was back flushed shortly before the run had ended to prevent high boiling point contaminants from entering the second column. The second column was a 15 m x 0.25 mm i.d. 0.25  $\mu\text{m}$  film thickness DB-5MS UI capillary column (p/n 19091S-431UI). The column was installed between the other end of the purged union and the ICP-QQQ transfer line connection inside the GC oven. Sample injections of 1  $\mu\text{L}$  volume were made under splitless conditions with the inlet held at 280 °C. GC operating parameters are detailed in a previous study [1].

**ICP-QQQ:**  $\text{O}_2$  mass-shift method was applied to detect P and S. The  $\text{O}_2$  flow rate was 0.2 mL/min. P and S were detected as  $\text{PO}^+$  and  $\text{SO}^+$ , respectively.

**Samples and preparation:** Three standard pesticide mixes were obtained from Ultra Scientific (Kingstown, RI, USA) and Agilent Technologies (p/n 5190-0468). The standard solutions were diluted with high purity grade acetonitrile to form intermediate solutions. These solutions were then used to prepare calibration standard solutions following serial dilutions in acetonitrile.

## Results and discussion

Figure 1 shows overlaid chromatograms for P and S in a mixed pesticide standard. The pesticides that contain more than one hetero-element can be identified easily.

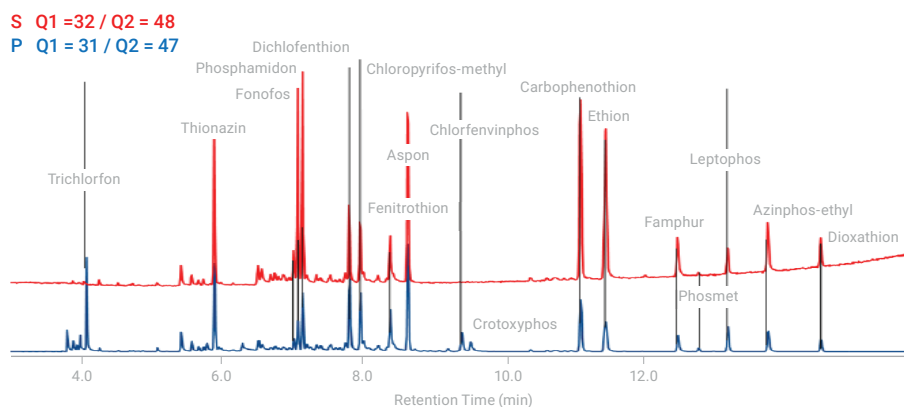


**Figure 1.** Chromatograms showing the heteroatom traces for P and S in the mixed pesticide standard, with identified pesticide compounds.

Reprinted with permission from *J. Agric. Food Chem.*, 2015, 63, 4478–4483. Copyright 2015 American Chemical Society.

Table 1 summarizes the retention time and compound detection limits (DLs) of the pesticides. DLs for pesticides using current GC/MS/MS instrumentation typically vary from about 0.1 to 10  $\mu\text{g/L}$  depending on the pesticide and instrument used. The data in Table 1 suggests that GC-ICP-QQQ offers similar or slightly lower DLs than GC/MS/MS for the determination of organophosphorus pesticides. For S-containing pesticides, detection limits are similar to, or slightly higher than DLs achieved by GC/MS/MS. All of the pesticides listed in Table 1, which were detected via their P content, were quantified well below the 10  $\mu\text{g/L}$  limit of quantitation (LOQ) required by most food safety laboratories.

**Table 1.** Detection limits as the compound for pesticides.

Pesticide	RT (min)	Compound DL (µg/L)	
		P	S
Trichlorfon	4.103	0.178	
Thionazin	5.926	0.221	11.93
Terbufos	7.071	0.718	9.708
Fonofos	7.185	0.455	7.917
Phosphamidon	7.299	0.923	
Dichlofenthion	7.858	0.362	15.8
Chloropyrifos-methyl	7.973	0.613	24.18
Fenitrothion	8.44	0.907	19.52
Aspon	8.705	0.200	9.912
Chlorfenvinphos	9.486	2.020	
Crotoxyphos	9.541	3.338	
Carbophenothion	11.158	0.583	9.585
Ethion	11.527	0.707	11.51
Famphur	12.547	2.206	20.61
Phosmet	12.851	3.829	
Leptophos	13.263	1.125	18.35
Azinphos-ethyl	13.827	1.812	21.33
Dioxathion	14.587	1.392	7.84

## Conclusion

The GC-ICP-QQQ method is suitable for the selective and sensitive detection of organophosphorus and organosulfur pesticides by measurement of their heteroatoms. Due to the significantly lower background of the Agilent 8800 ICP-QQQ, GC-ICP-QQQ provides good sensitivity performance for the determination of organophosphorus pesticides compared to GC/MS/MS.

## References

1. P. L. Wylie, C. Meng, A Method for the Trace Analysis of 175 Pesticides Using the Agilent Triple Quadrupole GC/MS/MS, Agilent publication, 2009, [5990-3578EN](#)
2. Jenny Nelson, Helene Hopfer, Fabio Silva, Steve Wilbur, Jianmin Chen, Kumi Shiota Ozawa, and Philip L. Wylie, Evaluation of GC-ICP-MS/MS as a New Strategy for Specific Heteroatom Detection of Phosphorus, Sulfur, and Chlorine Determination in Foods, *J. Agric. Food Chem.*, **2015**, DOI: 10.1021/jf506372e

## More information

Determination of pesticides in foods using phosphorus and sulfur detection by GC-ICP-QQQ, Agilent publication, [5991-6260EN](#)

# Petrochemicals

<b>Title</b>	<b>Page</b>
Determination of P, Si and S in acid digested lubricating oil using the Agilent 8800 triple quadrupole ICP-MS	337
Accurate sulfur quantification in organic solvents using isotope dilution mass spectrometry	342
Determination of chloride in crude oils using an Agilent 8900 ICP-QQQ	346
Single nanoparticle analysis of asphaltene solutions using ICP-QQQ	351
Gas chromatographic separation of metal carbonyls in carbon monoxide with detection using the Agilent 8800 ICP-QQQ	358



# Determination of P, Si and S in acid digested lubricating oil using the Agilent 8800 Triple Quadrupole ICP-MS

## Authors

Renata S. Amais<sup>1</sup>, Clarice D. B. Amaral<sup>1</sup>,  
Lucimar L. Fialho<sup>1</sup>, Daniela Schiavo<sup>2</sup>  
and Joaquim A. Nóbrega<sup>1</sup>

<sup>1</sup>Group of Applied Instrumental  
Analysis, Department of Chemistry,  
Federal University of São Carlos,  
São Carlos, SP, Brazil

<sup>2</sup>Agilent Technologies  
São Paulo, SP, Brazil

## Abstract

A new method is described for the accurate determination of silicon (Si), phosphorus (P), and sulfur (S) in lubricating oil samples using an Agilent 8800 Triple Quadrupole ICP-MS (ICP-QQQ). An optimized oxygen (O<sub>2</sub>) mass-shift method provided limits of detection for <sup>28</sup>Si, <sup>31</sup>P, <sup>32</sup>S and <sup>34</sup>S of 0.25, 0.01, 0.18 and 0.75 ppb, respectively. The method was successfully applied to the determination of Si, P and S in a lubricating oil standard reference material NIST 1848. Recoveries in the sample digests ranged from 96.4–103%.

## Introduction

Due to its high sensitivity and fast multi-element capabilities, inductively coupled plasma mass spectrometry (ICP-MS) is used increasingly in chemical analysis. However, spectral overlaps from isobaric concomitant species and polyatomic ions formed in the plasma can compromise ICP-MS sensitivity and accuracy in the determination of some elements (1).

For example, Si, P and S are difficult elements to determine at low levels by quadrupole based ICP-MS due to intense polyatomic interferences: <sup>28</sup>Si<sup>+</sup>, <sup>31</sup>P<sup>+</sup>, <sup>32</sup>S<sup>+</sup> and <sup>34</sup>S<sup>+</sup> suffer spectral overlaps from <sup>14</sup>N<sub>2</sub><sup>+</sup> and <sup>12</sup>C<sup>16</sup>O<sup>+</sup>, <sup>14</sup>N<sup>16</sup>OH<sup>+</sup>, <sup>16</sup>O<sub>2</sub><sup>+</sup> and <sup>16</sup>O<sup>18</sup>O<sup>+</sup>, respectively (2). Since the enthalpies of reaction for P<sup>+</sup> (-3.17 eV) and S<sup>+</sup> (-0.34 eV) with O<sub>2</sub> are negative and low for Si (0.11 eV) (3), some authors have studied the feasibility of using Collision/Reaction Cell (CRC-)ICP-MS with O<sub>2</sub> cell gas to determine these elements as oxide ions (4, 5, 6). The method of using a reaction product ion for the detection of an element is known as mass-shift mode. Conventional CRC-ICP-MS has no control of the ions that enter the cell or the reactions that occur in the cell. In contrast, the Agilent 8800 ICP-QQQ has a tandem mass spectrometer (MS/MS) configuration with two quadrupole mass filters, Q1 and Q2, positioned either side of the Octopole Reaction System (ORS<sup>3</sup>) cell. This configuration is designed to control the reactions in the cell for more effective removal of spectral interferences (Figure 1). In mass-shift mode using O<sub>2</sub> cell gas, Q1 is set to the mass of the target analyte ion so only the analyte and any on-mass interfering ions can enter the ORS<sup>3</sup> and react with the O<sub>2</sub> cell gas, ensuring a well controlled and more efficient reaction in the cell. The second quadrupole, Q2, is then set to the mass of the oxide ion of the element of interest, so rejecting any interfering ions that have not reacted with the cell gas and therefore remain at the original analyte mass. Balcaen et al. evaluated the MS/MS mass-shift mode of the 8800 ICP-QQQ for the low level determination of sulfur in ethanol-diluted biodiesel samples using isotope dilution (7).

In this study, mass-shift mode was evaluated for the low level analysis of Si, P and S in lubricating oil samples. We demonstrate that the 8800 Triple Quadrupole ICP-MS operating in MS/MS mode with O<sub>2</sub> as the reaction gas provides low Limits of Detection (LOD) for these difficult elements and enables their accurate determination in a complex matrix such as lubricating oil.

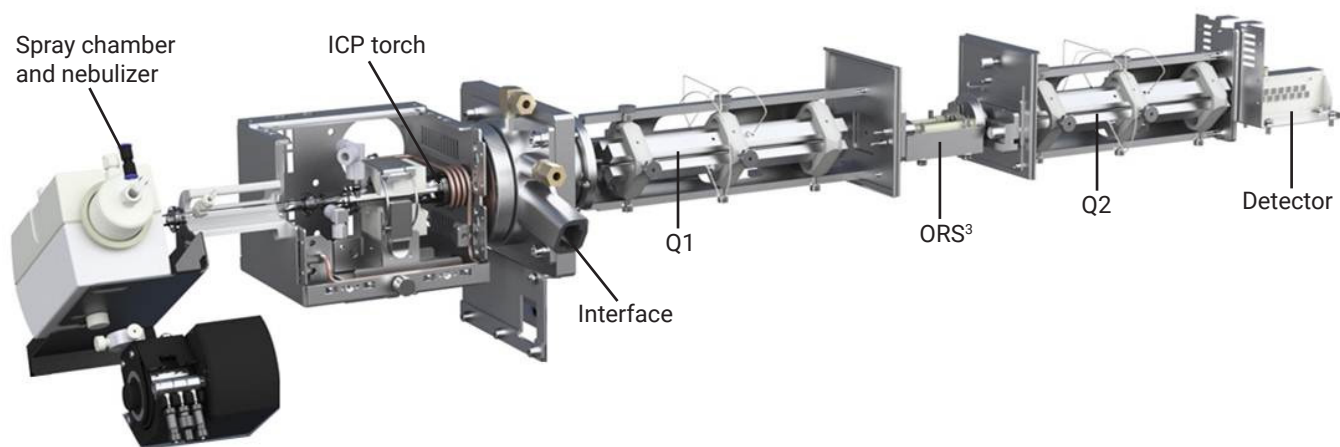


Figure 1. Schematic of the Agilent 8800 Triple Quadrupole ICP-MS

## Experimental

### Instrumentation

All measurements were carried using a standard Agilent 8800 Triple Quadrupole ICP-MS (option #100). The standard configuration is composed of an x-lens, a Peltier-cooled double-pass Scott-type spray chamber, a glass concentric nebulizer, and a one-piece quartz torch with 2.5 mm internal diameter (ID) injector. Instrument operating parameters are summarized in Table 1.

Table 1. Agilent 8800 ICP-QQQ operating conditions

Parameter	Value
RF power	1550 W
Sampling depth	8.0 mm
Carrier gas flow rate	1.08 L/min
Spray chamber temperature	2 °C
Cell gas	O <sub>2</sub>
Cell gas flow rate	0.5 mL/min
Mass pair (Q1, Q2)	(28, 44), (31, 47), (32, 48), (34, 50)

### Reagents and standard solutions

Deionized water (> 18.2 MΩ cm) obtained from a Milli-Q water purification system (Millipore, Bedford, MA, USA) was used to prepare all solutions. Nitric acid (Merck, Darmstadt, Germany) previously purified by a sub-boiling distillation system (Milestone, Sorisole, Italy) and 30% H<sub>2</sub>O<sub>2</sub> (Labsynth, Diadema, SP, Brazil) were used to digest the samples. Stock single element solutions containing 1000 mg/L of Si, P and S (Tec-Lab, Hexis, São Paulo, SP, Brazil) were used to prepare the calibration standard solutions by diluting in 1 % v/v HNO<sub>3</sub>.

### Samples and sample preparation

A lubricating oil standard reference material (SRM 1848, National Institute of Standard and Technology, Gaithersburg, MD, USA) was used to check the accuracy of the method. The SRM sample was microwave-assisted acid-digested (Milestone) using the following procedure. Aliquots of 0.25 g of the SRM 1848 were weighed directly in PTFE-PFA digestion vessels and 2.5 mL of concentrated HNO<sub>3</sub> was added to each flask. After standing for 30 min at room temperature, 2.5 mL of distilled–deionized water was added to the mixture. An additional pre-digestion

period of 30 min without any external heating was allowed before 3.0 mL of 30% H<sub>2</sub>O<sub>2</sub> was added to each digestion vessel. The microwave-assisted digestion of the samples was then carried out according to the heating program presented in Table 2. The digestion flasks were allowed to cool to room temperature and then the volume of each solution was made up to 13.0 mL with distilled–deionized water. The procedure was performed in triplicate and each sample digest was diluted 200x for Si and P and 2000x for S with distilled–deionized water.

**Table 2.** Heating program used in the microwave-assisted acid-digestion sample preparation procedure

Step	Applied power (W)	Time (min)	Temperature (°C)
1	250	2	80
2	0	3	80
3	550	4	120
4	650	5	180
5	750	5	200

## Results and discussion

### Figures of merit

The analytical performance of MS/MS mass-shift mode with O<sub>2</sub> reaction gas was evaluated for Si, P and S. O<sub>2</sub> gas flow rate was optimized at 0.50 mL/min gas. Calibration curves were prepared using calibration standard solutions ranging from 0.5 to 500 ppb (Figure 2). LODs of 0.25, 0.01, 0.18 and 0.75 ppb were obtained for <sup>28</sup>Si, <sup>31</sup>P, <sup>32</sup>S and <sup>34</sup>S respectively (Table 3) based on 10 consecutive blank measurements using the optimized acquisition conditions given in Table 1 and an integration time of 3 s.

**Table 3.** Limits of detection for Si, P and S obtained using the 8800 ICP-MS operating in O<sub>2</sub> mass-shift mode

Element	Mass pair (Q1, Q2)	Product ion	LOD (ppb)
Silicon	(28, 44)	<sup>28</sup> SiO <sup>+</sup>	0.25
Phosphorus	(31, 47)	<sup>31</sup> PO <sup>+</sup>	0.01
Sulfur	(32, 48)	<sup>32</sup> SO <sup>+</sup>	0.18
Sulfur	(34, 50)	<sup>34</sup> SO <sup>+</sup>	0.75

### Analytical application

The accuracy of the method for the determination of P, S, and Si in lubricating oil was evaluated by analyzing a digest of NIST 1848. The results are given in Table 4. The recoveries for all 3 analytes ranged from 96.4–103% indicating the effectiveness of the method to separate the analytes from the interferences. In MS/MS mode, non-target ions such as <sup>44</sup>Ca<sup>+</sup>, <sup>48</sup>Ca<sup>+</sup>, <sup>47</sup>Ti<sup>+</sup>, <sup>48</sup>Ti<sup>+</sup> or <sup>36</sup>Ar<sup>12</sup>C<sup>+</sup> (that would potentially overlap with the target product ions SiO<sup>+</sup>, PO<sup>+</sup> or SO<sup>+</sup>) are prevented from entering the ORS<sup>3</sup> by Q1, thus allowing the accurate and sensitive determination of these difficult elements in a complex matrix.

**Table 4.** Results of NIST 1848 analysis

	Certified (mg/kg)	Isotope	Mass pair (Q1, Q2)	Product ion	Determined conc. (mg/kg)	Recovery (%)
Silicon	50 <sup>a</sup> ± 2	<sup>28</sup> Si	(28, 44)	<sup>28</sup> Si <sup>16</sup> O <sup>+</sup>	48.2 ± 2.1	96.4
Phosphorus	7880 ± 280 <sup>b</sup>	<sup>31</sup> P	(31, 47)	<sup>31</sup> P <sup>16</sup> O <sup>+</sup>	7650 ± 120	97.0
Sulfur	23270 ± 43 <sup>b</sup>	<sup>32</sup> S	(32, 48)	<sup>32</sup> S <sup>16</sup> O <sup>+</sup>	24010 ± 820	103
		<sup>34</sup> S	(34, 50)	<sup>34</sup> S <sup>16</sup> O <sup>+</sup>	23985 ± 830	103

<sup>a</sup>Reference value

<sup>b</sup>Certified value

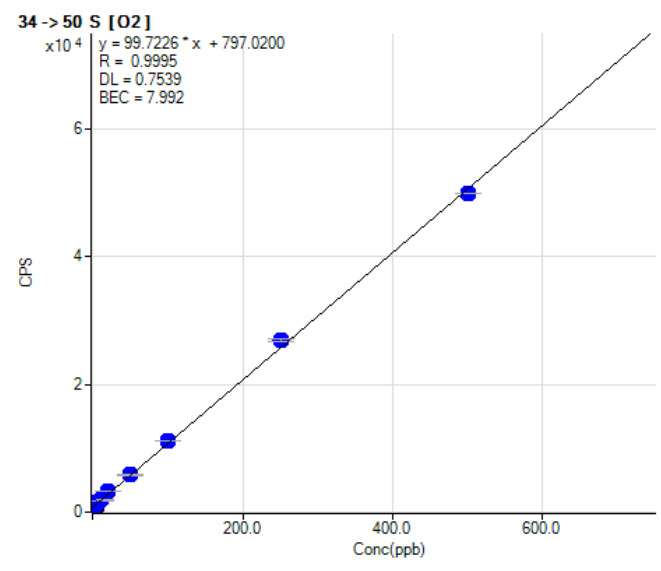
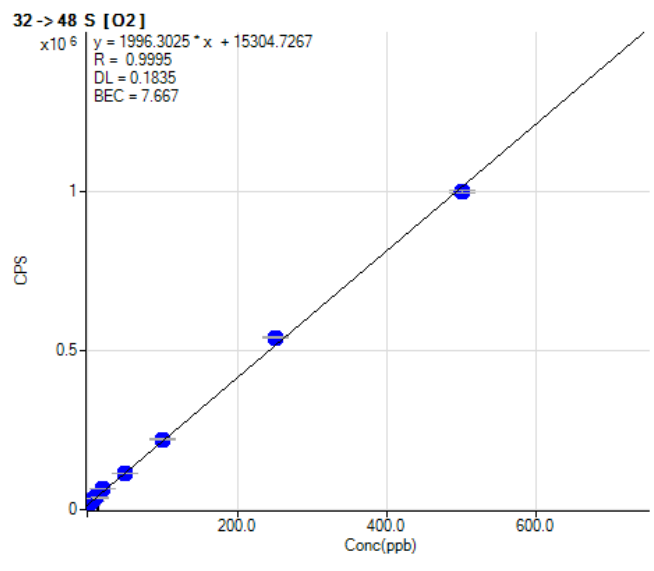
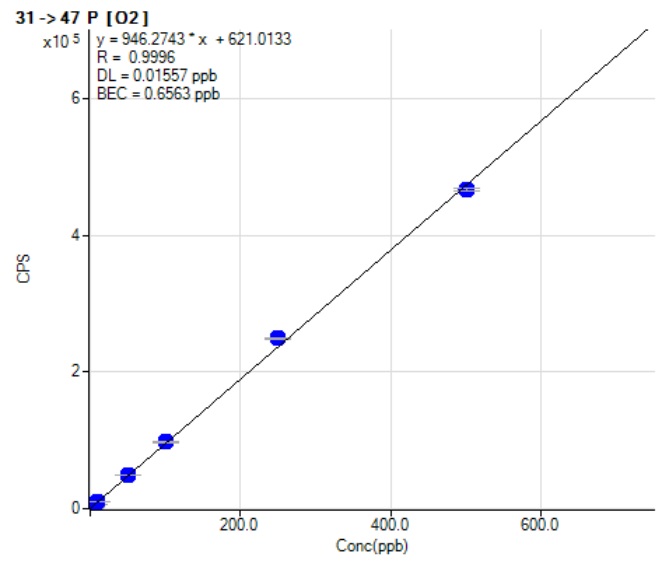
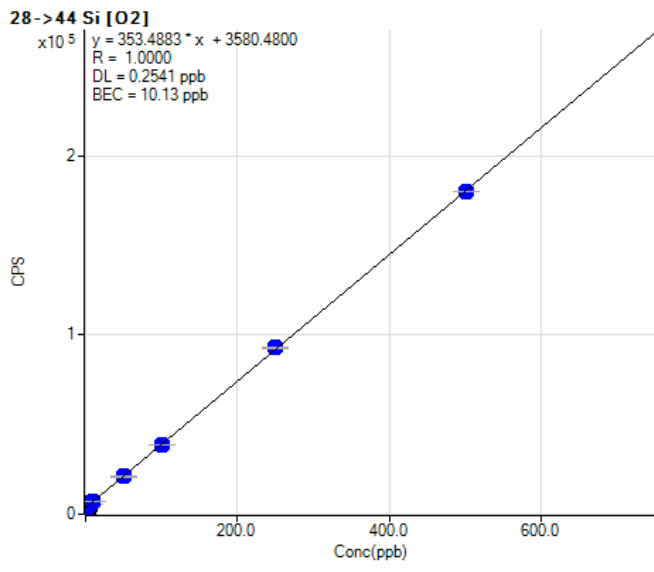


Figure 2. Calibration curves for  $^{28}\text{Si}^{16}\text{O}^+$ ,  $^{31}\text{P}^{16}\text{O}^+$ ,  $^{32}\text{S}^{16}\text{O}^+$  and  $^{34}\text{S}^{16}\text{O}^+$

## Conclusions

The Agilent 8800 ICP-QQQ operating in MS/MS mode with oxygen cell gas effectively removes spectral interferences allowing the determination of the challenging elements Si, P and S with sub-ppb ( $\mu\text{g}/\text{kg}$ ) LODs. By mass-shifting each of the 3 analytes by reaction with  $\text{O}_2$ , and detecting the oxide product ions, all potential interferences from polyatomic ions based on nitrogen and oxygen are removed. Also, any ions that might overlap the analyte product ions created in the cell are rejected by Q1, greatly improving the accuracy, reliability and ease of use of reaction gas mode. Si, P and S were accurately determined in a digested lubricating oil SRM, validating the applicability of the method to the most challenging sample types.

## Acknowledgments

The authors would like to acknowledge grants 2010/17387-7, São Paulo Research Foundation (FAPESP) for scholarship and fellowship provided to R.S.A.. J.A.N. is thankful to Conselho Nacional de Desenvolvimento Científico e Tecnológico (CNPq). We also acknowledge the technical support provided by Agilent Technologies.

## References

1. J. S. Becker, *Inorganic Mass Spectrometry: Principles and Applications*; Wiley: Chichester, 2008.
2. H. E. Taylor, *Inductively Coupled Plasma – Mass Spectrometry, Practices and Techniques*, Academic Press: San Diego, USA. 2001.
3. Agilent 8800 Triple Quadrupole ICP-MS: Understanding oxygen reaction mode in ICP-MS/MS. Application note: 5991-1708EN, 2012.
4. G. L. Donati, R. S. Amais, J. A. Nóbrega, Interference standard and oxide ion detection as strategies to determine phosphorus and sulfur in fuel samples by inductively coupled plasma quadrupole mass spectrometry. *J. Anal. At. Spectrom.*, 27, 1274-1279, 2012.
5. C.-H. Yang, S.-J. Jiang, Determination of B, Si, P and S in steels by inductively coupled plasma quadrupole mass spectrometry with dynamic reaction cell. *Spectrochim. Acta Part B*, 59, 1389-1394, 2004.
6. S. D. Tanner, V. I. Baranov, D. R. Bandura. Reaction cells and collision cells for ICP-MS: a tutorial review. *Spectrochim. Acta Part B*, 57, 1361-1452, 2002.
7. L. Balcaen, G. Woods, M. Resano, F. Vanhaecke, Accurate determination of S in organic matrices using isotope dilution ICP-MS/MS. *J. Anal. At. Spectrom.*, 28, 33-39, 2013.

# Accurate Sulfur Quantification in Organic Solvents using Isotope Dilution Mass Spectrometry

## Author

Glenn Woods

Agilent Technologies (UK) Ltd.

Based upon the published work

"Accurate determination of S in organic matrices using isotope dilution ICP-MS/MS" *J. Anal., At. Spectrom.*

2012 DOI: 10.1039/c2ja30265a by:

Lieve Balcaen and Frank Vanhaecke, Ghent University, Department of Analytical Chemistry, Ghent, Belgium

Martin Resano, University of Zaragoza, Department of Analytical Chemistry, Zaragoza, Spain

Glenn Woods, Agilent Technologies UK Ltd., 5500 Lakeside, Cheadle Royal Business Park, SK8 3GR, UK

## Keywords

sulfur, ID-MS, biodiesel, environmental, ethanol, NIST SRM 2773, oxygen mass-shift

## Introduction

Accurate measurement of sulfur in aqueous and organic media is relatively difficult for ICP-MS due to intense spectral interferences from polyatomic ions formed mainly from oxygen and nitrogen. Sulfur is an important element in environmental terms as it forms  $\text{SO}_x$  when combusted, contributing to acid rain and photochemical smog. It is also a catalyst poison for some industrial processes and its accurate measurement can be critical.

## Experimental

A quadrupole ICP-MS (ICP-QMS) with a collision/reaction cell set up for  $\text{O}_2$  mass-shift reaction chemistry can be used to avoid the  $^{16}\text{O}_2^+$  overlap on  $^{32}\text{S}^+$  by converting the  $\text{S}^+$  to  $\text{SO}^+$  reaction product ions that are then measured at a new mass ( $m/z$  48) that is free from the  $\text{O}_2^+$  overlap. However, in practice, this approach has been of relatively limited use, as ICP-QMS has no way to reject existing ions at the mass of the new analyte product ions, so not all of the interferences are eliminated, particularly when complex or variable matrices are investigated. There has also been some limited success reported by using Xe as a reaction gas to attenuate the  $\text{O}_2$ -based interference particularly on the  $^{34}\text{S}$  isotope. Neither of these approaches reduces the backgrounds significantly enough to allow reliable trace level measurement of S, and they do not necessarily preserve the S isotopic abundances. In this investigation, ethanol was used as an example organic solvent and the Agilent 8800 ICP-QQQ was used to determine S by ID-MS in a biodiesel reference material to assess the measurement accuracy of MS/MS mode with  $\text{O}_2$  mass-shift for S determination.

**Instrumentation:** Agilent 8800 #100 with Micromist nebulizer (free aspiration). For organic solvent analysis, a narrow injector torch with id 1.0 mm (G3280-80005) and Pt cones were used. 20%  $\text{O}_2$  balanced in Ar was introduced via an option gas flow line to prevent carbon build up.

**Plasma conditions:** Plasma conditions were optimized manually. (RF power = 1450 W, Carrier gas flow rate = 0.98 L/min, Option gas flow rate = 0.75 L/min and spray chamber temp. =  $-5^\circ\text{C}$ ).

**CRC conditions:**  $\text{O}_2$  gas at 0.4 mL/min, Octopole bias = -9 V, KED = -8 V.

**Sample:** Biodiesel certified reference material NIST SRM 2773.

## Results and discussion

When using mass-shift mode for sulfur (or any element) it is important to eliminate any potential interferences at the target mass of the reaction product ion, as well as on the primary element mass (the precursor ion). If the target mass suffers from interferences then the measurement would still be compromised. For sulfur, the corresponding isotopes are shifted as follows using  $M + 16$  u mass-shift:



Unfortunately, the  $\text{SO}^+$  product ion masses ( $m/z$  48, 49 and 50) can suffer from multiple interferences including  $\text{Ca}^+$ ,  $\text{Cr}^+$ ,  $\text{V}^+$ ,  $\text{Ti}^+$ ,  $\text{ArC}^+$  and  $\text{CCl}^+$  in natural samples. Furthermore, the  $^{33}\text{S}$  and  $^{34}\text{S}$  isotopes can suffer from overlaps due to other combinations of  $\text{SO}^+$  product ions, as well as pre-existing ions at the target mass. For example, the  $^{34}\text{S}^{16}\text{O}^+$  product ion formed at  $m/z$  50 is overlapped by  $^{32}\text{S}^{18}\text{O}^+$  and  $^{33}\text{S}^{17}\text{O}^+$ , as well as  $^{50}\text{Cr}^+$ ,  $^{50}\text{V}^+$ ,  $^{50}\text{Ti}^+$ ,  $^{38}\text{Ar}^{12}\text{C}^+$ , and  $^{13}\text{C}^{37}\text{Cl}^+$ . When operating the 8800 ICP-QQQ in MS/MS mass-shift mode, these overlaps are eliminated and the sulfur isotope pattern is preserved. Figure 1 provides a graphical representation of the ICP-QQQ setup and the method of interference elimination.

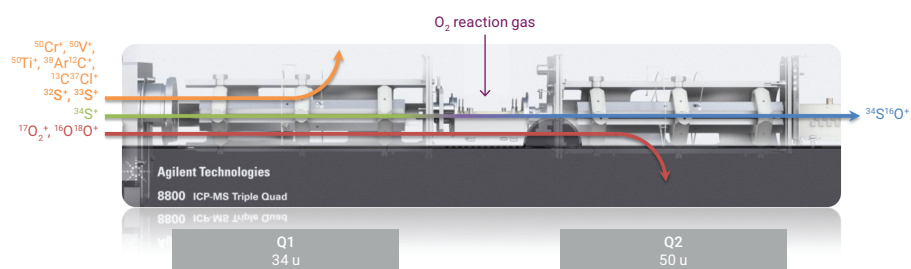


**Figure 1.** Mechanism of MS/MS mass-shift for sulfur isotope analysis. The mass difference between Q1 and Q2 is fixed at 16 u, so only the + <sup>16</sup>O-atom transition is observed – the other oxygen isotope transitions are eliminated so the original sulfur isotopic pattern is preserved.

This method would not be useful if the reaction were not quantitative, so to check for linearity, a blank ethanol sample was spiked with sulfur – see Figure 2. Despite the wide variation in absolute sensitivity for the different S isotopes, the BEC was the same for all three isotopes, indicating that the background is due to sulfur in the ethanol.

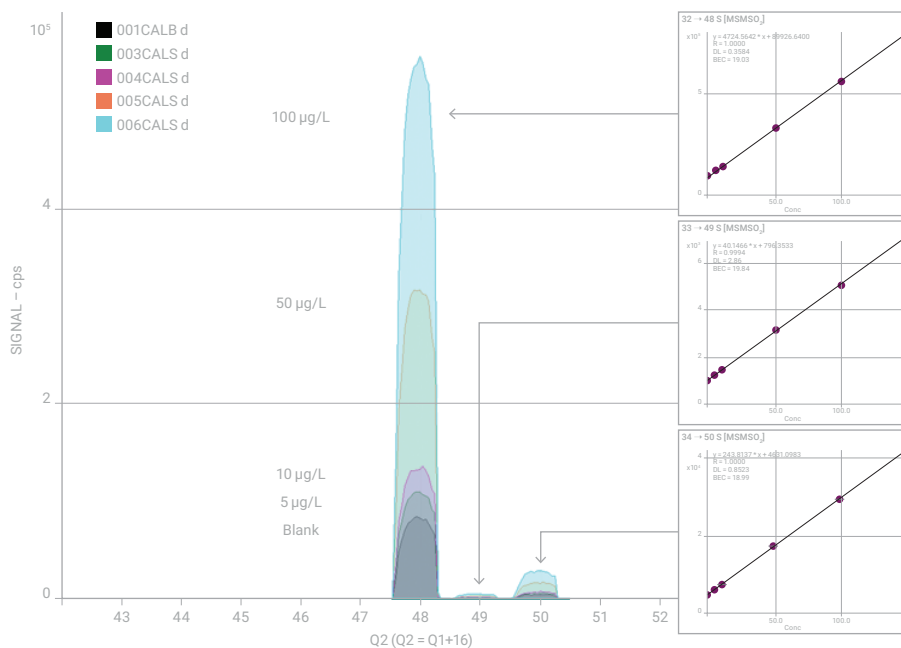


**Figure 2.** Ethanol with 0, 5, 10, 50 and 100 μg/L sulfur spikes and corresponding calibration curves.

An isotope dilution (ID) method was used to evaluate the accuracy of the 8800 ICP-QQQ MS/MS method, using a biodiesel certified reference material (NIST SRM 2773) and an enriched <sup>34</sup>S spike. The biodiesel sample was simply diluted into the ethanol solvent and the appropriate spike added. Reproducibility was tested by analyzing three separate samples of the CRM. The results are presented in Table 1. Repeat measurements were within the expected recovery limits for the material.

**Table 1.** Isotope dilution analysis of S in diluted biodiesel reference material NIST 2773.

Sample	S conc.(μg/g)
SRM 2773 - Certified	7.39 ± 0.39
SRM 2773 - measured 1	7.234
SRM 2773 - measured 2	7.227
SRM 2773 - measured 3	7.231
Average (measured)	7.231
Standard Deviation	0.003
95% confidence interval	7.231 ± 0.015



## Conclusion

Until the introduction of ICP-QQQ with MS/MS capability, it was impossible to obtain reliable results for reaction chemistry methods combined with an ID approach, using a quadrupole-based ICP-MS. The novel QQQ configuration of the 8800 ICP-QQQ enables operation in MS/MS mode, which ensures precise control over the reaction chemistry in the cell. This allows the unique isotopic information of the analyte to be retained, while removing the interferences that could affect both precursor and product ions of the target analyte.

# Determination of Chloride in Crude Oils using an Agilent 8900 ICP-QQQ

## Authors

Jenny Nelson

Agilent Technologies Inc.,  
Santa Clara, California, USA

Laura Poirier and Francisco Lopez-  
Linares

Chevron Energy Technology Company,  
Richmond, California, USA

Fast, accurate analysis of crude oils following direct dilution in an *o*-xylene-based diluent

## Introduction

As stated in a recent study, chlorinated compounds are often removed from crude oil refinery streams (1). To avoid corrosion and fouling during distillation, the concentration of chlorides in crude oil should be less than 1 mg/L. Despite its sensitivity, there are no ASTM standard test methods that use inductively coupled plasma mass spectrometry (ICP-MS) for the measurement of chloride in crude oils. However, ASTM D8110–17 test method specifies ICP-MS for the rapid determination of seven elements in distillate petroleum products (2). Because of its multi-element capabilities, ICP-MS is increasingly used to test petrochemical-based samples for a wide range of elements. It would be convenient to also use ICP-MS for the measurement of chloride.

The determination of chloride in complex matrices is challenging by conventional single quadrupole ICP-QMS. Petroleum crude oil and derivatives may contain sulfur (S), nitrogen (N), and oxygen (O) at variable concentrations, which could promote multiple interferences in the plasma. The  $^{35}\text{Cl}$  isotope (75.8% natural abundance) suffers polyatomic interferences from  $^{16}\text{O}^{18}\text{O}^1\text{H}^+$  and  $^{34}\text{S}^1\text{H}^+$ . Also, Cl is poorly ionized in the plasma because of its high first ionization potential of 12.967 eV, which affects the sensitivity of measurements by ICP-MS. Collision/reaction cells (CRCs) are used successfully to control many common polyatomic interferences in ICP-QMS. However, ICP-QMS cannot reduce the  $^{34}\text{S}^1\text{H}^+$  interference sufficiently to allow the accurate determination of Cl at trace levels in samples that contain a high level of S (1).

## Experimental

### Calibration standard and crude oil sample preparation

The calibration standards were prepared using different concentrations of a Cl organic solvent standard (Conostan, Quebec, Canada) prepared in a diluent. The diluent comprised 90 parts *o*-xylene (Fisher Scientific, NJ, USA) to 10 parts matrix modifier. The matrix modifier was made from mineral oil (80%, Fisher Scientific), a dispersant (20%, Chevron Oronite), and scandium (Sc) and yttrium (Y) spiked at 0.1 mg/kg as internal standards (Conostan, Quebec, Canada). Multiple calibration standards, ranging from 1 to 1000 mg/kg, were prepared by weight. The diluent (90% *o*-xylene to 10% matrix modifier) was run as a blank.

### Direct dilution

The composition of the 12 crude oil samples used in this study ranged from C (84 to 89 wt.%), H (10 to 14 wt.%), S (0.3 to 2.5 wt.%), and N (400 to 2500 mg/kg). The samples were diluted 1:5 or 1:10 (using diluent) to allow all Cl concentrations to fit within the calibration range. Standard Reference Material (SRM) NIST 1634c trace elements in fuel oil (Gaithersburg, MD, USA) was prepared at 1:5 and 1:10 dilution. All samples were shaken for two hours in a mechanical shaker. If any residue was seen on the vial walls, a vortex shaker was used to improve sample homogenization.

## Instrumentation

An Agilent 8900 ICP-QQQ (#100 for advanced applications) was used. The instrument was equipped with platinum sampling and skimmer cones, a concentric glass nebulizer, quartz spray chamber, and quartz torch with 1 mm injector. The diluted samples were introduced directly into the ICP-QQQ via a peristaltic pump fitted with solvent-resistant tubing (0.89 mm i.d., bought from Cole Parmer). Other parts were from the Agilent Organic Solvent Introduction kit (p/n G3280-60580). An optional gas flow of 20% O<sub>2</sub> in Ar was added to the carrier gas to prevent carbon building up on the interface cones. An *o*-xylene rinse was used between each sample to eliminate any carry-over from the sample introduction system.

Based on the findings of previous studies, hydrogen was used as a reactive cell gas for the determination of <sup>35</sup>Cl<sup>+</sup> (4, 5). Cl<sup>+</sup> reacts exothermically with H<sub>2</sub> to form HCl<sup>+</sup>, HCl<sup>+</sup> then continues to react via a chain reaction to form ClH<sub>2</sub><sup>+</sup>. This allows the use of the “mass-shift” approach, where the analyte reacts with a reaction gas in the cell to form a product ion, shifting it away from the interference. In this study, Q1 was set to *m/z* 35 to allow <sup>35</sup>Cl<sup>+</sup> ions to enter the CRC. The analyte ions then reacted with H<sub>2</sub> in the cell to form <sup>35</sup>Cl<sup>1</sup>H<sup>1</sup>H<sup>+</sup>, while the polyatomic interference ions (<sup>16</sup>O<sup>18</sup>O<sup>1</sup>H<sup>+</sup> and <sup>34</sup>S<sup>1</sup>H<sup>+</sup>) did not react with H<sub>2</sub>. Q2 was set to *m/z* 37, allowing the product of ion <sup>35</sup>ClH<sub>2</sub><sup>+</sup> to pass to the detector, free of interference.

ICP-QQQ instrument operating parameters are detailed in Table 1. For comparison purposes, chlorine was also measured using Instrumental Neutron Activation Analysis (INAA), which was carried out by EAI-Elemental Analysis, Inc, an elemental testing facility located in Lexington, KY, USA.

**Table 1.** ICP-QQQ operating conditions.

Parameter	Value
RF power (W)	1500
Nebulizer gas flow rate (L/min)	0.4
Sampling depth (mm)	8
Spray chamber temp (°C)	-2
Option gas flow rate (mL/min); Ar 80%, O <sub>2</sub> 20%	0.35 (35%)
Make up gas flow rate (L/min)	0.1
Nebulizer pump speed (rps)	0.1
H <sub>2</sub> cell gas flow rate (mL/min)	4.6
Octopole bias (V)	-18
Octopole RF (V)	180
Energy discrimination (V)	0
Monitored masses	Q1:35, Q2:37
Integration time (s)	3

## Results and discussion

The calibration plot for  $^{35}\text{Cl}$  is shown in Figure 1. Three sigma detection limits (DL), limits of quantification (LOQ), and background concentration (BEC) for  $^{35}\text{Cl}$  were determined by measuring a blank solution (*o*-xylene diluent containing a matrix modifier and internal standard) ten times. The results are shown in Table 2.

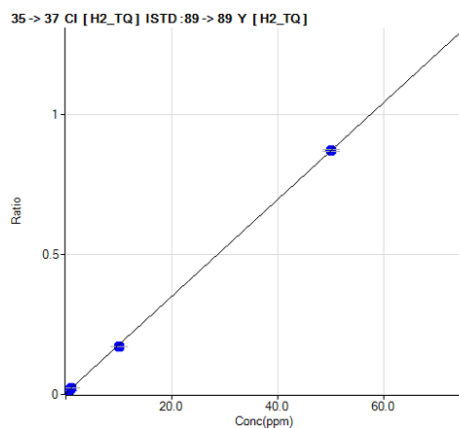


Figure 1. Calibration plot of Cl in *o*-xylene. Units: mg/kg (ppm).

Table 2. DL, LOQ, and BEC of  $^{35}\text{Cl}$  in a blank solution determined by ICP-QQQ in  $\text{H}_2$  mass-shift mode.

	Detection Limit (mg/kg)	LOQ (mg/kg)	BEC (mg/kg)
$^{35}\text{Cl}$	0.01	0.04	0.24

## Reference material analysis

Chlorine was determined in the petroleum feedstock SRM using the 8900 ICP-QQQ operating in  $\text{H}_2$  mass-shift mode. The reference value for chlorine in NIST 1634c is 45 mg/kg. The SRM was diluted in *o*-xylene at two different dilution factors. Other than carbon and hydrogen, real petroleum samples contain heteroatoms, S, N, and O, and metals such as V and Ni, among others. The sulfur content of NIST 1634c is around 2 wt.%, so the SRM is a useful test sample for ICP-QQQ given the likely interference on  $^{35}\text{Cl}$  by  $^{34}\text{S}^1\text{H}^+$ . As can be seen from the results presented in Table 3, excellent recoveries were obtained for  $^{35}\text{Cl}$ , irrespective of the dilution factor ( $100 \pm 10\%$ ). Since  $\text{H}_2$  effectively reacts with  $\text{Cl}^+$  to form  $\text{ClH}_2^+$ , the interferences on  $^{35}\text{Cl}$  can be avoided by measuring the product ion  $^{35}\text{ClH}_2^+$  at  $m/z$  37.

Table 3. Determination of Cl concentration in NIST 1634c SRM in *o*-xylene diluent using ICP-QQQ.

	Dilution Factor 5		Dilution Factor 10	
	Concentration (mg/kg)	*Recovery (%)	Concentration (mg/kg)	*Recovery (%)
$^{35}\text{Cl}$	44.33 $\pm$ 1.00	99	48.28 $\pm$ 1.89	107

\*NIST reference value for Cl = 45 mg/kg, S = 2 wt%

## Quantitative analysis of crude oil samples

Twelve petroleum crude oil samples with a sulfur content spanning from 0.38 up to 2.01 wt.% and hydrogen to carbon (H/C) ratio from 1.68 to 1.88 were analyzed by ICP-QQQ. The H/C provides an insight to the aromatic/paraffinic nature of the crude samples, which has implications for trading, processing, and stability of crude. The quantitative results for Cl measurements are given in Table 4.

**Table 4.** Determination of the Cl concentrations in 12 petroleum crude oil samples in *o*-xylene diluent using ICP-QQQ operating in H<sub>2</sub> mass-shift mode. Dilution factor 1:5. n = 3.

Sample	S (%)	H/C	<sup>35</sup> Cl Measured Concentration (mg/kg)	Sample	S (%)	H/C	<sup>35</sup> Cl Measured Concentration (mg/kg)
S1	0.38	1.84	22.32 ± 0.36	S7	1.19	1.78	24.80 ± 1.04
S2	0.38	1.85	12.80 ± 0.07	S8	1.19	1.78	20.78 ± 0.08
S3	0.38	1.86	22.84 ± 0.16	S9	1.97	1.71	48.33 ± 2.38
S4	0.38	1.88	6.15 ± 0.05	S10	1.99	1.68	18.25 ± 0.24
S5	0.50	1.85	33.89 ± 0.31	S11	2.01	1.70	50.35 ± 3.00
S6	0.59	1.87	24.87 ± 0.15	S12	2.01	1.71	17.68 ± 0.55

## Comparison of results

To further evaluate the accuracy of the ICP-QQQ method, quantitative results for Cl were compared with the results obtained by INAA. The results obtained for three crude samples are shown in Table 5.

**Table 5.** Comparison of measured Cl concentrations in crude oil samples obtained by ICP-QQQ (dilution factor 1:5) and INAA.

Sample	Measured Cl Concentration (mg/kg)	
	ICP-QQQ	INAA
S2	12.80 ± 0.07	14.40 ± 0.59
S4	6.19 ± 0.05	12.90 ± 0.53
S5	33.89 ± 0.31	25.30 ± 0.91

Depending on the sample, the agreement between the results obtained by ICP-QQQ and INAA was reasonably close. The agreement for sample S2 was around 89%, whereas it was slightly higher at 134% for sample S5. A similar observation was reported recently for these types of samples, using the same techniques (6). The low bias of the ICP-QQQ result for sample S4 suggests that the sample may contain solids or is heterogeneous. A qualitative XRF analysis of S4 suggested the presence of solids (most likely NaCl), which would explain why the ICP-QQQ result was low. It is likely that S4 wasn't fully solubilized or well dispersed in the *o*-xylene diluent.

## Conclusion

The Agilent 8900 ICP-QQQ is suitable for the determination of chlorine in petroleum crude samples. Despite the complex matrix, potential interferences on Cl ions originating from the crude petroleum samples were handled effectively using MS/MS technology. MS/MS enables more consistent and reliable reaction gas methods to be used for difficult elements, such as chlorine in complex matrices, than single quadrupole ICP-MS.

In this study, a BEC of 240 µg/kg was achieved for the most abundant Cl isotope, <sup>35</sup>Cl<sup>+</sup>, using mass-shift mode and H<sub>2</sub> cell gas. Interferences from <sup>16</sup>O<sup>18</sup>O<sup>1</sup>H<sup>+</sup> and <sup>34</sup>S<sup>1</sup>H<sup>+</sup> on <sup>35</sup>Cl<sup>+</sup> were avoided by measuring the product ion <sup>35</sup>ClH<sub>2</sub><sup>+</sup> at *m/z* 37.

A NIST trace element in fuel oil SRM and 12 crude oil samples were prepared for analysis using direct dilution. The specially prepared diluent contained o-xylene and a mineral oil matrix modifier, a dispersant, and internal standards. Excellent recoveries of Cl (99 and 107%) in the SRM were determined at two different dilution factors (5 and 10).

The petroleum crude samples were analyzed using ICP-QQQ, and some of the results were checked using INNA. The results show the importance of fully solubilized samples when using direct dilution as the sample preparation technique to avoid biased results due to the presence of particles.

Chloride was measured above the potential-corrosion trigger threshold of 1 mg/L in all 12 crude oil samples, indicating a risk of corrosion at refining facilities from the formation of HCl.

## References

1. Jenny Nelson, Laura Poirier, and Francisco Lopez-Linares, Determination of Chloride in Crude Oils by Direct Dilution using Inductively Coupled Plasma Tandem Mass Spectrometry (ICP-MS/MS), *J. Anal. At. Spectrom.*, 2019, Advance Article, DOI 10.1039/C9JA00096H
2. ASTM D8110–17 Standard Test Method for Elemental Analysis of Distillate Products by Inductively Coupled Plasma Mass Spectrometry (ICP-MS). ASTM International, West Conshohocken, PA, 2017, [www.astm.org/Standards/D8110.htm](http://www.astm.org/Standards/D8110.htm)
3. Handbook of ICP-QQQ Applications using the Agilent 8800 and 8900, Agilent publication, [5991-2802EN](#)
4. Naoki Sugiyama, Trace level analysis of sulfur, phosphorus, silicon and chlorine in NMP using the Agilent 8800 Triple Quadrupole ICP-MS, Agilent publication [5991-2303EN](#)
5. Kazumi Nakano, Ultra low-level determination of phosphorus, sulfur, silicon, and chlorine using the Agilent 8900 ICP-QQQ, Agilent publication, [5991-6852EN](#)
6. Adriana Doyle, Alvaro Saavedra, Maria Luiza B. Tristão, Márcio Nele, Ricardo Q. Aucélio, Direct chlorine determination in crude oils by energy dispersive X-ray fluorescence spectrometry: An improved method based on a proper strategy for sample homogenization and calibration with inorganic standards, *Spectrochimica Acta Part B*. 2011, 66, 368–372

## More information

For a full account of the method development, see Jenny Nelson, Laura Poirier, and Francisco Lopez-Linares, Determination of Chloride in Crude Oils by Direct Dilution using Inductively Coupled Plasma Tandem Mass Spectrometry (ICP-MS/MS), *J. Anal. At. Spectrom.*, 2019, Advance Article, DOI 10.1039/C9JA00096H

# Single nanoparticle analysis of asphaltene solutions using ICP-QQQ

## Authors

Jenny Nelson

Agilent Technologies, USA

Michiko Yamanaka

Agilent Technologies, Japan

Francisco Lopez-Linares, Laura Poirier,  
and Estrella Rogel

Chevron Energy Technology Company,  
USA

Agilent 8900 and ICP-MS MassHunter software module simplify spICP-MS analysis

## Introduction

Single Particle ICP-MS (spICP-MS) is increasingly being used to characterize the nanoparticle (NP) content of samples dispersed in an aqueous media (1–5). In several industries—including oil refining, petrochemicals, and semiconductor manufacturing—there is also interest in determining NPs in hydrocarbon matrices. In this study, we report a new method using triple quadrupole ICP-MS (ICP-QQQ) for the multi-element characterization of NPs in the heavy asphaltene fraction of petroleum (6). The method can be used to differentiate between metals present in NPs and the dissolved metal content. It will therefore extend the understanding of the role and form of metals present in crude oils and petroleum-based products. The method also has wider applicability to the characterization of NP populations in other hydrocarbon-based matrices, such as NMP, PGMEA, butyl acetate, and other organic solvents used in the semiconductor industry.

In spICP-MS analysis, the ICP-MS uses a fast time resolved acquisition mode to measure the signal generated by each NP as it passes through the plasma. The high sensitivity and low background noise of ICP-MS enables the signals generated from individual NPs to be distinguished, and these key performance characteristics are greatly enhanced with ICP-QQQ. The superior control of interferences achieved using tandem MS (MS/MS) operation means that ICP-QQQ is especially suitable for some of the elements of most interest in NP analysis, such as Si, Ti, Fe, S, and others.

The intensity of the NP signal peak is proportional to the size of the particle and the concentration (mass fraction) of the analyte element within the particle. The frequency of the individual NP signals is directly proportional to the number of NPs in the sample, allowing calculation of the NP size distribution, particle number, particle concentration, and dissolved metal concentration, all from a single ICP-MS measurement. Nanoparticle method setup, acquisition, calibration, and data reporting are simplified using the optional Single Nanoparticle Application Module of Agilent ICP-MS MassHunter software.

In this study, the spICP-MS acquisition mode of the Agilent 8900 ICP-QQQ was used to identify and characterize trace elements in asphaltenes—a complex class of high molecular weight hydrocarbons found in heavy oil fractions and bitumens. Asphaltenes are defined by their solubility class. They are soluble in aromatics such as benzene or toluene, but insoluble in lighter paraffins, such as *n*-pentane or *n*-heptane. Asphaltenes, together with waxes and resins, are of interest in petrochemical processing as they can deposit in equipment and pipelines leading to production problems. Asphaltenes also contain a high proportion of the metals in crude oil, including elements such as V and Ni, which act as catalyst poisons, affecting the oil refining process.

Iron- and Mo-based NPs were identified in the asphaltene samples. In contrast, V and Ni were found to be present mainly as dissolved metals, likely metal porphyrins and other organometallic species. Data is provided on the concentration and size distribution of Fe and Mo NPs in the asphaltene samples, and the levels of dissolved metals is also presented. The results highlight the potential of splCP-MS for the routine characterization of metal NPs—as well as dissolved metals—in asphaltenes, crude oils, petroleum-derived materials, and other organic sample-types.

## Experimental

### Reagents and samples

Trace metal grade purity chemicals were used throughout (6).

Three separate samples of asphaltene were obtained from different sources:

- Asphaltene A—a heavy Mexican crude oil (14° American Petroleum Institute, API).
- Asphaltene B—an asphaltenic deposit recovered from a submersible pump.
- Asphaltene C—an oxidized asphalt obtained from a commercial plant that produces specialty asphalts.

### Sample preparation

The asphaltenes were extracted from the sample matrix using n-heptane at a sample/solvent ratio of 1/20. The blended crude oil/heptane was heated to 80 °C. After one hour, the undissolved asphaltenes were recovered by filtering the mixture through a 0.8 µm membrane filter.

### Calibration standard preparation for total metals

Calibration standard solutions for direct analysis were prepared from Conostan (Quebec, Canada) S-21+K oil-based multi-element organometallic standard. The diluent comprised trace metal grade purity o-xylene (Fisher Scientific), a matrix modifier (made from mineral oil; Fisher Scientific), and a dispersant (Chevron Oronite). Scandium and yttrium were used as internal standards, spiked at 0.1 and 5 mg/kg, respectively.

Multiple calibration standards ranging from 1 to 1000 µg/kg for each of the target elements were prepared by weight from the 10 mg/kg Conostan multi-element standard and o-xylene diluent. The diluent solution was used as the blank for calibration.

### Nanoparticle reference materials and sample preparation

A 60 nm silver (Ag) NP reference material (nanoComposix) was used to calculate the nebulizer efficiency. The Ag NP reference material and the three asphaltene samples were diluted to a particle concentration of between 40 and 1000 ng/g with o-xylene (via propylene glycol methyl ether acetate, PGMEA). The solutions were sonicated for 5 min to ensure sample homogeneity. Elemental response factors were determined by measuring elemental standards for each target analyte (10.0 µg/g) prepared with o-xylene.



### Wet acid digestion for total metals

One to 5 g of each sample was heated on a hot plate at 100 °C for four hours with 1 to 2 mL of H<sub>2</sub>SO<sub>4</sub> (93–98 % w/w). The solution was then subjected to an ashing sequence, as described in reference 6. Six mL HCl (34 to 37 % w/w) and 2 mL HNO<sub>3</sub> (67 to 70 % w/w) were added, before further heating on a hot plate at 100 °C for 1 hour. Before analysis, Sc was added as an internal standard (to give a final Sc concentration of 5 mg/kg) and the solution was brought to a final volume of 25 mL with Milli-Q water.

### Instrumentation

An Agilent 8900 Triple Quadrupole ICP-MS (ICP-QQQ) equipped with the standard glass concentric nebulizer and Peltier-cooled quartz spray chamber was used. For the analysis of samples prepared in organic solvent (spICP-MS analysis and total metals determinations in the diluted asphaltene samples), an optional “organics” quartz torch with a 1 mm ID injector was used in place of the standard quartz torch, which has a 2.5 mm injector.

For the organic sample analyses, oxygen (20% in Ar) was added to the injector gas stream after the spray chamber. O<sub>2</sub> addition serves to decompose the carbon matrix thus avoiding carbon deposition on the interface cones. The more reactive plasma environment with O<sub>2</sub> addition requires the use of the more chemically resistant optional platinum-tipped sampling and skimmer cones.

The high sensitivity of the ICP-QQQ enabled the samples for NP analysis to be diluted by a factor between 1:2100 and 1:2700 in o-xylene. Applying a high dilution factor minimizes the risk of colloidal particles forming an agglomerate after nebulization. The dilution ensures that the NPs are dispersed in the solution so that each NP passes through the plasma separately from any other NPs. As a result, the signal peaks measured are each generated by a single particle event and not from multiple, overlapping particle signals.

Signal intensities for each NP target element were acquired in fast Time Resolved Analysis (fast TRA) mode using a dwell time of 0.1 ms (100 μs) per point, with no settling time between measurements. For Fe and Mo NPs, the signals were measured on-mass in MS/MS mode. For on-mass measurements, both quadrupoles (Q1 and Q2) were set to the target analyte ion mass of *m/z* 56 (for Fe) and *m/z* 95 (for Mo). Helium (He) cell gas was used in the 8900 ORS, to control the polyatomic interferences (mainly ArO on Fe at *m/z* 56). On-mass measurement with He cell gas was also used for the measurement of V and Ni (dissolved concentrations only—no NPs detected). ICP-QQQ operating conditions are given in Table 1.

**Table 1.** ICP-QQQ operating conditions.

Parameter	Value
RF power (W)	1600
Sampling depth (mm)	10
Carrier gas (L/min)	0.35
Spray chamber temperature (°C)	-5
Option gas (L/min) (Ar 80%, O <sub>2</sub> 20%)	0.35
Dwell time (ms)	0.1
He cell gas flow rate (mL/min)	5.0

## Simplified workflow

The optional Single Nanoparticle Application Module of the ICP-MS MassHunter software was used for NP data acquisition and analysis. The spICP-MS Method Wizard guides the user through the process of nanoparticle method setup, data acquisition, data analysis, and presentation of the NP results data.

## Nebulization efficiency

Nebulization efficiency is the ratio of the amount of analyte (aerosol) delivered to the plasma as a proportion of the amount of analyte (solution) entering the nebulizer. In this work, the nebulization efficiency was determined using the Ag NP reference material of known (60 nm) particle size. The reference material was first dispersed in PGMEA, and then further diluted in *o*-xylene. Nebulization efficiency, calculated from the certified size of Ag NP reference material, was found to be 0.065 or 6.5%.

## Results and discussion

### Nanoparticle size distributions

Nanoparticles containing Fe and Mo were detected in the asphaltene samples using the sp-ICP-MS method. By contrast, the signals for V and Ni were continuous, rather than the discrete signal pulses caused by the presence of clusters or particles of these elements. This finding indicates that V and Ni were most likely in the form of dissolved metal complexes. The TRA signal charts for Fe in sample B (Figure 1) and Mo in sample A (Figure 2) show the signal-intensity as a function of time. In spICP-MS, the peak area for each particle signal “plume” can be used to calculate the particle mass and therefore size.

According to the literature, the Fe NPs are most likely to be present as iron oxides ( $\text{Fe}_2\text{O}_3$  or  $\text{Fe}_3\text{O}_4$ ) (7) and pyrrhotite ( $\text{FeS}$ ) (8). The Mo NPs are most likely present as molybdenite ( $\text{MoS}_2$ ) (9), which is readily formed from oil-soluble Mo complexes present in heavy fractions from crude oils (10, 11).

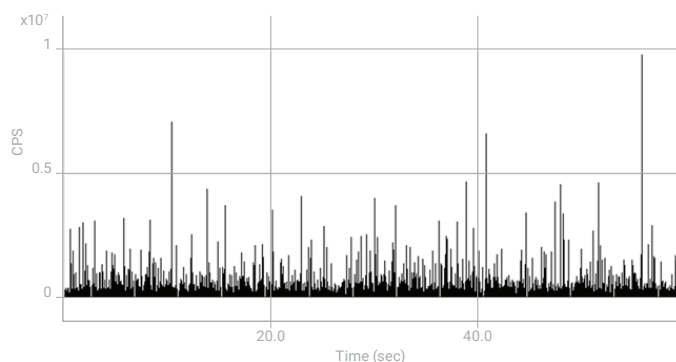


**Figure 1.** Asphaltene sample B: typical signals in counts per second (cps) for Fe ( $m/z$  56) as a function of time.

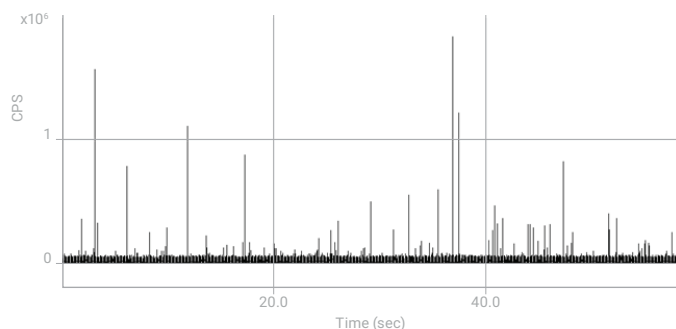


**Figure 2.** Asphaltene sample A: typical signals in counts per second (cps) for Mo ( $m/z$  95) as a function of time.

The Fe and Mo NP size distribution plots for the three different asphaltene samples were calculated on the assumption that the Fe NPs were composed of  $\text{Fe}_2\text{O}_3$ , and the Mo NPs were composed of  $\text{MoS}_2$ . As shown in Figure 3, the average size of the Fe NPs varied among the samples. In contrast, the particle size distributions for Mo NPs are similar, with an average particle diameter in the range 70 to 80 nm (Figure 4).

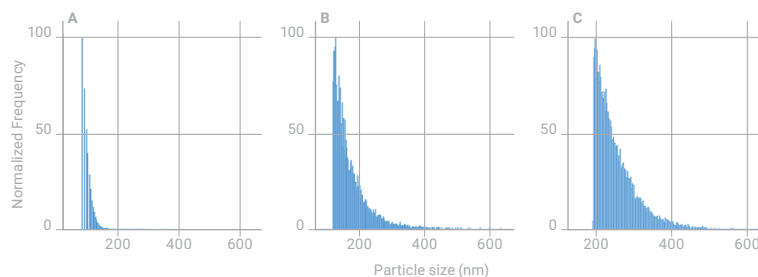


**Figure 3.** Comparison of size distributions for Fe NPs as  $\text{Fe}_2\text{O}_3$  in the three asphaltene samples: A, B, and C. Modified with permission from J. Nelson et al., *Energy Fuels*, 2017, 31 (11), 11971–11976. © 2017 American Chemical Society.

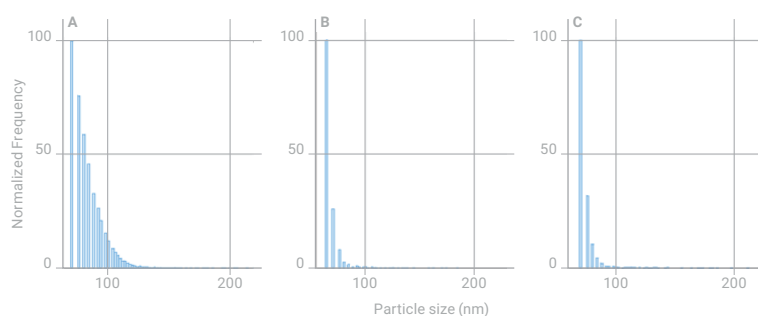


**Figure 4.** Comparison of size distributions for Mo NPs as  $\text{MoS}_2$  in the three asphaltene samples: A, B, and C. Modified with permission from J. Nelson et al., *Energy Fuels*, 2017, 31 (11), 11971–11976. © 2017 American Chemical Society.

### Concentration of the different forms of Fe and Mo

Uniquely, spICP-MS can distinguish between metal content that is contained in NPs (insoluble) and metal content that is dissolved in the sample matrix. The relative NP and soluble concentration data for Fe and Mo in the three asphaltene samples is given in Table 2. The data indicates that there was some variation in the distribution of metals among the asphaltene samples. In samples A and B, Fe was mostly present as NPs (76 and 91 wt. %, respectively), while in asphaltene sample C, less than half the Fe content was present as NPs. By contrast, Mo was almost all present as soluble forms (between 60 and 99 wt. %) in all three asphaltene samples, as shown in Table 2.

**Table 2.** Interference check results for  $^{48}\text{Ti}$  in various matrices, with and without cell gas.

Asphaltene samples	Iron concentration, mg/kg					Molybdenum concentration, mg/kg				
	NPs	Soluble	Total, spICP-MS	Total, direct dilution	Total, wet acid digestion	NPs	Soluble	Total, spICP-MS	Total, direct dilution	Total, wet acid digestion
A	54.0 (76%)	17.0	71.0	39.5	68.0	3.48	5.33 (60%)	8.81	39.7	40.4
B	173 (91%)	0.001	0.18	0.054	0.001	0.04	3.23 (99%)	3.27	0.78	0.52
C	457 (47%)	508	965	420	750	0.07	6.33 (99%)	6.40	5.89	6.22

Reprinted with permission from J. Nelson et al., *Energy Fuels*, 2017, 31 (11), 11971–11976. © 2017 American Chemical Society.

### **Total concentration of Fe and Mo**

The total concentrations of Fe and Mo from the spICP-MS analysis (sum of the particle concentration and the dissolved concentration) were compared to the total metal concentrations measured by direct dilution and wet acid digestion. The results, which are given in Table 2, indicate that there was some variation between the three separate results for total concentrations of Fe and Mo. The spICP-MS and acid digestion approaches gave similar results for total Fe in all three samples, with the direct dilution results being consistently lower. This low bias for Fe present as particles in samples prepared and introduced using direct dilution has been reported in the literature (12). A study using Laser Ablation-ICP-MS (13) has also shown that large particles are not completely vaporized and ionized in the plasma. This finding could account for the low recovery observed for Fe in the direct analysis of the diluted samples. The difference compared to the spICP-MS total concentration may be due to the way the relatively large particles in these asphaltene samples are calibrated in spICP-MS vs the effect of incomplete dissociation and ionization of these larger particles measured by direct dilution.

The concentrations for Mo following direct dilution compare well with those obtained using wet acid digestion. For sample C, the total concentration found using spICP-MS also agrees well. But for the other two samples, the spICP-MS results do not tally with the total Mo concentrations found by the dilution and digestion methods. Total Mo by spICP-MS was found to be lower in Sample A and higher in Sample B, compared to total Mo determined by the other two approaches. Further studies are underway to investigate the discrepancies in the total concentration values for Mo calculated using the spICP-MS method compared with direct dilution and wet acid digestion.

### **Conclusion**

Single particle-ICP-MS is becoming a widely used and well-established technique for the characterization of NPs in aqueous-based solutions. In this study, we show the potential for the spICP-MS methodology to be applied to complex hydrocarbon-based matrices of interest in petroleum refining and other industries.

The Agilent 8900 ICP-QQQ is especially suited to spICP-MS analysis because of its high sensitivity, low background, and unmatched control of spectral interferences. Setup and analysis for NP applications is facilitated by the optional Single Nanoparticle Application Module for ICP-MS MassHunter software.

Iron and molybdenum NPs were determined in three asphaltene samples from different sources associated with oil refining and petroleum-related product processing. No nickel or vanadium-containing NPs were detected in the heavy petroleum fractions suggesting that these elements are more likely to form dissolved organometallic complexes, such as porphyrins. This spICP-MS method is also able to differentiate between metal-containing NPs and dissolved metals.

Further work is in progress to expand the spICP-MS method for the routine characterization of metals in petroleum-derived samples, as well as in other hydrocarbon-based samples.

## References

1. S. Sannac, Single particle analysis of nanomaterials using the Agilent 7900 ICP-MS, Agilent publication, 2014, [5991-4401EN](#)
2. S. Wilbur, M. Yamanaka and S. Sannac, Characterization of nanoparticles in aqueous samples by ICP- MS, Agilent publication, 2015, [5991-5516EN](#)
3. M. Yamanaka, K. Yamanaka, T. Itagaki, S. Wilbur, Automated, high sensitivity analysis of single nanoparticle using the Agilent 7900 ICP-MS with Single Nanoparticle Application Module, Agilent publication, 2015, [5991-5891EN](#)
4. S. Nunez, H. Goenaga Infante, M. Yamanaka and T. Itagaki, Analysis of 10 nm gold nanoparticles using the high sensitivity of the Agilent 8900 ICP-QQQ, Agilent publication, 2016, [5991-6944EN](#)
5. M. Yamanaka and S. Wilbur, Accurate Determination of TiO<sub>2</sub> Nanoparticles in Complex Matrices using the Agilent 8900 ICP-QQQ, Agilent publication, 2017, [5991-8358EN](#)
6. J. Nelson, M. Yamanaka, F. A Lopez-Linares, L. Poirier, and E. Rogel, Characterization of dissolved metals and metallic nanoparticles in asphaltene solutions by Single Particle ICP-MS, *Energy Fuels*, **2017**, 31 (11), pp 11971–11976
7. L. Carbognani, Effects of iron compounds on the retention of oil polar hydrocarbons over solid sorbents, *Petroleum Science and Technology*, **2000**, 18, 335–360.
8. W. R. Biggs, R. J. Brown, J. Fetzer, Elemental profiles of hydrocarbon materials by size-exclusion chromatography/inductively coupled plasma atomic emission spectrometry, *Energy & Fuels*, **1987**, 1, 257–262.
9. F. L. Hess, Molybdenum Deposits. A Short Review, United States Geological Survey, Bulletin 761, p. 2, Government Printing Office, Washington 1924.
10. I. Watanabe, Y. Korai, I. Mochida, M. Otake, M. Yoshimoto, K. Sakanishi Behaviors of oil-soluble molybdenum complexes to form very fine MoS<sub>2</sub> particles in vacuum residue, *Fuel*, 2002, 81, 1515–1520.
11. I. Aydin, F. Aydin, C. Hamamci, Molybdenum speciation in asphaltite bottom ash (Seguruk, SE Anatolia, Turkey), *Fuel*, 2012, 95, 481–485.
12. L. Poirier, J. Nelson, G. Gilleland, S. Wall, L. Berhane, F. Lopez-Linares, Comparison of Preparation Methods for the Determination of Metals in Petroleum Fractions (1000 °F+) by Microwave Plasma Atomic Emission Spectroscopy, *Energy & Fuels*, **2017**, 31, 7809–7815.
13. M. Guillong, D. Günther, Effect of particle size distribution on ICP-induced elemental fractionation in laser ablation-inductively coupled plasma-mass spectrometry, *J. Anal. At. Spectrom.*, **2002**, 17, 831–837.

# Gas chromatographic separation of metal carbonyls in carbon monoxide with detection using the Agilent 8800 ICP-QQQ

## Authors

William M. Geiger, Blake McElmurry  
and Jesus Anguiano

CONSCI, Ltd., Pasadena, Texas, USA

## Introduction

Carbon monoxide (CO) gas is used in a number of industries and applications. For example, the semiconductor industry uses it to moderate the etch rate of silicon wafers and improve selectivity for greater control of the process. In pharmacology, CO has been used therapeutically to mitigate organ rejection in transplant patients. It can also be a major constituent in cogeneration gas or syngas. However, CO can form a metal carbonyl on contact with various metals including chromium, molybdenum, iron, nickel, cobalt, and several more. Iron carbonyl  $[\text{Fe}(\text{CO})_5]$  and nickel carbonyl  $[\text{Ni}(\text{CO})_4]$  are the most common examples [1].

Metal carbonyls are highly toxic and the therapeutic use of carbon monoxide can lead to exposure to carbonyls that may be more harmful than the CO itself. In the etching process, if a metallic carbonyl residue forms on the surface of the wafer, it can cause electronic device failure. Similarly, if CO is present at high levels in syngas, the deposition of carbonyls on gas turbine fan blades may lead to the catastrophic failure of the turbine. Because of the potential harm caused by metal carbonyls, it is important that the concentration of metal carbonyls in CO used in mixed gases is known or controlled before the gas is used.

Gas chromatography with electron capture detection (ECD) can be used for the analysis of nickel and iron carbonyl, with excellent sensitivity [2]. However, the method requires a laborious and complicated calibration strategy that can lead to poor accuracy due to errors introduced during sample handling and analysis. A novel approach using a GC coupled to a triple quadrupole ICP-MS (ICP-QQQ) operating in MS/MS mode offers an efficient and elegant alternative approach for the analysis of Ni, Fe and other metal carbonyls.

There are several challenges that need to be addressed for GC-ICP-QQQ analysis to be successful. Since metal carbonyl gas standards are not readily available, a calibration strategy must be developed. As both nickel and iron carbonyls can easily form or deposit on steel surfaces in a carbon monoxide matrix, a chromatographic system without metal in the flow path must be used to avoid erroneous measurements. Finally, for optimum performance, two tune conditions are required for the ICP-QQQ as the best performance for nickel is achieved using helium gas in the ORS collision/reaction cell, while performance for iron is superior with hydrogen cell gas.

## Experimental

### Instrumentation

An Agilent 7890B Gas Chromatograph was coupled to an Agilent 8800 Triple Quadrupole ICP-MS, using a combined gas/liquid introduction interface, as illustrated in Figure 1.

All sample wetted parts were composed of PEEK, including tubing, sampling lines, and a Valco 10 port gas sampling valve (GSV). The GSV was used to introduce two gas volumes to the GC column (Figure 2). A sample loop of 280  $\mu\text{L}$  was used for the introduction of the calibration standard or carbon monoxide sample, and a standard addition loop of 70  $\mu\text{L}$  was used as an internal calibration/check standard.

The combination GC-ICP-QQQ interface (with both GC effluent connection and conventional nebulizer/spray chamber) enabled the liquid standard solution or blank (introduced via the nebulizer) to be mixed with the gaseous effluent from the GC, before being passed to the plasma torch [3]. GC operating conditions are given in Table 1.

**Table 1.** Agilent 7890 GC conditions

Carrier	Helium @ 13 psig
Column	30 m x 0.53 mm x 1.5 $\mu\text{m}$ DB-5
Oven	40 °C Isothermal
Sample size	280 $\mu\text{L}$

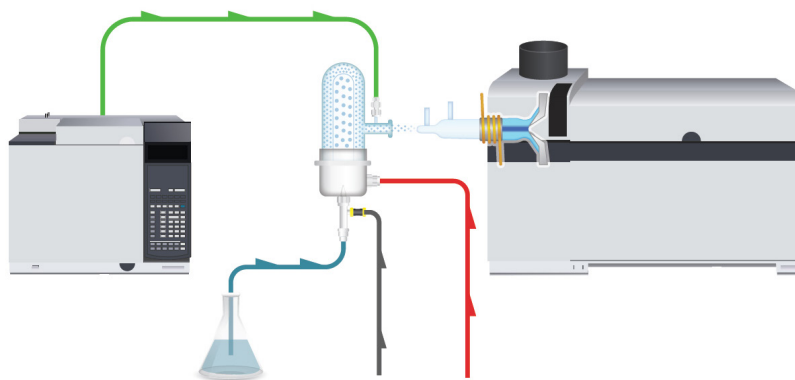


**Figure 1.** GC-ICP-QQQ interface for the simultaneous aspiration of liquid standard or blank and GC effluent

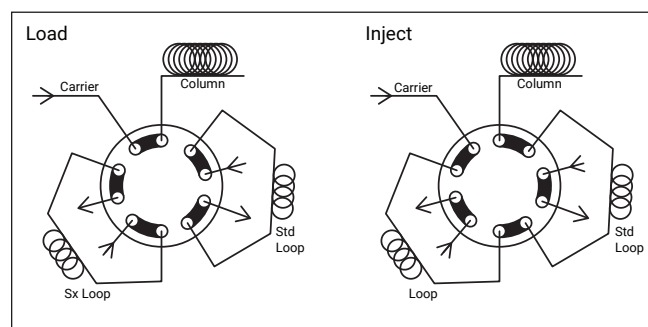


**Figure 2.** Valco 10 port PEEK gas sampling valve (GSV) flow path providing standard addition capability.

## Acquisition conditions

In this study, the 8800 ICP-QQQ was operated in MS/MS mode using helium as the collision gas for the on-mass measurement of Ni at  $m/z$  58 (integration time 0.1 seconds/mass). Hydrogen cell gas mode was used for the on-mass measurement of Fe at  $m/z$  56 (integration time 0.5 seconds/mass). Tuning conditions were almost identical for the two modes, the only differences were in the KED voltage and the cell gas flow. Bromine was determined in He mode at  $m/z$  79 (integration time 0.1 seconds/mass).

**Table 2.** Agilent 8800 ICP-QQQ operating conditions

	He mode	H <sub>2</sub> mode
RF power (W)		1550
Sample depth (mm)		8.0
Dilution gas flow (L/min)		0.2
Extract 1 (V)		0.0
Extract 2 (V)	-165.0	-160.0
Kinetic Energy Discrimination (V)	3.0	0.0
Cell gas flow (mL/min)	3.30	7.00
Integration time/mass (seconds)	Ni, Br: 0.1	Fe: 0.5

## Calibration

Calibration was performed by the aspiration of aqueous standards (Inorganic Ventures, Christiansburg, Virginia, USA, standard IV-ICPMS-71A) of nickel (0.17  $\mu$ moles/L), iron (0.18  $\mu$ moles/L), and a bromine standard (12.8  $\mu$ moles/L). This allowed the relative response of Ni and Fe to Br to be determined, as illustrated for Ni in Figure 3. In order to determine nickel or iron carbonyl concentrations, a gas standard of methyl bromide (101 ppb) was introduced to the GC via the GSV. Relative response factors were used to quantitate for the unknowns as illustrated in Figure 4 [4]. The methyl bromide gas phase standard was prepared at 101 ppb by dynamically diluting a higher level standard (certified as 9.90 ppm NIST traceable, sourced from United Specialty Gases, Houston, Texas, USA).

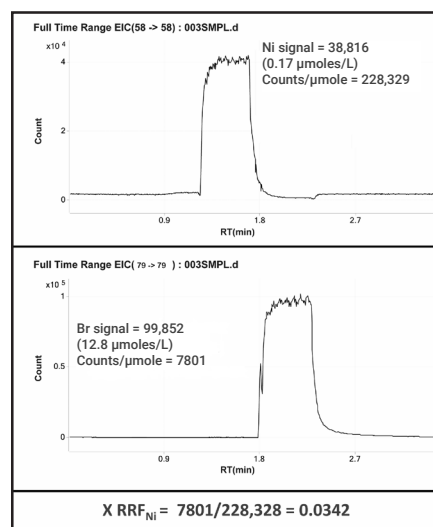


**Figure 3.** Calculation of relative response factor (RRF) for Ni, from aspiration of aqueous nickel and bromine standards

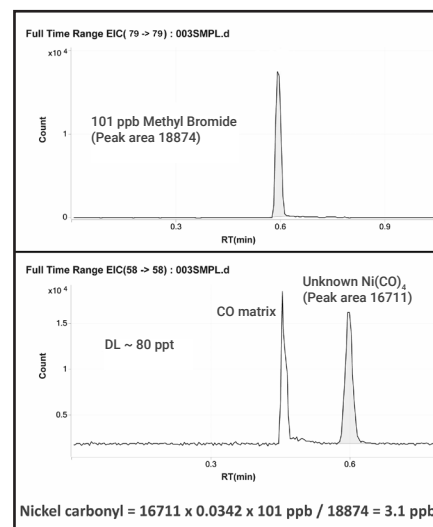


**Figure 4.** Analysis of known gas phase bromine standard as a surrogate standard for the determination of unknown nickel carbonyl.



The ICP-MS MassHunter software allows multiple tune conditions to be applied in series during a single time resolved analysis (TRA) acquisition. Mode switching allows the acquisition mass and cell mode to be changed mid-run, so nickel and iron can be measured under optimum conditions (using helium and hydrogen cell gas, respectively), in the same analytical run. As there is a reasonable interval between the elution of nickel carbonyl and iron carbonyl, there is sufficient time for switching tune conditions so that both elements can be measured from a single injection. Since two tune modes were used in the analysis (He mode for Ni and Br, and H<sub>2</sub> mode for Fe) there was a virtual gain in sensitivity when switching mode since only one mass was monitored at a time allowing for better signal averaging. This is illustrated in Figure 5.

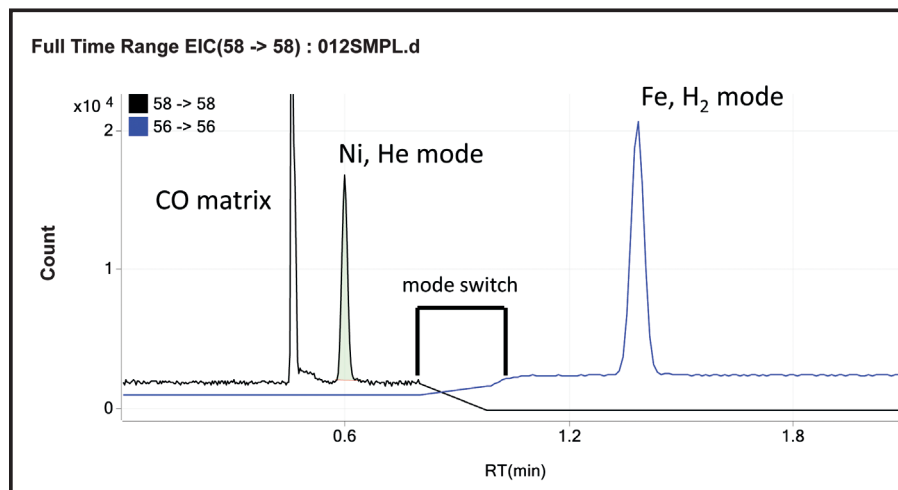


Figure 5. Tune mode switching for optimum measurement conditions during TRA acquisition.

### Limits of Detection

The detection limit (DL) for nickel carbonyl was estimated to be 80 ppt based on 2x signal-to-noise (S/N). Since the iron carbonyl peak is broader, the integration time was increased from 0.1 to 0.5 seconds/mass in the second tune so that the S/N ratio was improved. For comparison purposes, two different methods were used to establish the DL for iron carbonyl. A simple 2 x S/N calculation gave a DL of ~70 ppt. Applying a t-test to eight replicate analyses resulted in a more statistically valid value of 140 ppt. The nickel DL was improved at least twofold using He gas mode compared to no gas. Similarly, the DL for iron was improved about three fold using hydrogen versus helium as the cell gas.

An important matter in achieving very low detection limits, particularly for iron carbonyl, is the cleanliness of the blank solution. Figure 6 shows the signal plot for a suspect blank compared to a five level calibration. Note that the suspect blank is over 2 ppb on a weight basis, which would raise the noise level and therefore the detection limit for the gas phase analysis.

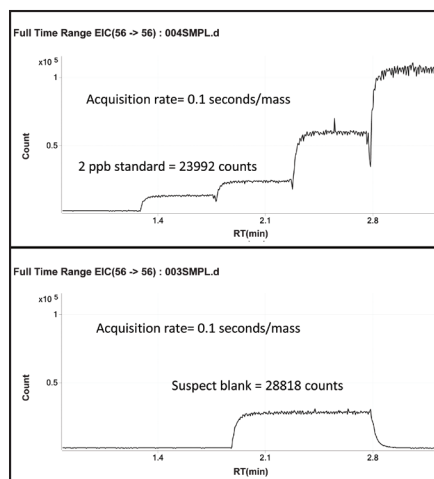


Figure 6. Aqueous standards (top) versus contaminated blank (bottom)

## Conclusions

The Agilent 8800 ICP-QQQ's ability to use multiple tune conditions in a single chromatographic analysis makes it possible to use optimum acquisition settings for each analyte. This enables the GC-ICP-QQQ to achieve excellent detection limits for nickel carbonyl and iron carbonyl, two of the most analytically challenging contaminants in carbon monoxide. The detection levels of 70-80 ppt are comparable to GC-ECD detection and are well below what is currently required by the various industries. However, the multi-element capability of ICP-QQQ ensures that other metal carbonyls can also be successfully measured with this method, including  $\text{Co}_2(\text{CO})_8$ ,  $\text{Cr}(\text{CO})_6$ ,  $\text{Mo}(\text{CO})_6$ , and  $\text{Fe}_2(\text{CO})_9$ .

The GC was interfaced to the ICP-QQQ via a second inlet connection to the standard ICP spray chamber, to allow simultaneous aspiration of an aqueous standard. This approach is essential to performing quantitative measurements of carbonyl species, for which gas phase standards are not typically available. The simultaneous aspiration of an aqueous standard also provides sufficient oxygen to prevent carbon buildup on the torch or cones from the carbon monoxide, avoiding the need to add additional oxygen.

## References

1. D.H. Stedman, D.A. Hikade, R. Pearson, Jr., E.D. Yalvac, *Science*, 1980, 208, 1029
2. A. Harper, *Analyst*, 1991, 149-151
3. E.M. Krupp, et. al., *Spectrochimica Acta Part 56*, 2001, 1233-1240
4. W.M. Geiger, M.W. Raynor, D. Cowles, *Trace Analysis of Specialty and Electronic Gases*, 2013, Wiley, Chapter 6, 182-185.

## Geology and geochemistry

Title	Page
Lead isotope analysis: removal of $^{204}\text{Hg}$ isobaric interference on $^{204}\text{Pb}$ using ICP-QQQ MS/MS reaction cell	364
Fractionation of sulfur isotope ratio analysis in environmental waters	368
Measurement of $^{87}\text{Sr}/^{86}\text{Sr}$ isotope ratios in rocks by ICP-QQQ in mass-shift mode	372
Direct strontium isotopic analysis of solid samples by LA-ICP-MS/MS	378
Resolution of $^{176}\text{Yb}$ and $^{176}\text{Lu}$ interferences on $^{176}\text{Hf}$ to enable accurate $^{176}\text{Hf}/^{177}\text{Hf}$ isotope ratio analysis using an Agilent 8800 ICP-QQQ with MS/MS	382

# Lead Isotope Analysis: Removal of $^{204}\text{Hg}$ Isobaric Interference on $^{204}\text{Pb}$ using ICP-QQQ MS/MS Reaction Cell

## Author

Glenn Woods  
Agilent Technologies, UK

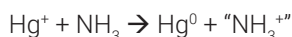
## Keywords

lead, isotope, ratio, geochronology, dating, mercury, artifacts, precious metals, food, ammonia, on-mass

## Introduction

Lead isotope ratio analysis is important as it is used for Pb-Pb dating in geochronology, and to trace the origin of artifacts, precious metals and even foodstuffs. The natural isotopic pattern of lead varies more than any other element in the periodic table, because three of its isotopes are formed from the radioactive decay of uranium ( $^{235}\text{U} \rightarrow ^{207}\text{Pb}$ ;  $^{238}\text{U} \rightarrow ^{206}\text{Pb}$ ) and thorium ( $^{232}\text{Th} \rightarrow ^{208}\text{Pb}$ ). The Pb isotopic pattern can therefore vary depending upon the geology of the rocks and minerals from which the lead was extracted, and the age of the material. In geochronology, the constant rate of U/Th decay allows the Pb/Pb, U/Pb and Th/Pb ratios to be used to date the age of rocks using a so-called geological clock.

When Pb ratios are measured, it is often necessary to correct for the lead naturally present in the sample, and the only non-radiogenic isotope of Pb ( $^{204}\text{Pb}$ ; natural or common lead), is used for this purpose. For Pb-Pb dating,  $^{204}\text{Pb}$  is the reference isotope against which the radiogenic isotopes are compared ( $^{206}\text{Pb}/^{204}\text{Pb}$ ;  $^{207}\text{Pb}/^{204}\text{Pb}$ ). Unfortunately,  $^{204}\text{Pb}$  is directly overlapped by an isotope of Hg ( $^{204}\text{Hg}$ ), which makes accurate measurement of  $^{204}\text{Pb}$  impossible by ICP-MS. Mass resolution of  $^{204}\text{Pb}$  from  $^{204}\text{Hg}$  is far beyond the capability of any commercial high-resolution (HR-) ICP-MS system, and until recently there has been no reliable chemical means to remove the Hg interference, so mathematical correction has been employed, which introduces error. Mercury does however undergo a gas-phase charge-transfer reaction with ammonia gas ( $\text{NH}_3$ ), a reaction that can be utilized in the collision/reaction cell of a suitably equipped ICP-MS as follows:



This reaction offers the potential to remove the  $^{204}\text{Hg}$  interference from  $^{204}\text{Pb}$ , and could be applied to either solution or laser-based ICP-MS analysis.

## Experimental

**Instrumentation:** Agilent 8800 #100.

**Plasma conditions:** Preset plasma/General purpose.

**Ion lens tune:** Soft extraction tune: Extract 1 = 0 V, Extract 2 = -170 V.

**CRC conditions:**  $\text{NH}_3$  gas (10% in He) at 1.7 mL/min, Octopole bias = -8 V, KED = -8 V.

**Acquisition parameters:** Three acquisition modes were compared:

- No gas: No reaction cell gas; Single Quad (SQ) mode with Q1 operating as an ion guide.
- NH<sub>3</sub> bandpass: Ammonia reaction gas; SQ mode with Q1 operating as a bandpass filter.
- NH<sub>3</sub> MS/MS: Ammonia reaction gas; MS/MS mode with Q1 operating as a mass filter at unit mass resolution.

## Results and discussion

### Removal of <sup>204</sup>Hg<sup>+</sup> interference on <sup>204</sup>Pb<sup>+</sup>

A preliminary study showed that Pb is almost unreactive with NH<sub>3</sub> cell gas (<0.5% loss of Pb signal) indicating that on-mass sensitivity for Pb should be maintained. On-mass measurement of Pb in NH<sub>3</sub> cell gas mode was therefore investigated in the presence of Hg at 10 ppb. Figure 1 displays the spectra obtained in no gas (left) and NH<sub>3</sub> cell gas (right) modes. The <sup>204</sup>Hg interference on <sup>204</sup>Pb can be clearly seen in the no gas spectrum, while it has been completely removed under NH<sub>3</sub> reaction mode with MS/MS. A perfect isotopic pattern match was confirmed for Pb in NH<sub>3</sub> mode.

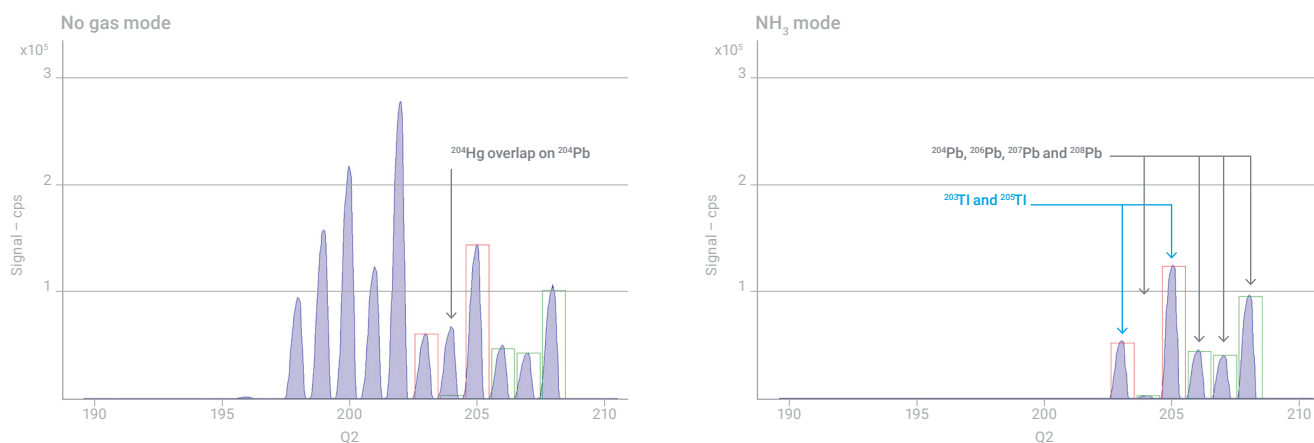


**Figure 1.** Standard solution (1 ppb each of Pb and Tl) spiked with 10 ppb Hg without cell gas (left) and with NH<sub>3</sub> (right) using MS/MS mode. Note the <sup>204</sup>Hg interference on <sup>204</sup>Pb in no gas mode.

## Effectiveness of MS/MS

The  $\text{NH}_3$  reaction that removes the  $^{204}\text{Hg}$  interference would also work in the reaction cell of a single quadrupole ICP-MS (ICP-QMS), but ammonia is a highly reactive gas and can produce many adduct cluster ions, for example from Rare Earth Elements (REEs), see Table 1. The complex matrix composition of many natural samples means that the results obtained with  $\text{NH}_3$  cell gas in ICP-QMS are often extremely unreliable. With the 8800 ICP-QQQ, MS/MS mode allows all the co-existing matrix elements to be rejected by Q1, so only the target ions ( $^{204}\text{Pb}$  and  $^{204}\text{Hg}$ ) enter the CRC. The  $\text{NH}_3$  reactions are therefore controlled and consistent, and no overlapping reaction product ions are formed from other elements in the sample.

**Table 1.** Some possible Rare Earth Element cluster ions that can form in the CRC of an ICP-QMS when using  $\text{NH}_3$  reaction gas – the list is by no means exhaustive.

Mass	Potential Cluster Ions of REE
204	$\text{Eu}(\text{NH}_3)_3$ ; $\text{Yb}(\text{NH}_3)_2$ ; $\text{Ce}(\text{NH}_3)_4$
205	$\text{Yb}(\text{NH}_3)_2$ ; $\text{Gd}(\text{NH}_3)_3$
206	$\text{Yb}(\text{NH}_3)_2$ ; $\text{Lu}(\text{NH}_3)_2$ ; $\text{La}(\text{NH}_3)_4$ ; $\text{Ce}(\text{NH}_3)_4$ ; $\text{Gd}(\text{NH}_3)_3$
207	$\text{La}(\text{NH}_3)_4$ ; $\text{Yb}(\text{NH}_3)_2$ ; $\text{Gd}(\text{NH}_3)_3$
208	$\text{Ce}(\text{NH}_3)_4$ ; $\text{Gd}(\text{NH}_3)_3$ ; $\text{Tb}(\text{NH}_3)_2$ ; $\text{Yb}(\text{NH}_3)_2$ ; $\text{Gd}(\text{NH}_3)_3$

To check the formation of cluster ions, the ICP-QQQ was operated with  $\text{NH}_3$  cell gas; “Single Quad bandpass” and MS/MS modes were compared for the measurement of a 50 ppb REE mix. Figures 2a and 2b display the spectra obtained using bandpass and MS/MS conditions, respectively.

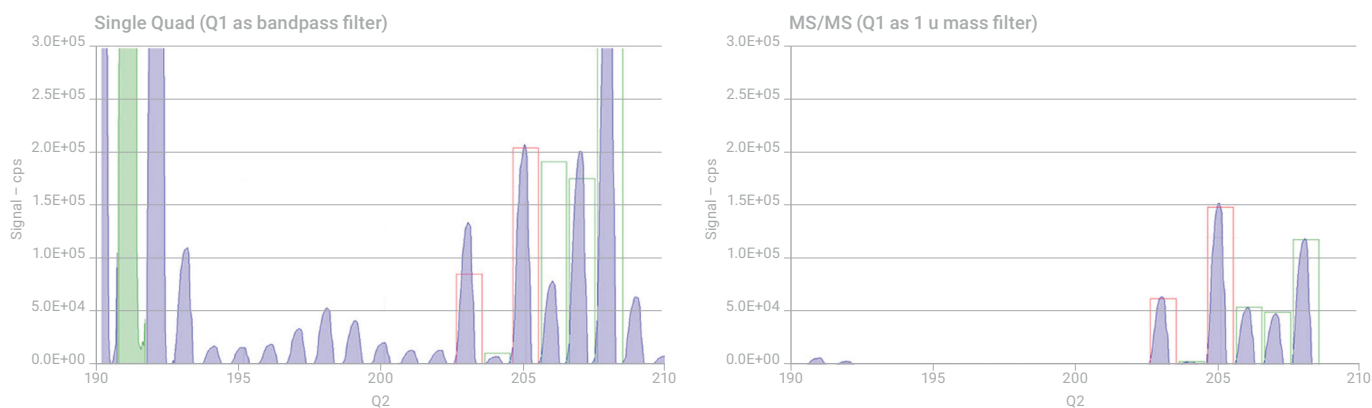


**Figure 2.** Cluster ion formation for 50 ppb REE standard in ammonia mode. Figure 2a (left): REE cluster ion formation using ammonia cell gas in bandpass mode; REE's are allowed into the cell if Q1 is operated as a bandpass filter. The REE cluster ions can be seen at all masses including those for Hg, Tl, Pb and Bi. Figure 2b (right): The identical sample under the same ammonia conditions but this time with Q1 operated at unit mass resolution (MS/MS mode). The REE's are removed from the ion beam before they can enter the cell and form reaction by-products.

### **$^{204}\text{Pb}/^{208}\text{Pb}$ isotope ratio analysis in presence of Hg**

To check the effectiveness of the  $^{204}\text{Hg}$  removal, the  $^{204}\text{Pb}/^{208}\text{Pb}$  ratio was measured in a 1 ppb lead solution spiked with increasing Hg concentration. Table 2 displays the measured Pb ratio results (without any mass bias correction), showing that the Pb isotope ratio remained constant, regardless of the Hg content.

**Table 2.** Uncorrected isotopic ratios measured in 1 ppb Pb solutions containing mercury at varying concentrations. The lead isotopic ratio 204/208 is not influenced by the presence of Hg.

	$^{204}\text{Pb}$	$^{208}\text{Pb}$	IR (204/208)
<b>Sample</b>		<b>CPS</b>	
Theoretical	NA	NA	0.02671
Pb	3518.5	136124.8	0.02585
Pb Hg 5 ppb	3510.0	139585.9	0.02515
Pb Hg 10 ppb	3439.2	132796.4	0.02590
Pb Hg 20 ppb	3464.8	134417.7	0.02578

### **Conclusion**

With the successful removal of the  $^{204}\text{Hg}$  interference on the natural  $^{204}\text{Pb}$  isotope, ICP-QQQ displays great promise for Pb/Pb and U/Pb dating and for other applications where accurate measurement of  $^{204}\text{Pb}$  is required.

# Fractionation of Sulfur Isotope Ratio Analysis in Environmental Waters

## Author

Naoki Sugiyama  
Agilent Technologies, Japan

## Keywords

sulfur, sulfur isotope ratio, isotope ratio analysis, fractionation, mass-shift

## Introduction

Sulfur isotope ratio (IR) data is a useful indicator in geochemical and biochemical studies [1]. In stable sulfur isotope analysis, the variation in the  $^{34}\text{S}/^{32}\text{S}$  IR is calculated and reported as a deviation or delta ( $\delta$ ) in  $^{34}\text{S}$  abundance relative to a standard material, the troilite (iron sulfide) mineral from the Canyon Diablo meteorite. This standard is referred to as  $\delta\text{VCDT}$  (Vienna Canyon Diablo Troilite). Natural variations in  $^{34}\text{S}$  abundance, expressed in parts per thousand or “per mil” (‰), can be of the order of -50‰ to +40‰ (and occasionally much greater), due to redox reaction [2]. In this study, triple quadrupole ICP-MS (ICP-QQQ) was investigated as a fast and simple technique for S IR analysis. ICP-QQQ is a tandem ICP-MS that can resolve spectral interferences using reaction cell technologies. Using the method described in this paper, ICP-QQQ can measure S at a low concentration (background equivalent concentration < 0.2 ppb in UPW) with high sensitivity ( $^{32}\text{S}$  > 10000 cps/ppb).

## Experimental

**Instrumentation:** Agilent 8900 Advanced Applications configuration ICP-QQQ with PFA nebulizer. Self-aspiration mode was used for better precision.

**Tuning:**  $\text{O}_2$  mass-shift method. Tuning conditions are summarized in Table 1.

**Method:** the following procedures were used for the accurate determination of sulfur IRs:

- Matrix matching: all samples were diluted by the matrix blank, which contained 50 ppm Ca and 100 ppm NaCl in 1%  $\text{HNO}_3$ .
- Concentration matching: each sample was diluted by the matrix blank to ~0.5 ppm S concentration. This dilution was done to remove any errors caused by signal count differences. For example, NASS 5 was diluted 2000 times and mineral water A was diluted 10 times.
- Mass bias correction: to correct mass bias (including mass-bias drift), sample-standard bracketing was applied. IR of 0.5 ppm IAEA-S-1 [3] was measured before and after the IR analysis of each sample. The average of the IRs for the standard was used to correct the mass-bias and the drift.

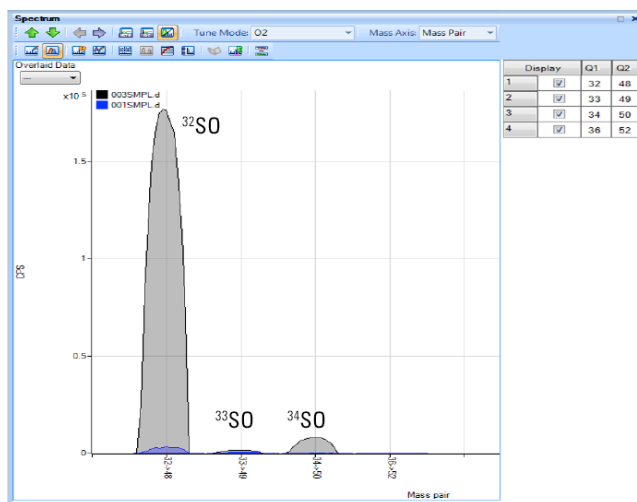


**Table 1.** ICP-QQQ tuning and method parameters.

	Tuning parameter	Unit	Value
Plasma	RF power	W	1550
	Sampling depth	mm	8.0
	Nebulizer gas flow rate	L/min	0.90
	Make-up gas flow rate	L/min	0.30
Lens	Extract 1	V	-80
	Extract 2	V	-150
	Omega	V	10.0
	Omega bias	V	-120
Cell	Octp Bias	V	-5.0
	Axial Acceleration	V	2.0
	KED	V	-8.0
	Cell gas		Oxygen
	Cell gas flow rate	mL/min	0.45
	Method parameter	Unit	Value
Data acquisition	Integration time	s	1 and 5 for <sup>32</sup> S and <sup>34</sup> S
	Number of sweeps	–	1000
	Number of replicates	–	10
Rinse	1% HNO <sub>3</sub> rinse	s	20
	50 ppm/100 ppm NaCl rinse	s	30
Sample load	Load time	s	30
	Stabilization time	s	30

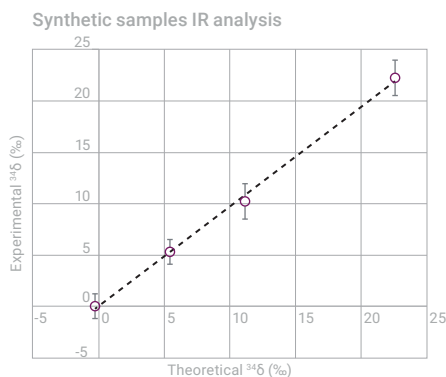
## Results and discussion

Figure 1 shows a spectrum of three sulfur isotopes in a blank and 10 ppb S standard measured by ICP-QQQ in  $O_2$  mass-shift mode. The two spectra show the low BEC of sulfur in the blank, which allows accurate S IR analysis.



**Figure 1.** Spectra of S isotopes measured in  $O_2$  mass-shift mode. The blank is indicated in blue and the 10 ppb S standard in grey. The spectra show that the BEC of the blank is < 200 ppt.

Synthetic samples were prepared and analyzed. Two standards, IAEA S-1 ( $^{34}\delta = -0.3\text{‰}$ ) and IAEA S-2 ( $^{34}\delta = +22.6\text{‰}$ ), were mixed to make four synthetic samples with a theoretical S IR of  $^{34}\delta = -0.3, 5.4, 11.2$  and  $22.6 \text{‰}$ . Each sample was measured six times, and the average IR and precision (as two times the standard deviation) were calculated. As shown by the linearity of Figure 2, the measured  $^{34}\delta$  values were in excellent agreement with the theoretical values.



**Figure 2.** Sulfur IR of four synthetic samples.

The developed method was used to analyze seven samples: sulfuric acid (Tampure AA-100); a Japan river water CRM, JSAC0301; a hot spring water, IKAHO; three mineral waters A, B, and C; and a seawater SRM, NASS-5. The concentration of S was first determined in each sample. The samples were then diluted with the matrix blank (50 ppm Ca + 100 ppm NaCl) to ~0.5 ppm of S. The IR of each sample was measured 10 times to determine the average value and precision (as two times the standard deviation). The results given in Figure 3 show  $\pm 1.2$  to  $\pm 1.7$  ‰ error.

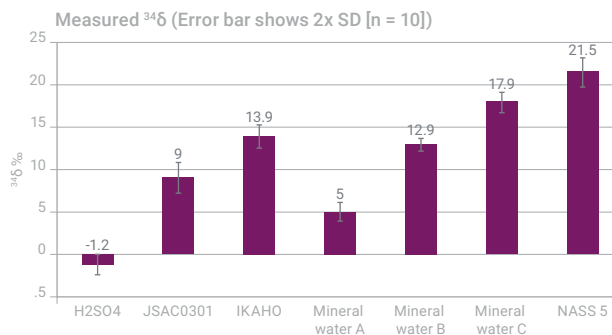


**Figure 3.** Measured  $\delta^{34}\text{S}$  of seven samples.

## Conclusion

The Agilent 8900 Advanced Applications configuration ICP-QQQ is ideally suited to  $^{34}\text{S}/^{32}\text{S}$  isotope ratio analysis. The analysis can provide valuable information for sample characterization in natural systems or to monitor anthropogenic impact. The 8900 ICP-QQQ provides a low background and high sensitivity for sulfur, which enabled a method to be developed that required the sample to be diluted with the matrix blank before analysis. The precision of the IRs achieved was excellent at 1.2–1.7 ‰ (as two times the standard deviation).

## References

1. J. Ryu, R.A. Zierenberg, R.A. Dahlgren et al., **2006**, *Chemical Geology* 229: 257-2722.
2. H.G. Thode, *Mineral. Soc. Amer. Spec.*, **1970**, Pap. 3: 133–144
3. National Institute of Standards and Technology certificate sheet for Reference Material 8554 -IAEA-S-1 (Sulfur Isotopes in Silver Sulfide)

## More information

Sulfur isotope fractionation analysis in mineral waters using an Agilent 8900 ICP-QQQ, Agilent publication [5991-7285EN](#)

# Measurement of $^{87}\text{Sr}/^{86}\text{Sr}$ Isotope Ratios in Rocks by ICP-QQQ in Mass-Shift Mode

## Authors

Xiaoming Liu<sup>1</sup>  
Yahui Yue<sup>1</sup>  
Yibo Yang<sup>1</sup>  
Shuofei Dong<sup>2</sup>

<sup>1</sup> Institute of Tibetan Plateau Research,  
Chinese Academy of Sciences, Beijing  
100085, China

<sup>2</sup> Agilent Technologies Co., Ltd. (China),  
Beijing 100102, China

The direct Agilent 8900 ICP-QQQ method removes need for chromatographic separation of  $^{87}\text{Sr}$  and  $^{87}\text{Rb}$

## Introduction

Triple quadrupole ICP-MS (ICP-QQQ) instrumentation is increasingly used for isotope ratio (IR) analysis studies (1–5). Geologists use radioactive isotopes that have long half-lives to date rocks and sediments, often with the choice of dating method dependent on the type of samples under investigation. For example, rubidium (Rb) is abundant in many potassium-containing rocks, so the Rb-strontium (Sr)  $\beta$ -decay scheme is used in geochronology studies of igneous, and sometimes metamorphic rocks and minerals (5, 6).

Strontium (Sr) has four naturally occurring isotopes:  $^{84}\text{Sr}$  (0.56% abundance),  $^{86}\text{Sr}$  (9.86% abundance),  $^{87}\text{Sr}$  (7.00% abundance), and  $^{88}\text{Sr}$  (82.58% abundance). While these are the four stable isotopes of Sr, the abundance of  $^{87}\text{Sr}$  varies over long periods of time due to the formation of radiogenic  $^{87}\text{Sr}$  following  $\beta$ -decay of  $^{87}\text{Rb}$ . The level of  $^{87}\text{Sr}$  compared to  $^{86}\text{Sr}$  is dependent on the original concentration of Rb in the environmental or geological system. Therefore,  $^{87}\text{Sr}/^{86}\text{Sr}$  IR measurements can also serve as a tracer of ecosystem processes (7).

Traditional IR measurement techniques such as thermal ionization mass spectrometry (TIMS) or multicollector inductively coupled plasma mass spectrometry (MC-ICP-MS) offer excellent accuracy and high precision for most IR studies. However, they are less efficient for the measurement of  $\beta$  decay product isotopes, due to isobaric interferences of the daughter isotope by their respective parent isotope. For example,  $^{87}\text{Sr}$  must be separated from  $^{87}\text{Rb}$  before analysis by TIMS or MC-ICP-MS to avoid the isobaric spectral overlap at mass 87. This process is labor-intensive and time consuming, especially for large sample numbers that are typical of geological and environmental survey studies. By contrast, no Rb/Sr separation is needed before analysis using ICP-MS/MS methodology, simplifying the analysis and improving sample throughput. ICP-MS/MS methods use “chemical resolution” to resolve isobaric interferences, as demonstrated in previous studies using Agilent ICP-QQQ instrumentation (1, 5).

In those studies, reactive gases were used in the collision/reaction cell (CRC) of the ICP-QQQ to separate the isobaric overlap from  $^{87}\text{Rb}$  on  $^{87}\text{Sr}$ , avoiding the need for chromatographic separation. Isobaric ion interferences can be separated using ICP-QQQ when the cell gas reacts quickly with one of the elements to form a product ion, while the other element does not react (or reacts slowly). Although reaction cell gases such as  $\text{CH}_3\text{F}$ ,  $\text{N}_2\text{O}$ , and  $\text{SF}_6$  provide a higher reaction rate with  $\text{Sr}^+$  than  $\text{O}_2$ ,  $\text{O}_2$  is more widely available in laboratories and is more suited to routine applications.

The aim of this study was to develop a fast, high throughput, routine method suitable for the accurate determination of  $^{87}\text{Sr}/^{86}\text{Sr}$  IR with precision below 0.1% RSD. To achieve the objective, an Agilent 8900 ICP-QQQ was operated in MS/MS mass-shift mode using  $\text{O}_2$  as the cell gas.

#### $^{87}\text{Sr}/^{86}\text{Sr}$ IR analysis by ICP-QQQ in $\text{O}_2$ mass-shift mode

The Agilent 8900 Triple Quadrupole ICP-MS (ICP-QQQ) uses two identical, full-sized quadrupoles (Q1 and Q2), one before and one after the ORS<sup>4</sup> reaction cell. Like the analyzer mass filter, Q2, Q1 operates in a high vacuum region, so it provides excellent resolution and abundance sensitivity. This allows precise selection of which ions enter the cell, ensuring the reactions used to resolve the analyte ions from their on-mass interferences are consistent and predictable. As shown in Figure 1, by setting Q1 to  $m/z$  87, only Rb-87 and Sr-87 enter the cell that is pressurized with  $\text{O}_2$ . In the cell,  $^{87}\text{Sr}^+$  reacts with  $\text{O}_2$  to form  $^{87}\text{Sr}^{16}\text{O}^+$  product ion, while  $^{87}\text{Rb}^+$  does not react. The second quadrupole (Q2) is set to  $m/z=103$ , which allows  $^{87}\text{Sr}^{16}\text{O}^+$  to pass to the detector, free of interference.

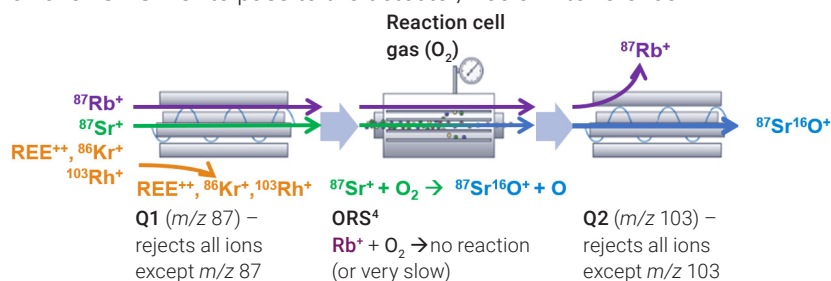


**Figure 1.** Determination of  $^{87}\text{Sr}$  as  $^{87}\text{Sr}^{16}\text{O}^+$  product ion using ICP-QQQ operating in mass-shift mode with  $\text{O}_2$  cell gas.

#### Efficiency of using mass-shift mode to separate Sr from Rb

When  $\text{Sr}^+$  ions react with  $\text{O}_2$  in the cell, not all  $\text{Sr}^+$  ions complete the reaction to form  $\text{SrO}^+$  ions during the short transit time in the cell. To optimize the  $\text{O}_2$  flow rate, counts per second (cps) of both  $^{86}\text{Sr}^+$  (at  $m/z$  86) and  $^{86}\text{Sr}^{16}\text{O}^+$  (at  $m/z$  102) were monitored. For the calculation, the measured cps of Q1 ( $m/z$  = 86)  $\rightarrow$  Q2 ( $m/z$  = 102) was divided by the cps of Q1 ( $m/z$  = 86)  $\rightarrow$  Q2 ( $m/z$  = 86). The mass-shift efficiency of Sr in  $\text{O}_2$  reaction mode ranged between the expected range of 10 and 14% (8). The variation was mainly due to instrument conditions on the day of measurement.

To evaluate whether  $^{87}\text{Rb}^{16}\text{O}^+$  formed in the cell sufficiently to affect the measurement of  $^{87}\text{Sr}^{16}\text{O}^+$ ,  $^{85}\text{Rb}$  was used as a proxy for  $^{87}\text{Rb}$ . The signals at  $m/z$  85 (for  $^{85}\text{Rb}^+$ ) and  $m/z$  101 (for  $^{85}\text{Rb}^{16}\text{O}^+$ ) were monitored during method development. First, Q1 and Q2 were both set to  $m/z$  = 85. The measured cps of  $^{85}\text{Rb}^+$  in the reference materials (RMs) and rock samples were between  $6 \times 10^5$  and  $4 \times 10^6$  (the cps of  $^{85}\text{Rb}^+$  in the solution blank was typically below 1). Then Q2 was set to  $m/z$  101 and the measured cps range was below 1, suggesting minimal formation of  $^{85}\text{Rb}^{16}\text{O}^+$  in the cell. Using the natural abundance of  $^{85}\text{Rb}$  (72.17%) and  $^{87}\text{Rb}$  (27.83%), we calculated that the conversion of  $^{87}\text{Rb}^+$  to  $^{87}\text{Rb}^{16}\text{O}^+$  would lead to a measured cps for  $^{87}\text{Rb}^{16}\text{O}^+$  at  $m/z$  = 103 below 0.4 cps.

In this study, the Sr concentration of the RMs and rock samples measured by ICP-QQQ were mostly around 100 ng/mL. This concentration is equivalent to over  $1 \times 10^5$  cps for  $^{87}\text{Sr}^+$  as  $^{87}\text{Sr}^{16}\text{O}^+$  ( $m/z$  = 103). Therefore, the interference effect of  $^{87}\text{Rb}^{16}\text{O}^+$  ( $m/z$  = 103) on  $^{87}\text{Sr}^{16}\text{O}^+$  ( $m/z$  = 103) is negligible in this study.

## Experimental

### Standards and sample preparation

To determine the accuracy and precision of the method, three US Geological Survey (USGS) RMs were used: Basalt, Columbia River (BCR-2), Basalt, Hawaiian Volcanic Observatory (BHVO-2), and Andesite (AGV-2). Twenty-three rock samples were analyzed in the study, including basalt (Rb/Sr concentration ratio 0.02–0.12), dolerite (Rb/Sr concentration ratio 0.04–0.10), andesite (Rb/Sr concentration ratio 0.76–0.87), and rhyolite (Rb/Sr concentration ratio 5.6–9.1).

All RMs and samples were prepared at the Institute of Tibetan Plateau Research, Chinese Academy of Sciences (ITP-CAS) using a classic pressurized acid digestion method for trace element measurements. Approximately 50 mg of each sample was digested using 1 mL each of purified HNO<sub>3</sub> and HF in a closed vessel oven, heated at 190 °C for 36 hours. Following the addition of 0.25 mL of HClO<sub>4</sub>, the sample was evaporated to incipient dryness on a hot plate at 130 °C. This procedure was repeated with the addition of 0.5 mL of HNO<sub>3</sub>. The sample was further heated at 170 °C until white fumes were seen. 0.5 mL of 40% HNO<sub>3</sub> was added, and the sample was oven-heated at 130 °C for 3 h. After cooling, 49.5 mL of de-ionized water was added to the sample, ready for analysis by ICP-QQQ.

### Instrumentation

An Agilent 8900 ICP-QQQ was used. The sample introduction system consisted of a quartz torch with 2.5 mm i.d. injector, a quartz spray chamber, glass concentric nebulizer, and nickel-tipped interface cones. Samples were introduced into the ICP-QQQ using a standard peristaltic pump and Agilent SPS 4 autosampler.

<sup>87</sup>Sr and <sup>86</sup>Sr were determined in mass-shift mode using O<sub>2</sub> as the cell gas. The isobaric interference on <sup>87</sup>Sr by <sup>87</sup>Rb was avoided by measuring the Sr product ions <sup>87</sup>Sr<sup>16</sup>O<sup>+</sup> and <sup>86</sup>Sr<sup>16</sup>O<sup>+</sup> at  $m/z=103$  and  $m/z=102$ , respectively. Typical instrument operating parameters are listed in Table 1.

Throughout the analytical workflow, a BCR-2 RM sample solution containing 100 ng/mL Sr was measured after every two or three samples to ensure that the mass bias calibration was up to date. Instrument mass bias occurs when ions of different element masses transmit through the ICP-MS with different efficiencies, resulting in inaccurate IR measurements. The Agilent ICP-MS MassHunter software automatically updates the mass bias.

**Table 1.** ICP-QQQ operating parameters and acquisition settings for <sup>87</sup>Sr/<sup>86</sup>Sr IR analysis.

Parameter	Setting
RF Power (W)	1550
Sampling Depth (mm)	8.0
Nebulizer Gas Flow Rate (L/min)	1.15
KED (V)	-6.0
Cell Gas Flow Rate (mL/min)	0.45 (30% of full scale)
Axial Acceleration (V)	1.0
Q1 → Q2 Masses ( $m/z$ )	86 → 102 87 → 103
Q2 Peak Pattern	1 point
Replicates	7
Sweeps	1000
Integration Time of Each Mass (s)	9

## Results and discussion

### Determination of $^{87}\text{Sr}/^{86}\text{Sr}$ IRs in the RMs

$^{87}\text{Sr}/^{86}\text{Sr}$  IRs were measured in BCR-2 and BHVO-2 RMs using the ICP-QQQ mass-shift method with  $\text{O}_2$  cell gas. To confirm that chromatographic separation of Sr wasn't needed for successful ICP-QQQ analysis, data was acquired with and without the Sr purification stage. Each RM was measured seven times in different batches or on different days, with seven replicate measurements.

The  $^{87}\text{Sr}/^{86}\text{Sr}$  ratio results in Figure 2 show that there was no significant difference in the results for BCR-2 and BHVO-2 with and without Sr purification. Both sets of measured data are within the literature reported values that were obtained using TIMS and MC-ICP-MS (9). The ICP-QQQ method is accurate enough to study  $^{87}\text{Sr}/^{86}\text{Sr}$  ratios in natural samples/systems with a wide range of  $^{87}\text{Sr}/^{86}\text{Sr}$  distributions. Also, the sample preparation procedure doesn't affect the precision of the ICP-QQQ measurements.

The error bars show two times the standard deviation (SD) of the average of seven separate measurements of the two RMs, which range between 0.0003 and 0.0005 ( $n=7$ ) or between 0.02 and 0.04% RSD. This deviation is significantly higher than the RSD of the MC-ICP-MS method. However, the results show that ICP-QQQ can distinguish  $^{87}\text{Sr}/^{86}\text{Sr}$  ratios of materials within 0.001 (i.e. 0.1%) precision.

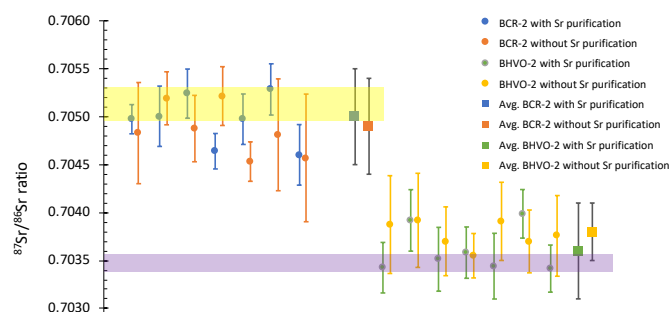


**Figure 2.** Comparison of the measured  $^{87}\text{Sr}/^{86}\text{Sr}$  ratios of BCR-2 and BHVO-2 with and without Sr purification column chemistry by ICP-QQQ with literature values (9) represented by the shaded bands. Circle symbols: average value of each measurement, the error bar is 1SD of the seven replicates of each measurement. Square symbols: the average value of the seven measurements of BCR-2 and BHVO-2, the error bar represents 2SD of the seven measurements.

### The effect of the Sr concentration in the samples

To optimize the level of sample dilution of the sample digests, we investigated the effects of the concentration of Sr in the rock samples on the analysis. Three fully digested rock samples (andesite, dolerite, and basalt) were diluted to give a Sr concentration between 60 and 350 ng/mL. A BCR-2 solution containing 100 ng/mL of Sr was used for online instrumental mass bias correction.

The results in Table 2 show that, within the measured concentration range, the Sr concentration doesn't significantly affect the  $^{87}\text{Sr}/^{86}\text{Sr}$  ratios of each type of sample. Therefore, the digested samples could potentially be diluted into a certain range, such as from 60 to 350 ng/mL, according to a standard operation procedure, simplifying the analysis.

**Table 2.** Measured  $^{87}\text{Sr}/^{86}\text{Sr}$  IRs of three different rock samples (one sample of each type of rock) with four different Sr concentrations.

Sample	Sr Concentration (ng/mL)	$^{87}\text{Sr}/^{86}\text{Sr}$ Ratio	2SD (n=3)
Basalt	70	0.7036	0.0009
	100	0.7055	0.0002
	175	0.7043	0.0008
	350	0.7060	0.0009
Dolerite	70	0.7035	0.0015
	100	0.7047	0.0009
	170	0.7039	0.0016
	340	0.7046	0.0008
Andesite	60	0.7114	0.0013
	100	0.7126	0.0006
	140	0.7120	0.0015
	280	0.7126	0.0014

### Analysis of Sr IRs of rock samples by ICP-QQQ

The 23 rock samples were analyzed in triplicate (n=3) using the ICP-QQQ mass-shift method, without Sr purification. As shown in Figure 3, the samples cover a large  $^{87}\text{Sr}/^{86}\text{Sr}$  ratio range from 0.705 to 0.748. This range is typical of common rocks (Figure 3), as well as minerals, waters, and plants (4).

The accuracy of the  $^{87}\text{Sr}/^{86}\text{Sr}$  ratio measurements obtained by ICP-QQQ was compared with data obtained by MC-ICP-MS. There was good agreement between the two methods (4), with a variation of between 0.00001 and 0.0016 of the mean of the  $^{87}\text{Sr}/^{86}\text{Sr}$  ratio. The variation wasn't dependent on the  $^{87}\text{Sr}/^{86}\text{Sr}$  ratio range.

The precision of the  $^{87}\text{Sr}/^{86}\text{Sr}$  ratio measured by ICP-QQQ varied between 0.0001 and 0.0019 (2SD, n=3) or between 0.01 and 0.13% (RSD, n=3). While this precision is lower than the precision of the MC-ICP-MS method, it is sufficient for applications with large  $^{87}\text{Sr}/^{86}\text{Sr}$  ratio differences, such as the identification of  $^{87}\text{Sr}/^{86}\text{Sr}$  ratio in between certain rock types. Andesite, rhyolite, and dolerite rock samples have significant  $^{87}\text{Sr}/^{86}\text{Sr}$  ratio variations, as shown in Figure 3. However, distinguishing rock types within a narrow range of  $^{87}\text{Sr}/^{86}\text{Sr}$  ratios, e.g., low  $^{87}\text{Sr}/^{86}\text{Sr}$  basalts, could be challenging.

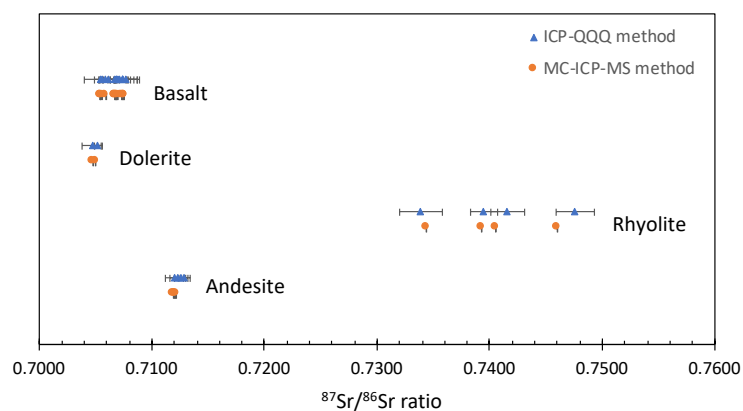


**Figure 3.**  $^{87}\text{Sr}/^{86}\text{Sr}$  IR distribution for typical rocks. Triangle symbol:  $^{87}\text{Sr}/^{86}\text{Sr}$  IR of ICP-QQQ method, error bar in 2SD (n=3). Circle symbol:  $^{87}\text{Sr}/^{86}\text{Sr}$  IR of MC-ICP-MS method, error bar in 2SD (n=3) which falls within the circle mark.



## Conclusion

The study has shown that the Agilent 8900 ICP-QQQ can be used for the accurate measurement of  $^{87}\text{Sr}/^{86}\text{Sr}$  isotope ratios in a range of rock samples. The isobaric interference of  $^{87}\text{Rb}$  on  $^{87}\text{Sr}$  was resolved using a mass-shift method with  $\text{O}_2$  cell gas. Because Sr reacts with oxygen at a much faster rate than Rb,  $^{87}\text{Sr}$  was measured as  $^{87}\text{Sr}^{16}\text{O}^+$ , free from interference from  $^{87}\text{Rb}$ . This method is simpler, faster, and less costly than TIMS or MC-ICP-MS methods, as both TIMS and MC-ICP-MS require chromatographic separation of Sr from Rb before analysis. The ICP-QQQ mass-shift method is also suited to nonspecialist laboratories that aren't equipped with TIMS or MC-ICP-MS.

The distribution of  $^{87}\text{Sr}/^{86}\text{Sr}$  IRs of natural samples is generally between 0.70 and 0.77, although it can range from 0.700 to 0.943 (4). The accuracy and precision of the ICP-MS/MS method is sufficient to differentiate between various sources when the  $^{87}\text{Sr}/^{86}\text{Sr}$  ratio varies by more than 0.001. Therefore, this method has the potential to be used in applications that require source identification, such as environmental pollutant source tracing, large-scale geological surveys, and agricultural product authenticity studies.

## More information

For detailed information, please see Liu, X, Dong, S, Yue, Y, et al.  $^{87}\text{Sr}/^{86}\text{Sr}$  isotope ratios in rocks determined by ICP-MS/MS in  $\text{O}_2$  mode without prior Sr purification. *Rapid Commun Mass Spectrom.* 2020, <https://doi.org/10.1002/rcm.8690>

## References

1. E. Bolea-Fernandez, L. Balcaen, M. Resano, F. Vanhaecke, Tandem ICP-mass spectrometry for Sr isotopic analysis without prior Rb/Sr separation. *J Anal At Spectrom.*, **2016**, 31, 303-310
2. Glenn Woods, Resolution of  $^{176}\text{Yb}$  and  $^{176}\text{Lu}$  interferences on  $^{176}\text{Hf}$  to enable accurate  $^{176}\text{Hf}/^{177}\text{Hf}$  isotope ratio analysis using an Agilent 8800 ICP-QQQ with MS/MS, Agilent publication, [5991-6752EN](https://doi.org/10.1002/5991-6752EN)
3. Glenn Woods, Lead isotope analysis: Removal of  $^{204}\text{Hg}$  isobaric interference from  $^{204}\text{Pb}$  using ICP-QQQ in MS/MS mode, Agilent publication, [5991-5270EN](https://doi.org/10.1002/5991-5270EN)
4. X. Liu, S. Dong, Y. Yue, et al.  $^{87}\text{Sr}/^{86}\text{Sr}$  isotope ratios in rocks determined by ICP-MS/MS in  $\text{O}_2$  mode without prior Sr purification. *Rapid Commun Mass Spectrom.*, **2020**, accessed May 2020, <https://doi.org/10.1002/rcm.8690>
5. T. Zack, K. J. Hogmalm, Laser ablation Rb/Sr dating by online chemical separation of Rb and Sr in an oxygen-filled reaction cell. *Chem Geol.* **2016**, 437, 120–133
6. G. Faure, J. L. Powell, Strontium Isotope Geology. *Springer-Verlag*, New York, **1972**
7. R. C. Capo, B. W. Stewart, O. A. Chadwick, Strontium isotopes as tracers of ecosystem processes: theory and methods. *Geoderma.* **1998**, 82, 197-225
8. Naoki Sugiyama and Kazumi Nakano, Reaction data for 70 elements using  $\text{O}_2$ ,  $\text{NH}_3$  and  $\text{H}_2$  gases with the Agilent 8800 Triple Quadrupole ICP-MS; Agilent publication, [5991-4585EN](https://doi.org/10.1002/5991-4585EN)
9. K.P. Jochum, U. Nohl, K. Herwig, E. Lammel, B. Stoll, A. W. Hofmann, GeoReM: A new geochemical database for reference materials and isotopic standards. *Geostand Geoanal Res.* **2005**, 29, 333–338

# Direct Strontium Isotopic Analysis of Solid Samples by LA-ICP-MS/MS

## Authors

Eduardo Bolea-Fernandez, Stijn J. M. Van Malderen, Lieve Balcaen, and Frank Vanhaecke, Ghent University, Belgium

Martín Resano, University of Zaragoza, Spain

## Keywords

isotopic analysis, LA-ICP-MS/MS, LA-ICP-QQQ, strontium, geology

## Introduction

Strontium has four stable isotopes:  $^{84}\text{Sr}$  (0.56%),  $^{86}\text{Sr}$  (9.86%),  $^{87}\text{Sr}$  (7.0%), and  $^{88}\text{Sr}$  (82.58%).  $^{87}\text{Sr}$  is either formed during nucleosynthesis with other stable Sr isotopes or via beta decay from  $^{87}\text{Rb}$  (half-life of  $4.88 \times 10^{10}$  years):  $^{87}\text{Rb} \rightarrow ^{87}\text{Sr} + \beta^- + \bar{\nu}$ . Consequently, a high  $^{87}\text{Sr}/^{86}\text{Sr}$  ratio is observed in rocks that are geologically old or which contain a high concentration of Rb (high Rb/Sr ratio). The  $^{87}\text{Sr}/^{86}\text{Sr}$  ratio has been widely studied and reported in geological studies [1].

Measuring the  $^{87}\text{Sr}/^{86}\text{Sr}$  ratio using mass spectrometry techniques is challenging because of the isobaric overlap of the signals from  $^{87}\text{Rb}$  and  $^{87}\text{Sr}$ . Chemical separation can be used to isolate Sr from Rb before analysis by ICP-MS. However, a simpler method uses triple quadrupole ICP-MS (ICP-QQQ) and chemical reaction in the CRC with a reactive gas. In this study, Laser Ablation coupled to ICP-QQQ (LA-ICP-QQQ) in MS/MS mode with  $\text{CH}_3\text{F}/\text{He}$  reaction gas was used to resolve the  $^{87}\text{Rb}$  interference on  $^{87}\text{Sr}$ . This approach allowed the direct Sr isotopic analysis of solid samples [2].

## Experimental

A preliminary study showed that better precision was obtained using wet plasma conditions. The experimental setup shown in Figure 1 was used throughout. De-ionized water was continuously aspirated using a standard nebulizer. The sample aerosol that was generated by the LA system was carried by helium gas. Before being delivered to the plasma, the dry aerosol was combined with the liquid aerosol in the spray chamber, which was chilled to 2 °C.

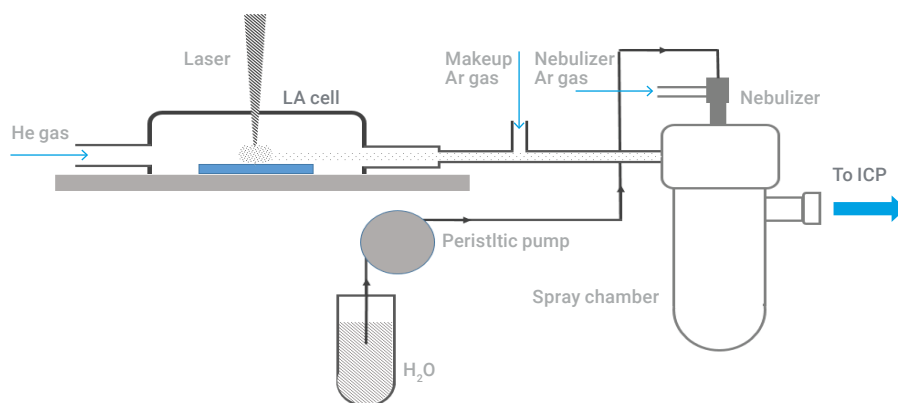


Figure 1. Schematic diagram of LA-ICP-QQQ using wet plasma conditions.

**Instrumentation:** An Analyte G2 193 nm ArF\*excimer-based LA-unit (Teledyne CETAC Technologies, USA) equipped with a HELEX 2 ablation cell was coupled to an Agilent 8800 #100. The ICP-QQQ was fitted with a standard sample introduction system.

**Method:** Tuning conditions and method parameters are given in Table 1.

**Reaction cell method:** The CH<sub>3</sub>F/He (1:9) cell gas was introduced via the ICP-QQQ's fourth cell gas mass flow channel (0-1 mL/min as O<sub>2</sub>). Rb<sup>+</sup> ions do not react with CH<sub>3</sub>F, whereas Sr<sup>+</sup> reacts with CH<sub>3</sub>F to form SrF<sup>+</sup>. Thus <sup>86</sup>Sr<sup>+</sup>, <sup>87</sup>Sr<sup>+</sup>, and <sup>88</sup>Sr<sup>+</sup> can be measured as the corresponding <sup>86</sup>SrF<sup>+</sup>, <sup>87</sup>SrF<sup>+</sup> and <sup>88</sup>SrF<sup>+</sup> reaction product ions, free from interference.

**Mass bias correction:** The instrumental mass bias was corrected for using a double correction approach: internal correction assuming a constant <sup>88</sup>Sr/<sup>86</sup>Sr isotope ratio (Russell's law, given below), followed by external correction in a sample-standard bracketing (SSB) approach using NIST 612 glass SRM.

$$R^{87\text{Sr}/86\text{Sr}}_{\text{sample, corrected}} = R^{87\text{Sr}/86\text{Sr}}_{\text{sample, measured}} \times (m^{87\text{Sr}}/m^{86\text{Sr}})^f$$

$$f = \ln [R^{88\text{Sr}/86\text{Sr}}_{\text{true}} / R^{88\text{Sr}/86\text{Sr}}_{\text{measured}}] / \ln [m^{88\text{Sr}}/m^{86\text{Sr}}]$$

**Samples:** Seven geological reference materials (RMs) were analyzed for their Sr isotopic composition. The RMs were selected to cover a wide range of matrix composition, Sr concentration, and Rb/Sr elemental ratio, as summarized in Table 2.

**Table 1.** LA-ICP-QQQ tuning conditions.

Laser Ablation		
Energy density	J/cm <sup>2</sup>	3.54
Repetition rate	Hz	40
Scan speed	µm/s	15
Beam size	µm	20-85
He carrier gas flow	L/min	0.42
ICP-QQQ		
RF power	W	1550
Sampling depth	mm	3.5
Nebulizer gas flow	L/min	1.0
Make-up gas flow	L/min	0.33
CH <sub>3</sub> F/He cell gas flow	mL/min	0.90
Dwell time per acquisition point	ms	300
Acquisition time per replicate	s	60
Number of replicates		12
Total analysis time per sample	min	15.55

## Results and discussion

### Removal of $^{87}\text{Rb}$ overlap using MS/MS mass-shift mode with $\text{CH}_3\text{F}/\text{He}$ cell gas

Seven RMs were selected to cover a wide range of Rb/Sr ratios. The  $^{87}\text{Sr}/^{86}\text{Sr}$  ratio was measured in each RM. For comparison purposes, the analysis was done using a no gas on-mass method and the  $\text{CH}_3\text{F}/\text{He}$  mass-shift method. Figure 2 shows the measured  $^{87}\text{Sr}/^{86}\text{Sr}$  and  $^{88}\text{Sr}/^{86}\text{Sr}$  ratios obtained with the two methods as a function of the Rb/Sr ratio.

With both methods, a constant  $^{88}\text{Sr}/^{86}\text{Sr}$  ratio was obtained regardless of the sample type. However, the measured  $^{87}\text{Sr}/^{86}\text{Sr}$  ratio increased in no gas mode, indicating an interference from  $^{87}\text{Rb}$  on  $^{87}\text{Sr}$ . In contrast, the  $^{87}\text{Sr}/^{86}\text{Sr}$  ratio measured in  $\text{CH}_3\text{F}/\text{He}$  mode remained constant, regardless of the Rb/Sr ratio, showing that the method was effective at removing the  $^{87}\text{Rb}$  isobaric overlap on  $^{87}\text{Sr}$ .

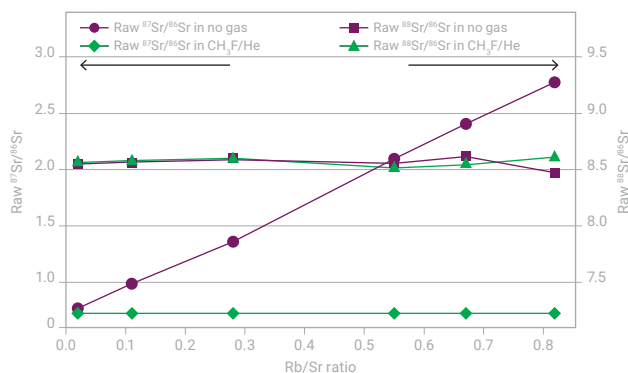


**Figure 2.**  $^{87}\text{Sr}/^{86}\text{Sr}$  and  $^{88}\text{Sr}/^{86}\text{Sr}$  isotope ratios measured using LA-ICP-QQQ in no gas and  $\text{CH}_3\text{F}/\text{He}$  cell gas modes. Reproduced from *J. Anal. At. Spectrom.*, 2016, 31, 464–472 with permission from the Royal Society of Chemistry.

### Determination of $^{87}\text{Sr}/^{86}\text{Sr}$ ratio in seven RMs

The method was used to determine the  $^{87}\text{Sr}/^{86}\text{Sr}$  ratio in seven RMs. The results are summarized in Table 2. After mass bias correction, excellent agreement was obtained between the measured  $^{87}\text{Sr}/^{86}\text{Sr}$  ratios and the recommended reference values, even in samples with a high Rb content.

**Table 2.**  $^{87}\text{Sr}/^{86}\text{Sr}$  isotope ratio results in seven reference materials.

Reference material	Type	Rb/Sr ratio	Chemical composition of the reference materials (%)								$^{87}\text{Sr}/^{86}\text{Sr}$ ratio				
			$\text{Al}_2\text{O}_3$	CaO	FeO	$\text{K}_2\text{O}$	MgO	MnO	$\text{Na}_2\text{O}$	$\text{SiO}_2$	Experimental	Recommended	Error (%)		
USGS BHVO-2G	Basalt	0.02	13.6	11.4	11.3	0.51	7.13	0.17	2.4	49.3	0.70351	$\pm 0.00034$	0.703469	$\pm 0.000007$	0.006
USGS NKT-1G	Nephelinite	0.03	10.5	13.4	12.2	1.27	14.2	0.24	3.85	38.9	0.70363	$\pm 0.00017$	0.703509	$\pm 0.000019$	0.017
USGS TB-1G	Basalt	0.11	17.12	6.7	8.67	4.52	3.51	0.18	3.56	54.29	0.70576	$\pm 0.00030$	0.705580	$\pm 0.000023$	0.026
USGS GSD-1G	Basalt	0.55	13.4	7.2	13.3	3	3.6		3.6	53.2	0.70924	$\pm 0.00029$	0.709416	$\pm 0.000050$	-0.025
USGS BCR-2G	Basalt	0.14	13.4	7.06	12.4	1.74	3.56	0.19	3.23	54.4	0.70486	$\pm 0.00038$	0.705003	$\pm 0.000004$	-0.020
MPI-DING T1-G	Diorite	0.28	17.1	7.1	6.44	1.96	3.75	0.127	3.13	58.6	0.70990	$\pm 0.00035$	0.710093	$\pm 0.000017$	-0.027
MPI-DING ATHO-G	Rhyolite	0.67	12.2	1.7	3.27	2.64	0.103	0.106	3.75	75.6	0.70310	$\pm 0.00026$	0.703271	$\pm 0.000015$	-0.024

Reproduced from *J. Anal. At. Spectrom.*, 2016, 31, 464–472 with permission from the Royal Society of Chemistry.

## Conclusion

LA-ICP-QQQ with wet plasma conditions can be used for the direct determination of the  $^{87}\text{Sr}/^{86}\text{Sr}$  isotope ratio in geological samples. The isobaric interference from  $^{87}\text{Rb}$  on  $^{87}\text{Sr}$  was overcome using MS/MS mass-shift mode with  $\text{CH}_3\text{F}/\text{He}$  cell gas. The  $\text{Sr}^+$  ions react in the CRC to form  $\text{SrF}^+$  reaction product ions, while  $\text{Rb}^+$  ions do not react.  $^{87}\text{Sr}/^{86}\text{Sr}$  ratios were accurately determined in seven reference materials, regardless of the matrix composition, Sr concentration, and Rb/Sr elemental ratio.

## References

1. R. A. Bentley, *J. Archaeol. Meth. Theor.*, **2006**, 13, 135–187.
2. E. Bolea-Fernandez, S. Van Malderen, L. Balcaen, M. Resano, and F. Vanhaecke, Laser ablation-tandem ICP-mass spectrometry (LA-ICP-MS/MS) for direct Sr isotopic analysis of solid samples with high Rb/Sr ratios, *J. Anal. At. Spectrom.*, **2016**, 31, 464–472

# Resolution of $^{176}\text{Yb}$ and $^{176}\text{Lu}$ interferences on $^{176}\text{Hf}$ to enable accurate $^{176}\text{Hf}/^{177}\text{Hf}$ isotope ratio analysis using ICP-QQQ with MS/MS

## Author

Glenn Woods  
Agilent Technologies, UK

## Keywords

Hafnium, Hf, geology, dating studies, rock dating, isotopic abundance

## Introduction

Hafnium  $^{176}\text{Hf}$  to  $^{177}\text{Hf}$  isotope ratio analysis can provide insight into the different geological events and processes that a mineral underwent during its formation/metamorphosis;  $^{176}\text{Hf}/^{177}\text{Hf}$  ratios are also used for geochronology dating studies. Isotope geochronology is a dating technique in which the age of a rock or mineral is derived from differences in the abundance of two isotopes of an element. Changes in isotopic abundance may be caused by isotopic (mass) fractionation, or by radioactive decay; in each case, the ratio acts as a geological clock, allowing the time that the mineral was formed to be estimated. Hf has lower mobility than lead (Pb) in metamict minerals such as zircon, xenotime, euxenite etc., so Hf isotope ratios can offer an alternative to Pb/Pb or Pb/U ratios for dating these minerals.

Of the Hf isotopes of interest,  $^{177}\text{Hf}$  is free from direct isobaric overlap from any other element and does not typically suffer from polyatomic interference from other co-existing elements. However, the second Hf isotope used in the isotope ratio calculation,  $^{176}\text{Hf}$ , suffers isobaric overlap from  $^{176}\text{Lu}$  and  $^{176}\text{Yb}$ , as shown in Figure 1. In order to obtain accurate Hf ratios, it is therefore necessary to separate the  $^{176}\text{Hf}$  signal from the overlapping Lu and Yb signals.

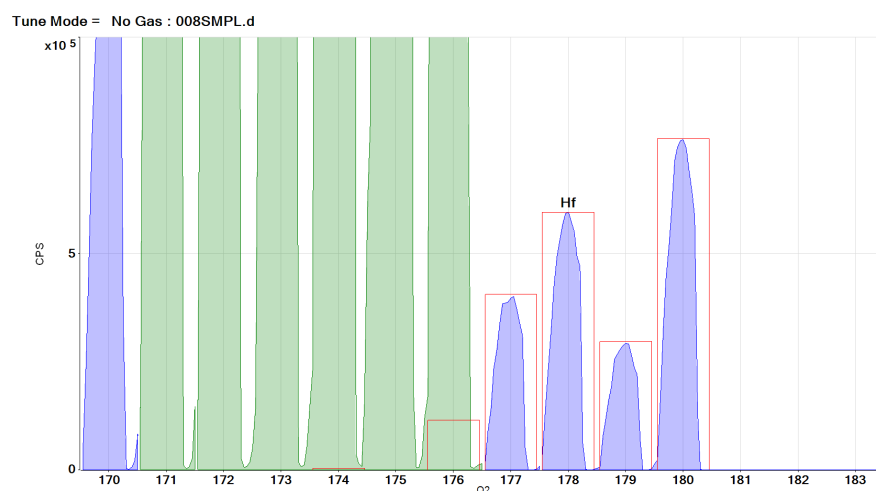


**Figure 1.** Hf (red peak template) in the presence of Lu and Yb matrix. The poor template fit for  $^{176}\text{Hf}$  (highlighted in blue outline) is due to the contribution from  $^{176}\text{Lu}$  and  $^{176}\text{Yb}$  to the signal at  $m/z$  176.

The mass resolution required to separate  $^{176}\text{Hf}$  from the Lu and Yb isobaric interferences ( $M/\Delta M$  of  $\sim 140,000$  for  $^{176}\text{Lu}$  and  $>150,000$  for  $^{176}\text{Yb}$ ) is far beyond the capability of commercial High Resolution Sector Field ICP-MS (SF-ICP-MS), so sample preparation (chemical separation) is required prior to analysis. In cases where chemical separation cannot be performed, for example in-situ measurement by Laser Ablation (LA), the Lu/Yb overlaps mean that accurate Hf isotope ratio analysis is not possible or must rely on mathematical corrections (and the errors they can introduce).

An alternative direct approach is “chemical” resolution within a collision/reaction cell (CRC), using specific gas phase ion-molecule reaction(s) that will either:

- React with the interfering ion to neutralize it or move it to a new mass.
- React with the analyte to create a new product ion at a different, non-interfered mass.

In this study, the second approach, known as “mass-shift”, was used. Hf reacts efficiently with ammonia cell gas to form Hf-ammonia cluster ions, while Lu and Yb are relatively unreactive. However, ammonia will react with the other Hf isotopes and other co-existing ions present in a typical sample matrix. These other ions also form ammonia-adduct ions, creating new interferences that vary depending on the matrix composition. These ammonia-adduct ions would interfere with the original Hf isotope pattern, making Hf isotope analysis unreliable, so control over the reaction process is essential.

The solution to this problem is to use a tandem mass spectrometer, which has an additional mass filter before the CRC. This extra mass filter prevents all ions apart from the target mass from entering the CRC, so the reaction chemistry is precisely controlled and unwanted side-reactions are avoided. This double mass filter approach is only possible with a tandem MS (or MS/MS) configuration, which provides unprecedented control of the ion/molecule reaction chemistry used in CRC-ICP-MS methods.

The Agilent 8800 and 8900 Triple Quadrupole ICP-MS (ICP-QQQ) instruments have an additional quadrupole mass filter (Q1), positioned in front of the CRC, with the capability of operating at unit mass resolution (MS/MS mode). In MS/MS operation, only a single mass-to-charge ratio ( $m/z$ ) is transmitted through Q1, so the other Hf isotopes and any co-existing elements are rejected before they can enter the CRC. Unwanted side-reactions and potentially overlapping product ions are therefore eliminated. This method was used to measure Hf isotope ratios in a variety of samples containing Lu, Yb and mixed rare earth elements (REE). For this proof of concept, all work was performed using solution sample introduction, which allowed a greater flexibility to test interference removal. However, the same cell gas and MS/MS method can also be applied successfully to sample analysis using laser ablation (LA-ICP-QQQ).

## Experimental

### Instrumentation

The Agilent 8800\* ICP-QQQ was configured with an SPS 4 autosampler and the standard sample introduction system consisting of a Micromist nebulizer (free aspiration), quartz spray chamber and torch, and Ni interface cones. Table 1 shows the key instrument parameters used for the analysis.

**Table 1.** Instrument parameters.

Parameter	Value
RF power	1550 W
Sampling depth	7.0 mm
Nebulizer gas	1.15 L/min
Spray chamber temp	2 °C
Ammonia (10% in He) cell gas	22% of full scale (~2.2 mL/min)
Octopole bias	-6.0 V
Energy discrimination	-8.0 V

### Samples and sample preparation

Due to the reactivity of ammonia, its use as a cell gas leads to a complex population of product ions, even in a simple sample matrix. However, selection of the most appropriate adduct ion is relatively simple with ICP-QQQ, by performing a Product Ion Scan. Unique to the MS/MS mode of operation, a Product Ion Scan uses a fixed mass setting for Q1, combined with a Q2 scan across the selected mass range. To identify useful  $^{176}\text{Hf}$ - ammonia product ions, Q1 was fixed to mass ( $m/z$ ) 176 u, and Q2 was scanned across the mass range from  $m/z$  170 to  $m/z$  260, while aspirating a solution of 5  $\mu\text{g/L}$  Hf. The resulting mass spectrum can be seen in Figure 2. Initially, the reaction product ion spectra may appear complex, but it should be noted that the use of a fixed mass setting for Q1 means that all these ammonia product ions are derived from the  $^{176}\text{Hf}$  isotope. The most abundant ammonia adduct ion was  $\text{Hf}(\text{NH})(\text{NH}_2)(\text{NH}_3)_3^+$ , which occurs at  $M + 82$  u ( $m/z$  258 for the  $^{176}\text{Hf}$  isotope); this adduct was selected as the preferred mass transition.

It should be noted that the Hf adduct ion used is sensitive to CRC conditions, particularly the acceleration voltage applied from the Octopole Bias. This parameter was optimized to a lower value than is typically used, in order to favor the preferred transition and maximize the yield of the desired product ion. The cell gas flow rate was then re-optimized using the ICP-MS MassHunter autotune routines to further improve the product ion signal.





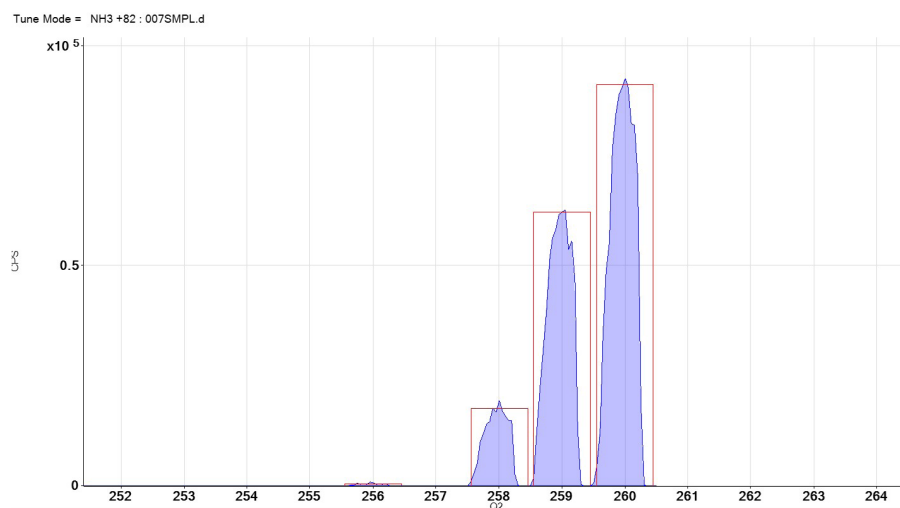


**Figure 4.** Neutral Gain Scan of the Hf isotopes as  $\text{Hf}(\text{NH})(\text{NH}_2)(\text{NH}_3)_3^+$  clusters; theoretical Hf isotopic abundances are shown in red, confirming that the isotope ratios are preserved in the product ion spectrum.

To simulate real-world sample analysis, several potential sources of interference were introduced to assess whether bias or new interferences were created.

The test solutions included:

- Hf standard (5 ppb) – also used for Mass Bias Calibration
- 100 ppb Yb and 5 ppb Hf
- 100 ppb Lu and 5 ppb Hf
- 100 ppb Yb + Lu and 5 ppb Hf
- Mixed 100 ppb “REE1” standard and 5 ppb Hf
- Mineral<sup>2</sup> sample with 100 ppb “REE1” and 5 ppb Hf

### Hf isotope ratio measurement

In order to provide comparative performance data, the ICP-QQQ was set to measure  $^{176}/^{177}\text{Hf}$  isotope ratios in three separate acquisition modes:

- No cell gas, “Single Quad” mode  
“Base” ICP-MS data not utilizing any mechanism to reduce isobaric overlaps
- $\text{NH}_3$  reaction gas, Single Quad Bandpass mode  
Non-MS/MS operation, allowing a limited mass range “window” into the CRC
- $\text{NH}_3$  reaction gas, MS/MS mode  
Q1 operating as a mass filter with unit mass resolution, allowing only a single m/z into the CRC

Table 2 displays the Hf isotope ratio (IR) data for each of the test solutions in each instrument mode. It can be seen that there was a large positive deviation from the expected ratio (i.e. the  $^{176}\text{Hf}$  signal was high relative to its theoretical abundance) in both of the Single Quad modes of operation (no gas mode and ammonia mode with bandpass filtering). This indicates that “Single Quad” operation did not resolve the Yb and Lu isobars at m/z 176, or stop the formation of new reaction product ion interferences.

1. Agilent Standard 8500-6944 containing La, Ce, Pr, Nd, Sm, Eu, Gd, Tb, Dy, Ho, Er, Tm, Yb, Lu, plus Sc, Y, Th.  
2. Natural mineral sample containing approximately 500 ppm Ca, 120 ppm Mg, 15 ppm Na, 5 ppm K, 1500 ppm  $\text{SO}_4$

By contrast, MS/MS mode with NH<sub>3</sub> cell gas gave consistent, accurate Hf IR data in all the sample matrices.

To visualize and further investigate the potential overlaps that could have caused the poor Hf isotope ratio performance in Single Quad mode, a mass scan of the mineral sample was performed using Single Quadrupole Bandpass mode with NH<sub>3</sub> reaction gas. The spectrum can be observed in Figure 5. The measured Hf isotopic pattern (far right of the spectrum) does not match the theoretical abundance template, showing that the Hf isotopes suffer overlap from new cell-formed cluster ions, due to the lack of control over the reaction processes. In a complex sample matrix, numerous cell-formed interferences are created, precluding the accurate analysis of many target product ions.

**Table 2.** <sup>176/177</sup>Hf isotope ratio (IR) data measured in samples containing various sources of interferences, using three different ICP-QQQ operating modes. The "deviation" is the error in the measured ratio relative to the true ratio of 0.282796.

Sample	No gas Single Quad		NH <sub>3</sub> Single Quad bandpass		NH <sub>3</sub> MS/MS	
	IR	Deviation	IR	Deviation	IR	Deviation
Hf 5 ppb	0.27981	0.989	0.28252	0.999	0.28196	0.997
Hf 5 ppb, Yb 100 ppb	15.25251	53.935	0.30461	1.077	0.28370	1.003
Hf 5 ppb, Lu 100 ppb	3.18739	11.271	1.06062	3.750	0.28051	0.992
Hf 5 ppb, Yb, Lu 100 ppb	18.51262	65.463	1.06267	3.758	0.28099	0.994
Hf 5 ppb, REE mix 100 ppb	15.26995	53.996	0.64603	2.284	0.28139	0.995
Hf 5 ppb, Mineral REE mix 100 ppb	16.16150	57.149	0.63479	2.245	0.28230	0.998

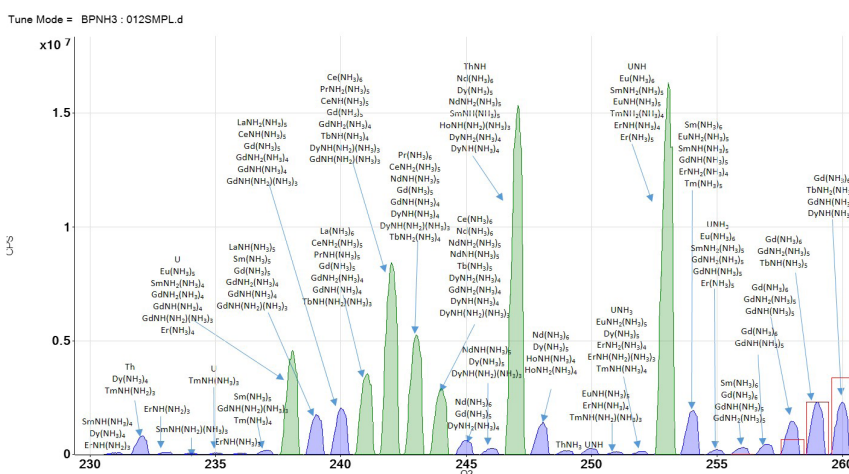


**Figure 5.** Mass spectrum of the mineral sample acquired under Single Quad Bandpass mode using ammonia as the reaction gas. The poor fit of the measured Hf isotopic pattern (far right) illustrates the interferences that occur in Single Quad mode. Some examples of cell-formed ammonia cluster ions are shown.

Many matrix elements and other analytes can react with ammonia to produce higher order reaction products, so MS/MS mode is essential to remove these precursor ions before they enter the cell and form new interferences.

The 8800 and 8900 ICP-QQQ use an additional quadrupole mass filter, operating at unit mass resolution and positioned before the CRC, to control which ions enter the reaction cell. This ensures unprecedented levels of control over the reaction processes that occur within the cell. MS/MS mode can quickly switch between on-mass measurement and off-mass measurement within a single acquisition, supporting multi-element analysis in each gas mode. Figure 6 shows the Hf isotopes measured using off-mass mode ( $Q2=Q1 + 82$  u) and the other masses measured on-mass ( $Q1=Q2$ ). The small, residual peaks for unreacted Th and U can be seen, along with ThO and UO. Most of the Th and U would have reacted with ammonia cell gas, forming adduct species that are not measured in MS/MS on-mass mode. Any undesired side reactions are eliminated before they can proceed, so the underlying analyte isotope ratios are preserved in the product ion spectrum.

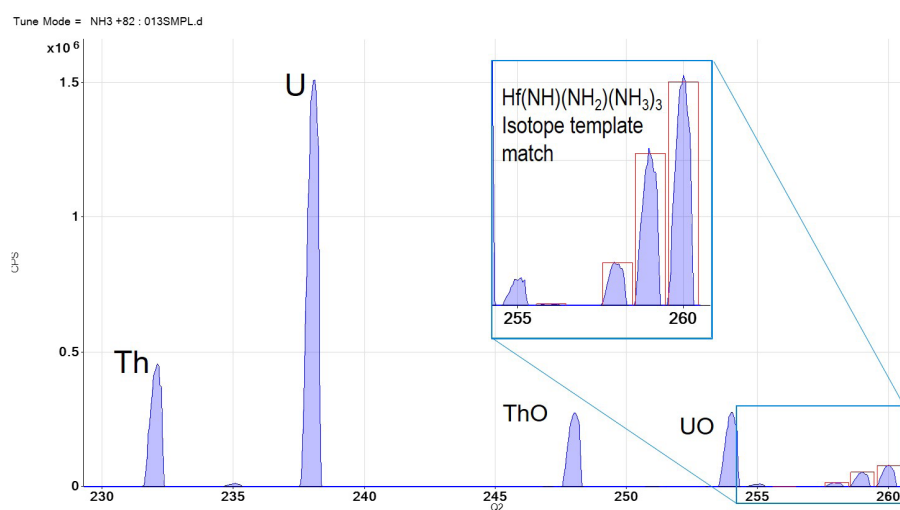


**Figure 6.** Mass spectrum of the mineral sample measured using  $\text{NH}_3$  mass-shift mode for Hf and on-mass mode for all other isotopes. The Hf isotopic pattern illustrates that all of the interferences that occurred in Single Quad mode (shown in Figure 5) have been resolved.

## Conclusion

The MS/MS capabilities of Agilent's ICP-QQQ measured Hf isotope ratios with excellent accuracy—even in samples containing high levels of co-existing and potentially interfering matrix elements.

The isobaric overlaps from  $^{176}\text{Lu}$  and  $^{176}\text{Yb}$  on  $^{176}\text{Hf}$  were eliminated using  $\text{NH}_3$  as the reaction gas. The reaction chemistry was controlled in the cell by operating the first quadrupole mass filter at unit mass resolution set to  $m/z$  176. This excluded all ions apart from those at  $m/z$  176 ( $^{176}\text{Lu}$ ,  $^{176}\text{Yb}$  and  $^{176}\text{Hf}$ ). Since only Hf reacts readily with  $\text{NH}_3$ ,  $^{176}\text{Hf}$  was free to be measured via its most appropriate cluster ion at  $m/z$  258, effectively avoiding the isobaric overlaps from Lu and Yb. Together with the corresponding ammonia cluster ion formed from the  $^{177}\text{Hf}$  isotope, this method allowed accurate Hf isotope analysis to be performed in a range of complex synthetic sample matrices.

In summary:

Chemical resolution using a reaction gas offers a powerful alternative to mass resolution, allowing access to isobars beyond the maximum resolution available with commercial High Resolution SF-ICP-MS.

Control over the reaction processes is essential to avoid new, unexpected interferences forming from the sample matrix and other coexisting elements and isotopes.

MS/MS technology affords unprecedented control over the reaction processes, greatly simplifying methodology regardless of the process or sample matrix.

Crucially, MS/MS operation allows access to higher order reaction product (cluster) ions, while still preserving the analyte's original isotopic information.

# Nuclear

Title	Page
Analysis of radioactive iodine-129 using MS/MS with O <sub>2</sub> reaction mode	391
Feasibility study on the analysis of radioisotopes: Sr-90 and Cs-137	395
Determination of trace <sup>236</sup> U as UOO <sup>+</sup> using ICP-QQQ O <sub>2</sub> mass-shift method	398
Measurement of neptunium in the presence of uranium: benefits of low abundance sensitivity and oxygen reaction mode	401
Direct analysis of zirconium-93 in nuclear site decommissioning samples by ICP-QQQ	404

# Analysis of Radioactive Iodine-129 Using MS/MS with Oxygen Reaction Mode

## Authors

Yasuyuki Shikamori, Kazumi Nakano  
and Naoki Sugiyama  
Agilent Technologies, Japan

## Keywords

radionuclide, iodine,  $^{129}\text{I}$ , environmental,  
nuclear, xenon, NIST 3231 Level I and  
II, abundance sensitivity, oxygen  
on-mass

## Introduction

Iodine-129 is a long-lived radionuclide (half-life of 15.7 My) which has been released into the environment as a result of human activities such as nuclear weapons testing, accidents at nuclear power plants and especially by emissions from spent nuclear fuel reprocessing plants. The determination of iodine-129 in environmental samples is very difficult by ICP-MS due to the element's relatively low sensitivity, the very low concentrations at which  $^{129}\text{I}$  must be determined, relative to potentially high levels of  $^{127}\text{I}$ , the high background caused by  $^{129}\text{Xe}$  impurities in the argon plasma gas, and possible polyatomic interference from  $^{127}\text{IH}_2^+$ . Iodine analysis is further complicated by the fact that it is rapidly volatilized from samples prepared using the acid digestions that are normal for ICP-MS analysis, so an alternative, alkaline sample solubilization and stabilization strategy is required. The isobaric interference from  $^{129}\text{Xe}^+$  can be significantly reduced using ICP-QMS with an Octopole Reaction Cell operated in  $\text{O}_2$  reaction mode, resulting in a measured ratio for  $^{129}\text{I}/^{127}\text{I}$  of  $10^{-7}$  in NIST 3231 SRM Level I (1). However, the problem of potential overlap due to tailing from  $^{127}\text{I}$  and  $^{127}\text{IH}$  remains, as the relative abundance of the  $^{129}\text{I}$  to  $^{127}\text{I}$  will typically exceed  $10^{-7}$ , which is of the same order as the abundance sensitivity (ability to separate adjacent peaks) of quadrupole ICP-MS (ICP-QMS). In order to overcome these challenges, ICP-QQQ operating in MS/MS mode with  $\text{O}_2$  reaction gas was applied to determine ultratrace levels of iodine-129 in aqueous samples.

## Experimental

**Instrumentation:** Agilent 8800 #100.

**Plasma conditions:** Preset plasma/Low matrix.

**Ion lens tune: Soft extraction tune:** Extract 1 = 0 V, Extract 2 = -190 V.

**CRC conditions:**  $\text{O}_2$  gas at 0.8 mL/min,  
Octopole bias = -18 V and KED = -1.5V. MS/MS  $\text{O}_2$  on-mass mode was applied to measure iodine-127 and iodine-129 (Q1 = Q2 = 127 for iodine-127; Q1 = Q2 = 129 for iodine-129).

**Reference materials and calibration standards:** Calibration standards were prepared by diluting  $^{129}\text{I}$  isotopic standards NIST SRM 3231 Level I and II (NIST, Gaithersburg MD, USA) with 0.5% TMAH in deionized water. The Level I Certified Value for  $^{129}\text{I}/^{127}\text{I} = 0.981 \times 10^{-6} \pm 0.012 \times 10^{-6}$ , Level II =  $0.982 \times 10^{-8} \pm 0.012 \times 10^{-8}$ . These reference materials were used to check the calibration linearity of the iodine isotopes and to validate the isotopic ratio of iodine-129 and iodine-127.

## Results and discussion

### Optimization of oxygen cell gas flow

The oxygen gas flow rate was optimized by varying the O<sub>2</sub> flow over the full range of the mass flow controller (0–1.12 mL/min), while monitoring the <sup>127,129</sup>I signal and blank intensity, as shown in Figure 1. As the flow rate of O<sub>2</sub> increases, the background signal (due to <sup>129</sup>Xe) at *m/z* = 129 decreases rapidly, and the iodine signal remains high, dramatically improving the DL for <sup>129</sup>I.

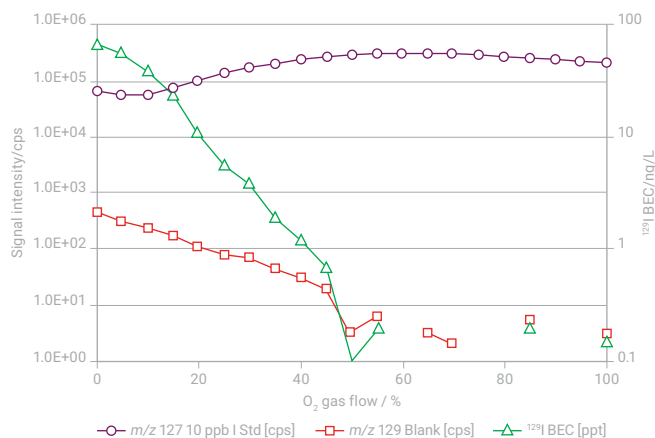


**Figure 1.** Profile of <sup>127</sup>I<sup>+</sup>, <sup>129</sup>Xe<sup>+</sup> signals and estimated <sup>129</sup>I BEC. For the BEC calculation, the sensitivity of <sup>129</sup>I was assumed to be the same as <sup>127</sup>I. Scale of O<sub>2</sub> flow: 100% = 1.12 mL/min.

### Abundance sensitivity

Scan spectra over the mass range 127 to 129, covering both <sup>127</sup>I and <sup>129</sup>I, were acquired for the two SRMs, NIST 3231 Level I and II, using the Agilent 8800 ICP-QQQ in MS/MS on-mass mode with O<sub>2</sub> reaction gas. The overlaid spectra are shown in Figure 2. Excellent abundance sensitivity can be seen, with the sides of the intense (>10<sup>9</sup> cps) <sup>127</sup>I peak reaching baseline with no tailing of <sup>127</sup>I<sup>+</sup> or <sup>127</sup>IH<sup>+</sup> on <sup>129</sup>I<sup>+</sup>.

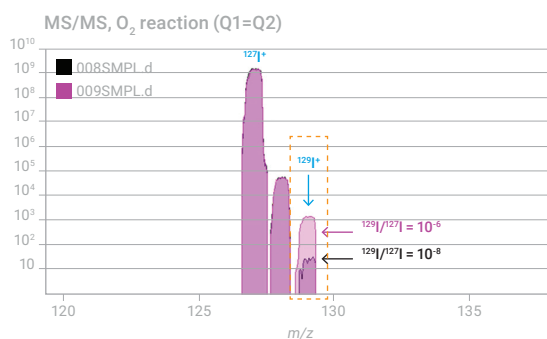


**Figure 2.** Iodine spectra showing both <sup>127</sup>I and <sup>129</sup>I acquired using MS/MS on-mass mode with O<sub>2</sub> cell gas. <sup>127</sup>IH<sup>+</sup> remains to some extent while <sup>127</sup>IH<sub>2</sub><sup>+</sup> is completely removed, as noted later.



### Calibration curves for <sup>127</sup>I and <sup>129</sup>I

In order to check the linearity of both iodine isotopes, different concentration solutions of NIST 3231 SRM Level I were prepared in 0.5% TMAH and analyzed as calibration standards, as shown in Figure 3. The BECs for <sup>127</sup>I and <sup>129</sup>I were 2.9 µg/L and 0.04 ng/L respectively, and the detection limits (3σ, n=10) were 0.26 µg/L for <sup>127</sup>I and 0.07 ng/L for <sup>129</sup>I.

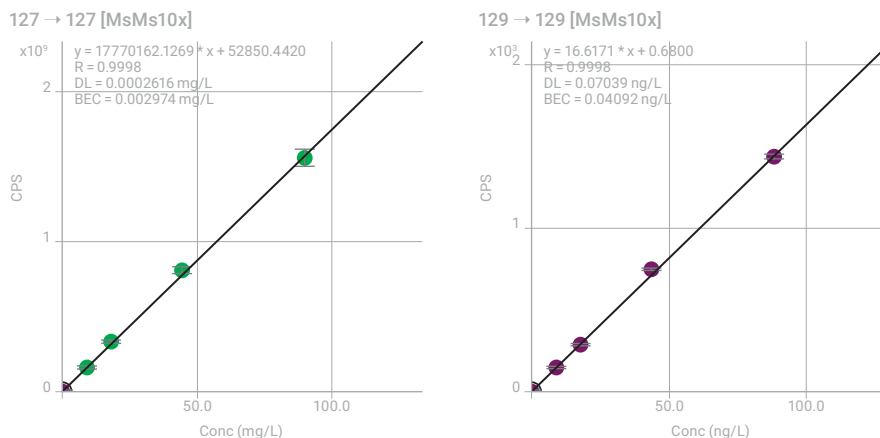


**Figure 3.** Calibration curve for iodine-127 (top) and iodine-129 (bottom) obtained from multiple dilutions of NIST 3231 SRM.

### Analysis of NIST 3231 SRM Level I and Level II

The <sup>129</sup>I/<sup>127</sup>I ratio in 10x diluted NIST 3231 SRM Levels I (<sup>129</sup>I/<sup>127</sup>I = 0.981 × 10<sup>-6</sup>) and II (<sup>129</sup>I/<sup>127</sup>I = 0.982 × 10<sup>-8</sup>) was measured using ICP-QQQ in MS/MS on-mass mode with O<sub>2</sub> cell gas. The results are summarized in Table 1. After subtracting the <sup>129</sup>I blank, the measured <sup>129</sup>I/<sup>127</sup>I ratio of NIST 3231 SRM Levels I and II corresponded well with the certified values of 0.981×10<sup>-6</sup> and 0.982×10<sup>-8</sup> respectively. The good agreement with the certified ratio indicates that the potential interference of <sup>127</sup>IH<sub>2</sub><sup>+</sup> on <sup>129</sup>I<sup>+</sup> is completely removed by O<sub>2</sub> reaction with MS/MS mode.

**Table 1.** Analytical results for NIST 3231 Level I and Level II.

Sample name	Dilution factor	Q1=Q2=127 CPS	Q1=Q2=129 CPS	<sup>129</sup> I/ <sup>127</sup> I	<sup>129</sup> I/ <sup>127</sup> I (average n = 5)	RSD (%)
NIST 3231 10 <sup>-6</sup> ( <sup>129</sup> I/ <sup>127</sup> I = 0.981 × 10 <sup>-6</sup> )	10	594,277,896	585.6	0.971 × 10 <sup>-6</sup>	0.981 × 10 <sup>-6</sup>	0.8
		592,633,576	597.4	0.994 × 10 <sup>-6</sup>		
		590,000,723	586.5	0.980 × 10 <sup>-6</sup>		
		593,387,443	588.5	0.978 × 10 <sup>-6</sup>		
		592,834,056	588.9	0.979 × 10 <sup>-6</sup>		
NIST 3231 10 <sup>-8</sup> ( <sup>129</sup> I/ <sup>127</sup> I = 0.982 × 10 <sup>-8</sup> )	10	608,737,949	15.1	1.12 × 10 <sup>-8</sup>	1.02 × 10 <sup>-8</sup>	7.2
		608,536,242	14.8	1.07 × 10 <sup>-8</sup>		
		602,626,536	14.2	0.979 × 10 <sup>-8</sup>		
		603,091,763	13.9	0.929 × 10 <sup>-8</sup>		
		603,250,003	14.5	1.03 × 10 <sup>-8</sup>		
NIST Blank	10	600,444,851	8.3	—	—	—

## Reference

1. The ultratrace determination of iodine 129 in aqueous samples using the 7700x ICP-MS with oxygen reaction mode, Agilent application note, 5990-8171EN.

## More information

The ultratrace determination of iodine 129 using the Agilent 8800 Triple Quadrupole ICP MS in MS/MS mode, Agilent publication, [5991-0321EN](#)

# Feasibility Study on the Analysis of Radioisotopes: Sr-90 and Cs-137

## Authors

Yasuyuki Shikamori and  
Kazumi Nakano  
Agilent Technologies, Japan

## Keywords

radioisotopes, radioactive,  
environmental, nuclear, strontium,  
<sup>90</sup>Sr, zirconium, cesium, <sup>137</sup>Cs, barium,  
abundance sensitivity, oxygen and  
hydrogen on-mass, nitrous oxide  
on-mass

## Introduction

ICP-MS can be an effective analytical tool for the analysis of long half-life radioisotopes due to its high sensitivity, speed of analysis, low sample consumption, and ease of sample preparation. The challenge for ICP-MS analysis of radioisotopes arises from interferences; not only by polyatomic ions but also atomic isobar ions that cannot be separated even by high-resolution (HR-) ICP-MS.

Trace analysis of the radionuclide <sup>90</sup>Sr (half-life = 28.74 years) in environmental samples is of great interest. <sup>90</sup>Sr is a main fission product that may be present in the environment following accidental releases from nuclear power plants. Geiger-Muller (GM) detectors or Liquid Scintillation Counters (LSC) are used to measure <sup>90</sup>Sr, though both techniques require complex chemical separation prior to analysis, or long integration times. ICP-MS is also used to measure <sup>90</sup>Sr, especially when a quick turn-around time is desired. However, detection limits of quadrupole ICP-MS are compromised by a spectral overlap from <sup>90</sup>Zr; in common with all direct isobaric interferences, the <sup>90</sup>Zr overlap is too close in mass to the <sup>90</sup>Sr to be resolved using sector field HR-ICP-MS, which is limited to a maximum resolution ( $M/\Delta M$ ) of 10,000. This note describes a method for measuring trace <sup>90</sup>Sr in the presence of <sup>90</sup>Zr using ICP-QQQ in MS/MS reaction mode. Since it isn't possible to obtain <sup>90</sup>Sr, a natural isotope of strontium (<sup>88</sup>Sr) was used to estimate the DL for <sup>90</sup>Sr. A similar approach was applied to <sup>137</sup>Cs (half-life = 30.0 years).

## Experimental

**Instrumentation:** Agilent 8800 #100.

**Plasma conditions:** Preset plasma/Low matrix.

**Ion lens tune:** Soft extraction tune: Extract 1 = 0 V, Extract 2 = -190 V.

**CRC and acquisition conditions:** The following conditions were used for the analysis of <sup>90</sup>Sr and <sup>137</sup>Cs:

- For <sup>90</sup>Sr: MS/MS on-mass mode (Q1 = Q2 = 90) with O<sub>2</sub> + H<sub>2</sub> cell gas: 1 mL/min of O<sub>2</sub> and 10 mL/min of H<sub>2</sub>, Octopole bias = -5 V and KED = -13 V.
- For <sup>137</sup>Cs: MS/MS on-mass mode (Q1 = Q2 = 137) with N<sub>2</sub>O cell gas: 7 mL/min of N<sub>2</sub>O (10% N<sub>2</sub>O balanced in He, introduced via the 3rd cell gas flow line), Octopole bias = -5 V and KED = -13 V.

## Results and discussion

### Radioactive Sr-90 ( $O_2 + H_2$ on-mass mode)

Figure 1 shows spectra of a solution containing Sr and Zr (natural isotopes) acquired on the 8800 ICP-QQQ operated in Single Quad mode (Q1 operated as an ion guide to emulate conventional quadrupole ICP-MS) with no cell gas (left), and in MS/MS mode with  $O_2 + H_2$  cell gas (right). As can be seen in the left hand spectrum, the overlap of  $^{90}Zr^+$  on  $^{90}Sr^+$  precludes the low-level determination of  $^{90}Sr$  by conventional quadrupole ICP-MS. The spectrum on the right indicates that  $^{90}Sr^+$  could be measured on-mass at  $m/z = 90$  free from interference by  $^{90}Zr^+$ , since  $Zr^+$  reacts readily with the  $O_2 + H_2$  gas to form  $ZrO^+$  and  $ZrO_2^+$ . The signal-to-noise ratio for  $^{90}Sr$  was improved by six orders of magnitude using MS/MS  $O_2 + H_2$  reaction cell mode.

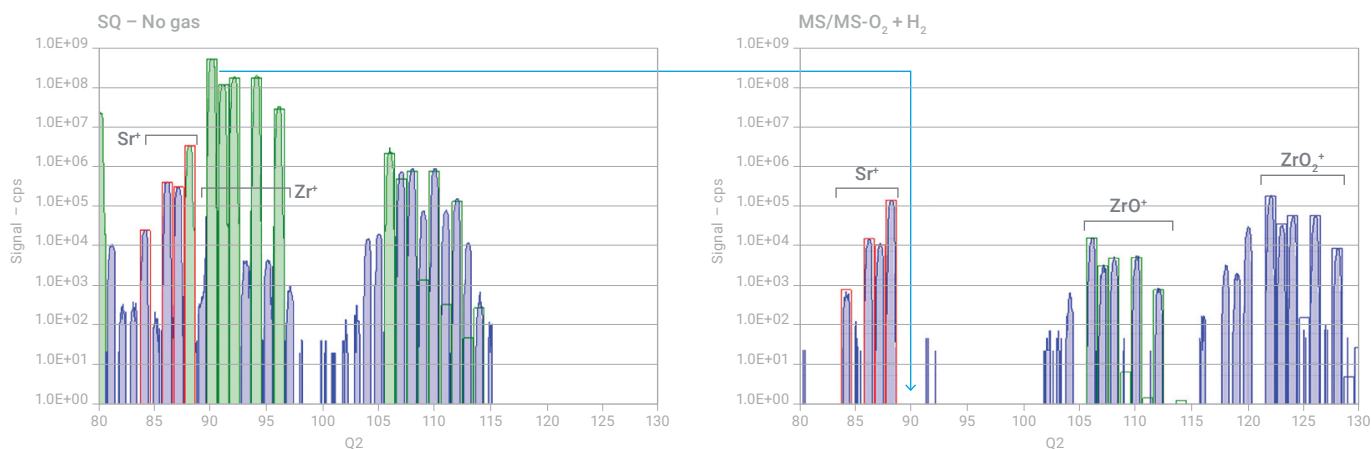


Figure 1. Mass spectra of a solution containing 20 ppb Sr + 5 ppm Zr: (left) SQ no gas mode and (right) MS/MS  $O_2 + H_2$  reaction mode.

Figure 2 is a spectrum of 100 ppm Sr acquired using MS/MS on-mass mode with  $O_2 + H_2$  reaction gas. The excellent abundance sensitivity (peak separation) of MS/MS mode can be confirmed. The peak sides reach the baseline with no tailing from the intense peak of the natural isotope of  $^{88}Sr^+$ . In addition, no  $^{88}SrHH^+$  at  $m/z = 90$  is formed in cell, even in a solution containing 100 ppm natural Sr.

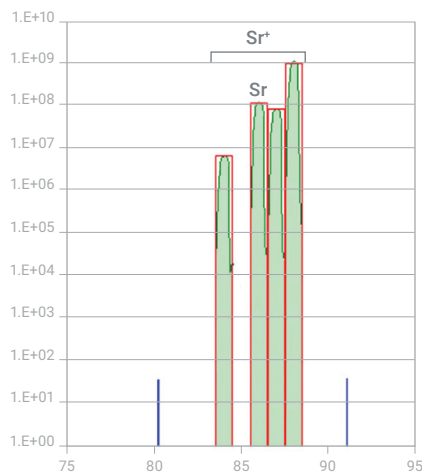
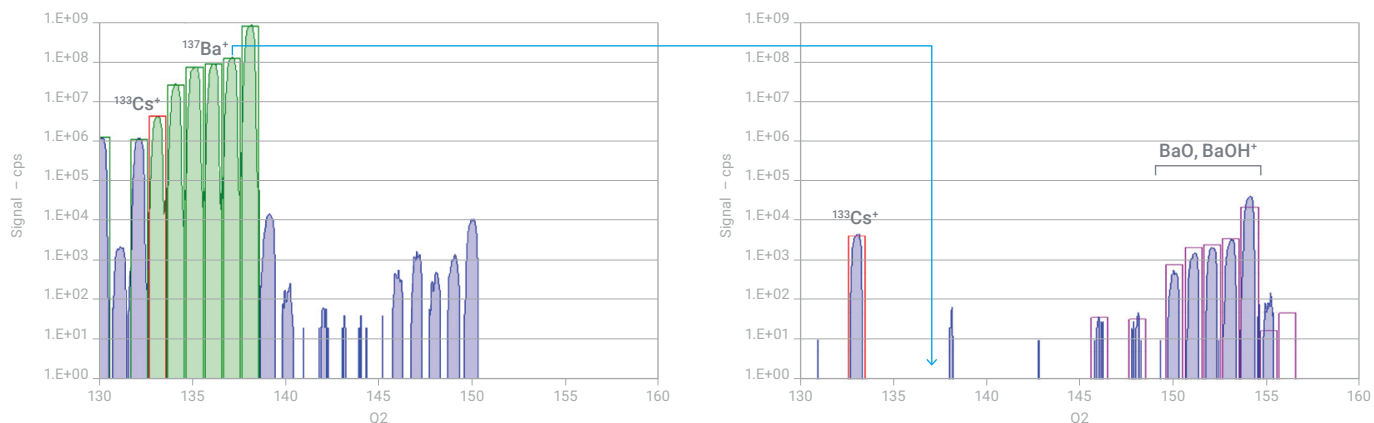


Figure 2. Spectrum of 100 ppm Sr solution acquired using MS/MS  $O_2 + H_2$  on-mass mode.

### Radioactive Cs-137 (N<sub>2</sub>O on-mass mode)

Figure 3 shows spectra of a solution containing Cs and Ba (natural isotopes) acquired on the 8800 ICP-QQQ operated in Single Quad mode with no gas mode (left), and in MS/MS mode with N<sub>2</sub>O cell gas (right). As can be seen in the left hand spectrum, the <sup>137</sup>Ba<sup>+</sup> overlap on <sup>137</sup>Cs<sup>+</sup> is a problem in conventional quadrupole ICP-MS. As with <sup>90</sup>Sr, the right hand spectrum shows that <sup>137</sup>Cs<sup>+</sup> could be measured on mass at *m/z* = 137, free from the <sup>137</sup>Ba<sup>+</sup> interference. Ba<sup>+</sup> reacts readily with N<sub>2</sub>O to form BaO<sup>+</sup> and BaOH<sup>+</sup> while a part of the Cs<sup>+</sup> analyte ion signal remains at its original mass (as shown by the substantial peak for <sup>133</sup>Cs in the right-hand spectrum).



**Figure 3.** Mass spectra of a solution containing 20 ppb Cs + 5 ppm Ba: (left) SQ no gas and (right) MS/MS N<sub>2</sub>O reaction mode.

### Estimated BEC and DL for Sr-90 and Cs-137

The BEC and DL for two radioisotopes, <sup>90</sup>Sr and <sup>137</sup>Cs, were estimated from these spectra as summarized in Table 1. This feasibility study demonstrates the potential of ICP-QQQ for the measurement of radioisotopes such as <sup>90</sup>Sr and <sup>137</sup>Cs.

**Table 1.** Estimated BEC and DL for <sup>90</sup>Sr and <sup>137</sup>Cs.

Radioisotope	BEC (ng/L)	DL (ng/L)
<sup>90</sup> Sr	0.08	0.23
<sup>137</sup> Cs	2.9	15

# Determination of Trace $^{236}\text{U}$ as $\text{UO}_2^+$ using ICP-QQQ Oxygen Mass-shift Method

## Author

Naoki Sugiyama  
Agilent Technologies, Japan

## Keywords

uranium, uranium-236,  $\text{O}_2$  cell gas, mass-shift, extended mass range

## Introduction

Uranium-236 is a long-lived radionuclide that is created from the naturally occurring trace isotope  $^{235}\text{U}$  (0.72% abundance) by thermal neutron capture. This process leads to a natural abundance of  $^{236}\text{U}$  in the range from  $10^{-14}$  to  $10^{-13}$  relative to the major  $^{238}\text{U}$  isotope ( $^{236}\text{U}/^{238}\text{U}$ ).  $^{236}\text{U}$  is also created during the process of uranium enrichment for nuclear fuel or weapons. The  $^{236}\text{U}/^{238}\text{U}$  ratio is increased up to  $10^{-3}$  in spent nuclear fuel, with background levels in the environment at around  $10^{-7}$  to  $10^{-8}$  as a result of global fallout. The  $^{236}\text{U}/^{238}\text{U}$  isotope ratio can therefore be used as a sensitive method to trace the accidental release of enriched uranium fuel, spent fuel, and nuclear waste.

The challenges for ICP-MS for this application are the interference on  $^{236}\text{U}^+$  by the hydride ion  $^{235}\text{UH}^+$ , and the contribution at  $m/z$  236 from tailing of the  $^{235}\text{U}^+$  and  $^{238}\text{U}^+$  peaks. The hydride overlap and peak tailing are more problematic in samples that have been enriched, as these samples contain a higher proportion of  $^{235}\text{U}$ . Uranium was measured via its dioxide ion,  $\text{UO}_2^+$ , due to the efficient conversion (almost 100%) of  $\text{U}^+$  to  $\text{UO}_2^+$  with  $\text{O}_2$  cell gas.

## Experimental

**Instrumentation:** Agilent 8900 Advanced Applications configuration ICP-QQQ with PFA nebulizer (p/n G3139-65100).

**Plasma tuning:** RF power = 1550 W, sampling depth = 8.0 mm, nebulizer gas flow rate = 0.80 L/min, make-up gas flow rate = 0.30 L/min, and peristaltic pump = 0.1 rps.

**Cell tuning:** Octopole bias = 0 V, KED = -10 V,  $\text{O}_2$  cell gas flow = 0 to 35% of full scale (0 to 0.53 mL/min).

**Sample preparation:** Uranium solutions were prepared at suitable concentrations by diluting SPEX multi element standard XSTC-331 (SPEX CertiPrep, Metuchen, NJ, USA) with de-ionized water. All samples, blank, and rinse solutions were spiked with high purity TAMAPURE 100  $\text{HNO}_3$  (Tama Kagaku, Saitama, Japan) to a concentration of 1%.

## Results and discussion

### UO<sup>+</sup> and UO<sub>2</sub><sup>+</sup> formation as a function of O<sub>2</sub> cell gas flow rate

The rate of formation of UO<sup>+</sup> and UO<sub>2</sub><sup>+</sup> was studied as a function of O<sub>2</sub> cell gas flow rate. A solution containing 10 ppb uranium (1000x dilution of XSTC-331) was introduced into the ICP-QQQ. The signals of <sup>238</sup>U<sup>+</sup>, <sup>238</sup>U<sup>16</sup>O<sup>+</sup>, and <sup>238</sup>U<sup>16</sup>O<sup>16</sup>O<sup>+</sup> were measured via three mass pairs (Q1→Q2) = (238→238), (238→254), and (238→270), and plotted against the O<sub>2</sub> cell gas flow rate. The octopole bias (Octp Bias) voltage was optimized to give the maximum UO<sub>2</sub><sup>+</sup> signal (0 V).

Figure 1 shows that UO<sup>+</sup> formation reaches a maximum at an O<sub>2</sub> flow rate of 5% of full scale (equivalent to 0.074 mL/min as O<sub>2</sub>). Above 0.075 mL/min flow rate, the formation of UO<sup>+</sup> decreased, while the formation of UO<sub>2</sub><sup>+</sup> increased, reaching a maximum at an O<sub>2</sub> flow of 22% of full scale (0.33 mL/min). This indicates the conversion of UO<sup>+</sup> to UO<sub>2</sub><sup>+</sup> via a chain reaction. The 8900 ICP-QQQ was optimized for highest sensitivity for the UO<sub>2</sub><sup>+</sup> product ion.

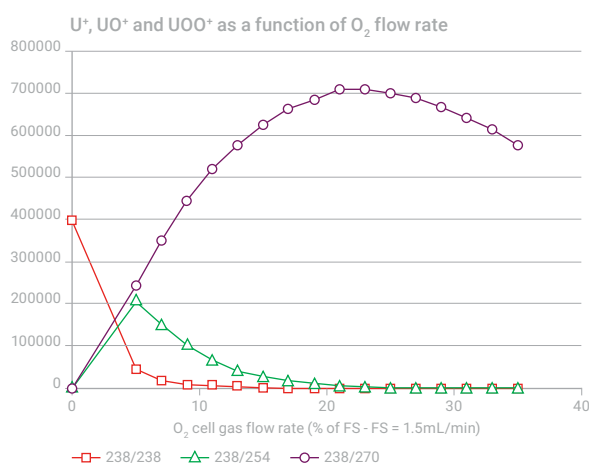


Figure 1. U<sup>+</sup> (238 → 238), UO<sup>+</sup> (238 → 254), and UO<sub>2</sub><sup>+</sup> (238 → 270) as a function of O<sub>2</sub> cell gas flow rate.

### Effect of product ion selection on hydride ion formation rate

The hydride ratio was measured at the optimal O<sub>2</sub> flow rate for U<sup>+</sup> and each of the U-oxide product ions: <sup>238</sup>UH<sup>+</sup>/<sup>238</sup>U<sup>+</sup>, <sup>238</sup>UOH<sup>+</sup>/<sup>238</sup>UO<sup>+</sup>, and <sup>238</sup>UO<sub>2</sub>H<sup>+</sup>/<sup>238</sup>UO<sub>2</sub><sup>+</sup>.

A sample containing 50 ppb U (200x diluted XSTC- 331) was introduced for the measurement of the hydride formation ratio. Ten replicate measurements were made, with integration times of 1 s and 10 s for the analyte and hydride ions respectively. The results are summarized in Table 1. The data shows that measuring UO<sup>+</sup> decreases the hydride ratio by a factor of ~20, while measuring UO<sub>2</sub><sup>+</sup> leads to more than a three orders of magnitude improvement, reducing the hydride ratio to 10<sup>-8</sup>.

## Uranium detection limit

The detection limit (DL) of U was estimated using the  $\text{UO}_2^+$  method. A blank solution was introduced and the signal of the mass pairs (236→268 and 238→270) corresponding to  $^{236}\text{U}^+ \rightarrow ^{236}\text{UO}_2^+$  and  $^{238}\text{U}^+ \rightarrow ^{238}\text{UO}_2^+$  were measured using an integration time of 10 s. The results in Table 2 are based on 10 replicate measurements. The DL for  $^{236}\text{U}$  was calculated from the concentration equivalent to three times the standard deviation of the background, using the sensitivity of  $^{238}\text{UO}_2^+$  given in Table 1 and the background for mass pair 236→268 in Table 2. The DL for uranium-236 was calculated to be 0.50 ppq (fg/g).

**Table 1.**  $\text{UH}^+/\text{U}^+$  ratios obtained by measuring uranium as  $\text{U}^+$ ,  $\text{UO}^+$ , and  $\text{UO}_2^+$ .

	$\text{O}_2$ cell gas flow rate (%)	$\text{U}^+$ analysis			$\text{UH}^+$ analysis			$\text{UH}^+/\text{U}^+$
		Mass pair for $\text{U}^+$	Counts	RSD	Mass pair for $\text{UH}^+$	Counts	RSD	
		Q1/Q2	cps	%	Q1/Q2	cps	%	
as $\text{U}^+$	0	238/238	24168974	2.8	239/239	1578.5	0.6	6.53E-05
as $\text{UO}^+$	5	238/254	14152816	4.2	239/255	48.9	4.3	3.46E-06
as $\text{UO}_2^+$	22	238/270	40527770	2.0	239/271	2.3	20.8	5.68E-08

**Table 2.** Uranium background noise.

236/268		238/270	
Counts	RSD	Counts	RSD
cps	%	cps	%
0.15	90.3	0.18	51.1

## Conclusion

The Agilent 8900 ICP-QQQ operating in MS/MS mode with  $\text{O}_2$  cell gas is suitable for the measurement of U via its reaction product ion  $\text{UO}_2^+$ . This approach was successful in reducing the contribution from the hydride ion (i.e.  $^{235}\text{UH}$  overlap on  $^{236}\text{U}$ ). The formation of  $^{235}\text{UH}$  was decreased by three orders of magnitude compared to direct, on-mass measurement of  $\text{U}^+$ . MS/MS mode with  $\text{O}_2$  cell gas gave a  $\text{UO}_2\text{H}^+/\text{UO}_2^+$  ratio in the  $10^{-8}$  range, without the use of a desolvation system. The results suggest that the approach could be successful in reducing the interference of  $^{235}\text{UH}^+$  on  $^{236}\text{U}^+$ , even in samples containing enriched U.

## More information

Using ICP-QQQ for  $\text{UO}_2^+$  product ion measurement to reduce uranium hydride ion interference and enable trace  $^{236}\text{U}$  isotopic analysis, Agilent publication [5991-6553EN](#)



# Measurement of Neptunium in the Presence of Uranium: Benefits of Low Abundance Sensitivity and Oxygen Reaction Mode

## Author

Glenn Woods  
Agilent Technologies, UK

## Keywords

neptunium, radiochemistry, abundance sensitivity, oxygen reaction mode

## Introduction

Neptunium is present in the environment at ultratrace levels due to natural neutron capture, nuclear bomb testing, and as a decay product of  $^{241}\text{Am}$ .  $^{241}\text{Am}$  is used in ionizing smoke detectors, radiography, and a neutron source, among other uses. By far the greatest quantity of Np is formed during energy production within uranium fission reactors. The predominant isotope formed is  $^{237}\text{Np}$ , with approximately 50 metric tonnes per annum being produced in nuclear waste. As the half-life of  $^{237}\text{Np}$  is ~2.14 billion years,  $^{237}\text{Np}$  in existence today is solely from the previously mentioned processes rather than remaining from the formation of the earth. However, the relatively long half-life ensures its persistence. Np will readily form aqueous solutions (more so than any other actinide element). It also attaches to particles and colloids rather than getting trapped in humic media (such as soil and peat). These properties mean that Np is fairly mobile once in the environment. Its high affinity for calcium-rich media causes it to concentrate within concrete, shells, etc.

Trace and ultratrace measurement of  $^{237}\text{Np}$  is hindered by the presence of uranium within the sample. The biggest potential interference comes from peak broadening of the adjacent  $^{238}\text{U}$  isotope. This Abundance Sensitivity (AS) interference is difficult to overcome. AS depends on the fundamental design of the spectrometer – such as the mass separation process (e.g. quadrupole or magnets), vacuum system, and electronics. Furthermore, minor but important polyatomic interferences from the hydrides of lighter U isotopes;  $^{236}\text{U}^1\text{H}$ ,  $^{235}\text{U}^1\text{H}_2$ ,  $^{235}\text{U}^2\text{H}$ ,  $^{234}\text{U}^1\text{H}^2\text{H}$  hinder the measurement of  $^{237}\text{Np}$ . Regardless of the interference source, its affect will vary depending on the concentration of uranium (and its isotope ratio), potentially causing false and variable measurements.

## Experimental

**Instrumentation:** An Agilent 8900 Advanced Applications configuration ICP-QQQ was used. The instrument version features Axial Acceleration across the ORS<sup>4</sup> collision/reaction cell that gives a higher product ion yield when using reaction chemistry.

**Tuning:** Np was measured under two sets of MS/MS conditions: on-mass (using no gas) and mass-shift (using  $\text{O}_2$  reaction gas). In the latter mode,  $^{237}\text{Np}$  is shifted away from the  $\text{UH}_x$  interferences allowing Np to be measured as the product ion  $\text{NpO}_2^+$ , free from interference, at  $m/z$  269.

**Calibration:** Np was spiked into a 10 mg/L (ppm) U matrix to produce a set of calibration standards at 0.0, 0.19, 0.95, 1.9, 19.0, 95.0 ng/L (ppt).

## Results and discussion

The Single Quad mass scan in Figure 1 shows the problem associated with AS when the U concentration is relatively high. As can be seen, the  $^{238}\text{U}$  peak overlaps the  $^{237}\text{Np}$  peak, impeding the trace level measurement of Np. Conversely when operating the ICP-QQQ in MS/MS mode, the peak overlap on Np is eliminated. This improvement is due to two separate mass separations taking place, improving the AS from  $\sim 10^{-7}$  to  $\ll 10^{-10}$ . The background is significantly reduced under MS/MS mode but not eliminated. Uranium can form various hydride interferences that are not related to (or removed by) AS. However, reaction chemistry can be used to remove interference-based background levels.

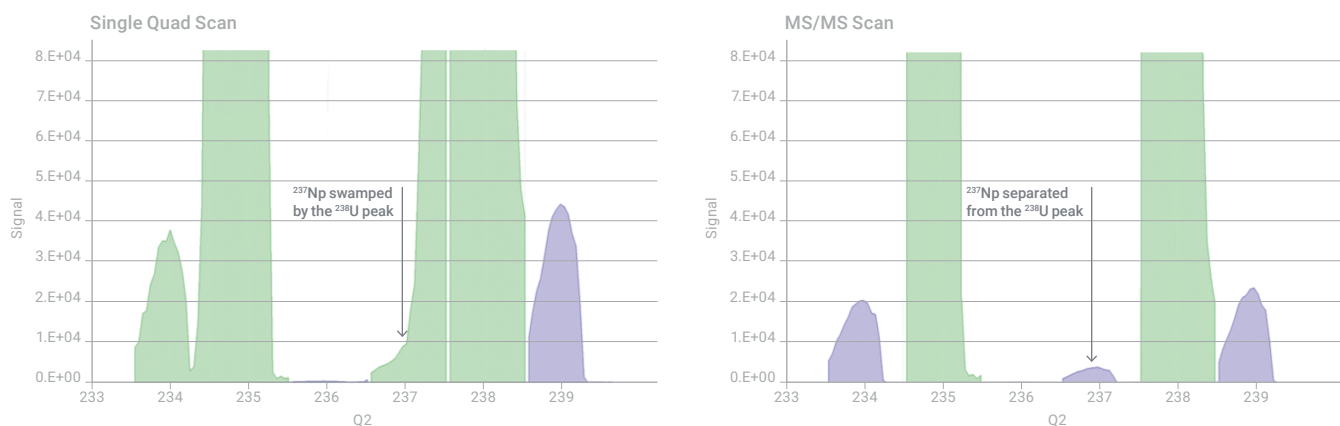


**Figure 1.** Spectrum of  $^{237}\text{Np}$  in presence of 10 ppm U. Left: Single Quad scan and Right: MS/MS mode. MS/MS mode eliminates the peak tail on the low mass side of the intense  $^{238}\text{U}$  peak.

To check the reaction efficiency of oxygen as a cell gas for this study, a spiked U matrix was measured under MS/MS mass-shift mode with  $\text{O}_2$  reaction gas. The Np spike was 1000x lower than the previous scans at 950 ppq (0.95 ng/L). Figure 2 shows the mass scan of the  $\text{NpO}_2$  (and  $\text{UO}_2$ ) product ions. It is worth noting that during quantitative analysis (rather than scanning, as shown in Figure 2), all the U isotopes would be eliminated by Q1, which would be set to  $m/z$  237. The conversion efficiency of Np to  $\text{NpO}_2$  was found to be 99%. Only 1% of total Np signal converted to  $\text{NpO}$ .

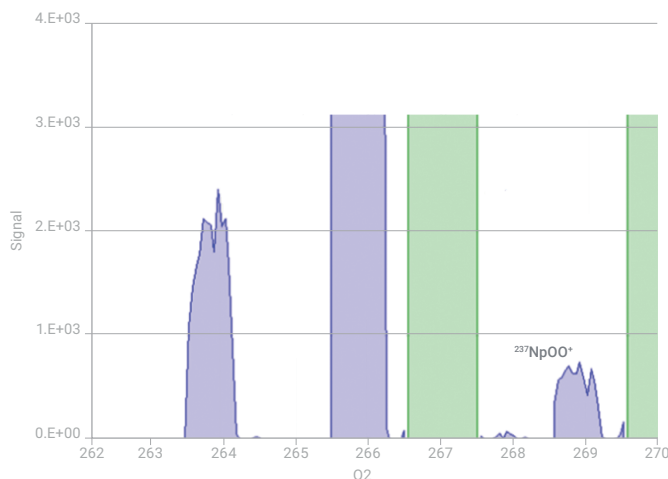


**Figure 2.** 950 ppt Np in 10 ppm U measured in MS/MS mass-shift mode with  $\text{O}_2$  cell gas.

Figure 3 shows the calibration graphs for Np in a 10 ppm U matrix generated in no gas mode (left) and oxygen reaction gas mode (right). Identical solutions were analyzed in both cases. The improvement in BEC and DL can be clearly seen in oxygen mass-shift mode. The DL and BEC under no gas conditions were 1.9 ppq and 2.4 ppq. Using O<sub>2</sub> mode and measuring Np as NpO<sub>2</sub> improved the DL to 0.56 ppq and the BEC to 0.32 ppq (pg/L).

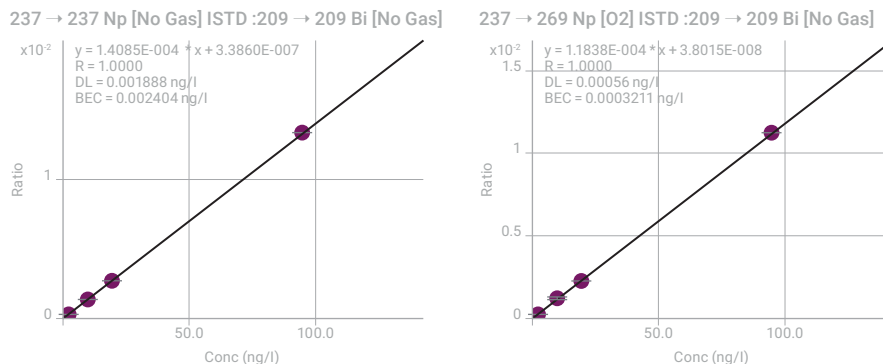


**Figure 3.** Np calibration in a 10 ppm U matrix. Left: no gas mode. Right: O<sub>2</sub> reaction gas mode – showing a 7.5x reduction in BEC. All UH-based interferences were avoided by measuring <sup>237</sup>Np as <sup>237</sup>Np<sup>16</sup>O<sub>2</sub>.

## Conclusion

The Agilent 8900 ICP-QQQ in MS/MS mode performs two mass selection steps, increasing the abundance sensitivity performance and allowing an ultratrace element to be measured in the proximity of a major matrix isotope. For the determination of Np, the removal of uranium-based interferences is essential, as U is present within the environment at significantly higher concentrations than Np. The unique MS/MS capability of the 8900 ICP-QQQ removes peak overlaps and uranium hydride-based interferences.

# Direct Analysis of Zirconium-93 in Nuclear Site Decommissioning Samples by ICP-QQQ

## Author

Heather Thompkins<sup>1</sup>

Ben Russell<sup>1</sup>

Sharon Goddard<sup>2</sup>

<sup>1</sup>Nuclear Metrology Group and

<sup>2</sup>Gas and Particle Metrology Group,  
National Physical Laboratory,  
Teddington, UK

Using MS/MS mass-shift mode to resolve <sup>93</sup>Zr from <sup>93</sup>Nb without chemical separation

## Introduction

Zirconium-93 is a long-lived radionuclide that is produced by nuclear fission of uranium and plutonium. It is also formed by neutron activation of stable zirconium in nuclear fuel cladding in pressurized water reactors. Therefore, <sup>93</sup>Zr is an important element to monitor during the decommissioning of nuclear sites. The long half-life of <sup>93</sup>Zr ( $1.61 \times 10^6$  years (1)) means it is a significant contributor to the total waste inventory over long timescales. Clearly, there is a need to accurately quantify <sup>93</sup>Zr in various complex decommissioning wastes as part of the initial site characterization process. Also, monitoring of waste repositories and the environment around nuclear sites following decommissioning is needed.

Zirconium-93 decays to stable <sup>93</sup>Nb by beta emission, but with a low decay energy that makes measurement by decay counting methods challenging. With its long-half-life, <sup>93</sup>Zr is well suited to measurement by ICP-MS (1 Bq/g is equivalent to  $1.1 \times 10^4$  pg/g), which offers a high throughput alternative to decay counting techniques. However, accurate measurement by ICP-MS is affected by the isobaric interference from <sup>93</sup>Nb (100% abundance), as well as potential radioactive <sup>93</sup>Mo, and polyatomic ion interference from <sup>92</sup>Mo<sup>1</sup>H<sup>+</sup> and <sup>92</sup>Zr<sup>1</sup>H<sup>+</sup>. The removal of these interferences traditionally requires time-consuming, multistage extraction and/or chromatographic separation before measurement, using a significant number of reagents and materials (2, 3). Also, since <sup>93</sup>Nb is monoisotopic, it is challenging for the analyst to be confident that complete interference removal has been achieved before measurement.

In this study, triple quadrupole ICP-MS (ICP-QQQ) was used for the rapid and direct low-level measurement of <sup>93</sup>Zr in decommissioning samples below International Atomic Energy Agency (IAEA) regulatory limits (4). Reactive gases were used in the collision/reaction cell (CRC) of the ICP-QQQ to separate the isobaric overlap from <sup>93</sup>Nb on <sup>93</sup>Zr, eliminating the need for chromatographic separation. Isobaric ion interferences can be separated using ICP-QQQ when the cell gas reacts quickly with one of the elements to form a product ion, while the other element does not react (or reacts slowly). This “chemical” resolution method significantly reduces the procedural time and secondary waste associated with decay counting and alternative mass spectrometric procedures. With its fast analysis times, ICP-QQQ offers a cost-effective method for the analysis of nuclear decommissioning samples.

## ICP-QQQ with MS/MS mode

ICP-QQQ is a well-established technique that is especially suitable for improved control of spectral, doubly charged ion, and isobaric interferences using reactive cell gas methods (5). Compared to conventional single quadrupole ICP-MS, ICP-QQQ has an additional mass filter before the CRC. This extra mass filter

prevents all ions apart from the target mass from entering the CRC, so the reaction chemistry in the cell can be controlled. This double mass filter approach is only possible with a tandem MS (or MS/MS) configuration, which provides unprecedented control of the ion-molecule reaction chemistry used in CRC-ICP-MS methods.

## Experimental

### Standards and sample preparation

Calibration standards were prepared by diluting an NPL-standardized  $^{93}\text{Zr}$  stock solution in 0.3 M  $\text{HNO}_3$  over a concentration range of 53.8 to  $1.1 \times 10^5$  pg/g (equivalent to  $5.0 \times 10^{-3}$  to 10.0 Bq/g). To provide matrix matched calibration standards, the same standards were also prepared in dissolved steel and aqueous decommissioning waste solutions. To determine the separation factor of  $^{93}\text{Zr}$  and  $^{93}\text{Nb}$ , increasing concentrations of  $^{93}\text{Nb}$  were spiked into 0.3 M  $\text{HNO}_3$  and steel solutions which contained the same concentration of  $^{93}\text{Zr}$ .

### Instrumentation

An Agilent 8800 Triple Quadrupole ICP-MS (ICP-QQQ) was used for all work on active samples containing  $^{93}\text{Zr}$ . The sample introduction system consisted of a quartz torch with 2.5 mm i.d. injector, a quartz spray chamber, glass concentric nebulizer, and nickel-tipped interface cones.

To separate  $^{93}\text{Zr}$  and  $^{93}\text{Nb}$  using ICP-QQQ, both  $\text{O}_2$  and  $\text{NH}_3$  cell gases were investigated. Helium was added as a buffer gas and  $\text{H}_2$  was also added to the cell to see if it enhanced product ion formation.

Instrument operating conditions were established using stable isotope standards. A 10 ng/g mixed stable element standard containing  $^{90}\text{Zr}$  and  $^{93}\text{Nb}$  was analyzed and product ion scans were obtained for each precursor ion mass. Q1 was first set to  $m/z$  90 (for Zr) and then  $m/z$  93 (for Nb), while Q2 was scanned to identify the most abundant product ions formed from reactions of  $^{90}\text{Zr}$  and  $^{93}\text{Nb}$  with each cell gas. The optimal cell gas for interference removal was found to be  $\text{NH}_3$  with He and  $\text{H}_2$ . The instrument conditions were then optimized for sensitivity, focusing on cell gas flow rate, octopole bias, and energy discrimination. The operating conditions (Table 1) were validated using active samples.

**Table 1.** 8800 ICP-QQQ operating conditions.

Parameter	Setting	
	Stainless Steel	Aqueous Waste Samples
Scan Mode	MS/MS (Q1=93, Q2=195)	
Plasma Conditions	HMI	General Purpose
Integration Time (s)	0.1	
Carrier Gas (L/min)	0.60	0.95
Dilution Gas (L/min)	0.35	0.00
Helium Flow Rate (mL/min)	2.0	
Hydrogen Flow Rate (mL/min)	3.0	
Ammonia Flow Rate (% of maximum flow rate)	15 (1.5 mL/min)	
Octopole Bias (V)	-2.8	
Energy Discrimination (V)	-9.0	
Octopole RF (V)	180	

## Results and discussion

### Calibration

The zirconium-93 calibration standards were analyzed using the 8800 ICP-QQQ using the General Purpose parameters in Table 1. The detection limit was calculated as 6.5 pg/g (0.6 mBq/g).

### Instrument sensitivity and interference removal

During method optimization using a 10 ng/g mixed stable element standard, different product ions were monitored to assess interference removal efficiency. The product ion scans identified multiple product ions using both O<sub>2</sub> and NH<sub>3</sub> as reaction gases. A Zr/Nb separation factor of > 5 × 10<sup>3</sup> was achieved using Zr-NH<sub>3</sub> product ions: Zr(NH<sub>3</sub>)<sub>2</sub>NH<sub>2</sub><sup>+</sup> (mass-shift of 50) and Zr(NH<sub>3</sub>)<sub>5</sub><sup>+</sup> (mass-shift of 85), and Zr-O<sub>2</sub> product ions: ZrO<sub>3</sub><sup>+</sup> (mass-shift of 48), and Zr(OH)<sub>3</sub><sup>+</sup> (mass-shift of 51). However, the optimal Zr/Nb separation was achieved with a mass shift of 102, measuring the product ion Zr(NH<sub>3</sub>)<sub>6</sub><sup>+</sup>. This finding agrees with a previous study that first demonstrated measurement of <sup>93</sup>Zr by ICP-QQQ (6).

Figure 1 shows that, if <sup>93</sup>Zr was measured on mass, Nb concentrations of 10 pg/g and above would contribute to the signal at *m/z* 93, leading to interference on <sup>93</sup>Zr (blue bars). By comparison, when mass 195 (<sup>93</sup>Zr(NH<sub>3</sub>)<sub>6</sub>) was monitored in MS/MS mass-shift mode, the background counts from Nb remained below 10 cps at concentrations up to 5 × 10<sup>4</sup> pg/g Nb (white bars). The results show the successful removal of the <sup>93</sup>Nb isobaric interference on <sup>93</sup>Zr up to 5 × 10<sup>4</sup> pg/g Nb, using the MS/MS mass-shift method.

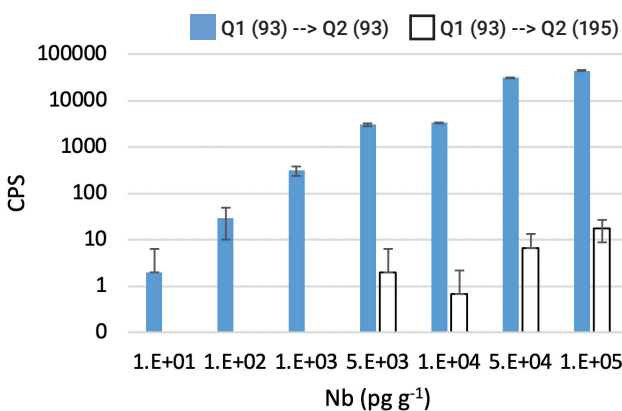


**Figure 1.** Background at *m/z* = 93 and 195 with increasing Nb concentration (Q1 set to *m/z* = 93 in both cases).

### Measurement of decommissioning samples

#### Spiked stainless steel

Inactive stainless steel dissolved in concentrated nitric acid was provided as part of a European Metrology Research Program (EMRP) project. Samples were evaporated to near-dryness and made up in an equal volume of 0.3 M HNO<sub>3</sub>. A further 1 in 10 dilution was made, giving approximately 20x total dilution (5% total dissolved solids, TDS). A semiquantitative scan of the sample was performed using the 8800 ICP-QQQ to determine the sample composition. The most abundant elements detected in the diluted solution were Fe (out of range), Cr (2 µg/g), Mg (20 µg/g), Ni (2.5 µg/g), Cu (10 µg/g), Mo and Sn (both 1 µg/g). The Nb concentration in the diluted steel samples ranged from 0.5 to 1.4 ×

10<sup>4</sup> pg/g. The steel samples were run using the optimized operating conditions for the measurement of <sup>93</sup>Zr (Table 1). No background was measured at *m/z*=195, which also demonstrates removal of any potential polyatomic ion interferences on <sup>93</sup>Zr from <sup>92</sup>Mo<sup>1</sup>H<sup>+</sup> and <sup>92</sup>Zr<sup>1</sup>H<sup>+</sup>.

The spiked steel samples (spiked with <sup>93</sup>Zr and <sup>93</sup>Nb) were initially run on the 8800 without dilution, using <sup>101</sup>Ru as an internal standard. However, even using the High Matrix Introduction (HMI) system with aerosol dilution on the 8800, the 5% steel matrix caused significant matrix deposition on the cones after running four to five samples. The nominal TDS limit for HMI is 3%. The matrix tolerance could potentially be improved with the UHMI available on the 8900 ICP-QQQ, which allows matrix levels up to 25% TDS to be analyzed.

Following a 1 in 10 dilution, the instrument sensitivity for the spiked steel was similar to the <sup>93</sup>Zr calibration standards. Figure 2 shows the calibration curve of <sup>93</sup>Zr in the dissolved stainless steel matrix, measured as Zr(NH<sub>3</sub>)<sub>6</sub><sup>+</sup>. The method detection limit (MDL) was 8.6 pg/g (0.8 mBq/g), which is significantly lower than the exemption limit of 10 Bq/g defined by IAEA/RS-G 1.7 (4).

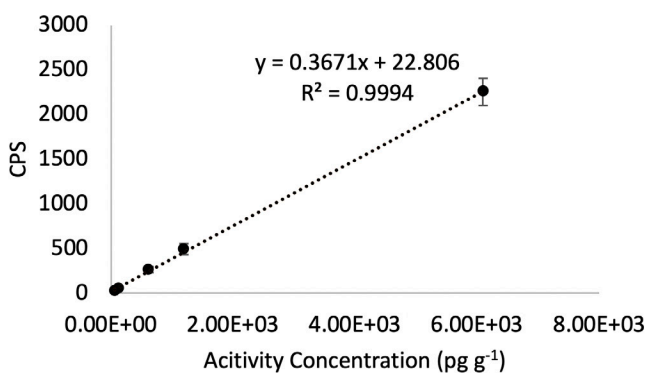


Figure 2. Dissolved stainless steel spiked with <sup>93</sup>Zr, measured as Zr(NH<sub>3</sub>)<sub>6</sub><sup>+</sup> using ICP-QQQ.

### Aqueous waste samples

Aqueous wastes containing a range of decommissioning radionuclides were measured without any sample treatment using the 8800 ICP-QQQ. General Purpose plasma conditions were used rather than HMI mode. The maximum Nb concentration was 1 × 10<sup>4</sup> pg/g, with a background of <20 cps at *m/z*=195, compared to ~40,000 cps when measured on mass at *m/z*=93 in He mode. The average ICP-MS/MS reaction cell interference removal factor (equivalent to the decontamination factor quoted for radiochemical separation experiments) was 3.5 × 10<sup>3</sup>, with an MDL of 1.1 pg/g (0.1 mBq/g). This DL is significantly below the IAEA out-of-scope limit, and the World Health Organisation (WHO) drinking water regulation limit of 0.1 Bq/mL (4, 7). The results show that this ICP-QQQ method is suitable for the direct measurement of <sup>93</sup>Zr in drinking water samples.

### Comparing the 8900 and 8800 ICP-QQQ

At NPL we also have access to a newer Agilent 8900 ICP-QQQ, but this instrument is in a laboratory that does not handle radioactive samples. To evaluate the relative performance of the 8800 and 8900, we used a stable, natural Zr standard to run a comparative test between the two instruments. For this comparison, the <sup>90</sup>Zr(NH<sub>3</sub>)<sub>6</sub><sup>+</sup> product ion was used as an analog of the target <sup>93</sup>Zr(NH<sub>3</sub>)<sub>6</sub><sup>+</sup> product ion. The 8900 was operated using the same General Purpose instrument operating conditions shown in Table 1.

The product ion scans obtained by the 8900 ICP-QQQ using the 10 ng/g mixed stable element standard agreed with the 8800 ICP-QQQ scan results. Both instruments identified  $\text{Zr}(\text{NH}_3)_6^+$  at  $m/z$  192 as the most intense  $^{90}\text{Zr}$  product ion, using a mass shift of 102. As shown in Table 2, measuring Zr as  $\text{Zr}(\text{NH}_3)_6^+$  offered the most efficient Nb interference removal method. The results also show that a maximum separation factor of >10,000 was achieved with the 8900 compared to 6,200 on the 8800. The 8900 also detected intense  $^{90}\text{Zr}$  product ions not detected on the 8800, most notably at  $m/z$  206 ( $^{90}\text{ZrN}(\text{NH}_3)_6$ ) and 207 ( $^{90}\text{ZrNH}(\text{NH}_3)_6$ ) (Table 2).

**Table 2.** Zr/Nb separation factors for 8800 and 8900 ICP-QQQ. Based on product ion scans of  $^{90}\text{Zr}$  and  $^{93}\text{Nb}$  in a 10 ng/g mixed stable element standard. Zr-90 counts were scaled to 100% abundance for this calculation.

Q1/Q2 ( $m/z$ )	90/155	90/159	90/175	90/176	90/177	90/192	90/206	90/207
Mass-shift	65	69	85	86	87	102	116	117
Zr/Nb Separation Factor (8800)	<1	<1	<1	1	4	6,200	<1	<1
Zr/Nb Separation Factor (8900)	2,300	470	715	155	400	10,200	2,800	4,300

The 8900 offers higher sensitivity and lower backgrounds compared to the 8800, as verified by the data presented in Table 3. The stable element calibration standards were measured by both instruments. The counts per second (cps) for the  $^{90}\text{Zr}(\text{NH}_3)_6$  product ion at  $m/z$  192 obtained by the 8900 were significantly higher than the 8800 (Table 3). The sensitivity improvement of the 8900 is due to more efficient ion transmission in the interface vacuum stage. Also, axial acceleration (0.5 V in this study) improves reaction product ion energy, overcoming collisional attenuation and space-charge effects.

**Table 3.** Difference in instrument sensitivity and instrument detection limit (IDL) for stable Zr standards.

Parameter	8800 ICP-QQQ		8900 ICP-QQQ	
	90/90	90/192	90/90	90/192
$^{90}\text{Zr}$ sensitivity (cps, 10 ng/g)	1,800	2,000	53,000	166,000
*IDL (pg/g)	6.5		0.1	
*IDL (mBq/g)	0.6		$8.8 \times 10^{-3}$	

\*IDLs were calculated from the 90/192 data.

## Conclusion

ICP-QQQ has been successfully used for the direct and accurate measurement of the long-lived radionuclide  $^{93}\text{Zr}$  in decommissioning samples below IAEA out-of-scope limits. Since ICP-QQQ with MS/MS uses reaction chemistry in the CRC to separate analytes and interferences, there was no need for a separation-step before measurement, simplifying and speeding up the analysis.

Both active and stable element standards containing Nb and Zr were used during method development. The study shows the Agilent 8800 ICP-QQQ with MS/MS can eliminate isobaric overlaps from  $^{93}\text{Nb}$  on  $^{93}\text{Zr}$  using  $\text{NH}_3/\text{H}_2$  as the reaction gas. Nb doesn't react with  $\text{NH}_3/\text{H}_2$  in the CRC, so Nb remains at  $m/z$  93, allowing  $^{93}\text{Zr}$  to be measured as  $^{93}\text{Zr}(\text{NH}_3)_6^+$  at  $m/z = 195$ , free from interference.

The integrated HMI aerosol dilution technology extends the matrix tolerance of Agilent ICP-QQQ for the analysis of high matrix samples. The 8800 was used to analyze  $^{93}\text{Zr}$  in dissolved steel (using HMI) and aqueous waste samples.



An MDL of less than 1 mBq/g was achieved in both matrices, which is several orders of magnitude lower than regulatory limits for decommissioning wastes and drinking water. The study showed that the newer Agilent 8900 ICP-QQQ offers higher sensitivity and lower backgrounds compared to the 8800.

Compared to decay counting techniques, ICP-QQQ reduces the preparation time of samples dramatically, with sample-throughput further improved by the short measurement times of the technique. The ICP-QQQ method will be beneficial to analysts working in nuclear decommissioning and environmental monitoring labs.

## References

1. Decay Data Evaluation Project, accessed September 2019, [http://www.nucleide.org/DDEP\\_WG/Nuclides/Zr-93\\_tables.pdf](http://www.nucleide.org/DDEP_WG/Nuclides/Zr-93_tables.pdf)
2. P. Cassette, F. Chartier, H. Isnard, C. Fréchet, I. Laszak, J. P. Degros, M. M. Bé, M. C. Lépy, I. Tartes, Determination of  $^{93}\text{Zr}$  decay scheme and half-life. *Applied Radiation and Isotopes*, 2010, 68 (1), 122–130
3. F. Chartier, H. Isnard, J. P. Degros, A. L. Faure, C. Fréchet, Application of the isotope dilution technique for  $^{93}\text{Zr}$  determination in an irradiated cladding material by multiple collector-inductively coupled plasma mass spectrometry. *Int. J. of Mass Spectrom.*, 2008, 270 (3), 127–133
4. IAEA Safety Standards Series Safety Guide No. RS-G 1.7 Application of the concepts of exclusion, exemption and clearance, accessed September 2019, [http://www-pub.iaea.org/MTCD/publications/PDF/Pub1202\\_web.pdf](http://www-pub.iaea.org/MTCD/publications/PDF/Pub1202_web.pdf)
5. Fourth Edition of Handbook of ICP-QQQ Applications using the Agilent 8800 and 8900, Agilent publication, [5991-2802EN](#)
6. P. Petrov, B. Russell, D. N. Douglas, H. Goenaga-Infante, Interference-free determination of sub ng kg<sup>-1</sup> levels of long-lived  $^{93}\text{Zr}$  in the presence of high concentrations ( $\mu\text{g kg}^{-1}$ ) of  $^{93}\text{Mo}$  and  $^{93}\text{Nb}$  using ICP-MS/MS. *Anal. Bioanal. Chem*, 2018, Volume 410 (3), 1029–1037
7. World Health Organisation Guidelines for Drinking Water Quality Fourth Edition, accessed September 2019, <https://apps.who.int/iris/bitstream/handle/10665/254637/9789241549950-eng.pdf%3bjsessionid=92EE6E44405FC8DBD781EA0B1C957B18?sequence=1>

## Clinical research

Title	Page
Manganese analysis in whole blood: expanding the analytical capabilities of ICP-MS	411
Measurement of titanium to assess joint replacements	415
Measurement of selenium in the presence of Gd-based MRI contrasting agents	418
Evaluation of the elemental content of a single cell using fast time-resolved analysis (TRA) ICP-MS	421

# Manganese Analysis in Whole Blood: Expanding the Analytical Capabilities of ICP-MS

## Author

Amir Liba  
Agilent Technologies, USA

## Keywords

manganese, whole blood, iron,  
abundance sensitivity, helium MS/MS

## Introduction

Analysis of clinical research samples is challenging due to their complex matrices. While ICP-MS is an immensely powerful multi-element analytical technique, it does suffer from some well-documented spectral interferences. Achieving low detection limits is limited by background signal from low level impurities and the presence of polyatomic interferences, which require the use of CRC technology for their removal. Although the use of CRC-ICP-MS has alleviated many of these analytical challenges, some spectral interferences remain problematic for quadrupole ICP-MS (ICP-QMS). One such interference is the signal overlap on  $^{55}\text{Mn}$  due to peak tailing from both  $^{54}\text{Fe}$  and  $^{56}\text{Fe}$ . Whole blood contains an average of 500 ppm of Fe, and with the level of Mn in whole blood being roughly 10 ppb, analytical results for Mn tend to bias high due to the significant signal tailing and overlap from the adjacent Fe peaks. In this work, we use the superior abundance sensitivity of the 8800 ICP-QQQ to remove any signal overlap from Fe, allowing accurate determination of Mn in whole blood.

## Experimental

**Instrumentation:** Agilent 8800 #100.

**Plasma conditions and ion lens tune:** Preset plasma/General purpose with soft extraction tune: Extract 1 = 0 V.

**Method:** Samples were analyzed using the 8800 ICP-QQQ in both Single Quad (SQ) mode and MS/MS mode. In this study, the mass range of interest (from  $m/z$  50 to 60) was scanned at twenty points per peak in both no gas and helium (He) modes. For the measurement of Mn in blood, MS/MS mode with on-mass measurement (Q2 set to the same mass as Q1) was used, with helium cell gas (typical flow of 4.3 mL/min) to remove polyatomic ion interferences such as  $\text{FeH}^+$  and  $\text{ArOH}^+$ .

**Sample preparation:** A 5 ppb solution of Mn was prepared from a stock of 1000 ppm Mn and either analyzed separately or spiked into "base" whole blood (low level Mn). Whole blood was diluted using an alkali matrix containing ammonium hydroxide, EDTA, Triton X-100, and butanol.

### Abundance sensitivity

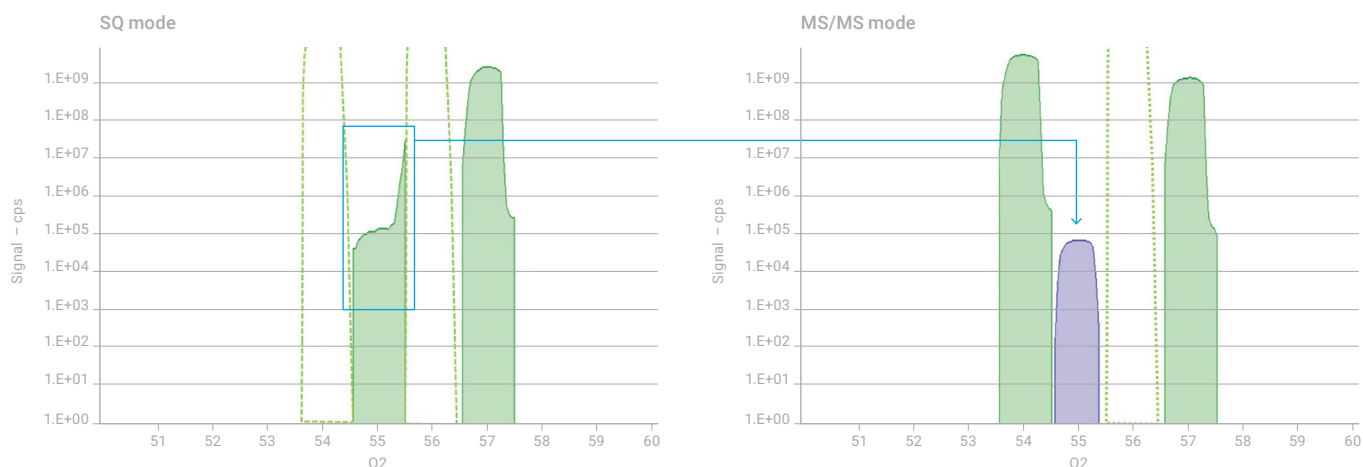
The abundance sensitivity (AS) of a mass spectrometer is the contribution that the signal at mass  $M$  makes to the signals at the adjacent masses ( $M\pm 1$ ), expressed as a ratio ( $M-1/M$  on the low-mass side and  $M+1/M$  on the high-mass side). Simply put, AS is the measure of the "peak tailing" to adjacent masses, which will contribute to a false positive signal, such as that seen on  $^{55}\text{Mn}$  (present at trace levels) from the large contribution from  $^{54}\text{Fe}$  and  $^{56}\text{Fe}$  (which exists at very high concentration) in whole blood. The abundance sensitivity of the best quadrupole ICP-MS systems is of the order of  $10^{-7}$ .

## Results and discussion

### Abundance sensitivity study in SQ and MS/MS mode

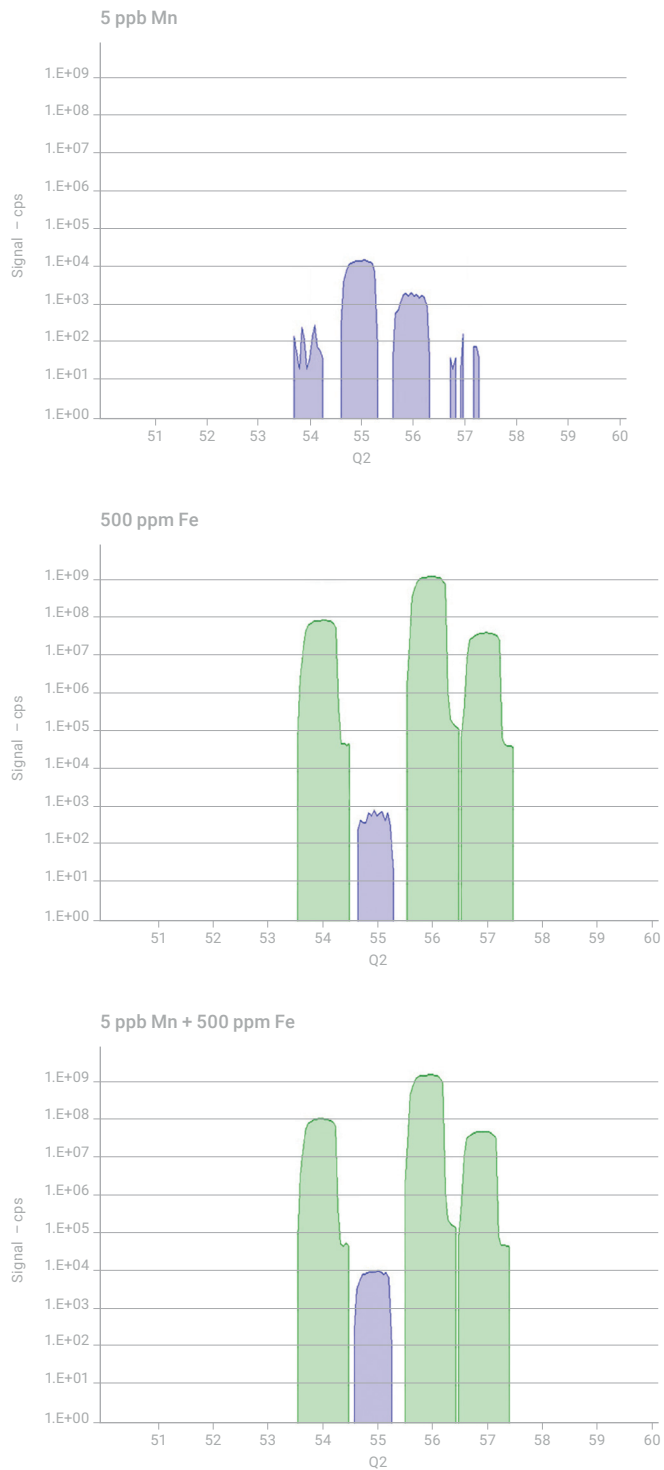
SQ and MS/MS spectra for a 500 ppm Fe solution acquired in no gas mode are shown in Figure 1. The spectrum on the right illustrates the improvement in peak-to-peak resolution of the 8800 ICP-QQQ operated in MS/MS mode. Although no interference removal for polyatomic ions was employed, the elimination of the contribution to mass 55 from adjacent peaks is clearly evident in MS/MS mode. The “flat-top” peak shapes are the result of the logarithmic scale.

Abundance sensitivity plays an important role when samples contain a large concentration of Fe. Figure 1 looks at the contribution of “peak tailing” on  $^{55}\text{Mn}$  due to high levels of Fe. The high concentration of Fe together with the  $\text{ArN}^+$  and  $\text{ArO}^+$  contribution in no gas mode resulted in the signals at 54 and 56 being over the range of the detector, and so they were automatically skipped. However, the signal contribution from  $^{56}\text{Fe}$  on mass 55 is clearly visible in the SQ mode (indicated by the blue box) while it is absent in the MS/MS mode.



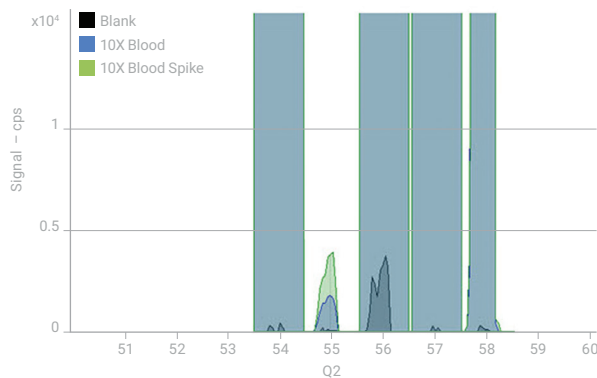
**Figure 1.** Comparison of no gas mode spectra for 500 ppm Fe solution, measured in SQ mode (left) and MS/MS mode (right). The signal colored blue was obtained in pulse counting while the green signal was obtained in analog mode. The dotted lines indicate over-range peaks (automatically skipped to protect the EM detector).

Figure 2 shows three spectra obtained in MS/MS mode with He cell gas. When He cell mode is used for interference removal, precise and accurate analysis is easily achieved. In He MS/MS mode, all interferences (arising from signal overlap from tailing of adjacent peaks and polyatomic ions isobaric interferences) are removed, yielding unbiased analysis and accurate results.



**Figure 2.** He MS/MS mode spectra: (top to bottom) 5 ppb Mn, 500 ppm Fe, and 5 ppb Mn + 500 ppm Fe

Figure 3 is an overlay of three spectra measured using He MS/MS mode; 1) Blank, 2) 10x whole blood, and 3) 500 ppt Mn spike in 10x whole blood. Table 1 summarizes the results of 10x diluted whole blood analysis and 500 ppt Mn spike recovery test. As shown, very low blank levels were achieved, <sup>55</sup>Mn was clearly resolved in the spectrum and good spike recoveries were obtained.



**Figure 3.** Spectra of three samples: blank, 10x diluted blood and 10x diluted blood spiked with 500 ppt Mn

**Table 1.** 10x diluted whole blood analysis results for Mn

	Blood sample	Blood sample + 500 ppt Mn	Spike recovery
	µg/L		%
Sample A	0.413	0.983	114
Sample B	0.432	0.924	98

## Conclusion

Quadrupole ICP-MS has been almost universally accepted for low level analysis of trace analytes in complex matrices. However, many challenging interferences remain unresolved, especially when trace analytes must be measured close to matrix element peaks in complex samples. The Agilent 8800 ICP-QQQ with MS/MS capability has abundance sensitivity better than  $10^{-10}$ , which enables the analysis of trace analytes (such as Mn) in the presence of a high concentration of adjacent elements (such as Fe).

For Research Use Only. Not for use in diagnostic procedures.

# Measurement of Titanium to Assess Joint Replacements

## Author

Glenn Woods  
Agilent Technologies (UK) Ltd.

## Keywords

titanium, biological, serum, urine,  
joint-replacement, Seronorm, ammonia  
mass-shift

## Introduction

Although titanium (Ti) has little or no direct biological role, it is widely used in dental, artificial/replacement joints, and surgical reconstruction applications. Its benefits include high strength, light weight, and the fact it is biocompatible. It is also used extensively as a pigment and abrasive polishing agent (as  $TiO_2$ ) and is used as an additive in foods and toothpaste due to its inertness and high opacity.

Metal-on-metal (rather than ceramic or polymer based) joint replacements can lead to the release of metal particles or ions. These can pass into the bloodstream and be excreted through urine. A raised concentration of Ti might therefore be a sign of degradation in Ti-based joint. It would be useful to develop a method that is able to determine the concentration of Ti at normal levels in biological fluids. This would allow identification of the basal or reference concentration, above which a raised level could be flagged for investigation.

## Experimental

The determination of Ti at ultratrace levels is challenging for conventional ICP-MS, due to the spectral interferences from sulfur (as SO), phosphorus (as PO), and calcium, which affect all the Ti isotopes. It is possible to use  $NH_3$  reaction cell gas to create a higher mass  $Ti^+$  product ion, separating the Ti from the interfering species. However, the use of highly reactive cell gases in single quadrupole ICP-MS (ICP-QMS) is prone to severe errors, as there is no way to control the ions that enter the CRC. This means that the reaction chemistry and the product ions created can change dramatically, with even slight differences in sample matrix or co-existing analyte concentrations. For this application, the 8800 ICP-QQQ was used to provide controlled reaction chemistry with ammonia as the reaction gas and measuring Ti as the  $TiNH_2(NH_3)_4^+$  cluster ion at the  $M + 84$  u transition.

**Instrumentation:** Agilent 8800 #100.

**Plasma conditions:** Preset plasma/General purpose.

**Ion lens tune:** Soft extraction tune: Extract 1 = 0 V, Extract 2 = -170 V.

**CRC conditions:**  $NH_3$  gas (10% in He) at 1.7 mL/min, Octopole bias = -8 V, KED = -8 V.

**Samples and sample preparation:** Certified reference materials of serum and urine were purchased from Seronorm (Norway). They were prepared in duplicate by 10x dilution into a basic diluent consisting of  $NH_4OH$  (0.5%),  $H_4$ -EDTA (0.01%), BuOH (2%) and Triton X-100 (0.01%) in ultrapure water. The same diluent was used to prepare the calibration standards, with no further matrix matching.

## Results and discussion

### Selection of product ion for Ti measurement

In order to select the most appropriate Ti cluster ions in  $\text{NH}_3$  mode, a product ion scan was performed for the  $^{48}\text{Ti}$  isotope by introducing a 10 ppb Ti solution (Figure 1). Q1 was set to  $m/z$  48, allowing only ions at the mass of the target precursor ion to enter the cell; Q2 was scanned over a selected mass range to measure all the product ions formed in the cell by  $\text{NH}_3$  reactions with  $^{48}\text{Ti}$ . Based upon this scan, the two most abundant cluster ions (Q1 + 84 u [ $\text{TiNH}_2(\text{NH}_3)_{3/4}^+$ ] and Q1 + 102 u [ $\text{Ti}(\text{NH}_3)_6^+$ ]) were selected for further study. For each of the two reaction transitions identified above, neutral gain scans (where Q1 and Q2 are scanned synchronously, with a set mass difference between them (Q2 = Q1 + 84 and Q2 = Q1 + 102 in this case)) were performed. These scans are shown in Figure 2 confirming the correct natural isotopic abundances for the different Ti isotopes. Without MS/MS capability, it would be impossible to preserve the isotopic information for this element due to inter-isotope overlaps from the Ti-ammonia adducts. The instrument cell conditions were optimized using simple  $\text{HNO}_3$  acidified Ti standards and applied to the analysis of the CRMs.

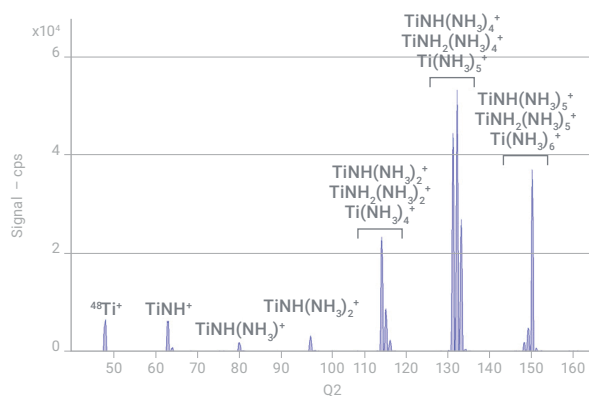


Figure 1. Product ion scan for  $^{48}\text{Ti}^+$  in  $\text{NH}_3$  mode

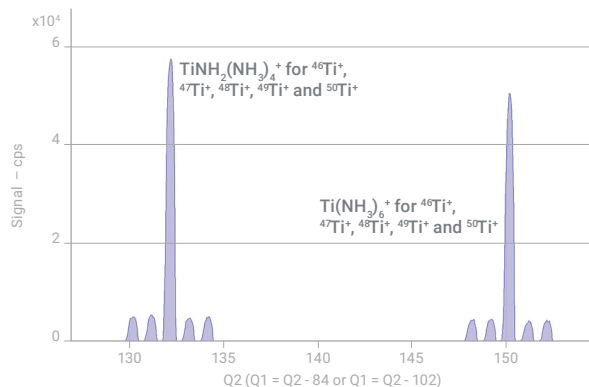


Figure 2. Neutral gain scan for two  $\text{Ti} \rightarrow \text{Ti}$  cluster ion transitions: For  $\text{TiNH}_2(\text{NH}_3)_{3/4}^+$  cluster ions, Q2 = Q1 + 84 u, and for  $\text{Ti}(\text{NH}_3)_6^+$  cluster ions, Q2 = Q1 + 102 u. The preservation of the natural Ti isotope abundance pattern ( $^{46}\text{Ti}^+$ ,  $^{47}\text{Ti}^+$ ,  $^{48}\text{Ti}^+$ ,  $^{49}\text{Ti}^+$  and  $^{50}\text{Ti}^+$ ) can be seen, confirming that MS/MS mode provides complete control over the complex Ti- $\text{NH}_3$  reaction chemistry.



Table 1 displays the results for the serum and urine CRMs measured against a the same calibration. In addition to the NH<sub>3</sub> cell gas mode, the 8800 ICP-QQQ was operated in no gas and He mode to provide comparative data. Three Ti isotopes were monitored for the same cluster ion transition, to give confirmation of the results.

**Table 1.** Urine and serum sample recovery (µg/L) for Ti in Seronorm CRM using TiNH<sub>2</sub>(NH<sub>3</sub>)<sub>4</sub><sup>+</sup> cluster

Sample Name	Target	<sup>47</sup> Ti [No gas]	<sup>47</sup> Ti [He]	47 -> 131 Ti [NH <sub>3</sub> ]	48 -> 132 Ti [NH <sub>3</sub> ]	49 -> 133 Ti [NH <sub>3</sub> ]
Urine blank	4.6 (2.2-7.0)	1989.79	41.44	2.80	2.79	2.92
Urine blank	4.6 (2.2-7.0)	2004.91	44.30	3.50	2.93	3.33
Urine trace elements		1789.92	51.41	14.81	15.27	14.42
Urine trace elements		1749.13	52.58	14.99	15.49	15.50
Serum L1	1.28 (0.86-1.80)	144.18	3.79	1.21	1.15	1.14
Serum L1	1.28 (0.86-1.80)	128.97	2.95	1.27	1.18	1.09
Serum L2		100.16	3.95	1.76	1.92	1.61
Serum L2		95.65	3.02	1.82	1.64	1.76

## Conclusion

Titanium was only certified in two of the four materials measured but the 8800 ICP-QQQ data were all comfortably within the measured ranges when operating under ammonia MS/MS mode, in contrast to no gas and He mode data. Importantly, the three Ti isotopes measured under ammonia MS/MS mode all gave equivalent data; this could indicate applicability of the method to the use of isotope-based analysis such as isotope dilution (ID) or isotope tracer analysis. The use of ammonia combined with MS/MS greatly simplifies the analysis of Ti in biological media for several isotopes. Furthermore, because MS/MS mode provides control over the reaction chemistry, no special attention needs to be paid to specific matrix matching regardless of the fluid investigated.

For Research Use Only. Not for use in diagnostic procedures.

# Measurement of Selenium in the Presence of Gadolinium-Based Magnetic Resonance Imaging Contrasting Agents

## Author

Glenn Woods  
Agilent Technologies (UK) Ltd.

## Keywords

selenium, MRI contrasting agents,  
gadolinium, molybdenum, zirconium,  
neutral gain scan, oxygen mass-shift

## Introduction

Selenium is an important micronutrient and is contained within several co-factors and enzyme systems.

Magnetic Resonance Imaging (MRI) is a commonly used radiology imaging technique. However, for some soft tissues, a “contrasting agent” is needed to improve the image quality to enable tissue differentiation. There are several contrasting agents which are salts or chelates of gadolinium (III) (Gd(III)), trade names are given in brackets:

Gadodiamide (Omniscan), Gadobenate (MultiHance), Gadopentetate (Magnevist), Gadoteridol (ProHance), Gadofosveset (Ablavar, formerly Vasovist), Gadoversetamide (OptiMARK), Gadoxetate (Eovist), Gadobutrol (Gadavist)

Unfortunately for analysis of samples by ICP-MS, Gd has a relatively low second ionization potential (12.09 eV) meaning it can form doubly-charged (Gd<sup>2+</sup>) ions in the plasma. These Gd<sup>2+</sup> ions appear at half their true mass, as a quadrupole separates ions based on their mass to charge ratio or  $m/z$ . This means that the Gd<sup>2+</sup> ions appear between  $m/z$  76 and 80 where they form interferences on all of the main analytical isotopes of Se. This is complicated to a greater extent as Gd has several odd-mass isotopes which form Gd<sup>2+</sup> interferences at half-mass values (e.g., <sup>155</sup>Gd<sup>2+</sup> would appear at  $m/z$  77.5). This makes the spectrum in the mass region of the Se isotopes quite complex when Gd is present in the sample. In a typical post-MRI sample, the Gd concentration can vary between zero to several thousand parts per billion (µg/L). Because of the variability in Gd level from sample to sample a simple mathematical correction cannot always be made or a constant “background” be assumed.

## Experimental

In order to avoid the Gd<sup>2+</sup> interference, Se<sup>+</sup> can be reacted with oxygen cell gas in the collision/reaction cell to produce SeO<sup>+</sup> product ions. The Se-O reaction is slightly endothermic ( $\Delta H_r = 0.71$  eV) which means that the reaction yield for SeO<sup>+</sup> would be relatively low. However, the bias voltage on the ORS can be adjusted to increase the ion energy, which improves the reaction yield significantly over a more “thermalized” approach. These conditions are referred to as high ORS bias conditions.

**Instrumentation:** Agilent 8800 #100.

**Plasma conditions:** Preset plasma/General purpose.

**Ion lens tune:** Soft extraction tune: Extract 1 = 0 V, Extract 2 = -170 V.

**CRC conditions:** O<sub>2</sub> gas at 0.3 mL/min, Octopole bias = -15 V, KED = -8 V.

## Results and discussion

### O<sub>2</sub> mass-shift method

Using O<sub>2</sub> mass-shift, the analyte is measured at M +16 u (e.g. <sup>78</sup>Se<sup>+</sup> is measured as <sup>78</sup>Se<sup>16</sup>O<sup>+</sup> at 94 u). With conventional quadrupole ICP-MS, any <sup>94</sup>Mo or <sup>94</sup>Zr present in the sample would interfere with the measurement at this mass. However, with ICP-QQQ in MS/MS mode, <sup>94</sup>Mo and <sup>94</sup>Zr are removed by Q1 as it is set to the mass of the Se<sup>+</sup> precursor ion at 78 u. The <sup>156</sup>Gd<sup>++</sup> remains at m/z 78 and so is eliminated by Q2, which is set to the SeO<sup>+</sup> product ion mass of 94 u. Even if Gd did form GdO<sup>++</sup> this would also be eliminated by Q2 as the apparent mass (m/z) of <sup>156</sup>Gd<sup>16</sup>O<sup>++</sup> is 172/2 (86 u). Figure 1 is a graphical representation of the MS/MS method.

To check for efficient conversion of Se<sup>+</sup> to SeO<sup>+</sup>, a neutral gain scan covering the mass range of all the SeO<sup>+</sup> product ions was performed for a 5 ppb Se solution. Figure 2 displays the isotope pattern of the +<sup>16</sup>O-atom transitions for all the Se isotopes, showing a perfect match with the theoretical isotopic abundances.

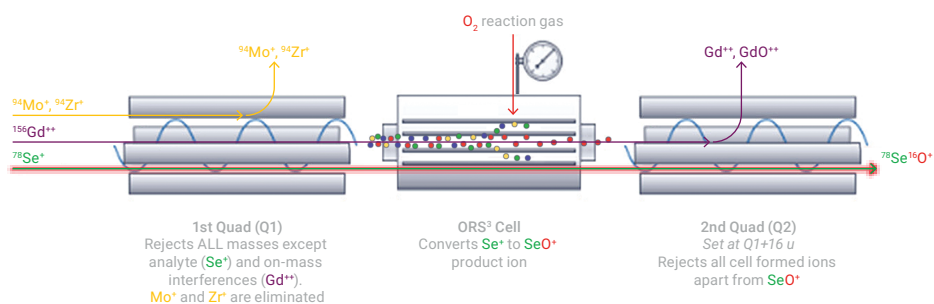


**Figure 1.** Representation of ICP-QQQ setup with Q1 set to 78 u and Q2 set to 94 u. Mo and Zr-based interferences are eliminated by Q1 and Gd<sup>++</sup> is eliminated by Q2 allowing the measurement of <sup>78</sup>Se as <sup>78</sup>Se<sup>16</sup>O<sup>+</sup>.

### Se measurement

Instrument cell conditions were optimized using a Se standard in a simple HNO<sub>3</sub> matrix. A serum matrix was prepared by 10x dilution into a basic diluent consisting of NH<sub>4</sub>OH (0.5%), H<sub>4</sub>-EDTA (0.01%), BuOH (2%) and Triton X-100 (0.01%) in ultrapure water. The sample was prepared unspiked and spiked with Gd equivalent to 250, 500 and 1000 µg/L in the original sample, and analyzed using the 8800 ICP-QQQ in no gas and O<sub>2</sub> mass-shift modes for comparison. The data is summarized in Table 1. The results show that, under no gas conditions, the apparent Se concentration is influenced by the variable Gd<sup>++</sup> interference. Recovery based upon the original unspiked sample demonstrates an over-recovery of almost 130% for the no gas data when Gd is at a concentration of 1000 µg/L. In contrast, the Se data measured with MS/MS mass-shift mode remains very consistent at all levels of Gd matrix. This shows that the O<sub>2</sub> mass-shift reaction allows accurate analysis of Se independent of the Gd concentration, indicating that the ICP-MS/MS approach is highly applicable to this relatively difficult measurement.

**Table 1.** Serum sample data and recovery for Se with variable Gd concentration. Recovery is calculated based on determined Se concentration in unspiked serum sample. All data is dilution corrected.

	No gas mode		O <sub>2</sub> mass-shift	
	Conc. ppb	Recovery %	Conc. ppb	Recovery %
Serum	93.64	NA	91.42	NA
Serum with 250 µg/L Gd	99.97	106.7	91.38	100.0
Serum with 500 µg/L Gd	112.1	120.0	91.70	100.3
Serum with 1000 µg/L Gd	121.1	129.3	91.78	100.4

For Research Use Only. Not for use in diagnostic procedures.

# Evaluation of the Elemental Content of a Single Cell using Fast Time-Resolved Analysis (TRA) ICP-MS

## Authors

Yu-ki Tanaka<sup>1</sup>, Yasumitsu Ogra<sup>1</sup>,  
Tetsuo Kubota<sup>2</sup>

<sup>1</sup>Graduate School of Pharmaceutical  
Sciences, Chiba University, Chiba,  
Japan

<sup>2</sup>Agilent Technologies, Inc.

Determination of Mg, P, Fe, and Zn in a single yeast, green alga, and red blood cell by Agilent 8900 ICP-QQQ

## Introduction

Advances in ICP-MS technology mean that elemental signals from single particle-like materials such as nanoparticles and living cells can now be detected, measured, and reported more easily. Known as single particle (SP-) or single-cell (SC-) ICP-MS, these techniques are of interest in a range of industries and fields of study, including semiconductor, environmental, foods, and clinical research. For successful SP/SC-ICP-MS analysis, the ICP-MS must be operated in fast time resolved analysis (TRA) mode. Suspension solutions containing particles or cells are introduced directly into the ICP through a nebulizer where they are decomposed, atomized, and ionized. The ion plume is detected within 1 ms, which is much faster than the signal integration time used in conventional ICP-MS measurements (10–100 ms). To measure the signals from individual single particles or single cells, the fast TRA mode of Agilent single quadrupole ICP-MS or Agilent triple quadrupole ICP-MS (ICP-QQQ) uses an integration time of 0.1 ms.

In this study, a precise quantification method was developed using SC-ICP-MS for the determination of biologically important elements, Mg, P, Fe, and Zn, in a single yeast, green alga, and red blood cell (RBC). To validate the accuracy of the SC-ICP-MS method, which measures intact cells, data was also obtained using a conventional “bulk” ICP-MS analysis method following acid digestion of the cells. The acid digestion step destroys the individual cell structure, so the reported metal concentration results are derived from the mean values measured from thousands of cells. Compared with bulk analysis, SC-ICP-MS requires significantly fewer cells owing to the enhanced signal-to-noise ratio (S/N) of the signal in fast TRA mode. Requiring fewer cells for a successful analysis is a major advantage of the technique, especially in applications such as biological and clinical research where sample volumes may be limited.

When samples with a complex matrix are analyzed by ICP-MS, matrix-based polyatomic interferences are more likely to form that affect the accurate measurement of some analytes. For example, in biological samples, phosphorus (<sup>31</sup>P) can be affected by high background noise at *m/z* 31 arising from interferences such as <sup>12</sup>C<sup>18</sup>OH<sup>+</sup>, <sup>14</sup>N<sup>16</sup>OH<sup>+</sup>, <sup>15</sup>N<sub>2</sub>H<sup>+</sup>, <sup>15</sup>N<sup>16</sup>O<sup>+</sup>, and <sup>13</sup>C<sup>18</sup>O<sup>+</sup>. Also, P has a high first ionization potential (IP) of 10.5 eV. The high IP means that a relatively low number of ions is formed in the argon plasma compared to elements with an IP between ~6 and 8 eV, leading to lower sensitivity.

The Agilent 8900 ICP-QQQ is suitable for SC-ICP-MS studies due to its high sensitivity, low background, and interference removal capabilities. The 8900 is a tandem MS instrument that uses MS/MS mode for reliable reaction chemistry in the collision/reaction cell (CRC) to resolve polyatomic ion interferences on

analytes such as P. Using MS/MS, the instrument can measure analytes 'on-mass' or in 'mass-shift' mode, as explained elsewhere (1, 2). A mass-shift method with O<sub>2</sub> cell gas is often used to measure <sup>31</sup>P via its oxide ion, <sup>31</sup>P<sup>16</sup>O<sup>+</sup>, at *m/z* 47 (3). MS/MS methods provide a reliable and reproducible way to avoid polyatomic ion interferences on analytes of interest.

To simplify SC-ICP-MS analysis using Agilent ICP-MS or ICP-QQQ instrumentation, Agilent has developed the Single Nanoparticle Application Module (p/n G5714A) for Agilent ICP-MS MassHunter instrument control software. The Agilent particle detection technique, which has been patented in the United States, provides clear signal distribution data even in biological samples that have a high ionic background arising from the cell-suspended solution.

In this study, SC-ICP-MS was evaluated as a potential technique for metabolism studies of essential elements in fungus, plant, and animal cells. It is an important area of research, as many elements are essential for cell health, and an imbalance, deficiency, or excess of certain metals may disrupt natural cell processes.

## Experimental

### Cell samples and chemicals

Three kinds of cells of approximately 1 to 5 μm in diameter were investigated, as shown in Figure 1. Commercially available dried yeast (*Saccharomyces cerevisiae*) was bought from Sala Akita Shirakami Corporation (Akita, Japan). Green unicellular alga, *C. reinhardtii* (NIES-3379) was obtained from Microbial Culture Collection at the National Institute for Environmental Studies (Tsukuba, Japan). Red blood cells were collected from 11-week-old male Wistar rats (Japan SLC Inc.). The cell samples were washed and suspended in 0.9% NaCl solution before analysis by SC-ICP-MS.

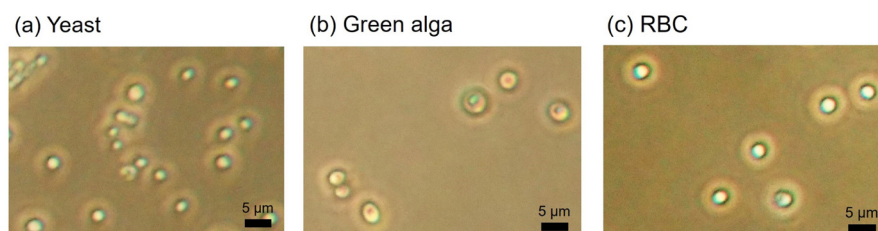


**Figure 1.** Microscopic images of three types of cell suspended in 0.9% NaCl solution.

Ionic standards were prepared by mixing single element standards for Mg, Si, P, Fe, and Zn. Details are given in Table 1. To matrix match the standards and samples, the 0.9% NaCl solution was added to each ionic standard.

**Table 1.** Details of the element standards and calibration range.

Element	Ionic Standard Concentration for SC-ICP-MS (ppb)	Calibration Range for Bulk Concentration Analysis (ppm)	Supplier
Mg	10	0–15	Kanto Chemical
Si	100	-	Kanto Chemical
P	1000	0–20	FUJIFILM Wako Pure Chemical
Fe	10	0–5	Kanto Chemical
Zn	10	0–1	Kanto Chemical

A SiO<sub>2</sub> nanoparticle certified reference material (Merck Sigma Aldrich) with a nominal internal particle diameter of 200 nm was diluted to 2 ppb in ultrapure water. The SiO<sub>2</sub> nanoparticle and ionic Si solutions were used to estimate nebulization efficiency.

### Instrumentation

For the SC-ICP-MS study, single cell samples were introduced into an 8900 ICP-QQQ using an MVX-7100 autosampler (Teledyne Cetac Technologies, Omaha, NE, USA), as shown in Figure 2. The 8900 was fitted with a MicroMist glass nebulizer and a Single-Cell Sample Introduction System (Glass Expansion, Victoria, Australia) total consumption spray chamber.

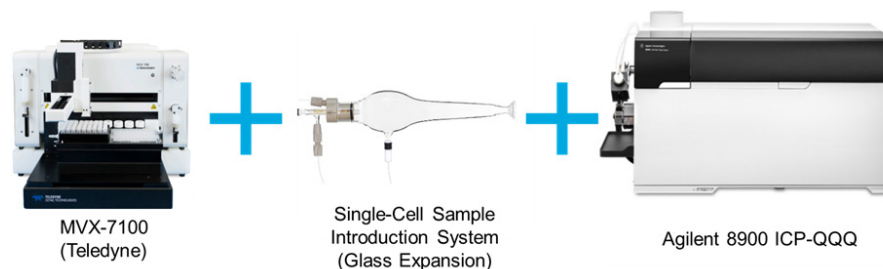


Figure 2. Configuration of SC-ICP-MS system.

For bulk concentration analysis, digested cell samples were introduced into an Agilent 8800 ICP-QQQ equipped with a standard sample introduction system. The method parameter settings of the two ICP-QQQ instruments are shown in Table 2. The same cell gases were used in both methods. Mg and Zn were measured in no gas mode. <sup>31</sup>P was measured as the <sup>31</sup>P<sup>16</sup>O product ion by operating the ICP-QQQ in O<sub>2</sub> mass-shift mode, and Fe and Si were measured on-mass in H<sub>2</sub> mode.

Table 2. ICP-QQQ operating conditions for the SC-ICP-MS and conventional bulk cell ICP-MS methods.

Parameter	Method					
	SC-ICP-MS			Bulk Concentration Analysis by ICP-MS		
ICP-QQQ Instrument Model	8900			8800		
RF Power (W)	1600			1550		
Nebulizer Gas/Make-up Gas (L/min)	0.65/0.20			1.0/0.3		
Cell Gas Mode	No gas	O <sub>2</sub>	H <sub>2</sub>	No gas	O <sub>2</sub>	H <sub>2</sub>
Cell Gas (mL/min)	-	0.38	5.5	-	0.38	5.5
Analytes*	<sup>24</sup> Mg, <sup>66</sup> Zn	<sup>31</sup> P**	<sup>56</sup> Fe, <sup>28</sup> Si	<sup>24</sup> Mg, <sup>66</sup> Zn	<sup>31</sup> P**	<sup>56</sup> Fe
Measurement Mode	Single particle			Full quantitative		
Integration Time (ms)	0.1			100		
Nebulization Efficiency (%)	~55			Not applicable		

\*All elements were measured in MS/MS mode.

\*\*MS/MS mass-shift mode with O<sub>2</sub> cell gas; the quadrupole mass filters, Q1 and Q2, were set to m/z 31 and 47, respectively.

### Sample preparation

The sample preparation procedure is described in detail elsewhere (4). The number of cells for the three cell types were counted using a Bürker-Türk hemocytometer. The measurements were used in the calculations of the bulk concentration analysis section of this note.

### Determination of the elemental content of a single cell

Four essential elements (Mg, P, Fe, and Zn) were measured in a single cell using SC-ICP-MS. The mass of each analyte element ( $m$ ) in a single cell was obtained using the following equation (eq. 1).

$$m = \frac{I_{\text{Cell}}}{(I_{\text{Std}} - I_{\text{Blk}})} \cdot f \cdot C_{\text{Std}} \cdot v$$

$I_{\text{Cell}}$ ,  $I_{\text{Std}}$ , and  $I_{\text{Blk}}$  represent signal intensity of a single cell, ionic standard, and 0.9% NaCl blank solution, respectively.  $f$ ,  $C_{\text{Std}}$ , and  $v$  denote nebulization/transport efficiency of the sample aerosol, concentration of ionic standard solution, and sample flow rate (0.015 mL/min), respectively.

Nebulization/transport efficiency ( $f$ ) was calculated from the signal intensities of  $^{28}\text{Si}$  measured in both an ionic Si solution and  $\text{SiO}_2$  nanoparticle suspension solution using equation (eq. 2).  $I_{\text{Si}}$  and  $I_{\text{Silica}}$  represent signal intensity of ionic Si solution and intensity of transient signals for  $\text{SiO}_2$ , respectively. Mass of Si ( $m_{\text{Silica}}$ ) in a single  $\text{SiO}_2$  nanoparticle was calculated from the radius (100 nm), density (2.63 g/cm<sup>3</sup>), and mass fraction (Si/SiO<sub>2</sub> ~ 28/60) of the  $\text{SiO}_2$  nanoparticle solution.  $C_{\text{Si}}$  is the concentration of ionic Si solution (100 ng/mL). In summary, the transport efficiency is calculated by comparing the sensitivity factor of  $^{28}\text{Si}$  between the ionic solution ( $(I_{\text{Si}} - I_{\text{Blk}})/C_{\text{Si}} \cdot v$ ) and the  $\text{SiO}_2$  nanoparticle ( $I_{\text{Silica}}/m_{\text{Silica}}$ ) solution.

$$f = \frac{m_{\text{Silica}}}{C_{\text{Si}} \cdot v} \cdot \frac{(I_{\text{Si}} - I_{\text{Blk}})}{I_{\text{Silica}}}$$

The Single Nanoparticle Application Module of the ICP-MS MassHunter software automatically performed all calculations.

### Bulk concentration analysis

A small aliquot (0.1 mL) of yeast, green alga, and RBC suspended in NaCl solution was digested with 0.5 mL HNO<sub>3</sub> (60%). The cell samples were prepared in a glass test tube, which was heated on a hot plate at 100 °C. The digested cell samples were diluted with Milli-Q water before elemental analysis by ICP-MS. The elemental concentrations were determined from external calibration curves. The elemental content per cell was calculated as follows:

$$\text{ICP-MS determined concentration (fg/mL)} / \text{counted cells (cell/mL)}$$



## Results and discussion

Transient signals for Mg, P, Fe, and Zn were detected in yeast, green alga, and RBC using the 8900 ICP-QQQ operating in fast TRA mode. Typical signal profiles are shown in Figure 3, using Fe and P as examples. A cell suspension solution with a cell density of  $\sim 10^6$  cells/mL provided enough signal for detection.

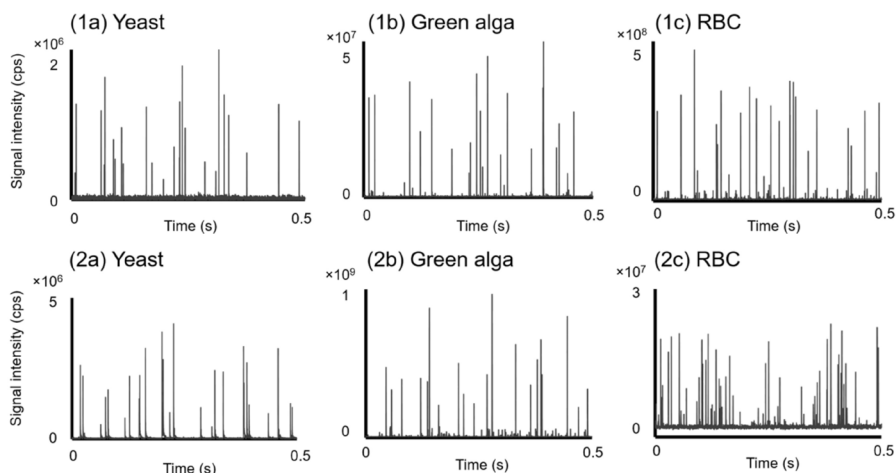


**Figure 3.** Signal profiles of Fe (top, 1a to 1c) and P (bottom, 2a to 2c) in the three types of cell obtained by ICP-QQQ in fast TRA mode.

The mass (fg/cell) of each element in a single cell was automatically calculated by the ICP-MS MassHunter software. The results can be displayed in a histogram of mass per cell against frequency of that mass. Figure 4 shows the Fe and P content of a single cell. Mass distributions of Fe and P in each of the three cells can be clearly distinguished from the background noise on the Y-axis.

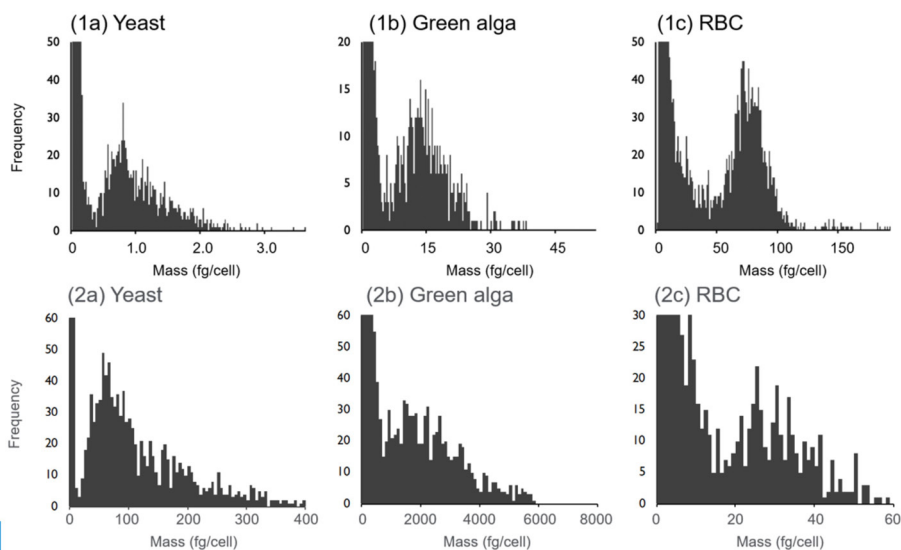


**Figure 4.** Histograms for the mass of Fe (top, 1a to 1c) and P (bottom, 2a to 2c) in a single cell.

A comparison of single cell (SC-ICP-MS, blue bars) and bulk cell (ICP-MS, yellow bars) results for Mg, P, Fe, and Zn is shown in Figure 5. The SC-ICP-MS results show that the average contents of each element varied significantly among the three types of cell.

Green alga was characterized by the higher Mg content than for yeast and RBC, possibly due to the presence of chlorophyll. Mg is required for photosynthesis in the cell. P and Zn in RBC were lower than in other two types of cells, since P and Zn are highly contained in the cell nucleus, and RBCs are enucleated during its differentiation. The higher Fe content of 70 fg in RBC may be due to the presence of hemoglobin.

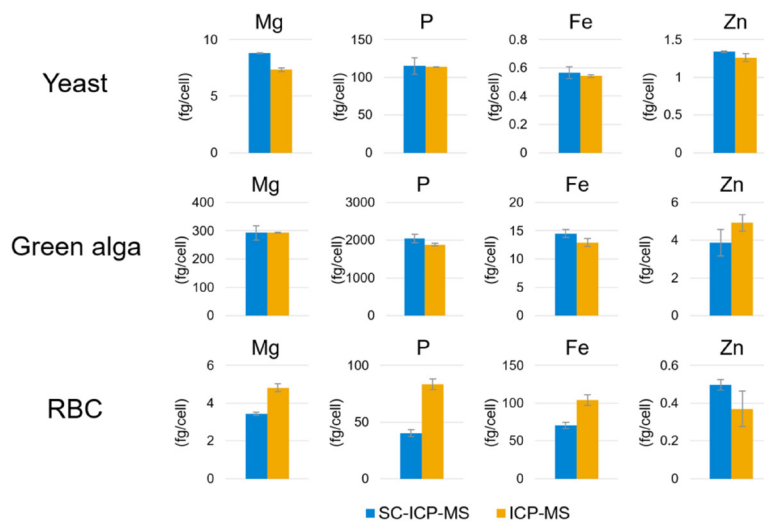


**Figure 5.** Elemental content of yeast (top), green alga (middle), and RBC (bottom).

For yeast and green alga, there was general agreement between the results obtained by SC-ICP-MS and the bulk analysis method (Figure 5) (4). In the RBC, the results obtained by SC-ICP-MS for P, Fe, and Zn were lower than the results obtained by bulk analysis. However, the SC-ICP-MS result for Fe in RBC was consistent with reference data (66.5 fg/cell) calculated using the certified Mean Cell Hemoglobin (MCH) value (5), as shown in Figure 6. Possibly the data from the bulk analysis included a contribution from elements in lysed RBC and/or serum in suspension, resulting in an over-estimation of the results for a single RBC. The confirmation of the Fe data suggests that SC-ICP-MS provides more accurate results than the conventional acid digestion bulk cell method for the determination of the elemental content of single cells.

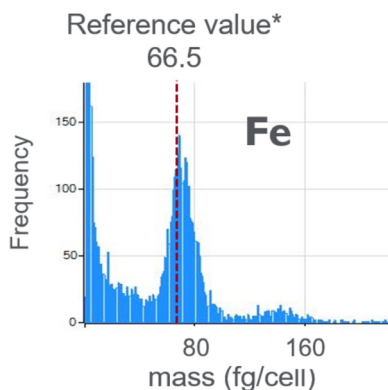


**Figure 6.** Fe mass in RBC measured by SC-ICP-MS.

*\*The reference value was calculated from the certified mean hemoglobin content in RBC for an 11-week-old male Wistar rat provided by the vendor.*

## Conclusion

The high sensitivity, low background, advanced interference removal capabilities, and fast TRA mode of the Agilent 8900 ICP-QQQ enabled the multi-element analysis of a single yeast, green alga, and red blood cell using SC-ICP-MS. All the calculations needed for the analysis of a single cell were automatically performed by the integrated Single Nanoparticle Application Module data analysis software for ICP-MS MassHunter.

The results for Mg, P, Fe, and Zn in yeast and green alga obtained by SC-ICP-MS and conventional bulk ICP-MS analysis were in good agreement, verifying the SC-ICP-MS method. The accuracy of the result for Fe in RBC by SC-ICP-MS was confirmed against a calculated reference value. Since SC-ICP-MS provided a more reliable result for Fe than conventional ICP-MS, the results for Mg, P, and Zn were also likely to be more accurate. By measuring the content of intact RBCs, SC-ICP-MS avoids contamination from elements originating from lysed RBC and/or serum in suspension, leading to more accurate results.

The study demonstrates the potential of SC-ICP-MS as a useful and powerful technique for the quantitative analysis of the elemental content of a single cell.

## References

1. E. Bolea-Fernandez, L. Balcaen, M. Resano, F. Vanhaecke. Overcoming spectral overlap via inductively coupled plasma-tandem mass spectrometry (ICP-MS/MS). A tutorial review, *J. Anal. At. Spectrom.*, **2017**, 32, 1660–1679, <https://doi.org/10.1039/C7JA00010C>
2. E. McCurdy, G. Woods, N. Sugiyama. Method Development with ICP-MS/MS: Tools and Techniques to Ensure Accurate Results in Reaction Mode, *Spectroscopy*, 2019 (9):20–27, <http://www.spectroscopyonline.com/method-development-icp-msms-tools-and-techniques-ensure-accurate-results-reaction-mode>
3. K. Nakano, Ultralow level determination of phosphorus, sulfur, silicon, and chlorine using the Agilent 8900 ICP-QQQ, Agilent publication, [5991-6852EN](https://pubs.aapm.org/doi/10.1118/1.509911)
4. Y. K. Tanaka, R. Iida, S. Takada, T. Kubota, M. Yamanaka, N. Sugiyama, Y. Abdelnour, Y. Ogra, Quantitative Elemental Analysis of a Single Cell by Using Inductively Coupled Plasma Mass Spectrometry in Fast Time-Resolved Analysis Mode. *Chem Bio Chem*, **2020**, 21 (22), 3266–3272, <https://doi.org/10.1002/cbic.202000358>
5. Japan SLC Inc., Wistar rat mean corpuscular haemoglobin (MCH), accessed October 2021, <http://www.jslc.co.jp/pdf/data/2007/wistar2007.pdf>

## Life science

<b>Title</b>	<b>Page</b>
Simultaneous quantitation of peptides and phosphopeptides by capLC-ICP-QQQ	429
Analysis of selenoproteins in rat serum using HPLC-ICP-QQQ	432
Absolute quantification of intact proteins in snake venom by capLC-ICP-QQQ	435

# Simultaneous Quantitation of Peptides and Phosphopeptides by capLC-ICP-QQQ

## Authors

Silvia Diez Fernández<sup>1</sup>, Naoki Sugiyama<sup>2</sup>, Jorge Ruiz Encinar<sup>1</sup> and Alfredo Sanz-Medel<sup>1</sup>

<sup>1</sup>Department of Physical and Analytical Chemistry, University of Oviedo, Spain,

<sup>2</sup>Agilent Technologies, Japan

## Keywords

proteins, peptides, phosphorus, phosphopeptides, sulfur, S-containing peptides, heteroatom, isotope ratio, pharmaceutical, clinical research, drugs, metabolites, environmental, pesticides, nanotechnology, nanoparticles, oxygen mass-shift

## Introduction

LC-MS/MS is used for the quantification of proteins in pharma/biopharma and clinical research. The approach generally relies on the use of synthetic, isotopically-labeled forms of each target protein and peptide, which are used as compound-specific standards for the quantitation of the corresponding target compound. In contrast, the high temperature plasma ionization source used in ICP-MS ensures that elemental response is practically independent of the original form of the compound in which the element occurs. This enables non-species-specific (or compound-independent) quantitation of compounds by measuring the signal for an element contained in the target compound. In this way, different proteins and peptides containing the heteroatoms S and P can be quantified using a known S- or P-containing compound as a generic standard. Unfortunately, with conventional quadrupole ICP-MS, the DLs for P and S are compromised by their high ionization potential and by multiple polyatomic interferences. The Agilent 8800 ICP-QQQ can effectively remove those interferences using reaction cell chemistry combined with the unique MS/MS mode, achieving excellent DLs for P and S even in organic solvents. This paper demonstrates the advantage of ICP-QQQ for the determination of proteins and peptides by measurement of P and S heteroatoms.

## Experimental

**Instrumentation:** An Agilent 8800 Triple Quadrupole ICP-MS was used with an Agilent 1260 Series low flow capillary LC system. The standard 2.5 mm internal diameter (id) injector torch was replaced with the narrow injector, 1.5 mm id torch (G3280-80080) used for the analysis of volatile organic solvents. The exit of the LC column was interfaced to the ICP-MS via an Agilent capillary LC interface kit (G3680A) featuring a total consumption nebulizer and micro-volume spray chamber. O<sub>2</sub> gas (20% O<sub>2</sub> in Ar) was supplied to the plasma as an option gas at 0.08 L/min to prevent carbon build-up on the interface cones. Agilent ICP-MS MassHunter chromatographic software was used for integrated control of the LC-ICP-MS system and for data analysis.

**CRC conditions:** O<sub>2</sub> cell gas flow rate at 0.35 mL/min, Octopole bias = -18 V and KED = -6 V.

**Acquisition conditions:** MS/MS O<sub>2</sub> mass-shift method was applied for P and S measurement as shown in Figure 1.

**LC conditions:** An Agilent Zorbax SB C18 (5 μm, 150 x 0.3 mm) reverse phase column was used with a flow rate of 5 μL/min. Mobile phases of water (A) and acetonitrile (B) were used for a gradient elution with the following profile: 0-3 min: 1% B; 3-35 min: 1-60% B linear. Both mobile phases contained 0.1% formic acid and 10 ppb Ge as ISTD and for tuning. The injection volume was 2 μL.

**Reagents:** Bis-4-nitro-phenyl phosphate (BNPP, 99% purity) and methionine ( $\geq 99\%$  purity) (Sigma- Aldrich, Steinheim, Germany) were used as calibration standards for phosphopeptides and S-containing peptides respectively. Amino acid sequences of the phosphopeptides were LRRRA-pS-LG and KRS-pY-EEHIP, and the S-containing peptides were A-C-TPER-M-AE and VP-M-LK. All peptides were purchased from AnaSpec (Fremont, CA, USA) with purity  $\geq 95\%$ .

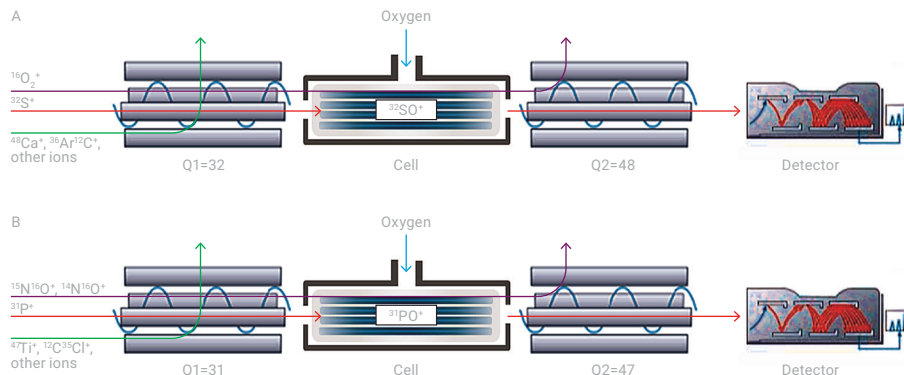


**Figure 1.** 8800 ICP-QQQ MS/MS operation in mass-shift mode to remove interferences on S (A) and P (B).

## Results and discussion

### Calibration and DL

Calibration standards containing 25, 50, 100 and 200 ng/mL (ppb) of both P and S (BNPP and methionine, respectively) were injected and measured. Excellent linearity and RSD of  $<4\%$  was obtained.

The chromatogram for the 50 ng/mL standard was used for signal to noise (S/N) and DL calculation. The DL achieved was 0.10 ng/mL for P and 0.18 ng/mL for S. As the injection volume was 2  $\mu\text{L}$ , the DLs in absolute weight were calculated to be 6.6 fmol and 11 fmol for P and S, respectively.

### Measurement of phosphopeptides and S-containing peptides

Finally, a sample containing a mixture of phosphopeptides and S-containing peptides was analyzed. The sample was also spiked with the standards methionine and BNPP for non-species-specific calibration. The chromatogram shown in Figure 2 illustrates the excellent peak shape and S/N obtained, demonstrating the exciting potential of ICP-QQQ for quantitative protein and peptide analysis using measurement of P- and S-heteroatoms.

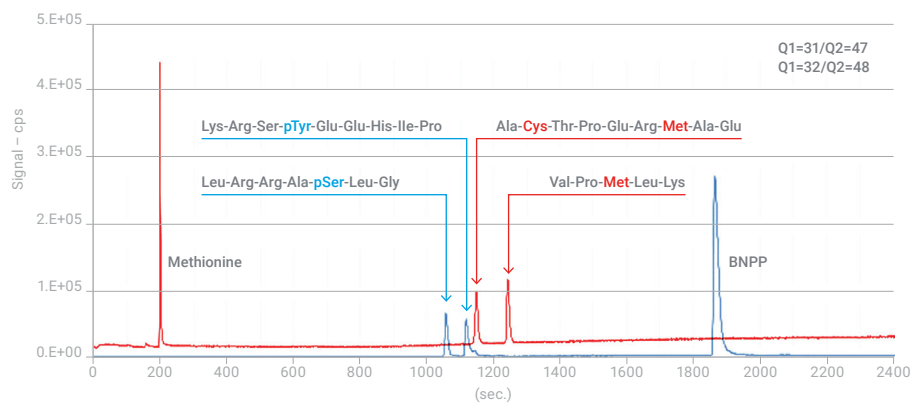


**Figure 2.** Chromatogram of phosphopeptides and S-containing peptides. Sample: 45 ng/mL of two phosphopeptides and two S-containing peptides, and 105 ng/mL of BNPP and methionine (conc. as P or S).

### More information

Simultaneous quantitation of peptides and phosphopeptides by capLC-ICP-MS using the Agilent 8800 Triple Quadrupole ICP-MS, Agilent publication, [5991-1461EN](#)

For Research Use Only. Not for use in diagnostic procedures.

# Analysis of Selenoproteins in Rat Serum using HPLC-ICP-QQQ

## Authors

Yasumi Anan, Yoshiko Hatakeyama,  
Maki Tokumoto, Yasumitsu Ogra  
Showa Pharmaceutical University,  
Tokyo, Japan

## Keywords

selenium, selenoprotein P, Sel P,  
glutathione peroxidase, eGPx, GPx-3,  
serum, biological, rat, mouse, hamster,  
guinea pig, speciation, mass-shift  
method, oxygen reaction mode

## Introduction

Selenium (Se) is an essential micronutrient in animals and is present in several of the key proteins found in plasma. Two selenoproteins which contain Se as selenocysteine (SeCys) in their primary structures, extracellular glutathione peroxidase (eGPx, GPx-3) and selenoprotein P (Sel P), have been detected in animal plasma. Other Se-containing proteins which have Se incorporated into their peptide sequence as selenomethionine (SeMet), are also detected because animals are unable to discriminate SeMet from methionine (Met). The most abundant Se-containing protein in human plasma is albumin. However, some studies have indicated that no or little Se-containing albumin is detected in the blood plasma of experimental animals compared to human plasma [1-3]. This can be explained by the fact that humans ingest Se mainly as SeMet, whereas the major Se species in the feeds given to experimental animals is inorganic Se, such as selenite and selenate.

The three most abundant Se isotopes,  $^{80}\text{Se}$  (49.6%),  $^{78}\text{Se}$  (23.8%), and  $^{76}\text{Se}$  (9.36%), suffer from interference by several polyatomic ions originating from the Ar plasma, namely,  $^{40}\text{Ar}^{40}\text{Ar}^+$ ,  $^{40}\text{Ar}^{38}\text{Ar}^+$ , and  $^{38}\text{Ar}^{38}\text{Ar}^+$ , respectively.  $^{77}\text{Se}$  is also subject to interference by  $^{40}\text{Ar}^{37}\text{Cl}^+$  when chloride is present in the sample matrix, as is the case with biological samples. Sample matrix components such as S, Ca and K may also contribute polyatomic overlaps on isotopes of Se, for example  $^{39}\text{K}^{37}\text{Cl}^+$  on  $^{76}\text{Se}^+$ ,  $^{32}\text{S}_2^{16}\text{O}^+$ ,  $^{32}\text{S}^{16}\text{O}_3^+$  and  $^{40}\text{Ca}_2^+$  on  $^{80}\text{Se}^+$ , and  $^{79/81}\text{BrH}^+$  on  $^{80/82}\text{Se}^+$ .

ICP-QQQ can operate with oxygen cell gas and mass-shift mode, using O-atom addition to move the analyte ions away from the interference for detection at  $M+16$  u. For example,  $^{78}\text{Se}^+$  is measured as  $^{78}\text{Se}^{16}\text{O}^+$  at 94 u;  $^{80}\text{Se}^+$  is measured at 96 u; and  $^{82}\text{Se}^+$  is measured at 98 u. The aim of this study is to evaluate the performance of ICP-QQQ for the speciation of Se in rat serum.

## Experimental

**Instrumentation:** Agilent 8800 #100 was used with an HPLC system.

**CRC conditions:**  $\text{O}_2$  cell gas at a flow rate of 0.30 mL/min.

**Acquisition conditions:** MS/MS  $\text{O}_2$  mass-shift method:  
Se signals were monitored as  $\text{SeO}^+$  at  $m/z$  94, 96, and 98

**LC conditions:** A multi-mode gel filtration column, Shodex Asahipak GS-520HQ (7.5 i.d. x 300 mm, with a guard column, 7.5 i.d. x 75 mm, Showa Denko, Tokyo, Japan), was used. A 200  $\mu\text{L}$  aliquot of serum sample was injected onto the column and then eluted with 50 mmol/L Tris-HCl, pH 7.4, at a flow rate of 0.6 mL/min. The eluate emerging from the column was introduced directly into the nebulizer of the ICP-QQQ.

**Reagents:** The instrument was tuned using an inorganic Se standard. Tris(hydroxymethyl) aminomethane (TRIZMA base and TRIZMA HCl) were purchased from Sigma (St. Louis, MO, USA).



## Results and discussion

### Elution profiles of Se in rat serum

Blood was collected from the experimental rats after one week; the blood was separated by centrifugation, and the serum samples were stored at  $-30\text{ }^{\circ}\text{C}$  prior to analysis by LC-ICP-QQQ. Two well-separated Se peaks were detected at retention times of 11.7 and 14.3 min (Figure 1). The former and latter peaks were assignable to eGPx and Sel P, respectively, per a previous study [4]. It was reported that albumin was eluted at the retention time of 15.0-16.0 min on this column [5]. However, we did not detect a Se peak at a retention time of 15.0-16.0 min, suggesting that SeMet was not incorporated into albumin in place of Met.

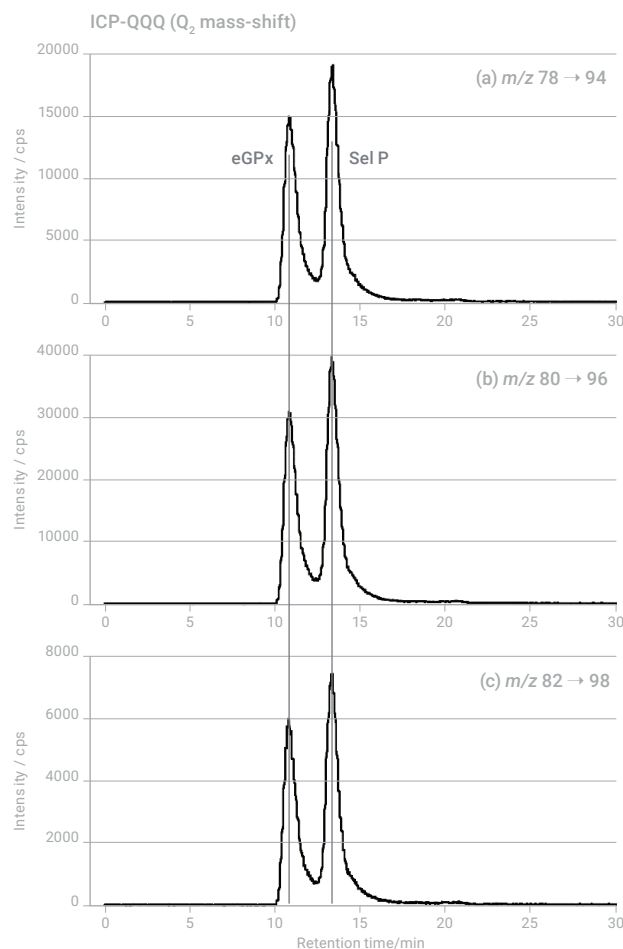


**Figure 1.** Elution profiles of Se in rat serum. A 200- $\mu\text{L}$  aliquot of a rat serum sample was injected into a GS-520HQ column and the eluate was monitored by ICP-QQQ (a-c) at  $m/z$  94 (a), 96 (b), and 98 (c).

## Conclusion

Two major selenoproteins, eGPx and Sel P, in rat serum were well separated on an HPLC column. ICP-QQQ was a more accurate detector for the speciation of serum selenoproteins than conventional quadrupole ICP-MS, because the ICP-QQQ analysis was completely free of interferences originating from the Ar plasma source and any matrix elements.

## References

1. P. Óscar, and R. Łobiński, *Talanta*, 2007, 71, 1813.
2. Y. Kobayashi, Y. Ogra, and K. T. Suzuki, *J. Chromatogr. B Biomed. Sci. Appl.*, 2001, 760, 73.
3. H. Koyama, Y. Kasanuma, C. Y. Kim, A. Ejima, C. Watanabe, H. Nakatsuka, and H. Satoh, *Tohoku J Exp Med*, 1996, 178, 17.
4. Y. Anan, Y. Hatakeyama, M. Tokumoto, and Y. Ogra, *Anal. Sci.*, 2013, 29, 787.
5. Y. Tsuji, T. Mikami, Y. Anan, and Y. Ogra, *Metallomics*, 2010, 2, 412.

## More information

Analysis of selenoproteins in rat serum by Triple Quadrupole ICP-MS, Agilent publication, [5991-2750EN](#)

For Research Use Only. Not for use in diagnostic procedures.

# Absolute Quantification of Intact Proteins in Snake Venom by capLC-ICP-QQQ

## Authors

Francisco Calderon-Celis, Jorge Ruiz Encinar, Alfredo Sanz-Medel

Department of Physical and Analytical Chemistry, University of Oviedo, Spain

Juan Jose Calvete

Instituto de Biomedicina de Valencia, Consejo Superior de Investigaciones Cientificas (CSIC), Valencia, Spain

## Introduction

Venoms are complex biological fluids that contain unique mixtures of peptides and proteins. Identifying and quantifying the composition of venoms is of increasing scientific interest. It is especially important to characterize the toxins responsible for the severe biological effects of the venom on humans. Better understanding of the symptoms of envenoming would help with the development of effective therapies. Also, venoms are being investigated as potential sources of new compounds in drug development.

In this study, an absolute quantification method suitable for the direct quantification of intact proteins was applied to the analysis of the venom of the Mozambique spitting cobra (*Naja mossambica*). This cobra is one of the most dangerous snakes in Africa. The cobra's venom is mainly toxic to cells (cytotoxic), causing swelling of the bite wound that may evolve into tissue necrosis and gangrene [1, 2]. The cytotoxic components of the cobra venom have been identified mainly as members of the three-finger toxin (3FTx) and phospholipase A2 (PLA2) protein families [3, 4].

The methodology was based on capillary liquid chromatography (capLC) coupled to a triple quadrupole ICP-MS (ICP-QQQ). Absolute protein quantification was achieved by measuring the sulfur heteroelement in the proteins, calibrated using online isotope dilution analysis (IDA). ICP-QQQ uses MS/MS mode to control reaction chemistry in the collision/reaction cell (CRC), giving consistent removal of spectral interferences using reactive cell gases [5]. Efficient removal of spectral overlaps using MS/MS allows access to multiple isotopes of biologically important elements such as iron, sulfur, and selenium. ICP-QQQ enables the quantification of metalloproteins and peptides using IDA, without the need for compound-specific calibration standards [6, 7].

Most proteins (> 95%) contain sulfur from methionine and cysteine residues [8, 9], but sulfur determination is difficult by conventional single-quadrupole ICP-MS. The challenges are due to the element's high ionization potential (10.4 eV) that leads to low sensitivity, and the occurrence of spectral interferences from multiple polyatomic ions that overlap all isotopes of sulfur. ICP-QQQ provides low backgrounds and high sensitivity, and removes multiple matrix interferences using MS/MS, freeing up the three most abundant S isotopes for accurate measurement using IDA.

In this study, capLC-ICP-QQQ was used for the quantitative analysis of intact proteins, isolated, and present in simple mixtures. The method was also applied to the analysis and quantification of the major toxins comprising the venom proteome of the Mozambique spitting cobra.

## Experimental

### Reagents and samples

Methionine and BOC-Met-OH (Sigma-Aldrich, Germany) were used as standards. Bovine serum albumin (BSA), transferrin,  $\beta$ -casein, and cytochrome C (Sigma-Aldrich, Germany); and intact monoclonal antibody (mAb) Mass Check Standard (Waters, USA) were used as protein standards in the recovery study. Other reagents included sulfur (1000 mg/L S) ICP standard (Merck KGaA, Germany); solid isotopically enriched  $^{34}\text{S}$  (Isoflex USA); and sodium hydroxide (VWR Chemicals Belgium). Lyophilized *Naja mossambica* venom was obtained from the specialist venom supplier Latoxan S.A.S., France. The venom was collected from a snake from Tanzania, and was stored at  $-20\text{ }^{\circ}\text{C}$  before use. All solutions were prepared in Milli-Q water (ChemLabor Millipore system, with  $0.22\text{ }\mu\text{m}$  filter, Millipak - Millipore). Mobile phase B was prepared in acetonitrile (ACN) Optima<sup>®</sup> LC/MS (Fischer Scientific, USA). Formic acid (FA) was bought from Merck KGaA (Germany).

### Instrumentation

Capillary LC separation was performed using an Agilent 1200 Series HPLC system fitted with a BIOShell<sup>™</sup> A400 C4,  $3.4\text{ }\mu\text{m}$ ,  $150\text{ mm} \times 0.3\text{ mm}$  reversed-phase column (Sigma-Aldrich, Germany) and autosampler. Chromatographic column and post-column connections comprised Agilent PEEK-coated fused silica capillaries  $200\text{ mm} \times 100\text{ }\mu\text{m}$  id (ICP and syringe connection) and  $50\text{ }\mu\text{m}$  (column connection), and a  $0.03''$  ( $0.8\text{ mm}$ ) Agilent zero-dead volume T-connector. Post-column flow was provided by a syringe pump system kdScientific (Holliston, MA, USA). The column was heated using a Spark Holland oven (Mistral, The Netherlands) to improve chromatographic efficiency.

Sulfur isotope measurements were carried out using an Agilent 8800 Triple Quadrupole ICP-MS (ICP-QQQ). The capLC column was connected to the ICP-QQQ using the Agilent capillary LC interface kit (Agilent product number G3680A). The kit consists of a total consumption nebulizer with single pass spray chamber. Enriched  $^{34}\text{S}$  was added to the LC eluate solution post-column to allow sulfur quantification by IDA [10]. Sulfur isotopes were measured by ICP-QQQ using an oxygen mass-shift MS/MS method which successfully resolves a range of interferences on both the  $^{32}\text{S}$  and  $^{34}\text{S}$  isotopes. BOCMet-OH was used as the internal standard (IS) to correct for any injection errors. capLC-ICP-QQQ operating conditions are given in Table 1.

**Table 1.** capLC-ICP-QQQ operating conditions.

ICP-QQQ		
RF power (W)	1550	
Sampling depth (mm)	8.0	
Carrier gas flow rate (L/min)	0.85	
Makeup gas flow rate (L/min)	0.00	
O <sub>2</sub> cell gas flow rate (mL/min)	0.16	
Data acquisition ion pairs, Q1 (S <sup>+</sup> ) » Q2 (SO <sup>+</sup> ) mass ( <i>m/z</i> )	32 → 48 34 → 50	
capLC		
Chromatographic flow rate (μL/min)	4.5; 3.5*	
Mobile phase A	H <sub>2</sub> O/0.2% FA	
Mobile phase B	AcN/0.2% FA	
Temperature (°C)	80	
Chromatographic gradient	Time range (Min)	% mobile phase B
BSA and Intact mAb standards	0	2
	2	2
	16	60
	18	90
<i>Naja mossambica</i> sample	0	1.5
	8	1.5
	10	10
	40	30
	47	90

\* Conditions for measurement of venom sample

## Results and discussion

### Absolute protein quantification

Absolute quantification of proteins was achieved through the measurement of sulfur by capHPLC-ICP-QQQ, with postcolumn IDA. Two individual protein samples (BSA and mAb) were spiked with BOC-Met-OH IS. Quantitative ID (mass purity) results for BSA,  $95 \pm 5\%$  ( $n=3$ ), compared well with the sample purity data provided by the manufacturer ( $\geq 98\%$ ). The ID mass purity result for Intact mAb was  $77 \pm 4\%$  ( $n=3$ ).

To confirm the accuracy and specificity of the ICP-MS/MS analysis, digests of the two protein standards were quantified using external calibration of sulfur. The results obtained by external calibration were  $96 \pm 1\%$  for BSA and  $79 \pm 2\%$  for Intact mAb. These results are in good agreement with the ID mass purity results for BSA and Intact mAb shown above.

## Quantitative analysis of snake venom proteome

The method was applied to the analysis and quantification of the proteins present in a snake venom sample. Before analysis, chromatographic recovery was calculated by measuring the sulfur mass of a sample eluting from the chromatographic column and comparing this to the sulfur mass recorded directly by flow injection (FI). Chromatographic recovery for a series of protein standards (cytochrome C,  $\beta$ -casein, transferrin, BSA, Intact mAb) was higher than 98%. For the *Naja mossambica* protein content, it was  $99 \pm 1\%$  ( $n=3$ ). The total sulfur mass content corresponded almost exactly to the sum of the sulfur contained in the different venom protein peaks detected via their sulfur heteroelement content (Figure 1). The excellent recovery obtained for the complex sample shows that quantitative protein recoveries for the chromatographic column are species (individual protein) independent.

Parallel capLC-ESI-MS analysis was used to identify the proteins from their molecular weight, according to database information (Table 2). By identifying the proteins, it was possible to know the S-to-protein stoichiometry of each peak. This information was then used to translate the measured sulfur mass into individual protein quantities, in  $\mu\text{mol}$  protein per gram of venom sample. The quantified results are summarized in Table 2.

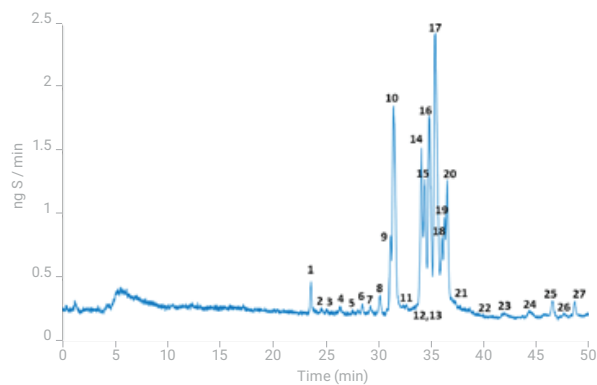


**Figure 1.** capLC-ICP-QQQ mass flow chromatogram of *Naja mossambica* venom. All the venom protein species eluted between 20 and 50 min (S detection). The 27 sulfur-containing peaks are numbered—see Table 2 for More information.

Reprinted with permission from *Anal. Chem.*, 2016, 88 (19), 9699–9706. Copyright 2016 American Chemical Society.

**Table 2.** Matching of the masses of protein peaks from *Naja mossambica* venom to known protein families. Closest available protein species, estimated exact mass, and calculated concentration are listed. Uncertainty corresponds to one standard deviation (n=3).

Peak	Family	Closest homolog	Mol wt (Da)	$\mu\text{mol protein/g venom sample}$
1	3FTx	–	7064.2	1.99 $\pm$ 0.06
2	3FTx	~P29179	7417.4	0.471 $\pm$ 0.066
3	3FTx	~P29179	7451.6	0.325 $\pm$ 0.040
4	3FTx	~P01420	6892.4	1.10 $\pm$ 0.13
5	3FTx	~Q9W6W6	7786.4	< 0.1
6	3FTx	~P01452	7277.3	0.680 $\pm$ 0.050
7	3FTx	~P01452	7306.3	0.668 $\pm$ 0.057
8	3FTx	–	7246.2	1.35 $\pm$ 0.10
9	3FTx	P25517	6832.4	5.09 $\pm$ 0.28
10	3FTx	P01452	6704.3	19.0 $\pm$ 0.8
11	3FTx	–	6686.3	0.183 $\pm$ 0.035
12	3FTx	–	6829.3	0.220 $\pm$ 0.039
13	3FTx	–	6687.3	< 0.1
14	PLA2	P00604	13280.9	7.76 $\pm$ 0.32
15	3FTx	P01470	6882.4	9.54 $\pm$ 0.27
16	3FTx	P25517	6813.3	16.2 $\pm$ 0.4
17	3FTx	P01467	6814.3	27.8 $\pm$ 0.8
18	3FTx	~P01469	7046.4	5.13 $\pm$ 0.26
19	PLA2	P00604	13237.8	3.40 $\pm$ 0.14
20	PLA2	P00002	13196.6	7.35 $\pm$ 0.33
21	PLA2	–	13179.7	0.805 $\pm$ 0.049
22	Minor	–	42000	0.102 $\pm$ 0.009
23	Endonuclease	–	30000	0.619 $\pm$ 0.050
24	SVMP	Q10749	46700	0.165 $\pm$ 0.009
25	SVMP	Q10750	46700	0.264 $\pm$ 0.013
26	SVMP	Q10751	46700	0.097 $\pm$ 0.006
27	SVMP	Q10752	46700	0.257 $\pm$ 0.006

Reprinted with permission from Anal. Chem., 2016, 88 (19), 9699–9706.  
Copyright 2016 American Chemical Society.

## Conclusion

The capLC-ICP-QQQ method uses measurement of sulfur by IDA to enable the absolute quantification of intact proteins without the need for protein-specific standards.

Agilent ICP-QQQ instrumentation is especially suited for IDA analysis of S as it uses MS/MS to remove multiple spectral interferences from several S isotopes using an oxygen mass shift method. By adding enriched  $^{34}\text{S}$  post-column and spiking each sample with a generic S-containing internal standard, multiple S isotopes can be measured as  $\text{SO}^+$  product ions. MS/MS ensures that each S isotope mass enters the CRC in isolation, so no interfering product ions can be formed from the other isotopes of S. This approach allows the sulfur content of the proteins to be determined by IDA.

The method was applied successfully to the quantification and mass purity confirmation of protein standards. If quantitative chromatographic recoveries can be assured, it is even possible to quantify nonpure protein samples using this method. The potential of the methodology for the quantification of intact proteins present in relatively complex samples was demonstrated by separating and quantifying 27 proteins in snake venom.

## References

1. D. A. Warrell, *Lancet*, 2010, 375, 77–88.
2. J.M. Gutiérrez, D. Williams, H.W Fan, D.A. Warrell, *Toxicon*, 2010, 56 (7), 1223-1235
3. D. Petras, L. Sanz, Á. Segura, M. Herrera, M. Villalta, D. Solano, M. Vargas, G. León, D. A. Warrell, R. D. G. Theakston, R. A. Harrison, N. Durfa, A. Nasidi, J. M. Gutiérrez, and J. J. Calvete, *J. Proteome Res.* 2011, 10 (3), 1266–1280.
4. I. Méndez, J.M. Gutiérrez, Y. Angulo, J.J. Calvete, B. Lomonte, *Toxicon*, 2011, 58 (6–7), 558–564.
5. Technical Overview of Agilent 8900 Triple Quadrupole ICP-MS, Agilent publication, 2016, 5991-6942EN
6. Y. Anan, Y. Hatakeyama, M. Tokumoto, and Y. Ogra, Analysis of selenoproteins in rat serum by Triple Quadrupole ICP-MS, Agilent publication, 2013, 5991-2750EN
7. P. De Raeve, J. Bianga, Fast and accurate absolute quantification of proteins and antibodies using Isotope Dilution-Triple Quadrupole ICP-MS. Agilent publication, 2016, 5991-6118EN
8. M. Wind, A. Wegener, A. Eisenmenger, R. Keller, W.D. Lehmann, *Angewandte Chemie International*, 2003, 42:3425–3427
9. H. Zhang, W. Yan, R Aebersold, *Current Opinions Chem. Biol.* 2004, 8 (1) 66–75
10. F. Calderon-Celis, S. Diez-Fernandez, J. M. Costa-Fernandez, J. R. Encinar, J.J. Calvete, and A. Sanz-Medel, *Elemental Mass Spectrometry for Absolute Intact Protein Quantification without Protein-Specific Standards: Application to Snake Venomics*, *Anal. Chem.*, 2016, 88 (19), 9699–9706.

## More information

The full results of the study were published in: Francisco Calderón-Celis et al., *Elemental Mass Spectrometry for Absolute Intact Protein Quantification without Protein-Specific Standards: Application to Snake Venomics*, *Anal. Chem.*, 2016, 88 (19), 9699–9706.

For Research Use Only. Not for use in diagnostic procedures.



# Pharmaceutical

Title	Page
Quantitative analysis of active pharmaceutical ingredients using heteroatoms as elemental labels	442
Fast and accurate absolute-quantification of proteins and antibodies using ID-ICP-QQQ	446
Determination of diclofenac and its related compounds using RP-HPLC-ICP-QQQ	449
Characterization of rare earth elements used for radiolabeling applications by ICP-QQQ	456

# Quantitative Analysis of Active Pharmaceutical Ingredients using Heteroatoms as Elemental Labels

## Authors

Naoki Sugiyama<sup>1</sup>, Yasumi Anan<sup>2</sup> and Yasumitsu Ogra<sup>2</sup>

<sup>1</sup>Agilent Technologies, Tokyo, Japan,

<sup>2</sup>Showa Pharmaceutical University, Tokyo, Japan

## Keywords

protein, heteroatom, API, monoclonal antibody, mAb, sulfonamide, sulfur, zoledronic acid hydrate, phosphorus, clonidine hydrochloride, chlorine, mass-shift, oxygen reaction mode, hydrogen reaction mode

## Introduction

Organic molecules and proteins can be detected and quantified indirectly using ICP-MS to measure a heteroatom “tag” element contained within the targeted compound. For example, a large number of Active Pharmaceutical Ingredients (API) contain sulfur (S), phosphorus (P) or halogens. Unfortunately, S, P and the halogens have high first ionization potentials so they are poorly ionized in the ICP-MS plasma, leading to low sensitivity. S, P and chlorine (Cl) are also difficult to measure by conventional quadrupole ICP-MS (ICP-QMS) due to intense spectral interferences. As a result, accurate analysis of S, P, and the halogens at the analytical ranges that are relevant to pharmaceutical molecules is nearly impossible to achieve by ICP-QMS. However, ICP-QQQ operating in MS/MS reaction cell mode can be applied to resolve these spectral interferences, allowing the quantification of S, P and Cl at far lower levels (biologically relevant concentrations) than was previously possible by ICP-QMS.

In this study, five APIs and a monoclonal antibody (mAb) were analyzed using ICP-QQQ. The targeted compounds included small ( $m = 250\text{--}320$  Da) and large ( $m = 146$  kDa for the mAb) molecules.

## Experimental

**Instrumentation:** An Agilent 8800 ICP-QQQ #100 was coupled to an Agilent 1260 Infinity Bio-inert HPLC system with quaternary pump (G5611A) and autosampler (G5667A). An HPLC flow rate of 0.4 mL/min and an injection volume of 20  $\mu$ L were applied throughout the study.

**CRC conditions:** O<sub>2</sub> at 0.3 mL/min. H<sub>2</sub> flow at 3.0 mL/min. Octopole bias = -4 V and KED = -8 V.

**Acquisition conditions:** MS/MS O<sub>2</sub> mass-shift method for S and P measurement and H<sub>2</sub> mass-shift method for Cl measurement.

**LC conditions:** Two types of columns were used: an Agilent ZORBAX plus C18, 2.1 x 100 mm, 3.5  $\mu$ m (Agilent # 959793-902) was used for the analysis of the small molecules, and an Agilent Bio SEC-3 300 Å, 4.6 x 150 mm, 3  $\mu$ m (Agilent # 5190-2514) was employed for the mAb analysis.

**Reagents:** Sulfamethizole, sulfamethazine, sulfamethoxazole, zoledronic acid hydrate and clonidine hydrochloride were purchased from Sigma Aldrich (St. Louis, MO, US). The monoclonal antibody (IgG2a) was obtained from Agilent Technologies (Agilent #200473).

## Results and discussion

### Sulfur-containing APIs

Three sulfonamide APIs, sulfamethizole, sulfamethazine and sulfamethoxazole, were dissolved separately in methanol or methanol/water. Each sample was filtered, diluted with the LC mobile phase of 13% acetonitrile with 0.1% formic acid, and injected into the HPLC using an isocratic separation. The resulting overlaid chromatograms are shown in Figure 1. The method detection limit (MDL) for the compound sulfamethizole was calculated to be 23 nM (6.3 ppb as the compound and 1.5 ppb as S).

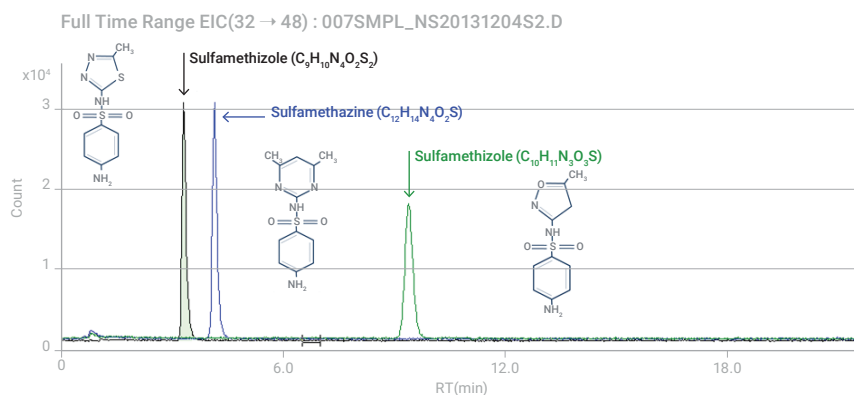


**Figure 1.** Overlaid chromatograms of three sulfur-containing APIs. The concentration of S in all three APIs injected is 100 ppb.

Antibodies are glycoproteins that contain about 1% sulfur and are therefore excellent targets for quantification via sulfur determination by ICP-QQQ. A mAb (IgG2a) obtained from Agilent was diluted with UPW and injected into the HPLC. An isocratic mobile phase of 50 mM phosphate buffer adjusted to pH 7.0 was used. Figure 2 shows the overlaid chromatograms obtained for two different concentrations of IgG2a. The MDL was calculated to be 14 nM (40 ng) as the compound.

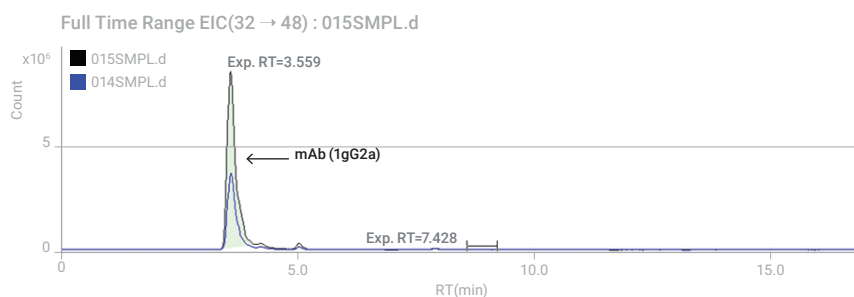


**Figure 2.** Overlaid chromatograms of 0.5 mg/mL and 1.0 mg/mL mAb (IgG2a) obtained by HPLC-ICP-QQQ.

### Phosphorus-containing API

ZOMETA® is a commercial phosphorus-containing drug. It contains zoledronic acid monohydrate ( $C_5H_{10}N_2O_7P_2 \cdot H_2O$ ). A 5 mL vial of commercially supplied ZOMETA® (containing 4.264 mg of the API) was prepared by diluting the drug 2000-fold with the LC mobile phase to give a final API concentration of 426.4 µg/L. The isocratic mobile phase consisted of a 70:30 mixture of A: 6 mM tetra-butyl-ammonium bromide and 5 mM acetic acid adjusted to pH 6.5 with  $NH_3(aq)$ , and B: 95% MeOH. A calibration curve was prepared using zoledronic acid monohydrate standards, and the API in the sample was quantified based on the response for P compared to the external calibration. The concentration of the API in the sample was determined to be 433 ng/mL, which is a recovery of 102%. The MDL for the drug compound was calculated to be 25 nM (144 pg; 7.2 ppb as compound and 1.5 ppb as P).

### Chlorine-containing API

Catapres® is a commercial drug that contains clonidine hydrochloride ( $C_9H_9Cl_2N_3 \cdot HCl$ ). A tablet of Catapres® (containing 75 µg of the API) was dissolved in 50 mL water and sonicated for 60 minutes. The solution was then filtered and analyzed by HPLC-ICP-QQQ. A calibration curve was prepared by analyzing clonidine hydrochloride standards, and the API in the sample was quantified by external calibration. The isocratic HPLC method used a mobile phase consisting of 20% acetonitrile with 0.1% formic acid adjusted to pH 7.0 by  $NH_3(aq)$ . The calibration curve for Cl measured as  $^{35}ClH_2^+$  at  $m/z$  37 and the chromatogram of clonidine hydrochloride measured in the Catapres® sample are presented in Figure 3. The concentration of the API in the sample was determined to be 1444 ppb, which is a recovery of 96%. The MDL of the compound was 146 nM (780 pg; 39 ppb as compound and 15 ppb as Cl).

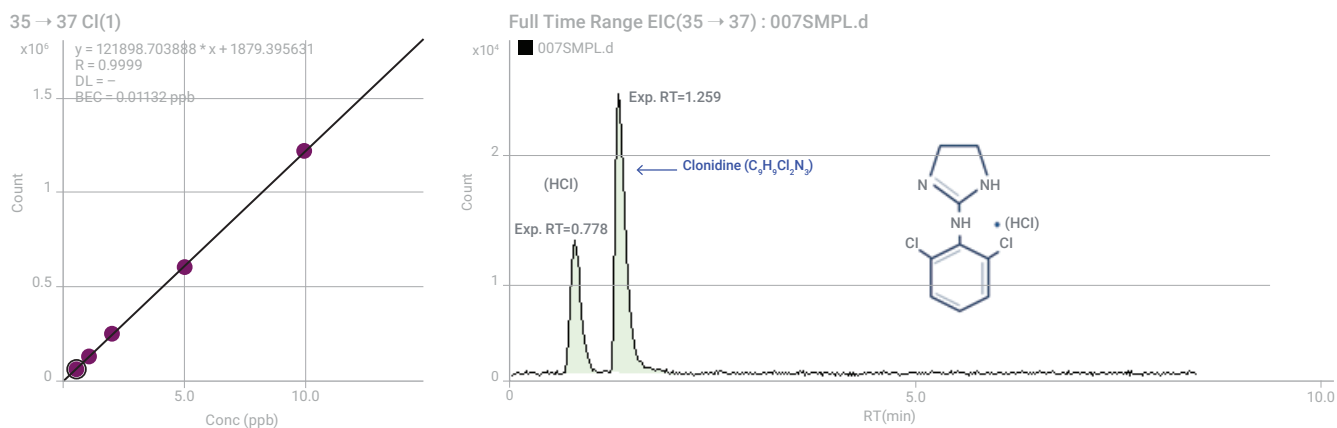


**Figure 3.** (Top) Calibration curve for Cl (measured as  $^{35}ClH_2^+$ ) in clonidine hydrochloride ( $C_9H_9Cl_2N_3 \cdot HCl$ ) standards. (Bottom) Chromatogram of clonidine hydrochloride in Catapres® sample

## Conclusion

The advanced capability of the Agilent 8800 ICP-QQQ operating in MS/MS mode has been successfully applied to the analysis of APIs and mAb, based on the measurement of the heteroatoms S, P and Cl – an analysis that is normally carried out using molecular-MS techniques. These preliminary studies are presented here in order to demonstrate the potential use of HPLC-ICP-QQQ in drug development and post manufacturing QA/QC control.

For Research Use Only. Not for use in diagnostic procedures.

# Fast and Accurate Absolute-quantification of Proteins and Antibodies using ID-ICP-QQQ

## Authors

Philippe De Raeve, Juliusz Bianga  
Quality Assistance S.A., Contract  
Research Organization, Belgium

## Keywords

proteins, antibody, absolute-  
quantification, isotope dilution,  
ICP-MS/MS, ICP-QQQ

## Introduction

Triple quadrupole ICP-MS (ICP-QQQ) dramatically improves the efficiency and reliability of removing spectral interferences on a wider number of elements than conventional ICP-MS. Challenging elements such as sulfur (S), which suffer intense spectral overlaps, can be analyzed at low levels by ICP-QQQ. Furthermore, the effective removal of spectral overlaps allows access to multiple isotopes of elements, enabling quantification of metalloproteins and peptides using isotope dilution mass spectrometry (IDMS) analysis. IDMS is an absolute quantification technique that eliminates the requirement for compound-specific calibration standards. It allows accurate quantification without the need for a reference standard, which is a major benefit of ID-ICP-MS/MS for life science research, where many compounds are unknown.

In this study, we evaluated an Agilent 8800 ICP-QQQ and isotope dilution analysis (ID-ICP-QQQ) of sulfur, for the quantification of NIST Bovine Serum Albumin (BSA) 927e standard reference material (SRM) [1] and a monoclonal antibody, trastuzumab.

## Experimental

**Instrumentation:** An Agilent 8800 #100 was used.

**Acquisition conditions:** two sulfur isotopes,  $^{32}\text{S}$  and  $^{34}\text{S}$ , were measured in MS/MS mass-shift mode with oxygen ( $\text{O}_2$ ) reaction gas.

**Plasma conditions:** RF power = 1550 W, nebulizer gas flow rate = 0.25 L/min, and dilution gas flow rate of 0.85 L/min.

**Double isotope dilution method:** in a simple ID method, a sample containing an unknown amount of S, which is primarily composed of the major  $^{32}\text{S}$  isotope (94.93% abundance), is spiked with a known amount of a certified enriched isotopic standard solution containing  $^{34}\text{S}$ . An aliquot of the resulting solution is analyzed, and the ratio of  $^{34}\text{S}$  to  $^{32}\text{S}$  is measured. From the measured ratio and the known amount of  $^{34}\text{S}$  added, it is possible to calculate the amount of  $^{32}\text{S}$  and therefore the total S concentration (based on natural isotopic abundances) in the original sample.

However, as the  $^{34}\text{SO}_4^{2-}$  spiking solution used in this study was prepared by oxidation of a powder of  $^{34}\text{S}$  sulfur, the exact concentration of  $^{34}\text{S}$  present in the spike was unknown. Therefore, a high accuracy technique known as double IDMS was employed in this study per Equation 1. The concentration of  $^{34}\text{S}$  in the  $\text{H}_2^{34}\text{SO}_4$  solution was determined by reverse IDMS, using a National Institute of Standards and Technology (NIST) certified solution of  $\text{SO}_4$  with a natural sulfur isotopic abundance as the reference standard.

$$w_x = w_z \cdot \frac{m_y \cdot m_z}{m_x \cdot m_{y'}} \cdot \frac{R_y - R_{xy}}{R_{xy} - R_x} \cdot \frac{R_{zy} - R_z}{R_y - R_{zy}}$$

- x refers to the sample
- y and y' refer to the  $^{34}\text{SO}_4$  spiking solution
- z refers to the NIST  $\text{SO}_4$  standard solution
- $w_x$  is the sulfur mass fraction ( $\mu\text{g/g}$ ) in the sample
- $w_z$  is the sulfur mass fraction ( $\mu\text{g/g}$ ) in the NIST  $\text{SO}_4$  standard solution
- $m_i$  is the mass of sample, standard, or spiking solution
- $R_i$  is the  $^{34}\text{S}/^{32}\text{S}$  ratio measured by ICP-QQQ in the unspiked and spiked solutions
- $R_x$  is the  $^{34}\text{S}/^{32}\text{S}$  ratio measured in the sample solution
- $R_y$  is the  $^{34}\text{S}/^{32}\text{S}$  ratio measured in the spiking solution
- $R_z$  is the  $^{34}\text{S}/^{32}\text{S}$  ratio measured in the  $\text{SO}_4$  standard solution
- $m_x$  is spiked with  $m_y$  and ratio  $R_{xy}$  is measured
- $m_z$  is spiked with  $m_{y'}$  and ratio  $R_{zy}$  is measured

**Equation 1.** The double IDMS equation used in this study.

**Samples:** Sample solutions were prepared by microwave digestion. First, an amount of sample (BSA standard and trastuzumab solution) estimated to contain approximately 50  $\mu\text{g}$  sulfur was weighed into a disposable glass tube. 50  $\mu\text{g}$  of  $^{34}\text{S}$  (as  $\text{H}_2^{34}\text{SO}_4$ ) was added, followed by 2 mL of 69%  $\text{HNO}_3$ , 0.5 mL of 37%  $\text{HCl}$ , and 1 mL of 30 %  $\text{H}_2\text{O}_2$ . Once the microwave digestion program had finished, the digest was transferred and diluted to 50 mL with  $\text{H}_2\text{O}$ . The concentration of S in solution was about 1 ppm.

A standard was also prepared for the double IDMS method. 50  $\mu\text{g}$  of a 1000 mg/L sulfur ICP-MS standard (natural isotopic abundance) was weighed into another glass tube. The above procedure was then carried out.

## Results and discussion

Six samples of NIST BSA 927e were quantified using the ID-ICP-MS/MS method. The average recovery to the certified value (67.38  $\pm$  1.38 g/L as S) was 101.26 % and the RSD of six analyses was 0.22%.

Matrix effects were also investigated. The same amount of BSA was spiked with different formulation ingredients. The solutions were then digested and analyzed. The results in Figure 1 show good recoveries were obtained for S in all matrix solutions.

Trastuzumab is a monoclonal antibody (mAb) that was quantified using the developed method. The average recovery to expected value (21 mg/mL as S) was 97.8% and the RSD of three analyses was 0.02%.

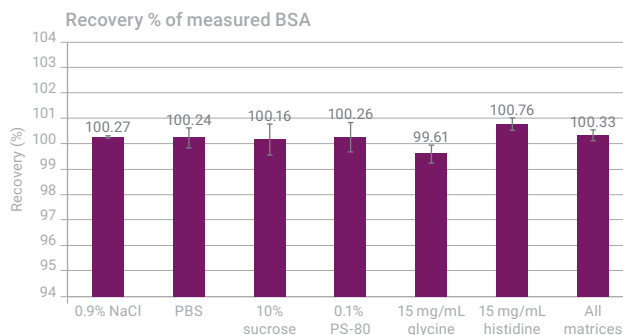


**Figure 1.** Recovery % (average of n = 3) of measured BSA in various matrix solutions. The error bars show the standard deviation of the three analyses.

## Conclusion

The Agilent 8800 ICP-QQQ with MS/MS mode provides high analytical sensitivity and effective interference reduction for the determination of multiple sulfur isotopes. This capability allows the accurate analysis of biological molecules that contain sulfur, using isotope dilution analysis. The ID-ICP-QQQ method is suitable for the accurate and precise quantitative analysis of biological molecules, such as pure proteins and antibodies, without the need for compound-specific calibration standards.

## References

1. National Institute of Standards & Technology SRM 927e certificate
2. P. De Raeve, J. Bianga, Agilent publication, 2015, 5991-6118EN

## More information

Fast and accurate absolute-quantification of proteins and antibodies using Isotope Dilution-Triple Quadrupole ICP-MS, Agilent publication, 2015, [5991-6118EN](#)

For Research Use Only. Not for use in diagnostic procedures.



# Determination of Diclofenac and Its Related Compounds using RP-HPLC-ICP-QQQ

## Authors

Balazs Klencsar<sup>1</sup>, Lieve Balcaen<sup>1</sup>,  
Filip Cuyckens<sup>2</sup>, Frederic Lynen<sup>3</sup>,  
Frank Vanhaecke<sup>1</sup>

<sup>1</sup> Ghent University,  
Department of Analytical  
Chemistry, Belgium

<sup>2</sup> Janssen R&D,  
Pharmacokinetics, Dynamics  
& Metabolism, Belgium

<sup>3</sup> Ghent University,  
Department of Organic and  
Macromolecular Chemistry,  
Belgium

Compound structure-independent quantification of drugs

## Introduction

Quantitative drug metabolite profiling is an important application in the pharmaceutical industry. Researchers involved in drug development require an analytical technique with a response that is independent of compound structure. This compound-independent response enables accurate quantification of the drug and its metabolites, without requiring compound-specific calibration. Currently, radiolabeling techniques followed by HPLC separation and radiodetection are used for this application, but a simpler, quicker, and safer alternative approach is desirable.

The very high temperature plasma ion source and elemental ion-based measurement of ICP-MS enables compound structure-independent quantification, so individual standards for the metabolites of the (candidate) drug are not required. ICP-MS also links seamlessly with chromatography systems, for example HPLC, for speciation studies.

HPLC-ICP-MS is used in a wide range of applications, including speciation studies of metals and metalloids, such as arsenic, mercury, selenium, chromium, and antimony [1]. However, many drugs contain nonmetal heteroatoms such as phosphorus, sulfur, chlorine, fluorine, or bromine, rather than metals and metalloids. The determination of these nonmetals is difficult by conventional single quadrupole ICP-MS, due to poor ionization, spectral overlaps, high backgrounds, or a combination of these factors. Except for F, these “difficult” elements can be measured accurately at low levels by triple quadrupole ICP-MS (ICP-QQQ) operating in MS/MS mode with a reactive cell gas. Reversed phase (RP) HPLC coupled to ICP-QQQ can introduce further analytical challenges due to the changing composition of the mobile phase during the gradient elution. In this study, it was necessary to compensate for the effect of gradient elution on the instrumental response during the RP-HPLC-ICP-QQQ analysis [2].

This note describes the quantitative determination of the drug diclofenac and its related degradation compounds. Diclofenac is a prescription non-steroidal anti-inflammatory drug (NSAID). Compounds were quantified based on measurement of the Cl heteroatom using RP-HPLC-ICP-QQQ.

Chlorine is not a typical analyte for ICP-MS, due to its poor ionization, high background signal, and the presence of intense spectral overlaps. The element's very high first ionization potential of 12.967 eV means that Cl atoms are only converted to positive ions (Cl<sup>+</sup>) with an efficiency of about 0.13 % in an argon plasma operating at a nominal temperature of 7000 K. Chlorine is also a common contaminant in the laboratory, either from handling of sample containers, sample preparation equipment, or instrument hardware. Also, HCl acid is commonly used for stabilization of many elements, and chlorine tablets are often used as a biocidal treatment in deionized water systems, leading to high background.

Finally, both isotopes of Cl ( $^{35}\text{Cl}$  and  $^{37}\text{Cl}$ ) suffer from polyatomic interference from polyatomic ions including  $\text{O}_2\text{H}^+$ ,  $\text{SH}^+$ , and  $\text{ArH}^+$ .

## Experimental

### Samples

Diclofenac sodium (99.9% purity) and 4'-hydroxydiclofenac (99.0% purity) were bought from Sigma-Aldrich (St. Louis, MO, USA). Mixed working solutions containing diclofenac sodium and 4'-hydroxydiclofenac were used for method development, external standard calibration, and method validation. Full details are given in Reference 2. Diclofenac was synthetically degraded to generate degradation products covering a broad hydrophobicity range [2]. The synthetically degraded diclofenac samples were used as part of the mass balance study.

Sample preparation details are given in Reference 2.

### Instrumentation

An 8800\* Triple Quadrupole ICP-MS (ICP-QQQ) was used for all measurements; the instrument was fitted with a PFA nebulizer and platinum cones. The spray chamber was set to a temperature of  $-1\text{ }^\circ\text{C}$  and a plasma torch with a 1.0 mm internal diameter injector was used. These changes helped ensure plasma stability with the high vapor pressure from the volatile organic acetonitrile-based mobile phase. Oxygen (20%  $\text{O}_2$  in Ar) was added to the carrier gas flow at 0.20 L/min to prevent the build-up of carbon on the interface.

To address the spectral overlaps on Cl, the major isotope  $^{35}\text{Cl}$  (75.78% abundance) was measured by ICP-QQQ in MS/MS mode using a mass-shift method with  $\text{H}_2$  cell gas. In this mode, ICP-QQQ avoids the interferences on  $^{35}\text{Cl}$  by measuring the product ion  $^{35}\text{ClH}_2^+$  at  $m/z$  37 [3]. ICP-QQQ operating conditions and acquisition parameters are given in Table 1.

**Table 1.** ICP-QQQ operating conditions and acquisition parameters.

Parameter	Value
RF power (W)	1570
Ar carrier gas flow rate (L/min)	0.30
Optional gas (20% $\text{O}_2$ in Ar) mass flow controller setting	20% (0.2 L/min)
Spray chamber temp ( $^\circ\text{C}$ )	-1
$\text{H}_2$ cell gas flow rate (mL/min)	3.5
Monitored transitions/masses, Q1 $\rightarrow$ Q2 ( $m/z$ )	35 ( $\text{Cl}^+$ ) $\rightarrow$ 37 ( $\text{ClH}_2^+$ )
Data collection mode	TRA
Integration time (s)	0.4 for $m/z$ 37

The ICP-QQQ was coupled to an Agilent 1260 Infinity HPLC System equipped with an Agilent 1260 Infinity Vacuum Degasser, an Agilent 1260 Infinity Binary Pump, an Agilent 1260 Infinity Autosampler, an Agilent 1290 Infinity Thermostatted Column Compartment, and an Agilent 1290 Infinity Series 2-position/10-port Microvalve. Column details and operating conditions are given in Table 2.

\* The 8800 ICP-MS has been superseded by the 8900 model.

To compensate for the increased sensitivity for Cl caused by the changing level of acetonitrile during the gradient elution, a mathematical correction was applied to the Cl response (measured as  $^{35}\text{ClH}_2^+$ ). The correction was based on the measured variation of the Cl response with increasing acetonitrile concentration, as shown in Figure 1.

The chromatographic peaks for the drug and metabolite compounds were identified by retention times (RT), and each peak area was then integrated. The organic solvent concentration at the RT of each peak was calculated from the LC gradient program. The appropriate response factor for each peak was then determined from the organic solvent concentration and the response curve. Finally, the corrected Cl concentration of each peak was calculated based on the peak area and the corresponding response factor.

**Table 2.** HPLC operating conditions.

Online preconcentration	
Analytical column	1570
Eluent A	0.1% (v/v) formic acid in MQ water
Eluent B	0.1% (v/v) formic acid in acetonitrile
Gradient	-1
Flow rate (mL/min)	1.0
Sample temp (°C)	5
Column temp (°C)	22–23 (room temp)
Injection volume (µL)	50

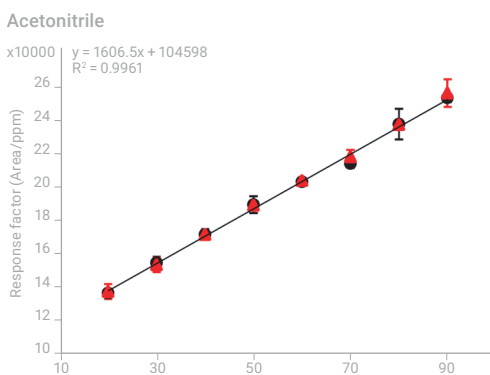


**Figure 1.** Measured response curve demonstrating the Cl ionization enhancement effect caused by the organic solvent (acetonitrile) content of the mobile phase. The Cl response measured by ICP-QQQ is shown for both inorganic Cl and diclofenac-Cl (95% confidence intervals, n = 3). The response factor was found to be independent of the chemical form, as expected.

## Method Development and Method Validation

### Selectivity

Compound selectivity—the ability of a technique to distinguish an individual compound from other (often related) compounds—was confirmed by comparing the chromatograms shown in Figure 2. The chromatograms include (i) a blank, (ii) a mixture of 4'-hydroxydiclofenac and diclofenac, each at a concentration equivalent to 1 mg/L (ppm) Cl (iii) synthetically degraded diclofenac at a concentration equivalent to 10 mg/L Cl, and (iv) synthetically degraded diclofenac (at 10 mg/L Cl) spiked with 4'-hydroxydiclofenac (at 1 mg/L Cl).

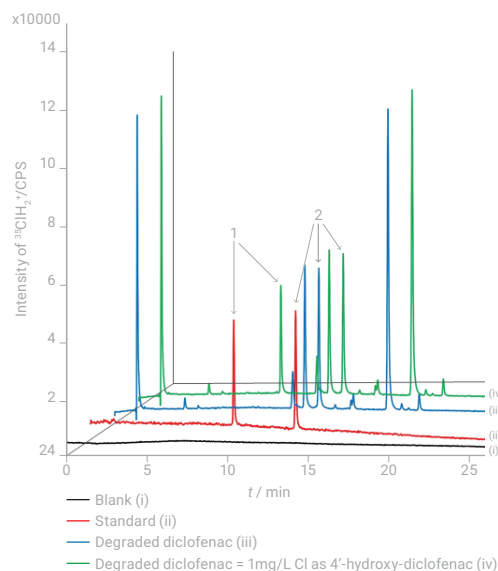


**Figure 2.** Chlorine chromatograms for (i) a blank, (ii) 4'-hydroxydiclofenac plus diclofenac, each at a concentration equivalent to 1 mg/L Cl, (iii) synthetically degraded diclofenac at 10 mg/L Cl, and (iv) synthetically degraded diclofenac at 10 mg/L Cl, spiked with 4'-hydroxydiclofenac at 1 mg/L Cl. Peak 1: 4'-hydroxydiclofenac; peak 2: diclofenac; other peaks: degradation products with unknown chemical structure.

### Accuracy and precision

Accuracy and precision were investigated by spiking blank plasma with 4'-hydroxydiclofenac and diclofenac at three concentration levels (three replicates at each level). The recovery was determined for both compounds. To assess the precision of the method, both intraday and interday precision were studied. As summarized in Table 3, excellent results were obtained with recoveries between 90-100% and RSDs below 4%.

**Table 3.** Accuracy and precision of the results for 4'-hydroxydiclofenac and diclofenac spiked into plasma matrix.

Cl conc (mg/L)	Recovery (%)		Intraday precision (RSD%)		Interday precision (RSD%)	
	4'-hydroxy-diclofenac	Diclofenac	4'-hydroxy-diclofenac	Diclofenac	4'-hydroxy-diclofenac	Diclofenac
0.5	92.4	97.5	2.7	3.2	3.1	2.5
1.0	95.0	97.2	1.8	1.8	1.9	2.3
3.0	91.9	91.8	0.2	0.3	0.3	0.6

### Linearity and Limit of Quantitation

The linearity of the method was tested by injecting diclofenac standard solutions at concentrations equivalent to between 0.05 and 5.0 mg/L Cl. Excellent linearity was achieved with an  $R^2 > 0.99$  and with the origin included in the 95% confidence interval of the intercept.

The limit of quantification (LOQ) was determined according to the signal-to-noise (S/N) method described in the ICH Q2(R1) guidelines (Part II, section 7.2). The LOQ for diclofenac was a compound concentration equivalent to 0.05 mg/L Cl.

### Mass balance study

The mass balance study was performed using a blank solution and a plasma matrix. Each solution was spiked with synthetically degraded diclofenac at a level equivalent to a nominal total Cl concentration of 10 mg/L (the actual total spike amounts are shown in Table 4). The total Cl content of all the compounds in the spiked samples was measured and the concentration and recovery results are given in Table 4.

The recovery for the total Cl content was excellent, both in the absence and presence of the plasma matrix (92 and 93 %, respectively). This matrix-independent response was further confirmed by comparing the results separately for each degradation product peak with and without the plasma matrix. The relative percent differences (RPDs) observed were mostly less than 5%. Slightly higher differences—up to 12% RPD—were observed for compounds that were present at levels close to the LOQ of 0.05 mg/L. It can be concluded that the plasma matrix does not introduce any bias to the results obtained using this method.

**Table 4.** Comparison of mass balance studies with and without plasma sample matrix.

RT/min	v/v % of acetonitrile*	Cl conc without plasma (mg/L)	Cl conc with plasma (mg/L)	Relative difference (%)**
1.4	30.0	2.10	2.10	0.0
4.4	38.3	0.10	0.10	-2.3
11.1	57.1	0.43	0.44	3.3
11.8	59.2	1.29	1.30	1.5
12.7	61.6	1.25	1.27	1.0
14.7	67.2	0.07	0.07	-9.3
14.8	67.6	0.15	0.14	-5.6
17.0	73.6	2.89	2.94	1.5
18.9	79.0	0.15	0.16	0.2
Measured total Cl content (mg/L)		8.49	8.57	
True spike amount (mg/L)		9.21	9.21	
Recovery (%)		92.2	93.1	

\*The eluent composition in which the compound with the indicated retention time is eluted.

\*\*Results in spiked plasma, relative to the values obtained without plasma matrix.

## Enhancing Sensitivity for Cl

### Online sample preconcentration

To improve the sensitivity of the method and enable metabolite profiling of low-dose Cl-based drugs, a simple sample preconcentration procedure was used. The drug-related compounds present in plasma were trapped on a trapping column (Waters XBridge BEH C18 4.6x20 mm; 3.5  $\mu$ m) before analytical separation and ICP-QQQ detection. No additional sample pretreatment was required. The injection volume was increased to 1500  $\mu$ L to load the preconcentration column. More details can be found in Reference 2. Using preconcentration, the LOQ for diclofenac was equivalent to 0.002 mg/L Cl – a 25-fold improvement. Plasma blanks were spiked with 4'-hydroxydiclofenac and diclofenac at three concentration levels between 0.005 and 0.05 mg/L Cl (5 to 50  $\mu$ g/L, ppb). Excellent recoveries between 94 and 98% were obtained for both compounds at all concentration levels, as shown in Table 5.

**Table 5.** Recoveries obtained for 4'-hydroxydiclofenac and diclofenac in the presence of plasma matrix, when using a simple sample preconcentration procedure.

Cl conc ( $\mu$ g/L, ppb)	Recovery (%)	
	4'-hydroxydiclofenac	Diclofenac
5	95.7	96.7
30	97.8	95.7
50	97.4	93.9

### Conclusion

A reversed phase HPLC-ICP-QQQ method has been successfully used for the compound-independent quantitative determination of diclofenac and its related compounds. Based on the measurement of the Cl heteroatom, the new HPLC-ICP-QQQ approach is quicker, simpler, and safer than the traditional radiolabeling HPLC technique.

Since Cl has a high first ionization potential and is poorly ionized in the ICP plasma, ICP-MS sensitivity is usually low. This was overcome using a simple online sample preconcentration procedure. The drug-related compounds from a larger injection volume of plasma were trapped on the preconcentration column, leading to a 25-fold improvement in the LOQ of Cl. This step broadens the application to metabolite profiling of low-dose pharmaceutical drugs containing Cl at sub mg/L levels.

### References

1. Handbook of Hyphenated ICP-MS Applications, Agilent publication, 2012, 5989-9473EN
2. Balazs Klencsar, Lieve Balcaen, Filip Cuyckens, Frederic Lynen, Frank Vanhaecke, *Analytica Chimica Acta* 974, 2017, 43–53
3. Naoki Sugiyama, Trace level analysis of sulfur, phosphorus, silicon and chlorine in NMP using the Agilent 8800 Triple Quadrupole ICP-MS, Agilent publication, 2013, [5991-2303EN](#)

### More information

For a full account of this application, see Balazs Klencsar, Lieve Balcaen, Filip Cuyckens, Frederic Lynen, Frank Vanhaecke, Development and validation of a novel quantification approach for gradient elution reversed phase high-performance liquid chromatography coupled to tandem ICP-mass spectrometry (RP-HPLC-ICP-MS/MS) and its application to diclofenac and its related compounds, *Analytica Chimica Acta* 974, 2017, 43–53, doi.org/10.1016/j.aca.2017.04.030.

For Research Use Only. Not for use in diagnostic procedures.

# Characterization of Rare Earth Elements used for Radiolabeling Applications by ICP-QQQ

## Authors

B. Russell<sup>1</sup>, P. Ivanov<sup>1</sup>

B. Webster<sup>1,2</sup>, D. Read<sup>1,2</sup>

<sup>1</sup>Nuclear Metrology Group, National Physical Laboratory, Teddington, UK

<sup>2</sup>School of Chemistry and Chemical Engineering, University of Surrey, Guildford, UK

Analysis of radiogenic REE isotopes in bulk REE matrices

## Introduction

Radiolabeling refers to a technique where a compound or substance is labeled (or tagged) with a radioactive isotope of an element. The labeled material can then be used for controlled delivery of the radiation emitted by the active isotope, or detected and traced from the radioactivity of the isotopic label.

The use of radiolabeled materials is growing steadily, with the market for radiolabeled pharmaceutical compounds expected to be worth over 5 billion US dollars by 2024 (1). Elements that can form useful radioisotopes include the lanthanides – also known as rare earth elements (REEs). Radio-lanthanide compounds are used in pharmaceutical and imaging applications.

To meet the rising demand for radio-lanthanides, there is a critical need for analytical techniques to support the production of traceable, high purity, labeled lanthanides (2). Production scale chemical purification and labeling of radio-lanthanides is challenging though, because all the lanthanides have similar chemical properties and tend to behave as a consistent group. To prepare a pure radio-lanthanide, it is necessary to accurately characterize the chemical composition of the non-radioactive natural or isotopically enriched starting material used. Before a candidate starting material can be used for routine radionuclide production, each batch must be tested and validated to ensure that radionuclide yields will be of the desired quantity and quality (3). To carry out this level of quality assurance (QA), accurate analytical procedures are needed, particularly to determine the level of trace lanthanide contaminants in the pure lanthanide starting material. Since any impurities need to be removed, the QA data is also useful to guide the design of robust, reproducible chemical separation methods (4). Determining the type and quantity of impurities present in the starting material also helps manufacturers predict whether unwanted radioactive side-products will be produced during irradiation.

Table 1 lists several radio-lanthanide product isotopes that have chemical and radioactive decay properties that make them suitable for applications in radiolabeling. In most of these examples, the starting material is a different element to the intended radio-lanthanide product isotope. This avoids the radio-lanthanide product isotope being affected by high concentrations of a stable isotope of the same element in the irradiated target, which cannot be removed by subsequent chemical separation. Typically, the radionuclides are produced by irradiating a lanthanide or lanthanide oxide starting material target at a nuclear reactor or cyclotron facility. For example, terbium-155 can be produced from gadolinium (III) oxide ( $Gd_2O_3$ ) starting material in a cyclotron. The stable isotope  $^{155}Gd$  is converted to the radioisotope  $^{155}Tb$  via a (p, n) reaction, where a proton enters the nucleus and a neutron leaves the nucleus simultaneously.



**Table 1.** Starting materials and production route for radio-lanthanides used in labeling applications.

Radio-lanthanide	Starting Material*	Possible Nuclear Reaction Production Route**
<sup>153</sup> Sm	<sup>152</sup> Sm	<sup>152</sup> Sm(n, γ) → <sup>153</sup> Sm
<sup>149</sup> Tb	<sup>151</sup> Eu	<sup>151</sup> Eu( <sup>3</sup> He, 5n) → <sup>149</sup> Tb
<sup>155</sup> Tb	<sup>155</sup> Gd	<sup>155</sup> Gd(p, n) → <sup>155</sup> Tb
<sup>161</sup> Tb	<sup>160</sup> Gd	<sup>160</sup> Gd(n, γ) <sup>161</sup> Gd → <sup>161</sup> Tb + β-
<sup>166</sup> Ho	<sup>164</sup> Dy	<sup>164</sup> Dy(n, γ) <sup>165</sup> Dy(n, γ) <sup>166</sup> Dy → <sup>166</sup> Ho + β-
<sup>169</sup> Er	<sup>168</sup> Er	<sup>168</sup> Er(n, γ) → <sup>169</sup> Er
<sup>177</sup> Lu	<sup>176</sup> Yb	<sup>176</sup> Yb(n, γ) <sup>177</sup> Yb → <sup>177</sup> Lu + β-

\* Starting materials are often isotopically enriched targets.

\*\*n (neutron), p (proton), γ (gamma), <sup>3</sup>He (helium-3).

The accurate characterization of REE materials is challenging for conventional single quadrupole ICP-MS. The REEs form hydride (MH<sup>+</sup>), oxide (MO<sub>x</sub><sup>+</sup>), and hydroxide (MOH<sup>+</sup>) polyatomic ions in the plasma or during ion extraction, and these polyatomic ions can overlap the measured isotopes of other REEs. High intensity REE matrix element peaks can also cause peak tail overlaps on trace REE isotopes measured at adjacent masses. This peak tailing effect, known as the abundance sensitivity (AS), is different for different types of mass spectrometer. On commercial single quadrupole ICP-MS instruments, the AS is typically 10<sup>-7</sup>, which means that every 10 million counts at a high intensity peak contributes one count to the adjacent masses. This AS performance means that an intense major element peak can cause peak tailing overlaps on trace analytes at adjacent masses when measured by single quadrupole ICP-MS.

Compared to single quadrupole ICP-MS, Agilent triple quadrupole ICP-MS (ICP-QQQ) instruments offer superior resolution of polyatomic interferences using reactive cell gases. This performance improves accuracy in complex sample types, including analysis of trace REEs in geological samples and materials applications (5, 6). Also, Agilent ICP-QQQ instruments use a tandem mass spectrometer configuration (MS/MS) with two full-sized quadrupole mass analyzers, Q1 and Q2, both housed in high vacuum regions. Two mass filtering steps reduce peak tail overlaps, as the overall AS in MS/MS is the product of the AS of the two quadrupoles, so 10<sup>-7</sup> × 10<sup>-7</sup>, or 10<sup>-14</sup> (7).

Previous studies suggest that ICP-QQQ methods can improve the accuracy of analysis of trace impurities in the lanthanide starting materials/targets used for radio-lanthanide production. Also, assessment of the concentration of impurities in the starting material recovered after chemical separation of the radioisotope could allow for re-use of the recovered material.

The chemical separation methods used to purify radio-lanthanide isotopes can be designed and optimized using stable isotopes of each lanthanide, rather than the radioactive material. ICP-QQQ can be used to measure the intended lanthanide product element at trace (ppt) levels in the presence of a high concentration (ppm level) of the bulk target material. This capability enables realistic testing of the separation scheme while using cheap, safe, and readily available natural REE materials.

In this study, several pairs of trace REE analytes and adjacent mass neighboring REE matrix elements relevant to radio-lanthanide production were measured by ICP-QQQ. The samples included materials that are typically used as irradiation targets for radio-lanthanide production. The use of ICP-QQQ for optimizing radiochemical separation of target lanthanides, and for measuring REE impurities in irradiated targets, was also demonstrated. The developed methods will enable

end users to compile a REE impurity profile of materials of relevance to the production of radionuclides for labeling applications.

## Experimental

### Sample preparation

For the detection limit (DL) study, calibration standards from 1 ppt to 100 ppb were prepared for each trace REE in solutions containing 10 ppm of the neighboring REE matrix element. All solutions were stabilized with 2% HNO<sub>3</sub>. These bulk-trace lanthanide pairs are summarized in Table 2. Similar solutions were prepared to test the extraction chromatography-based chemical separation procedures.

**Table 2.** Pairs of natural REE matrix elements and trace REE analytes used for preparation of calibration standard sets to test resolution of adjacent mass interferences.

Bulk REE Matrix (Isotopic abundance, %)	Trace REE Analyte (Isotopic abundance, %)
<sup>139</sup> La (99.91)	<sup>140</sup> Ce (88.45)
<sup>140</sup> Ce (88.45)	<sup>141</sup> Pr (100)
<sup>158</sup> Gd (24.84)	<sup>159</sup> Tb (100)
<sup>164</sup> Dy (28.18)	<sup>165</sup> Ho (100)
<sup>165</sup> Ho (100)	<sup>166</sup> Er (33.61)
<sup>168</sup> Er (26.78)	<sup>169</sup> Tm (100)
<sup>174</sup> Yb (31.83)	<sup>175</sup> Lu (97.41)

The performance of the ICP-QQQ MS/MS method with O<sub>2</sub> cell gas was investigated using analysis of Tb in the presence of a Gd matrix. Gadolinium (III) oxide powder (Gd<sub>2</sub>O<sub>3</sub>, 99.999 % purity) was gently dissolved in 8 M HNO<sub>3</sub>, evaporated to dryness, and then redissolved in 2% HNO<sub>3</sub> to give a final concentration of 10 ppm Gd.

Irradiated Gd<sub>2</sub>O<sub>3</sub> targets were dissolved in concentrated HNO<sub>3</sub>. To determine the target radio-lanthanide activity levels and any other radionuclides produced, an aliquot was taken for measurement by gamma spectrometry. Following this analysis the sample was left for enough time to allow short-lived radionuclides to decay, after which the stable REE impurities were determined by ICP-QQQ.

### Instrumentation

An Agilent 8800 ICP-QQQ was used in this study. The 8800 was equipped with a standard sample introduction system comprising a glass concentric nebulizer, a quartz spray chamber, a quartz torch with 2.5 mm i.d. injector, and nickel-tipped interface cones. The general instrument operating conditions are summarized in Table 3.

**Table 3.** ICP-QQQ operating parameters.

Parameter	Setting
Scan Mode	MS/MS
Plasma Conditions	Low matrix
RF Power (W)	1550
Extract 1 (V)	0
Extract 2 (V)	-175
Reaction Cell Gas	Oxygen
Oxygen Flow Rate (mL/min)	0.3 (30% of full-scale)
Octopole Bias (V)	-5.0
Energy Discrimination (V)	-7.0
Octopole RF (V)	200

## Results and discussion

### Instrument sensitivity and interference removal

To remove the matrix element hydride and peak tailing interferences for each of the trace REE analytes investigated, the 8800 ICP-QQQ was operated in MS/MS mode with O<sub>2</sub> cell gas. To compare the performance of single quadrupole ICP-MS, the measurements were also performed using the 8800 in single quad mode, where Q1 does not perform any mass selection.

Using the example of trace Tb analysis in a Gd matrix, Tb was measured as the product ion <sup>159</sup>Tb<sup>16</sup>O<sup>+</sup> at *m/z* 175 using mass shift. In single quad mode, the <sup>158</sup>Gd<sup>1</sup>H and <sup>158</sup>Gd tailing interferences were not effectively avoided using O<sub>2</sub> cell gas. A 10 ppm Gd standard gave a signal at *m/z* = 175 of approximately 1.3×10<sup>6</sup> counts per second (cps). This high background meant Tb could not be measured at concentrations below 100 ppt.

Using MS/MS mode with Q1 and Q2 set to *m/z* = 159 and 175, respectively, the *m/z* 175 background signal in the 10 ppm Gd matrix was reduced to ~4,400 cps, which enabled accurate low-level Tb measurement. Using MS/MS, a detection limit of 2.1 ppt was achieved for Tb in the 10 ppm Gd matrix with background subtraction (Figure 1).

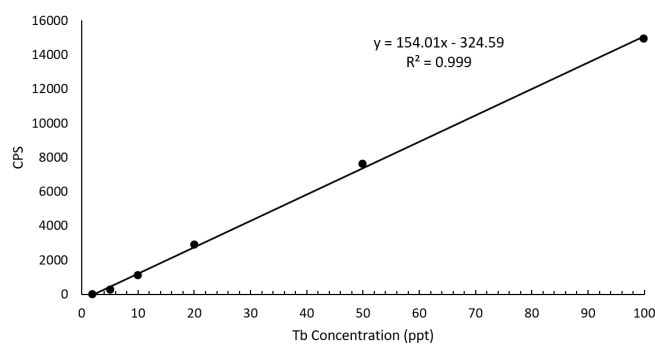


**Figure 1.** Calibration for Tb in the presence of 10 ppm <sup>158</sup>Gd. Tb measured as <sup>159</sup>Tb<sup>16</sup>O<sup>+</sup> by ICP-MS/MS in O<sub>2</sub> mass-shift mode.

A similar trend was seen for the other trace lanthanides listed in Table 4. Operating the 8800 in MS/MS with on-mass or mass-shift mode using O<sub>2</sub> cell gas, DLs in the low ppt range were achieved for most analytes. Only Ho (measured at *m/z* 165) in a Dy (164) matrix and Er (166) in a Ho (165) matrix showed higher DLs, up to 1.1 ppb in the case of Ho in Dy. The ppt level DLs are equivalent to purity levels of up to 2.1×10<sup>-7</sup> relative to the 10 ppm concentration of each respective matrix element. This sensitivity is significantly better than the purity information currently provided by the manufacturers of lanthanide powders. The purity analysis also provides valuable information about possible radionuclides that may be formed from contaminants during irradiation of the lanthanide starting material powders.

The single O<sub>2</sub> cell gas mode used for this study gave acceptable data for all trace lanthanides studied. The DLs for some REEs, e.g., trace Ho in Dy, could be improved by further optimizing the cell conditions or using an alternative reaction gas such as N<sub>2</sub>O or NH<sub>3</sub> (6).

**Table 4.** Detection limits achieved by 8800 ICP-QQQ for trace REEs in REE matrices. Analysis based on measurement of natural, stable isotope elemental standards.

Trace Element (Measured isotope)	Q1 / Q2	Matrix Element (10 ppm)	DL of Trace Element (ppt)
Ce (140)	140/156	<sup>139</sup> La	12.2
Pr (141)	141/157	<sup>140</sup> Ce	11.9
Tb (159)	159/175	<sup>158</sup> Gd	2.1
Ho (165)	165/181	<sup>164</sup> Dy	1100
Er (166)	166/182	<sup>165</sup> Ho	186
Tm (169)	169/185	<sup>168</sup> Er	2.3
Lu (175)	175/191	<sup>174</sup> Yb	9.3

### Measurement of lanthanide oxide samples

The concentrations of trace lanthanides in a solution containing 10 ppm Gd<sub>2</sub>O<sub>3</sub> powder were determined using the 8800 ICP-QQQ with O<sub>2</sub> cell gas. As shown in Figure 2, most REEs were measured on-mass. Only <sup>159</sup>Tb, <sup>172</sup>Yb, and <sup>175</sup>Lu were measured as oxide product ions in mass-shift mode to avoid interferences from <sup>158</sup>Gd<sup>1</sup>H at *m/z* 159, <sup>156</sup>Gd<sup>16</sup>O at *m/z* 172, and <sup>158</sup>Gd<sup>16</sup>O<sup>1</sup>H at *m/z* 175 (Figure 2).

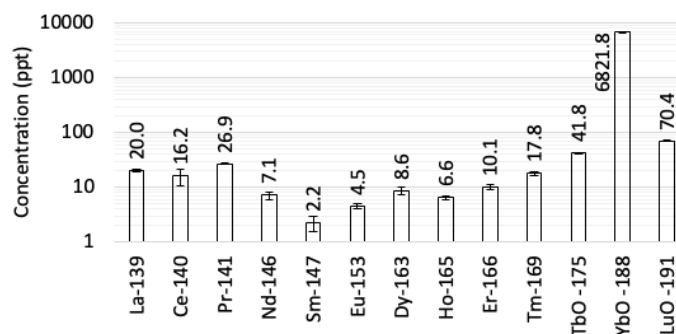


**Figure 2.** Impurity profile and ICP-MS measurement uncertainties (2σ) of Gd<sub>2</sub>O<sub>3</sub> powder used for irradiation.

Elemental standard solutions are used to test chemical separation procedures, so the same ICP-QQQ method was used to measure impurities in a Gd single-element ICP standard. The results are shown in Figure 3. The relatively high measured concentration of YbO in the powder and ICP standard suggests that the interference from <sup>156</sup>Gd<sup>16</sup>O and <sup>156</sup>Gd<sup>16</sup>O<sub>2</sub> on <sup>172</sup>Yb and <sup>172</sup>Yb<sup>16</sup>O, respectively, were not fully resolved. Yb is also not very reactive with oxygen cell gas, leading to low sensitivity for the YbO<sup>+</sup> product ion. The method could potentially be improved through further optimizing the cell conditions or using an alternative cell gas such as N<sub>2</sub>O or NH<sub>3</sub> (6, 7).

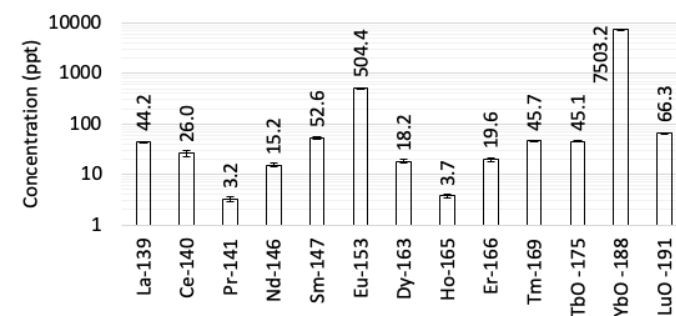


**Figure 3.** Impurity profile and ICP-MS measurement uncertainties (2σ) of a Gd ICP standard using 8800 ICP-QQQ in MS/MS mode with O<sub>2</sub> cell gas.

## Chemical separation results

Operating the 8800 in MS/MS mode with  $O_2$  cell gas and using stable element analogs in place of short-lived radioactive samples enables the optimization of separation procedures under realistic conditions. Realistic conditions refer to the separating of a trace level target lanthanide in the presence of high concentrations of a neighboring lanthanide. This approach enables the development of robust radiochemical procedures before testing with active samples. It also avoids the cost and safety issues of handling active materials during method development.

In this study, Tb was separated from Gd using an extraction chromatography column packed with a LN (lanthanide) resin (50–100  $\mu\text{m}$  particle size, Triskem International). Figure 4 shows an elution profile for Gd and Tb at a  $4.5 \times 10^4$  excess of Gd. Gd was expected to elute with 0.75 M  $\text{HNO}_3$ , while Tb was expected to be retained until conditions were switched to 1.0 M  $\text{HNO}_3$  (8). To check if the separation scheme had been effective, each 1 mL fraction was collected and measured using ICP-MS/MS in  $O_2$  mass-shift mode. The results showed that a small amount of  $^{159}\text{Tb}$  was recovered in the  $^{158}\text{Gd}$  fraction.

The effectiveness of the ICP-QQQ method to resolve Tb from Gd has been demonstrated using trace Tb standards in a Gd matrix. This performance gives confidence that the signal at  $m/z$  159 seen in the Gd fraction was due to trace  $^{159}\text{Tb}$  eluting together with the Gd, rather than an interference from  $^{158}\text{Gd}^1\text{H}$ . Also, based on the starting concentration of Tb added to the column, the total Tb recovery was  $<100\%$ , suggesting little or no contribution from Gd to the measured Tb signal.

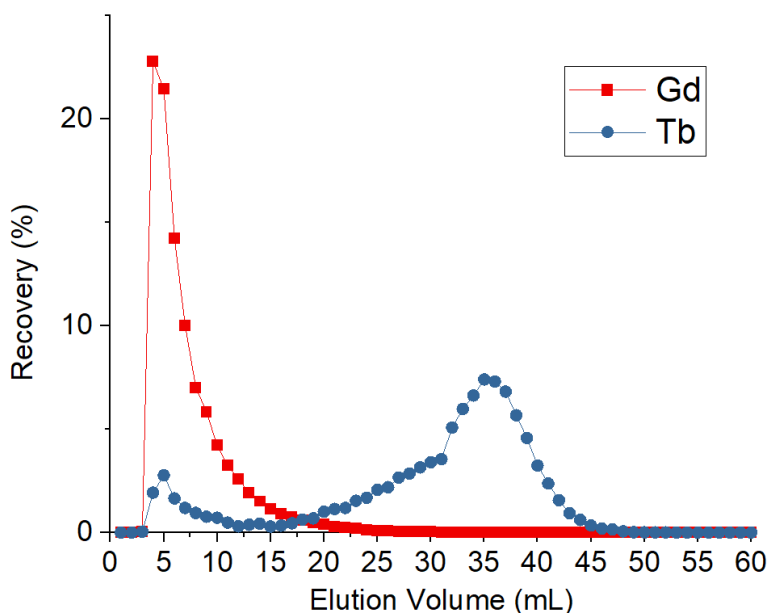


Figure 4. Elution profile for Tb and Gd.

## Measurement of impurities in irradiated samples

A compacted  $\text{Gd}_2\text{O}_3$  powder target was irradiated to produce  $^{155}\text{Tb}$  (half-life of 5.32 days). The irradiated target was then dissolved in concentrated  $\text{HNO}_3$  and an aliquot was used to measure the activity level of  $^{155}\text{Tb}$  and other short-lived radionuclides by gamma spectrometry. After leaving the sample enough time for the radioisotopes to decay, the stable REE isotopes remaining in the  $\text{Gd}_2\text{O}_3$  sample were measured using ICP-QQQ.

Lanthanum and Ce were the only REE contaminants detected in the final sample at concentrations of  $\sim 13.1$  and  $3.5$  ppm, respectively. However, the concentration of both La and Ce was reduced to below background levels after chemical separation. The detection of La and Ce in the irradiated  $\text{Gd}_2\text{O}_3$  powder shows the potential for stable and long-lived radionuclide impurities to be formed during irradiation. The findings illustrate the importance of chemical separation in the production of high purity radio-lanthanides.

The ICP-QQQ method can be used for post-separation analysis of the final radio-lanthanide product to assess the concentration of stable impurities still present, and to help assess the effectiveness of the chemical separation. Depending on the application, enriched or recycled target materials may be used that contain lanthanides at non-natural abundances, which will affect the level of impurities that can be measured. The measurement of such impurities is important as a QA measure, as high concentrations of impurities can lead to competition for the chelating agent used, which can reduce the radiolabeling efficiency.

## Conclusion

The use of radio-lanthanides is of increasing interest in pharmaceutical and imaging applications. Preparation of high purity radio-lanthanides often requires separation of the low concentration target isotope from the high concentration stable REE matrix. To check the purity of the starting REE materials, the Agilent 8800 ICP-QQQ was operated in MS/MS mode with  $\text{O}_2$  cell gas to measure all REE impurities in high-purity REE matrices. The ICP-QQQ method was much more effective at removing REE matrix-based polyatomic and peak tailing interferences compared to single quadrupole ICP-MS.

The measurement of trace levels of Tb in the presence of bulk Gd was used as an example. The results obtained from analyzing stable element standards showed that the method was useful for a range of radio-lanthanides.

Overall, the ICP-MS/MS method improved accuracy and confidence of the measurements needed for a complete REE impurity profile of materials used in the production of radionuclides for pharmaceutical and imaging applications. The study has shown that the method is suitable for:

- The measurement of REE impurities in the starting powders used for irradiation.
- Optimizing chemical separation conditions using stable element analogs.
- Assessing the REE impurities present in the irradiated target material post-irradiation.

## References

1. Markets and Markets, Nuclear Medicine/Radiopharmaceuticals Market by Type (Diagnostic (SPECT - Technetium, PET- F-18), Therapeutic (Beta Emitters – I-131, Alpha Emitters, Brachytherapy – Y-90)), Application (Oncology, Cardiology) - Global Forecast to 2024, accessed online August 2020, <https://www.marketsandmarkets.com/Market-Reports/radiopharmaceuticals-market-417.html>
2. M. Van de Voorde *et al.* Radiochemical processing of nuclear-reactor-produced radio lanthanides for medical applications. *Coordination Chemistry Reviews* **2019**, 382 (1), 103–125
3. The International Pharmacopoeia, Ninth Edition. <https://apps.who.int/phint/en/p/docf/>
4. B. Webster *et al.* Chemical Purification of Terbium-155 from Pseudo-Isobaric Impurities in a Mass Separated Source Produced at CERN, *Nature Scientific Reports* **2019**, 9, 1–9
5. N. Sugiyama, Removal of hydride ion interferences (MH<sup>+</sup>) on Rare Earth Elements using the Agilent 8800 Triple Quadrupole ICP-MS, Agilent publication, [5991-1481EN](#)
6. N. Sugiyama and G. Woods, Direct measurement of trace rare earth elements (REEs) in high-purity REE oxide using the Agilent 8800 Triple Quadrupole ICP-MS with MS/MS mode. Agilent publication, [5991-0892EN](#)
7. N. Sugiyama, Direct Analysis of Ultratrace Rare Earth Elements in Environmental Waters by ICP-QQQ, Agilent publication, [5994-1785EN](#)
8. F. Monroy-Guzman and E. J. Salinas, Separation of Micro-Macrocomponent Systems: Ho-Dy and Lu-Yb by Extraction Chromatography, *J. Mex. Chem. Soc.*, **2015**, 59, 143–150

# Glossary

## A

<b>Acquisition conditions</b>	Parameters including: Peak profile, mass, integration time, scan number and replicate.
<b>ADME</b>	Acronym of absorption, distribution, metabolite, and excretion studies.
<b>Ammonia, NH<sub>3</sub></b>	A reaction gas used in the collision/reaction cell. NH <sub>3</sub> is a very reactive gas, which is used both in on-mass methods and mass-shift methods to remove/avoid interferences.
<b>amu</b>	Atomic mass unit. An obsolete, non-SI unit that is still in common use in its abbreviated form "amu", meaning the same thing as "unified atomic mass unit" (u) or Dalton (Da). All are used to indicate the atomic mass of ions, atoms or molecules, based on the carbon 12 standard.
<b>API, Active Pharmaceutical Ingredient</b>	An API is a compound in a drug which has remedy effects on the target disorder.
<b>AS, abundance sensitivity</b>	The measure of an analyzer's ability to separate adjacent peaks differing greatly in intensity. Agilent ICP-QQQ with MS/MS operation delivers unmatched peak separation (abundance sensitivity <math><10^{-10}</math>), as the resolution performance is the product of the abundance sensitivity of the two quadrupoles.
<b>ASX-520</b>	Autosampler suitable for medium to high sample throughput applications, with rack configurations providing up to 360 vial positions (up to 720 with the extended rack XLR-8 version).
<b>Axial Acceleration</b>	A function of the ion guide to accelerate/decelerate ions along the axis of the ion guide.

## B

<b>Bandpass</b>	Mode of operation of a multipole ion guide, where both a low-mass cut-off and high-mass cut-off are applied, rejecting ions below and above a certain $m/z$ . A bandpass filter passes a "window" of masses (typically covering a 20-30 $m/z$ range) through the ion guide, and is therefore distinct from a mass filter, which is capable of unit mass resolution (single $m/z$ mass selection).
-----------------	---



**Batch** The acquisition batch contains all the information required for a sample analysis or experiment, including peripump program, tuning conditions, acquisition parameters, sample list and data analysis (calibration) parameters. The data analysis (DA) batch contains the measured results for the batch of samples, and includes the calibration plots, internal standard signals and QC flags.

**BEC, Background Equivalent Concentration** The magnitude of a signal in a blank, expressed as a concentration.

**BED, Background Equivalent Diameter** BED is the diameter equivalent to the background noise in single particle analysis.

## C

**Charge transfer** A reaction mechanism that relies on the exchange of charge between ions and cell gas molecules,  
e.g.,  $\text{Ar}^+ + \text{NH}_3 \rightarrow \text{Ar} + \text{NH}_3^+$

**Collision mode** A cell mechanism to remove interferences either by collisional dissociation or by kinetic energy discrimination (KED). With KED, ions entering the collision/reaction cell collide with the cell gas (such as helium). Since polyatomic ions have a larger ionic cross-section than mono-atomic analyte ions at the same mass, the polyatomic ions undergo more collisions than the analyte ions, and so lose more energy. By the cell exit, the lower energy ions (the polyatomics) can be separated from the higher energy (analyte) ions by applying a bias voltage "step". This is known as kinetic energy discrimination (KED).

**Cool plasma** A technique used to reduce interferences. Under low temperature plasma (cool plasma) conditions, the formation of interferences such as  $\text{Ar}^+$ ,  $\text{ArO}^+$  and  $\text{ArH}^+$  is suppressed, allowing the detection of  $\text{Ca}^+$ ,  $\text{Fe}^+$  and  $\text{K}^+$  at the trace level. Typical RF power for cool plasma is 600-900 W.

**CRGS, Carrier gas** Carrier gas is an Ar gas supply flowing through the nebulizer to convert a liquid sample into a fine aerosol. It is a tuning parameter of the plasma.

**CRC, Collision/ Reaction Cell** Device used to remove interferences from the ion beam, using settings such as cell gas, cell gas flow rate, octopole bias voltage, KED bias and deflection lens.

## D

<b>DL</b>	Abbreviation of Detection Limit. Also called LOD (limit of detection). Usually calculated as the concentration that is equivalent to 3 times the standard deviation (SD) of the background signal.
<b>Desolvation system</b>	A device to remove solvent from the aerosol generated by the nebulizer.
<b>DIGS, Dilution Gas</b>	Argon gas flow added to the carrier gas via a dilution gas port located between the torch and the spray chamber. A dilution gas is used for Aerosol Dilution with HMI or UHMI. The gas supply used for the DiGS can also be switched automatically to add the gas flow to the spray chamber instead (known as make-up gas or MUGS). It is a tuning parameter of the plasma.
<b>DMPK: Drug Metabolism and Pharmacokinetics</b>	An approach used to assess the effectiveness and safety of a drug under development.
<b>Dynamic range or analytical working range</b>	The range of linearity of an analytical instrument. Agilent ICP-QQQ instruments are fitted with an advanced, dual-mode, discrete dynode electron multiplier (DDEM) that provides a full nine orders dynamic range under standard operating conditions.
<b>Dwell time</b>	The period of time that the analytical instrument accumulates the signal.
<b>E</b>	
<b>Enthalpy of reaction, <math>\Delta H_r</math></b>	Amount of energy (heat) absorbed or released by a reaction. When $\Delta H_r$ is positive ( $\Delta H_r > 0$ ), the reaction is endothermic, meaning energy is required (absorbed) for the reaction to occur. When $\Delta H_r$ is negative ( $\Delta H_r < 0$ ), the reaction is exothermic, meaning energy is released by the reaction, which is spontaneous.
<b>G</b>	
<b>GC Interface kit</b>	Agilent's GC-ICP-MS interface features a fully heated inert transfer line and separately heated inert torch injector that provides reliable separation of volatile compounds.
<b>H</b>	
<b>HMI, High Matrix Introduction</b>	HMI Aerosol Dilution technology is standard on Agilent ICP-QQQ, extending the TDS range to % level, while eliminating the added cost, time and potential errors of conventional liquid dilution.
<b>UHMI, Ultra High Matrix Introduction</b>	Agilent's second generation aerosol dilution system, which allows the direct analysis of 25% NaCl solutions.

<b>Hard extraction</b>	A tuning condition when a negative voltage is applied to the extraction lens. Hard extraction provides higher sensitivity at lower plasma temperature than soft extraction. Cool plasma conditions require hard extraction.
<b>Helium mode, He mode</b>	See collision mode.
<b>HR-ICP-MS, high-resolution ICP-MS</b>	Also known as magnetic sector, sector field or double focusing. Magnetic sector based ICP-MS instruments are capable of resolution ( $M/\Delta M$ ) of up to 10,000 and are able to resolve most polyatomic species from analytes at the same nominal mass.
<b>I</b>	
<b>I-AS, Integrated Auto sampler</b>	Integrated, covered auto sampler with pumped rinse station; ideal for ultratrace analysis and small sample volumes (as low as 0.5 mL). Flexible rack configurations offer a maximum capacity of 89 vials, plus 3 rinse vials.
<b>ICP</b>	Inductively coupled plasma, generated by applying a high-power radio frequency (RF) field to a flow of argon gas. The plasma is a high temperature ion source, up to 10,000 K maximum and around 7,500 K in the central channel.
<b>ICP-MS</b>	Inductively coupled plasma mass spectrometer or spectrometry.
<b>ICP-QQQ</b>	Abbreviation for triple quadrupole ICP-MS.
<b>IDA, ID, ID-MS</b>	Isotope Dilution Analysis or Isotope Dilution Mass Spectrometry is a highly accurate method to quantify elements based on the change in isotope ratio that results from the spiking of an unknown sample with a spike enriched in one isotope of the target analyte. Because each sample result is based on the measurement of the change in ratio in that sample, rather than relative to a response in a separate calibration standard, IDMS results are also directly traceable to certified standards, which reduces uncertainty.
<b>Inert Sample Introduction kit</b>	O-ring-free and manufactured from PFA for the lowest contamination levels. Demountable torch with Pt or sapphire injector options. HF resistant, and suitable for high-purity reagents.
<b>Interferences – spectral</b>	Direct overlap from a different element with an isotope at the same nominal mass (isobar), or overlap from a polyatomic ion, or doubly-charged ions resulting from the loss of two electrons instead of just one. Because the quadrupole separates ions based on $m/z$ (mass over charge ratio), a doubly-charged ion ( $M^{2+}$ ) will appear at mass $M/2$ .

<b>Ion guide</b>	Operation of an ion lens where no mass rejection is performed. Applies to simple electrostatic ion lenses, and also to multipole ion guides operated with no low- or high-mass cut-off.
<b>IP, Ionization Potential</b>	The first ionization potential of the element is the energy required to remove one electron from a neutral atom and is specific for each element. Most elements are largely converted (>90%) to singly-charged ions in an argon plasma. Elements with a low second IP will also form some doubly-charged ions.
<b>IR, Isotope Ratio</b>	Ratio of abundance of two isotopes of an element.
<b>Isobar</b>	Refers to isotopes of different elements that appear at the same nominal mass. These overlaps occur when atoms of two different elements (i.e. different number of protons in the nucleus, so different atomic number) each have an isotope with the same atomic weight (same total number of protons plus neutrons in the nucleus, e.g. $^{204}\text{Pb}$ and $^{204}\text{Hg}$ ).
<b>Isobaric interferences</b>	Overlaps that occur at the same mass (see isobar). These overlaps/interferences can be resolved by reaction chemistry (e.g. $\text{NH}_3$ is used to separate Pb from the Hg overlap), but cannot be separated by high-resolution ICP-MS; separation of $^{204}\text{Pb}$ from $^{204}\text{Hg}$ would require a resolution of around 500,000 (50x higher than can be achieved by any commercial high-resolution ICP-MS).
<b>Isotope</b>	A specific form (atomic weight) of an element. Many elements have atoms with different atomic weights, such as Pb 204, 206, 207 and 208; these are called isotopes. The different isotopes of Pb all have 82 protons in the nucleus (Pb has atomic number 82) but a different number of neutrons, so the atomic weight is different for each isotope.
<b>ISTD, internal standard</b>	Internal standards are commonly used in ICP-MS, particularly where samples vary in composition from the calibration standards. Changes in sample transport, nebulization efficiency and signal intensity (long-term drift) would all lead to errors, which may be corrected if an ISTD element with similar behavior is used as a reference.

## K

**KED, Kinetic Energy Discrimination** KED is used to discriminate the analyte ion of interest from interfering ion(s) by the difference of kinetic energy. Refer to collision mode. KED is also used as a tuning parameter of CRC conditions:  $KED = (Q2 \text{ bias voltage}) - (\text{octopole bias voltage})$ .

## L

**LA, Laser Ablation** Method used for the direct analysis of solid samples using a laser to vaporize the sample before introduction to the plasma.

**LC speciation kits** Sample introduction kits to facilitate LC coupling and provide turn-key methods for common speciation applications. A Capillary-LC connection kit is also available.

## M

**MUGS, Make-up gas** Make-up gas refers to Ar gas applied to the spray chamber to increase/adjust total injector gas flow rate. It is a tuning parameter of the plasma.

**MS/MS mode** Acquisition mode unique to Agilent ICP-QQQ. MS/MS mode operates Q1 as a unit (1 amu window) mass filter and Q2 is also set to the single mass of the target ion or reaction product ion.

**Mass balance** Balance between the amount of a substance introduced into the system and excreted from the system.

**Mass pair** MS/MS mode requires a mass setting for Q1 and Q2. The selected mass settings for Q1 and Q2 are known as the mass pair. For example when As is measured in O<sub>2</sub> mode, Q1 is set to the precursor ion (As<sup>+</sup>) at  $m/z$  75 and Q2 is set to the product ion (AsO<sup>+</sup>) at  $m/z$  91. 75 --> 91 is the mass pair for As in O<sub>2</sub> mode.

**Mass filter** Generic term for any mass analyzer capable of unit mass resolution. Note that the ion guide used in the CRC of some quadrupole mass spectrometers appears physically similar to a quadrupole mass filter. However, these ion guides cannot provide unit mass resolution because of the ion scattering effect at the higher pressures present in the CRC.

**Mass spectrum** See spectrum.

**Mass-shift method** A method where the analyte ion is reactive and is moved to a new mass free from the original interference. Sometimes referred to as "indirect" measurement, e.g. Se<sup>+</sup> reacts with O<sub>2</sub> in the cell and is converted to SeO<sup>+</sup>. It can then be detected free from the original interference of ArAr<sup>+</sup>.

**MH, MassHunter software** Software package that provides comprehensive instrument control for the Agilent ICP-QQQ and accessories, and integrated data processing.

<b>m-lens</b>	An optional lens of the Agilent 8900. It provides a low BEC for alkaline elements like K and Na under hot plasma conditions.
<b>Monoclonal antibody, mAb</b>	Antibody produced by identical antibody-forming cell, which binds to a certain antigen.
<b>MSA, Method of Standard Additions (also known as StdAdd)</b>	A calibration solution is spiked at multiple levels directly into the unknown sample, giving a calibration of response against added concentration. MSA eliminates matrix effects by calibrating in the sample matrix.
<b>Multiquad ICP-MS, Multi-quadrupole ICP-MS.</b>	Any ICP-MS instrument that incorporates more than one quadrupole. This can apply to a triple quadrupole ICP-MS that uses two quadrupole analyzer mass filters (Q1 and Q2), for example. It can also apply to a single quadrupole ICP-MS that uses a quadrupole ion guide in the collision reaction cell.

## N

<b>Nanoparticle, NP</b>	Sub-microscale particles with at least one dimension in the size range from 1 to 100 nm.
<b>Neutral Gain Scan</b>	Q1 and Q2 scan together, a fixed mass-shift apart. For example, Q2 scans at Q1 + 16 amu for O-atom addition reactions.

## O

<b>O<sub>2</sub>, oxygen</b>	A reaction gas used with the Agilent ICP-QQQ. A number of elements can be measured in mass-shift method using O <sub>2</sub> , e.g. Se <sup>+</sup> can be measured as SeO <sup>+</sup> using O <sub>2</sub> cell gas. O <sub>2</sub> is also added to the plasma carrier gas to decompose the carbon matrix when organic solvents are analyzed.
<b>Octopole bias (OctP Bias)</b>	A CRC parameter. It is the bias voltage applied to the octopole ion guide, which determines the collision energy of analyte ions with cell gas molecules.
<b>OIDA, on-line isotope dilution analysis</b>	A very powerful and useful development of traditional isotope dilution, using on-line addition of the isotope spike. Removes the time consuming step of spiking enriched-isotope standards into each separate sample.
<b>On-mass method</b>	A method where reactive interferences are removed to allow an unreactive analyte to be measured at its original mass. Sometimes referred to as "direct" measurement, e.g., the interference of GdO <sup>+</sup> on Yb <sup>+</sup> can be removed by the reaction of GdO <sup>+</sup> with NH <sub>3</sub> .
<b>Organics kit</b>	Contains the sample introduction parts needed to run volatile organic solvents. Includes organics torch, solvent-resistant drain kit and uptake tubing.

<b>ORS</b>	Agilent's CRC design is known as the Octopole Reaction System. It is a temperature-controlled collision/reaction cell with octopole ion guide and four cell gas lines as standard on the Agilent ICP-QQQ. Provides maximum flexibility in collision and reaction modes, and uses a small internal volume cell to ensure rapid cell gas switching and high ion transmission.
<b>ORS<sup>4</sup></b>	Fourth generation Octopole Reaction System.
<b>Oxygen atom abstraction or oxygen atom transfer</b>	Reaction mechanism associated with the use of oxygen in the collision reaction cell.
<b>P</b>	
<b>Preset method</b>	Preset methods are provided in the ICP-MS MH software. These built-in methods cover a range of predefined operating conditions to suit different applications. Using a preset method, a user can create a new batch with minimum or no customization.
<b>Preset plasma</b>	Preset plasma conditions are a function of ICP-MS MH software. The software provides several predefined plasma conditions that users can select according to the application. This greatly simplifies system optimization by automatically tuning and calibrating the plasma parameters, rather than the user having to set a number of individual plasma tuning parameters. There are three preset plasma conditions that can be selected depending on the sample matrix: Low matrix, general purpose and HMI/UHMI.
<b>Polyatomic, polyatomic ion</b>	A molecular ion (an ion composed of more than one atom) that arises in the plasma or during ion extraction, and can appear at the same nominal mass as analyte ions. Polyatomics are usually interferences (such as ArO <sup>+</sup> ).
<b>Precursor ion scan</b>	Q1 scans a user set mass range, while Q2 is set to a single fixed mass, measuring all the reaction product ions at that mass, formed from the different ions entering the cell as Q1 scans the mass range.
<b>Product ion scan</b>	Q1 is set to a fixed precursor ion mass, while Q2 scans a user set mass range measuring all reaction product ions formed from that single precursor ion.

## Q

**Quadrupole bias (QP Bias or Qpole Bias)** Bias voltage applied to the Q2 rods. Used in conjunction with the Octopole bias to provide a bias voltage “step” at the cell exit, usually to reject unwanted low energy ions from the ion beam.

**Quantitation or quantification** Quantitative results are produced by comparing signal intensities of elements in the sample to those generated by calibration standards.

**Q1** First quadrupole in the configuration of the Agilent ICP-QQQ. Q1 is positioned in front of the ORS, to control the ions that are passed to the cell and enable MS/MS operation.

**Q2** Second quadrupole in the configuration of the Agilent ICP-QQQ. Q2 filters the ions that emerge from the cell exit, passing only the target analyte ions to the detector.

## R

**Rare Earth Elements, REEs** Comprise 17 elements: Sc, Y, La, Ce, Pr, Nd, (Pm), Sm, Eu, Gd, Tb, Dy, Ho, Er, Tm, Yb, and Lu.

**Resolution** The ability of a mass filter to separate adjacent masses. Defined as  $M/\Delta M$ ; the mass of the target peak/the mass difference to the nearest adjacent peak that can be separated. Sometimes also quoted as the width of the peak at a given peak height (e.g. 0.75 u at 10% peak height).

## S

**SEMI** Semiconductor Equipment and Materials International standards are international standards for materials, chemicals and manufacturing devices used in microelectronics industries.

**Single particle (sp) analysis** In this handbook, spICP-MS analysis refers to particle size measurement using the signal generated from a single particle.

**Single Quadrupole MS, ICP-QMS** Conventional ICP-MS containing a single quadrupole mass filter.

**Single Quad mode, SQ mode** Q1 operates as a wide band mass filter. SQ mode emulates conventional quadrupole ICP-MS.

**Speciation measurement** Combination of chromatographic techniques with ICP-MS as a detector to determine the chemical form of elements in the sample.



**Spectrum (mass spectrum)** After separation by the final mass filter (Q2), the ions are detected by an electron multiplier. The detector electronics count and store the total signal for each mass ( $m/z$ ), creating a mass spectrum. The spectrum that is produced provides a simple and accurate qualitative representation of the sample. The magnitude of each peak is directly proportional to the concentration of an element in a sample.

**STS, ShieldTorch System** A technique to eliminate capacitive coupling between the RF coil and plasma, keeping the plasma potential low and energy distribution of ions narrow. The technique is crucial for cool plasma and collision mode.

## T

**TDS, total dissolved solids** The total summed concentration of all non-volatile, dissolved inorganic and organic substances in a liquid. The nominal matrix tolerance of ICP-MS instruments is 0.2 % TDS. On Agilent ICP-MS system, this can be extended to approximately 3% TDS with HDMI, and up to approximately 25% with UHDMI.

**Triple quadrupole ICP-MS** ICP-MS with a tandem MS configuration, featuring a quadrupole mass filter (Q1) in front of the collision/reaction cell (CRC), which is followed by a second quadrupole mass filter (Q2).

## U

**Unified atomic mass unit (u)** Equivalent to Dalton (Da) and the obsolete but still widely used atomic mass unit (amu). All are used to indicate the atomic mass of ions, atoms or molecules, based on the carbon 12 standard.

**UPW** Ultra Pure Water, purified by ion exchange to remove trace contaminants. Used for preparation of standards and for sample dilution for ultratrace analysis

## V

**Venomics** The study of venoms via genomic, proteomic, and transcriptomic approaches.

Learn more:

[www.agilent.com/chem/icpms](http://www.agilent.com/chem/icpms)

Buy online:

[www.agilent.com/chem/store](http://www.agilent.com/chem/store)

U.S. and Canada

**1-800-227-9770**

[agilent\\_inquiries@agilent.com](mailto:agilent_inquiries@agilent.com)

Europe

[info\\_agilent@agilent.com](mailto:info_agilent@agilent.com)

Asia Pacific

[inquiry\\_lsca@agilent.com](mailto:inquiry_lsca@agilent.com)

**For Research Use Only. Not for use in diagnostic procedures.**

DE71430128

This information is subject to change without notice.

© Agilent Technologies, Inc. 2022  
Published in the USA, July 4, 2022  
5991-2802EN

